

CONFERENCE COLLECTION

5TH WORLD CONFERENCE ON MARINE BIODIVERSITY

Understanding the current state and importance of
biodiversity in the marine environment



PeerJ
Life & Environment

A *PeerJ Life & Environment* Conference Collection in
association with the World Conference on
Marine Biodiversity

Peer Reviewed Research Articles

Biogeography, diversity and environmental relationships of shelf and deep-sea benthic Amphipoda around Iceland

Anne-Nina Lörz, Stefanie Kaiser, Jens Oldeland, Caroline Stolter, Karlotta Kürzel, Saskia Brix

A new threat to local marine biodiversity: filamentous mats proliferating at mesophotic depths off Rapa Nui

Javier Sellanes, Matthias Gorny, Germán Zapata-Hernández, Gonzalo Alvarez, Praxedes Muñoz, Fadia Tala

Dongsha Atoll is an important stepping-stone that promotes regional genetic connectivity in the South China Sea

Shang Yin Vanson Liu, Jacob Green, Dana Briggs, Ruth Hastings, Ylva Jondelius, Skylar Kensinger, Hannah Leever, Sophia Santos, Trevor Throne, Chi Cheng, Hawis Madduppa, Robert J. Toonen, Michelle R. Gaither, Eric D. Crandall

The modelled distribution of corals and sponges surrounding the Salas y Gómez and Nazca ridges with implications for high seas conservation

Samuel Georgian, Lance Morgan, Daniel Wagner

Adding pieces to the puzzle: insights into diversity and distribution patterns of Cumacea (Crustacea: Peracarida) from the deep North Atlantic to the Arctic Ocean

Carolin Uhlir, Martin Schwentner, Kenneth Meland, Jon Anders Kongsrud, Henrik Glenner, Angelika Brandt, Ralf Thiel, Jörundur Svavarsson, Anne-Nina Lörz, Saskia Brix

Microplastic ingestion by commercial marine fish from the seawater of Northwest Peninsular Malaysia

Yuen Hwei Foo, Sharnietha Ratnam, Er Vin Lim, Masthurah Abdullah, Vincent J. Molenaar, Aileen Tan Shau Hwai, Shoufeng Zhang, Hongjun Li, Norlaila Binti Mohd Zanuri

Habitat variability and faunal zonation at the Ægir Ridge, a canyon-like structure in the deep Norwegian Sea

Saskia Brix, Stefanie Kaiser, Anne-Nina Lörz, Morgane Le Saout, Mia Schumacher, Frederic Bonk, Hronn Egilsdottir, Steinunn Hilma Olafsdottir, Anne Helene S. Tandberg, James Taylor, Simon Tewes, Joana R Xavier, Katrin Linse

Related Content

Navigating paths through science as early career researchers: A WCMB panel discussion

Navigating Early Careers as Women in Marine Science: A WCMB panel discussion

PeerJ Awards Winners

Interview with Dr. Shang Yin Vanson Liu

5th World Conference on Marine Biodiversity Collection Introduction

The *5th World Conference on Marine Biodiversity Collection* - published in the *PeerJ Life & Environment journal* - collates research presented at the 2020 edition of the *WCMB series*, which was held virtually by the University of Auckland, New Zealand in December of that year.

The WCMB series first started in 2008, and has become a major focal assembly for sharing research outcomes, management and policy issues, as well as discussions on the role of biodiversity in sustaining ocean ecosystems. This meeting brings together scientists, practitioners, and policy makers to discuss and advance our understanding of the importance and current state of biodiversity in the marine environment.

The 5th edition of the WCMB saw over 400 delegates from 45 countries attend the 3-day conference.



5th World Conference
on Marine Biodiversity
AUCKLAND | 13-16 DECEMBER 2020

The WCMB has continued its association with PeerJ, from a collection of abstracts for the 4th WCMB to this collection of full research articles from the 5th WCMB, along with sponsoring four Early Career Researchers awards.

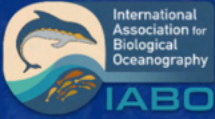
The 6th WCMB will be hosted by the Centre for Marine & Coastal Studies (CEMACS) of Universiti Sains Malaysia in Penang, Malaysia.

Mark Costello, 5th WCMB convenor.



IABO Hub

The publishing community of the
International Association for Biological
Oceanography



IABO Hub

PeerJ and the International Association for Biological Oceanography have been working together to create the IABO Hub: the publishing home of the International Association for Biological Oceanography.

Visit the IABO Hub

The Hub features the latest research published by members of IABO.

“Through the IABO Hub we hope to boost the scientific impact of the IABO community by lowering the costs of publishing Open Access, enhancing the visibility of research conducted by our members, facilitate networking experiences within our association and developing a Hub Cooperative Publishing Fund to support early-career researchers and IABO members from countries of emerging economies”

- Enrique Montes, President of the International Association for Biological Oceanography.

IABO Members receive publishing discounts, and can access and contribute to a Cooperative Publishing Fund. Submissions to the Hub are assessed by the Hub Editorial Team, made up of IABO members, to ensure that the research featured is of interest to the IABO community. Approved manuscripts are peer reviewed and published in the Open Access journal *PeerJ Life & Environment*.

To read more about PeerJ Hubs, please visit: <https://peerj.com/hubs>



PeerJ Publishing



PeerJ

PeerJ is a modern and streamlined publisher, built for the internet age. Our mission is to give researchers the publishing tools and services they want, with a unique and exciting experience. All of our seven journals are Gold Open Access and are widely read and cited, with over 500,000 monthly views and 48,500 content alert subscribers. We have published 12,844 peer-reviewed articles since 2013.



Prestigious
Editorial Board



High-Impact
Research



Quality
Peer Review



Rapid
Publishing



Optimum
Discoverability



PeerJ Life & Environment



PeerJ
Life & Environment

PeerJ's flagship journal, publishing primary research and reviews in biology, life sciences, environmental sciences, and medicine. High-quality, developmental peer review, coupled with industry leading customer service and an award-winning submission system, means PeerJ Life & Environment is the optimal choice for your research.

Impact Factor: 3.06
Citescore: 4.7

Scimago Ranking: 0.766
SNIP: 1.074

PeerJ Conference Collections are free for conference organisers and can increase the visibility of both the event and the research presented during the meeting. If you are organising a conference and would like to consider a PeerJ Conference Collection, email us at communities@peerj.com.

Biogeography, diversity and environmental relationships of shelf and deep-sea benthic Amphipoda around Iceland

Anne-Nina Lörz¹, Stefanie Kaiser², Jens Oldeland³, Caroline Stolter⁴, Karlotta Kürzel⁵ and Saskia Brix⁶

¹ Institute for Marine Ecosystems and Fisheries Science, Universität Hamburg, Hamburg, Germany

² Faculty of Biology and Environmental Protection, Department of Invertebrate Zoology and Hydrobiology, University of Łódź, Lodz, Poland

³ Eco-Systems, Hamburg, Germany

⁴ Department Biology, Zoological Institute, Universität Hamburg, Hamburg, Germany

⁵ Department Biology, Universität Hamburg, Hamburg, Germany

⁶ Deutsches Zentrum für Marine Biodiversität, Senckenberg Nature Research Society, Hamburg, Germany

ABSTRACT

The waters around Iceland, bounding the Northern North Atlantic and the Nordic seas, are a region characterized by complex hydrography and seabed topography. This and the presence of the Greenland-Iceland-Faroe-Scotland ridge (GIFR) are likely to have a major impact on the diversity and distribution of the benthic fauna there. Biodiversity in this region is also under increasing threat from climate-induced changes, ocean warming and acidification in particular, affecting the marine realm. The aim of the present study was to investigate the biodiversity and distributional patterns of amphipod crustaceans in Icelandic waters and how it relates to environmental variables and depth. A comprehensive data set from the literature and recent expeditions was compiled constituting distributional records for 355 amphipod species across a major depth gradient (18–3,700 m). Using a 1° hexagonal grid to map amphipod distributions and a set of environmental factors (depth, pH, phytobiomass, velocity, dissolved oxygen, dissolved iron, salinity and temperature) we could identify four distinct amphipod assemblages: A Deep-North, Deep-South, and a Coastal cluster as well as one restricted to the GIFR. In addition to depth, salinity and temperature were the main parameters that determined the distribution of amphipods. Diversity differed greatly between the depth clusters and was significantly higher in coastal and GIFR assemblages compared to the deep-sea clusters north and south of the GIFR. A variety of factors and processes are likely to be responsible for the perceived biodiversity patterns, which, however, appear to vary according to region and depth. Low diversity of amphipod communities in the Nordic basins can be interpreted as a reflection of the prevailing harsh environmental conditions in combination with a barrier effect of the GIFR. By contrast, low diversity of the deep North Atlantic assemblages might be linked to the variable nature of the oceanographic environment in the region over multiple spatio-temporal scales. Overall, our study highlights the importance of amphipods as a constituent part of Icelandic benthos. The strong responses of amphipod communities to certain water

Submitted 30 March 2021

Accepted 13 July 2021

Published 11 August 2021

Corresponding author

Anne-Nina Lörz, Anne-Nina.

Loerz@uni-hamburg.de

Academic editor

Mark Costello

Additional Information and
Declarations can be found on
page 27

DOI [10.7717/peerj.11898](https://doi.org/10.7717/peerj.11898)

© Copyright

2021 Lörz et al.

Distributed under

Creative Commons CC-BY 4.0

OPEN ACCESS

mass variables raise the question of whether and how their distribution will change due to climate alteration, which should be a focus of future studies.

Subjects Biodiversity, Biogeography, Ecology, Marine Biology, Zoology

Keywords Amphipoda, Biodiversity, Biogeography, Deep sea, North Atlantic, Arctic, Water masses, Benthic

INTRODUCTION

Human impacts on the world's oceans are fundamentally altering the biogeography and biodiversity of marine communities (*Lotze et al., 2006; Halpern et al., 2008*). Cumulating effects of climate change, resource exploitation and pollution are particularly pronounced in the Northern Hemisphere, and some of these changes have already evoked significant biotic responses, such as shifts in distribution and abundance (e.g., *Harley et al., 2006; Jones et al., 2014; Birchenough et al., 2015; Hiddink, Burrows & García Molinos, 2015*). The pace and strength of global warming and increased atmospheric CO₂ may be faster and greater in the ocean than in the terrestrial realm (*Burrows et al., 2011*), but our knowledge of the consequences for the marine biota is limited (*Richardson & Poloczanska, 2008*). Uncovering distribution patterns of species and the identification of the ecological and evolutionary factors and processes responsible for them is therefore vital for predicting biodiversity responses to global change.

A complex array of mechanisms have been identified to determine the distribution of species on multiple spatial and temporal scales (*Leibold et al., 2004*). Abiotic variables confine the space that species occupy according to their physiological limits (*Chase & Leibold, 2003*). Species' dispersal capacity alongside their evolutionary heritage defines the size of their realized distribution (*Grantham, Eckert & Shanks, 2003; Hilário et al., 2015; Baco et al., 2016*). Finally, biological relationships are known to structure spatial patterns of species in many ways, such as those associated with competitors, consumers, and facilitators (*Jablonski, 2008; Bascompte, 2009*).

Environmental differences may be less obvious in the deep sea (>200 m) than in the shallows. It is now clear, though, that there is considerable spatial and temporal variation in the physical and biological properties to which species are exposed and which determine their distribution. Processes associated with sediment properties, temperature, salinity, nutrient input and dissolved oxygen are among the main drivers for structuring biodiversity and its geographical distribution (*Levin et al., 2001; Schnurr et al., 2018*). However, there is still a lack of understanding of distribution boundaries in the marine realm and even less so in the deep sea (*Lourie & Vincent, 2004; Rex et al., 2005*), making it difficult to predict how communities will respond in the wake of a changing ocean.

The waters around Iceland and adjoining seas represent a spatially heterogeneous environment with steep gradients that promote distinct habitats and related communities. As a boundary region between temperate North Atlantic, and polar waters, they are also considered to be very susceptible to climatic changes (*Astthorsson, Gislason & Jonsson, 2007; Eiríksson et al., 2011*). Iceland is located on top of the mid-Atlantic ridge and is

criss-crossed by several topographic barriers that determine the flow of water masses and ultimately the distribution of species. At the forefront is the Greenland-Iceland-Faroe ridge (GIFR), which stretches from Scotland and the Faroes *via* Iceland to Greenland, and restricts the exchange of water masses between the warm, salty North Atlantic waters and the cold and less salty Nordic Seas (Hansen *et al.*, 2008). As a result, seabed temperature and salinity differ strongly between areas north and south of the GIFR, which, in turn, can lead to marked differences in species compositions (Weisshappel & Svavarsson, 1998; Weisshappel, 2000; Bett, 2001; Weisshappel, 2001; Brix & Svavarsson, 2010; Dauvin *et al.*, 2012; Jochumsen, Schnurr & Quadfasel, 2016; Schnurr *et al.*, 2018). Alterations of the physicochemical environment, including temperature rise, ocean acidification, and salinity, have already been observed around Iceland (Astthorsson, Gislason & Jonsson, 2007; Olafsson *et al.*, 2009; Seidov *et al.*, 2015; Jochumsen, Schnurr & Quadfasel, 2016). Knowledge on the most important environmental parameters structuring deep-sea benthic communities would therefore allow prediction of future changes for those communities.

Amphipod crustaceans are very common and diverse across marine benthic habitats (Just, 1980; De Broyer & Jazdzewski, 1996; Lörz, 2010; Stransky & Brandt, 2010; Brix *et al.*, 2018; Jazdzewska *et al.*, 2018), and also in Icelandic waters (Weisshappel, 2000; Weisshappel, 2001; Dauvin *et al.*, 2012; Brix *et al.*, 2018). Their occurrence in a wide variety of marine environments, in turn translates into a diverse feeding types that comprise detritivores, suspension-feeders, predators, and scavengers amongst others (Guerra-García *et al.*, 2014). But they also play a central role in the marine food web (*e.g.*, Lörz, 2010; Nyssen *et al.*, 2002). Amphipods, as a member of the crustacean superorder Peracarida, have a brooding life style, from which a limited dispersal capacity is derived for most species making them potentially very susceptible to environmental change (*e.g.*, Jablonski & Roy, 2003; but see Lucey *et al.*, 2015). Exceptions are purely pelagic species (*e.g.*, within the Hyperiidea) or species of the highly mobile scavenging guild.

The aim of this study was to identify the main factors influencing the distribution and biodiversity of marine amphipods in the waters around Iceland. This could provide hints as to which variables could most importantly affect distribution changes as a result of climate change. For this purpose, a comprehensive data—set from the literature and recent expeditions was compiled constituting distributional records for 355 species across a major depth gradient (18–3,700 m). These come from historical missions, in particular the Danish Ingolf expedition (1895 and 1896), which carried out sampling in Icelandic and West Greenlandic waters (Stephensen, 1944b), but mainly from sampling as part of BIOICE (Benthic Invertebrates of Icelandic Waters) and IceAGE (Icelandic marine Animals: Genetics and Ecology) projects (*e.g.*, Brix *et al.*, 2014). Earlier community analyses of the Icelandic amphipod fauna identified depth as a strong driver of species distributions, but water mass properties were also important (Dauvin *et al.*, 2012; Brix *et al.*, 2018). In this regard, the GIFR appears to act as a major, albeit surmountable distributional barrier (Weisshappel & Svavarsson, 1998; Weisshappel, 2000; Weisshappel, 2001; Dauvin *et al.*, 2012; Brix *et al.*, 2018). Therefore, we tested whether geographical

distinctions of Iceland, mainly determined by the GIFR and depth, are mirrored by the distribution of benthic amphipods.

MATERIALS & METHODS

Amphipoda data

We compiled data on occurrences and abundance of 355 amphipod species for 532 localities from the literature. The following expeditions and respective data sources were used: extensive literature search, data from BIOICE and IceAGE expeditions. The assembled dataset was highly heterogenous regarding sampling effort and method, time, location and date of the different expeditions. Many only listed one or two species, in particular the historic data from *e.g.*, [Boeck \(1861\)](#), [Hansen \(1887\)](#) and [Stephensen \(1933, 1938, 1942, 1944a, 1944b\)](#) only providing occurrence data. However, other had high abundances of individuals (max: 2,709) and high species richness (max: 72). Due to this high heterogeneity, we aggregated the data at a coarser spatial resolution.

A common approach is to construct a coarse rectangular grid in which species occurrences are joined. We constructed a hexagonal grid using QGIS ([QGIS Development Team, 2019](#)) with a horizontal diameter of 1° per grid cell. Within each grid cell, the occurrence and abundance information were pooled, so that a grid cell contained information from multiple localities but species were not double counted, yet the sum of the abundances per species could be calculated. Hexagonal grids have several advantages over rectangular grids, *e.g.*, symmetric neighbourhood relations or reduced edge effects ([Birch, Oom & Beecham, 2007](#)). For our study the most compelling reason to favour a hexagonal grid was the match of the polygons to the coastlines of Iceland and Greenland. Hexagonal grids provided a much better fit to this jagged pattern with an appropriate size, whereas rectangular grid cells would have to be much smaller and would then be too small for the purposes of our sampling. Given the case that many of our samples were near the coast, the hexagonal design clearly improved our sampling design.

Environmental layers

We extracted twelve variables from the Bio-Oracle 2.0 database ([Assis et al., 2018](#)) using the *sdmpredictors* package ([Bosch, Tyberghein & De Clerck, 2018](#)). Variables were chosen to represent major environmental deep-sea gradients ([Table 1](#)). All variables, except minimum depth, represented long-term maximum values modelled at minimum depths on a raster with 7 km² resolution per cell. In order to use the parameters on the same spatial scale as the species data, we aggregated the raster data to the scale of the hexagonal grid cells by calculating the mean raster value for each grid cell. Hexagons then represented the summed species abundances and averaged environmental data.

We analysed the environmental data for multicollinearity on the level of the hexagons. We calculated a Pearson correlation matrix (AppS1) for all environmental layers and removed all layers with a Pearson's *r* above 0.75. As expected, we found strong correlation between parameters of the same information type, *i.e.*, Chl-*a* and primary productivity or all nutrient related parameters. Finally, we retained the following parameters: depth, pH, phytobiomass, velocity, dissolved oxygen, dissolved iron, salinity and temperature.

Table 1 Environmental parameters.

Acronym	Parameter	Units	Source
depth	Bathymetry	meters	GEBCO URL: http://gebco.net Bathymetry URL: http://www.emodnet-bathymetry.eu/
chl _a	Chlorophyll concentration	mg/m ²	Global Ocean Biogeochemistry NON ASSIMILATIVE Hindcast (PISCES) URL: http://marine.copernicus.eu/
vel	Current velocity	m/s	Global Ocean Physics Reanalysis ECMWF ORAP5.0 (1979–2013) URL: http://marine.copernicus.eu/
dO ₂	Dissolved oxygen concentration	μmol/m ²	Global Ocean Biogeochemistry NON ASSIMILATIVE Hindcast (PISCES) URL: http://marine.copernicus.eu/
dFe	Dissolved iron concentration	μmol/m ²	Global Ocean Biogeochemistry NON ASSIMILATIVE Hindcast (PISCES) URL: http://marine.copernicus.eu/
dP	Phosphate concentration	μmol/m ²	Global Ocean Biogeochemistry NON ASSIMILATIVE Hindcast (PISCES) URL: http://marine.copernicus.eu/
dNO ₃	Nitrate concentration	μmol/m ²	Global Ocean Biogeochemistry NON ASSIMILATIVE Hindcast (PISCES) URL: http://marine.copernicus.eu/
temp	Sea water temperature	degrees Celcius	Global Ocean Physics Reanalysis ECMWF ORAP5.0 (1979–2013) URL: http://marine.copernicus.eu/
phybio	Carbon phytoplankton biomass	μmol/m ²	Global Ocean Biogeochemistry NON ASSIMILATIVE Hindcast (PISCES) URL: http://marine.copernicus.eu/
prod	Primary production	g/m ² /day	Global Ocean Biogeochemistry NON ASSIMILATIVE Hindcast (PISCES) URL: http://marine.copernicus.eu/
Salinity	Sea water salinity	PSS	Global Ocean Physics Reanalysis ECMWF ORAP5.0 (1979–2013) URL: http://marine.copernicus.eu/
SiO ₄	Silicate concentration	μmol/m ²	Global Ocean Biogeochemistry NON ASSIMILATIVE Hindcast (PISCES) URL: http://marine.copernicus.eu/

Note:

Environmental parameters initially extracted from the BIO-ORACLE 2.0 database. All parameters are long-term maxima at minimum depth, except bathymetry, which represents the deepest (=minimum) depth measured.

We kept salinity although it was correlated with temperature as it is an important parameter to structuring deep-sea communities around Iceland (*e.g.*, [Weisshappel & Svavarsson, 1998](#)).

Environmental cluster analysis

We hypothesized that deep-sea regions with similar environmental conditions would have a similar benthic fauna. Hence, we clustered the hexagonal grid cells based on the reduced set of the averaged environmental layers into a small set of environmentally homogenous regions. We used the *mclust* package ([Scrucca et al., 2016](#)) to conduct model-based hierarchical clustering using finite Gaussian Mixtures. The clustering algorithm compares 14 differently shaped types of Gaussian covariance structures representing different kinds of elliptical shapes ordered by an increasing complexity. The different models are compared using the Bayesian Information Criterion ([Burnham & Anderson, 2002](#)) choosing the model with the lowest complexity. Based on the plot of the different BIC models for possible cluster sizes from 2 to 10 (S3), we identified the optimal cluster as that one with highest regionalization capacity, *i.e.*, having a low number of clusters but already touching the plateau of the curve, signalling little differences in the model fit. We further confirmed the optimal number of clusters using a bootstrapped sequential likelihood ratio

test ([Scrucca et al., 2016](#)) by comparing an increasing number of cluster sizes. Finally, we calculated mean, standard deviation, minimum and maxima for each parameter and cluster combination. This was done to allow an interpretation of the environmental conditions representing the clusters.

Taxonomic data

To interpret the overlap between clusters in terms of species composition, we first performed a constrained analysis of principal coordinates (CAP) ([Anderson & Willis, 2003](#)) with presence absence information and the Jaccard distance measure. CAP is an ordination technique, that allows to visualize similarities in sites based on species composition and environmental correlates. The ordination diagram was visually inspected by plotting the sites encircled by hulls on the first two axes. We further calculated the ANOSIM statistic on presence/absence transformed species data. ANOSIM is a non-parametric method to measure the community-wise overlap between different clusters ([Clarke, 1993](#)). It yields a statistic called R that is in the range from 0 to 1 with values of R below 0.5 indicating strong overlap. The statistic is tested for significance using a permuted p -value ($n = 9,999$). R-values above 0.75 indicate largely non-overlapping clusters with strongly different species composition. Both analyses were performed using the vegan package ([Oksanen et al., 2019](#)).

To identify characteristic species for each cluster, we identified all species being positively associated with one specific cluster or combinations of clusters using the *multipatt* function of the *indicpecies* package ([Cáceres & Legendre, 2009](#)). We used the group-size corrected Indicator Value (IndVal.g) as a measure of association. The null hypothesis tested is that the association of a species is not higher in a specific cluster than in the other clusters. This function calculates a p -value based on 9,999 permutations, which is not corrected for multiple testing. However, as we are not interested in the number of indicator species, but in whether a species has a high association to a cluster or not, the p -values do not have to be adjusted ([De Cáceres, Legendre & Moretti, 2010](#)). After the analysis, species with high association values were extracted as lists for each cluster combination. The resulting species-cluster relationship was compared with literature and information from the World Register of Marine Species (WoRMS) database ([Horton et al., 2021](#)).

Diversity

We aimed to compare amphipod diversity between the different clusters. However, due to different numbers of samples ($n = 136$), *i.e.*, hexagonal cells, that contained the species data, clusters were not directly comparable in terms of diversity. Hence, we conducted a combined rarefaction-extrapolation analysis based on Hill numbers ([Chao, Chiu & Jost, 2014](#)). The concept of comparing species diversity using Hill numbers stems from the fact that most diversity indices are measures of entropy, such as Shannon or Simpson and do not translate directly into a diversity measure although often applied in such a way ([Jost, 2006](#)). Yet three well known measures of diversity *i.e.*, species richness, Shannon and Simpson diversity ([Shannon & Weaver, 1949](#); [Simpson, 1949](#)) can be generalized by a

formula derived by Hill (Jost, 2006; Chao, Chiu & Jost, 2014) which orders the indices along an order of q , *i.e.*, $q = 0, 1, 2$ translating to richness, Shannon and Simpson, respectively. This order reflects an increasing importance of the evenness component of diversity, while the richness component becomes less effective. This means that for richness, there is no effect of abundance on the diversity measure, while for the Simpson index, rare species only have little effect on the estimated diversity values. Hence, the Simpson index is often thought to be the most robust index, when number of individuals strongly differ, as is the case here. The diversity information is transformed into a common measure of diversity, the effective number of species, which is the number of species having equal abundances that would be required to reach *e.g.*, the Shannon entropy value of the sample. This measure allows comparisons of all three different indices having the same unit, the effective number of species. We performed the analysis using the iNEXT package (Hsieh, Ma & Chao, 2016) based on the summed abundance vectors per species and cluster.

When studying deep-sea organisms, the most important indirect environmental gradient is depth in meters. In order to evaluate the diversity pattern related to depth we studied the original data from the different stations ($n = 532$) and expeditions. First, we calculated a Poisson Generalized Linear Model (GLM) to quantify the relationship between the number of species per station and depth in meters. Then we split the depth gradient in 100-m intervals to study the trend of the maximum number of species across the depth gradient.

RESULTS

General

The total number of amphipod individuals analyzed is $n = 71,108$. The assembled dataset contained 355 species from 141 genera and 44 families (Tab. 2). From these, 101 species were only be identified to the genus level, where species were given a numerical code. The original number of stations from the expeditions ($n = 532$) were reduced to a set of 136 one-degree wide hexagonal cells in order to reduce the heterogeneity in the dataset. These hexagonal cells were clustered according to their environmental conditions. The entire dataset is available *via* Peer J supplement as well as Pangaea (GfBIO) <https://doi.pangaea.de/10.1594/PANGAEA.931959> (Lörz *et al.*, 2021).

Environmental clusters

The *mclust* algorithm identified six clusters to be the optimal configuration according to BIC and the likelihood ratio tests. However, when aggregating the species data to six clusters, this would result in clusters with disproportionately large differences in samples per cluster. Hence, we reduced the final number of clusters to four (Fig. 1). As the clustering is hierarchical, and the four-cluster solution is not much worse in terms of BIC we were confident that this aggregation is more informative with regard to the species than the six-cluster solution which would have split the northern and southern clusters into separate regions for the specific basins (the six cluster map is shown in the Supplementary Data). The four-cluster solution also provides a good overview of the large-scale spatial

Table 2 Amphipoda species.

Nr	Species	Authority	Family
1	<i>Abludomelita gladiosa</i>	(Spence Bate, 1862)	Melitidae
2	<i>Abludomelita obtusata</i>	(Montagu, 1813)	Melitidae
3	<i>Acanthonotozoma cristatum</i>	(Ross, 1835)	Acanthonotozomatidae
4	<i>Acanthonotozoma serratum</i>	(O. Fabricius, 1780)	Acanthonotozomatidae
5	<i>Acanthostepheia malmgreni</i>	(Goës, 1866)	Oedicerotidae
6	<i>Aceroides latipes</i>	(G.O. Sars, 1883)	Oedicerotidae
7	<i>Aeginella spinosa</i>	Boeck, 1861	Caprellidae
8	<i>Aeginina longicornis</i>	(Krøyer, 1843)	Caprellidae
9	<i>Ambasia atlantica</i>	(H. Milne Edwards, 1830)	Ambasiidae
10	<i>Ampelisca aequicornis</i>	Bruzelius, 1859	Ampeliscidae
11	<i>Ampelisca amblyops</i>	G.O. Sars, 1891	Ampeliscidae
12	<i>Ampelisca compacta</i>	Norman, 1882	Ampeliscidae
13	<i>Ampelisca eschrichtii</i>	Krøyer, 1842	Ampeliscidae
14	<i>Ampelisca gibba</i>	G.O. Sars, 1883	Ampeliscidae
15	<i>Ampelisca islandica</i>	Bellan-Santini & Dauvin, 1996	Ampeliscidae
16	<i>Ampelisca macrocephala</i>	Liljeborg, 1852	Ampeliscidae
17	<i>Ampelisca odontoplax</i>	G. O. Sars, 1879	Ampeliscidae
18	<i>Ampelisca</i> sp. A	Krøyer, 1842	Ampeliscidae
19	<i>Ampelisca</i> sp. B	Krøyer, 1842	Ampeliscidae
20	<i>Ampelisca uncinata</i>	Chevreaux, 1887	Ampeliscidae
21	<i>Amphilochoides boeckii</i>	G.O. Sars, 1892	Amphiloichidae
22	<i>Amphilochoides serratipes</i>	(Norman, 1869)	Amphiloichidae
23	<i>Amphiloichus anoculus</i>	Tandberg & Vader, 2018	Amphiloichidae
24	<i>Amphiloichus hamatus</i>	(Stephensen, 1925)	Amphiloichidae
25	<i>Amphiloichus manudens</i>	Spence Bate, 1862	Amphiloichidae
26	<i>Amphiloichus</i> sp. A	Spence Bate, 1862	Amphiloichidae
27	<i>Amphiloichus</i> sp. B	Spence Bate, 1862	Amphiloichidae
28	<i>Amphiloichus</i> sp. C	Spence Bate, 1862	Amphiloichidae
29	<i>Amphiloichus tenuimanus</i>	Boeck, 1871	Amphiloichidae
30	<i>Amphithopsis longicaudata</i>	Boeck, 1861	Calliopiidae
31	<i>Andaniella pectinata</i>	G.O. Sars, 1883	Stegocephalidae
32	<i>Andaniexis abyssi</i>	(Boeck, 1871)	Stegocephalidae
33	<i>Andaniexis lupus</i>	Berge & Vader, 1997	Stegocephalidae
34	<i>Andaniexis</i> sp. A	Stebbing, 1906	Stegocephalidae
35	<i>Andaniopsis nordlandica</i>	(Boeck, 1871)	Stegocephalidae
36	<i>Andaniopsis pectinata</i>	(G.O. Sars, 1883)	Stegocephalidae
37	<i>Anonyx</i> sp. A	Krøyer, 1838	Uristidae
38	<i>Apherusa glacialis</i>	(Hansen, 1888)	Calliopiidae
39	<i>Apherusa sarsii</i>	Shoemaker, 1930	Calliopiidae
40	<i>Apherusa</i> sp. A	Walker, 1891	Calliopiidae
41	<i>Apherusa</i> sp. B	Walker, 1891	Calliopiidae

Table 2 (continued)

Nr	Species	Authority	Family
42	<i>Apherusa</i> sp. C	Walker, 1891	Calliopiidae
43	<i>Apherusa</i> sp. D	Walker, 1891	Calliopiidae
44	<i>Argissa hamatipes</i>	(Norman, 1869)	Argissidae
45	<i>Arrhinopsis</i> sp. A	Stappers, 1911	Oedicerotidae
46	<i>Arrhis phyllonyx</i>	(Sars, 1858)	Oedicerotidae
47	<i>Arrhis</i> sp. A	Stebbing, 1906	Oedicerotidae
48	<i>Astyra abyssii</i>	Boeck, 1871	Stilipedidae
49	<i>Astyra</i> sp. A	Boeck, 1871	Stilipedidae
50	<i>Austrosyrhoe septentrionalis</i>	Stephensen, 1931	Synopiidae
51	<i>Austrosyrhoe</i> sp. A	K.H. Barnard, 1925	Synopiidae
52	<i>Autonoe borealis</i>	(Myers, 1976)	Aoridae
53	<i>Bathymedon longimanus</i>	(Boeck, 1871)	Oedicerotidae
54	<i>Bathymedon obtusifrons</i>	(Hansen, 1883)	Oedicerotidae
55	<i>Bathymedon saussurei</i>	(Boeck, 1871)	Oedicerotidae
56	<i>Bathymedon</i> sp. A	G.O. Sars, 1892	Oedicerotidae
57	<i>Bruzelia</i> sp. A	Boeck, 1871	Synopiidae
58	<i>Bruzelia tuberculata</i>	G.O. Sars, 1883	Synopiidae
59	<i>Byblis crassicornis</i>	Metzger, 1875	Ampeliscidae
60	<i>Byblis erythrops</i>	G.O. Sars, 1883	Ampeliscidae
61	<i>Byblis gaimardii</i>	(Krøyer, 1846)	Ampeliscidae
62	<i>Byblis medialis</i>	Mills, 1971	Ampeliscidae
63	<i>Byblis minuticornis</i>	Sars, 1879	Ampeliscidae
64	<i>Byblis</i> sp. A	Boeck, 1871	Ampeliscidae
65	<i>Byblisoides bellansantinae</i>	Peart, 2018	Ampeliscidae
66	<i>Calliopiopus laeviusculus</i>	(Krøyer, 1838)	Calliopiidae
67	<i>Camacho faroensis</i>	Myers, 1998	Aoridae
68	<i>Caprella ciliata</i>	G.O. Sars, 1883	Caprellidae
69	<i>Caprella dubia</i>	Hansen, 1887	Caprellidae
70	<i>Caprella microtuberculata</i>	G. O. Sars, 1879	Caprellidae
71	<i>Caprella rinki</i>	Stephensen, 1916	Caprellidae
72	<i>Caprella septentrionalis</i>	Krøyer, 1838	Caprellidae
73	<i>Chevreuxius grandimanus</i>	Bonnier, 1896	Aoridae
74	<i>Cleippides bicuspis</i>	Stephensen, 1931	Calliopiidae
75	<i>Cleippides quadricuspis</i>	Heller, 1875	Calliopiidae
76	<i>Cleippides tricuspis</i>	(Krøyer, 1846)	Calliopiidae
77	<i>Cleonardo</i> sp. A	Stebbing, 1888	Eusiridae
78	<i>Cleonardopsis</i> sp. A	K.H. Barnard, 1916	Amathillopsidae
79	<i>Corophiidira</i> sp. A	Leach, 1814 (<i>sensu</i> Lowry & Myers, 2013)	Corophiidira
80	<i>Cressa carinata</i>	Stephensen, 1931	Cressidae
81	<i>Cressa jeanjusti</i>	Krapp-Schickel, 2005	Cressidae
82	<i>Cressa minuta</i>	Boeck, 1871	Cressidae

(Continued)

Table 2 (continued)

Nr	Species	Authority	Family
83	<i>Cressa quinquedentata</i>	Stephensen, 1931	Cressidae
84	<i>Cressina monocuspis</i>	Stephensen, 1931	Cressidae
85	<i>Deflexilodes norvegicus</i>	(Boeck, 1871)	Oedicerotidae
86	<i>Deflexilodes rostratus</i>	(Stephensen, 1931)	Oedicerotidae
87	<i>Deflexilodes subnudus</i>	(Norman, 1889)	Oedicerotidae
88	<i>Deflexilodes tenuirostratus</i>	(Boeck, 1871)	Oedicerotidae
89	<i>Deflexilodes tessellatus</i>	(Schneider, 1883)	Oedicerotidae
90	<i>Deflexilodes tuberculatus</i>	(Boeck, 1871)	Oedicerotidae
91	<i>Dulichia</i> sp. A	Krøyer, 1845	Dulichidae
92	<i>Dulichia spinosissima</i>	Krøyer, 1845	Dulichidae
93	<i>Dulichopsis</i> sp. A	Laubitz, 1977	Dulichidae
94	<i>Dyopedos porrectus</i>	Spence Bate, 1857	Dulichidae
95	<i>Dyopedos</i> sp. A	Spence Bate, 1857	Dulichidae
96	<i>Epimeria (Epimeria) loricata</i>	G.O. Sars, 1879	Epimeriidae
97	<i>Epimeria (Epimeria)</i> sp. A	Costa in Hope, 1851	Epimeriidae
98	<i>Erichthonius megalops</i>	(Sars G.O., 1879)	Ischyroceridae
99	<i>Eusirella elegans</i>	Chevreaux, 1908	Eusiridae
100	<i>Eusirogenes</i> sp. A	Stebbing, 1904	Eusiridae
101	<i>Eusirogenes</i> sp. B	Stebbing, 1904	Eusiridae
102	<i>Eusirus bathybius</i>	Schellenberg, 1955	Eusiridae
103	<i>Eusirus biscayensis</i>	Bonnier, 1896	Eusiridae
104	<i>Eusirus holmii</i>	Hansen, 1887	Eusiridae
105	<i>Eusirus longipes</i>	Boeck, 1861	Eusiridae
106	<i>Eusirus minutus</i>	G.O. Sars, 1893	Eusiridae
107	<i>Eusirus propinquus</i>	Sars, 1893	Eusiridae
108	<i>Eusirus</i> sp. A	Krøyer, 1845	Eusiridae
109	<i>Eusirus</i> sp. B	Krøyer, 1845	Eusiridae
110	<i>Eusirus</i> sp. C	Krøyer, 1845	Eusiridae
111	<i>Eusirus</i> sp. D	Krøyer, 1845	Eusiridae
112	<i>Eusyrophoxus</i> sp. A	Gurjanova, 1977	Phoxocephalidae
113	<i>Gammaropsis</i> sp. A	Lilljeborg, 1855	Photidae
114	<i>Gitana abyssicola</i>	G.O. Sars, 1892	Amphilochidae
115	<i>Gitana rostrata</i>	Boeck, 1871	Amphilochidae
116	<i>Gitana sarsi</i>	Boeck, 1871	Amphilochidae
117	<i>Gitana</i> sp. A	Boeck, 1871	Amphilochidae
118	<i>Gitanopsis arctica</i>	G.O. Sars, 1892	Amphilochidae
119	<i>Gitanopsis bispinosa</i>	(Boeck, 1871)	Amphilochidae
120	<i>Gitanopsis inermis</i>	(G.O. Sars, 1883)	Amphilochidae
121	<i>Gitanopsis</i> sp. A	G.O. Sars, 1892	Amphilochidae
122	<i>Glorandaniotes eilae</i>	(Berge & Vader, 1997)	Stegocephalidae
123	<i>Gronella groenlandica</i>	(Hansen, 1888)	Tryphosidae

Table 2 (continued)

Nr	Species	Authority	Family
124	<i>Halice abyssii</i>	Boeck, 1871	Pardaliscidae
125	<i>Halice</i> sp. A	Boeck, 1871	Pardaliscidae
126	<i>Halicoides</i> sp. A	Walker, 1896	Pardaliscidae
127	<i>Halicoides tertia</i>	(Stephensen, 1931)	Pardaliscidae
128	<i>Halirages fulvocinctus</i>	(M. Sars, 1858)	Calliopiidae
129	<i>Halirages quadridentatus</i>	G.O. Sars, 1877	Calliopiidae
130	<i>Halirages</i> sp. A	Boeck, 1871	Calliopiidae
131	<i>Haliragoides inermis</i>	(G.O. Sars, 1883)	Calliopiidae
132	<i>Haploops carinata</i>	Liljeborg, 1856	Ampeliscidae
133	<i>Haploops dauvini</i>	Peart, 2018	Ampeliscidae
134	<i>Haploops islandica</i>	Kaïm-Malka, Bellan-Santini & Dauvin, 2016	Ampeliscidae
135	<i>Haploops kaimmalkai</i>	Peart, 2018	Ampeliscidae
136	<i>Haploops setosa</i>	Boeck, 1871	Ampeliscidae
137	<i>Haploops similis</i>	Stephensen, 1925	Ampeliscidae
138	<i>Haploops</i> sp. A	Liljeborg, 1856	Ampeliscidae
139	<i>Haploops tenuis</i>	Kannevorff, 1966	Ampeliscidae
140	<i>Haploops tubicola</i>	Liljeborg, 1856	Ampeliscidae
141	<i>Hardametopa nasuta</i>	(Boeck, 1871)	Stenothoidae
142	<i>Harpinia abyssii</i>	G.O. Sars, 1879	Phoxocephalidae
143	<i>Harpinia antennaria</i>	Meinert, 1890	Phoxocephalidae
144	<i>Harpinia crenulata</i>	(Boeck, 1871)	Phoxocephalidae
145	<i>Harpinia crenuloides</i>	Stephensen, 1925	Phoxocephalidae
146	<i>Harpinia laevis</i>	Sars, 1891	Phoxocephalidae
147	<i>Harpinia mucronata</i>	G. O. Sars, 1879	Phoxocephalidae
148	<i>Harpinia pectinata</i>	Sars, 1891	Phoxocephalidae
149	<i>Harpinia propinqua</i>	Sars, 1891	Phoxocephalidae
150	<i>Harpinia</i> sp. A	Boeck, 1876	Phoxocephalidae
151	<i>Harpinia</i> sp. B	Boeck, 1876	Phoxocephalidae
152	<i>Harpinia</i> sp. C	Boeck, 1876	Phoxocephalidae
153	<i>Harpinia</i> sp. D	Boeck, 1876	Phoxocephalidae
154	<i>Harpinia</i> sp. E	Boeck, 1876	Phoxocephalidae
155	<i>Harpinia</i> sp. F	Boeck, 1876	Phoxocephalidae
156	<i>Harpinia</i> sp. G	Boeck, 1876	Phoxocephalidae
157	<i>Harpinia</i> sp. H	Boeck, 1876	Phoxocephalidae
158	<i>Harpinia truncata</i>	Sars, 1891	Phoxocephalidae
159	<i>Harpiniopsis similis</i>	Stephensen, 1925	Phoxocephalidae
160	<i>Hippomedon gorbunovi</i>	Gurjanova, 1929	Tryphosidae
161	<i>Hippomedon propinquus</i>	G.O. Sars, 1890	Tryphosidae
162	<i>Idunella aeqvicornis</i>	(G.O. Sars, 1877)	Liljeborgiidae
163	<i>Idunella</i> sp. A	G.O. Sars, 1894	Liljeborgiidae
164	<i>Ischyrocerus anguipes</i>	Kroyer, 1838	Ischyroceridae

(Continued)

Table 2 (continued)

Nr	Species	Authority	Family
165	<i>Ischyrocerus latipes</i>	Krøyer, 1842	Ischyroceridae
166	<i>Ischyrocerus megacheir</i>	(Boeck, 1871)	Ischyroceridae
167	<i>Ischyrocerus megalops</i>	Sars, 1894	Ischyroceridae
168	<i>Jassa</i> sp. A	Leach, 1814	Ischyroceridae
169	<i>Kerguelenia borealis</i>	G.O. Sars, 1891	Kergueleniidae
170	<i>Laetmatophilus</i> sp. A	Bruzelius, 1859	Podoceridae
171	<i>Laetmatophilus tuberculatus</i>	Bruzelius, 1859	Podoceridae
172	<i>Laothoes meinerti</i>	Boeck, 1871	Calliopiidae
173	<i>Laothoes pallaschi</i>	Coleman, 1999	Calliopiidae
174	<i>Laothoes</i> sp. A	Boeck, 1871	Calliopiidae
175	<i>Lepechinella arctica</i>	Schellenberg, 1926	Lepechinellidae
176	<i>Lepechinella grimi</i>	Thurston, 1980	Lepechinellidae
177	<i>Lepechinella helgii</i>	Thurston, 1980	Lepechinellidae
178	<i>Lepechinella skarphedini</i>	Thurston, 1980	Lepechinellidae
179	<i>Lepechinella victoriae</i>	Johansen & Vader, 2015	Lepechinellidae
180	<i>Lepechinelloides karii</i>	Thurston, 1980	Lepechinellidae
181	<i>Lepidepecreum</i> sp. A	Spence Bate & Westwood, 1868	Tryphosidae
182	<i>Leptamphopus sarsi</i>	Vanhöffen, 1897	Calliopiidae
183	<i>Leptophoxus falcatus</i>	(G.O. Sars, 1883)	Phoxocephalidae
184	<i>Leucothoe lilljeborgi</i>	Boeck, 1861	Leucothoidae
185	<i>Leucothoe</i> sp. A	Leach, 1814	Leucothoidae
186	<i>Leucothoe spinicarpa</i>	(Abildgaard, 1789)	Leucothoidae
187	<i>Leucothoe vaderotti</i>	Krapp-Schickel, 2018	Leucothoidae
188	<i>Liljeborgia fissicornis</i>	(Sars, 1858)	Liljeborgiidae
189	<i>Liljeborgia pallida</i>	(Spence Bate, 1857)	Liljeborgiidae
190	<i>Liljeborgia</i> sp. A	Spence Bate, 1862	Liljeborgiidae
191	<i>Lysianella petalocera</i>	G.O. Sars, 1883	Tryphosidae
192	<i>Megamoera dentata</i>	(Krøyer, 1842)	Melitidae
193	<i>Megamphopus raptor</i>	Myers, 1998	Photidae
194	<i>Melphidippa borealis</i>	Boeck, 1871	Melphidippidae
195	<i>Melphidippa goesi</i>	Stebbing, 1899	Melphidippidae
196	<i>Melphidippa macrura</i>	G.O. Sars, 1894	Melphidippidae
197	<i>Melphidippa</i> sp. A	Boeck, 1871	Melphidippidae
198	<i>Melphidippa</i> sp. B	Boeck, 1871	Melphidippidae
199	<i>Metacaprella horrida</i>	(Sars G.O., 1877)	Caprellidae
200	<i>Metandania wimi</i>	Berge, 2001	Stegocephalidae
201	<i>Metopa abyssalis</i>	Stephensen, 1931	Stenothoidae
202	<i>Metopa boeckii</i>	Sars, 1892	Stenothoidae
203	<i>Metopa bruzelii</i>	(Goës, 1866)	Stenothoidae
204	<i>Metopa leptocarpa</i>	G.O. Sars, 1883	Stenothoidae
205	<i>Metopa norvegica</i>	(Liljeborg, 1851)	Stenothoidae

Table 2 (continued)

Nr	Species	Authority	Family
206	<i>Metopa palmata</i>	Sars, 1892	Stenothoidae
207	<i>Metopa robusta</i>	Sars, 1892	Stenothoidae
208	<i>Metopa rubrovittata</i>	G.O. Sars, 1883	Stenothoidae
209	<i>Metopa sinuata</i>	Sars, 1892	Stenothoidae
210	<i>Metopa</i> sp. A	Boeck, 1871	Stenothoidae
211	<i>Metopa</i> sp. B	Boeck, 1871	Stenothoidae
212	<i>Metopa</i> sp. C	Boeck, 1871	Stenothoidae
213	<i>Metopa</i> sp. D	Boeck, 1871	Stenothoidae
214	<i>Metopa</i> sp. E	Boeck, 1871	Stenothoidae
215	<i>Monoculodes latimanus</i>	(Goës, 1866)	Oedicerotidae
216	<i>Monoculodes latissimanus</i>	Stephensen, 1931	Oedicerotidae
217	<i>Monoculodes packardi</i>	Boeck, 1871	Oedicerotidae
218	<i>Monoculodes</i> sp. A	Stimpson, 1853	Oedicerotidae
219	<i>Monoculodes</i> sp. B	Stimpson, 1853	Oedicerotidae
220	<i>Monoculodes</i> sp. C	Stimpson, 1853	Oedicerotidae
221	<i>Monoculodes</i> sp. D	Stimpson, 1853	Oedicerotidae
222	<i>Monoculodes</i> sp. E	Stimpson, 1853	Oedicerotidae
223	<i>Monoculodes</i> sp. F	Stimpson, 1853	Oedicerotidae
224	<i>Monoculodes</i> sp. G	Stimpson, 1853	Oedicerotidae
225	<i>Monoculopsis longicornis</i>	(Boeck, 1871)	Oedicerotidae
226	<i>Neopleustes boeckii</i>	(Hansen, 1888)	Pleustidae
227	<i>Neopleustes pulchellus</i>	(Krøyer, 1846)	Pleustidae
228	<i>Neopleustes</i> sp. A	Stebbing, 1906	Pleustidae
229	<i>Nicippe tumida</i>	Bruzelius, 1859	Pardaliscidae
230	<i>Nototropis smitti</i>	(Goës, 1866)	Atylidae
231	<i>Nototropis</i> sp. A	Costa, 1853	Atylidae
232	<i>Odius carinatus</i>	(Spence Bate, 1862)	Ochlesidae
233	<i>Oedicerina ingolfi</i>	Stephensen, 1931	Oedicerotidae
234	<i>Oedicerina</i> sp. A	Stephensen, 1931	Oedicerotidae
235	<i>Oediceropsis brevicornis</i>	Lilljeborg, 1865	Oedicerotidae
236	<i>Oediceropsis</i> sp. A	Lilljeborg, 1865	Oedicerotidae
237	<i>Oediceros borealis</i>	Boeck, 1871	Oedicerotidae
238	<i>Onisimus plautus</i>	(Krøyer, 1845)	Uristidae
239	<i>Orchomene macroserratus</i>	Shoemaker, 1930	Tryphosidae
240	<i>Orchomene pectinatus</i>	G.O. Sars, 1883	Tryphosidae
241	<i>Orchomene</i> sp. A	Boeck, 1871	Tryphosidae
242	<i>Pacifoculodes pallidus</i>	(G.O. Sars, 1892)	Oedicerotidae
243	<i>Paradulichia typica</i>	Boeck, 1871	Dulichiiidae
244	<i>Paramphilochooides odontonyx</i>	(Boeck, 1871)	Amphilochoidae
245	<i>Paramphithoe hystrix</i>	(Ross, 1835)	Paramphithoidae
246	<i>Parandania gigantea</i>	(Stebbing, 1883)	Stegocephalidae

(Continued)

Table 2 (continued)

Nr	Species	Authority	Family
247	<i>Paraphoxus oculatus</i>	(G. O. Sars, 1879)	Phoxocephalidae
248	<i>Parapleustes assimilis</i>	(G.O. Sars, 1883)	Pleustidae
249	<i>Parapleustes bicuspis</i>	(Krøyer, 1838)	Pleustidae
250	<i>Pardalisca abyssi</i>	Boeck, 1871	Pardaliscidae
251	<i>Pardalisca cuspidata</i>	Krøyer, 1842	Pardaliscidae
252	<i>Pardalisca</i> sp. A	Krøyer, 1842	Pardaliscidae
253	<i>Pardalisca</i> sp. B	Krøyer, 1842	Pardaliscidae
254	<i>Pardalisca</i> sp. C	Krøyer, 1842	Pardaliscidae
255	<i>Pardalisca tenuipes</i>	G.O. Sars, 1893	Pardaliscidae
256	<i>Pardaliscoides tenellus</i>	Stebbing, 1888	Pardaliscidae
257	<i>Paroediceros curvirostris</i>	(Hansen, 1888)	Oedicerotidae
258	<i>Paroediceros lynceus</i>	(M. Sars, 1858)	Oedicerotidae
259	<i>Paroediceros propinquus</i>	(Goës, 1866)	Oedicerotidae
260	<i>Periocolodes longimanus</i>	(Spence Bate & Westwood, 1868)	Oedicerotidae
261	<i>Phippsia gibbosa</i>	(G.O. Sars, 1883)	Stegocephalidae
262	<i>Phippsia roemeri</i>	Schellenberg, 1925	Stegocephalidae
263	<i>Photis reinhardi</i>	Krøyer, 1842	Photidae
264	<i>Phoxocephalus holbolli</i>	(Krøyer, 1842)	Phoxocephalidae
265	<i>Pleustes (Pleustes) panoplus</i>	(Krøyer, 1838)	Pleustidae
266	<i>Pleustes tuberculatus</i>	Spence Bate, 1858	Pleustidae
267	<i>Pleusymtes pulchella</i>	(G.O. Sars, 1876)	Pleustidae
268	<i>Pleusymtes</i> sp. A	J.L. Barnard, 1969	Pleustidae
269	<i>Pontocrates arcticus</i>	G.O. Sars, 1895	Oedicerotidae
270	<i>Pontocrates</i> sp. A	Boeck, 1871	Oedicerotidae
271	<i>Proaeginina norvegica</i>	(Stephensen, 1931)	Caprellidae
272	<i>Probolooides gregaria</i>	(G.O. Sars, 1883)	Stenothoidae
273	<i>Protellina ingolfi</i>	Stephensen, 1944	Caprellidae
274	<i>Protoaeginella muriculata</i>	Laubitz & Mills, 1972	Caprellidae
275	<i>Protomeдея fasciata</i>	Krøyer, 1842	Corophiidae
276	<i>Pseudo bioice</i>	(Berge & Vader, 1997)	Stegocephalidae
277	<i>Pseudotiron</i> sp. A	Chevreaux, 1895	Synopiidae
278	<i>Rhachotropis aculeata</i>	(Lepechin, 1780)	Eusiridae
279	<i>Rhachotropis arii</i>	Thurston, 1980	Eusiridae
280	<i>Rhachotropis distincta</i>	(Holmes, 1908)	Eusiridae
281	<i>Rhachotropis gislii</i>	Thurston, 1980	Eusiridae
282	<i>Rhachotropis gloriosae</i>	Ledoyer, 1982	Eusiridae
283	<i>Rhachotropis helleri</i>	(Boeck, 1871)	Eusiridae
284	<i>Rhachotropis inflata</i>	(G.O. Sars, 1883)	Eusiridae
285	<i>Rhachotropis kergueleni</i>	Stebbing, 1888	Eusiridae
286	<i>Rhachotropis leucophthalma</i>	G.O. Sars, 1893	Eusiridae
287	<i>Rhachotropis macropus</i>	G.O. Sars, 1893	Eusiridae

Table 2 (continued)

Nr	Species	Authority	Family
288	<i>Rhachotropis northriana</i>	d'Udekem d'Acoz, Vader & Legezinska, 2007	Eusiridae
289	<i>Rhachotropis oculata</i>	(Hansen, 1887)	Eusiridae
290	<i>Rhachotropis palporum</i>	Stebbing, 1908	Eusiridae
291	<i>Rhachotropis proxima</i>	Chevreur, 1911	Eusiridae
292	<i>Rhachotropis</i> sp. A	S.I. Smith, 1883	Eusiridae
293	<i>Rhachotropis</i> sp. B	S.I. Smith, 1883	Eusiridae
294	<i>Rhachotropis</i> sp. C	S.I. Smith, 1883	Eusiridae
295	<i>Rhachotropis</i> sp. D	S.I. Smith, 1883	Eusiridae
296	<i>Rhachotropis thordisae</i>	Thurston, 1980	Eusiridae
297	<i>Rhachotropis thorkelli</i>	Thurston, 1980	Eusiridae
298	<i>Rostroculodes borealis</i>	(Boeck, 1871)	Oedicerotidae
299	<i>Rostroculodes kroyeri</i>	(Boeck, 1870)	Oedicerotidae
300	<i>Rostroculodes longirostris</i>	(Goës, 1866)	Oedicerotidae
301	<i>Scopelocheirus</i> sp. A	Spence Bate, 1857	Scopelocheiridae
302	<i>Sicafodia iceage</i>	Campean & Coleman, 2017	Sicafodiidae
303	<i>Sicafodia</i> sp. A	Just, 2004	Sicafodiidae
304	<i>Siphonoecetes typicus</i>	Krøyer, 1845	Ischyroceridae
305	<i>Socarnes bidenticulatus</i>	(Spence Bate, 1858)	Lysianassidae
306	<i>Socarnes vahlii</i>	(Krøyer, 1838)	Lysianassidae
307	<i>Stegocephalina wagini</i>	(Gurjanova, 1936)	Stegocephalidae
308	<i>Stegocephaloides auratus</i>	(G.O. Sars, 1883)	Stegocephalidae
309	<i>Stegocephaloides barnardi</i>	Berge & Vader, 1997	Stegocephalidae
310	<i>Stegocephaloides christianiensis</i>	Boeck, 1871	Stegocephalidae
311	<i>Stegocephalus ampulla</i>	(Phipps, 1774)	Stegocephalidae
312	<i>Stegocephalus inflatus</i>	Krøyer, 1842	Stegocephalidae
313	<i>Stegocephalus similis</i>	Sars, 1891	Stegocephalidae
314	<i>Stegocephalus</i> sp. A	Krøyer, 1842	Stegocephalidae
315	<i>Stegocephalus</i> sp. B	Krøyer, 1842	Stegocephalidae
316	<i>Stegonomadia biofar</i>	(Berge & Vader, 1997)	Stegocephalidae
317	<i>Stegonomadia idae</i>	(Berge & Vader, 1997)	Stegocephalidae
318	<i>Stegoplax longirostris</i>	G.O. Sars, 1883	Cyproideidae
319	<i>Stegoplax</i> sp. A	G.O. Sars, 1883	Cyproideidae
320	<i>Stenopleustes latipes</i>	(M. Sars, 1858)	Pleustidae
321	<i>Stenopleustes malmgreni</i>	(Boeck, 1871)	Pleustidae
322	<i>Stenopleustes nodifera</i>	(G.O. Sars, 1883)	Pleustidae
323	<i>Stenopleustes</i> sp. A	G.O. Sars, 1893	Pleustidae
324	<i>Stenothoe marina</i>	(Spence Bate, 1857)	Stenothoidae
325	<i>Stenothoe megacheir</i>	(Boeck, 1871)	Stenothoidae
326	<i>Stenothoe</i> sp. A	Dana, 1852	Stenothoidae
327	<i>Stenothoe</i> sp. B	Dana, 1852	Stenothoidae
328	<i>Stenothoe</i> sp. C	Dana, 1852	Stenothoidae

(Continued)

Table 2 (continued)

Nr	Species	Authority	Family
329	<i>Stenothoe</i> sp. D	Dana, 1852	Stenothoidae
330	<i>Stephobruzelia dentata</i>	(Stephensen, 1931)	Synopiidae
331	<i>Synchelidium haplocheles</i>	(Grube, 1864)	Oedicerotidae
332	<i>Synchelidium intermedium</i>	Sars, 1892	Oedicerotidae
333	<i>Synchelidium</i> sp. A	G.O. Sars, 1892	Oedicerotidae
334	<i>Syrrhoe crenulata</i>	Goës, 1866	Synopiidae
335	<i>Syrrhoe</i> sp. A	Goës, 1866	Synopiidae
336	<i>Syrrhoites pusilla</i>	Enequist, 1949	Synopiidae
337	<i>Syrrhoites serrata</i>	(G.O. Sars, 1879)	Synopiidae
338	<i>Syrrhoites</i> sp. A	G.O. Sars, 1893	Synopiidae
339	<i>Themisto gaudichaudii</i>	Guérin, 1825	Hyperiidae
340	<i>Thorina elongata</i>	Laubitz & Mills, 1972	Caprellidae
341	<i>Thorina spinosa</i>	Stephensen, 1944	Caprellidae
342	<i>Tiron spiniferus</i>	(Stimpson, 1853)	Synopiidae
343	<i>Tmetonyx cicada</i>	(Fabricius, 1780)	Uristidae
344	<i>Tmetonyx</i> sp. A	Stebbing, 1906	Uristidae
345	<i>Tryphosella schneideri</i>	(Stephensen, 1921)	Tryphosidae
346	<i>Tryphosella</i> sp. A	Bonnier, 1893	Tryphosidae
347	<i>Unciola laticornis</i>	Hansen, 1887	Unciolidae
348	<i>Unciola leucopis</i>	(Krøyer, 1845)	Unciolidae
349	<i>Unciola planipes</i>	Norman, 1867	Unciolidae
350	<i>Urothoe elegans</i>	Spence Bate, 1857	Urothoidae
351	<i>Westwoodilla brevicealcar</i>	Goës, 1866	Oedicerotidae
352	<i>Westwoodilla caecula</i>	(Spence Bate, 1857)	Oedicerotidae
353	<i>Westwoodilla megalops</i>	(G.O. Sars, 1883)	Oedicerotidae
354	<i>Westwoodilla</i> sp. A	Spence Bate, 1862	Oedicerotidae
355	<i>Xenodice</i> sp. A	Boeck, 1871	Podoceridae

Note:

Amphipoda species, authorities and family.

pattern. There is a “Coastal” cluster ($n = 34$ cells) which is always close to the coastline and is characterized by shallow depth, high amounts of dissolved iron and phytobiomass and warm, oxygen-rich waters with a high current speed (Fig. 2). The second cluster resembles the GIFR ($n = 55$), which spreads from west to east and separates the northern and southern basis. In many points it is similar to the coastal cluster but is deeper and with less dissolved iron, oxygen, and phytobiomass. The other two clusters are called “Deep South” ($n = 19$) and “Deep North” ($n = 28$) as they represent the deep-sea regions around Iceland. They differ strongly from the first two clusters by having very low values for many parameters. “Deep North” differs from “Deep South” by being much colder, with almost no current velocity. Further, “Deep North” has a much higher amount of dissolved oxygen and pH. The lowest depths of around 3,400 m are observed in the Aegir ridge. These four

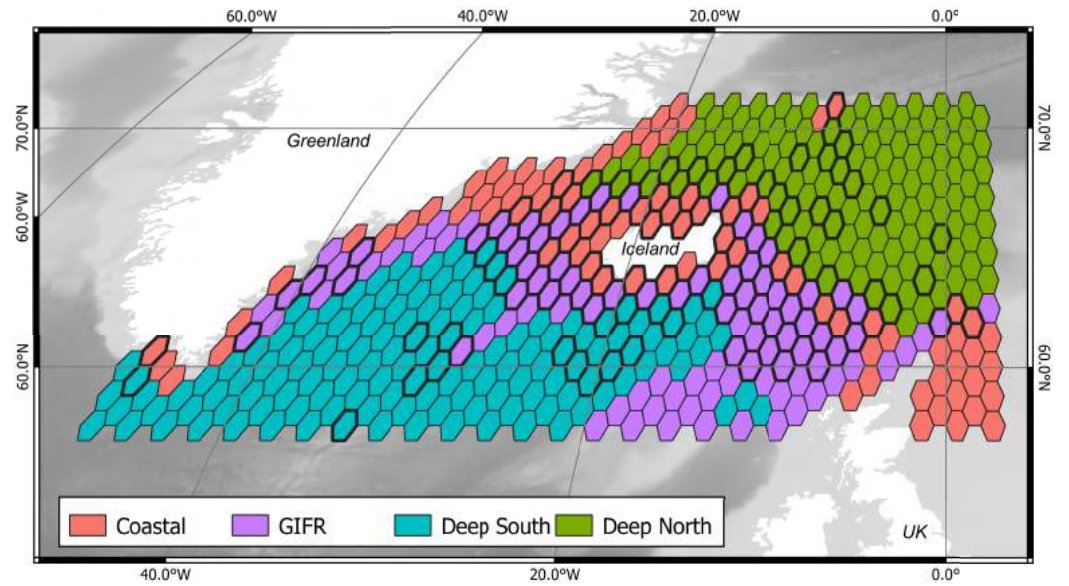


Figure 1 Four environmental clusters. Map of the outlines for four identified environmental clusters in the North Atlantic. The Greenland-Faroe-Iceland ridge (GIFR) extends from west to east and is, like the coastal cluster, partly interrupted due to the coarse resolution of the hexagonal cells of 1° in east-west direction, ($n = 469$). [Full-size](#) DOI: 10.7717/peerj.11898/fig-1

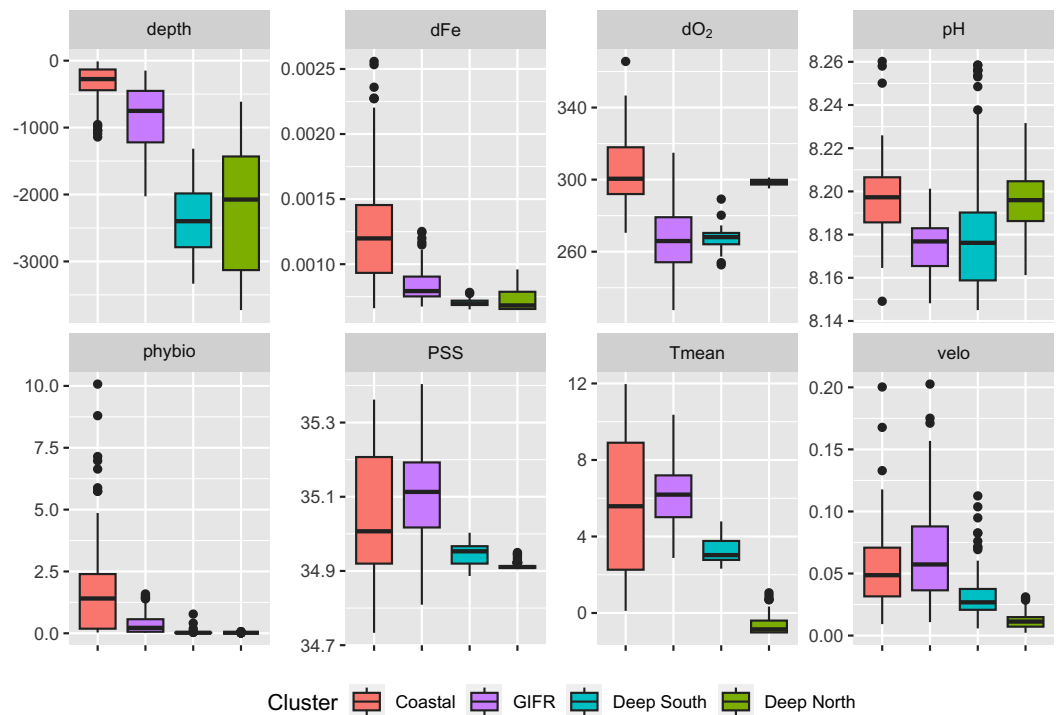


Figure 2 Environmental parameters. Characterization of the four environmental clusters by the environmental parameters with box-whisker plots. For abbreviations refer to Table 1. An extended table with numeric information can be found in the appendix. [Full-size](#) DOI: 10.7717/peerj.11898/fig-2

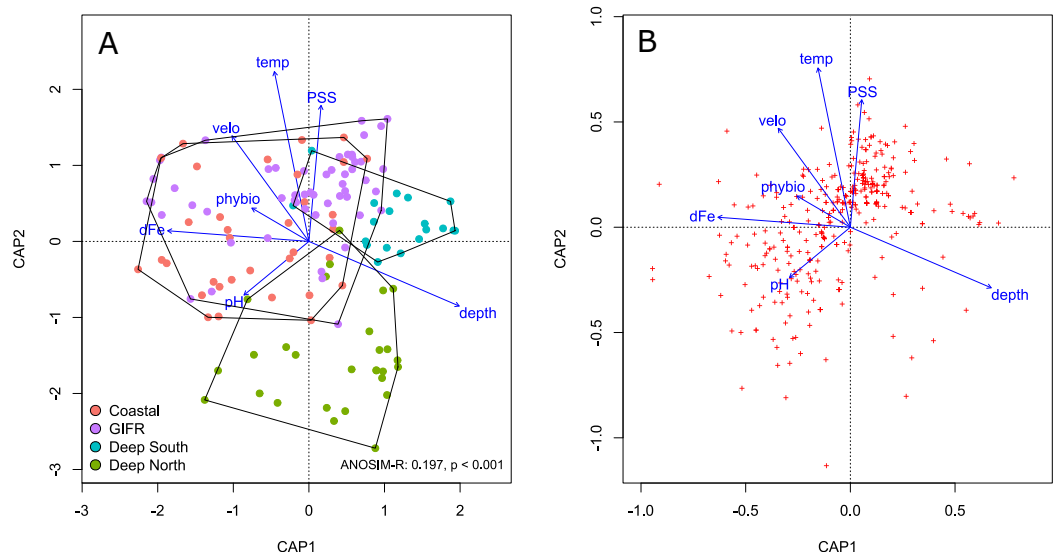


Figure 3 Constrained analysis of principal coordinates. Constrained analysis of principal coordinates (CAP) based on Jaccard distances. (A) Scaling is based on site scores, (B) scaling is based on species scores (red dots)—note the differences of the axes. Arrows point into the direction of largest correlation with species and site scores. The 0,0 coordinate reflects the centroid of each variable. The environmental clusters still overlap considerably in their species composition as reflected by the low ANOSIM-R statistic. [Full-size !\[\]\(75ae59747fbf764049bf5489c82fb3e0_img.jpg\) DOI: 10.7717/peerj.11898/fig-3](https://doi.org/10.7717/peerj.11898/fig-3)

clusters thus characterize the environmental conditions around Iceland on a regional spatial scale.

Constrained ordination

We conducted a constrained ordination to verify the amount of variation explained in the species data by the environmental information contained at the level of the hexagonal cells. The constrained axes of the ordination explained 11% of the total variation, while 89% is explained by the 357 unconstrained axes. According to a permutation test of the marginal effects of each environmental variable carried out using the *anova.cca* function of the *vegan* package, the most important environmental variables were temperature ($F = 2.34$, $p < 0.001$), depth ($F = 2.123$, $p < 0.001$), and salinity ($F = 2.01$, $p < 0.001$).

The four different clusters strongly overlapped in ordination space (Fig. 3A). The ANOSIM-R value of 0.197 signals considerable similarity in species composition between the clusters. All clusters overlap in the centre of the diagram; their large spread indicates strong heterogeneity. The deep-sea clusters overlapped less than the coastal and GIFR-cluster. In general, the first constrained axis represented the depth gradient, which was in contrast to all other variables. Salinity, temperature and pH characterized the second constrained axes, with pH being in contrast to temperature and salinity (Fig. 3A). The species pattern clumped near the centroid of the ordination diagram (Fig. 3B) indicating that many species are found in intermediate environmental conditions. Fewer species have a clear centroid in deeper waters, instead many species favour higher temperatures and an above average salinity. Large variation appears in the direction of pH and dissolved iron, as indicated by the strong scatter of species centroids (Fig. 3B).

Indicator species analysis

To characterize the different clusters with regard to faithful species, *i.e.*, so-called indicator species we conducted a multipattern indicator species analysis. We compared 15 different combinations with an increasing number of clusters. From 355 species, we identified 56 to have a strong association to one or more clusters. Forty-three species were associated to one cluster only, while twelve and one species were associated to two and three clusters, respectively (Table 3). Only two species were found for the GIFR cluster, but more species from GIFR appear in combination with other clusters.

Three of the clusters, the Deep North, the Deep South and the Coastal have indicator species belonging to the genus *Rhachotropis*. While different species of a genus might be specialized on different diets, all *Rhachotropis* species are very good swimmers (Lörz, 2010). The Deep South cluster has four *Rhachotropis* as indicator species. While the GIFR cluster only had two endobenthic species, belonging to the family Ampeliscidae, which are not considered strong swimmers (Peart, 2018), the combined GIFR and coastal cluster indicate *Rhachotropis aculeata* (Lepechin, 1780) as an indicator—a species that is known to have a circum-Arctic distribution (Lörz et al., 2018). *Caprella microtuberculata* G. O. Sars, 1879 and *Aeginella spinosa* Boeck, 1861 are indicator species of the combined coastal and GIFR cluster. These two species belong to the amphipod group Caprellidae, skeleton or ghost shrimps, which are known for their clinging lifestyle. The indicator species with the highest values, over 0.5, are *Cleippides quadricuspis* Heller, 1875 from the Deep North, *Eusirus holmi* Hansen, 1887 from the combined Coastal and Deep North cluster and *Rhachotropis thordisae* Thurston, 1980 from the Deep South cluster—these three species are all large amphipods of several cm body length and known as predators (Lörz et al., 2018).

Diversity

The number of aggregated hexagonal cells differed for each cluster, hence we had to apply a rarefaction and extrapolation analysis to make the three diversity measures comparable. The rarefaction of the summed abundances revealed that the two clusters “coastal” and “GIFR” have about twice the number of species than the deep-sea clusters (Fig. 4A). This even holds when only the lowest comparable value of approximate 10,000 individuals is considered. Although there were so many individuals per cluster, the curves do not level off, indicating that still more sampling would be required to reach a plateau in species richness. The Shannon diversity (Fig. 4B) considers the richness-abundance component of diversity. The “coastal” and “GIFR” clusters are at the same level of 60 effective species; the deep-sea clusters again have a much lower diversity, *i.e.*, almost three times lower. All curves reach a plateau, indicating that there is little more diversity to expect when abundances are considered. Hence, only rare species might be added by future sampling. Considering the Simpson diversity (Fig. 4C), *i.e.*, when no rare species but only dominant species have an influence on the diversity measure, then the “coastal” cluster becomes the most diverse cluster while the “GIFR” is only half as diverse as the coastal cluster.

The richness pattern across the depth gradient showed high variation at depths above 1,500 m with richness values up to 79 species per station (Fig. 5A). Most of the stations

Table 3 Indicator value analysis for all combinations of the environmental clusters. The group-size corrected Indicator Value (IndVal.g) represent the association value of a species with a given cluster. The p -value is based on 999 permutations. Asterisks code for p -values at significance levels of 5% (*) and 1% (**).

Cluster	Nr.	Species	IndVal.g	p -value	
Coastal	1	<i>Rhachotropis oculata</i>	0.400	0.005	
	2	<i>Westwoodilla caecula</i>	0.383	0.015	
	3	<i>Ampelisca macrocephala</i>	0.368	0.010	**
	4	<i>Deflexilodes tessellatus</i>	0.368	0.035	*
	5	<i>Harpinia</i> sp. E	0.343	0.020	*
	6	<i>Monoculodes</i> sp. A	0.343	0.015	*
	7	<i>Westwoodilla megalops</i>	0.343	0.030	*
	8	<i>Harpinia pectinata</i>	0.328	0.020	*
	9	<i>Bathymedon obtusifrons</i>	0.319	0.035	*
Deep North	10	<i>Monoculodes latimanus</i>	0.297	0.045	*
	1	<i>Cleippides quadricuspis</i>	0.642	0.005	**
	2	<i>Bruzelia dentata</i>	0.463	0.005	**
	3	<i>Rhachotropis</i> sp. A	0.392	0.005	**
	4	<i>Paroedicerus curvirostris</i>	0.375	0.015	*
	5	<i>Deflexilodes tenuirostratus</i>	0.349	0.040	*
	6	<i>Halirages quadridentata</i>	0.344	0.025	*
	7	<i>Monoculopsis longicornis</i>	0.344	0.025	*
Deep South	8	<i>Oedicerina</i> sp.	0.327	0.025	*
	1	<i>Rhachotropis thordisae</i>	0.559	0.005	**
	2	<i>Rhachotropis proxima</i>	0.499	0.010	**
	3	<i>Eusirus bathybius</i>	0.459	0.010	**
	4	<i>Lepechinelloides karii</i>	0.459	0.005	**
	5	<i>Rhachotropis gislii</i>	0.459	0.005	**
	6	<i>Protoaeginella muriculata</i>	0.401	0.010	**
	7	<i>Cleonardopsis</i> sp.	0.397	0.005	**
	8	<i>Lepechinella grimi</i>	0.397	0.005	**
	9	<i>Lepechinella helgii</i>	0.397	0.010	**
	10	<i>Lepechinella skarpheini</i>	0.397	0.010	**
	11	<i>Rhachotropis thorkelli</i>	0.397	0.010	**
	12	<i>Neopleustes boeckii</i>	0.365	0.010	**
	13	<i>Neopleustes</i> sp.	0.324	0.010	**
	14	<i>Sicafodia</i> sp.	0.324	0.010	**
	15	<i>Eusirus</i> sp. C	0.300	0.020	*
	16	<i>Rhachotropis aislui</i>	0.300	0.040	*
17	<i>Rhachotropis gloriosae</i>	0.300	0.035	*	
GFIR	1	<i>Ampelisca odontoplax</i>	0.348	0.03	*
	2	<i>Haploops tenuis</i>	0.302	0.05	*
Coastal + Deep North	1	<i>Eusirus holmi</i>	0.509	0.005	**
	2	<i>Halirages fulvocincta</i>	0.490	0.050	*
	3	<i>Arrhis phyllonyx</i>	0.458	0.005	**
	4	<i>Andaniella pectinata</i>	0.430	0.005	**
	5	<i>Paroedicerus propinquus</i>	0.372	0.040	*
	6	<i>Halirages elegans</i>	0.359	0.030	*
	7	<i>Harpiniopsis similis</i>	0.347	0.035	*

Table 3 (continued)

Cluster	Nr.	Species	IndVal.g	p-value
Coastal + GFIR	1	<i>Aeginella spinosa</i>	0.559	0.005 **
	2	<i>Rhachotropis aculeata</i>	0.467	0.025 *
	3	<i>Caprella microtuberculata</i>	0.462	0.010 **
	4	<i>Harpinia propinqua</i>	0.459	0.030 *
Deep South + Deep North	1	<i>Liljeborgia pallida</i>	0.349	0.045 *
	2	<i>Ampelisca islandica</i>	0.329	0.025 *
Coastal + Deep South + Deep North	1	<i>Amphilochus anoculus</i>	0.424	0.035 *

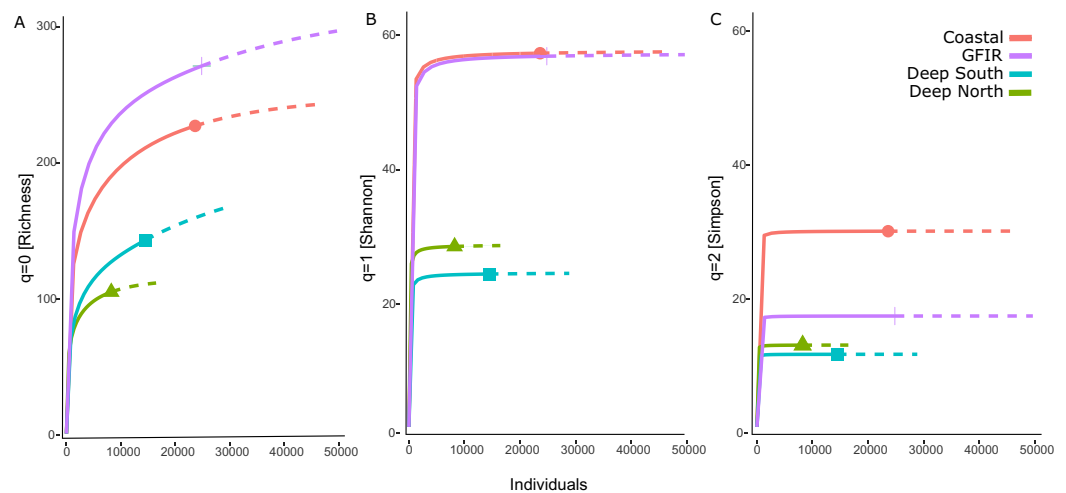


Figure 4 Rarefaction-extrapolation of diversity indices per cluster. The diversity indices (A) richness, (B) Shannon, and (C) Simpson, represent an increasing importance of abundant species. The unit of the y-axis is the effective number of species. [Full-size !\[\]\(bbdef48f99f824c7a2021d7c299fdec3_img.jpg\) DOI: 10.7717/peerj.11898/fig-4](https://doi.org/10.7717/peerj.11898/fig-4)

recorded rather few species *i.e.*, up to 10 species with an average of 20 species at the shallowest parts (18 m) and an estimated richness of eight species at the lowest depths. The trend for the maximum number of species aggregated per 100-m interval showed an unimodal pattern with a peak at depths around 500 m and a much lower richness at depths lower than 1,000 m (Fig. 5B). These figures support the finding that the Coastal and GFIR clusters are much more diverse than the deep-sea clusters (Fig. 5C).

DISCUSSION

Environmental and historical imprints on amphipod distributions

Distributional groupings given in the present study corresponded to earlier findings, in which distinctive boundaries between a northern and a southern deep-sea fauna were inferred, while the composition of the shallow-water fauna (<500 m) around Iceland was very similar (Weisshappel & Svavarsson, 1998; Weisshappel, 2000; Bett, 2001; Weisshappel, 2001). Unsurprisingly, the spatial distribution of amphipods appeared to be most strongly influenced by bathymetry, salinity and seafloor temperature. The latter two were interconnected and indicative of particular water masses (Puerta *et al.*, 2020).

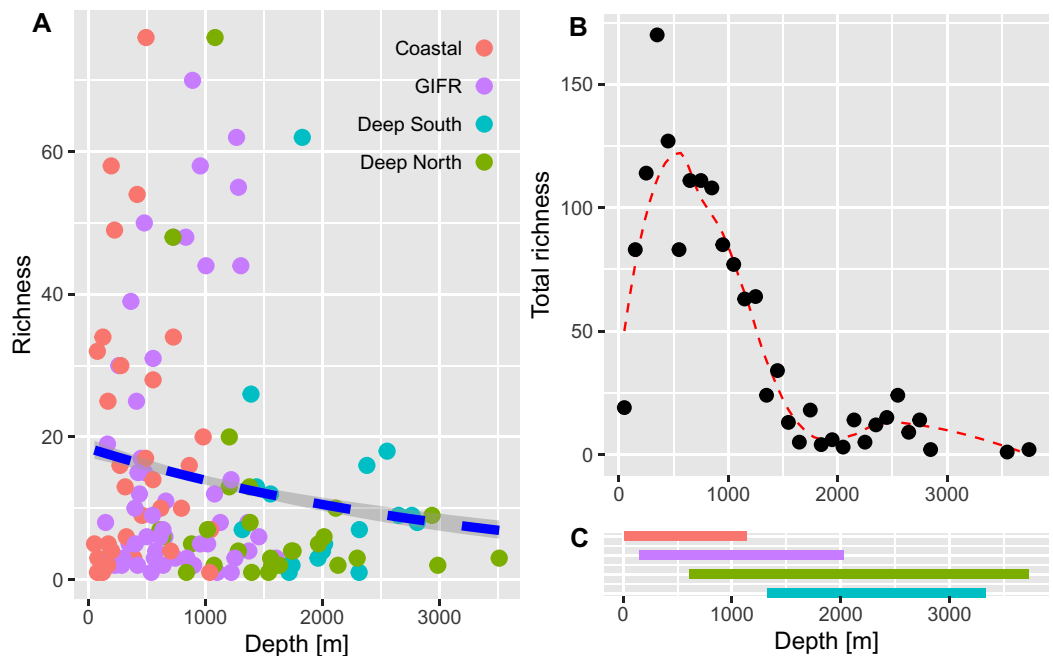


Figure 5 Amphipod species diversity pattern along a depth gradient. (A) Richness values per station and coloured according to the environmental clusters. The blue dashed line represents the Poisson GLM. (B) Maximum number of amphipod species per 100-m interval. A Loess smoother represented by the red dashed line is plotted to better visualize the pattern. (C) Bars show the depth ranges in meters for each of the four environmental clusters. Colours according to the legend in (A).

Full-size [DOI: 10.7717/peerj.11898/fig-5](https://doi.org/10.7717/peerj.11898/fig-5)

The presence of the GIFR is known as an effective barrier to disrupt the dispersal of benthic organisms between the North Atlantic and the Nordic seas (*Weisshappel & Svavarsson, 1998; Brix & Svavarsson, 2010; Schnurr et al., 2018*). With a saddle depth averaging 600 m in the Strait of Denmark and 480 m between Iceland and the Faroe Islands and a maximum depth of c. 840 m, the depth increases towards the abyssal basins on each side of the ridge exceeding 3,000 m. Depth, or rather ecological and environmental variables that change with depth, such as hydrostatic pressure, temperature, food availability, or competition, have been demonstrated to have a large impact on species distributions (*Rex & Etter, 2010; Brown & Thatje, 2011; Tittensor et al., 2011*). In contrast, there are several examples of amphipod species, mostly within the more motile scavenger and predator guilds, with large depth distributions and thus at least the intrinsic capability to overcome topographical barriers (*Lacey et al., 2018; Lörz, Jazdzewska & Brandt, 2018; Weston et al., 2021*).

The GIFR also marks the transition between different bodies of water, and hence the effects of depth and water mass properties are intertwined. Generally, physical and chemical water mass attributes such as temperature, salinity, pH, organic matter, and dissolved oxygen play critical roles in structuring benthic communities including microbes, fish, crustaceans, corals, and sponges (*Koslow, 1993; Weisshappel & Svavarsson, 1998; Brix & Svavarsson, 2010; Schnurr et al., 2018; Puerta et al., 2020; Roberts et al., 2021*). Reasons for this involve physiological tolerances of larvae, juveniles and adults towards

certain environmental conditions, dispersal constraints invoked by density differences or current shear, as well as enhanced nutrient input linked to hydrography ([Puerta et al., 2020](#); [Roberts et al., 2021](#)).

Obviously, cold sub-zero temperatures in the Nordic sea basins restrict species distributions, as only few species are pre-adapted to such low temperatures while withstanding high hydrostatic pressures ([Svavarsson, Stromberg & Brattegard, 1993](#); [Brown & Thatje, 2011](#)). This is supported by the fact that many amphipod species in our study prefer moderate conditions, at least in terms of temperature. Initially, however, species originating from the North Atlantic had to overcome the GIFR and enter the Nordic seas against the overflow water from the Denmark Strait and Faroe Bank Channel ([Yasuhara et al., 2008](#)), the latter being limited to species with broad bathymetric distributions or eurytherm “shallow”-water taxa. The presence of the GIFR is thereby inevitably linked to the opening of the North-east Atlantic about 55 Mya, representing a barrier between the Nordic seas and North Atlantic ever since ([Hjartarson, Erlendsson & Blischke, 2017](#)). Alternatively, species from the North Pacific had to cross the Bering Strait sill, and experience subsequent trans-Arctic migration ([Hardy et al., 2011](#)). While the shelf fauna represents a mixture of North Pacific, North Atlantic and to a lesser extent endemic Arctic fauna (e.g., [Svavarsson, Stromberg & Brattegard, 1993](#); [Hardy et al., 2011](#)), large parts of the contemporary deep-sea fauna of the Arctic and Nordic seas likely originate from the North Atlantic (e.g., [Bluhm et al., 2011](#) and citations therein; [Svavarsson, Stromberg & Brattegard, 1993](#)).

In our indicator analysis, species were identified based on their predominant affiliation to certain oceanographic conditions. Identifying areas of endemism, [Arfianti & Costello \(2020\)](#) defined our study area as part of a larger region that comprised North American boreal, Arctic and North Pacific areas. Our results, however, are consistent with the view that the deep-sea fauna of the Nordic seas appears to originate from shelf genera or less pronounced deep-sea taxa that were able to cross the GIFR ([Dahl, 1979](#); [Just, 1980](#); [Svavarsson, Stromberg & Brattegard, 1993](#)). The study by [Arfianti & Costello \(2020\)](#) contained data for the entire Arctic and sub-Arctic regions, encompassing both shelf and deep-sea areas, with the first reportedly representing a mixture of Atlantic, Arctic and Pacific elements (see above). Contrasting distribution patterns in hyperbenthic Eusiridae and Calliopiidae represent good examples to illustrate the barrier effect of the ridge; the family Eusiridae, which is more prevalent in deep water, has only a few species north of the GIFR, which is in contrast to the shallow water family Calliopiidae, whose species diversity is higher in the north ([Weisshappel, 2000](#); [Weisshappel, 2001](#)). Overall, [Svavarsson, Stromberg & Brattegard \(1993\)](#) describe the deep-sea fauna of the Arctic and Nordic seas as very young, probably less than 100,000 yrs. old, due to the presence of the ridge and the adverse conditions prevailing in the northern regions (“topographic and environmental filtering”). Accordingly, little time remained for speciation and formation of endemic species ([Svavarsson, Stromberg & Brattegard, 1993](#)).

Our coastal amphipod assemblage, as well as the one associated with the GIFR, consisted of indicator species with broad North Atlantic distributions. Over the past millennia the biogeography of northern latitudes had been shaped by recurring glacial

cycles (Darby, Polyak & Bauch, 2006). During the last glacial maximum (ending about 6,000 yrs ago; Darby, Polyak & Bauch, 2006) Arctic shelves were largely covered by grounded ice sheets forcing the fauna towards more southerly (North Atlantic) ice-free areas or deeper waters (Dunton, 1992; Darby, Polyak & Bauch, 2006). The latter may have become the ancestors of today's Nordic deep-sea fauna (Nesis, 1984). While evidence exists that at least parts of the shelf had remained ice-free and thus served as glacial refugia, notably here Iceland and the Faroe Islands (Maggs et al., 2008; Hardy et al., 2011), most species must have recolonized the previously ice-covered areas rather swiftly. Given the close overlap of coastal and GIFR fauna in our study, the ridge could have provided a potential shallow-water link for brooding taxa that has promoted the recolonization from suitable ice-free habitats.

Diversity trends

The comparison of the diversity between the environmental clusters showed that the diversity of the shallow clusters (coastal and GIFR) was higher than that of the deep clusters north and south of the ridge. While species richness had the highest number of effective species (Fig. 4A), its sole use is usually not encouraged as it is heavily affected by sample size and shows high sensitivity in recording rare species (Jost, 2006). There were some profound differences between Hill numbers—species richness, Shannon, and Simpson diversity—likely because each of these indices scales rarity differently (Chao, Chiu & Jost, 2014; Roswell, Dushoff & Winfree, 2021; Figs. 4B, 4C). The fact that none of the richness-based rarefaction curves has stabilized yet, could therefore be an artifact; many species have only been found once, either because they could not be identified to species level or because only a small number of individuals were sampled during the historical missions. The Simpson index, on the other hand, is considered as being most robust when sampling effort differs strongly between samples, since it largely reflects patterns in the most common species (Jost, 2006). Shannon diversity can be seen as a intermediate measure in terms of its responses to sample size and rarity (Roswell, Dushoff & Winfree, 2021). Overall, though, all estimates applied have their merits and pitfalls, and typically using all three indices provides the best representation of the diversity in a given area (Roswell, Dushoff & Winfree, 2021). Nevertheless, a consistent pattern of a higher diversity in the shallows—relative to the deep clusters—was evident in all three indices. In the same way, analysis of the entire data set showed an unimodal pattern, with richness peaking at around 500 m, and then a sharp decline in richness with increasing depth (Fig. 5). Compared to other studies that often show a peak between 2,000–3,000 m (cf. Rex & Etter, 2010 and citations therein), maximum richness in amphipods of the Nordic Seas seems to be much shallower and to resemble patterns in isopods from the same area (Brix et al., 2018, but see Svarvarsson, 1997). However, it should be noted here that differences in sampling intensity between grid cells and depth were a confounding factor in our study and the results therefore will have to be reassessed with additional future sampling.

Combined historical and ecological explanations have been utilized to interpret the overall low diversity of the Nordic basins compared to the other deep-sea regions

(*Svavarsson, Stromberg & Brattegard, 1993; Bluhm et al., 2011*). In general, it is believed that variation in energy supply (temperature and productivity) affect deep-sea diversity (e.g., *Woolley et al., 2016; Yasuhara & Danovaro, 2016; Jöst et al., 2019*). However, cold temperatures *per se* do not seem to have a negative impact on diversity, since benthic communities at sub-zero temperatures in the Southern Ocean abyss appear to be extraordinarily rich (*Brandt et al., 2007*), but when coupled with the very low productivity and geographical isolation of the Nordic basins, the diversity of invertebrates is relatively low (*Svavarsson, Stromberg & Brattegard, 1993; Egilsdottir, McGinty & Gudmundsson, 2019; Jöst et al., 2019*). In addition, antagonistic effects of high hydrostatic pressure and low temperatures that prevail in the deep Nordic Sea basins could explain the low diversity there (*Brown & Thatje, 2011, 2014*).

Notably, the diversity of the “Deep South” cluster in our study was as low as that of the Deep North, which contrasts with the perception of an impoverished Nordic deep-sea fauna (*Bouchet & Warén, 1979; Dahl, 1979; Rex et al., 1993; Svavarsson, 1997; Weissshappel & Svavarsson, 1998; Jöst et al., 2019*). Although amphipods are typically less well presented in the deep sea (e.g., when compared to isopods; *Lörz, Kaiser & Bowden, 2013*), their ‘deficiency’ in Nordic waters was established earlier. For example, *Dahl (1979)* found that gammaridean species in the Norwegian Sea is a mere 20% of that in the North Atlantic. Yet, it is not clear whether this is a valid conclusion, since pure richness comparisons are very susceptible to differences in sample sizes and sample effort (see discussion above). In addition, different taxa north and south of the ridge can have different diversity patterns resulting e.g., from their different evolutionary histories, lifestyles (brooding vs. broadcaster) or physiological scope. This becomes very evident in isopods, a sister group of the amphipods, where the diversity of the deep North Atlantic exceeds that of the Nordic seas (*Svavarsson, 1997*).

Although not strictly comparable, but in line with our results, *Egilsdottir, McGinty & Gudmundsson (2019)*, found local deep-sea diversity of bivalve and gastropod molluscs north and south of the GIFR to be equally low. They attributed this to specific oceanographic conditions prevailing at the deep southern stations. In addition, changes in environmental conditions in the course of past glacial maxima in the northern North Atlantic and in the North Sea were associated with cyclical changes of low (glacial) and relatively increased (interglacial) diversity (*Cronin & Raymo, 1997; Yasuhara et al., 2014*). The related environmental consequences of these climatic changes, in particular variation in bottom-water temperature, seasonality and meltwater runoff, evidently had a strong impact on deep-sea diversity, with recent deep-sea fauna still in the process of recovering from these events (*Rex et al., 1993; Cronin & Raymo, 1997; Wilson, 1998; Yasuhara et al., 2008; Yasuhara et al., 2014*; but see *Jöst et al., 2019* and citations therein).

Compared to the deep-sea cluster, the diversity of the shallower coastal and GIFR clusters was considerably higher (Fig. 4A). This is in stark contrast to an allegedly poor amphipod fauna, for example when compared to the South polar region (*Arfianti & Costello, 2020*). Although a direct comparison with other regions at complementary depth is still pending, it is already clear that the shelf and upper slope amphipod fauna on the border between the North Atlantic and North Sea, consisting of more than 300

effective species, is not depleted (Fig. 4A). In comparison, *De Broyer & Jazdzewska (2014)* counted ~560 amphipod species for the entire Antarctic region (south of the Polar front), which is considered to have a significantly higher amphipod diversity relative to high northern latitudes (*Arfianti & Costello, 2020*). In addition, through the application of molecular techniques, but also additional sampling, especially of the deeper and less frequently explored areas, more species are likely to be discovered for the northern region (*Bluhm et al., 2011; Jazdzewska et al., 2018; Lörz, Jazdzewska & Brandt, 2018; Schwentner & Lörz, 2020*). We admit the comparison is slightly misleading, as cryptic species are discovered across all environments at similar rates (*Pfenninger & Schwenk, 2007*), plus different geological histories, oceanographic settings, and the size of the Arctic vs. Antarctica, among other things represent additional confounders. We thus believe that the diversity of the northern regions should not be underestimated and presumably occupies globally at least a middle ranking.

CONCLUSIONS

In amphipods, water mass properties appear to be the main force in delineating species distributions at the boundary between the North Atlantic and the Nordic seas, with the GIFR additionally hindering the exchange of deep-sea species between northern and southern deep-sea basins. This pattern is largely congruent for all benthic but also hyperbenthic amphipod families. Different factors are likely responsible for driving deep-sea diversity on each side of the ridge. While impoverished amphipod communities in the Nordic basins are likely to be due to topographical and environmental barrier effects, the southern deep-sea assemblage shows similarly low diversity, presumably a response to variation in the oceanographic environment over a range of temporal and spatial scales. In addition, bathymetric sampling constraints need to be considered.

Since the Cenozoic Era (c. 65 mya) and more recently, the areas of the northern North Atlantic and the Nordic seas have undergone profound climatic changes, from greenhouse to icehouse conditions and vice versa, shaping the composition and distribution of the marine biota (*Piepenburg, 2005; Horton et al., 2020*). Distinct temperature thresholds for the Arctic and boreal benthic species point towards future range shifts (restrictions vs. extensions), which will have a strong impact on the diversity in the region (*Renaud et al., 2015*). Our data showed a high salinity and temperature-driven distribution of the amphipod assemblages, which also applies to a number of other taxa (*Brix & Svavarsson, 2010; Schnurr et al., 2018; Egilsdottir, McGinty & Gudmundsson, 2019; Jöst et al., 2019*). Additional environmental variables may prove important in explaining diversity and distribution, including seasonality in productivity, pH and ice cover (*Yasuhara et al., 2012*). These are especially the ones that are predicted to change first due to recent climate changes (e.g., *Hoegh-Guldberg & Bruno, 2010*).

In our study, amphipods were highlighted as an important benthic component in Icelandic waters. Since climate change is supposed to have an impact on several organizational levels (populations, species, communities), in future studies, we aim to investigate the interaction of local and regional processes on amphipod diversity as well as

species-specific responses to better understand potential effects of climate change in the Nordic seas.

ACKNOWLEDGEMENTS

We submitted the data to GFBIO and OBIS (Oceanographic Biodiversity Information System) and are grateful for their processing. We thank all crew and scientific teams for all efforts taking, sorting and identifying the samples. Furthermore, we acknowledge the data management of the IceAGE Amphipoda in the local DZMB database by Antje Fischer and Karen Jeskulke during two amphipod determination workshops in 2016 and 2017.

ADDITIONAL INFORMATION AND DECLARATIONS

Funding

Anne-Nina Lörz was financed by the German Science Foundation project IceAGE Amphipoda (LO2543/1-1). Stefanie Kaiser received a grant from the Narodowa Agencja Wymiany Akademickiej (NAWA, Poland) under the ULAM program. Financial support for two amphipod determination workshops from IceAGE expeditions was given by the Volkswagenstiftung to Saskia Brix and Anne-Nina Lörz. The funders had no role in study design, data collection and analysis, decision to publish, or preparation of the manuscript.

Grant Disclosures

The following grant information was disclosed by the authors:
German Science Foundation project IceAGE Amphipoda: LO2543/1-1.
Narodowa Agencja Wymiany Akademickiej (NAWA, Poland).
ULAM.

Competing Interests

The authors declare that they have no competing interests. Jens Oldeland is a freelancing environmental data scientist.

Author Contributions

- Anne-Nina Lörz conceived and designed the experiments, analyzed the data, authored or reviewed drafts of the paper, and approved the final draft.
- Stefanie Kaiser analyzed the data, authored or reviewed drafts of the paper, and approved the final draft.
- Jens Oldeland performed the experiments, analyzed the data, prepared figures and/or tables, authored or reviewed drafts of the paper, and approved the final draft.
- Caroline Stolter performed the experiments, prepared figures and/or tables, and approved the final draft.
- Karlotta Kürzel performed the experiments, prepared figures and/or tables, and approved the final draft.
- Saskia Brix conceived and designed the experiments, authored or reviewed drafts of the paper, and approved the final draft.

Data Availability

The following information was supplied regarding data availability:

The data are available in the [Supplemental Files](#).

The data is also available at Pangaea: Lörz, Anne-Nina; Brix, Saskia; Oldeland, Jens; Coleman, Charles Oliver; Peart, Rachel; Hughes, Lauren; Andres, Hans Georg; Kaiser, Stefanie; Stolter, Caroline; Kürzel, Karlotta; Vader, Wim; Tandberg, Anne Helene; Stransky, Bente; Svavarsson, Jörundur; Guerra-García, José-Manuel; Krapp-Schickel, Traudl (2021): Marine Amphipoda and environmental occurrence around Iceland. <https://doi.pangaea.de/10.1594/PANGAEA.931959>.

Supplemental Information

Supplemental information for this article can be found online at <http://dx.doi.org/10.7717/peerj.11898#supplemental-information>.

REFERENCES

- Anderson MJ, Willis TJ. 2003.** Canonical analysis of principal coordinates: a useful method of constrained ordination for ecology. *Ecology* **84**(2):511–525
DOI [10.1890/0012-9658\(2003\)084\[0511:CAOPCA\]2.0.CO;2](https://doi.org/10.1890/0012-9658(2003)084[0511:CAOPCA]2.0.CO;2).
- Arfianti T, Costello MJ. 2020.** Global biogeography of marine amphipod crustaceans: latitude, regionalization, and beta diversity. *Marine Ecology Progress Series* **638**:83–94
DOI [10.3354/meps13272](https://doi.org/10.3354/meps13272).
- Assis J, Tyberghein L, Bosch S, Verbruggen H, Serrão EA, De Clerck O. 2018.** Bio-ORACLE v2.0: extending marine data layers for bioclimatic modelling. *Global Ecology and Biogeography* **27**(3):277–284 DOI [10.1111/geb.12693](https://doi.org/10.1111/geb.12693).
- Astthorsson OS, Gislason A, Jonsson S. 2007.** Climate variability and the Icelandic marine ecosystem. *Deep Sea Research Part II: Topical Studies in Oceanography* **54**(23–26):2456–2477
DOI [10.1016/j.dsr2.2007.07.030](https://doi.org/10.1016/j.dsr2.2007.07.030).
- Baco AR, Etter RJ, Ribeiro PA, Von der Heyden S, Beerli P, Kinlan BP. 2016.** A synthesis of genetic connectivity in deep-sea fauna and implications for marine reserve design. *Molecular Ecology* **25**(14):3276–3298 DOI [10.1111/mec.13689](https://doi.org/10.1111/mec.13689).
- Bascompte J. 2009.** Mutualistic networks. *Frontiers in Ecology and the Environment* **7**(8):429–436
DOI [10.1890/080026](https://doi.org/10.1890/080026).
- Bett BJ. 2001.** UK atlantic margin environmental survey: introduction and overview of bathyal benthic ecology. *Continental Shelf Research* **21**(8–10):917–956
DOI [10.1016/S0278-4343\(00\)00119-9](https://doi.org/10.1016/S0278-4343(00)00119-9).
- Birch CP, Oom SP, Beecham JA. 2007.** Rectangular and hexagonal grids used for observation, experiment and simulation in ecology. *Ecological Modelling* **206**(3–4):347–359
DOI [10.1016/j.ecolmodel.2007.03.041](https://doi.org/10.1016/j.ecolmodel.2007.03.041).
- Birchenough SN, Reiss H, Degraer S, Mieszkowska N, Borja Á, Buhl-Mortensen L, Braeckman U, Craeymeersch J, De Mesel I, Kerckhof F. 2015.** Climate change and marine benthos: a review of existing research and future directions in the North Atlantic. *Wiley Interdisciplinary Reviews: Climate Change* **6**(2):203–223 DOI [10.1002/wcc.330](https://doi.org/10.1002/wcc.330).
- Bluhm BA, Gebruk AV, Gradinger R, Hopcroft RR, Huettmann F, Kosobokova KN, Sirenko BI, Weslawski JM. 2011.** Arctic marine biodiversity: an update of species richness and examples of biodiversity change. *Oceanography* **24**(3):232–248 DOI [10.5670/oceanog.2011.75](https://doi.org/10.5670/oceanog.2011.75).

- Boeck A. 1861.** Bemaerkninger angaaende de ved de norske kyster forekommende Amphipoder. *Forhandlinger ved de Skandinaviske Naturforskeres Mfte* **8**:631–677.
- Bosch S, Tyberghein L, De Clerck O. 2018.** *sdmpredictors: species distribution modelling predictor datasets*. R package version 0.2. 8. Available at <https://CRAN.R-project.org/package=sdmpredictors>.
- Bouchet P, Warén A. 1979.** Planktotrophig larval development in deep-water gastropods. *Sarsia* **64**(1–2):37–40 DOI [10.1080/00364827.1979.10411360](https://doi.org/10.1080/00364827.1979.10411360).
- Brandt A, Gooday AJ, Brandão SN, Brix S, Brökeland W, Cedhagen T, Choudhury M, Cornelius N, Danis B, De Mesel I, Diaz RJ, Gillan DC, Ebbe B, Howe JA, Janussen D, Kaiser S, Linse K, Malyutina M, Pawlowski J, Raupach M, Vanreusel A. 2007.** First insights into the biodiversity and biogeography of the Southern Ocean deep sea. *Nature* **447**(7142):307–311 DOI [10.1038/nature05827](https://doi.org/10.1038/nature05827).
- Brix S, Lörz A-N, Jażdżewska AM, Hughes L, Tandberg AHS, Pabis K, Stransky B, Krapp-Schickel T, Sorbe JC, Hendrycks E, Vader W, Frutos I, Horton T, Jażdżewski K, Peart R, Beermann J, Coleman CO, Buhl-Mortensen L, Corbari L, Havermans C, Tato R, Campan AJ. 2018.** Amphipod family distributions around Iceland. *ZooKeys* **731**(1–2):41–53 DOI [10.3897/zookeys.731.19854](https://doi.org/10.3897/zookeys.731.19854).
- Brix S, Meissner K, Stransky B, Halanych KM, Jennings RM, Kocot KM, Svavarsson J. 2014.** The IceAGE project—a follow up of BIOICE. *Polish Polar Research* **35**:141–150.
- Brix S, Svavarsson J. 2010.** Distribution and diversity of desmosomatid and nannoniscid isopods (Crustacea) on the Greenland–Iceland–Faeroe Ridge. *Polar Biology* **33**(4):515–530 DOI [10.1007/s00300-009-0729-8](https://doi.org/10.1007/s00300-009-0729-8).
- Brown A, Thatje S. 2011.** Respiratory response of the deep-sea amphipod *Stephonyx biscayensis* indicates bathymetric range limitation by temperature and hydrostatic pressure. *PLOS ONE* **6**(12):e28562 DOI [10.1371/journal.pone.0028562](https://doi.org/10.1371/journal.pone.0028562).
- Brown A, Thatje S. 2014.** Explaining bathymetric diversity patterns in marine benthic invertebrates and demersal fishes: physiological contributions to adaptation of life at depth. *Biological Reviews* **89**:406–426.
- Burnham KP, Anderson DR. 2002.** *Model selection and multimodel inference: a practical information-theoretic approach*. New York: Springer.
- Burrows MT, Schoeman DS, Buckley LB, Moore P, Poloczanska ES, Brander KM, Brown C, Bruno JF, Duarte CM, Halpern BS. 2011.** The pace of shifting climate in marine and terrestrial ecosystems. *Science* **334**(6056):652–655 DOI [10.1126/science.1210288](https://doi.org/10.1126/science.1210288).
- Cáceres MD, Legendre P. 2009.** Associations between species and groups of sites: indices and statistical inference. *Ecology* **90**(12):3566–3574 DOI [10.1890/08-1823.1](https://doi.org/10.1890/08-1823.1).
- Chase JM, Leibold MA. 2003.** *Ecological niches*. Chicago: Chicago University Press.
- Clarke KR. 1993.** Non-parametric multivariate analyses of changes in community structure. *Austral Ecology* **18**(1):117–143 DOI [10.1111/j.1442-9993.1993.tb00438.x](https://doi.org/10.1111/j.1442-9993.1993.tb00438.x).
- Chao A, Chiu C-H, Jost L. 2014.** Unifying species diversity, phylogenetic diversity, functional diversity, and related similarity and differentiation measures through Hill numbers. *Annual Review of Ecology, Evolution, and Systematics* **45**(1):297–324 DOI [10.1146/annurev-ecolsys-120213-091540](https://doi.org/10.1146/annurev-ecolsys-120213-091540).
- Cronin TM, Raymo ME. 1997.** Orbital forcing of deep-sea benthic species diversity. *Nature* **385**(6617):624–627 DOI [10.1038/385624a0](https://doi.org/10.1038/385624a0).
- Dahl E. 1979.** Deep-sea carrion feeding amphipods: evolutionary patterns in niche adaptation. *Oikos* **33**(2):167–175 DOI [10.2307/3543994](https://doi.org/10.2307/3543994).

- Darby DA, Polyak L, Bauch HA. 2006.** Past glacial and interglacial conditions in the Arctic Ocean and marginal seas—a review. *Progress in Oceanography* 71(2–4):129–144 DOI 10.1016/j.pocean.2006.09.009.
- Dauvin J-C, Alizier S, Weppe A, Guðmundsson G. 2012.** Diversity and zoogeography of Icelandic deep-sea Ampeliscidae (Crustacea: Amphipoda). *Deep Sea Research Part I: Oceanographic Research Papers* 68:12–23 DOI 10.1016/j.dsr.2012.04.013.
- De Broyer C, Jazdzewski K. 1996.** Biodiversity of the Southern Ocean: towards a new synthesis for the Amphipoda (Crustacea). *Bollettino del Museo Civico di Storia Naturale di Verona* 20:547–568.
- De Broyer C, Jazdzewska A. 2014.** Biogeographic patterns of Southern Ocean benthic Amphipods. In: De Broyer C, Koubbi P, eds. *Biogeographic Atlas of the Southern Ocean*. Cambridge: Scientific Committee on Antarctic Research, 155–165.
- De Cáceres M, Legendre P, Moretti M. 2010.** Improving indicator species analysis by combining groups of sites. *Oikos* 119(10):1674–1684 DOI 10.1111/j.1600-0706.2010.18334.x.
- Dunton K. 1992.** Arctic biogeography: the paradox of the marine benthic fauna and flora. *Trends in Ecology & Evolution* 7(6):183–189 DOI 10.1016/0169-5347(92)90070-R.
- Egilsdóttir H, McGinty N, Gudmundsson G. 2019.** Relating depth and diversity of Bivalvia and Gastropoda in two contrasting sub-arctic marine regions. *Frontiers in Marine Science* 6:129 DOI 10.3389/fmars.2019.00129.
- Eiríksson J, Knudsen KL, Larsen G, Olsen J, Heinemeier J, Bartels-Jónsdóttir HB, Jiang H, Ran L, Símonarson LA. 2011.** Coupling of palaeoceanographic shifts and changes in marine reservoir ages off North Iceland through the last millennium. *Palaeogeography, Palaeoclimatology, Palaeoecology* 302(1–2):95–108 DOI 10.1016/j.palaeo.2010.06.002.
- Grantham BA, Eckert GL, Shanks AL. 2003.** Dispersal potential of marine invertebrates in diverse habitats: ecological archives A013-001-A1. *Ecological Applications* 13:108–116 DOI 10.1890/1051-0761(2003)013[0108:DPOMII]2.0.CO;2.
- Guerra-García J, De Figueroa JT, Navarro-Barranco C, Ros M, Sánchez-Moyano J, Moreira J. 2014.** Dietary analysis of the marine Amphipoda (Crustacea: Peracarida) from the Iberian Peninsula. *Journal of Sea Research* 85:508–517 DOI 10.1016/j.seares.2013.08.006.
- Halpern BS, Walbridge S, Selkoe KA, Kappel CV, Micheli F, D'Agrosa C, Bruno JF, Casey KS, Ebert C, Fox HE, Fujita R, Heinemann D, Lenihan HS, Madin EMP, Perry MT, Selig ER, Spalding M, Steneck R, Watson R. 2008.** A global map of human impact on marine ecosystems. *Science* 319(5865):948–952 DOI 10.1126/science.1149345.
- Hansen HJ. 1887.** Malacostraca marina Groenlandiae occidentalis: oversigt over det vestlige Grønlands fauna af malakostrake havkrebssdyr. *Videnskabelige Meddelelser fra Dansk Naturhistorisk Forening* 2–7:5–226.
- Hansen B, Østerhus S, Turrell WR, Jónsson S, Valdimarsson H, Hátún H, Olsen SM. 2008.** The inflow of Atlantic water, heat, and salt to the nordic seas across the Greenland-Scotland ridge. In: Dickson RR, Meincke J, Rhines P, eds. *Arctic-Subarctic Ocean Fluxes*. Dordrecht: Springer.
- Hardy SM, Carr CM, Hardman M, Steinke D, Corstorphine E, Mah C. 2011.** Biodiversity and phylogeography of Arctic marine fauna: insights from molecular tools. *Marine Biodiversity* 41(1):195–210 DOI 10.1007/s12526-010-0056-x.
- Harley CD, Randall Hughes A, Hultgren KM, Miner BG, Sorte CJ, Thornber CS, Rodriguez LF, Tomanek L, Williams SL. 2006.** The impacts of climate change in coastal marine systems. *Ecology Letters* 9(2):228–241 DOI 10.1111/j.1461-0248.2005.00871.x.
- Heller C. 1875.** Neue Crustaceen und Pycnogoniden: Gesammelt während der k.k. österr.-ungar. Nordpol-Expedition. *Vorläufige Mittheilung—Sitzungsberichte der*

- Mathematisch-Naturwissenschaftlichen Classe der Kaiserlichen Akademie der Wissenschaften in Wien* 71:609–612.
- Hiddink JG, Burrows MT, García Molinos J. 2015.** Temperature tracking by North Sea benthic invertebrates in response to climate change. *Global Change Biology* 21(1):117–129 DOI 10.1111/gcb.12726.
- Hilário A, Metaxas A, Gaudron SM, Howell KL, Mercier A, Mestre NC, Ross RE, Thurnherr AM, Young C. 2015.** Estimating dispersal distance in the deep sea: challenges and applications to marine reserves. *Frontiers in Marine Science* 2:6 DOI 10.3389/fmars.2015.00006.
- Hjartarson Á, Erlendsson Ö, Blischke A. 2017.** The Greenland–Iceland–Faroe Ridge Complex. *Geological Society, London, Special Publications* 447(1):127–148 DOI 10.1144/SP447.14.
- Hoegh-Guldberg O, Bruno JF. 2010.** The impact of climate change on the world's marine ecosystems. *Science* 328(5985):1523–1528 DOI 10.1126/science.1189930.
- Horton T, Lowry J, De Broyer C, Bellan-Santini D, Coleman CO, Corbari L, Costello MJ, Daneliya M, Dauvin JC, Fišer C, Gasca R, Grabowski M, Guerra-García JM, Hendrycks E, Hughes L, Jaume D, Jazdzewski K, Kim YH, King R, Krapp-Schickel T, LeCroy S, Lörz ANA-N, Mamos T, Senna AR, Serejo C, Sket B, Souza-Filho JF, Tandberg AH, Thomas JD, Thurston M, Vader W, Väinölä R, Vonk R, White K, Zeidler W. 2021.** World Amphipoda Database—Amphipoda: accessed through: World Register of Marine species. Available at <http://www.marinespecies.org/aphia.php?p=taxdetails&id=1135> (accessed 3 May 2021).
- Horton T, Thurston MH, Vlierboom R, Gutteridge Z, Pebody CA, Gates AR, Bett BJ. 2020.** Are abyssal scavenging amphipod assemblages linked to climate cycles? *Progress in Oceanography* 184(3):102318 DOI 10.1016/j.pocean.2020.102318.
- Hsieh T, Ma K, Chao A. 2016.** iNEXT: an R package for rarefaction and extrapolation of species diversity (Hill numbers). *Methods in Ecology and Evolution* 7(12):1451–1456 DOI 10.1111/2041-210X.12613.
- Jablonski D. 2008.** Biotic interactions and macroevolution: extensions and mismatches across scales and levels. *Evolution: International Journal of Organic Evolution* 62(4):715–739 DOI 10.1111/j.1558-5646.2008.00317.x.
- Jablonski D, Roy K. 2003.** Geographical range and speciation in fossil and living molluscs. *Proceedings of the Royal Society of London. Series B: Biological Sciences* 270(1513):401–406 DOI 10.1098/rspb.2002.2243.
- Jazdzewska AM, Corbari L, Driskell A, Frutos I, Havermans C, Hendrycks E, Hughes L, Lörz A-N, Stransky B, Tandberg AHS, Vader W, Brix S. 2018.** A genetic fingerprint of Amphipoda from Icelandic waters—the baseline for further biodiversity and biogeography studies. *ZooKeys* 55(9):55–73 DOI 10.3897/zookeys.731.19931.
- Jochumsen K, Schnurr SM, Quadfasel D. 2016.** Bottom temperature and salinity distribution and its variability around Iceland. *Deep Sea Research Part I: Oceanographic Research Papers* 111:79–90 DOI 10.1016/j.dsr.2016.02.009.
- Jones DO, Yool A, Wei CL, Henson SA, Ruhl HA, Watson RA, Gehlen M. 2014.** Global reductions in seafloor biomass in response to climate change. *Global Change Biology* 20(6):1861–1872 DOI 10.1111/gcb.12480.
- Jöst AB, Yasuhara M, Wei CL, Okahashi H, Ostmann A, Martínez Arbizu P, Mamo B, Svavarsson J, Brix S. 2019.** North Atlantic gateway: test bed of deep-sea macroecological patterns. *Journal of Biogeography* 46(9):2056–2066 DOI 10.1111/jbi.13632.
- Jost L. 2006.** Entropy and diversity. *Oikos* 113(2):363–375 DOI 10.1111/j.2006.0030-1299.14714.x.
- Just J. 1980.** *Amphipoda (Crustacea) of the Thule area, northwest Greenland: faunistics and taxonomy*. Copenhagen: Museum Tusulanum Press.

- Koslow JA. 1993. Community structure in North Atlantic deep-sea fishes. *Progress in Oceanography* 31(3):321–338 DOI 10.1016/0079-6611(93)90005-X.
- Lacey NC, Mayor DJ, Linley TD, Jamieson AJ. 2018. Population structure of the hadal amphipod *Bathycallisoma (Scopelocheirus) schellenbergi* in the Kermadec Trench and New Hebrides Trench, SW Pacific. *Deep Sea Research Part II: Topical Studies in Oceanography* 155:50–60 DOI 10.1016/j.dsr2.2017.05.001.
- Leibold MA, Holyoak M, Mouquet N, Amarasekare P, Chase JM, Hoopes MF, Holt RD, Shurin JB, Law R, Tilman D. 2004. The metacommunity concept: a framework for multi-scale community ecology. *Ecology Letters* 7(7):601–613 DOI 10.1111/j.1461-0248.2004.00608.x.
- Lepechin I. 1780. Tres Oniscorum Species descriptae ab I Lepechin. In: *Acta Academiae scientiarum imperialis petropolitanae*. Petropoli: Typis Academiae Scientiarum, 1778–1786.
- Levin LA, Etter RJ, Rex MA, Gooday AJ, Smith CR, Pineda J, Stuart CT, Hessler RR, Pawson D. 2001. Environmental influences on regional deep-sea species diversity. *Annual Review of Ecology and Systematics* 32(1):51–93 DOI 10.1146/annurev.ecolsys.32.081501.114002.
- Lotze HK, Lenihan HS, Bourque BJ, Bradbury RH, Cooke RG, Kay MC, Kidwell SM, Kirby MX, Peterson CH, Jackson JB. 2006. Depletion, degradation, and recovery potential of estuaries and coastal seas. *Science* 312(5781):1806–1809 DOI 10.1126/science.1128035.
- Lourie SA, Vincent AC. 2004. Using biogeography to help set priorities in marine conservation. *Conservation Biology* 18(4):1004–1020 DOI 10.1111/j.1523-1739.2004.00137.x.
- Lucey NM, Lombardi C, DeMarchi L, Schulze A, Gambi MC, Calosi P. 2015. To brood or not to brood: are marine invertebrates that protect their offspring more resilient to ocean acidification? *Scientific Reports* 5(1):1–7 DOI 10.1038/srep12009.
- Lörz A-N. 2010. Deep-sea *Rhachotropis* (Crustacea: Amphipoda: Eusiridae) from New Zealand and the Ross Sea with key to the Pacific, Indian Ocean and Antarctic species. *Zootaxa* 2482:22–48.
- Lörz A-N, Brix S, Oldeland J, Coleman C, Peart R, Hughes L, Andres HG, Kaiser S, Kürzel K, Vader W, Tandberg AH, Stransky B, Svavarsson J, Guerra-García JM, Krapp-Schickel T. 2021. Marine Amphipoda and environmental occurrence around Iceland. *PANGAEA*. Available at <https://doi.pangaea.de/10.1594/PANGAEA.931959>.
- Lörz A-N, Jażdżewska AM, Brandt A. 2018. A new predator connecting the abyssal with the hadal in the Kuril-Kamchatka Trench, NW Pacific. *PeerJ* 6(5):e4887 DOI 10.7717/peerj.4887.
- Lörz A-N, Kaiser S, Bowden D. 2013. Macrofaunal crustaceans in the benthic boundary layer from the shelf break to abyssal depths in the Ross Sea (Antarctica). *Polar Biology* 36(3):445–451 DOI 10.1007/s00300-012-1269-1.
- Lörz A-N, Tandberg AHS, Willassen E, Driskell A. 2018. *Rhachotropis* (Eusiroidea, Amphipoda) from the North East Atlantic—Amphipoda from the IceAGE-Project (Icelandic marine Animals: Genetics and Ecology). *ZooKeys* 731:75–101 DOI 10.3897/zookeys.731.19814.
- Maggs CA, Castilho R, Foltz D, Henzler C, Jolly MT, Kelly J, Olsen J, Perez KE, Stam W, Väinölä R, Viard F, Wares J. 2008. Evaluating signatures of glacial refugia for North Atlantic benthic marine taxa. *Ecology* 89:108–122 DOI 10.1890/08-0257.1.
- Nesis K. 1984. A hypothesis on the origin of western and eastern Arctic distribution areas of marine bottom animals. *Soviet Journal of Marine Biology* 9:235–243.
- Nyssen F, Brey T, Lepoint G, Bouqueneau J-M, De Broyer C, Dauby P. 2002. A stable isotope approach to the eastern Weddell Sea trophic web: focus on benthic amphipods. *Polar Biology* 25(4):280–287 DOI 10.1007/s00300-001-0340-0.
- Oksanen J, Blanchet FG, Friendly M, Kindt R, Legendre P, McGlenn D, Minchin PR, O'Hara RB, Simpson GL, Solymos P, Stevens MHH, Szoecs E, Wagner H. 2019. *vegan*:

community ecology package. R package version 2.5-6. Available at <https://CRAN.R-project.org/package=vegan>.

- Olafsson J, Olafsdottir SR, Benoit-Cattin A, Danielsen M, Arnarson TS, Takahashi T. 2009.** Rate of Iceland Sea acidification from time series measurements. *Biogeosciences* **6(11)**:2661–2668 DOI [10.5194/bg-6-2661-2009](https://doi.org/10.5194/bg-6-2661-2009).
- Pearl RA. 2018.** Ampeliscidae (Crustacea, Amphipoda) from the IceAGE expeditions— Amphipoda from the IceAGE-Project (Icelandic marine Animals: Genetics and Ecology). *ZooKeys* **731**:145–173 DOI [10.3897/zookeys.731.19948](https://doi.org/10.3897/zookeys.731.19948).
- Pfenninger M, Schwenk K. 2007.** Cryptic animal species are homogeneously distributed among taxa and biogeographical regions. *BMC Evolutionary Biology* **7(1)**:1–6 DOI [10.1186/1471-2148-7-121](https://doi.org/10.1186/1471-2148-7-121).
- Piepenburg D. 2005.** Recent research on Arctic benthos: common notions need to be revised. *Polar Biology* **28(10)**:733–755 DOI [10.1007/s00300-005-0013-5](https://doi.org/10.1007/s00300-005-0013-5).
- Puerta P, Johnson C, Carreiro-Silva M, Henry L-A, Kenchington E, Morato T, Kazanidis G, Rueda JL, Urrea J, Ross S, Wei C-L, González-Irusta JM, Arnaud-Haond S, Orejas C. 2020.** Influence of water masses on the biodiversity and biogeography of deep-sea benthic ecosystems in the North Atlantic. *Frontiers in Marine Science* **7**:239 DOI [10.3389/fmars.2020.00239](https://doi.org/10.3389/fmars.2020.00239).
- QGIS Development Team. 2019.** *QGIS geographic information system*. Chicago: Open Source Geospatial Foundation.
- Renaud PE, Sejr MK, Bluhm BA, Sirenko B, Ellingsen IH. 2015.** The future of Arctic benthos: expansion, invasion, and biodiversity. *Progress in Oceanography* **139(7)**:244–257 DOI [10.1016/j.pocean.2015.07.007](https://doi.org/10.1016/j.pocean.2015.07.007).
- Rex MA, Crame JA, Stuart CT, Clarke A. 2005.** Large-scale biogeographic patterns in marine mollusks: a confluence of history and productivity? *Ecology* **86(9)**:2288–2297 DOI [10.1890/04-1056](https://doi.org/10.1890/04-1056).
- Rex MA, Etter RJ. 2010.** *Deep-sea biodiversity: pattern and scale*. Cambridge: Harvard University Press.
- Rex MA, Stuart CT, Hessler RR, Allen JA, Sanders HL, Wilson GD. 1993.** Global-scale latitudinal patterns of species diversity in the deep-sea benthos. *Nature* **365(6447)**:636–639 DOI [10.1038/365636a0](https://doi.org/10.1038/365636a0).
- Richardson AJ, Poloczanska ES. 2008.** Under-resourced, under threat. *Science* **320(5881)**:1294–1295 DOI [10.1126/science.1156129](https://doi.org/10.1126/science.1156129).
- Roberts E, Bowers D, Meyer H, Samuelson A, Rapp H, Cárdenas P. 2021.** Water masses constrain the distribution of deep-sea sponges in the North Atlantic Ocean and Nordic Seas. *Marine Ecology Progress Series* **659**:75–96 DOI [10.3354/meps13570](https://doi.org/10.3354/meps13570).
- Roswell M, Dushoff J, Winfree R. 2021.** A conceptual guide to measuring species diversity. *Oikos* **130(3)**:321–338 DOI [10.1111/oik.07202](https://doi.org/10.1111/oik.07202).
- Sars GO. 1879.** Crustacea et Pycnogonida nova in itinere 2do et 3tio expeditionis Norvegicae anno 1877 & 78 collecta (prodromus descriptionis). *Archiv for Mathematik og Naturvidenskab* **4**:427–476.
- Schnurr S, Osborn KJ, Malyutina M, Jennings R, Brix S, Driskell A, Svavarsson J, Arbizu PM. 2018.** Hidden diversity in two species complexes of munnopsid isopods (Crustacea) at the transition between the northernmost North Atlantic and the Nordic Seas. *Marine Biodiversity* **48(2)**:813–843 DOI [10.1007/s12526-018-0877-6](https://doi.org/10.1007/s12526-018-0877-6).
- Schwentner M, Lörz A-N. 2020.** Population genetics of cold-water coral associated Pleustidae (Crustacea, Amphipoda) reveals cryptic diversity and recent expansion off Iceland. *Marine Ecology* **42(1)**:e12625 DOI [10.1111/maec.12625](https://doi.org/10.1111/maec.12625).

- Scrucca L, Fop M, Murphy TB, Raftery AE. 2016. mclust 5: clustering, classification and density estimation using Gaussian finite mixture models. *The R Journal* 8(1):289 DOI 10.32614/RJ-2016-021.
- Seidov D, Antonov J, Arzayus K, Baranova O, Biddle M, Boyer T, Johnson D, Mishonov A, Paver C, Zweng M. 2015. Oceanography north of 60 °N from World Ocean Database. *Progress in Oceanography* 132(41):153–173 DOI 10.1016/j.pocean.2014.02.003.
- Shannon CE, Weaver W. 1949. *The mathematical theory of communication*. Urbana and Chicago: University of Illinois Press.
- Simpson EH. 1949. Measurement of diversity. *Nature* 163(4148):688 DOI 10.1038/163688a0.
- Stephensen K. 1933. The Godthaab expedition 1928: Amphipoda. *Meddelelser om Grønland* 79:1–88.
- Stephensen K. 1938. The Amphipoda of N. Norway and Spitsbergen with adjacent waters. *Tromsø Museums Skrifter* 3(2):141–278.
- Stephensen K. 1942. The Amphipoda of N. Norway and Spitsbergen with adjacent waters. *Tromsø Museums Skrifter* 3(3):363–526.
- Stephensen K. 1944a. The Zoology of East Greenland: Amphipoda. *Meddelelser om Grønland* 121:1–165.
- Stephensen K. 1944b. Crustacea Malacostraca VIII: Amphipoda IV. *The Danish Ingolf Expedition* 3:1–54.
- Stransky B, Brandt A. 2010. Occurrence, diversity and community structures of peracarid crustaceans (Crustacea, Malacostraca) along the southern shelf of Greenland. *Polar Biology* 33(6):851–867 DOI 10.1007/s00300-010-0785-0.
- Svavarsson JR. 1997. Diversity of isopods (Crustacea): new data from the Arctic and Atlantic Oceans. *Biodiversity & Conservation* 6(11):1571–1579 DOI 10.1023/A:1018322704940.
- Svavarsson J, Stromberg J-O, Brattegard T. 1993. The deep-sea asellote (Isopoda, Crustacea) fauna of the Northern Seas: species composition, distributional patterns and origin. *Journal of Biogeography* 20(5):537–555 DOI 10.2307/2845725.
- Thurston MH. 1980. Abyssal benthic Amphipoda (Crustacea) from the East Iceland Basin—1: the genus Rhachotropis. *Bulletin of the British Museum (Natural History), Zoology* 38(1):43–67 DOI 10.5962/p.12605.
- Tittensor DP, Rex MA, Stuart CT, McClain CR, Smith CR. 2011. Species–energy relationships in deep-sea molluscs. *Biology Letters* 7(5):718–722 DOI 10.1098/rsbl.2010.1174.
- Weisshappel JB. 2000. Distribution and diversity of the hyperbenthic amphipod family Eusiridae in the different seas around the Greenland–Iceland–Faeroe–Ridge. *Sarsia* 85(3):227–236 DOI 10.1080/00364827.2000.10414575.
- Weisshappel JB. 2001. Distribution and diversity of the hyperbenthic amphipod family Calliopiidae in the different seas around the Greenland–Iceland–Faeroe–Ridge. *Sarsia* 86(2):143–151 DOI 10.1080/00364827.2001.10420469.
- Weisshappel J, Svavarsson J. 1998. Benthic amphipods (Crustacea: Malacostraca) in Icelandic waters: diversity in relation to faunal patterns from shallow to intermediate deep Arctic and North Atlantic Oceans. *Marine Biology* 131(1):133–143 DOI 10.1007/s002270050304.
- Weston JN, Peart RA, Stewart HA, Ritchie H, Piertney SB, Linley TD, Jamieson AJ. 2021. Scavenging amphipods from the Wallaby–Zenith Fracture Zone: extending the hadal paradigm beyond subduction trenches. *Marine Biology* 168(1):1–14 DOI 10.1007/s00227-020-03798-4.

- Wilson GD. 1998.** Historical influences on deep-sea isopod diversity in the Atlantic Ocean. *Deep Sea Research Part II: Topical Studies in Oceanography* 45(1-3):279-301 DOI [10.1016/S0967-0645\(97\)00046-5](https://doi.org/10.1016/S0967-0645(97)00046-5).
- Woolley SN, Tittensor DP, Dunstan PK, Guillera-Arroita G, Lahoz-Monfort JJ, Wintle BA, Worm B, O'Hara TD. 2016.** Deep-sea diversity patterns are shaped by energy availability. *Nature* 533(7603):393-396 DOI [10.1038/nature17937](https://doi.org/10.1038/nature17937).
- Yasuhara M, Cronin TM, Demenocal PB, Okahashi H, Linsley BK. 2008.** Abrupt climate change and collapse of deep-sea ecosystems. *Proceedings of the National Academy of Sciences of the United States of America* 105(5):1556-1560 DOI [10.1073/pnas.0705486105](https://doi.org/10.1073/pnas.0705486105).
- Yasuhara M, Danovaro R. 2016.** Temperature impacts on deep-sea biodiversity. *Biological Reviews* 91(2):275-287 DOI [10.1111/brv.12169](https://doi.org/10.1111/brv.12169).
- Yasuhara M, Hunt G, Van Dijken G, Arrigo KR, Cronin TM, Wollenburg JE. 2012.** Patterns and controlling factors of species diversity in the Arctic Ocean. *Journal of Biogeography* 39(11):2081-2088 DOI [10.1111/j.1365-2699.2012.02758.x](https://doi.org/10.1111/j.1365-2699.2012.02758.x).
- Yasuhara M, Okahashi H, Cronin T, Rasmussen T, Hunt G. 2014.** Deep-sea biodiversity response to deglacial and Holocene abrupt climate changes in the North Atlantic Ocean. *Global Ecology and Biogeography* 23(9):957-967 DOI [10.1111/geb.12178](https://doi.org/10.1111/geb.12178).

A new threat to local marine biodiversity: filamentous mats proliferating at mesophotic depths off Rapa Nui

Javier Sellanes^{1,2}, Matthias Gorny³, Germán Zapata-Hernández^{1,2,4}, Gonzalo Alvarez^{5,6}, Praxedes Muñoz¹ and Fadia Tala^{1,6,7}

¹Departamento de Biología Marina, Facultad de Ciencias del Mar, Universidad Católica del Norte, Coquimbo, Coquimbo, Chile

²Millennium Nucleus for Ecology and Sustainable Management of Oceanic Islands (ESMOI), Universidad Católica del Norte, Coquimbo, Coquimbo, Chile

³Oceana, Santiago, Chile

⁴Programa de Doctorado en Biología y Ecología Aplicada (BEA), Universidad Católica del Norte, Coquimbo, Coquimbo, Chile

⁵Departamento de Acuicultura, Universidad Católica del Norte, Coquimbo, Coquimbo, Chile

⁶Centro de Investigación y Desarrollo Tecnológico en Algas y otros Recursos Biológicos (CIDTA), Facultad de Ciencias del Mar, Universidad Católica del Norte, Coquimbo, Coquimbo, Chile

⁷Instituto Milenio en Socio-Ecología Costera (SECOS), Santiago, Chile

ABSTRACT

Mesophotic and deeper habitats (~40 to 350 m in depth) around Rapa Nui (Easter Island) were investigated using a remotely operated vehicle. We observed extensive fields of filamentous cyanobacteria-like mats covering sandy substrates and mostly dead mesophotic *Leptoseris* spp. reefs. These mats covered up to 100% of the seafloor off Hanga Roa, the main village on the island, located on its western side. The highest mortality of corals was observed at depths between 70 and 95 m in this area. Healthy *Leptoseris* reefs were documented off the northern and southeastern sides of the island, which are also the least populated. A preliminary morphologic analysis of samples of the mats indicated that the assemblage is composed of at least four filamentous taxa, including two cyanobacteria (cf. *Lyngbya* sp. and *Pseudoanabaena* sp.), a brown alga (*Ectocarpus* sp.), and a green alga (*Cladophora* sp.). An ongoing eutrophication process is suggested as a potential driver of the proliferation of these filamentous mats off Hanga Roa village.

Submitted 1 April 2021
Accepted 3 August 2021
Published 24 August 2021

Corresponding author
Javier Sellanes, sellanes@ucn.cl

Academic editor
Xavier Pochon

Additional Information and
Declarations can be found on
page 11

DOI 10.7717/peerj.12052

© Copyright
2021 Sellanes et al.

Distributed under
Creative Commons CC-BY 4.0

OPEN ACCESS

Subjects Ecology, Marine Biology, Natural Resource Management, Environmental Contamination and Remediation, Environmental Impacts

Keywords Cyanophyceae, Lepstoseris, Mesophotic reefs, Marine conservation, Easter Island, Polynesia

INTRODUCTION

Mesophotic coral ecosystems are deep reef communities that typically occur at a depth range of 30 or 40 to over 150 m (*Baker et al., 2016*). They are formed mainly by coral taxa adapted to living in low-light conditions and often also include other structure-forming taxa, such as sponge and macroalgae species (*Baker et al., 2016; Slattery & Lesser, 2021*). These ecosystems are now recognized as ecologically distinct and independent from their shallower counterparts and contain a substantial diversity of unique biota that is still

unexplored in most parts of the world (Rocha *et al.*, 2018). The lack of knowledge about these deep coral ecosystems is a consequence of the difficulty of accessing the depths at which they occur, as technical diving (e.g., rebreather diving using trimix) or sophisticated submarine equipment (e.g., remotely operated vehicles, autonomous drop-cams, or manned submersibles) are required to carry out research. Mesophotic coral ecosystems are vulnerable to a series of anthropogenic stressors, such as fishing, thermal stress, diseases, pollution, invasive species, the marine aquarium trade, oil and gas exploration, cables, and pipelines (Andradi-Brown *et al.*, 2016).

Rapa Nui (Easter Island; 27°07'S, 109°22'W), which formed ~0.8 Mya, is a remote island located at the westernmost end of the large chain of seamounts comprising the Salas y Gómez ridge, relatively close to the East Pacific Rise (Rodrigo, Díaz & González-Fernández, 2014). Located in the easternmost apex of the Polynesian triangle, it is recognized for the high overall endemism levels of its coastal marine fishes (~22%; Randall & Cea, 2010) and invertebrate taxa (4% to 34%; see Fernandez *et al.*, 2014). However, this unique marine biodiversity is severely threatened by several anthropogenic impacts, including overfishing (Zylich *et al.*, 2014), plastic pollution (Hidalgo-Ruz *et al.*, 2021), exacerbated tourism (Figueroa & Rotarou, 2016), coastal erosion and terrestrial runoff (Mieth & Bork, 2005), and potential pollution from the percolation of domestic sewage and landfill contaminants into aquifers (Rosa, 2013).

Recently (2015–2018), through the use of a remotely operated vehicle (ROV), we have been able to access unexplored marine habitats (from ~40 to 350 m deep) around the island, as well as at nearby seamounts, allowing for a first assessment of the biodiversity of mesophotic ecosystems and deeper sites (Easton *et al.*, 2019), generation of new records of fauna, including fishes (e.g., Easton *et al.*, 2017) and echinoderms (Mecho *et al.*, 2019), and reports of vast fields of the solitary mesophotic mushroom coral *Cycloseris vaughani* (Hoeksema, Sellanes & Easton, 2019). In these surveys, a chance discovery was the presence of dense and extensive fields of filamentous mats, covering the seafloor and nearby reefs at mesophotic depths at several locations around the island. It is known that cyanobacteria are a common constituent of coral reef ecosystems (Stal, 2000) and play an important role in nitrogen fixation and primary production (Charpy *et al.*, 2012). However, under certain conditions, they can undergo massive proliferation, affecting the health of the ecosystem (Bakker *et al.*, 2017; Ford *et al.*, 2017). These events have been associated with variation in irradiance, nutrient supply, and other natural and anthropogenic disturbances (Ford *et al.*, 2018). These proliferation events seem to be increasing at a global scale because of alterations in local biogeochemical cycles related to climate change (Paul, 2008; Paerl & Paul, 2012). These filamentous mats could develop into such dense blooms that they could even wash ashore, producing a mass accumulation, as reported by Nagle & Paul (1999) for Guam. At this location, benthic marine cyanobacterial blooms often occur in the presence of diverse assemblages of herbivorous fishes and urchins, but the underlying factors causing these proliferations, as well as the interaction mechanisms between grazers and these mats (since cyanobacteria are known to produce feeding-deterrent compounds), are still poorly understood (Cissell, Manning & McCoy, 2019; Ford *et al.*, 2021). In addition, cyanobacteria have been directly linked with ciguatera fish poisoning outbreaks (Laurent *et al.*, 2008),

and mats can create suitable habitats for other toxic microalgae, including toxin-producing dinoflagellates, thus generating co-occurring blooms (Paerl & Otten, 2013). Although several microalgae species are not toxic, their growth could produce low oxygen conditions as a consequence of organic matter accumulation and associated degradation processes in the bottom water, thus affecting the benthic communities (Albert et al., 2012). It is also possible that the rise of fixed nitrogen may modify its budget in the system, promoting the growth of macroalgae, further increasing the organic matter content within the sediments, and decreasing porewater oxygen content (Brocke et al., 2015; Brocke et al., 2018). In some environments, mats form associations with sulfate-reducing bacteria, producing sulfide, which is toxic for corals and establishes black band disease (Myers & Richardson, 2009; Charpy et al., 2012).

It has also been reported that in littoral reefs, green algae (chlorophytes) are common indicators of eutrophication (Barile, 2004). Most of the species in this group proliferate due to increased nutrient inputs, tolerate a wide range of environmental conditions, aggressively compete against sensitive corals, and have sub-lethal effects on several of the biological functions of corals (Koop et al., 2001; Fabricius, 2005; Birrel et al., 2008).

In this context, the aims of the present study were: (1) to provide a first approach to the spatial coverage of filamentous mats in the benthic ecosystem around Rapa Nui, (2) to evaluate the extent of the mesophotic coral reefs potentially impacted by these mats, and (3) to provide a preliminary description of the taxonomic composition of these mats.

MATERIALS AND METHODS

Rapa Nui is a triangular-shaped island, delimited by the volcanoes Rano Kau in the southwest, Terevaka in the north, and Poike in the east, with Hanga Roa, the main village, located on the western side (Fig. 1). Aiming to have a representative spatial and bathymetric (~40 to 350 m deep) characterization of the mesophotic habitats on the three sides of the island, a remotely operated vehicle (ROV), controlled from local fishing boats, was deployed in 56 mostly independent sites around the island. There were 18 deployments each in January 2018 and 2019, and 20 during November and December 2019 (Fig. 1). The ROV, model Commander MKII (Mariscope Meerestechnik, Kiel, Germany), was equipped with two laser pointers, 10 cm apart, and a front-pointing HD video camera (Panasonic SD 909), angled at 45° and recording at 30 fps with a resolution of 1920 × 1080 pixels. The videos were analyzed at half their normal speed using GOM Player 2.3.19 (GOM & Company; <https://www.gomlab.com/>).

As mentioned in the Introduction, some of the results of these and previous ROV surveys have been presented elsewhere (Easton et al., 2017; Easton et al., 2019; Hoeksema, Sellanes & Easton, 2019; Mecho et al., 2019), for selected biotic components. For the present study, however, the focus was to evaluate the spatial coverage of filamentous mats in the benthic ecosystem, and the extent of mesophotic reefs potentially impacted by these mats, as well as their overall health conditions. The presence and coverage of filamentous mats were assessed semi-quantitatively by observing the seafloor in a stepwise manner as the ROV advanced over the ground along transects. Bottom-time varied between 10 and 42 min

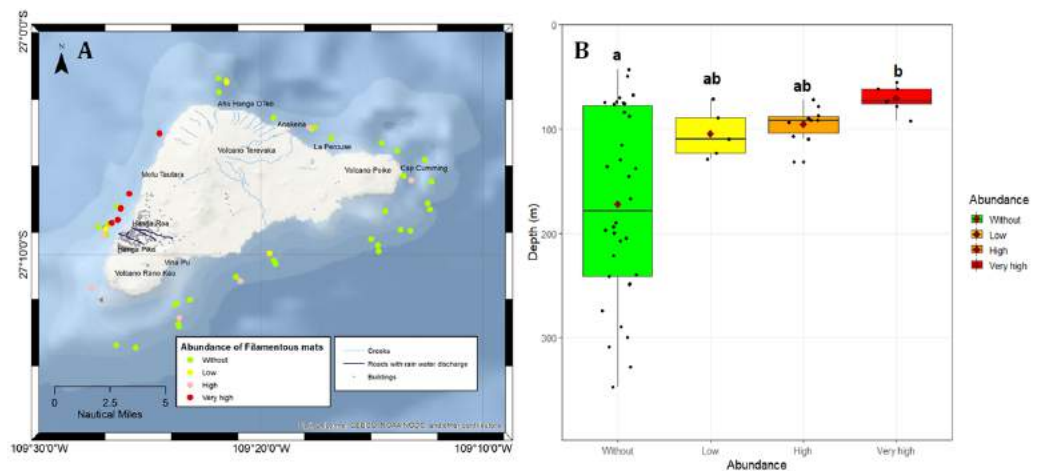


Figure 1 Map of Rapa Nui showing the main features of the island, the sites surveyed in the present study, and the extent of coverage of filamentous mats at these sites. (A) Abundance of filamentous mats in the benthic ecosystems at the survey sites. (B) Depth range of the remotely operated vehicle stations for each category of filamentous mat coverage used in this study. Green: no mats observed, yellow: low coverage, orange: high coverage, and red: very high coverage. The box plots show the mean (red diamonds), median (horizontal black line), and lower and upper quartiles; the whiskers indicate the depth range for each category. The letters (a, b) indicate homogenous groups identified using the Wilcoxon *post hoc* test.

Full-size [DOI: 10.7717/peerj.12052/fig-1](https://doi.org/10.7717/peerj.12052/fig-1)

(mean: 25 min) per transect. In general, a portion of 10 to 20 min of video, considering mainly those segments in which the ROV was displaced at a steady velocity and a suitable distance from the bottom, was selected and analyzed per site. For each transect, we analyzed an area of at least 10 m^2 , corresponding to ~ 15 non-overlapping frames. We exclusively analyzed those frames when the ROV was approximately 25 cm above the ground or in front of the reefs. As calibrated with the ROV on land, at these distances the images covered an area of $\sim 0.65 \text{ m}^2$ (width $\sim 117 \text{ cm} \times$ height $\sim 65 \text{ cm}$).

According to the extent to which the bottom or the coral was covered by filamentous mats, the transects were cataloged into four groups: (1) without patches of filamentous mats, (2) low coverage (less than 50% coverage in at least five non-overlapping frames of the video of a transect), (3) high coverage (50% to 75% coverage in at least five frames of the video of a transect), and (4) very high coverage (100% coverage). Statistical comparisons of the mean depth between the four categories of filamentous mat coverage were evaluated using the Kruskal-Wallis test. *Post hoc* analyses were performed using pairwise comparisons with the Wilcoxon rank sum test and the *p*-value was adjusted using the Holm method (Holm, 1979). Before comparisons, normality and homogeneity of variance were tested using the Shapiro–Wilk and Levene tests, respectively. Statistical analyses were performed using RStudio (R Studio Team, 2020), specifically the “car” package (Fox & Weisberg, 2019) and the “ggplot2” package for boxplots (Wickham, 2016).

We used the same ROV survey approximation to assess the extent of live coral coverage as a proxy for coral health status. Three categories were considered: (1) a healthy reef with $>75\%$ of the corals alive, (2) some damage with 25% to 75% of the corals alive, and (3) mostly damaged with $<25\%$ of the corals alive (mainly dead corals or fragments). Dead

corals were easily identified by their generally greenish or darker colors. Some were also covered by filaments.

To characterize the taxonomic composition of the filamentous mat assemblage, in May 2019, a small benthic trawl with a horizontal aperture of 30 cm was deployed at a site off Hanga Roa, where patches with 100% coverage were frequent. Mat samples were fixed using a 4% aqueous solution of formaldehyde (ACS Reagent; Sigma-Aldrich, St. Louis, MO, USA). For morphological characterization, filaments were observed using an Olympus IX71 inverted microscope equipped with phase contrast and epifluorescence (Olympus Co., Tokyo, Japan). Micrographs were taken using a camera ProgRes C3 (JENOPTIK AG, Jena, Germany), and measurements of cells (length and width) were carried out using ProgRes® CapturePro (JENOPTIK AG) analytical software. Monographic publications, floristic studies, and systematic articles were used for taxonomic identification of the macroalgae composing the mats, at least to the genus level (*Santelices, 1989; Loiseaux-de Goër & Noailles, 2008; Cormaci, Furnari & Alongi, 2014; Ramirez et al., 2018*). Guides and systematic articles were used to identify the cyanobacteria inhabiting the mat samples (*Komarek & Anagnostidis, 2007; Yu et al., 2015; Brocke et al., 2018; Zubia et al., 2019*). The identification of taxa was performed at the genus or species complex level.

Sample collection was performed with permission Res. Ext No. 41/2016 and No. 3314/2017 from SUBPESCA (National Fishing Authority of Chile) granted to the Universidad Católica del Norte. This project was also presented to the local *Consejo del Mar de Rapa Nui* (Council of the Sea of Rapa Nui), which permitted the capture of underwater footage and sampling around the island.

RESULTS

The ROV transects around the island covered a depth range of 43 to 347 m. This allowed us to visualize the spatial and bathymetric distribution of sites with different levels of filamentous mat coverage (Figs. 1 and 2), and the distribution of mesophotic reefs and their health status around the island (Fig. 3). Mesophotic corals were represented by reef-forming *Porites lobata* and *Pocillopora* spp. at shallower depths (<60 m), *Leptoseris* spp., and *C. vaughani* at depths between 70 and 117 m, and sea-whips (*Stichopathes* spp.) between 127 and 327 m (Fig. 2). Other scleractinians were occasionally sighted deeper than 120 m (e.g., cup corals), but they were too small to identify using ROV images.

Spatial distribution of filamentous mats and corals

Filamentous mats were absent (category: without) from 34 of the studied sites around Rapa Nui, and low to very high coverage was observed at the remaining 22 sites, commonly on the western side of the island (Fig. 1A) and in water shallower than ~130 m (Fig. 1B). Statistical comparisons confirmed the significant differences between the depths of the mat-coverage categories (Kruskal-Wallis, $\chi^2 = 12.9$, $df = 3$, $p = 0.005$), in particular between the categories without and very high (Wilcoxon test, $p = 0.023$; Fig. 1B). Other comparisons between categories were not significant (Wilcoxon test, $p > 0.05$). Indeed, high coverage was observed in the northwest corner (close to Hanga O'teo) at a depth of

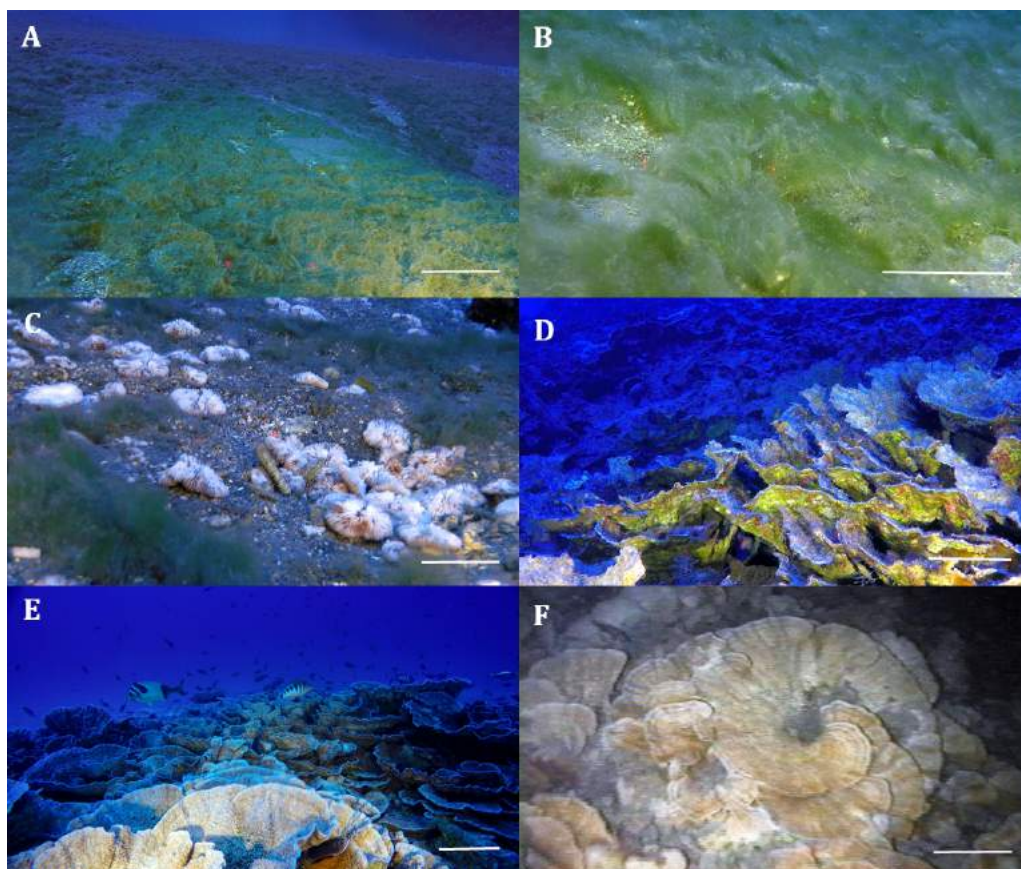


Figure 2 Remotely operated vehicle (ROV) images of the filamentous mats and mesophotic reefs off Rapa Nui. (A) Field of filamentous mats at ~80 m deep off Hanga Roa, Rapa Nui. (B) Close up view of the filaments. (C) Filaments among *Cycloseris vaughani* individuals. (D) Dead *Leptoseris* reef ~80 m deep overgrown by filaments. (E) Healthy *Leptoseris* reef off Anakena 80 m deep. (F) Healthy *Leptoseris* reef off Hanga Roa filmed during prospective ROV surveys during the “CIMAR-5 Islas” cruise conducted in 1999. Scale bars: 10 cm (A, B, C) and 25 cm (D, E, F). Images: Matthias Gorny, OCEANA.

Full-size  DOI: [10.7717/peerj.12052/fig-2](https://doi.org/10.7717/peerj.12052/fig-2)

123 m, and high and very high coverages were observed mainly off Hanga Roa (Fig. 1B) from 70 to 95 m deep.

Corals were observed in 50% of the 56 transects (Fig. 3A), and *Leptoseris* was present in 11 of them. Off Hanga Roa, the location where filamentous mats were most frequent, they were observed covering the sediments (Figs. 2A, 2B), fringing fields of the zooxanthellate mushroom coral *C. vaughani* (Figs. 2C, 3A; see also Hoeksema, Sellanes & Easton, 2019), and close by dead *Leptoseris* reefs (~80 m deep), which were also overgrown by filamentous mats (Fig. 2D). Healthy *Leptoseris* reefs were documented mainly off the northern and southeastern parts of the island (e.g., near Anakena, La Perouse, and Vinapú) at depths of 68 to 82 m (Fig. 3B). Of the six locations with the healthiest *Leptoseris* reefs, four of them had no filamentous mats, or a sporadic presence of them, whereas at the three sites where the reefs were completely dead, filamentous mat coverage was high or very high (see also Supplemental Information).

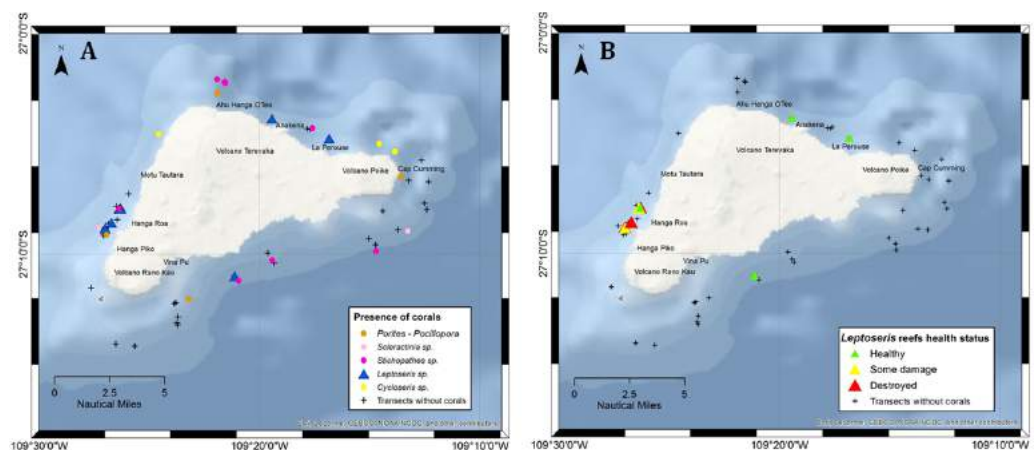


Figure 3 Transects surveyed off Rapa Nui in the present study showing sites with mesophotic corals. (A) Map showing the main mesophotic coral taxa at each site. (B) Health status of *Leptoseris* reefs indicated by color: green = healthy (no noticeable impact), yellow = some damage (25%–75% of corals damaged), and red = destroyed (only dead corals or fragments observed).

Full-size [DOI: 10.7717/peerj.12052/fig-3](https://doi.org/10.7717/peerj.12052/fig-3)

Taxonomic characterization of the filamentous mat assemblage

Morphological analyses of samples of mats collected off Hanga Roa indicated that mats are an assemblage of at least four taxa: one Chlorophyta (*Cladophora* sp.), one Ochrophyta (*Ectocarpus* sp.), and two Cyanobacteria (*Lyngbya* s.l. ([sensu lato] and *Pseudoanabaena* sp.) (Fig. 4) as follows:

Cladophora sp. (Figs. 4A, 4B): thallus of green to light green branched uniseriate filaments with 2–3 cm in total length. Basal part of the filaments fixed to the substrate by a primary rhizoid. Presence of unilateral branches inserted laterally or obliquely on the filament. Principal axis constituted by cylindrical cells measuring of $998.9 \pm 69.2 \mu\text{m}$ in length and $223.3 \pm 9.5 \mu\text{m}$ in diameter. Apical cells cylindrical, round ended with a diameter of $250.0 \pm 7.6 \mu\text{m}$ and length of $701.8 \pm 76.0 \mu\text{m}$. Zoosporangia were not observed.

Ectocarpus sp. (Figs. 4C, 4D): thallus of light brown to olive sparingly branched filament 0.1–0.5 cm in total length. Cells conform to uniseriate filaments ending in a rounded apical cell. Cells barrel-shaped, $50.0 \pm 7.3 \mu\text{m}$ in length, and $14.1 \pm 3.4 \mu\text{m}$ in diameter. Plurilocular sporangia were present, elongated with cylindroconical form, 80–130 μm in length and 20–30 μm in diameter.

Lyngbya s.l. (Figs. 4E, 4F): thallus caespitose, brownish-red, filaments slightly curved, sheet colorless, lamellated with apices not attenuated at the end. Trichome not constricted at the cross-wall, cylindrical cells very short $3.5 \pm 0.3 \mu\text{m}$ in length and $7.1 \pm 0.1 \mu\text{m}$ in diameter, sheath $1.6 \pm 0.3 \mu\text{m}$, end cells rotund, calyptra absent.

Pseudoanabaena sp. (Figs. 4G, 4H): trichomes solitary or crowded in clusters, straight or almost straight, pale blue–green. Cells barrel-shaped, $2.8 \pm 0.8 \mu\text{m}$ in length and $1.2 \pm 0.1 \mu\text{m}$ in diameter, intensely constricted at cross walls, no heterocysts or sheath, end cells round.

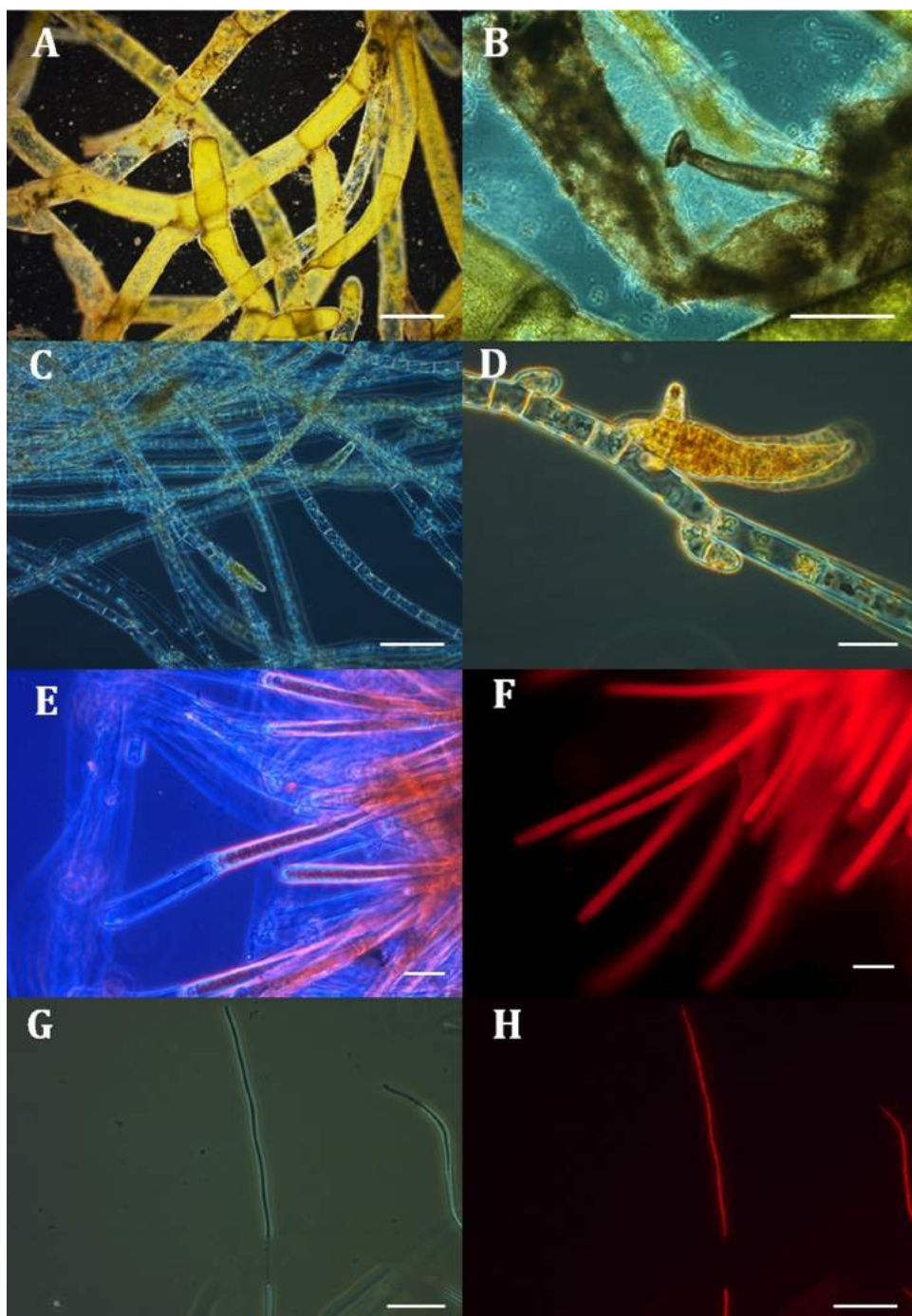


Figure 4 Micrographs of four filamentous taxa in samples from mats collected off Hanga Roa, Rapa Nui at mesophotic depths. A–E and G were photographed using phase-contrast and F and H using epifluorescence techniques. (A, B) *Cladophora* sp. (C, D) *Ectocarpus* sp. (E, F) *Lyngbya* s.l. (G, H) *Pseudoanabaena* sp. Scale bars represent (A): 500 μ m, (B): 200 μ m, (C): 100 μ m, (D): 30 μ m, (E and F): 20 μ m, and (G) and H: 30 μ m.

Full-size  DOI: 10.7717/peerj.12052/fig-4

DISCUSSION

Although we have provided only a preliminary taxonomic characterization of the filamentous mats covering sandy areas and dead mesophotic reefs off Rapa Nui, our findings indicate that these mats are composed of at least two cyanobacteria. We are aware of, and recognize the limitations associated with our approach to identifying mat taxa, based only on morphology. As indicated by *Komárek (2016)*, *Lyngbya*, *Okeania*, and *Moorea* cannot be distinguished from each other using light microscopy. Thus, we refer to *Lyngbya* s.l. ([sensu lato]) and suggest that genetic analysis is needed to clarify this classification. Cyanobacteria-dominated microbial mats are known to be typical components of coral reef systems and often undergo massive proliferation (*Stal, 2000*). These events have been associated with natural processes (e.g., variation in irradiance), but mostly with anthropogenic disturbances that increase nutrient concentrations in the marine environment (*Ford et al., 2017*). The highest coverage of mats was observed mainly off Hanga Roa village, which has the highest concentration of the island's human population (7,750 inhabitants; <http://www.ine.cl>) and where most tourists engage in recreational activities. *Figueroa & Rotarou (2016)* reported ~20,000 visitors per year in the late 1990s, whereas ~150,000 were reported during 2019 (<http://www.sernatur.cl>), representing an approximately eight-fold increase over the last two decades. Factors such as overtourism, the absence of a wastewater collection and treatment system (most of the residences have cesspools and a minor proportion have septic tanks), and the unlined landfill (*Rosa, 2013*) potentially pose a great threat to the marine environment off Hanga Roa village, owing to the potential input of organic matter, nutrients, and contaminants. Pollutants can reach the sea by runoff or percolation to aquifers that eventually discharge into the sea. On Rapa Nui, submarine groundwater discharges are ubiquitous in intertidal environments around the island (*Brosnan, Becker & Lipo, 2018*), and could hypothetically also seep through deeper sediments (*Montgomery EL & Associates INC, 2011*), potentially conducting nutrients of anthropogenic origin directly to mesophotic habitats. Indeed, very low salinities (4.7–16.8 psu) have been measured in the overlying water of unperturbed sediment cores obtained off Hanga Roa where filamentous mats proliferate, further suggesting percolation of pollutants to aquifers in the area (P. Muñoz, unpublished data). A similar situation has been observed at the western flank of Hawai'i Island, where freshwater from onshore aquifers can flow through permeable fractured basalts, mix with seawater to form freshened groundwater, and seep into offshore (mesophotic) benthic areas (*Attias et al., 2020*). Furthermore, the observation of low salinity bottom water is concomitant with relatively high NO_3^- concentrations (1.87 and 3.03 μM), compared to two other sites where nitrate concentrations were undetectable in overlying waters with normal salinities (~35 psu) (P. Muñoz, unpublished data). Therefore, it is feasible that the benthic fluxes and submarine groundwater discharges could channel nutrients to mesophotic depths, enhancing algal and cyanobacterial growth, to the detriment of corals. A similar situation, albeit caused by groundwater nutrients derived from bird guano, was observed in the coral reefs of Heron Island (Great Barrier Reef, Australia; *McMahon & Santos, 2017*). In addition to the potential impacts of pollutants, the permanent coastal erosion around Rapa Nui and

terrestrial runoff during rainy seasons (May to October) could also increase nutrient inputs to the coastal environments, including ammonia, nitrate, and silicate, which are known to have negative consequences for corals (D'Angelo & Wiedenman, 2014). Furthermore, the volcanic origin of Rapa Nui, together with enhanced erosion could also increase the iron concentration in the marine ecosystem. Iron from shipwrecks has been found to directly drive cyanobacteria expansion in iron-limited reefs in the Pacific (Kelly et al., 2012; Mangubhai & Obura, 2018). Increased iron added to a decrease in the N:P ratio could even further stimulate the proliferation of cyanobacteria (Ford et al., 2018).

Regarding mesophotic reefs, two species of the genus *Leptoseris* have been reported for Rapa Nui, *L. scabra* and *L. solida*, both collected in 1999 off Hanga Roa at depths of 43 m and 80 to 100 m, respectively (Glynn et al., 2007). Given the depth of our observations as well as the plate-like structure of the colonies, as indicated by Glynn et al. (2007), the damaged reef off Hanga Roa village was probably composed mainly of *L. solida*. A piece of evidence, also obtained in November 1999 during the first ROV survey ever done off Hanga Roa at ~80 m deep, suggests that the same *Leptoseris* reef that is currently dead was healthy ~20 years ago (Fig. 2D; Gorny & Retamal, 2000). In the present study, live *Leptoseris* reefs were documented mainly off the northern and southeastern sides of the island (e.g., Anakena, La Perouse, and Vinapú).

Despite the circumstantial indication of the health status of the mesophotic reefs off Hanga Roa a few decades ago, the ecological impacts on the biodiversity and ecosystem functioning associated with anthropogenic causes are still unknown and need further investigation in the short term. Further research should address a more detailed taxonomic characterization of these mats, for example, through molecular techniques; assessment of the seasonal, spatial, and structural patterns of the assemblage; their eventual role in reef deterioration; recognition of eutrophication mechanisms; and long-term monitoring of dissolved organic matter and nutrient dynamics. These studies are encouraged to inform the implementation of effective and integrated land-sea management actions, including a wastewater treatment system. This information should also be key to inform the implementation of management strategies of the recently created Marine Protected Area of Multiple Uses (MPA-MU) of Rapa Nui, currently the largest in Latin America. This protected area encompasses ~579,000 km² (Paredes et al., 2019) and aims to protect this unique world biodiversity heritage site. In addition, this study will also serve as a baseline for future studies of changes in the mesophotic ecosystem off Rapa Nui after closure of the island to tourism, from March 2020 to date, due to the COVID-19 pandemic.

CONCLUSIONS

Based on opportunistic video observations, we provide the first report of filamentous mats covering sandy areas and dead mesophotic reefs (*Leptoseris* spp.) off Rapa Nui. A preliminary morphological analysis of mat samples suggested that the assemblage is constituted by at least four filamentous taxa, including two cyanobacteria (*Lyngbya* s.l. and *Pseudoanabaena* sp.), a brown alga (*Ectocarpus* sp.), and a green alga (*Cladophora* sp.). Whereas a highly damaged, even completely dead, *Leptoseris* reef was observed in

the waters off the main village on the western side of the island, reefs in much healthier conditions were observed off the less populated northern and southeastern parts of the island (e.g., Anakena, La Perouse, and Vinapú). Circumstantial evidence indicates that the *Leptoseris* reef off Hanga Roa was alive ~20 years ago. Our preliminary evidence suggests a link between ongoing eutrophication associated with human population expansion and deficient management of wastewater and urban runoff on the western side of the island, the proliferation of filamentous mats, and consequent damage to mesophotic *Leptoseris* reefs.

ACKNOWLEDGEMENTS

We thank Poky Tane Haoa, Ricardo Hito, and Enrique Hey from the Rapa Nui community. We also thank Erin Easton and Ariadna Mecho for their collaboration during fieldwork, and Maria Valladares and Valentina Hevia for helping with the collection of the samples. Our thanks go to Bert Hoeksema for his valuable comments on a very early version of this manuscript, as well as to Amanda Ford, Marc Slattery, and an anonymous reviewer.

ADDITIONAL INFORMATION AND DECLARATIONS

Funding

This work was supported by grants FONDECYT 1180694 and 1181153, as well as funding from the ANID- Millennium Science Initiative ESMOI. Germán Zapata-Hernández was funded by CONICYT-PCHA/ Doctorado Nacional/2015-21151249 and Beca de Postdoctorado MINEDUC UCN-19101 N° 002. Oceana Chile contributed to the funding of the expeditions and provided the ROV. The funders had no role in study design, data collection and analysis, decision to publish, or preparation of the manuscript.

Grant Disclosures

The following grant information was disclosed by the authors:

FONDECYT: 1180694, 1181153.

ANID- Millennium Science Initiative ESMOI.

CONICYT-PCHA/ Doctorado Nacional: 2015-21151249.

Beca de Postdoctorado MINEDUC: UCN-19101 No 002.

Oceana Chile.

Competing Interests

The authors declare there are no competing interests.

Author Contributions

- Javier Sellanes and Matthias Gorny conceived and designed the experiments, performed the experiments, analyzed the data, prepared figures and/or tables, authored or reviewed drafts of the paper, and approved the final draft.
- Germán Zapata-Hernández and Gonzalo Alvarez performed the experiments, analyzed the data, prepared figures and/or tables, authored or reviewed drafts of the paper, and approved the final draft.

- Praxedes Muñoz conceived and designed the experiments, performed the experiments, analyzed the data, authored or reviewed drafts of the paper, and approved the final draft.
- Fadia Tala performed the experiments, analyzed the data, authored or reviewed drafts of the paper, and approved the final draft.

Field Study Permissions

The following information was supplied relating to field study approvals (i.e., approving body and any reference numbers):

Sample collection was performed with permission Res. Ext N° 41/2016 and N° 3314/2017 from SUBPESCA (National Fishing Authority of Chile) granted to the Universidad Católica del Norte. This project was also presented to the local Consejo del Mar de Rapa Nui (Council of the Sea of Rapa Nui), which permitted the capture of underwater footage and sampling around the island.

Data Availability

The following information was supplied regarding data availability:

The raw data are available in the [Supplementary File](#).

Supplemental Information

Supplemental information for this article can be found online at <http://dx.doi.org/10.7717/peerj.12052#supplemental-information>.

REFERENCES

- Albert S, Dunbabin M, Skinner M, Moore B. 2012.** Benthic shift in a Solomon Islands' lagoon: corals to cyanobacteria. In: *Proceedings of the 12th international coral reef symposium, Cairns, Australia*.
- Andradi-Brown D, Laverick J, Bejarano I, Bridge T, Colin PL, Eyal G, Jones R, Kahng SE, Reed J, Smith TB, Spalding H, Well E, Wood E. 2016.** Threats to mesophotic coral ecosystems and management options. In: Baker EK, Puglise KA, Harris PT, eds. *Mesophotic coral ecosystems—a lifeboat for coral reefs?* Nairobi and Arendal: The United Nations Environment Programme and GRID-Arendal, 67–82. Available at https://coastalscience.noaa.gov/data_reports/threats-to-mesophotic-coral-ecosystems-and-management-options/.
- Attias E, Thomas D, Sherman D, Ismail K, Constable S. 2020.** Marine electrical imaging reveals novel freshwater transport mechanism in Hawai'i. *Science Advances* 6(48):eabd4866 DOI 10.1126/sciadv.abd4866.
- Baker E, Puglise KA, Colin PL, Harris PT, Kahng SE, Rooney JJ, Sherman C, Slattery M, Spalding HL. 2016.** What are mesophotic coral ecosystems? In: Baker EK, Puglise KA, Harris PT, eds. *Mesophotic coral ecosystems—A lifeboat for coral reefs?* Nairobi and Arendal: The United Nations Environment Programme and GRID-Arendal, pp. 98.
- Bakker D, Van Duyl F, Bak R, Nugues MM, Nieuwland G, Meesters E. 2017.** 40 Years of benthic community change on the Caribbean reefs of Curacao

- and Bonaire: the rise of slimy cyanobacterial mats. *Coral Reefs* **36**:355–367
[DOI 10.1007/s00338-016-1534-9](https://doi.org/10.1007/s00338-016-1534-9).
- Barile PJ. 2004.** Evidence of anthropogenic nitrogen enrichment of the littoral waters of East Central Florida. *Journal of Coastal Research* **20**:137–1245.
- Birrel C, McCook L, Willis B, Diaz-Pulido G. 2008.** Effects of benthic algae on the replenishment of corals and the implications for the resilience of coral reefs. *Oceanography and Marine Biology: An Annual Review* **46**:25–63.
- Brocke HJ, Piltz B, Herz N, Abed RMM, Palinska KA, John U, Haan JD, De Beer D, Nugues MM. 2018.** Nitrogen fixation and diversity of benthic cyanobacterial mats on coral reefs in Curaçao. *Coral Reefs* **37**(3):861–874 [DOI 10.1007/s00338-018-1713-y](https://doi.org/10.1007/s00338-018-1713-y).
- Brocke HJ, Polerecky L, De Beer D, Weber M, Claudet J, Nugues MM. 2015.** Organic matter degradation drives benthic cyanobacterial mat abundance on Caribbean Coral Reefs. *PLOS ONE* **10**(5):e0125445 [DOI 10.1371/journal.pone.0125445](https://doi.org/10.1371/journal.pone.0125445).
- Brosnan T, Becker MW, Lipo CP. 2018.** Coastal groundwater discharge and the ancient inhabitants of Rapa Nui (Easter Island), Chile. *Hydrogeology Journal* **27**:519–534
[DOI 10.1007/s10040-018-1870-7](https://doi.org/10.1007/s10040-018-1870-7).
- Charpy I, Casareto BE, Langlade MJ, Suzuki Y. 2012.** Cyanobacteria in coral reef ecosystems: a review. *Journal of Marine Sciences* **2012**:259571 [DOI 10.1155/2012/259571](https://doi.org/10.1155/2012/259571).
- Cissell EC, Manning JC, McCoy SJ. 2019.** Consumption of benthic cyanobacterial mats on a Caribbean coral reef. *Scientific Reports* **9**:12693 [DOI 10.1038/s41598-019-49126-9](https://doi.org/10.1038/s41598-019-49126-9).
- Cormaci M, Furnari G, Alongi G. 2014.** Flora marina bentónica del Mediterráneo: Chlorophyta. *Bollettino Delle Sedute Della Accademia Gioenia di Scienze Naturali in Catania* **47**:11–436.
- D'Angelo C, Wiedenman J. 2014.** Impacts of nutrient enrichment on coral reefs: new perspectives and implications for coastal management and reef survival. *Current Opinion in Environmental Sustainability* **7**:82–93 [DOI 10.1016/j.cosust.2013.11.029](https://doi.org/10.1016/j.cosust.2013.11.029).
- Easton EE, Gorny M, Mecho A, Sellanes J, Gaymer CF, Slapding HL, Aburto J. 2019.** Chile and the Salas y Gómez Ridge. In: Loya Y, Puglise KA, Bridge TCL, eds. *Mesophotic coral ecosystems*. Cham: Springer International Publishing, 477–490
[DOI 10.1007/978-3-319-92735-0](https://doi.org/10.1007/978-3-319-92735-0).
- Easton EE, Sellanes J, Gaymer CF, Morales N, Gorny M, Berkenpass E. 2017.** Diversity of deep-sea fishes of the Easter Island Ecoregion. *Deep-Sea Research Part II* **137**:78–88 [DOI 10.1016/j.dsr2.2016.12.006](https://doi.org/10.1016/j.dsr2.2016.12.006).
- Fabricius K. 2005.** Effects of terrestrial runoff on the ecology of corals and coral reefs: review and synthesis. *Marine Pollution Bulletin* **50**:125–146
[DOI 10.1016/j.marpolbul.2004.11.028](https://doi.org/10.1016/j.marpolbul.2004.11.028).
- Fernandez M, Pappalardo P, Rodriguez Ruiz MC, Castilla JC. 2014.** Synthesis of the state of knowledge about species richness of macroalgae, macroinvertebrates and fishes in coastal and oceanic waters of Easter and Salas y Gomez islands. *Latin American Journal of Aquatic Research* **42**(4):760–802 [DOI 10.3856/vol42-issue4-fulltext-7](https://doi.org/10.3856/vol42-issue4-fulltext-7).
- Figueroa E, Rotarou ES. 2016.** Sustainable development or eco-collapse: lessons for tourism and development from Easter Island. *Sustainability* **8**:1093
[DOI 10.3390/su8111093](https://doi.org/10.3390/su8111093).

- Ford AK, Bejarano S, Nugues MM, Visser PM, Albert S, Ferse SCA. 2018.** Reefs under siege—the rise, putative drivers, and consequences of benthic cyanobacterial mats. *Frontiers in Marine Science* 5:18 DOI [10.3389/fmars.2018.00018](https://doi.org/10.3389/fmars.2018.00018).
- Ford A, Van Hoytema N, Moore B, Pandiha L, Wild C, Ferse S. 2017.** High sedimentary oxygen consumption indicates that sewage input from small islands drives benthic community shifts on overfished reefs. *Environmental Conservation* 44(4):405–414 DOI [10.1017/S0376892917000054](https://doi.org/10.1017/S0376892917000054).
- Ford AK, Visser PM, Van Herk MJ, Jongepier E, Bonito V. 2021.** First insights into the impacts of benthic cyanobacterial mats on fish herbivory functions on a nearshore coral reef. *Scientific Reports* 11:7147 DOI [10.1038/s41598-021-84016-z](https://doi.org/10.1038/s41598-021-84016-z).
- Fox J, Weisberg S. 2019.** *An R companion to applied regression*. 3rd edition. Thousand Oaks: Sage.
- Glynn PW, Wellington GM, Riegl B, Olson DB, Borneman E, Wieters EA. 2007.** Diversity and biogeography of the scleractinian coral fauna of Easter Island (Rapa Nui). *Pacific Science* 61:67–90 DOI [10.1353/psc.2007.0005](https://doi.org/10.1353/psc.2007.0005).
- Gorny M, Retamal M. 2000.** Estudio sobre la biodiversidad del megabentos De Isla De Pascua y Salas y Gómez mediante video subacuático, Libro De Resúmenes. Taller sobre los resultados del Crucero Cimar-Fiordo 5. Valparaíso. 119–121. Available at www.cona.cl/pub/libros_RS_CIMAR/LRP_cimar5.zip (accessed on 16 August 2021).
- Hidalgo-Ruz V, Luna-Jorquera G, Eriksen M, Frick H, Miranda-Urbina D, Porflitt-Toro M, Rivadeneira M, Robertson CJR, Scofield RP, Serratos J, Suazo CG, Thiel M. 2021.** Factors (type, colour, density, and shape) determining the removal of marine plastic debris by seabirds from the South Pacific Ocean: is there a pattern? *Aquatic Conservation: Marine and Freshwater Ecosystem* 31:389–407 DOI [10.1002/aqc.3453](https://doi.org/10.1002/aqc.3453).
- Hoeksema BW, Sellanes J, Easton EE. 2019.** A high-latitude, mesophotic *Cycloseris* field at 85 m depth off Rapa Nui (Easter Island). *Bulletin of Marine Science* 95(1):101–102 DOI [10.5343/bms.2018.0053](https://doi.org/10.5343/bms.2018.0053).
- Holm S. 1979.** A simple sequentially rejective multiple test procedure. *Scandinavian Journal of Statistics* 6:65–70.
- Kelly LW, Barott KL, Dinsdale E, Friedlander AM, Nosrat B, Obura D, Sala E, Sandin SA, Smith JE, Vermeij MJA, Williams GJ, Willner D, Rohwer F. 2012.** Black reefs: iron-induced phase shifts on coral reefs. *The ISME Journal* 6:638–649 DOI [10.1038/ismej.2011.114](https://doi.org/10.1038/ismej.2011.114).
- Komárek J. 2016.** A polyphasic approach for the taxonomy of cyanobacteria: principles and applications. *European Journal of Phycology* 51:346–353 DOI [10.1080/09670262.2016.1163738](https://doi.org/10.1080/09670262.2016.1163738).
- Komarek J, Anagnostidis K. 2007.** *Süßwasserflora von Mitteleuropa, Bd. 19/2: Cyanoprokaryota. Bd. 2 / Part 2, Oscillatoriales*. Germany: Springer Spektrum.
- Koop K, Booth D, Broadbent A, Drodie J, Bucher D, Capone D, Coll J, Dennison W, Erdmann M, Harrison P, Hoegh-Guldberg O, Hutchings P, Jones GB, Larkum AWD, O’Neil J, Steven A, Tentori E, Ward S, Williamson J, Yellowless D. 2001.** ENCORE: the effect of nutrient enrichment on coral reefs,

- Synthesis of results and conclusions. *Marine Pollution Bulletin* **42**:91–120
DOI [10.1016/S0025-326X\(00\)00181-8](https://doi.org/10.1016/S0025-326X(00)00181-8).
- Laurent D, Kerbrat AS, Darius HT, Girard E, Golubic S, Benoit E, Sauviat MP, Chinain M, Molgo J, Pauillac S. 2008.** Are cyanobacteria involved in Ciguatera Fish Poisoning-like outbreaks in New Caledonia? *Harmful Algae* **7**:827–838
DOI [10.1016/j.hal.2008.04.005](https://doi.org/10.1016/j.hal.2008.04.005).
- Loiseaux-de Goër S, Noailles MC. 2008.** *Algues De Roscoff*. Roscoff: CNRS - Les éditions de la Station Biologique de Roscof, 215.
- Mangubhai S, Obura DO. 2018.** Silent killer: black reefs in the Phoenix Islands protected area. *Pacific Conservation Biology* **25**(2):213–214.
- McMahon A, Santos IR. 2017.** Nitrogen enrichment and speciation in a coral reef lagoon driven by groundwater inputs of bird guano. *Journal of Geophysical Research Oceans* **122**:7218–7236 DOI [10.1002/2017JC012929](https://doi.org/10.1002/2017JC012929).
- Mecho A, Easton EE, Sellanes J, Gorny M, Mah C. 2019.** Unexplored diversity of the mesophotic echinoderm fauna of the Easter Island Ecoregion. *Marine Biology* **166**:91 DOI [10.1007/s00227-019-3537-x](https://doi.org/10.1007/s00227-019-3537-x).
- Mieth A, Bork H-R. 2005.** History, origin and extent of soil erosion on Easter Island (Rapa Nui). *Catena* **63**:244–260 DOI [10.1016/j.catena.2005.06.011](https://doi.org/10.1016/j.catena.2005.06.011).
- Montgomery EL & Associates Inc. 2011.** *Condiciones hidrogeológicas Isla De Pascua, Chile*. Dirección general de aguas, pp 48.
- Myers J, Richardson L. 2009.** Adaptation of cyanobacteria to the sulfide-rich microenvironment of black band disease of coral. *FEMS Microbiology Ecology* **67**:242–251
DOI [10.1111/j.1574-6941.2008.00619.x](https://doi.org/10.1111/j.1574-6941.2008.00619.x).
- Nagle DG, Paul VJ. 1999.** Production of secondary metabolites by filamentous tropical marine cyanobacteria: ecological functions of the compounds. *Journal of Phycology* **35**:1412–1421 DOI [10.1046/j.1529-8817.1999.3561412.x](https://doi.org/10.1046/j.1529-8817.1999.3561412.x).
- Paerl HW, Otten TG. 2013.** Harmful cyanobacterial blooms: causes, consequences and controls. *Microbial Ecology* **65**:995–1010 DOI [10.1007/s00248-012-0159-y](https://doi.org/10.1007/s00248-012-0159-y).
- Paerl H, Paul V. 2012.** Climate change: links to global expansion of harmful cyanobacteria. *Water Research* **46**(5):1349–1363 DOI [10.1016/j.watres.2011.08.002](https://doi.org/10.1016/j.watres.2011.08.002).
- Paredes F, Flores D, Figueroa A, Gaymer C, Aburto J. 2019.** Science, capacity building and conservation knowledge: The empowerment of the local community for marine conservation in Rapa Nui. *Aquatic Conservation: Marine and Freshwater Ecosystem* **13**:130–137 DOI [10.1002/aqc.3114](https://doi.org/10.1002/aqc.3114).
- Paul VJ. 2008.** Global warming and cyanobacterial harmful algal blooms. In: Hudnell HK, ed. *Advances in experimental medicine and biology*. 619. New York: Springer.
- Ramirez ME, Bulboa C, Contreras L, Mora AM. 2018.** *Algas marinas De Quintay*. RiL Editores.
- Randall JE, Cea A. 2010.** *Shore fishes of Easter Island*. Hawai'i, USA: University of Hawai'i Press.
- R Studio Team. 2020.** *RStudio: integrated Development for R*. Boston: RStudio, Inc.
Available at <http://www.rstudio.com/>.

- Rocha LA, Pinheiro HT, Shepherd B, Papastamatiou YP, Luiz OJ, Pyle RL, Bongaerts P. 2018.** Mesophotic coral ecosystems are threatened and ecologically distinct from shallow water reefs. *Science* **361**:281–284 DOI [10.1126/science.aaq1614](https://doi.org/10.1126/science.aaq1614).
- Rodrigo C, Díaz J, González-Fernández A. 2014.** Origin of the Easter Submarine Alignment: morphology and structural lineaments. *Latin American Journal of Aquatic Research* **42**(4):857–870 DOI [10.3856/vol42-issue4-fulltext-12](https://doi.org/10.3856/vol42-issue4-fulltext-12).
- Rosa K. 2013.** A hydrologic overview and discussion of sources of groundwater pollution on Rapa Nui. *Rapa Nui Journal* **27**(2):51–59.
- Santelices B. 1989.** *Algas Marinas De Chile*. Santiago: Ediciones Universidad Católica de Chile.
- Slattery M, Lesser MP. 2021.** Gorgonians are foundation species on sponge-dominated Mesophotic Coral Reefs in the Caribbean. *Frontiers in Marine Science* **8**:654268 DOI [10.3389/fmars.2021.654268](https://doi.org/10.3389/fmars.2021.654268).
- Stal LJ. 2000.** Cyanobacterial mats and stromatolites. In: Whitton PA, Potts M, eds. *The ecology of cyanobacteria: their diversity in time and space*. Dordrecht: Kluwe Academic, 61–120.
- Wickham H. 2016.** *ggplot2: elegant graphics for data analysis*. New York: Springer-Verlag.
- Yu G, Zhu M, Chen Y, Pan Q, Chai W, Li R. 2015.** Polyphasic characterization of four species of *Pseudanabaena* (Oscillatoriales, Cyanobacteria) from China and insights into polyphyletic divergence within the *Pseudanabaena* genus. *Phytotaxa* **192**(1):1–12 DOI [10.11646/phytotaxa.192.1.1](https://doi.org/10.11646/phytotaxa.192.1.1).
- Zubia M, Vieira C, Palinska KA, Roué M, Gaertner J-C, Zloch I, Grellier M, Golubic S. 2019.** Benthic cyanobacteria on coral reefs of Moorea Island (French Polynesia): diversity response to habitat quality. *Hydrobiologia* **843**(1):61–78 DOI [10.1007/s10750-019-04029-8](https://doi.org/10.1007/s10750-019-04029-8).
- Zylich K, Harper S, Licandeo R, Vega R, Zeller D, Pauly D. 2014.** Fishing in Easter Island, a recent history (1950–2010). *Latin American Journal of Aquatic Research* **42**(4):845–856 DOI [10.3856/vol42-issue4-fulltext-11](https://doi.org/10.3856/vol42-issue4-fulltext-11).

Dongsha Atoll is an important stepping-stone that promotes regional genetic connectivity in the South China Sea

Shang Yin Vanson Liu^{1,2}, Jacob Green^{3,4}, Dana Briggs³, Ruth Hastings³, Ylva Jondelius³, Skylar Kensinger^{3,5}, Hannah Leever³, Sophia Santos³, Trevor Throne³, Chi Cheng², Hawis Madduppa⁶, Robert J. Toonen⁷, Michelle R. Gaither⁸ and Eric D. Crandall^{3,9}

¹ Dongsha Atoll Research Station, College of Marine Sciences, National Sun Yat-sen University, Kaohsiung City, Taiwan

² Department of Marine Biotechnology and Resources, National Sun Yat-Sen University, Kaohsiung City, Taiwan

³ School of Natural Sciences, California State University, Monterey Bay, California, United States

⁴ Department of Biological and Environmental Science, University of Rhode Island, Kingston, Rhode Island, United States

⁵ Department of Molecular, Cellular and Developmental Biology, University of California, Santa Cruz, Santa Cruz, California, United States

⁶ Department of Marine Science and Technology, Institut Pertanian Bogor, Bogor, Indonesia

⁷ Hawai'i Institute of Marine Biology, University of Hawai'i at Mānoa, Kane'ohe, Hawai'i, United States

⁸ Department of Biology, University of Central Florida, Orlando, Florida, United States

⁹ Department of Biology, Pennsylvania State University, University Park, Pennsylvania, United States

ABSTRACT

Background: Understanding region-wide patterns of larval connectivity and gene flow is crucial for managing and conserving marine biodiversity. Dongsha Atoll National Park (DANP), located in the northern South China Sea (SCS), was established in 2007 to study and conserve this diverse and remote coral atoll. However, the role of Dongsha Atoll in connectivity throughout the SCS is seldom studied. In this study, we aim to evaluate the role of DANP in conserving regional marine biodiversity.

Methods: In total, 206 samples across nine marine species were collected and sequenced from Dongsha Atoll, and these data were combined with available sequence data from each of these nine species archived in the Genomic Observatories Metadatabase (GEOME). Together, these data provide the most extensive population genetic analysis of a single marine protected area. We evaluate metapopulation structure for each species by using a coalescent sampler, selecting among panmixia, stepping-stone, and island models of connectivity in a likelihood-based framework. We then completed a heuristic graph theoretical analysis based on maximum dispersal distance to get a sense of Dongsha's centrality within the SCS.

Results: Our dataset yielded 111 unique haplotypes across all taxa at DANP, 58% of which were not sampled elsewhere. Analysis of metapopulation structure showed that five out of nine species have strong regional connectivity across the SCS such that their gene pools are effectively panmictic (mean pelagic larval duration (PLD) = 78 days, sd = 60 days); while four species have stepping-stone metapopulation structure, indicating that larvae are exchanged primarily between

Submitted 19 April 2021
Accepted 4 August 2021
Published 31 August 2021

Corresponding authors
Shang Yin Vanson Liu,
syvliu@mail.nsysu.edu.tw
Eric D. Crandall, eric.d.
crandall@gmail.com

Academic editor
Nicholas Jeffery

Additional Information and
Declarations can be found on
page 18

DOI 10.7717/peerj.12063

© Copyright
2021 Liu et al.

Distributed under
Creative Commons CC-BY 4.0

OPEN ACCESS

nearby populations (mean PLD = 37 days, sd = 15 days). For all but one species, Dongsha was ranked within the top 15 out of 115 large reefs in the South China Sea for betweenness centrality. Thus, for most species, Dongsha Atoll provides an essential link for maintaining stepping-stone gene flow across the SCS.

Conclusions: This multispecies study provides the most comprehensive examination of the role of Dongsha Atoll in marine connectivity in the South China Sea to date. Combining new and existing population genetic data for nine coral reef species in the region with a graph theoretical analysis, this study provides evidence that Dongsha Atoll is an important hub for sustaining connectivity for the majority of coral-reef species in the region.

Subjects Biodiversity, Conservation Biology, Evolutionary Studies, Marine Biology, Zoology
Keywords Indo-Pacific, Migration models, Larval dispersal, Marine connectivity, Phylogeography, Marine metapopulations, Stepping-stones

INTRODUCTION

With coral reefs and their communities in accelerating global decline ([Hughes et al., 2003, 2018](#)), governments around the world have established Marine Protected Areas (MPAs) as a way to counteract this trend ([Selig & Bruno, 2010](#)). It is now quite clear that MPAs, especially when planned as part of a network, can increase biodiversity, enhance the biomass of fished species, and promote ecosystem resilience ([Emslie et al., 2015](#); [Mellin et al., 2016](#); [Sala et al., 2021](#)). When properly sized and spaced, a network of MPAs can protect coral reef populations, and an adequate fraction of their larval offspring that disperse to nearby MPAs, ensuring both long-term community persistence and fisheries spillover ([Gaines et al., 2010](#); [Krueck et al., 2017](#)). However, while there are a few robust examples of MPA networks planned at the regional level ([Gleason et al., 2013](#); [Emslie et al., 2015](#)), most MPAs are singletons implemented by regional governments for local benefit only ([Gaines et al., 2010](#)).

Singleton MPAs are still valuable for the conservation and resilience of local coral reef communities and maintaining local fisheries through larval export and adult spillover ([Lester et al., 2009](#); [Mellin et al., 2016](#)). However, it remains crucial to evaluate, post hoc, their role in conserving regional marine biodiversity. Does the MPA serve as a useful intergenerational stepping-stone that can augment demographic and genetic connectivity among regional reefs ([McCook et al., 2009](#))? Coalescent samplers are a family of population genetic models that allow a relatively quick and inexpensive way to make such an evaluation ([Crandall, Treml & Barber, 2012](#); [Selkoe et al., 2016](#); [Crandall et al., 2019b](#)). In a likelihood-based model selection framework, such methods can distinguish between models of effective panmixia (high regional gene flow) and metapopulation models in which larvae disperse only to nearby populations (stepping-stone model) or to all sampled populations (island model; [Beerli & Palczewski, 2010](#)).

Understanding the role of a given MPA in region-wide connectivity patterns requires genetic data from many species from inside the MPA and from the surrounding populations. Fortunately, a working group of the Diversity of the Indo-Pacific Network has

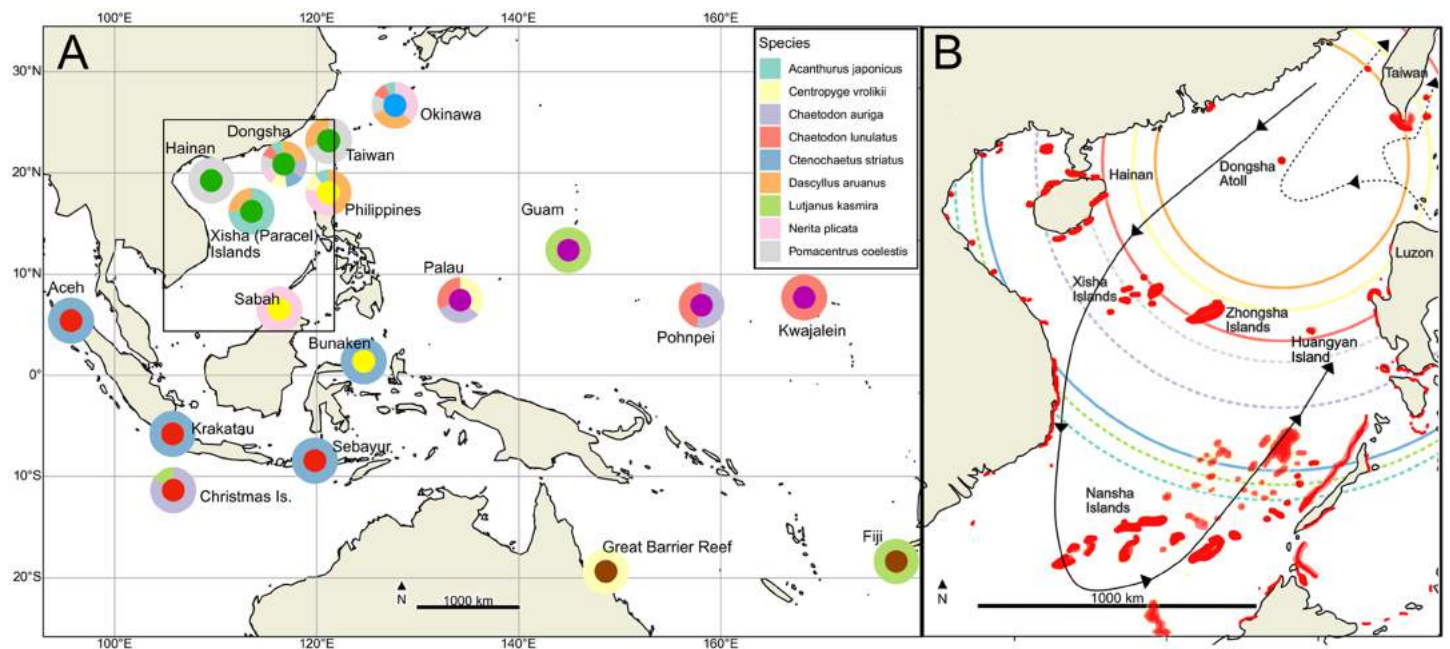


Figure 1 Sampling map. (A) Map of all sampled locations. Outer rings are colored by which species were sampled at a locality, while inner circles are keyed to regional colors in Fig. 3. (B) Inset of South China Sea showing coral reefs in red following Zhao *et al.* (2016) and Dorman *et al.* (2016). Summer surface circulation patterns (solid line with arrows; winter circulation is roughly reversed) and Kuroshio Current intrusion (dotted line with arrows) follow Hu *et al.* (2000). Open circles are colored by species, and give estimates of maximum larval dispersal distances given mean summer surface current speed of 18.7 km/day (Hu *et al.*, 2000) and PLD s given in Table 1. Solid circles indicate species for which a stepping-stone model was selected, and dashed lines indicate species for which panmixia was selected. Maps were generated from the public domain Natural Earth raster with the Cartopy v0.11.2 package for Python (Met Office, 2014). [Full-size !\[\]\(4f0005c8f9850885df208c45b0c231fa_img.jpg\) DOI: 10.7717/peerj.12063/fig-1](https://doi.org/10.7717/peerj.12063/fig-1)

compiled a genetic database comprising over 38,000 individuals from more than 230 species (DIPnet; Crandall *et al.*, 2019a), stored within the Genomic Observatories Metadatabase (GEOME; Deck *et al.*, 2017; Riginos *et al.*, 2020). This open database provides the opportunity to test various biogeography, speciation, and connectivity hypotheses across a wide taxonomic swath of species comprising Indo-Pacific communities, without the need to sample every location and every species by a single research group.

Located 340 km southeast of Hong Kong and 850 km southwest of Taipei, Dongsha Atoll, with an area of about 600 km², is the largest and oldest atoll in the South China Sea (SCS; Fig. 1), (Dai, 2004). The atoll is of strategic political importance in that it sits in the Taiwan Strait, a major trade route between East and Southeast Asia. The atoll also hosts important coral reef habitats in the northern South China Sea, providing necessary fishing opportunities for the people of China, Taiwan, and Vietnam (Dai, 2004). For this reason, the Dongsha Atoll National Park (DANP) was established in 2004 by the Taiwanese government. The DANP encompasses 3,537 km² of marine habitat (Cheng *et al.*, 2020), and its establishment has helped to mitigate the impact of massive bleaching events in 1998 and overfishing at the atoll, which were negatively impacting coral cover and biodiversity (Fang, 1998; Soong, Dai & Lee, 2002; Dai, 2004). With proper enforcement and regional cooperation in place since 2007, a general survey of marine resources in the

DANP in 2011 showed that both terrestrial and marine ecological resources are gradually recovering ([Dai, 2012](#)). Contradicting these results, [Cheng et al. \(2020\)](#) detected a dramatic 34% decrease in coral coverage since the DANP was established, with an alarming reduction in the abundance of branching corals indicating an overall simplification of habitat types. Although the effect of the establishment of the DANP on community biodiversity and health is still under debate, how these conservation efforts might have impacted other reefs in the South China Sea and beyond is poorly understood.

In the present study, we added sequence data from nine coral reef species sampled within the DANP to existing datasets in GEOME to test metapopulation hypotheses regarding the role of each species' Dongsha population in the greater context of the Indo-Pacific. We then used a graph theoretical analysis based on maximum dispersal distances to more closely examine Dongsha's role as an intergenerational stepping-stone within the South China Sea.

MATERIALS & METHODS

Sampling and sequencing

We selected nine target species from the Genomic Observatories Metadatabase (GEOME; [Deck et al., 2017](#)) based on the availability of genetic data from nearby populations and their common occurrence at Dongsha Atoll, including eight reef fishes and the intertidal gastropod *Nerita plicata* ([Table 1](#)). In March of 2017, tissue samples for these nine species were collected at Dongsha by SCUBA divers using spears in the case of reef fish species, or by hand in the case of the gastropod. Tissues were preserved in 95% ethanol. The field sampling of the present study is under the permit number 0000691 which was approved by the Marine National Park Headquarters in Taiwan.

Mitochondrial DNA (mtDNA) amplification and sequencing were conducted at California State University Monterey Bay as part of the Molecular Ecology and Evolution capstone research course in Fall of 2017. Marker choice was made based on the data available in GEOME and included the mitochondrial Cytochrome Oxidase I, Cytochrome-B, and the Control Region. In each case, published primers were used (see [Table 1](#) for details). DNA was extracted in a 10% Chelex® (Biorad) solution following [Walsh, Metzger & Higuchi \(1991\)](#). Polymerase chain reactions (PCR) were conducted in 25 µL reactions with 2.5 µL of 10x PCR buffer, two µL MgCl₂ (25 mM), 2.5 µL dNTPs (8 mM), 1.25 µL of each 10 mM primer, one µL of DNA template, and 0.625 U of AmpliTaq (Applied Biosystems, Waltham, MA, USA). Thermocycling conditions were the same across species, only differing in annealing temperature: initial denature for 2 min at 95 °C; followed by 35 cycles of denaturation at 95 °C for 15 s; annealing at T °C for 30 s (where T is given in [Table 1](#)); and elongation at 72 °C for 1 min; with a final elongation step at 72 °C for 7 min. PCR products were checked on a 1% agarose gel using GelRed (Biotium, Fremont, CA, USA). Successful PCR products were sent to the MCLab (South San Francisco; mclab.com) for cleanup, cycle sequencing (both directions), and sequencing on an ABI 3730 DNA Sequencer. Forward and reverse reads for each sample were proofread and aligned using Geneious 9.1.8 software. Complementary sequence data from four or five nearby populations were downloaded for each species from the GEOME database ([Fig. 1](#)).

Table 1 Species names, estimated pelagic larval durations, and primers and annealing temperatures used for PCR.

Scientific name (dataset citation)	Common name	Maximum pelagic larval duration (days)	mtDNA Locus (base pairs) & Primers used	Annealing temp (°C)
<i>Acanthurus japonicus</i> (DiBattista et al., 2016)	Japanese surgeonfish	62 (for <i>A. triostegus</i> ; McCormick, 1999)	Cytochrome-B (491) Cytb9/Cytb7 (DiBattista et al., 2016)	62
<i>Centropyge vrolikii</i> (DiBattista et al., 2012)	Pearlscale angelfish	29 (Thresher & Brothers, 1985)	Cytochrome-B (575) CLFM_FOR/CLFM_REV (DiBattista et al., 2012)	58
<i>Chaetodon auriga</i> (DiBattista et al., 2015)	Threadfin butterflyfish	48 (Wilson & McCormick, 1999)	Cytochrome-B (668) Cytb9/Cytb7 (DiBattista et al., 2013)	56
<i>Chaetodon lunulatus</i> (Waldrop et al., 2016)	Oval butterflyfish	35 (Soeparno et al., 2012)	Cytochrome-B (605) Cytb9/Cytb7 (Waldrop et al., 2016)	50
<i>Ctenochaetus striatus</i>	Striated surgeonfish	59 (Wilson & McCormick, 1999)	Control Region (316) CR-A/CR-E (Lee et al., 1995)	50
<i>Dascyllus aruanus</i> (Liu et al., 2014)	Whitetail dascyllus	26 (Thresher, Colin & Bell, 1989)	Cytochrome-B (1058) GluDG-L/H16460 (Palumbi et al., 1991)	56
<i>Lutjanus kasmira</i> (Gaither et al., 2010)	Bluestripe snapper	60 (Baensch, 2014)	Cytochrome-B (446) Cytb9/Cytb7 (DiBattista et al., 2013)	48
<i>Nerita plicata</i> (Crandall et al., 2008)	Whorled nerite	~180 (Underwood, 1978)	Cytochrome Oxidase I (613) LCO-1490/HCO-1498 (Folmer et al., 1994)	50
<i>Pomacentrus coelestis</i> (Liu et al., 2012)	Neon damselfish	39 (Wilson & McCormick, 1999)	Control Region (337) CR-A/CR-E (Lee et al., 1995)	50

Sequences for each species were aligned and trimmed to a common length using the muscle algorithm with default parameters implemented in Geneious v9 (Biomatters) and exported to FASTA format.

Population genetic analysis

We used the pegas (Paradis, 2010) and strataG (Archer, Adams & Schneiders, 2017) population genetic packages to read the FASTA-formatted data into R and identify unique haplotypes. We then utilized these packages to estimate standard genetic diversity statistics for the Dongsha population of each species. Haplotype diversity and the number of haplotypes unique to Dongsha were calculated using the *exptdHet*, *privateAlleles* functions in strataG. Fu's F_s , a statistic which identifies populations with an excess of recent substitution events caused by demographic growth, genetic hitchhiking, or background selection (Fu, 1997), was calculated using the *fusFS* functions in the same package.

Nucleotide diversity was measured using the *nuc.div* function in *pegas*. The significance of F_s was determined with 1,000 coalescent simulations of neutrality in Arlequin 3.5 (Excoffier & Lischer, 2010). Haplotype diversity, nucleotide diversity, and percentage of private haplotypes (unique to a given population) were also averaged across all nearby sampled populations, and a two-sided *t*-test was used to determine if the Dongsha populations' genetic diversity was significantly different from the nearest sampled populations.

Pairwise Φ_{ST} , a sequence analog of F_{ST} (Excoffier, Smouse & Quattro, 1992), was calculated with *pairwiseTest* in *strataG* with significance determined by 1,000 randomly drawn permutations of the data to represent the null hypothesis of no genetic structure. Finally, pairwise matrices were visualized in *ggplot2* and as non-metric dimensional scaling (NMDS) plots to represent the distances in two-dimensional space using the *metaMDSiter* function in the R package *vegan* (Oksanen et al., 2017), using a hybrid model of monotone and linear regression for Φ_{ST} values lower than 0.1. For both visualizations, negative values were corrected to zero, and for NMDS, zero or negative values had a very small positive value added to them. To visualize whether there is a geographic pattern of haplotype distribution, we defined samples used in this study into six regional groups (Fig. 1). Median joining networks with these regional colors were created using *PopArt* (Leigh & Bryant, 2015). All analyses are detailed at <https://github.com/ericcrandall/dongsha/>.

We also estimated the marginal likelihood of three different metapopulation models for the nine species in *Migrate-n* 3.6.11 (Beerli & Felsenstein, 2001; Beerli & Palczewski, 2010; Fig. 2): (a) extremely high levels of larval dispersal (proportion of migrants (m) > 0.1) throughout the sampled range yielding effective panmixia, (b) slightly restricted larval dispersal ($m < 0.1$) represented by an *n*-island model with equal population sizes and equal migration between all population pairs, (c) restricted larval dispersal such that larvae are only exchanged between neighboring populations or regions as represented in a stepping-stone model (two populations were determined to be neighboring if no other sampled populations would serve as a likely intermediate stepping-stone).

Migrate-n analysis followed methods developed in Crandall et al. (2019b). FASTA-formatted datasets were converted to *Migrate-n* format using *PGDSpider* 2.0.5.1 (Lischer & Excoffier, 2012). For each species, we found optimal parameters (gamma shape parameter, transition transversion ratio and base frequencies) for an HKY + G model of molecular evolution using the *modelTest* function in the R package *phangorn* (Schliep, 2011). The gamma shape parameter was discretized to four categories using the *discrete.gamma* function from the same package. All models had identical, windowed exponential priors on Θ (lower bound: 1×10^{-5} , upper bound: 1×10^{-1} , mean: 0.01) and m/μ (lower bound: 1×10^{-4} , upper bound: 1×10^6 , mean: 1×10^5) parameters. We used four heated chains with temperatures of 1, 1.5, 3, and 1×10^5 to ensure a thorough search of parameter space, thereby enabling an estimate of model marginal likelihood via path sampling (Beerli & Palczewski, 2010). *Migrate-n* was set to optimize on the m/μ parameter rather than the joint parameter $N_e m$ (to avoid correlations with the Θ ($= N_e \mu$) parameters), and with an inheritance scalar that reflected the haploid, uniparental

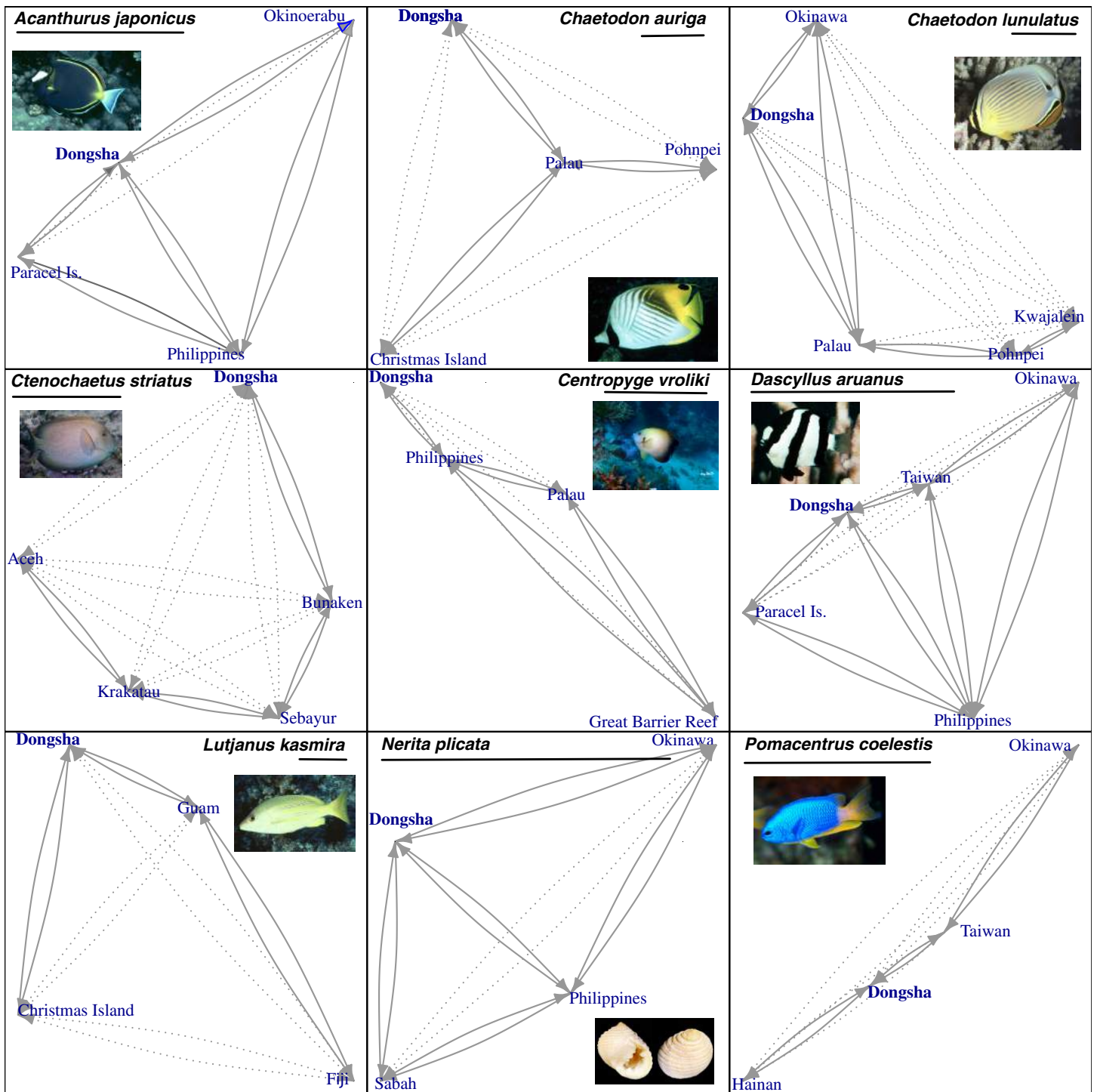


Figure 2 Visualization of all metapopulation models tested for each species. Visualization of all metapopulation models tested for each species. Black lines below each species name indicate a distance of 1,000 km. Blue text indicates sampled sites which are arranged in geographic space. Dotted lines with arrows connect every pair of sample sites and indicate directional migration (gene flow) parameters included in the n-island model while solid lines with arrows indicate directional migration parameters included in the stepping-stone model. The model of panmixia treated all sampled localities as a single population. [Full-size !\[\]\(e9a8f24c99f9e61762929d210c22c223_img.jpg\) DOI: 10.7717/peerj.12063/fig-2](https://doi.org/10.7717/peerj.12063/fig-2)

transmission of mtDNA. For each model, the coolest chain explored fifty million genealogies, sampling every 500 iterations, and discarding the first five million genealogies as burn-in.

Each Migrate-n run comprised three replicates of fifty million genealogies to yield a single estimate of marginal likelihood. Each run was then repeated three times, to yield three independent estimates of metapopulation model marginal likelihood from nine replicate runs. The Bezier-corrected estimate of model marginal likelihood (which approximates the marginal likelihood from a larger number of heated chains) was harvested from each outfile and averaged across the three independent replicate runs. Mean Bezier-corrected marginal likelihoods were converted to relative model probabilities and Bayes factors following *Johnson & Omland (2004)*. To account for variance in mean marginal likelihoods across the three replicate runs, a permutation *t*-test was run to compare the mean marginal likelihoods of the first and second ranked models, following *Crandall et al. (2019b)*. Parameter files for each species and each model, as well as code for interpreting the output, are available in the Github repository, within the `migrate_analysis` directory.

We then asked to what extent the models selected for each species by Migrate-n were a product of the maximum pelagic larval duration (PLD), especially given the spatially heterogeneous sampling of surrounding populations. Because only two of three possible models were selected by all nine species, we constructed a logistic regression model using values for maximum PLDs from the literature ([Table 1](#)) and great-circle distances from Dongsha Atoll to both the nearest and furthest sampled populations for each species, calculated with the Raster package (*Hijmans, 2021*) in R: $p(\text{Migrate Model}) \sim \text{Maximum PLD} + \text{Closest Distance} + \text{Furthest Distance}$. We used backward BIC model selection in the R package MASS (*Venables & Ripley, 2002*) to select the best model.

Graph theoretical analysis

To better place our results in the geographical context of the South China Sea, we undertook a graph theoretical analysis of the potential for larval dispersal in this region. We developed two rasters ([Fig. 1B](#)) representing (1) coral reef areas and (2) land areas of continents and islands of the South China Sea from [Fig. 1](#) of *Zhao et al. (2016)* and [Fig. 1A](#) of *Dorman et al. (2016)*, and projected both rasters into UTM coordinates (zone 50N) with 1 km resolution using the raster package. We then imported these rasters into Graphab 2.6 (*Foltête, Clauzel & Vuidel, 2012*), defining the reef areas with at least 25 hectares as habitat patches, and the land areas as a cost raster with each pixel costing 10,000. Graphab then generated a linkset between reef patches for each species using a maximum dispersal distance calculated as the product of maximum PLD ([Table 1](#)) and the mean current speed of 18.7 km/day given by *Hu et al. (2000)*. The basic binary simple (undirected) graph generated by Graphab from this linkset was then imported into the igraph package for R (*Csardi & Nepusz, 2006*), which we used to measure betweenness centrality, defined as the fraction of shortest paths between all patches which pass through a given reef patch. *Estrada & Bodin (2008)* have shown that betweenness centrality is an important measure of the overall importance of a patch to the large-scale connectivity of a

Table 2 Genetic diversity statistics including haplotype diversity (h), nucleotide diversity (π) and Fu's F_S for each sampled Dongsha population in comparison to regional means.

Species	Dongsha N	# Haplotypes	Private haplotypes	% Private	Regional mean % private	h	Regional mean h	π	Regional mean π	F_S
<i>A. japonicus</i>	14	9	3	21.43	12.96	0.88	0.86	0.006	0.004	-3.53
<i>C. auriga</i>	28	6	2	7.14	7.06	0.51	0.56	0.001	0.001	-4.16
<i>C. lunulatus</i>	19	4	1	5.26	13.92	0.56	0.66	0.004	0.005	2.19
<i>C. striatus</i>	26	24	21	80.77	75.03	0.99	0.99	0.025	0.023	-15.44
<i>C. vrolikii</i>	24	12	9	37.50	29.37	0.79	0.80	0.003	0.003	-7.45
<i>D. aruanus</i>	44	13	5	11.36	14.63	0.79	0.75	0.002	0.002	-5.19
<i>L. kasmira</i>	6	6	4	66.67	16.20**	1*	0.59	0.007**	0.002	-3.03
<i>N. plicata</i>	24	22	19	79.17	77.98	0.99	1.00	0.011	0.013	-14.99
<i>P. coelestis</i>	21	15	9	42.86	63.94**	0.90**	1.00	0.010**	0.014	-10.07

Note:

Significant deviations from regional means are noted at * $p < 0.05$ (*) and ** $p < 0.01$. Significantly low F_S values (compared to neutral coalescent simulations) at $p < 0.02$ are denoted in bold.

landscape. We also used igraph to measure the diameter of each species' graph, as the minimum number of larval-dispersal steps connecting the two most distant points. It is important to emphasize that this approach is not equivalent to a biophysical model of larval dispersal such as found in [Dorman et al. \(2016\)](#), and most dispersal is expected to occur at much shorter distances ([Cowen et al., 2000](#)). However, since genetic structure is very sensitive to dispersal at the tails of the larval dispersal kernel ([Grosberg & Cunningham, 2001](#)), this approach might provide an approximate understanding of potential gene flow in the South China Sea.

RESULTS

We sequenced a total of 206 tissue samples from Dongsha across the nine species. Sequence length varied from 316 bp (Control Region, *Ctenochaetus striatus*) to 1,058 bp (Cytochrome-B, *Dascyllus aruanus*). A total of 111 unique haplotypes across all nine species were detected (Table 2). Within our dataset, 58% of these haplotypes were apparently private to Dongsha Atoll (at least within the local region sampled from GEOME), ranging from 5% in the oval butterflyfish *Chaetodon lunulatus* to ~80% in the whorled nerite *Nerita plicata* and the striated surgeonfish *Ctenochaetus striatus*. The bluestripe snapper *Lutjanus kasmira* had significantly elevated genetic diversity (h, π and % private alleles) at Dongsha compared to the rest of the region; however, this may be an artifact of low sample size. The neon damselfish *Pomacentrus coelestis* had significantly lower genetic diversity (h, π , and % private alleles) at Dongsha than the surrounding populations. All but three species had Fu's F_S values that were significantly negative at the recommended alpha of $p < 0.02$ ([Fu, 1997](#)), indicating a departure from neutrality due to an excess of recent mutations at the tips of the genealogy. Median-joining haplotype networks showed no clear geographic pattern of haplotype distribution for any species (Fig. 3). In addition, all haplotype networks showed a star-like topology providing visual confirmation of the low Fu's F_S values and evidence of either recent

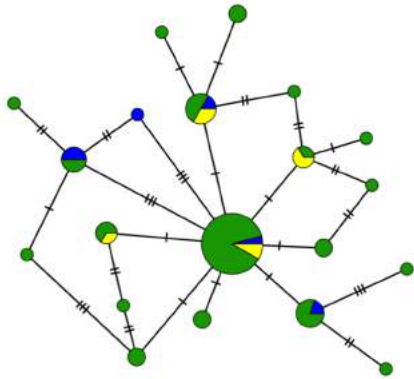
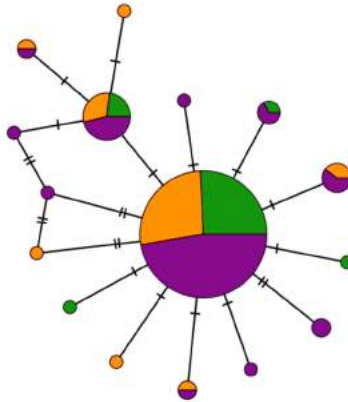
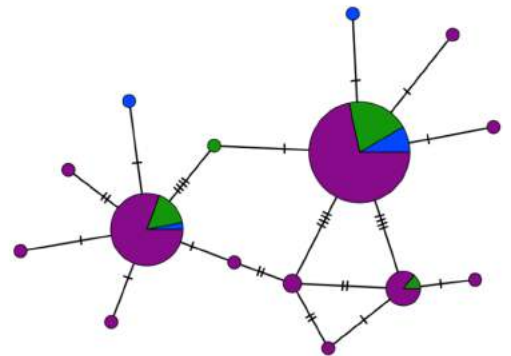
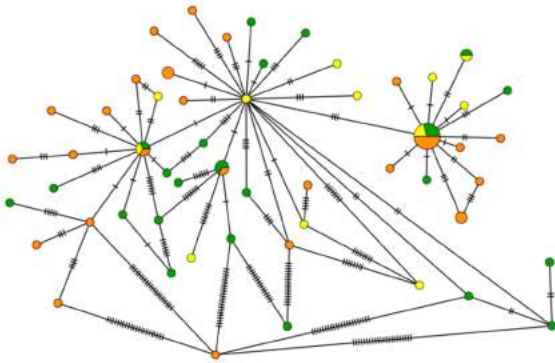
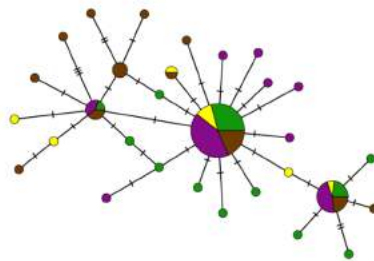
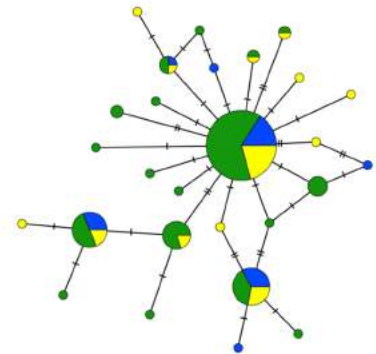
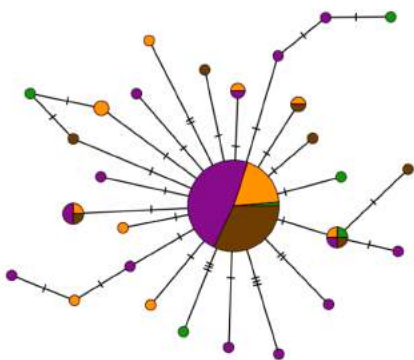
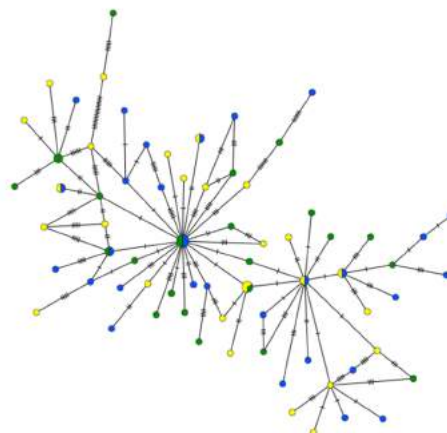
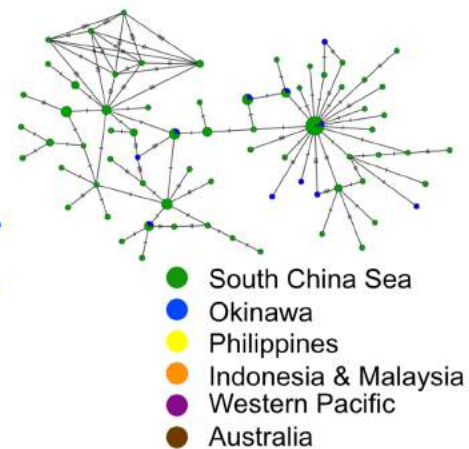
Acanthurus japonicus (CytB)*Chaetodon auriga* (CytB)*Chaetodon lunulatus* (CytB)*Ctenochaetus striatus* (CR)*Centropyge vroliki* (CytB)*Dascyllus aruanus* (Cyt B)*Lutjanus kasmira* (CytB)*Nerita plicata* (CO1)*Pomacentrus coelestis* (CR)

Figure 3 Haplotype networks of nine species. Median-joining networks for all nine species. Each circle represents a haplotype, with the frequency of the haplotype indicated by the circle's size (scale varies across species). Pie charts indicate each haplotype's distribution across sampling sites. Lines indicate possible mutational changes between haplotypes, with hash marks representing more than one change.

Full-size  DOI: 10.7717/peerj.12063/fig-3

natural selection or population expansion. The combined data set used in this study has been shared with location and date metadata in GEOME (geome-db.org) within the “Reef Species of Dongsha Atoll” expedition of the Diversity of the Indo-Pacific Project, with GUID: <https://n2t.net/ark:/21547/Dos2>. By clicking “Query All Reef Species of Dongsha Atoll Samples”, the fasta file can be downloaded through the download option next to “map” option.

Pairwise Φ_{ST} values varied from 0 (found in every dataset) to 0.202 in different taxa across Indo-Pacific (Fig. S1). In the Japanese surgeonfish, *Acanthurus japonicus* significant genetic structures were found between Okinoerabu (near Okinawa Island), Philippines, and Xisha. In addition, the Dongsha population of *L. kasmira* was highly and significantly structured with all other populations. However, low sample size in the Okinoerabu population of *A. japonicus* ($n = 6$) and the Dongsha population of *L. kasmira* ($n = 6$) curtails our ability to interpret the significance of these observations of high Φ_{ST} . The only other significant value of Φ_{ST} (0.077) for a Dongsha population was with the Xisha Islands in the whitetail dascyllus, *Dascyllus aruanus*. On average, the Dongsha population of each species had 1.9 positive pairwise Φ_{ST} values out of a total of 3 or 4 populations that it was measured against. Due to the lack of co-sampling of each species at these other sites, there were no clear geographic patterns in Dongsha’s genetic structuring with other populations. NMDS plots (Fig. S2) generally showed a similar lack of correlation with geography, except for perhaps *C. striatus* and *C. lunulatus*. This general lack of geographic signal in genetic structure is a common feature in the Indo-Pacific (Gaither et al., 2011; Crandall et al., 2019a) and marine population genetic datasets in general (Selkoe & Toonen, 2011; Selkoe et al., 2016).

Relative probabilities for each of three metapopulation models tested by Migrate-n are depicted in Fig. 4. Following guidelines laid out by Kass & Raftery (1995), Migrate-n found strong support for a metapopulation model wherein the Dongsha population acts as an important regional stepping-stone for oval butterflyfish (*Chaetodon lunulatus*; 5.42×10^9 : 1 odds against panmixia; see Table 3), striated surgeonfish (*Ctenochaetus striatus*; 1.78×10^8 : 1 odds against panmixia; see Table 3, Fig. 4), and substantial support for a stepping-stone model in the pearlscale angelfish (*Centropyge vroliki*; 12:1 odds against panmixia). The whitetail damselfish (*Dascyllus aruanus*) had modest support for a stepping-stone model (4:1 odds against panmixia), but the mean log-likelihood for this model was not significantly higher than that for panmixia ($p = 0.15$), leaving this result ambiguous. Datasets from the five other species strongly and unambiguously supported a regional model of effective panmixia (Table 3).

Backward stepwise model selection found that maximal and minimal distances between Dongsha and other sampled populations were not important predictors of whether Migrate-n selected a stepping-stone model. Maximum PLD was the only important predictor in explaining when Migrate-n selected a stepping-stone model over panmixia, with an improvement of 4.12 units of log-likelihood between the full model and one with PLD only. The resultant model was significant ($p = 0.0473$), with the coefficient indicating that for every day increase in PLD, there is a 9.3% decrease in the odds of selecting a stepping-stone model (95% CI [0.002–23]; Fig. 5).

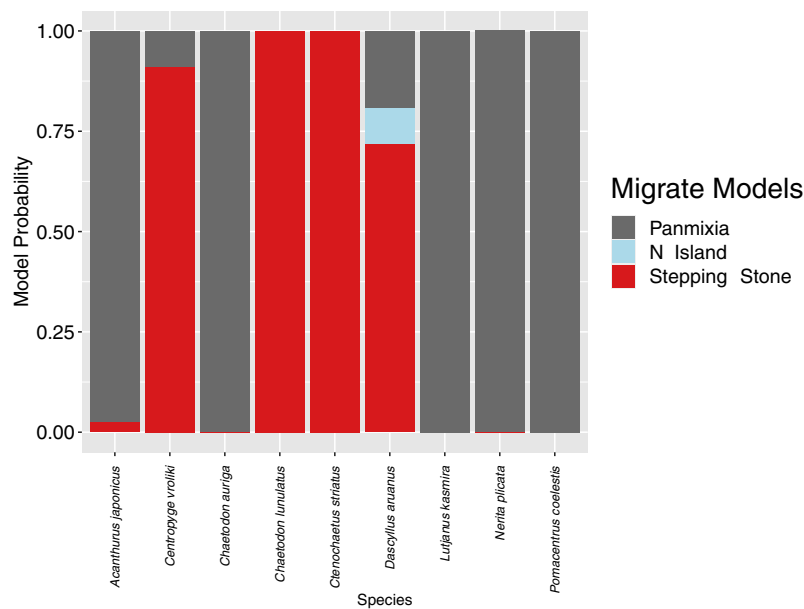


Figure 4 Relative probability of each of four metapopulation hypotheses. Relative probability of each of four metapopulation hypotheses depicted in Fig. 2 for each of nine species sampled at Dongsha as calculated from Migrate-n marginal likelihoods averaged across three replicate runs.

Full-size DOI: 10.7717/peerj.12063/fig-4

Table 3 Most probable (1°) and second most probable (2°) models and their relative probabilities for each species, followed by the *P*-value of a one-tailed permutation *t*-test of the alternate hypothesis that the mean ln-likelihood of the 1° model is significantly higher than the mean of the 2° model.

Species	1° Model	1° Probability	2° Model	2° Probability	p 1° Mean > 2° Mean	2 Ln Bayes Factor 1°/2°	Odds 1°:2°
<i>A. japonicus</i>	Panmixia	0.992	Stepping-stone	0.008	0.05	9.55*	118.4:1
<i>C. auriga</i>	Panmixia	1.000	Stepping-stone	0.000	0.05	19.29*	1.54 × 10 ⁴ :1
<i>C. lunulatus</i>	Stepping-stone	1.000	Panmixia	0.000	0.05	44.83*	5.42 × 10 ⁹ :1
<i>C. striatus</i>	Stepping-stone	1.000	Panmixia	0.000	0.05	37.99*	1.78 × 10 ⁸ :1
<i>C. vrolikii</i>	Stepping-stone	0.921	Panmixia	0.079	0.05	4.90	11.6:1
<i>D. aruanus</i>	Stepping-stone	0.742	Panmixia	0.169	0.15	2.96	4.4:1
<i>L. kasmira</i>	Panmixia	1.000	Stepping-stone	0.000	0.05	441.07*	6.0 × 10 ⁹⁵ :1
<i>N. plicata</i>	Panmixia	1.000	Stepping-stone	0.000	0.05	15.92*	2.86 × 10 ³ :1
<i>P. coelestis</i>	Panmixia	1.000	Stepping-stone	0.000	0.05	123.10*	5.37 × 10 ²⁶ :1

Note:

Loge Bayes Factor indicates the relative probability of the best model relative to the second best model, with values greater than six indicating a strong weight of evidence (odds > 20:1, indicated with *), and values greater than three indicating substantial support (bolded, *Kass & Raftery, 1995*). *P*-values indicate the outcome of a permutation *t*-test comparing the log-likelihoods of the two top-ranked models across three replicated Migrate-n runs, bolded at alpha of 0.05.

Graphab found 115 reef patches greater than 25 hectares in the South China Sea. These patches were connected with a minimum graph diameter of one larval dispersal step (*Nerita plicata*) or a maximum of seven generational steps for *Dascyllus aruanus* (Fig. 6). Graph diameter was highly correlated with PLD ($r^2 = 0.61$), so we do not present a separate logistic regression for its ability to predict whether a species had a stepping-stone model. Out of 115 reef patches, Dongsha was always ranked in the top 15 reef patches for

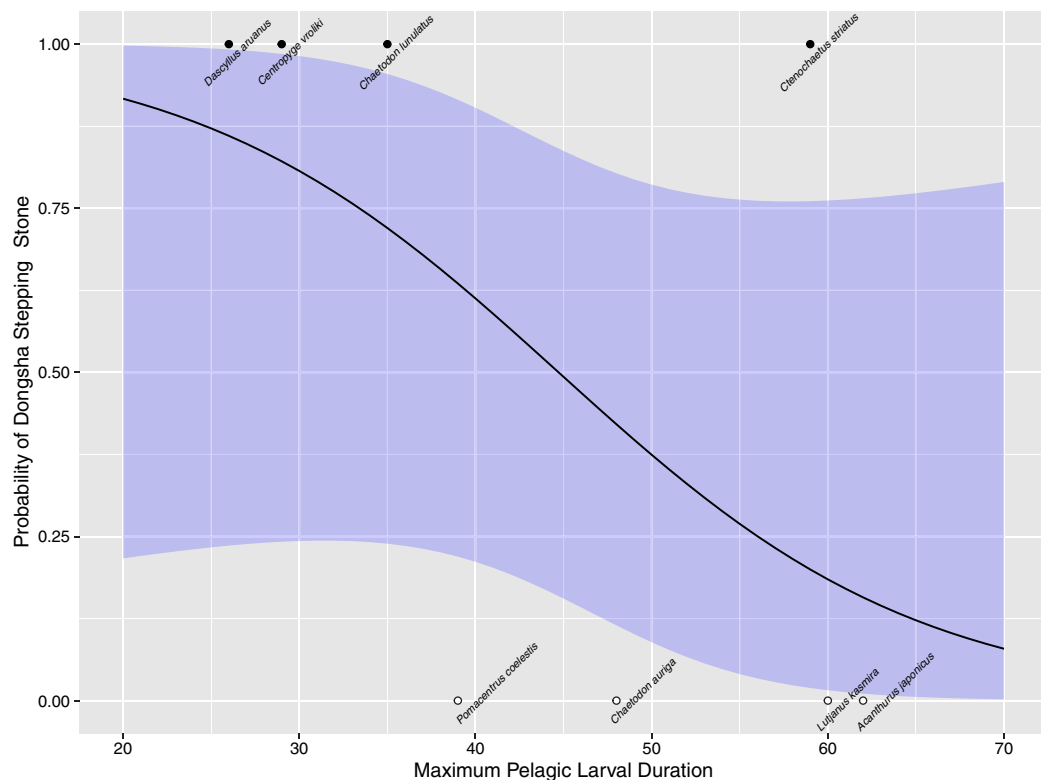


Figure 5 Logistic regression model. Logistic regression model for: Migrate-n model ~ maximum PLD, with 95% confidence intervals constructed as $1.96 \times$ standard error. The model is shown between 20 and 70 days larval duration to avoid extrapolation. Black circles show species with datasets that selected a stepping-stone model, while open circles show species datasets that selected a model of effective panmixia. [Full-size !\[\]\(4c749bfbab8fa9907970332693c435a8_img.jpg\) DOI: 10.7717/peerj.12063/fig-5](https://doi.org/10.7717/peerj.12063/fig-5)

betweenness centrality, ranging from the 3rd most important reef (*Chaetodon lunulatus* and *Pomacentrus coelestis*) and the 14th most important reef (*Dascyllus aruanus*) for this metric. The only reefs with consistently higher rankings were found in the Xisha Islands, the Zhongsha Islands, and Huangyan Island (Fig. 6).

DISCUSSION

While this genetic analysis of nine coral reef species represents a relatively small proportion of the thousands of species comprising the Dongsha Atoll National Park community, it is also the most extensive analysis attempted to put a protected single reef community into the broader ecological and evolutionary context of the Indo-Pacific to date. Overall, our analysis indicates that over evolutionary timescales, Dongsha populations are well-connected with the rest of the South China Sea and indeed with the rest of the Indo-Pacific and maintain genetic diversities that do not significantly deviate from average (except for *P. coelestis*, see discussion below). Furthermore, for marine species with mean PLDs less than 40 days (the vast majority; Strathman, 1987; Shanks, 2009), Dongsha Atoll provides a valuable stepping-stone that is consistently within the top 15 reef patches for promoting regional genetic and demographic connectivity within the South China Sea (Figs. 5 and 6).

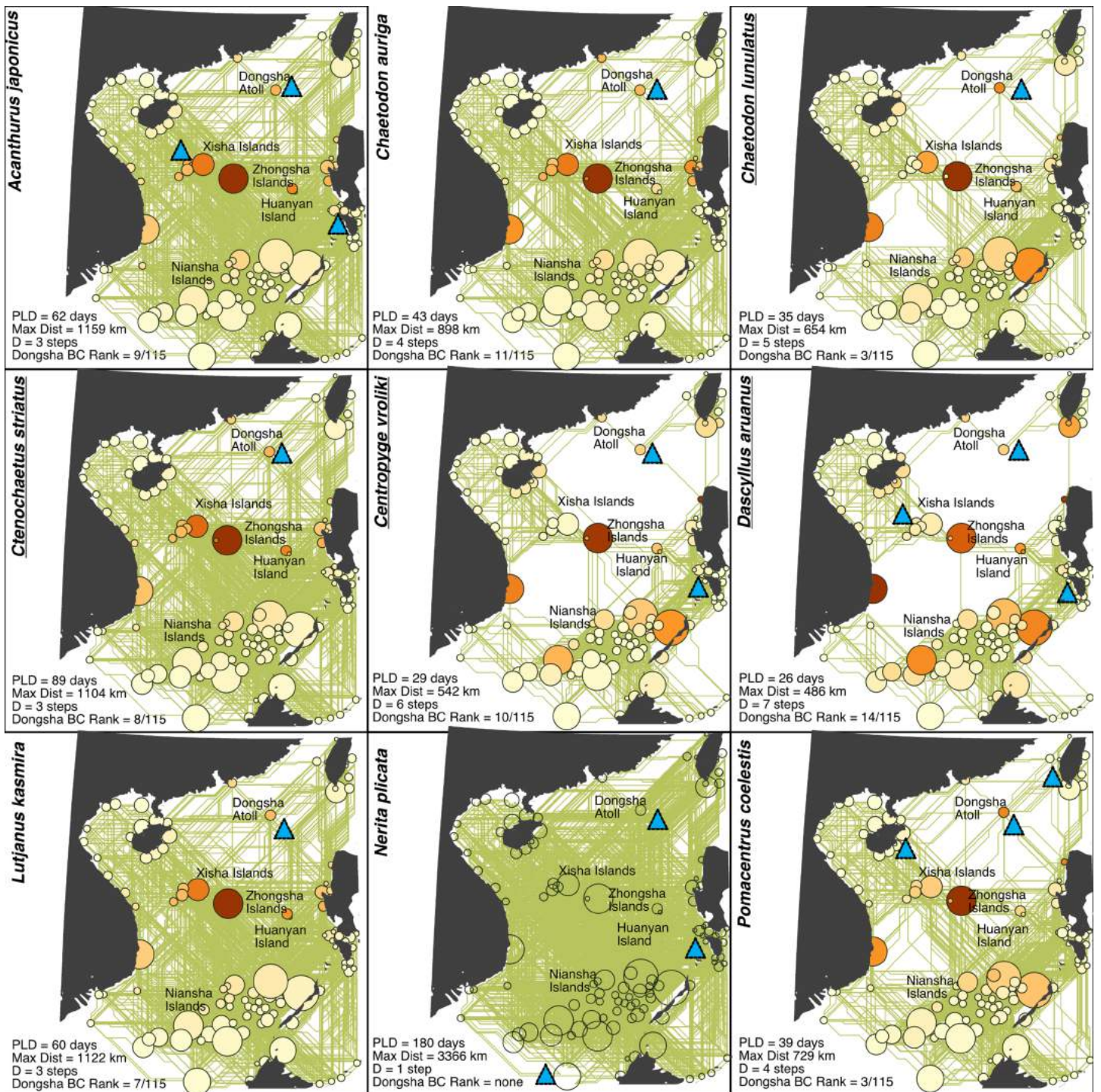


Figure 6 Undirected binary simple graphs between 115 South China Sea reef patches with areas greater than 25 hectares. Circle sizes are proportional to the approximate reef area of each patch, while darker colors indicate a higher relative betweenness centrality for a given patch. Blue triangles indicate a genetic sample for that species. Yellow lines show shortest overwater paths between reef patches that could potentially be connected by larval dispersal assuming a maximum distance given in the lower right corner. Additional statistics in the lower right corner include pelagic larval duration (PLD), graph diameter (D) as the shortest number of larval dispersal event required to cross the longest distance between reef patches for a given species and the ranking of betweenness centrality (BC) for Dongsha out of 115 reef patches. Genetic data for species with underlined names supported a stepping-stone model of dispersal. [Full-size DOI: 10.7717/peerj.12063/fig-6](https://doi.org/10.7717/peerj.12063/fig-6)

Genetic population structure between Dongsha Atoll and nearby populations, as measured by the sequence-based F_{ST} analog Φ_{ST} , was generally low and non-significant (Fig. S1). This finding is congruent with the results of connectivity studies targeting damselfishes between the SCS and Kuroshio regions which showed low and non-significant genetic structure among the Xisha (Paracel) Islands, Dongsha, and Taiwan (Liu et al., 2011, 2014, 2019). Failure to reject panmixia is generally common in marine species (Waples, 1998; Kinlan & Gaines, 2003), has been found consistently in the Indo-Pacific (Keyse et al., 2014; Crandall et al., 2019a), and is traditionally interpreted as evidence for relatively high levels of gene flow due to larval dispersal. However, these summary statistics can often be zero even when there has not been gene flow in thousands of generations (Faurby & Barber, 2012; Crandall et al., 2019a), and they do not provide any information about metapopulation structure.

Five of the nine species surveyed here demonstrate strong regional connectivity in the South China Sea such that their gene pools are well-mixed (effective panmixia; mean SCS graph diameter for these species = 3.0 intergenerational dispersal events, sd = 1.22). In contrast, the coalescent approach employed here clearly distinguishes these from the four species that have some regional metapopulation structure (stepping-stone; Table 3, Fig. 4). This latter group generally has shorter PLDs (mean PLD = 37 days, sd = 15 days) than the former group (mean PLD = 78 days, sd = 60 days), meaning that it will take more generations to cross the SCS (mean SCS graph diameter for these species = 5.25 intergenerational dispersal events, sd = 1.70). For these shorter PLD species, Dongsha Atoll provides an important intergenerational stepping-stone for maintaining gene flow across the SCS (highly ranked betweenness centrality for all species except *N. plicata*; Fig. 6). Furthermore, Fig. 5 demonstrates a significant relationship between PLD and metapopulation structure (albeit with wide confidence intervals) with a sharply increasing probability that a species will have a metapopulation structure that relies on Dongsha Atoll as PLD decreases to about 40 days or less. Below, we discuss the oceanographic context of the SCS as it relates to our findings.

Oceanographic circulation patterns in the SCS and larval dispersal

The seasonal circulation patterns in the SCS are mainly driven by monsoon winds and comprise several cyclonic/anticyclonic eddies. In contrast, northeastward monsoons and southwestward monsoons prevail during winter and summer, respectively (Hu et al., 2000, Fig. 1B). During winter, most currents are northeastward and turn east of Natuna Islands toward the west coast of Luzon in the Philippines. Meanwhile, the Kuroshio intrusion splits into two currents, with one branch moving toward Dongsha and another toward Xisha Islands (Paracel Islands), then turns northward to pass along the Taiwan coast. During summer, most of the currents flow southwestward, with a mean current velocity of 18.7 km/day, while the southwestward monsoon weakens the Kuroshio Intrusion.

Given this circulation pattern, Fig. 6 provides heuristic estimates of the maximum dispersal distances for larvae of each species during the summer, when most corals and fish are spawning (Liu, 2011; Ho, 2017). For example, even larvae from the species with the

shortest PLD (*Dascyllus aruanus*; 26 days) should be able to drift to the nearest reefs 230 km away near Hong Kong, or to Taiwan, 433 km away (*D. aruanus*; Figs. 1B and 6). In contrast, species with the longest PLD (*Nerita plicata*; 180 days) should be able to reach anywhere in the SCS in a single larval dispersal event. These estimates are heuristic because the vast majority of larvae released at Dongsha or elsewhere will not be advected over the maximal distance due to diffusion and mortality (Cowen *et al.*, 2000). On the other hand, it is possible that larvae may occasionally be advected beyond the depicted maximum distance by infrequent events such as typhoons or by the extension of their larval duration beyond what has been measured (McCormick, 1999). In the present study, Zongsha seems to act as an important hub for the connectivity in the area between Xisha, Zhongsha and Huangyang Island as revealed in Fig. 6. Liu, Hsin & Cheng (2020) suggested that the seasonal dynamic of eddies may facilitate the dispersal of marine organisms in this area which may support the role of Zongsha in term of population connectivity. Meanwhile, the heuristic estimates in Figs. 1B and 6 are useful in showing that, in general, the species for which a stepping-stone model of metapopulation structure was selected are only able to reach neighboring reefs, while those for which panmixia was selected have the capacity to disperse widely in the SCS and beyond.

Moreover, more sophisticated biophysical modeling of larval dispersal in the South China Sea indicates a clear regional structure for species with a PLD of 40 days or less (Melbourne-Thomas *et al.*, 2011; Dorman *et al.*, 2016; Liu, Hsin & Cheng, 2020). Although focused on the central and southern SCS, Melbourne-Thomas *et al.* (2011) modeled particles with 30 or 40 day PLD, active or passive dispersal with a rate of mortality of 0.1 to 0.2 per day, and showed that all particles released from the Nansha Islands (*i.e.*, Spratly or Kalayaan islands) settled either in the Nanshas or in western Palawan. Using more particles, slightly more realistic biological parameters, and tracking particles released from the Nanshas for 90 days or until settlement, Dorman *et al.* (2016) got similar results, with most particles staying in the Nanshas or moving eastward to Palawan, but they also showed limited connectivity from the Nanshas to the Xishas and Northern Luzon, especially during the Fall when currents shift to the northeast. Finally, Liu, Hsin & Cheng (2020) simulated benthic currents at 200-400 m depth over 60 days to show little connectivity between deep-sea coral (*Deltocyathus magnificus*) populations near Dongsha and the Xisha Islands, which was confirmed by clear genetic structure in microsatellites.

The significant relationship between PLD and the existence of metapopulation structure demonstrated here (Fig. 5) has wide confidence intervals due to two species. A metapopulation model of effective panmixia was selected for the neon damselfish, *Pomacentrus coelestis* despite having a maximum PLD of 39 days, while a stepping-stone model was most probable for *C. striatus*, even though it has a maximum PLD of 59 days (Wilson & McCormick, 1999). Although the best model for explaining metapopulation structure did not include sampling distance as a factor, we suggest that heterogeneous sampling may have played a role in the models that were selected for at least these two species. The nearest sampled population to Dongsha for the *P. coelestis* dataset was 411 km

away in Taiwan, while the furthest was 1,304 km away in Okinawa. Furthermore, the fact that the Dongsha sample of *P. coelestis* deviated from average regional diversities suggests that our sample of this species may be non-representative. The low genetic diversities in Table 2 may be due to cohesive dispersal among related larvae (Robitzch, Saenz-Agudelo & Berumen, 2020) since the specimens that we collected were juveniles around the same size and collected at the same location. Therefore, the haplotypes identified from these samples may derive from a relatively small number of parents. For *C. striatus*, even the nearest sampled population was much further than Okinawa, 2,280 km away in Bunaken near Sulawesi, while the furthest sampled population was 3,217 km away near Krakatau in the Sunda Strait. Given these heterogeneous sampling distances and the possibly non-representative sample of *P. coelestis*, it is easier to understand how a stepping-stone model was inferred over large distances for *C. striatus* while a model of panmixia was selected over short distances for *P. coelestis*. Future efforts to comparatively model metapopulation structure should standardize sampling to the extent that it is possible.

CONCLUSIONS

For the relatively low cost of adding mitochondrial sequence data from nine coral reef species sampled within the national park at Dongsha Atoll to existing datasets we were able to successfully test metapopulation hypotheses of larval dispersal and gene flow for each of these reef species. While it is important to acknowledge that these results derive from only a single genetic locus, results from initial mitochondrial surveys are often borne out by multi-locus analyses (Bowen *et al.*, 2014). Our results from both population genetic and graph theoretical analysis demonstrate that Dongsha is likely a key stepping-stone for promoting genetic and demographic connectivity among reefs in the northern South China Sea, especially for species with PLDs less than 40 days. Therefore, reinforcement of the management by Marine National Park Headquarters is crucial to reduce the fishing pressure (*i.e.*, illegal poaching) and maintain Dongsha populations. Meanwhile, research efforts need to be increased to better understand the role of Dongsha Atoll in connectivity partners across the region. Missing from these analyses are the habitat-building scleractinian corals and seagrasses that are essential to the long-term health of these threatened ecosystems. A comprehensive program to sample and sequence coral reef species throughout the South China Sea could provide a more detailed and empirical understanding of the valuable protections afforded by protected areas such as Dongsha Atoll.

ACKNOWLEDGEMENTS

We thank the technicians of the Dongsha Atoll Research Station (DARS), as well as Margaret Geissler and Melanie Chu at CSU Monterey Bay for their assistance in the field and laboratory and for logistical support. We thank Paul Barber for sharing previously unpublished data for *C. striatus* into GEOME.

ADDITIONAL INFORMATION AND DECLARATIONS

Funding

This research was financially supported by the Ministry of Science and Technology, Taiwan (MOST) and the National Science Foundation (NSF) under 109-2119-M-110 -003 and NSF-DEB#1457848, respectively. The funders had no role in study design, data collection and analysis, decision to publish, or preparation of the manuscript.

Grant Disclosures

The following grant information was disclosed by the authors:

Ministry of Science and Technology, Taiwan (MOST) and National Science Foundation (NSF): 109-2119-M-110 -003 and NSF-DEB#1457848.

Competing Interests

Robert J. Toonen is an Academic Editor for PeerJ.

Author Contributions

- Shang Yin Vanson Liu conceived and designed the experiments, performed the experiments, analyzed the data, prepared figures and/or tables, authored or reviewed drafts of the paper, and approved the final draft.
- Jacob Green performed the experiments, analyzed the data, prepared figures and/or tables, authored or reviewed drafts of the paper, and approved the final draft.
- Dana Briggs performed the experiments, analyzed the data, prepared figures and/or tables, authored or reviewed drafts of the paper, and approved the final draft.
- Ruth Hastings performed the experiments, analyzed the data, prepared figures and/or tables, authored or reviewed drafts of the paper, and approved the final draft.
- Ylva Jondelius performed the experiments, analyzed the data, prepared figures and/or tables, authored or reviewed drafts of the paper, and approved the final draft.
- Skylar Kensinger performed the experiments, analyzed the data, prepared figures and/or tables, authored or reviewed drafts of the paper, and approved the final draft.
- Hannah Leever performed the experiments, analyzed the data, prepared figures and/or tables, authored or reviewed drafts of the paper, and approved the final draft.
- Sophia Santos performed the experiments, analyzed the data, prepared figures and/or tables, authored or reviewed drafts of the paper, and approved the final draft.
- Trevor Throne performed the experiments, analyzed the data, prepared figures and/or tables, authored or reviewed drafts of the paper, and approved the final draft.
- Chi Cheng performed the experiments, analyzed the data, prepared figures and/or tables, authored or reviewed drafts of the paper, and approved the final draft.
- Hawis Madduppa performed the experiments, authored or reviewed drafts of the paper, and approved the final draft.
- Robert J. Toonen conceived and designed the experiments, performed the experiments, authored or reviewed drafts of the paper, and approved the final draft.

- Michelle R. Gaither conceived and designed the experiments, performed the experiments, authored or reviewed drafts of the paper, and approved the final draft.
- Eric D. Crandall conceived and designed the experiments, performed the experiments, analyzed the data, prepared figures and/or tables, authored or reviewed drafts of the paper, and approved the final draft.

Animal Ethics

The following information was supplied relating to ethical approvals (*i.e.*, approving body and any reference numbers):

The species used in this study are non-regulated animals. Therefore, there is no relevant provision for the ethical review process in Taiwan.

Field Study Permissions

The following information was supplied relating to field study approvals (*i.e.*, approving body and any reference numbers):

Field experiments were approved by the Marine National Park Headquarters (Taiwan) under permit number 0000691.

Data Availability

The following information was supplied regarding data availability:

The combined data set used in this study has been shared with location and date metadata in GEOME (geome-db.org) within the “Reef Species of Dongsha Atoll” expedition of the Diversity of the Indo-Pacific Project, with GUID, available at: <https://n2t.net/ark:/21547/Dos2>. By clicking “Query All Reef Species of Dongsha Atoll Samples”, the FASTA file can be downloaded through the download option next to “map” option.

Supplemental Information

Supplemental information for this article can be found online at <http://dx.doi.org/10.7717/peerj.12063#supplemental-information>.

REFERENCES

- Archer FI, Adams PE, Schneiders BB. 2017. STRATAG: an R package for manipulating, summarizing and analysing population genetic data. *Molecular Ecology Resources* 17(1):5–11 DOI 10.1111/1755-0998.12559.
- Baensch F. 2014. The Hawaii Larval fish project. *Coral* 11(2):64–77.
- Beerli P, Felsenstein J. 2001. Maximum likelihood estimation of a migration matrix and effective population sizes in n subpopulations by using a coalescent approach. *Proceedings of the National Academy of Sciences of the United States of America-Biological Sciences* 98:4563–4568.
- Beerli P, Palczewski M. 2010. Unified framework to evaluate panmixia and migration direction among multiple sampling locations. *Genetics* 185(1):313–326 DOI 10.1534/genetics.109.112532.
- Bowen BW, Shanker K, Yasuda N, Celia M, Malay MC, von der Heyden S, Paulay G, Rocha LA, Selkoe KA, Barber PH, Williams ST, Lessios HA, Crandall ED, Bernardi G, Meyer CP, Carpenter KE, Toonen RJ. 2014. Phylogeography unplugged: comparative surveys in the genomic era. *Bulletin of Marine Science* 90(1):13–46 DOI 10.5343/bms.2013.1007.

- Cheng Y-R, Chin C-H, Lin D-F, Wang C-K. 2020.** The probability of an unrecoverable coral community in Dongsha Atoll Marine National Park due to recurrent disturbances. *Sustainability* **12**(21):9052 DOI [10.3390/su12219052](https://doi.org/10.3390/su12219052).
- Cowen RK, Lwiza KM, Sponaugle S, Paris CB, Olson DB. 2000.** Connectivity of marine populations: open or closed? *Science* **287**(5454):857–859 DOI [10.1126/science.287.5454.857](https://doi.org/10.1126/science.287.5454.857).
- Crandall ED, Frey MA, Grosberg RK, Barber PH. 2008.** Contrasting demographic history and phylogeographical patterns in two Indo-Pacific gastropods. *Molecular Ecology* **17**:611–626.
- Crandall ED, Riginos C, Bird CE, Liggins L, Trembl E, Beger M, Barber PH, Connolly SR, Cowman PF, DiBattista JD, Eble JA, Magnuson SF, Horne JB, Kochzius M, Lessios HA, Liu SYV, Ludt WB, Madduppa H, Pandolfi JM, Toonen RJ. 2019a.** Contributing members of the diversity of the Indo-Pacific Network, Gaither MR, The molecular biogeography of the Indo-Pacific: testing hypotheses with multispecies genetic patterns. *Global Ecology and Biogeography* **58**:403–418.
- Crandall ED, Toonen RJ, ToBo Laboratory, Selkoe KA. 2019b.** A coalescent sampler successfully detects biologically meaningful population structure overlooked by F-statistics. *Evolutionary Applications* **12**(2):255–265 DOI [10.1111/eva.12712](https://doi.org/10.1111/eva.12712).
- Crandall ED, Trembl EA, Barber PH. 2012.** Coalescent and biophysical models of stepping-stone gene flow in neritid snails. *Molecular Ecology* **21**(22):5579–5598 DOI [10.1111/mec.12031](https://doi.org/10.1111/mec.12031).
- Csardi G, Nepusz T. 2006.** The igraph software package for complex network research. *Interjournal. Complex Systems* **2006**:1695.
- Dai C. 2004.** Dong-sha Atoll in the South China Sea: past, present and future. In: *Changing Islands - Changing Worlds, Kinmen Island, Taiwan*. 10.
- Dai CF. 2012.** *Natural resources and management strategy analysis of Dongsha Atoll Natural Park*. Kaohsiung: Marine National Park Headquarters. [in Chinese].
- Dorman JG, Castruccio FS, Curchitser EN, Kleypas JA, Powell TM. 2016.** Modeled connectivity of *Acropora millepora* populations from reefs of the Spratly Islands and the greater South China Sea. *Coral Reefs* **35**(1):169–179 DOI [10.1007/s00338-015-1354-3](https://doi.org/10.1007/s00338-015-1354-3).
- DiBattista JD, Berumen ML, Gaither MR, Rocha LA, Eble JA, Choat JH, Craig MT, Skillings DJ, Bowen BW. 2013.** After continents divide: comparative phylogeography of reef fishes from the Red Sea and Indian Ocean. *Journal of Biogeography* **40**(6):1170–1181 DOI [10.1111/jbi.12068](https://doi.org/10.1111/jbi.12068).
- DiBattista JD, Waldrop E, Bowen BW, Schultz JK, Gaither MR, Pyle RL, Rocha LA. 2012.** Twisted sister species of pygmy angelfishes: discordance between taxonomy, coloration, and phylogenetics. *Coral Reefs* **31**(3):839–851 DOI [10.1007/s00338-012-0907-y](https://doi.org/10.1007/s00338-012-0907-y).
- DiBattista JD, Waldrop E, Rocha LA, Craig MT, Berumen ML, Bowen BW. 2015.** Blinded by the bright: a lack of congruence between colour morphs, phylogeography and taxonomy for a cosmopolitan Indo-Pacific butterflyfish, *Chaetodon auriga*. *Journal of Biogeography* **42**(10):1919–1929 DOI [10.1111/jbi.12572](https://doi.org/10.1111/jbi.12572).
- DiBattista JD, Whitney J, Craig MT, Hobbs J-PA, Rocha LA, Feldheim KA, Berumen ML, Bowen BW. 2016.** Surgeons and suture zones: Hybridization among four surgeonfish species in the Indo-Pacific with variable evolutionary outcomes. *Molecular Phylogenetics and Evolution* **101**:203–215 DOI [10.1016/j.ympev.2016.04.036](https://doi.org/10.1016/j.ympev.2016.04.036).
- Deck J, Gaither MR, Ewing R, Bird CE, Davies N, Meyer C, Riginos C, Toonen RJ, Crandall ED. 2017.** The Genomic Observatories Metadatabase (GeOMe): a new repository for field and sampling event metadata associated with genetic samples. *PLOS Biology* **15**(8):e2002925 DOI [10.1371/journal.pbio.2002925](https://doi.org/10.1371/journal.pbio.2002925).

- Emslie MJ, Logan M, Williamson DH, Ayling AM, MacNeil MA, Ceccarelli D, Cheal AJ, Evans RD, Johns KA, Jonker MJ, Miller IR, Osborne K, Russ GR, Sweatman HPA. 2015. Expectations and outcomes of reserve network performance following re-zoning of the great barrier reef marine park. *Current Biology* 25(8):983–992 DOI 10.1016/j.cub.2015.01.073.
- Estrada E, Bodin Ö. 2008. Using network centrality measures to manage landscape connectivity. *Ecological Applications* 18(7):1810–1825 DOI 10.1890/07-1419.1.
- Excoffier L, Lischer HE. 2010. Arlequin suite ver 3.5: a new series of programs to perform population genetics analyses under Linux and Windows. *Molecular Ecology Resources* 10:564–567.
- Excoffier L, Smouse PE, Quattro JM. 1992. Analysis of molecular variance inferred from metric distances among DNA haplotypes: application to human mitochondrial DNA restriction data. *Genetics* 131:479–491.
- Fang LS. 1998. The status of marine ecology in Dongsha Atoll. In: *Proceedings of the European-Asian Workshop on Investigation and Management of Mediterranean and South China Sea Coastal Zone, Hong Kong, China*.
- Faurby S, Barber PH. 2012. Theoretical limits to the correlation between pelagic larval duration and population genetic structure. *Molecular Ecology* 21(14):3419–3432 DOI 10.1111/j.1365-294X.2012.05609.x.
- Folmer O, Black M, Hoeh W, Lutz R, Vrijenhoek R. 1994. DNA primers for amplification of mitochondrial cytochrome c oxidase subunit I from diverse metazoan invertebrates. *Molecular Marine Biology and Biotechnology* 3:294–299.
- Foltête J-C, Clauzel C, Vuidel G. 2012. A software tool dedicated to the modelling of landscape networks. *Environmental Modelling & Software* 38:316–327.
- Fu YX. 1997. Statistical tests of neutrality of mutations against population growth, hitchhiking and background selection. *Genetics* 147:915–925.
- Gaines SD, White C, Carr MH, Palumbi SR. 2010. Designing marine reserve networks for both conservation and fisheries management. *Proceedings of the National Academy of Sciences of the United States of America* 107(43):18286–18293 DOI 10.1073/pnas.0906473107.
- Gaither MR, Toonen RJ, Robertson DR, Planes S, Bowen BW. 2010. Genetic evaluation of marine biogeographical barriers: perspectives from two widespread Indo-Pacific snappers (*Lutjanus kasmira* and *Lutjanus fulvus*). *Journal of Biogeography* 37:133–147 DOI 10/cxj9v7.
- Gaither MR, Jones SA, Kelley C, Newman SJ, Sorenson L, Bowen BW. 2011. High connectivity in the deepwater snapper *Pristipomoides filamentosus* (Lutjanidae) across the Indo-Pacific with isolation of the Hawaiian Archipelago. *PLOS ONE* 6(12):e28913 DOI 10.1371/journal.pone.0028913.
- Gleason M, Fox E, Ashcraft S, Vasques J, Whiteman E, Serpa P, Saarman E, Caldwell M, Frimodig A, Miller-Henson M, Kirlin J, Ota B, Pope E, Weber M, Wiseman K. 2013. Designing a network of marine protected areas in California: achievements, costs, lessons learned, and challenges ahead. *Ocean & Coastal Management* 74(1):90–101 DOI 10.1016/j.ocecoaman.2012.08.013.
- Grosberg RK, Cunningham CW. 2001. Genetic structure in the sea: from populations to communities. In: Bertness MD, Gaines SD, Hay M, eds. *Marine Population Ecology*. Sunderland, MA: Sinauer Associates, 61–84.
- Hijmans RJ. 2021. raster: geographic data analysis and modeling. Available at <https://CRAN.R-project.org/package=raster>.
- Ho Y-N. 2017. Larval fish assemblages in the lagoon of Dongsha Atoll. Master thesis, National Sun Yat-sen University.

- Hu J, Kawamura H, Hong H, Qi Y. 2000. A review on the currents in the South China Sea: seasonal circulation, South China Sea warm current and Kuroshio intrusion. *Journal of Oceanography* 56(6):607–624 DOI 10.1023/A:1011117531252.
- Hughes TP, Baird AH, Bellwood DR, Card M, Connolly SR, Folke C, Grosberg R, Hoegh-Guldberg O, Jackson JBC, Kleypas J, Lough JM, Marshall P, Nystrom M, Palumbi SR, Pandolfi JM, Rosen B, Roughgarden J. 2003. Climate change, human impacts, and the resilience of coral reefs. *Science* 301(5635):929–933 DOI 10.1126/science.1085046.
- Hughes TP, Kerry JT, Baird AH, Connolly SR, Dietzel A, Eakin CM, Heron SF, Hoey AS, Hoogenboom MO, Liu G, McWilliam MJ, Pears RJ, Pratchett MS, Skirving WJ, Stella JS, Torda G. 2018. Global warming transforms coral reef assemblages. *Nature* 556(7702):492–496 DOI 10.1038/s41586-018-0041-2.
- Johnson JB, Omland KS. 2004. Model selection in ecology and evolution. *Trends in Ecology & Evolution* 19:101–108.
- Kass RE, Raftery AE. 1995. Bayes factors. *Journal of the American Statistical Association* 90(430):773–795 DOI 10.1080/01621459.1995.10476572.
- Keyse J, Crandall ED, Toonen RJ, Meyer CP, Trembl EA, Riginos C. 2014. The scope of published population genetic data for Indo-Pacific marine fauna and future research opportunities in the region. *Bulletin of Marine Science* 90(1):47–78 DOI 10.5343/bms.2012.1107.
- Kinlan BP, Gaines SD. 2003. Propagule dispersal in marine and terrestrial environments: a community perspective. *Ecology* 84(8):2007–2020 DOI 10.1890/01-0622.
- Krueck NC, Ahmadia GN, Green A, Jones GP, Possingham HP, Riginos C, Trembl EA, Mumby PJ. 2017. Incorporating larval dispersal into MPA design for both conservation and fisheries. *Ecological Applications* 27(3):925–941 DOI 10.1002/eap.1495.
- Lee WJ, Conroy J, Howell WH, Kocher TD. 1995. Structure and evolution of teleost mitochondrial control regions. *Journal of Molecular Evolution* 41(1):54–66 DOI 10.1007/BF00174041.
- Lester S, Halpern B, Grorud-Colvert K, Lubchenco J, Ruttenberg B, Gaines S, Aíramé S, Warner R. 2009. Biological effects within no-take marine reserves: a global synthesis. *Marine Ecology Progress Series* 384:33–46 DOI 10.3354/meps08029.
- Leigh JW, Bryant D. 2015. Popart: full-feature software for haplotype network construction. *Methods in Ecology and Evolution* 6:1110–1116.
- Lischer HEL, Excoffier L. 2012. PGDSpider: an automated data conversion tool for connecting population genetics and genomics programs. *Bioinformatics* 28:298–299.
- Liu S-T. 2011. Studies on the factors which restrict acroporids recovering in the lagoon of Dongsha Atoll. Master thesis, National Sun Yat-sen University.
- Liu SYV, Wang CH, Shiao JC, Dai CF. 2011. Population connectivity of neon damselfish, *Pomacentrus coelestis*, inferred from otolith microchemistry and mtDNA. *Marine and Freshwater Research* 61(12):1416–1424 DOI 10.1071/MF10079.
- Liu SYV, Dai CF, Allen GR, Erdmann MV. 2012. Phylogeography of the neon damselfish *Pomacentrus coelestis* indicates a cryptic species and different species origins in the West Pacific Ocean. *Marine Ecology Progress Series* 458:155–167 DOI 10.3354/meps09648.
- Liu SYV, Chang FT, Borsa P, Chen WJ, Dai CF. 2014. Phylogeography of the humbug damselfish, *Dascyllus aruanus* (Linnaeus, 1758): evidence of Indo-Pacific vicariance and genetic differentiation of peripheral populations. *Biological Journal of the Linnean Society* 113(4):931–942 DOI 10.1111/bij.12378.

- Liu SYV, Tuanmu MN, Rachmawati R, Mahardika GN, Barber PH. 2019. Integrating phylogeographic and ecological niche approaches to delimitating cryptic lineages in the blue-green damselfish (*Chromis viridis*). *PeerJ* 7(5):e7384 DOI 10.7717/peerj.7384.
- Liu SYV, Hsin YC, Cheng YR. 2020. Using particle tracking and genetic approaches to infer population connectivity in the deep-sea scleractinian coral *Deltocyathus magnificus* in the South China sea. *Deep Sea Research Part I: Oceanographic Research Papers* 161(3):103297 DOI 10.1016/j.dsr.2020.103297.
- McCook L, Almany GR, Berumen ML, Day J, Green AL, Jones GP, Leis JM, Planes S, Russ GR, Sale PF, Sale PF, Thorrold SR. 2009. Management under uncertainty: guide-lines for incorporating connectivity into the protection of coral reefs. *Coral Reefs* 28(2):353–366 DOI 10.1007/s00338-008-0463-7.
- McCormick MI. 1999. Delayed metamorphosis of a tropical reef fish (*Acanthurus triostegus*): a field experiment. *Marine Ecology Progress Series* 176:25–38 DOI 10.3354/meps176025.
- Melbourne-Thomas J, Johnson CR, Alino PM, Geronimo RC, Villanoy CL, Gurney GG. 2011. A multi-scale biophysical model to inform regional management of coral reefs in the western Philippines and South China Sea. *Environmental Modelling and Software* 26(1):66–82 DOI 10.1016/j.envsoft.2010.03.033.
- Mellin C, MacNeil MA, Cheal AJ, Emslie MJ, Caley MJ. 2016. Marine protected areas increase resilience among coral reef communities. *Ecology Letters* 19(6):629–637 DOI 10.1111/ele.12598.
- Met Office. 2014. Cartopy: a cartographic python library with a Matplotlib interface. Available at <https://scitools.org.uk/cartopy>.
- Oksanen J, Blanchet FG, Friendly M, Kindt R, Legendre P, McGlenn DJ, Minchin PR, O'Hara RB, Simpson G, Solymos P, Stevens HH, Szoecs E, Wagner H. 2017. vegan: Community Ecology Package. R package version 2.4-4. Available at <http://CRAN.R-project.org/package=vegan>.
- Palumbi SR, Martin AP, Romano S, Mcmilan WO, Stice L, Grabowski G. 1991. *The simple fool's guide to PCR*. Honolulu, HI: University of Hawaii.
- Paradis E. 2010. pegas: an R package for population genetics with an integrated-modular approach. *Bioinformatics* 26(3):419–420 DOI 10.1093/bioinformatics/btp696.
- Riginos C, Crandall ED, Liggins L, Gaither MR, Ewing RB, Meyer C, Andrews KR, Euclide PT, Titus BM, Therkildsen NO, Salces-Castellano A, Stewart LC, Toonen RJ, Deck J. 2020. Building a global genomics observatory: using geome (the genomic observatories metadata) to expedite and improve deposition and retrieval of genetic data and metadata for biodiversity research. *Molecular Ecology Resources* 20:1458–1469.
- Robitzch V, Saenz-Agudelo P, Berumen ML. 2020. Travel with your kin ship! Insights from genetic sibship among settlers of a coral damselfish. *Ecology and Evolution* 10(15):8265–8278.
- Sala E, Mayorga J, Bradley D, Cabral RB, Atwood TB, Auber A, Cheung W, Costello C, Ferretti F, Friedlander AM, Gaines SD, Garilao C, Goodell W, Halpern BS, Hinson A, Kaschner K, Kesner-Reyes K, Leprieur F, McGowan J, Morgan LE, Mouillot D, Palacios-Abrantes J, Possingham HP, Rechberger KD, Worm B, Lubchenco J. 2021. Protecting the global ocean for biodiversity, food and climate. *Nature* 592:397–402.
- Schliep KP. 2011. phangorn: phylogenetic analysis in R. *Bioinformatics* 27:592–593.
- Selig ER, Bruno JF. 2010. A global analysis of the effectiveness of marine protected areas in preventing coral loss. *PLOS ONE* 5:e9278.
- Selkoe KA, Toonen RJ. 2011. Marine connectivity: a new look at pelagic larval duration and genetic metrics of dispersal. *Marine Ecology Progress Series* 436:291–305 DOI 10.3354/meps09238.

- Selkoe KA, D'Aloia CC, Crandall ED, Iacchei M, Liggins L, Puritz JB, von der Heyden S, Toonen RJ. 2016. A decade of seascape genetics: contributions to basic and applied marine connectivity. *Marine Ecology Progress Series* 554:1–19 DOI 10.3354/meps11792.
- Shanks AL. 2009. Pelagic Larval duration and dispersal distance revisited. *Biological Bulletin* 216(3):373–385 DOI 10.1086/BBLv216n3p373.
- Soong K, Dai CF, Lee CP. 2002. Status of pratas atoll in south china sea. In: *Proceedings of the 4th Conference on the Protected Areas of East Asia (IUCN/WCPA/EA-4)*, Taipei, Taiwan.
- Soeparno Nakamura Y, Shibuno T, Yamaoka K. 2012. Relationship between pelagic larval duration and abundance of tropical fishes on temperate coasts of Japan. *Journal of Fish Biology* 80:346–357.
- Strathman MF. 1987. *Reproduction and development of marine invertebrates of the Northern Pacific coast*. Seattle: University of Washington Press.
- Thresher RE, Brothers EB. 1985. Reproductive ecology and biogeography of indo-west pacific angelfishes (pisces: pomacanthidae). *Evolution* 39:878–887.
- Thresher R, Colin P, Bell L. 1989. Planktonic duration, distribution and population structure of Western and Central Pacific damselfishes (Pomacentridae). *Copeia* 1989:420–434.
- Underwood AJ. 1978. An experimental evaluation of competition between three species of intertidal prosobranch gastropods. *Oecologia* 33:185–202.
- Venables WN, Ripley BD. 2002. *Modern applied statistics*. New York: Springer.
- Walsh PS, Metzger DA, Higuchi R. 1991. Chelex 100 as a medium for simple extraction of DNA for PCR-based typing from forensic material. *Biotechniques* 10:506–513.
- Waples RS. 1998. Separating the wheat from the chaff: patterns of genetic differentiation in high gene flow species. *Journal of Heredity* 89(5):438–450 DOI 10.1093/jhered/89.5.438.
- Waldrop E, Hobbs J-PA, Randall JE, DiBattista JD, Rocha LA, Kosaki RK, Berumen ML, Bowen BW. 2016. Phylogeography, population structure and evolution of coral-eating butterflyfishes (Family Chaetodontidae, genus Chaetodon, subgenus Corallochaetodon). *Journal of Biogeography* 43(6):1116–1129 DOI 10.1111/jbi.12680.
- Wilson DT, McCormick MI. 1999. Microstructure of settlement-marks in the otoliths of tropical reef fishes. *Marine Biology* 134:29–41.
- Zhao M, Yu K, Shi Q, Yang H, Riegl B, Zhang Q, Yan H, Chen T, Liu G, Lin Z. 2016. The coral communities of Yongle atoll: status, threats and conservation significance for coral reefs in South China Sea. *Marine and Freshwater Research* 67(12):1888 DOI 10.1071/MF15110.

Guiding high seas conservation efforts by modelling coral and sponge habitat



SEAMOUNT RIDGES WITH RICH AND DIVERSE MARINE LIFE

The **Salas y Gómez and Nazca ridges** are two seamount chains off the coast of South America. The ridges contain more than **110 seamounts**, with summit depths ranging between over 3,000 meters to just a few meters below the surface.

The ridges support an exceptionally rich diversity of marine life, including whales, corals and many other ecologically important species. The region also has the highest level of endemism found in any marine environment. For many groups of organisms, nearly half of the species that live there are not found anywhere else on Earth.



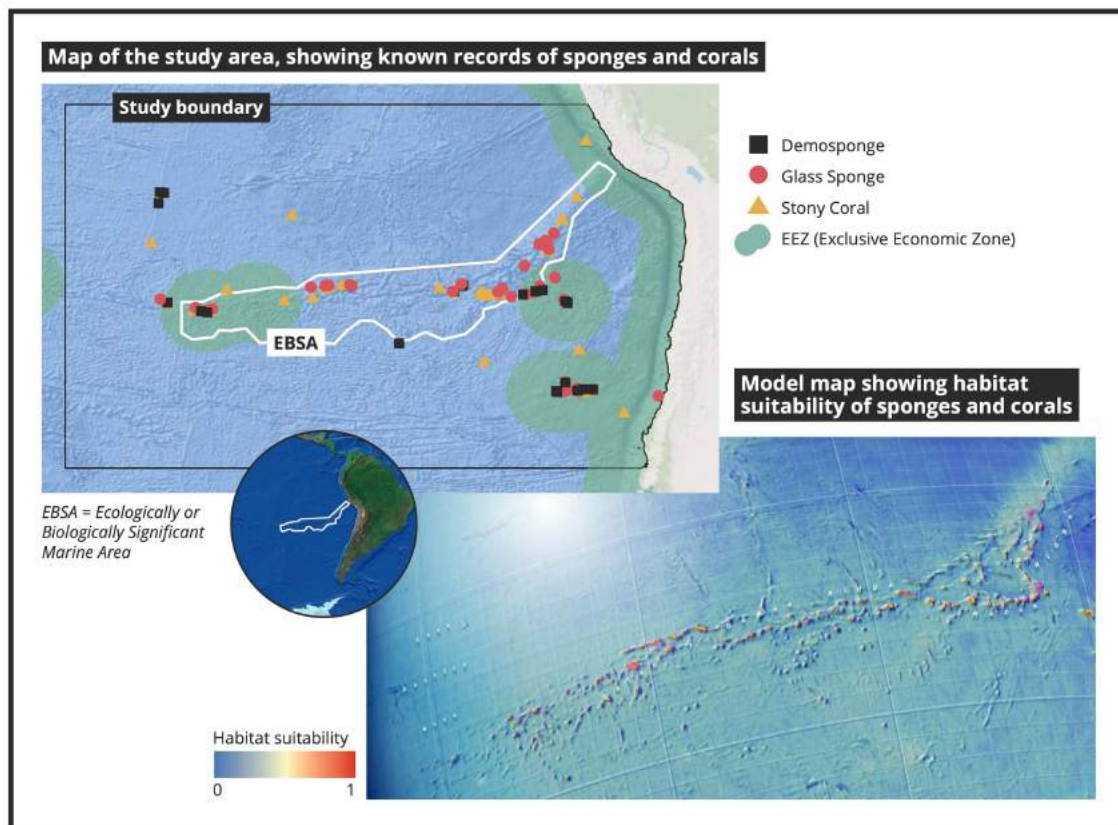
PROTECTING THE PRISTINE SEAMOUNTS

Despite some historical fishing in the region, the seamounts are relatively pristine. They are an excellent conservation opportunity to protect a global biodiversity hotspot before it is degraded. One **obstacle for effective protection is the scarcity of observational data from the region's deeper waters.**



MODELING DEEP-WATER CORAL AND SPONGE HABITAT

As a first step in mapping biodiversity along the ridges, we created **models that predict the distribution of sponges and corals.** These organisms create complex structures where diverse marine life is able to flourish.



Our models predict that the seamounts along both ridges contain highly suitable habitats for sponges and corals. This suggests that the ridges offer widespread suitable habitat for diverse marine life.

Our results strongly suggest that we must act quickly to protect these fragile habitats before they are damaged by human activities.

The modeled distribution of corals and sponges surrounding the Salas y Gómez and Nazca ridges with implications for high seas conservation

Samuel Georgian¹, Lance Morgan¹ and Daniel Wagner²

¹ Marine Conservation Institute, Seattle, Washington, United States

² Conservation International, Center for Oceans, Arlington, Virginia, United States of America

ABSTRACT

The Salas y Gómez and Nazca ridges are two adjacent seamount chains off the west coast of South America that collectively contain more than 110 seamounts. The ridges support an exceptionally rich diversity of benthic and pelagic communities, with the highest level of endemism found in any marine environment. Despite some historical fishing in the region, the seamounts are relatively pristine and represent an excellent conservation opportunity to protect a global biodiversity hotspot before it is degraded. One obstacle to effective spatial management of the ridges is the scarcity of direct observations in deeper waters throughout the region and an accompanying understanding of the distribution of key taxa. Species distribution models are increasingly used tools to quantify the distributions of species in data-poor environments. Here, we focused on modeling the distribution of demosponges, glass sponges, and stony corals, three foundation taxa that support large assemblages of associated fauna through the creation of complex habitat structures. Models were constructed at a 1 km² resolution using presence and pseudoabsence data, dissolved oxygen, nitrate, phosphate, silicate, aragonite saturation state, and several measures of seafloor topography. Highly suitable habitat for each taxa was predicted to occur throughout the Salas y Gómez and Nazca ridges, with the most suitable habitat occurring in small patches on large terrain features such as seamounts, guyots, ridges, and escarpments. Determining the spatial distribution of these three taxa is a critical first step towards supporting the improved spatial management of the region. While the total area of highly suitable habitat was small, our results showed that nearly all of the seamounts in this region provide suitable habitats for deep-water corals and sponges and should therefore be protected from exploitation using the best available conservation measures.

Submitted 23 February 2021

Accepted 23 July 2021

Published 24 September 2021

Corresponding author

Samuel Georgian, samuel.

georgian@marine-conservation.org

Academic editor

Matteo Zucchetta

Additional Information and
Declarations can be found on
page 24

DOI [10.7717/peerj.11972](https://doi.org/10.7717/peerj.11972)

© Copyright

2021 Georgian et al.

Distributed under

Creative Commons CC-BY 4.0

OPEN ACCESS

Subjects Conservation Biology, Ecology, Ecosystem Science, Marine Biology, Environmental Impacts

Keywords Cold-water corals, Sponge, Deep sea, Species distribution modeling, Habitat suitability, Conservation, Areas beyond national jurisdiction

INTRODUCTION

The Salas y Gómez and Nazca ridges are two adjacent seamount chains stretching more than 2,900 km off the coasts of Peru and Chile ([Fig. 1](#)) (reviewed in [Wagner et al., 2021](#)).

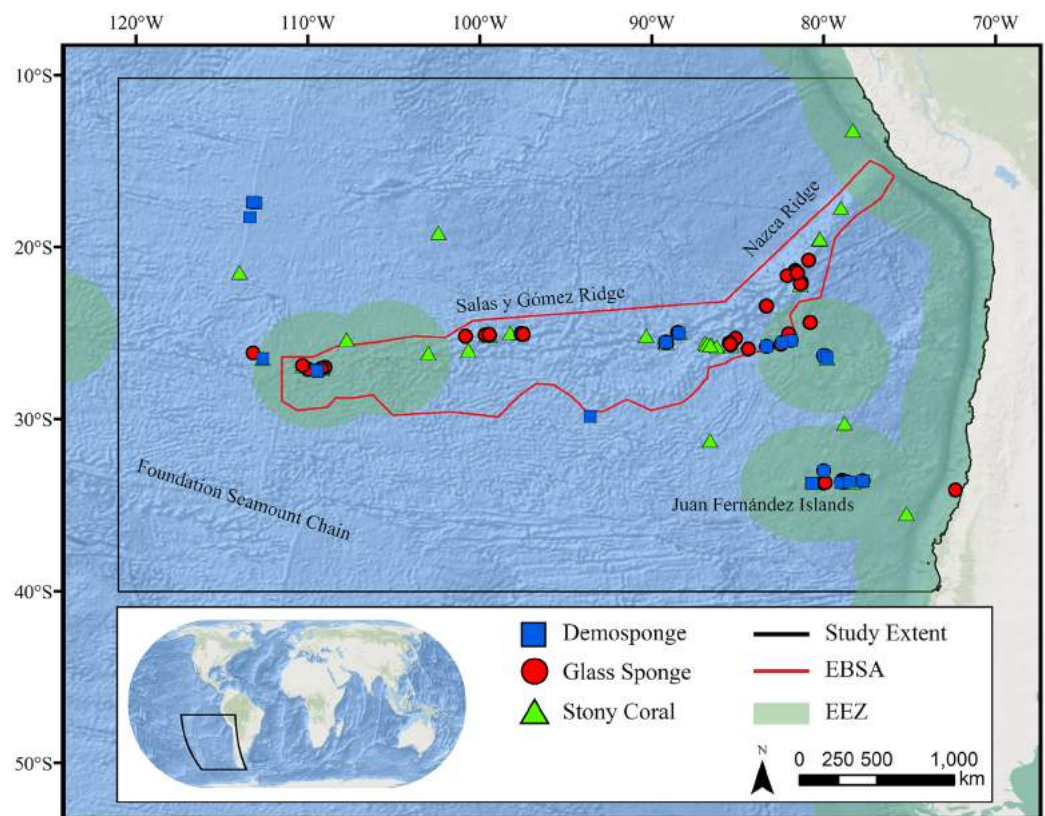


Figure 1 Map of the study area. The map shows the modeling extent, distribution of occurrence records for demosponges, glass sponges, and stony corals, national exclusive economic zones (EEZs), and Ecologically or Biologically Significant Marine Area (EBSA) designation.

Full-size DOI: [10.7717/peerj.11972/fig-1](https://doi.org/10.7717/peerj.11972/fig-1)

Combined, the ridges contain more than 110 seamounts that were created between 2–27 million years ago by a geological hotspot located on the western edge of the Salas y Gómez Ridge (Parin, Mironov & Nesis, 1997; Steinberger, 2002). The limited exploration that has been accomplished along the ridges has revealed exceptionally high biodiversity as well as unusually high endemism, due in part to its isolation from South America by the Humboldt Current System and the Atacama Trench (Parin, 1991; Comité Oceanográfico Nacional de Chile, 2017). More than 40% of known fish and invertebrate species are endemic to the region, the highest level of marine endemism in the world (Parin, Mironov & Nesis, 1997; Friedlander et al., 2016). New species have frequently and recently been discovered on the ridges (e.g., Andrade, Hormazábal & Correa-Ramírez, 2014; Sellanes et al., 2019; Shepherd et al., 2020; Diaz-Diaz et al., 2020), indicating that many new species remain to be discovered. The waters surrounding the Salas y Gómez and Nazca ridges provide important feeding grounds and migratory pathways for an array of important species, including billfish, sharks, sea turtles, seabirds and marine mammals (Weichler et al., 2004; Shillinger et al., 2008; Yanez et al., 2009; Hucke-Gaete et al., 2014; CBD, 2017; Serratos et al., 2020). On the seamounts and neighboring island habitats, diverse benthic communities form around

shallow-water, mesophotic (Easton et al., 2019), and deep-water coral and sponge reefs (Hubbard & Garcia, 2003; Easton et al., 2019; Friedlander et al., 2021).

Deep-water corals and sponges are critical foundation species found in every ocean basin. The complex, three-dimensional habitat structures they produce support thousands of associated species including other invertebrates and commercially important fish (Rogers, 1999; Costello et al., 2005; Cordes et al., 2008; Kenchington, Power & Koen-Alonso, 2013). In addition to habitat creation, corals and sponges provide other critical ecosystem services including the alteration of local current regimes (Dorschel et al., 2007; Mienis et al., 2009), carbon cycling and long-term sequestration (Oevelen et al., 2009; Kahn et al., 2015), and nutrient cycling (Wild et al., 2008; Tian et al., 2016). Deep-water corals and sponges are also being increasingly used as avenues for research purposes ranging from biomedical research (e.g., Hill, 2003; Müller et al., 2004) to reconstructing paleoclimate archives of climate change, pollution, and nutrients (Smith et al., 2000; Williams et al., 2006; Cao et al., 2007). The slow growth rates (Prouty et al., 2011), extreme longevity (Roark et al., 2009; Fallon et al., 2010), and life history strategies (e.g., low recruitment; Doughty, Quattrini & Cordes, 2014) make these taxa extremely sensitive to anthropogenic disturbance, and the recovery of damaged communities may take many decades, centuries, or even longer (see Ramirez-Llodra et al., 2011; Baco, Roark & Morgan, 2019). Considering the extreme logistical difficulties and costs associated with restoration efforts in these remote habitats (Van Dover et al., 2014), improved conservation measures are urgently needed to protect these fragile ecosystems before long-term damage occurs.

Like most marine biodiversity hotspots, the Salas y Gómez and Nazca ridges are threatened by a variety of ongoing or imminent anthropogenic disturbances, including commercial fishing, marine debris and plastic pollution, seabed mining, and climate change (reviewed in Wagner et al., 2021). Despite these threats and the clear biological value of the ridges, protecting their sensitive benthic communities from anthropogenic disturbance is a complex challenge. Over 73% of the ridges are located in areas beyond national jurisdiction (ABNJ), commonly known as the high seas, where no one country has sole management responsibility and hence international cooperation is necessary. While the portions of the ridge located within the Chilean and Peruvian exclusive economic zones (EEZs) have several established marine protected areas (MPAs) (MPAtlas, 2021), the high seas portions of the ridges are more loosely regulated by intergovernmental agencies including the International Seabed Authority (ISA), the International Maritime Organization (IMO), the Inter-American Tropical Tuna Commission (IATTC), and the South Pacific Regional Fisheries Management Organisation (SPRFMO), which regulate seabed mining, shipping, and fishing, respectively. Despite ongoing United Nations negotiations to better protect vulnerable marine ecosystems (VMEs) on the high seas (UNGA, 2007; Rogers & Gianni, 2010), there is no legal mechanism to establish high seas MPAs that are applicable to all States or sectors. Industrial fishing occurs in an estimated 48% of ABNJ, with fisheries pushing into deeper waters each year as stocks deplete in shallower waters (Visalli et al., 2020). Commercial fishing in waters surrounding the Salas y Gómez and Nazca ridges has been relatively limited historically (Wagner et al., 2021), providing a unique opportunity to protect this diverse region before it is irrevocably

damaged. However, effecting strong protection in ABNJ is difficult due to the lack of clear legal mechanisms, competing interests, and lack of sufficient data in lesser-explored regions (Gjerde *et al.*, 2021).

Species distribution models, also referred to as habitat suitability models, are important tools that help characterize the distribution and niche of taxa in data-poor regions. These models can be particularly useful for deep-water taxa on the high seas, where extremely limited surveys have occurred relative to shallow-water coastal areas (Fujioka & Halpin, 2014; Ortuño Crespo *et al.*, 2019), and data availability is a considerable obstacle to improved conservation management and scientific advancement (Vierod, Guinotte & Davies, 2014; Wagner *et al.*, 2020). Species distribution models statistically couple the known distribution of species with relevant environmental parameters to predict niche and distribution in unsurveyed geographic regions or under varying environmental conditions (Guisan & Zimmermann, 2000; Miller, 2010). Quantifying the biogeographic distribution of ecologically important or threatened species is critical for designing and implementing management plans, shaping future research and exploration efforts, and assessing past, present, and future anthropogenic impacts. Increasingly, species distribution models are being developed specifically to inform marine conservation and management (e.g., Rowden *et al.*, 2017; Georgian, Anderson & Rowden, 2019) or to predict responses to recent anthropogenic disturbances (e.g., Georgian *et al.*, 2020). Models have been successfully developed for a large variety of benthic taxa, including global models for stony corals (Davies & Guinotte, 2011), black corals (Yesson *et al.*, 2017), octocorals (Yesson *et al.*, 2012), and gorgonian corals (Tong *et al.*, 2013), as well as large-scale regional sponge models (e.g., Knudby, Kenchington & Murillo, 2013; Chu *et al.*, 2019). Given their status as foundation species, and the frequent classification of these taxa as indicators of VMEs, which SPRFMO and other fishery management organizations are mandated with identifying and protecting (e.g., Penney, Parker & Brown, 2009), it is critical to quantify their distribution.

An improved understanding of the spatial distribution of key taxa throughout the Salas y Gómez and Nazca ridges is necessary for the evidence-based conservation of the region. The suitability modeling in this study will inform ongoing efforts to identify and prioritize key conservation targets along the ridges (see Wagner *et al.*, 2021), reinforcing the increasingly clear need to protect sensitive benthic fauna in the region from further exploitation and disturbance from anthropogenic sources. In addition to conservation planning, these models will also support future expedition planning, and will improve our understanding of the niche of cold-water corals and sponges throughout the region.

MATERIALS & METHODS

Study area

The study area encompassed a large region (15,991,101 km²) of the southeast Pacific Ocean centered on the Salas y Gómez and Nazca ridges off the coasts of Peru and Chile (Fig. 1). This area contains 755 seamounts and guyots covering a total area of 561,452 km² (3.5% of the total area; geomorphology data from Harris *et al.*, 2014). The region includes

an area that has been recognized as an Ecologically or Biologically Significant Marine Area (EBSA) by the Conference of the Parties to the Convention of Biological Diversity (CBD, 2014). The EBSA extends around the ridges (Fig. 1) and includes roughly 285 seamounts and guyots covering a total area of 294,225 km² (17.2% of the EBSA area). The region is bounded on the eastern side by the Atacama Trench, which along with the Humboldt Current System isolates the ridges from South America (Von Dassow & Collado-Fabbri, 2014). The Nazca Ridge is comprised primarily of a large plateau, while the Salas y Gómez Ridge is mostly comprised of a series of smaller seamounts, escarpments, and ridge features (Fig. S21). Seamounts and features farther east along the ridges are progressively older and deeper (Rodrigo, Díaz & González-Fernández, 2014). Closer to the South American coast, a series of deep-water canyons extends into the Atacama Trench, while farther offshore the terrain is dominated by a series of large spreading ridges as well as smaller seamounts, ridges, and escarpments. The study area is primarily categorized as abyssal, with the Atacama Trench extending into hadal environments and small areas along the coasts, islands, and shallower seamounts extending upwards onto the slope and shelf (Fig. S22).

Occurrence records

Geo-referenced coral and sponge records were obtained from the Ocean Biodiversity Information System (OBIS, 2020), the NOAA Deep-Sea Coral and Sponge Database (NOAA, 2020), and records from recent expeditions to the area (J. Sellanes and E. Easton, 2020, unpublished data). All records were obtained as presence-only records, with duplicate records removed prior to analysis. The bulk of records were focused on the Salas y Gómez and Nazca ridges, with another cluster of records in the neighboring Juan Fernández Islands region. We chose to focus on three higher taxonomic groupings that are often key foundation species on seamounts: stony corals (Order: Scleractinia, $n = 233$), demosponges (Class: Demospongiae, $n = 275$), and glass sponges (Class: Hexactinellida, $n = 134$) (Tables S3–S5).

Pseudoabsence records

Species distribution models are ideally constructed using either presence-absence or abundance datasets (Winship et al., 2020). However, obtaining high-quality, true absence data is often difficult or impossible in remote environments, and particularly for deeper-water species. Even when absences are recorded, they may reflect the lack of systematic observations throughout the entire study area rather than true absence (particularly given the narrow field of view of most submersibles or towed camera arrays and similar issues with other sampling techniques such as tows or dredges). Inferring suitable habitat from absence data may also be misleading due to dispersal limitation, biotic interactions, or historical disturbances (e.g., Hirzel et al., 2002). Researchers are increasingly developing methods that account for the lack of true absence data by using sophisticated methods to produce better-than-random pseudoabsence or background data (e.g., Iturbide et al., 2015).

One of the primary limitations with species distribution models, and especially with presence-only models, is sampling bias in the occurrence data (*Kramer-Schadt et al., 2013; Syfert, Smith & Coomes, 2013*). Although often unaccounted for, sampling bias can introduce significant errors into models, affecting both their performance and ecological interpretability (e.g., *Syfert, Smith & Coomes, 2013*). We chose to reduce the effects of sampling bias by creating pseudoabsence data that has the same bias found in the presence data (*Elith, Kearney & Phillips, 2010; Huang, Brooke & Li, 2011; Fitzpatrick, Gotelli & Ellison, 2013*). To mirror the sampling bias that likely exists in our presence records, we created a two-dimensional kernel density estimate of sampling effort based on the presence locations for each taxon (Figs. S6–S8). Pseudoabsence records ($n = 10,000$) were sampled using this density estimate as a probability grid, resulting in a set of unique, sample-bias corrected pseudoabsences for each taxon.

Environmental data

Within the study area, a suite of 44 environmental variables known to influence the distribution of corals and sponges were constructed for use in models (Table 1). Bathymetry for the study area were obtained from the SRTM30+ dataset (*Becker et al., 2009; Sandwell et al., 2014*) at a resolution of 0.0083° (approximately 1 km) and used in the creation of several additional layers.

A number of terrain metrics were derived from this bathymetry layer to define the shape of the seafloor. Slope, roughness, aspect, general curvature, cross-sectional curvature, and longitudinal curvature were calculated using the ArcGIS (v10.8, ESRI) toolkit ‘DEM Surface Tools’ (v2; *Jenness, 2004; Jenness, 2013*). Slope was measured in degrees and calculated using the 4-cell method (*Jones, 1998*). Aspect represents the compass direction of the steepest slope and was converted to an index of eastness using a sine transformation and an index of northness using a cosine transformation. Curvature metrics assess the likely flow of water across a feature, with positive values generally indicating convex features that cause water to accelerate and diverge, in contrast to concave features where water would be expected to decelerate and converge. Roughness is a measure of topographical complexity, calculated here as the ratio of surface area to planimetric area, with more positive values indicating more complex terrain. The Topographic Position Index (TPI) was calculated using the toolkit Land Facet Corridor Designer (v1.2; *Jenness, Brost & Beier, 2013*). TPI assesses the relative height of features compared to the surrounding seafloor, with positive areas indicating locally elevated features and negative values indicating depressions. TPI is scale dependent, and was calculated at scales of 1,000, 5,000, 10,000, 20,000, 30,000, 40,000 and 50,000 m. Finally, the Vector Ruggedness Measure (*Hobson, 1972; Sappington, Longshore & Thompson, 2007*), which calculates terrain heterogeneity, was calculated with a neighborhood size of 3, 5, 7, 9, 15, 17 and 21 using the Benthic Terrain Modeler (v3.0; *Walbridge et al., 2018*).

To complement the suite of terrain metrics, large-scale geomorphological features expected to provide suitable habitat for corals and sponges were obtained from *Harris et al. (2014)*, including seamounts, guyots, canyons, ridges, spreading ridges, plateaus and escarpments. See Fig. S21 for a map of geomorphological features in the study area.

Table 1 Environmental variables used in model creation.

Variable name	Included in final models	Units	Native resolution	Reference
Bathymetry		meters	0.0083°	<i>Becker et al., 2009</i> <i>Sandwell et al., 2014</i>
Terrain Metrics				
Aspect–Eastness			0.0083°	<i>Jenness, 2013</i>
Aspect–Northness			0.0083°	<i>Jenness, 2013</i>
Curvature–General			0.0083°	<i>Jenness, 2013</i>
Curvature–Cross-Sectional			0.0083°	<i>Jenness, 2013</i>
Curvature–Longitudinal			0.0083°	<i>Jenness, 2013</i>
Roughness			0.0083°	<i>Jenness, 2013</i>
Slope	X	degrees	0.0083°	<i>Jenness, 2013</i>
Topographic Position Index (TPI)	X		0.0083°	<i>Jenness, Brost & Beier, 2013</i>
Vector Ruggedness Measure (VRM)	X			
Geomorphological Features				
Seamount				<i>Harris et al., 2014</i>
Guyot				<i>Harris et al., 2014</i>
Canyon				<i>Harris et al., 2014</i>
Ridge				<i>Harris et al., 2014</i>
Spreading Ridge				<i>Harris et al., 2014</i>
Plateaus				<i>Harris et al., 2014</i>
Escarpment				<i>Harris et al., 2014</i>
Benthic Conditions				
Total alkalinity		$\mu\text{mol l}^{-1}$	$3.6 \times 0.8\text{--}1.8^\circ$	<i>Steinacher et al. (2009)</i>
Dissolved inorganic carbon		$\mu\text{mol l}^{-1}$	$3.6 \times 0.8\text{--}1.8^\circ$	<i>Steinacher et al. (2009)</i>
Omega aragonite (Ω_A)	X		$3.6 \times 0.8\text{--}1.8^\circ$	<i>Steinacher et al. (2009)</i>
Omega calcite (Ω_C)			$3.6 \times 0.8\text{--}1.8^\circ$	<i>Steinacher et al. (2009)</i>
Dissolved oxygen	X	ml l^{-1}	1°	<i>Garcia et al. (2013a)</i>
Salinity		pss	0.25°	<i>Zweng et al., 2013</i>
Temperature		$^\circ\text{C}$	0.25°	<i>Locarnini, 2013</i>
Phosphate	X	$\mu\text{mol l}^{-1}$	1°	<i>Garcia et al. (2013a)</i>
Silicate	X	$\mu\text{mol l}^{-1}$	1°	<i>Garcia et al. (2013b)</i>
Nitrate	X	$\mu\text{mol l}^{-1}$	1°	<i>Garcia et al. (2013b)</i>
Particulate organic carbon (POC)	X	$\text{g C m}^{-2} \text{year}^{-1}$	0.05°	<i>Lutz et al. (2007)</i>
Regional current velocity		m s^{-1}	0.5°	<i>Carton, Giese & Grodsky (2005)</i>
Vertical current velocity		m s^{-1}	0.5°	<i>Carton, Giese & Grodsky (2005)</i>
Surface Conditions				
Chlorophyll <i>a</i>		mg m^{-3}	4 km	Aqua Modis (NOAA)
Sea Surface Temperature		$^\circ\text{C}$	4 km	Aqua Modis (NOAA)

Note:

Not all variables were retained in the final models produced. ‘Reference’ refers to either the tool used to create the variable (terrain metrics) or the original data source (other variables).

Data describing benthic conditions at the seafloor were obtained from the World Ocean Atlas (v2; 2013), including temperature, dissolved oxygen, salinity, nitrate, phosphate, and silicate. Carbonate data including dissolved inorganic carbon (DIC), total alkalinity,

and the saturation states of calcite and aragonite, were obtained from [Steinacher et al. \(2009\)](#). Current data describing regional horizontal and vertical current velocities were obtained from the Simple Ocean Data Assimilation model (SODA v3.4.1; [Carton & Giese, 2008](#)). Particulate organic carbon (POC) flux to the seafloor was obtained from [Lutz et al. \(2007\)](#). Raw benthic data layers were transformed to match the extent and resolution of the other environmental variables using the upscaling approach developed by [Davies & Guinotte \(2011\)](#). This upscaling technique incorporates bathymetry data to approximate conditions at the seafloor and has previously been demonstrated to work effectively on both global and regional scales for a variety of data ([Yesson et al., 2012](#); [Georgian, Anderson & Rowden, 2019](#)). The upscaled WOA data (dissolved oxygen, nitrate, phosphate and silicate) were compared to quality-controlled bottom-water bottle data from the Global Ocean Data Analysis Project (GLODAP v2.2019) to assess how much error may have been present in the raw WOA datasets or introduced *via* our upscaling approach (see [Fig. S23](#)).

Surface conditions were assessed as chlorophyll *a* and mean sea surface temperature data obtained from the Aqua MODIS program ([Aqua MODIS, 2018](#)). Both layers were calculated as the mean value from 2002–2016 at a resolution of 4 km, and resampled to match the extent and resolution of the other environmental layers with no additional interpolation.

Modeling techniques

Models were constructed using four different techniques that have proven successful in modeling the distribution of cold-water corals and sponges: Boosted Regression Tree (BRT), Generalized Additive Models (GAM), Maximum Entropy (Maxent), and Random Forest (RF). For each modeling technique, the sampling-bias corrected set of pseudoabsences ($n = 10,000$) was used in place of either true absences or random pseudoabsences. Each model outputs a habitat suitability score between 0–1, with higher scores indicating more suitable habitat. While often erroneously referred to as the probability of occurrence, this score does not represent a true probability of occurrence in presence-only models due to the lack of true absences and nonsystematic observation of the study area. The refinement of model parameters, final model, model evaluations, and model outputs (*e.g.*, variable importance and response curves) were completed using ‘biomod2’ ([Thuiller et al., 2016](#)), ‘gbm’ ([Ridgeway, 2004](#)), ‘dismo’ ([Hijmans et al., 2017](#)), ‘mgcv’ ([Wood & Wood, 2015](#)), and ‘randomForest’ ([Liaw & Wiener, 2002](#)) in R (v3.6.1; [R Core Team, 2019](#)).

Boosted Regression Tree (BRT) models rely on binary splits in a regression-tree structure to define the response of species occurrence or abundance to environmental variables ([Elith, Leathwick & Hastie, 2008](#)), and have been successfully used to model the distribution of deep-sea fauna (*e.g.*, [Rowden et al., 2017](#); [Georgian, Anderson & Rowden, 2019](#)). The minimum number of trees was set at 1,000, and a Bernoulli distribution of the presence-pseudoabsence data was assumed. Tree complexity was set to three to allow limited interactions between terms.

Maxent ([Phillips, Anderson & Schapire, 2006](#)) is a machine learning, presence-only modeling algorithm that has been shown to outperform other presence-only models

([Elith et al., 2006](#); [Tittensor et al., 2009](#)) and even presence-absence models ([Reiss et al., 2011](#)). Default model settings were used except the maximum number of iterations was increased to 500 to ensure that models converged. In addition, the regularization parameter (default of $\beta = 1$) was experimentally tested using values of $\beta = 1$ –10. Regularization is a smoothing function that controls the complexity of models, with higher values resulting in simpler models with fewer parameters. An ultimate value of $\beta = 5$ was chosen for all taxa based on the performance of preliminary models. Previous Maxent modeling of cold-water corals has shown that increasing β improves model performance in areas or conditions outside of the training data, essentially by preventing the model from overfitting to its training data ([Georgian, Shedd & Cordes, 2014](#)).

A Generalized Additive Model (GAM) is a type of generalized linear model that employs smoothing functions for each explanatory variable ([Hastie & Tibshirani, 1986](#)). GAM has frequently been used to model the distribution and niche of a variety of marine species including corals and sponges (e.g., [Rooper et al., 2014](#)). A binomial distribution of the presence-pseudoabsence data was assumed. Various types of smoothers and degrees of freedom allowed were explored in preliminary models, resulting in a thin plate regression spline smoothing function with 12 degrees of freedom used for all variables and modeling runs. Testing higher degrees of freedom (ranging from 4–15) resulted in small improvements in model performance but increased computational time, with no significant model improvements above 12 degrees of freedom (in general agreement with the findings of [Wood, 2017](#)).

Random Forest (RF) models ([Breiman, 2001](#)) are a classification or regression, tree-based algorithm that relies on a random selection of explanatory variables and an internal bootstrapping metric to produce and then combine a large number of trees. Default parameters were used except the number of trees was increased to 501 and tree depth was limited to a value of ten to prevent overfitting to the training data. Various tree depths (1–20) were investigated in preliminary models, and a tree depth of ten was ultimately selected as it appeared to improve model performance while preventing models from strongly overfitting to the training data. Tuning tree depth appropriately has been shown to improve model performance without significantly affecting computational time ([Duroux & Scornet, 2018](#)), with larger than default values often yielding the best results ([Segal, 2003](#)). It should be noted however that other studies have produced better results by limiting tree depth ([Nadi & Moradi, 2019](#)), suggesting that the correct tuning value may be dependent on the dataset used as well as how other model parameters are tuned in conjunction. The optimal value of ‘mtry’ was also experimentally altered in preliminary models, however, the default value (the square root of the number of explanatory variables) consistently performed well and was therefore used across all model runs.

Each modeling approach (BRT, Maxent, GAM and RF) is fundamentally distinct and depends on different structures and assumptions. Therefore, each will produce different habitat suitability maps that may reflect tradeoffs in various aspects of model performance, making it difficult to accurately determine which, if any, model type is superior ([Robert et al., 2016](#)). To create a more robust final model, we generated an

ensemble model for each taxon based on a performance-weighted average of habitat suitability scores from each model type. The BRT, Maxent, GM, and RF model for each taxon were combined using a weighted average of habitat suitability, with weights based on model performance (AUC scores).

Model testing

Models were tested using a ten-fold cross-validation procedure that randomly partitioned occurrences into 20% test data and 80% training data. Metrics of model performance were calculated for each run and averaged across all ten runs, however, final models were trained using the entire dataset. Model performance was assessed through a combination of Area Under the Curve (AUC) and the true skill statistic (TSS). AUC is a threshold-independent performance measure that in presence-only models indicates the probability that the model correctly ranks occurrences over background locations.

A random model has a theoretical AUC of 0.5, and while the maximum AUC is generally unknowable in presence-only models it is always less than 1 ([Wiley et al., 2003](#); [Phillips, Anderson & Schapire, 2006](#)). The TSS metric is similar to the conventionally reported kappa, but is independent of species prevalence as well as the size of the validation dataset ([Allouche, Tsoar & Kadmon, 2006](#)). TSS ranges from -1 to +1 with negative values indicating more random performance and positive values indicating better performance. To fine-tune model parameters (see above), the Akaike Information Criterion (AIC) was also used to assess model performance. AIC helps assess the tradeoff between goodness of fit and simplicity of models, and is therefore commonly used for model selection.

A similar ten-fold cross validation approach was used to estimate the spatial uncertainty of the models by randomly withholding 20% of occurrence and pseudoabsence data from model construction with replacement between runs. Uncertainty was then assessed as the standard deviation of habitat suitability scores across all ten model runs. This approach does not account for all possible sources of uncertainty, but provides a useful spatial measure of how sensitive the model is to the sampling of occurrence data and the construction of the pseudoabsence dataset.

Variable selection

The inclusion of highly correlated variables in species distribution models can reduce model performance and make the results more difficult to interpret ecologically ([Tittensor et al., 2009](#); [Huang, Brooke & Li, 2011](#)). Therefore, we employed a variable selection process to refine our original list of 44 environmental layers to a more parsimonious list of less-correlated variables. Variable selection was based on (1) preliminary model testing including predicted variable importance and impact on overall model performance for BRT, Maxent, GAM, and RF models, (2) correlation and clustering among variables, and (3) known biological importance for each taxon. When variables were highly correlated (Pearson's correlation coefficients >0.7) and clustered together (see [Figs. S1](#) and [S2](#)), preference was given to the variable that exhibited the best model performance, was less-correlated with other variables, clustered more independently, or was considered to be more biologically relevant.

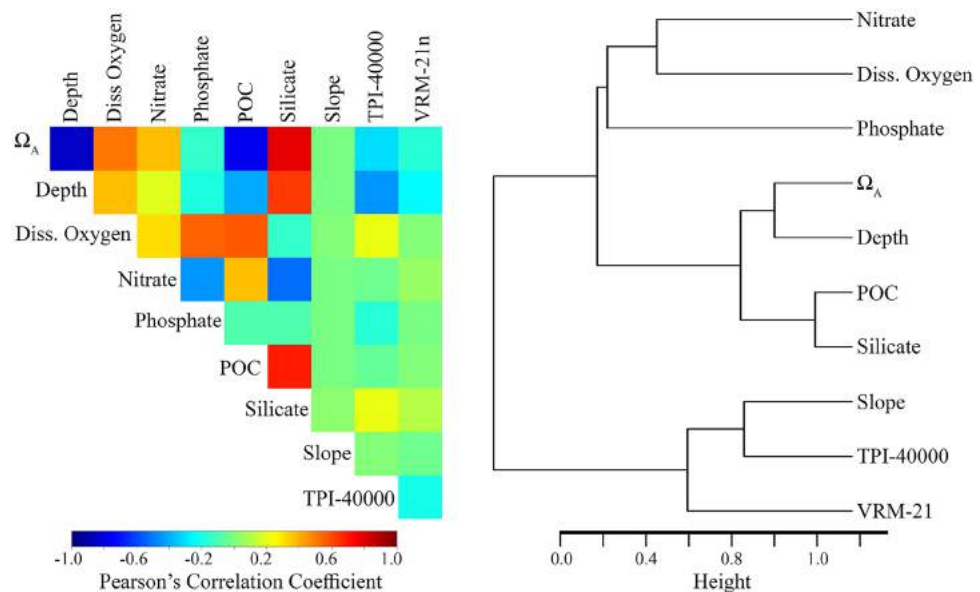


Figure 2 Relationship among the final set of environmental variables used to train the models. Depth was excluded from the final models but was included here for reference. Silicate was only included for demosponges and glass sponges. Ω_A was only included for stony corals. Left: Pearson's correlation coefficients among variables. Right: Cluster dendrogram showing the conceptual relationship among variables, with variables containing similar information clustering closer together. See Figs. S1 and S2 for the correlations and clustering of all environmental variables considered for modeling.

Full-size DOI: [10.7717/peerj.11972/fig-2](https://doi.org/10.7717/peerj.11972/fig-2)

Depth was artificially removed despite high model performance due to its high correlation with several, more biologically-relevant variables. The saturation state of aragonite (Ω_A) was included for stony corals due to moderate to high performance in preliminary models and known importance for structuring cold-water coral distributions (e.g., *Georgian, Shedd & Cordes, 2014; Georgian et al., 2016a*). Silicate concentration was included for both demosponges and glass sponges due to the inclusion of silicate in their skeletal structures and high performance in preliminary models. POC was retained despite relatively high correlations with both silicate (-0.684) and Ω_A (0.769) due to the known biological importance of all three variables and performance in preliminary models. However, it should be noted that ecological interpretations can be difficult when variables are highly correlated.

The final variable set included eight variables for each taxon, including dissolved oxygen, nitrates, phosphates, slope, TPI calculated at a scale of 40,000 m (TPI-40000), VRM calculated with a neighborhood size of 21 (VRM-21), POC, silicate (demosponge and glass sponges only), and Ω_A (stony corals only). Within the final variable set for each taxon, the highest correlation among variables was -0.684 (POC and silicate), and variables clustered relatively independently compared with the original set (Fig. 2 and Table S1).

RESULTS

Model performance

The models performed well across all taxa and modeling algorithms (Table 2). The 10-fold cross-validation procedure produced test AUC scores that were generally above 0.9, with a

Table 2 Model performance as evaluated by the AUC, and TSS metrics.

Taxa	Model	Test data		Training data	
		AUC	TSS	AUC	TSS
Demosponges	BRT	0.939 ± 0.02	0.783 ± 0.04	0.937	0.799
	GAM	0.976 ± 0.01	0.912 ± 0.03	0.974	0.799
	Maxent	0.975 ± 0.03	0.625 ± 0.06	0.817	0.524
	RF	0.837 ± 0.01	0.932 ± 0.03	0.998	0.959
	Ensemble	–	–	0.988	0.916
Glass sponges	BRT	0.868 ± 0.02	0.718 ± 0.04	0.872	0.739
	GAM	0.904 ± 0.04	0.770 ± 0.05	0.929	0.763
	Maxent	0.902 ± 0.04	0.738 ± 0.06	0.904	0.679
	RF	0.948 ± 0.04	0.862 ± 0.07	0.993	0.961
	Ensemble	–	–	0.968	0.770
Stony corals	BRT	0.915 ± 0.03	0.821 ± 0.07	0.924	0.842
	GAM	0.956 ± 0.03	0.827 ± 0.06	0.964	0.855
	Maxent	0.931 ± 0.03	0.820 ± 0.06	0.939	0.822
	RF	0.965 ± 0.02	0.901 ± 0.04	0.980	0.940
	Ensemble	–	–	0.973	0.845

Notes:

Higher values (closer to one) indicate better model performance in each metric. Each metric was calculated using test data during a ten-fold cross-validation procedure withholding 20% of records for testing, and also for the full model using all available training data. Test value are given as the mean ± standard deviation across 10 model runs.

lowest score of 0.837 (RF model for demosponges). Test TSS scores were similarly high, with an average TSS score of 0.809 across all model types and taxa. Test scores did not change considerably among different cross-validation runs, suggesting that ten runs were sufficient to capture the variation caused by withholding different testing data. Glass sponge models performed slightly worse across all modeling types (average test AUC of 0.905 and training AUC of 0.925), followed by demosponges (average test AUC of 0.932 and training AUC of 0.942). Stony corals performed the best by a small margin with an average test AUC of 0.942 and training AUC of 0.952.

Test data revealed that GAM and Maxent models consistently performed slightly better than BRT and RF models. When looking at the evaluation metrics for the final models built using all available training data, RF consistently outperformed the other approaches, consistently having the highest AUC and TSS scores. However, when looking at test scores during cross-validation, RF scores dropped considerably, suggesting that RF models were slightly overfitting to the training data despite optimization of model parameters. In contrast, Maxent models, which generally performed slightly worse than RF models when using training data, had little to no decrease in scores when using testing data, in some cases even performing better against testing data. This suggests that the optimization of the Maxent regularization parameter ($\beta = 5$, default = 1) was successful in reducing model complexity to appropriate levels without a large effect on overall model performance. Testing and training scores were similar for BRT and GAM models, with a very slight decrease in most testing scores. BRT and RF models generally had the lowest

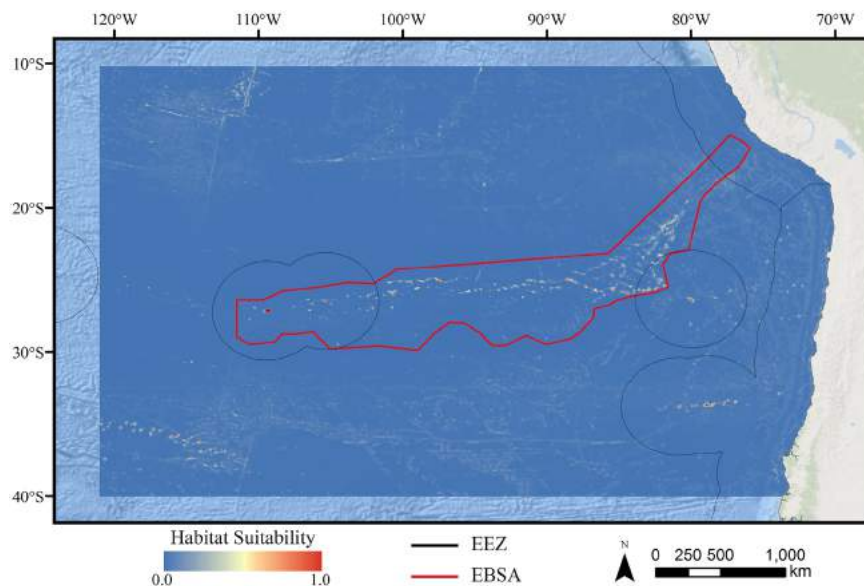


Figure 3 Predicted habitat suitability for the demosponge ensemble model. Warmer colors indicate more suitable habitat. [Full-size !\[\]\(87edba4eab630c1543c7b8d21a38a53f_img.jpg\) DOI: 10.7717/peerj.11972/fig-3](https://doi.org/10.7717/peerj.11972/fig-3)

uncertainty (Figs. S24–S35) compared to GAM and Maxent models, although GAM uncertainty was highly spatially restricted to very small areas of highly suitable habitat.

The full ensemble models performed well, with an AUC of 0.988 for demosponges, 0.968 for glass sponges, and 0.973 for stony corals. It is interesting that the demosponge ensemble model performed the best by a small margin, when the individual models performed slightly worse than the models for stony corals. This suggests that the ensemble modeling approach was successful in reducing potential structural inadequacies, lack of ideal model optimization, or bias in each model type that may affect the outputs (Robert *et al.*, 2016). In general, the scores for the ensemble models suggest that they outperformed GAM, Maxent, and BRT models, but performed slightly worse than the RF model. However, this is likely because RF models were overfitting slightly, producing artificially elevated training scores. Collectively, the performance metrics suggest that the ensemble models were the best for each taxon.

Distributions

For all three taxa, areas with high predicted habitat suitability were largely restricted to small pockets clustered around the Salas y Gómez and Nazca ridges, the eastern portion of the Foundation Seamount Chain, and the waters around the Juan Fernández Islands (Figs. 3–5). Glass sponges and stony corals also had strips of low-moderate suitability along the South American coast and along the west flank of the Atacama Trench. Stony corals models also predicted low-moderate suitability on a large spreading ridge along the East Pacific Rise, although there were few highly suitable areas (see Fig. S21). Within the Salas y Gómez and Nazca ridges, suitability predictions were remarkably similar among the three taxa, with highly suitable habitat coinciding with the flanks and summits of most seamount, knoll, and ridge features (see Fig. 6). However, glass sponges appeared to have

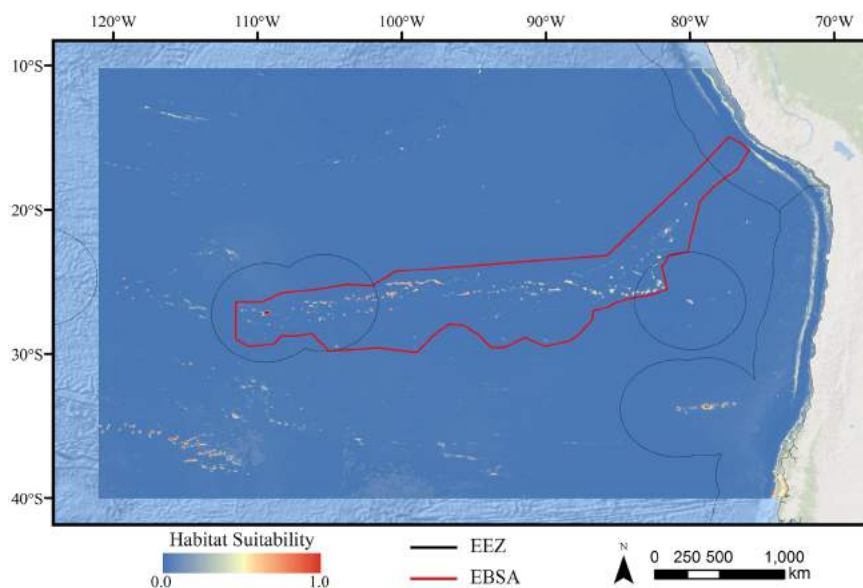


Figure 4 Predicted habitat suitability for the glass sponge ensemble model. Warmer colors indicate more suitable habitat.

Full-size [DOI: 10.7717/peerj.11972/fig-4](https://doi.org/10.7717/peerj.11972/fig-4)

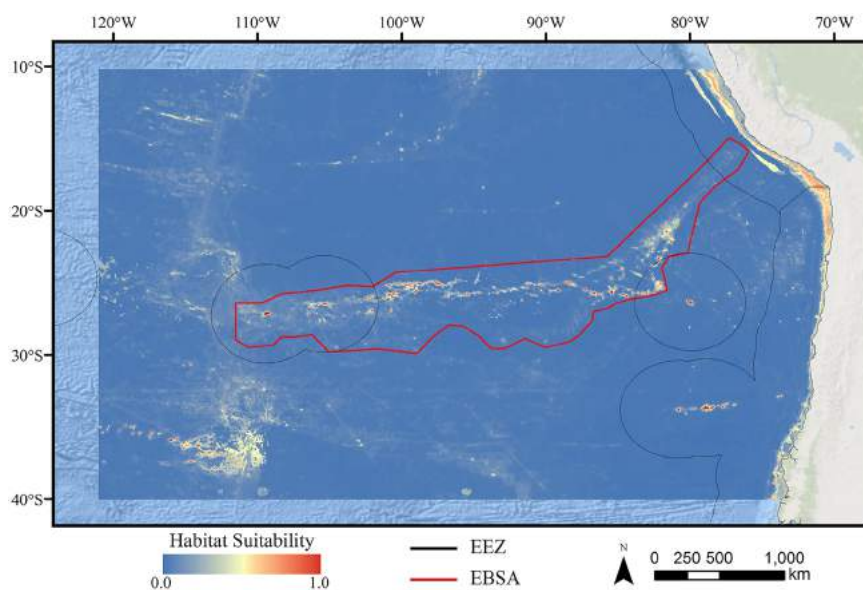


Figure 5 Predicted habitat suitability for the stony coral ensemble model. Warmer colors indicate more suitable habitat.

Full-size [DOI: 10.7717/peerj.11972/fig-5](https://doi.org/10.7717/peerj.11972/fig-5)

higher suitability predicted on the steeper sides of large seafloor features, while demosponges and stony corals were predicted to occur on the flanks and especially on the summits of the same features.

When the predicted distribution of each taxon was assessed against the large-scale geomorphological classifications (*Harris et al., 2014*, see [Fig. S21](#)), a clear preference for escarpments, ridges, seamounts, guyots, and plateaus (primarily along the Nazca Ridge) emerged ([Table S2](#)). BRT and RF models typically predicted narrow distributions clustered

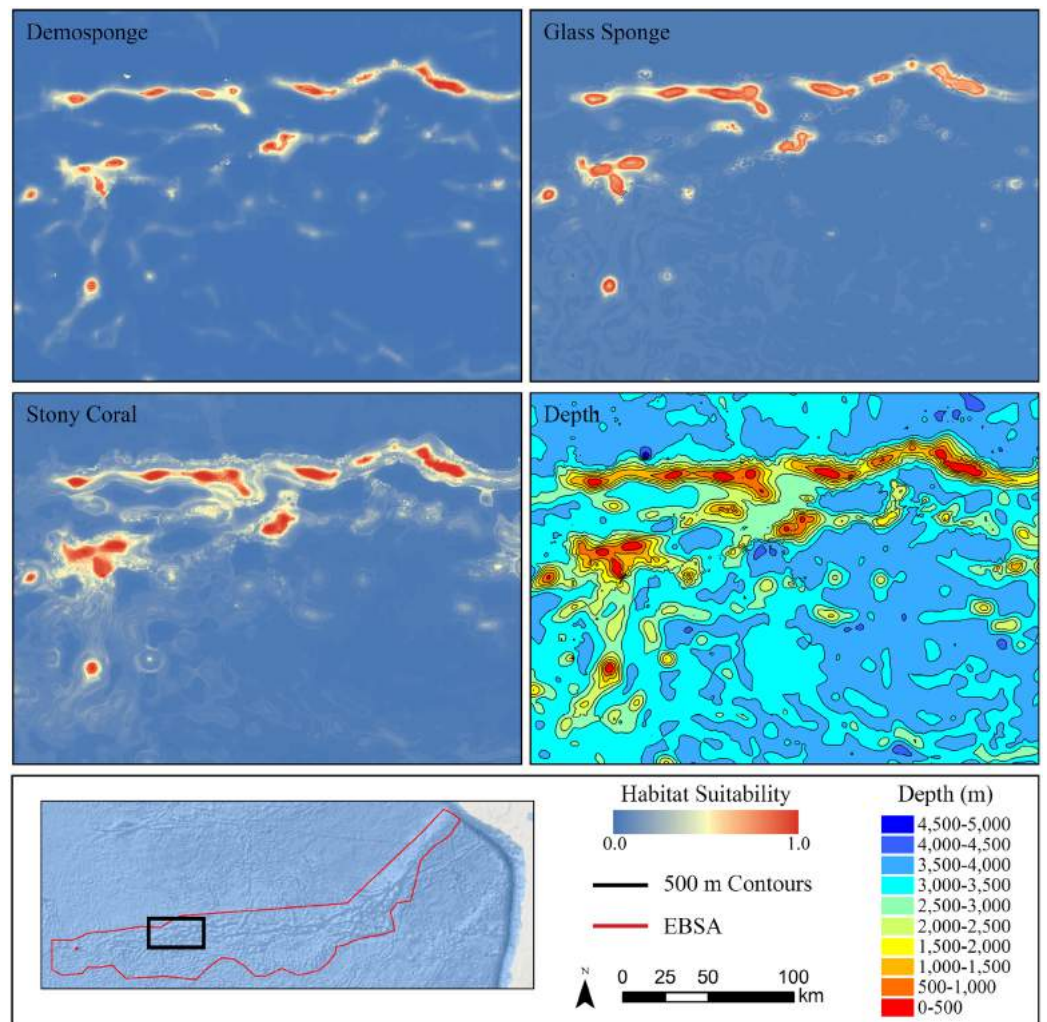


Figure 6 Ensemble models for demosponges, glass sponges, and stony corals showing a subset of highly suitable seamounts on the western side of the Salas y Gómez Ridge. Depth with 500 m contours is shown in the last panel for reference. [Full-size !\[\]\(67dcee5a7af814623519cd06e5005e63_img.jpg\) DOI: 10.7717/peerj.11972/fig-6](https://doi.org/10.7717/peerj.11972/fig-6)

almost exclusively on seamounts and other large terrain features, while Maxent and GAM also predicted areas of low-moderate suitability in bands along the coast, spreading ridges, and smaller-scale terrain features throughout the region (Figs. S9–S20). While the highly suitability regions were remarkably similar among modeling types, structural differences or assumptions in each model type did affect the overall suitability predictions, lending additional support for the creation and use of ensemble models rather than relying on a single model. It should be noted that model uncertainty was generally highest in areas with higher predicted habitat suitability (Figs. S24–S35), as well as in more coastal areas, suggesting that additional field surveys may improve models in these areas.

Niche

The niche of each taxa was assessed *via* a combination of variable contribution to the models (Table 3), response curves showing how predicted suitability changes over a range

Table 3 Percent variable contributions to each model.

Taxa	Model	Ω_A	Dissolved oxygen	Nitrate	Phosphate	POC	Silicate	Slope	TPI-40,000	VRM-21
Demosponges	BRT	–	0.0	0.4	0.3	3.7	8.5	0.1	86.0	1.0
	GAM	–	19.0	15.9	4.2	16.7	27.4	3.8	7.4	5.6
	Maxent	–	0.0	0.0	2.4	19.3	0.2	2.3	50.4	25.4
	RF	–	0.6	4.5	5.8	6.5	35.5	1.9	37.4	7.7
Glass sponges	BRT	–	0.1	0.3	0.1	12.5	78.3	7.3	0.6	0.9
	GAM	–	0.9	8.5	25.7	3.3	52.5	5.0	3.5	0.6
	Maxent	–	3.2	3.5	0.8	1.0	62.8	11.8	4.3	12.7
	RF	–	3.5	5.7	7.9	26.8	31.1	13.6	7.5	3.9
Stony corals	BRT	80.3	0.1	0.1	0.0	0.4	–	0.3	18.1	0.6
	GAM	48.9	1.0	1.6	37.4	5.2	–	0.5	2.4	2.9
	Maxent	89.7	0.1	0.0	0.0	4.8	–	0.3	0.0	5.1
	RF	54.1	2.2	7.0	3.2	1.6	–	1.1	28.6	2.2

Note:

Ω_A was only included in stony coral models. Silicate was only included in demosponge and glass sponge models. POC=particulate organic carbon.

TPI-40,000 = topographic position index calculated at the 40,000 m scale. VRM-21 = vector ruggedness measure calculated with a neighborhood size of 21. The top three variables for each model are highlighted in bold.

of environmental conditions (Fig. 7), and bean plots showing the environmental conditions occurring in the known distribution of each taxa compared to background conditions (Figs. S3–S5).

Terrain metrics consistently contributed a considerable amount of information in each model. Across all model types for demosponges, slope contributed an average of 2% of information, TPI-40,000 contributed an average of 45.3%, and VRM-21 contributed an average of 9.9%. For glass sponges, slope contributed an average of 9.4%, TPI-40,000 contributed an average of 4.0%, and VRM-21 contributed an average of 4.5%. For stony corals, slope contributed an average of 0.6%, TPI-40,000 contributed an average of 12.3%, and VRM-21 contributed an average of 2.7%. Considered jointly, terrain comprised between 15.5–57.3% of information for each taxon, suggesting that the shape of the seafloor is an important component of their niche. Response curves and bean plots suggest that stony corals and demosponges have a clear preference for elevated TPI values (indicating large-scale elevated features). All three taxa show a preference for elevated VRM values (indicating more varied terrain). Interestingly, VRM-21 correlated and clustered with seamounts (Pearson's coefficient of 0.5; Figs. S1 and S2), indicating that at this scale, VRM-21 was a likely an indicator of features similar in topography to seamounts, guyots, and knolls. Bean plots showed that the known distribution of all three taxa coincides with higher slope values of approximately 5–20 degrees compared with background data, however, response curves indicated a more complex relationship. Demosponges exhibited a small preference for elevated slopes, while glass sponges had a large preference for slopes up to approximately 15 degrees, and then a lower preference for steeper slopes. Stony corals had a negative affinity for slopes steeper than 5°.

Silicate was the highest performing variable for glass sponge models (average contribution of 56.2 across model types), and the second highest for demosponges (average

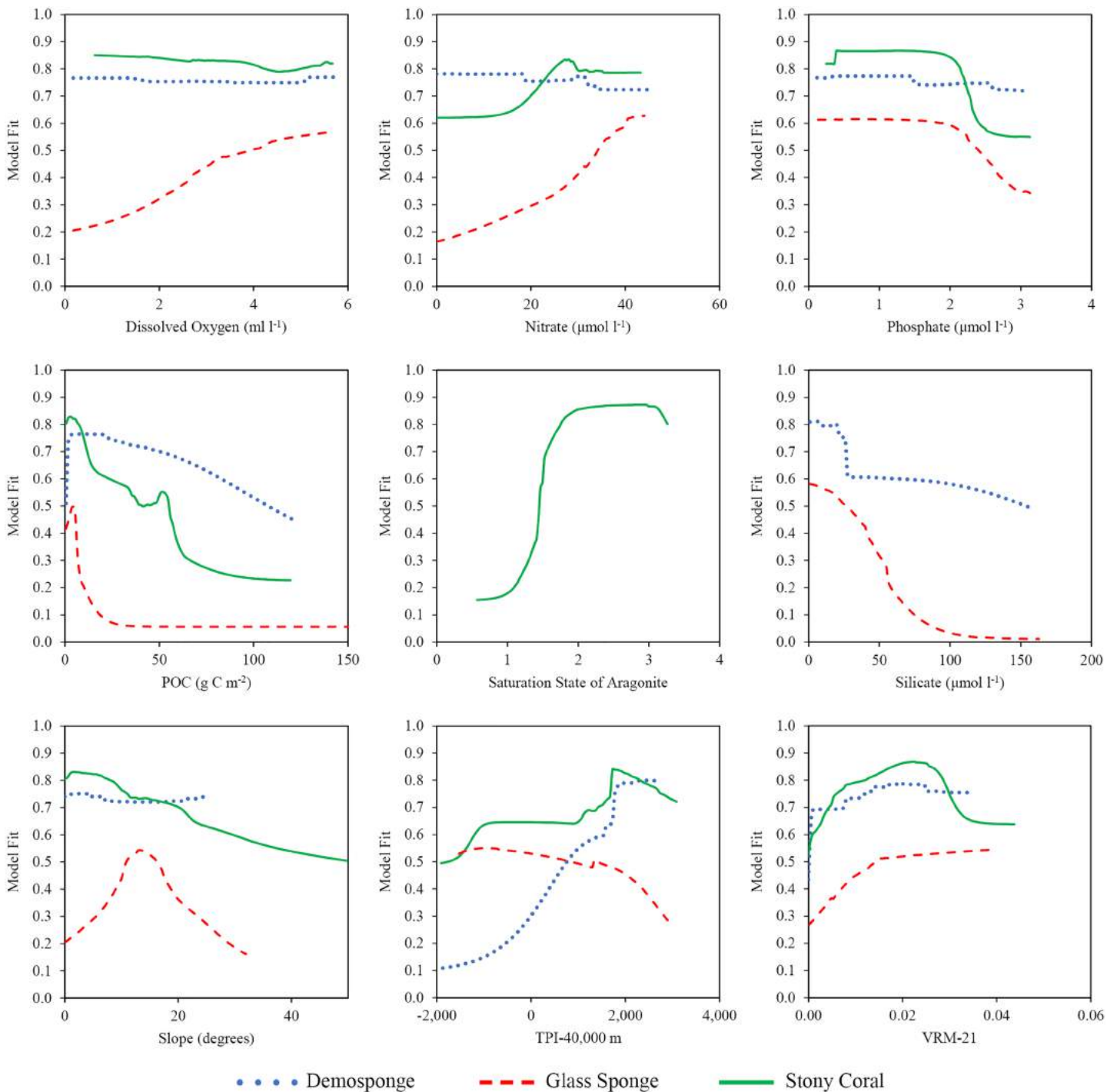


Figure 7 Response curves showing how the model fit changes over the range of each environmental variable. Values were calculated for the final variable set using the ensemble model for each taxa. Silicate was only included in demosponge and glass sponge models, and Ω_A was only included in the stony coral model. [Full-size DOI: 10.7717/peerj.11972/fig-7](https://doi.org/10.7717/peerj.11972/fig-7)

contribution of 17.9% across model types). Response curves indicated that both sponge taxa have a large drop-off in predicted suitability once silicate values exceed approximately 30–40 $\mu\text{mol l}^{-1}$, and bean plots show that both taxa occur at lower than expected silicate

values relative to the background environment. It should be noted that silicate had high correlations with other retained variables, including POC (Pearson's coefficient of -0.684) and nitrates (Pearson's coefficient of 0.538), which complicates the ecological interpretation of these results.

For stony corals, Ω_A contributed by far the most information in each model type with an average of 68.3% across all models. A clear preference in both response curves and bean plots for elevated Ω_A values above 1.5 indicated a need for a supersaturated environment. All three taxa were also moderately-highly influenced by POC, with response curves indicating a small spike in suitability between $0-10 \text{ g C m}^{-2}$, and then a rapid decrease in suitability at higher concentrations. However, an analysis of the bean plots indicates that POC values $> 5 \text{ g C m}^{-2}$ are rare in the study area, and that all three taxa occur at higher than expected concentrations compared with background values.

Dissolved oxygen, nitrate, and phosphate concentrations were only moderately important in the models for each taxon, generally only entering the top three variables in GAM models, which typically included more moderate contributions from all variables rather than receiving large contributions for a few variables. Response curves indicated that glass sponges preferred elevated dissolved oxygen concentrations, while demosponges and stony corals did not have a clear response. Both sponge taxa appeared to moderately prefer higher nitrate values, while stony corals indicated a small preference for lower values. All three taxa exhibited a moderate preference for lower phosphate concentrations.

DISCUSSION

Overview

In order to better inform the spatial management of fisheries and other human activities in the Salas y Gómez and Nazca ridges, we developed ensemble species distribution models for three taxa that are frequently classified as indicator taxa for VMEs (e.g., [Penney, Parker & Brown, 2009](#); [Parker, Penney & Clark, 2009](#): demosponges, glass sponges, and stony corals). These taxa act as critical foundation species in deep waters due to their habitat creation and other critical ecosystem services ([Roberts et al., 2009](#)). These areas are VMEs due to their susceptibility to disturbance based on the fragility, rarity, functional significance, and life history traits of their members ([FAO, 2009](#)). The United Nations require that states and associated intergovernmental agencies identify and protect VMEs, including the closure of fisheries when necessary ([UNGA, 2007](#)). A better understanding of the spatial distribution and niche of key VME taxa is a critical step towards enacting protection for these fragile and diverse habitats.

The models show that only a small portion of the total study area contained moderately or highly suitable habitat, with the most suitable habitat clustered around topographic highs along the Salas y Gómez and Nazca ridges, the waters around the Juan Fernández Islands, and the Foundation Seamount Chain. The patchy nature of the predicted distribution of all three taxa highlights the difficulties in achieving optimal spatial management with limited observation data, and reinforces the need for species distribution modeling to fill in key knowledge gaps. While the total area of highly suitable seafloor was predicted to be small, these patches extend over large distances, necessitating a regional

conservation approach. It is also important to note that most large-scale features (e.g., seamounts, guyots, ridges, and escarpments) were predicted to be highly suitable for all three taxa, particularly within the Salas y Gómez and Nazca ridges. Surveys in the area have shown that seamounts along the ridges have unique assemblages, including species not found elsewhere along the ridges (*Comité Oceanográfico Nacional de Chile, 2017*), further supporting the argument that protecting all of these features should be a high priority for conservation.

Influence of environmental conditions

Elevated and more complex seafloor topography has long been known to exert a strong influence on the success of many benthic species including corals and sponges (e.g., *Rowden et al., 2017; Chu et al., 2019*). As suspension and filter feeders, corals and sponges are heavily reliant on local and regional currents to increase food supply (*Purser et al., 2010*), transport larva (*Piepenburg & Müller, 2004*), and prevent sedimentation of both tissues and benthic surfaces required for recruitment (*Rogers, 1994*). Elevated and complex terrain affect current regimes in ways that can be favorable for the recruitment and success of cold-water corals and sponges (*Masson et al., 2003; Bryan & Metaxas, 2006*). Accordingly, all three taxa in our study appeared to have a strong affinity for seamounts, guyots, ridges, and escarpments, with a clear preference for high TPI and VRM values (indicating locally elevated and complex surfaces).

It was surprising that stony corals appeared to prefer flatter surfaces, while both sponge groups preferred steeper slopes. The response of stony corals to slope may be explained by the low variable contribution of slope to the stony coral model, and the larger contribution of other terrain features. However, a closer examination of the habitat suitability predictions around large seafloor features showed that stony corals appeared to prefer the summits of seamounts and flat-topped guyots to their steeper flanks, suggesting that this relationship may reflect a real preference for being on the tops, rather than the sides, of large terrain features. In contrast, highly suitable glass sponge habitats clustered preferentially on the steeper slopes of large features while also showing a preference for steeper slopes. The flanks and summits of seamounts can contain drastically different environmental conditions due to depth gradients, extreme hydrological forces, exposure to oxygen-minimum zones, and the topography and sediment type of the summit (*Clark et al., 2010*). Further observations on a finer scale than achieved here are necessary to confirm and explain this pattern.

The waters surrounding the Salas y Gómez and Nazca ridges are generally oligotrophic (*Von Dassow & Collado-Fabbri, 2014; González et al., 2019*) and oxygen-poor (*Espinoza-Morriberón et al., 2019*), suggesting that these variables could play large roles in determining species distributions throughout the region. Nitrate and phosphate only contributed a low-moderate amount of information to the models for each taxon, although response curves did indicate that both sponge taxa had an apparent preference for higher nitrate and lower phosphate concentrations. However, research suggests that phosphate and nitrate uptake in sponges is negligible and unlikely to significantly limit distribution (*Yahel et al., 2007; Perea-Blazquez, Davy & Bell, 2012*).

Dissolved oxygen concentration is frequently suggested as being critically important for cold-water corals (*Dodds et al., 2007; Lunden et al., 2014*) and sponges (*Whitney et al., 2005*). However, it generally did not contribute considerable information to the models in this study, and only glass sponges demonstrated a notable increase in suitability in response to higher dissolved oxygen concentrations. For stony corals and demosponges, this may suggest that dissolved oxygen is not a limiting factor in the region, congruent with other work showing that cold-water coral communities can grow successfully even in very low oxygen conditions (e.g., approximately 2.5 ml l^{-1} at deep-water reefs in the Gulf of Mexico; *Georgian et al., 2016a*). Similarly, research suggests that some sponges can tolerate periods of hypoxia, although they do so at the expense of other metabolic functioning (*Leys & Kahn, 2018*). In contrast, low dissolved oxygen concentrations have been suggested to be the primary limiting growth factor for glass sponge reefs in some regions (*Leys et al., 2004*), suggesting that dissolved oxygen may partially limit their distribution on the Salas y Gómez and Nazca ridges.

POC flux to the seafloor represents a proxy for food supply to benthic communities and is critically important for the success of deep-water corals and sponges (*Wagner et al., 2011; Kahn et al., 2015*). POC contributed significantly to the models for all taxa in this study, with suitability predicted to be highest at POC fluxes between approximately $5\text{--}50 \text{ g C m}^{-2}$. It was surprising that habitat suitability for each taxon actually decreased after POC fluxes of approximately 50 g C m^{-2} . However, correlations with other variables including depth, dissolved oxygen, temperature, Ω_A , and silicate may explain this trend. POC values greater than 50 g C m^{-2} were also spatially rare within the study region, with higher values almost exclusively occurring in shallower, coastal waters. In the offshore regions containing deep-water coral and sponge habitats, POC flux was extremely low (generally $<10 \text{ g C m}^{-2}$), suggesting that these communities may be food limited by default. However, corals and sponges may also uptake dissolved organic carbon (DOC) (*Weisz, Lindquist & Martens, 2008; Gori et al., 2014*), or receive food from the lateral transport of POC (e.g., *Rowe et al., 2008*), potentially decoupling the relationship between vertical POC flux to the seafloor and food supply.

Stony corals produce their hard skeletons using the aragonite form of calcium carbonate, with this mineral often serving as the foundation of entire deep-water ecosystems. The saturation state of aragonite (Ω_A) represents the tendency for aragonite to form or dissolve in seawater, with values >1 indicating supersaturated waters where formation is thermodynamically favored. In our study, Ω_A was the dominant contributing variable in each model type for stony corals, with response curves indicating a clear preference for supersaturated Ω_A values above approximately 1.5. This conforms with numerous field surveys (*Lunden et al., 2014; Georgian et al., 2016a*), experimental results (*Georgian et al., 2016b; Kurman et al., 2017*), and modeling studies (e.g., *Guinotte et al., 2006; Davies & Guinotte, 2011*) suggesting that aragonite supersaturation is a primary requirement for the growth and success of deep-water stony corals. While survival is still possible in undersaturated waters (*Thresher et al., 2011*), there are large energetic costs associated with calcifying under these conditions (*McCulloch et al., 2012; Wall et al., 2015*),

which generally require additional resources *via* increased feeding rates (Georgian *et al.*, 2016b).

While silicate was important in both sponge models, it was surprising that demosponge and glass sponge suitability was lower in areas with higher silicate concentrations, as both taxa produce extensive silicate skeletal materials (as much as 80% of the dry weight of glass sponges can be made up of silicate; Chu *et al.*, 2011). Previous work has found clear links between sponge distributions and silicate concentrations (*e.g.*, Whitney *et al.*, 2005; Howell *et al.*, 2016), with silicate uptake becoming more energetically costly when environmental concentrations are low (Krasko *et al.*, 2000). However, extensive glass sponge reefs have been documented at similar silicate concentrations (approximately 50 $\mu\text{mol l}^{-1}$; Chu *et al.*, 2011) that still coincided with predicted high suitability in our study, with response curves indicating a steep decline in suitability in concentrations starting only around 30 $\mu\text{mol l}^{-1}$. This suggests that it is possible that once a minimum concentration of silicate is reached, there is little additional biological benefit to growing in higher concentrations, allowing the relative importance of other variables to become more important. This finding aligns well with previous research suggesting that a lower silicate level of approximately 30–40 $\mu\text{mol l}^{-1}$ may be the lower limit for optimal sponge growth (Leys *et al.*, 2004).

It is also possible that the lower native resolutions of the nutrient, POC, aragonite saturation state, and dissolved oxygen datasets (see Table 1) precluded a more important role in the models, as well as potentially complicating their ecological interpretability. In addition, as comparisons of interpolated layers were not perfectly correlated with water-controlled bottle data from GLODAP (Fig. S23), it is likely that the environmental layers used in our study contain small errors, or that these data are temporally variable. These potential sources of error may complicate the ecological interpretation of these variables, especially when variables are already moderately to highly correlated with other variables (whether included or excluded in final models; see Table S1). However, bean plots and response curves generally demonstrated a strong habitat preference for most key variables, suggesting that these variables are more important on regional scales where the effects of small errors should be negligible. Future work should be completed to improve variable resolution and validate these data in order to more accurately assess how these environmental conditions affect the distribution and niche of these taxa throughout the region. Improved datasets would also considerably improve our ability to predict and map the potential shift in suitable habitat under future scenarios expected with ongoing warming, ocean acidification, shifts in primary productivity, and deoxygenation.

Threats

Anthropogenic impacts to deep-sea environments are increasing at an unprecedented rate and scale (reviewed in Ramirez-Llodra *et al.*, 2011). Despite their remote offshore location, the Salas y Gómez and Nazca ridges are not immune to the risks posed by human activities, including commercial fishing, pollution, climate change, and potential seabed mining (reviewed by Wagner *et al.*, 2021). Bottom fisheries are frequently cited as one

of the most damaging activities for deep-water coral and sponge habitats (*Watling & Norse, 1998; Pusceddu et al., 2014*), given the indiscriminate and destructive nature of the trawls, lines, and other equipment used. Suitable habitat for corals and sponges often overlaps with bottom fisheries due to the strong association of many demersal fish species with seamounts and similar features, as well as with the habitat structures created by corals and sponges themselves (*Baillon et al., 2012; Kutti et al., 2014*). The Salas y Gómez and Nazca ridges have been sporadically but not heavily trawled in the past, with a bottom trawl closure for orange roughy enacted by SPRFMO in 2006 (reviewed in *Tingley & Dunn, 2018*). Long-lining and pelagic fisheries do target the ridges, but for most target species, fishing effort in the region has been historically low (*Wagner et al., 2021*). Therefore, this area presents a unique opportunity to implement strong protections before widespread and irrevocable damage occurs.

Like every major marine habitat studied, the Salas y Gómez and Nazca ridges are affected by marine debris pollution including abandoned fishing gear and plastics, with the bulk of materials stemming from high seas fisheries in the South Pacific (*Luna-Jorquera et al., 2019*) or coastal regions *via* the confluence of the Humboldt Current System and the South Pacific Subtropical Gyre (*Thiel et al., 2018*). Plastic pollution alone is estimated to affect more than 97 species in the region through entanglement and ingestion, including fish, sea turtles, seabirds, and marine mammals. While the harmful effects of marine debris are better documented in pelagic species, microplastics have been found to significantly reduce the growth and feeding of deep-water corals, and derelict fishing gear causes physical damage to deep-water reefs and harms mobile fauna *via* ghost fishing (*Chapron et al., 2018; La Beur et al., 2019*).

Seabed mining is a new but imminent threat to many deep-sea environments including the Salas y Gómez and Nazca ridges. Deposits of cobalt, manganese, and polymetallic massive sulfides are known to exist on or near the ridges (*Hein et al., 2013; Miller et al., 2018; García et al., 2020*), leaving this area susceptible to future mining interests. While seabed mineral extraction has not yet occurred, rising demand for minerals coupled with technological advances in mining equipment are rapidly increasing global interest in the mining industry. If allowed to occur, seabed mining will cause widespread and serious harm to sensitive benthic habitats *via* the physical disruption of the seafloor and sedimentation of neighboring habitats (*Van Dover et al., 2017*).

One of the largest threats to most marine habitats is anthropogenic emissions, which are driving unprecedented rates of warming, deoxygenation, acidification, and decreased productivity in deep-sea environments (*Mora et al., 2013*). For coral and sponge habitats along the Salas y Gómez and Nazca ridges that already experience average or seasonally low dissolved oxygen, low Ω_A , high temperatures, or low POC flux, climate change may rapidly render even highly suitable habitats unviable for the long-term survival of these taxa. If the rate of environmental change is faster than species can adapt or acclimate, the distribution of many fauna may be considerably reduced, potentially resulting in widespread ecosystem collapse (*e.g., Ullah et al., 2018*). Climate change will also exacerbate local stressors including fishing and pollution, reducing both the resiliency of ecosystems as well as their ability to recover from disturbances. However, marine protected areas are

increasingly viewed as a viable tool to mitigate the results of climate change (*Mumby & Harborne, 2010; Micheli et al., 2012; Roberts et al., 2017*).

Implications for high seas conservation and management

ABNJ, commonly known as the high seas, cover more than 61% of the global ocean surface and 73% of its volume. These remote ocean areas are not only vast, but also critical for sustaining life on Earth, as they contain nearly 90% of the total ocean biomass, produce nearly half of the oxygen, and capture over 1.5 billion tons of carbon dioxide each year (*Van den Hove & Moreau, 2007; Global Ocean Commission, 2014; Laffoley et al., 2014*). Yet only 1.3% of ABNJ are currently protected within marine protected areas (*MPAtlas, 2021*), despite widespread and rapidly increasing threats. The lack of high seas protections is in large part due to the makeshift legal framework that is currently in place to protect ABNJ (*Molenaar & Elferink, 2009; Gjerde et al., 2016*), as well as the lack of awareness that important ecosystems exist within these remote ocean areas. The results of this study indicate that deep-sea corals and sponges, which build the foundation for some of the most abundant and diverse communities in the deep sea (*Rogers, 1999; Costello et al., 2005; Kenchington, Power & Koen-Alonso, 2013*), are widespread on seamounts and ridges located in high seas waters of the South Pacific. Given the ecological importance of deep-sea corals and sponges, and their high vulnerability to human impacts, areas that host these communities should be protected from exploitation using the best available conservation measures. Regional fishery management organizations that manage fisheries in this region, namely SPRFMO and IATTC, as well as the ISA which manages seabed mining in international waters globally, already have established mechanisms to protect sensitive marine habitats. Commercial fishing in this region has been very limited in recent years, and deep-sea mineral exploration has not occurred (*Wagner et al., 2021*), providing a time-sensitive opportunity to protect this region without significantly impacting those industries. We thus urge member States of SPRFMO, IATTC, and ISA to close this region to fishing and mining activities before it is too late.

CONCLUSIONS

The scarcity of data concerning the distribution of key habitat-forming fauna represents an obstacle to conservation efforts. We found that highly suitable habitat for demosponges, glass sponges, and stony corals likely occurs throughout the study area, particularly on large terrain features including seamounts, guyots, ridges, and escarpments of the Salas y Gómez and Nazca ridges. When previously visited during the limited expeditions to the area, these taxa were found to support abundant and diverse ecosystems housing a wide array of associated species (e.g., *Comité Oceanográfico Nacional de Chile, 2017*). It is our hope that these models will inform expedition planning and future research, improve our understanding of the niche and distribution of key taxa, and be considered in a science-based spatial management plan for the region. Anthropogenic disturbance in the deep sea is increasing at an alarming rate, making it imperative to enact strong, permanent protection before these communities are irrevocably damaged.

ACKNOWLEDGEMENTS

We are grateful for species occurrence records provided by Javier Sellanes (Universidad Católica del Norte) and Erin Easton (The University of Texas Rio Grande Valley). In addition, we are grateful to the NOAA Deep-sea Coral Data Portal and the Ocean Biodiversity Information System for their continued efforts to collect and publish taxonomic records, as well as to all of the researchers who have shared their data through these programs.

ADDITIONAL INFORMATION AND DECLARATIONS

Funding

This work was funded through the Coral Reefs of the High Seas Coalition by Conservation International, the Paul M. Angell Foundation, Alan Eustace, and Tom and Currie Barron. There was no additional external funding received for this study. The funders had no role in study design, data collection and analysis, decision to publish, or preparation of the manuscript.

Grant Disclosures

The following grant information was disclosed by the authors:

Coral Reefs of the High Seas Coalition.

Conservation International.

Paul M. Angell Foundation, Alan Eustace, and Tom and Currie Barron.

Competing Interests

The authors declare that they have no competing interests.

Author Contributions

- Samuel Georgian conceived and designed the experiments, performed the experiments, analyzed the data, prepared figures and/or tables, authored or reviewed drafts of the paper, and approved the final draft.
- Lance Morgan conceived and designed the experiments, authored or reviewed drafts of the paper, and approved the final draft.
- Daniel Wagner conceived and designed the experiments, authored or reviewed drafts of the paper, secured project funding, and approved the final draft.

Data Availability

The following information was supplied regarding data availability:

Data are available at Dryad: Georgian, Samuel (2021), The modeled distribution of corals and sponges surrounding the Salas y Gómez and Nazca ridges with implications for high seas conservation, Dryad, Dataset, DOI [10.5061/dryad.vdncjsxtc](https://doi.org/10.5061/dryad.vdncjsxtc).

Supplemental Information

Supplemental information for this article can be found online at <http://dx.doi.org/10.7717/peerj.11972#supplemental-information>.

REFERENCES

- Allouche O, Tsoar A, Kadmon R. 2006. Assessing the accuracy of species distribution models: prevalence, kappa and the true skill statistic (TSS). *Journal of Applied Ecology* 43(6):1223–1232 DOI 10.1111/j.1365-2664.2006.01214.x.
- Andrade I, Hormazábal S, Correa-Ramírez M. 2014. Time-space variability of satellite chlorophyll-a in the Easter Island Province, Southeastern Pacific Ocean. *Latin American Journal of Aquatic Research* 42(4):871–887 DOI 10.3856/vol42-issue4-fulltext-13.
- Aqua MODIS. 2018. NASA goddard space flight center, Ocean ecology laboratory, Ocean biology processing group—2018: moderate-resolution imaging spectroradiometer (MODIS) Aqua Chlorophyll and Sea Surface temperature data; 2018 reprocessing. Greenbelt, MD, USA: NASA OB.DAAC.
- Baco AR, Roark EB, Morgan NB. 2019. Amid fields of rubble, scars, and lost gear, signs of recovery observed on seamounts on 30- to 40-year time scales. *Science Advances* 5(8):eaaw4513 DOI 10.1126/sciadv.aaw4513.
- Baillon S, Hamel JF, Wareham VE, Mercier A. 2012. Deep cold-water corals as nurseries for fish larvae. *Frontiers in Ecology and the Environment* 10(7):351–356 DOI 10.1890/120022.
- Becker JJ, Sandwell DT, Smith WHF, Braud J, Binder B, Depner J, Fabre D, Factor J, Ingalls S, Kim S-H, Ladner R, Marks K, Nelson S, Pharaoh A, Trimmer R, Von Rosenberg J, Wallace G, Weatherall P. 2009. Global bathymetry and elevation data at 30 arc seconds resolution: SRTM30_PLUS. *Marine Geodesy* 32(4):355–371 DOI 10.1080/01490410903297766.
- Breiman L. 2001. Random forests. *Machine Learning* 45(1):5–32 DOI 10.1023/A:1010933404324.
- Bryan TL, Metaxas A. 2006. Distribution of deep-water corals along the North American continental margins: relationships with environmental factors. *Deep Sea Research Part I: Oceanographic Research Papers* 53(12):1865–1879 DOI 10.1016/j.dsr.2006.09.006.
- Cao L, Fairbanks RG, Mortlock RA, Risk MJ. 2007. Radiocarbon reservoir age of high latitude North Atlantic surface water during the last deglacial. *Quaternary Science Reviews* 26(5–6):732–742 DOI 10.1016/j.quascirev.2006.10.001.
- Carton JA, Giese BS, Grodsky SA. 2005. Sea level rise and the warming of the oceans in the Simple Ocean Data Assimilation (SODA) ocean reanalysis. *Journal of Geophysical Research: Oceans* 110:C09006 DOI 10.1029/2004JC002817.
- Carton JA, Giese BS. 2008. A reanalysis of ocean climate using Simple Ocean Data Assimilation (SODA). *Monthly Weather Review* 136(8):2999–3017 DOI 10.1175/2007MWR1978.1.
- CBD. 2014. Decision adopted by the Conference of the Parties to the Convention on Biological Diversity. In: *Conference of the Parties to the Convention on Biological Diversity Twelfth Meeting: Pyeongchang, Republic of Korea, 6–17 October 2014—Agenda item 21*. 59.
- CBD. 2017. Ecologically or Biologically Significant Areas (EBSAs)—Dorsal de Nazca y de Salas y Gómez (Salas y Gómez and Nazca Ridges). 8. Available at <https://chm.cbd.int/database/record?documentID=204100>.
- Chapron L, Peru E, Engler A, Ghiglione JF, Meistertzheim AL, Pruski AM, Purser A, Vétion G, Galand PE, Lartaud F. 2018. Macro-and microplastics affect cold-water corals growth, feeding and behaviour. *Scientific Reports* 8(1):1–8 DOI 10.1038/s41598-018-33683-6.
- Chu JW, Maldonado M, Yahel G, Leys SP. 2011. Glass sponge reefs as a silicon sink. *Marine Ecology Progress Series* 441:1–14 DOI 10.3354/meps09381.
- Chu JW, Nephin J, Georgian S, Knudby A, Rooper C, Gale KS. 2019. Modelling the environmental niche space and distributions of cold-water corals and sponges in the Canadian

- northeast Pacific Ocean. *Deep Sea Research Part I: Oceanographic Research Papers* **151**:103063 DOI 10.1016/j.dsr.2019.06.009.
- Clark MR, Rowden AA, Schlacher T, Williams A, Consalvey M, Stocks KI, Rogers AD, O'Hara TD, White M, Shank TM, Hall-Spencer JM. 2010. The ecology of seamounts: structure, function, and human impacts. *Annual Review of Marine Science* **2**(1):253–278 DOI 10.1146/annurev-marine-120308-081109.
- Comité Oceanográfico Nacional de Chile. 2017. Crucero CIMAR 22 Islas Oceánicas (13 de octubre al 14 de noviembre de 2016) resultados preliminares. 130. Available at <http://www.cona.cl/cimar22/librocimar22.pdf>.
- Cordes EE, McGinley MP, Podowski EL, Becker EL, Lessard-Pilon S, Viada ST, Fisher CR. 2008. Coral communities of the deep Gulf of Mexico. *Deep Sea Research Part I: Oceanographic Research Papers* **55**(6):777–787 DOI 10.1016/j.dsr.2008.03.005.
- Costello MJ, McCrea M, Freiwald A, Lundälv T, Jonsson L, Bett BJ, Van Weering TCE, De Haas H, Murray Roberts J, Allen D. 2005. Role of cold-water *Lophelia pertusa* coral reefs as fish habitat in the NE Atlantic. In: Freiwald A, Roberts JM, eds. *Cold-Water Corals and Ecosystems*. Berlin, Heidelberg: Springer, 771–805.
- Davies AJ, Guinotte JM. 2011. Global habitat suitability for framework-forming cold-water corals. *PLOS ONE* **6**(4):e18483.
- Diaz-Diaz OF, Rozbaczylo N, Sellanes J, Tapia-Guerra JM. 2020. A new species of Eunice Cuvier, 1817 (Polychaeta: Eunicidae) from the slope of the Desventuradas Islands and seamounts of the Nazca Ridge, southeastern Pacific Ocean. *Zootaxa* **4860**(2):zootaxa.4860.2.4 DOI 10.11646/zootaxa.4860.2.4.
- Dodds LA, Roberts JM, Taylor AC, Marubini F. 2007. Metabolic tolerance of the cold-water coral *Lophelia pertusa* (Scleractinia) to temperature and dissolved oxygen change. *Journal of Experimental Marine Biology and Ecology* **349**(2):205–214.
- Dorschel B, Hebbeln D, Foubert A, White M, Wheeler AJ. 2007. Cold-water coral carbonate mound hydrodynamics and facies distributions: instrumentation and model development. *Marine Geology* **244**(1–4):184–195.
- Doughty CL, Quattrini AM, Cordes EE. 2014. Insights into the population dynamics of the deep-sea coral genus *Paramuricea* in the Gulf of Mexico. *Deep Sea Research Part II: Topical Studies in Oceanography* **99**:71–82.
- Duroux R, Scornet E. 2018. Impact of subsampling and tree depth on random forests. *ESAIM: Probability and Statistics*. **22**:96–128 DOI 10.1051/ps/2018008.
- Easton EE, Gorny M, Mecho A, Sellanes J, Gaymer CF, Spalding HL, Aburto J. 2019. Chile and the Salas y Gómez ridge. In: *Mesophotic Coral Ecosystems*. Cham: Springer, 477–490.
- Elith J, Graham CH, Anderson RP, Dudík M, Ferrier S, Guisan A, Hijmans RJ, Huettmann F, Leathwick JR, Lehmann A, Li J, Lohmann LG, Loiselle BA, Manion G, Moritz C, Nakamura M, Nakazawa Y, Overton JMM, Townsend Peterson A, Phillips SJ, Richardson K, Scachetti-Pereira R, Schapire RE, Soberón J, Williams S, Wisz MS, Zimmermann NE. 2006. Novel methods improve prediction of species' distributions from occurrence data. *Ecography* **29**(2):129–151 DOI 10.1111/j.2006.0906-7590.04596.x.
- Elith J, Kearney M, Phillips S. 2010. The art of modelling range-shifting species. *Methods in Ecology and Evolution* **1**(4):330–342 DOI 10.1111/j.2041-210X.2010.00036.x.
- Elith J, Leathwick JR, Hastie T. 2008. A working guide to boosted regression trees. *Journal of Animal Ecology* **77**(4):802–813 DOI 10.1111/j.1365-2656.2008.01390.x.

- Espinoza-Morriberón D, Echevin V, Colas F, Tam J, Gutierrez D, Graco M, Ledesma J, Quispe-Ccalluari C. 2019.** Oxygen variability during ENSO in the tropical South Eastern Pacific. *Frontiers in Marine Science* 5:526.
- Fallon SJ, James K, Norman R, Kelly M, Ellwood MJ. 2010.** A simple radiocarbon dating method for determining the age and growth rate of deep-sea sponges. *Nuclear Instruments and Methods in Physics Research Section B: Beam Interactions with Materials and Atoms* 268(7–8):1241–1243.
- FAO. 2009.** *International guidelines for the management of deep-sea fisheries in the high seas*. Rome: Food and Agriculture Organization.
- Fitzpatrick MC, Gotelli NJ, Ellison AM. 2013.** MaxEnt versus MaxLike: empirical comparisons with ant species distributions. *Ecosphere* 4(5):1–15.
- Friedlander AM, Ballesteros E, Caselle JE, Gaymer CF, Palma AT, Petit I, Varas E, Wilson AM, Sala E. 2016.** Marine biodiversity in Juan Fernández and Desventuradas Islands, Chile: global endemism hotspots. *PLOS ONE* 11(1):e0145059.
- Friedlander AM, Goodell W, Giddens J, Easton EE, Wagner D. 2021.** Deep-sea biodiversity at the extremes of the Salas y Gómez and Nazca ridges with implications for conservation. *PLOS ONE* 16(6):e0253213.
- Fujioka E, Halpin PN. 2014.** Spatio-temporal assessments of biodiversity in the high seas. *Endangered Species Research* 24(2):181–190.
- Garcia HE, Locarnini RA, Boyer TP, Antonov JI, Mishonov AV, Baranova OK, Zweng MM, Reagan JR, Johnson DR. 2013a.** World ocean atlas 2013—volume 3, dissolved oxygen, apparent oxygen utilization, and oxygen saturation. In: Levitus S, Mishonov A, eds. *NOAA Atlas NESDIS 75*, 27. Available at <https://repository.library.noaa.gov/view/noaa/14849>.
- Garcia HE, Locarnini RA, Boyer TP, Antonov JI, Baranova OK, Zweng MM, Reagan JR, Johnson DR. 2013b.** World ocean atlas 2013—volume 4: dissolved inorganic nutrients (phosphate, nitrate, silicate). In: Levitus S, Mishonov A, eds. *NOAA Atlas NESDIS 76*, 25. Available at <https://repository.library.noaa.gov/view/noaa/14850>.
- García M, Correa Drubi J, Maksaev V, Townley Callejas B. 2020.** Potential mineral resources of the Chilean offshore: an overview. *Andean Geology* 47(1):1–13
DOI 10.5027/andgeoV47n1-3260.
- Georgian SE, Anderson OF, Rowden AA. 2019.** Ensemble habitat suitability modeling of vulnerable marine ecosystem indicator taxa to inform deep-sea fisheries management in the South Pacific Ocean. *Fisheries Research* 211:256–274.
- Georgian SE, DeLeo D, Durkin A, Gomez CE, Kurman M, Lunden JJ, Cordes EE. 2016a.** Oceanographic patterns and carbonate chemistry in the vicinity of cold-water coral reefs in the Gulf of Mexico: Implications for resilience in a changing ocean. *Limnology and Oceanography* 61(2):648–665.
- Georgian SE, Dupont S, Kurman M, Butler A, Strömberg SM, Larsson AI, Cordes EE. 2016b.** Biogeographic variability in the physiological response of the cold-water coral *Lophelia pertusa* to ocean acidification. *Marine Ecology* 37(6):1345–1359.
- Georgian SE, Kramer K, Saunders M, Shedd W, Roberts H, Lewis C, Fisher C, Cordes E. 2020.** Habitat suitability modelling to predict the spatial distribution of cold-water coral communities affected by the Deepwater Horizon oil spill. *Journal of Biogeography* 47(7):1455–1466.
- Georgian SE, Shedd W, Cordes EE. 2014.** High-resolution ecological niche modelling of the cold-water coral *Lophelia pertusa* in the Gulf of Mexico. *Marine Ecology Progress Series* 506:145–161 DOI 10.3354/meps10816.
- Gjerde K, Reeve L, Harden-Davies H, Ardron J, Dolan R, Durussel C, Earle S, Jimenez J, Kalas P, Laffoley D, Oral N, Page R, Chantal Ribeiro M, Rochette J, Spadone A, Thiele T,**

- Thomas HL, Wagner D, Warner R, Aulani Wilhelm T, Wright G. 2016.** Protecting Earth's last conservation frontier: scientific, management and legal priorities for MPAs beyond national boundaries. *Aquatic Conservation Marine and Freshwater Ecosystems* **26(S2)**:45–60.
- Gjerde KM, Wright G, Durussel C, Gjerde KM, Wright G. 2021.** *Strengthening high seas governance through enhanced environmental assessment processes: a case study of mesopelagic fisheries and options for a future BBNJ treaty.* STRONG High Seas Project, Potsdam, Germany: Institute for Advanced Sustainability Studies e. V. (IASS).
- Global Ocean Commission. 2014.** *From decline to recovery: a rescue package for the global ocean.* Oxford: Global Ocean Commission.
- González CE, Escribano R, Bode A, Schneider W. 2019.** Zooplankton taxonomic and trophic community structure across biogeochemical regions in the eastern South Pacific. *Frontiers in Marine Science* **5**:498.
- Gori A, Grover R, Orejas C, Sikorski S, Ferrier-Pagès C. 2014.** Uptake of dissolved free amino acids by four cold-water coral species from the Mediterranean Sea. *Deep Sea Research Part II: Topical Studies in Oceanography* **99**:42–50.
- Guinotte JM, Orr J, Cairns S, Freiwald A, Morgan L, George R. 2006.** Will human-induced changes in seawater chemistry alter the distribution of deep-sea scleractinian corals? *Frontiers in Ecology and the Environment* **4(3)**:141–146.
- Guisan A, Zimmermann NE. 2000.** Predictive habitat distribution models in ecology. *Ecological Modelling* **135(2–3)**:147–186.
- Harris PT, Macmillan-Lawler M, Rupp J, Baker EK. 2014.** Geomorphology of the oceans. *Marine Geology* **352(10)**:4–24 DOI [10.1016/j.margeo.2014.01.011](https://doi.org/10.1016/j.margeo.2014.01.011).
- Hastle TJ, Tibshirani R. 1986.** Generalized additive models (with discussion). *Statist. Sci* **1**:336–337.
- Hein JR, Mizell K, Koschinsky A, Conrad TA. 2013.** Deep-ocean mineral deposits as a source of critical metals for high-and green-technology applications: comparison with land-based resources. *Ore Geology Reviews* **51(Part. 1)**:1–14 DOI [10.1016/j.oregeorev.2012.12.001](https://doi.org/10.1016/j.oregeorev.2012.12.001).
- Hijmans RJ, Phillips S, Leathwick J, Elith J, Hijmans MRJ. 2017.** Package 'dismo'. *Circles* **9(1)**:1–68.
- Hill RT. 2003.** Microbes from marine sponges: a treasure trove of biodiversity for natural products discovery. In: *Microbial Diversity and Bioprospecting.* Washington, DC: ASM Press, 177–190.
- Hirzel AH, Hausser J, Chessel D, Perrin N. 2002.** Ecological-niche factor analysis: how to compute habitat-suitability maps without absence data? *Ecology* **83(7)**:2027–2036 DOI [10.1890/0012-9658\(2002\)083\[2027:ENFAHT\]2.0.CO;2](https://doi.org/10.1890/0012-9658(2002)083[2027:ENFAHT]2.0.CO;2).
- Hobson RD. 1972.** Surface roughness in topography: a quantitative approach. In: Chorley RJ, ed. *Spatial Analysis in Geomorphology.* London: Methuen & Co., 221–245.
- Howell KL, Piechaud N, Downie AL, Kenny A. 2016.** The distribution of deep-sea sponge aggregations in the North Atlantic and implications for their effective spatial management. *Deep Sea Research Part I: Oceanographic Research Papers* **115(C10)**:309–320 DOI [10.1016/j.dsr.2016.07.005](https://doi.org/10.1016/j.dsr.2016.07.005).
- Huang Z, Brooke B, Li J. 2011.** Performance of predictive models in marine benthic environments based on predictions of sponge distribution on the Australian continental shelf. *Ecological Informatics* **6(3–4)**:205–216 DOI [10.1016/j.ecoinf.2011.01.001](https://doi.org/10.1016/j.ecoinf.2011.01.001).
- Hubbard DK, Garcia M. 2003.** The corals and coral reefs of Easter Island—a preliminary look. In: *Easter Island.* Boston, MA: Springer, 53–77.

- Hucke-Gaete R, Aguayo-Lobo A, Yancovic-Pakarati S, Flores M. 2014.** Marine mammals of Easter Island (Rapa Nui) and Salas y Gómez Island (Motu Motiro Hiva), Chile: a review and new records. *Latin American Journal of Aquatic Research* **42**(4):743–751
DOI [10.3856/vol42-issue4-fulltext-5](https://doi.org/10.3856/vol42-issue4-fulltext-5).
- Iturbide M, Bedia J, Herrera S, Del Hierro O, Pinto M, Gutiérrez JM. 2015.** A framework for species distribution modelling with improved pseudo-absence generation. *Ecological Modelling* **312**(7):166–174 DOI [10.1016/j.ecolmodel.2015.05.018](https://doi.org/10.1016/j.ecolmodel.2015.05.018).
- Jenness JS. 2004.** Calculating landscape surface area from digital elevation models. *Wildlife Society Bulletin* **32**(3):829–839 DOI [10.2193/0091-7648\(2004\)032\[0829:CLSAFD\]2.0.CO;2](https://doi.org/10.2193/0091-7648(2004)032[0829:CLSAFD]2.0.CO;2).
- Jenness J. 2013.** *DEM surface tools*. Flagstaff: Jenness Enterprises.
- Jenness J, Brost B, Beier P. 2013.** *Land facet corridor designer*. Fort Collins: USDA Forest Service Rocky Mountain Research Station.
- Jones KH. 1998.** A comparison of algorithms used to compute hill slope as a property of the DEM. *Computers & Geosciences* **24**(4):315–323.
- Kahn AS, Yahel G, Chu JW, Tunnicliffe V, Leys SP. 2015.** Benthic grazing and carbon sequestration by deep-water glass sponge reefs. *Limnology and Oceanography* **60**(1):78–88.
- Kenchington E, Power D, Koen-Alonso M. 2013.** Associations of demersal fish with sponge grounds on the continental slopes of the northwest Atlantic. *Marine Ecology Progress Series* **477**:217–230.
- Knudby A, Kenchington E, Murillo FJ. 2013.** Modeling the distribution of *Geodia* sponges and sponge grounds in the Northwest Atlantic. *PLOS ONE* **8**(12):e82306.
- Kramer-Schadt S, Niedballa J, Pilgrim JD, Schröder B, Lindenborn J, Reinfelder V, Stillfried M, Heckmann I, Scharf AK, Augeri DM, Cheyne SM, Hearn AJ, Ross J, Macdonald DW, Mathai J, Eaton J, Marshall AJ, Semiadi G, Rustam R, Bernard H, Alfred R, Samejima H, Duckworth JW, Breitenmoser-Wuersten C, Belant JL, Hofer H, Wilting A. 2013.** The importance of correcting for sampling bias in MaxEnt species distribution models. *Diversity and Distributions* **19**(11):1366–1379.
- Krasko A, Lorenz B, Batel R, Schröder HC, Müller IM, Müller WE. 2000.** Expression of silicatein and collagen genes in the marine sponge *Suberites domuncula* is controlled by silicate and myotrophin. *European Journal of Biochemistry* **267**(15):4878–4887.
- Kurman MD, Gomez CE, Georgian SE, Lunden JJ, Cordes EE. 2017.** Intra-specific variation reveals potential for adaptation to ocean acidification in a cold-water coral from the Gulf of Mexico. *Frontiers in Marine Science* **4**:111.
- Kutti T, Bergstad OA, Fosså JH, Helle K. 2014.** Cold-water coral mounds and sponge-beds as habitats for demersal fish on the Norwegian shelf. *Deep Sea Research Part II: Topical Studies in Oceanography* **99**:122–133.
- La Beur L, Henry LA, Kazanidis G, Hennige S, McDonald A, Shaver MP, Roberts JM. 2019.** Baseline assessment of marine litter and microplastic ingestion by cold-water coral reef benthos at the East Mingulay Marine Protected Area (Sea of the Hebrides, western Scotland). *Frontiers in Marine Science* **6**:80.
- Laffoley D, Baxter JM, Thevenon F, Oliver J. 2014.** The significance and management of natural carbon stores in the open ocean. IUCN Global Marine and Polar Programme. Available at <https://portals.iucn.org/library/sites/library/files/documents/2014-049.pdf>.
- Leys SP, Kahn AS. 2018.** Oxygen and the energetic requirements of the first multicellular animals. *Integrative and Comparative Biology* **58**(4):666–676.

- Leys SP, Wilson K, Holeton C, Reiswig HM, Austin WC, Tunnicliffe V. 2004. Patterns of glass sponge (Porifera, Hexactinellida) distribution in coastal waters of British Columbia. *Canada Marine Ecology Progress Series* 283:133–149.
- Liaw A, Wiener M. 2002. Classification and regression by randomForest. *R news* 2(3):18–22.
- Locarnini RA, Mishonov AV, Antonov JI, Boyer TP, Garcia HE, Baranova OK, Zweng MM, Paver CR, Reagan JR, Johnson DR, Hamilton M, Seidov D. 2013. World Ocean Atlas 2013, volume 1: temperature. In: Levitus S, Mishonov A, eds. *NOAA Atlas NESDIS 73*, 40. Available at <https://repository.library.noaa.gov/view/noaa/14847>.
- Luna-Jorquera G, Thiel M, Portflitt-Toro M, Dewitte B. 2019. Marine protected areas invaded by floating anthropogenic litter: an example from the South Pacific. *Aquatic Conservation: Marine and Freshwater Ecosystems* 29:245–259.
- Lunden JJ, McNicholl CG, Sears CR, Morrison CL, Cordes EE. 2014. Acute survivorship of the deep-sea coral *Lophelia pertusa* from the Gulf of Mexico under acidification, warming, and deoxygenation. *Frontiers in Marine Science* 1:78.
- Lutz MJ, Caldeira K, Dunbar RB, Behrenfeld MJ. 2007. Seasonal rhythms of net primary production and particulate organic carbon flux to depth describe the efficiency of biological pump in the global ocean. *Journal of Geophysical Research: Oceans* 112(C10011):1–26.
- MPAtlas. 2021. Marine Conservation Institute. Seattle, WA. Available at www.mpatlas.org (accessed 18 February 2021).
- Masson DG, Bett BJ, Billett DSM, Jacobs CL, Wheeler AJ, Wynn RB. 2003. The origin of deep-water, coral-topped mounds in the northern Rockall Trough, Northeast Atlantic. *Marine Geology* 194(3–4):159–180.
- McCulloch M, Trotter J, Montagna P, Falter J, Dunbar R, Försterra G, López Correa M, Maier C, Rüggeberg A, Taviani M. 2012. Resilience of cold-water scleractinian corals to ocean acidification: boron isotopic systematics of pH and saturation state up-regulation. *Geochimica et Cosmochimica Acta* 87:21–34.
- Micheli F, Saenz-Arroyo A, Greenley A, Vazquez L, Montes JAE, Rossetto M, De Leo GA. 2012. Evidence that marine reserves enhance resilience to climatic impacts. *PLOS ONE* 7(7):e40832.
- Mienis F, De Stigter HC, De Haas H, Van Weering TCE. 2009. Near-bed particle deposition and resuspension in a cold-water coral mound area at the Southwest Rockall Trough margin, NE Atlantic. *Deep Sea Research Part I: Oceanographic Research Papers* 56(6):1026–1038.
- Miller J. 2010. Species distribution modeling. *Geography Compass* 4(6):490–509.
- Miller KA, Thompson KF, Johnston P, Santillo D. 2018. An overview of seabed mining including the current state of development, environmental impacts, and knowledge gaps. *Frontiers in Marine Science* 4:418.
- Molenaar EJ, Elferink AGO. 2009. Marine protected areas in areas beyond national jurisdiction—the pioneering efforts under the OSPAR convention. *Utrecht Law Review* 5:5.
- Mora C, Wei C-L, Rollo A, Amaro T, Baco AR, Billett D, Bopp L, Chen Q, Collier M, Danovaro R, Gooday AJ, Grupe BM, Halloran PR, Ingels J, Jones DOB, Levin LA, Nakano H, Norling K, Ramirez-Llodra E, Rex M, Ruhl HA, Smith CR, Sweetman AK, Thurber AR, Tjiputra JF, Usseglio P, Watling L, Wu T, Yasuhara M. 2013. Biotic and human vulnerability to projected changes in ocean biogeochemistry over the 21st century. *PLOS Biology* 11(10):e1001682.
- Mumby PJ, Harborne AR. 2010. Marine reserves enhance the recovery of corals on Caribbean reefs. *PLOS ONE* 5(1):e8657.

- Müller WE, Schröder HC, Wiens M, Perovic-Ottstadt S, Batel R, Müller IM. 2004. Traditional and modern biomedical prospecting: part II—the benefits. *Evidence-Based Complementary and Alternative Medicine* 1(2):133–144.
- Nadi A, Moradi H. 2019. Increasing the views and reducing the depth in random forest. *Expert Systems with Applications* 138(11):112801 DOI 10.1016/j.eswa.2019.07.018.
- NOAA. 2020. NOAA National Database for Deep-Sea Corals and Sponges. NOAA Deep Sea Coral Research & Technology Program. Available at <https://deepseacoraldata.noaa.gov/>.
- OBIS. 2020. Ocean Biodiversity Information System. Intergovernmental Oceanographic Commission of UNESCO. Available at www.obis.org.
- Oevelen DV, Duineveld G, Lavaleye M, Mienis F, Soetaert K, Heip CH. 2009. The cold-water coral community as hotspot of carbon cycling on continental margins: a food-web analysis from Rockall Bank (northeast Atlantic). *Limnology and Oceanography* 54(6):1829–1844 DOI 10.4319/lo.2009.54.6.1829.
- Ortuño Crespo GO, Dunn DC, Gianni M, Gjerde K, Wright G, Halpin PN. 2019. High-seas fish biodiversity is slipping through the governance net. *Nature Ecology & Evolution* 3(9):1273–1276 DOI 10.1038/s41559-019-0981-4.
- Parin NV. 1991. Fish fauna of the Nazca and Sala y Gomez submarine ridges, the easternmost outpost of the Indo-West Pacific zoogeographic region. *Bulletin of Marine Science* 49(3):671–683.
- Parin NV, Mironov AN, Nesis KN. 1997. Biology of the Nazca and Sala y Gomez submarine ridges, an outpost of the Indo-West Pacific fauna in the eastern Pacific Ocean: composition and distribution of the fauna, its communities and history. *Advances in Marine Biology* 32(1):145–242 DOI 10.1016/S0065-2881(08)60017-6.
- Parker SJ, Penney AJ, Clark MR. 2009. Detection criteria for managing trawl impacts on vulnerable marine ecosystems in high seas fisheries of the South Pacific Ocean. *Marine Ecology Progress Series* 397:309–317.
- Penney AJ, Parker SJ, Brown JH. 2009. Protection measures implemented by New Zealand for vulnerable marine ecosystems in the South Pacific Ocean. *Marine Ecology Progress Series* 397:341–354.
- Perea-Blazquez A, Davy SK, Bell JJ. 2012. Estimates of particulate organic carbon flowing from the pelagic environment to the benthos through sponge assemblages. *PLOS ONE* 7(1):e29569.
- Phillips SJ, Anderson RP, Schapire RE. 2006. Maximum entropy modeling of species geographic distributions. *Ecological Modelling* 190(3–4):231–259.
- Piepenburg D, Müller B. 2004. Distribution of epibenthic communities on the Great Meteor Seamount (North-east Atlantic) mirrors pelagic processes. *Archive of Fishery and Marine Research* 51(1–3):55–70.
- Prouty NG, Roark EB, Buster NA, Ross SW. 2011. Growth rate and age distribution of deep-sea black corals in the Gulf of Mexico. *Marine Ecology Progress Series* 423:101–115.
- Purser A, Larsson AI, Thomsen L, Van Oevelen D. 2010. The influence of flow velocity and food concentration on *Lophelia pertusa* (Scleractinia) zooplankton capture rates. *Journal of Experimental Marine Biology and Ecology* 395(1–2):55–62.
- Pusceddu A, Bianchelli S, Martín J, Puig P, Palanques A, Masqué P, Danovaro R. 2014. Chronic and intensive bottom trawling impairs deep-sea biodiversity and ecosystem functioning. *Proceedings of The National Academy of Sciences of The United States of America* 111(24):8861–8866.
- R Core Team. 2019. *R: a language and environment for statistical computing*. Vienna, Austria: R Foundation for Statistical Computing. Available at <https://www.R-project.org/>.

- Ramirez-Llodra E, Tyler PA, Baker MC, Bergstad OA, Clark MR, Escobar E, Levin LA, Menot L, Rowden AA, Smith CR, Van Dover CL. 2011. Man and the last great wilderness: human impact on the deep sea. *PLOS ONE* 6(8):e22588.
- Reiss H, Cunze S, König K, Neumann H, Kröncke I. 2011. Species distribution modelling of marine benthos: a North Sea case study. *Marine Ecology Progress Series* 442:71–86 DOI 10.3354/meps09391.
- Ridgeway G. 2004. *The gbm package*. Vienna, Austria: R Foundation for Statistical Computing.
- Roark EB, Guilderson TP, Dunbar RB, Fallon SJ, Mucciarone DA. 2009. Extreme longevity in proteinaceous deep-sea corals. *Proceedings of the National Academy of Sciences of the United States of America* 106(13):5204–5208.
- Robert K, Jones DO, Roberts JM, Huvenne VA. 2016. Improving predictive mapping of deep-water habitats: considering multiple model outputs and ensemble techniques. *Deep Sea Research Part I: Oceanographic Research Papers* 113:80–89.
- Roberts CM, O’Leary BC, McCauley DJ, Cury PM, Duarte CM, Pauly D, Sáenz-Arroyo A, Sumaila UR, Wilson RW, Worm B, Castilla JC. 2017. Marine reserves can mitigate and promote adaptation to climate change. *Proceedings of the National Academy of Sciences of the United States of America* 114(24):6167–6175.
- Roberts JM, Wheeler A, Freiwald A, Cairns S. 2009. *Cold-water corals: the biology and geology of deep-sea coral habitats*. Cambridge: Cambridge University Press.
- Rodrigo C, Díaz J, González-Fernández A. 2014. Origin of the Easter Submarine Alignment: morphology and structural lineaments. *Latin American Journal of Aquatic Research* 42(4):857–870 DOI 10.3856/vol42-issue4-fulltext-12.
- Rogers AD. 1994. The biology of seamounts. *Advances in Marine Biology* 30:305–350.
- Rogers AD. 1999. The biology of *Lophelia pertusa* (Linnaeus 1758) and other deep-water reef-forming corals and impacts from human activities. *International Review of Hydrobiology* 84(4):315–406.
- Rogers AD, Gianni M. 2010. *The implementation of UNGA resolutions 61/105 and 64/72 in the management of Deep-Sea fisheries on the high Seas—report prepared for the Deep-Sea Conservation Coalition*. London, United Kingdom: International Programme on the State of the Ocean, 97.
- Rooper CN, Zimmermann M, Prescott MM, Hermann AJ. 2014. Predictive models of coral and sponge distribution, abundance and diversity in bottom trawl surveys of the Aleutian Islands. *Alaska Marine Ecology Progress Series* 503:157–176.
- Rowden AA, Anderson OF, Georgian SE, Bowden DA, Clark MR, Pallentin A, Miller A. 2017. High-resolution habitat suitability models for the conservation and management of vulnerable marine ecosystems on the Louisville Seamount Chain, South Pacific Ocean. *Frontiers in Marine Science* 4:335.
- Rowe GT, Morse J, Nunnally C, Boland GS. 2008. Sediment community oxygen consumption in the deep Gulf of Mexico. *Deep Sea Research Part II: Topical Studies in Oceanography* 55(24–26):2686–2691.
- Sandwell DT, Müller RD, Smith WH, Garcia E, Francis R. 2014. New global marine gravity model from CryoSat-2 and Jason-1 reveals buried tectonic structure. *Science* 346(6205):65–67.
- Sappington JM, Longshore KM, Thompson DB. 2007. Quantifying landscape ruggedness for animal habitat analysis: a case study using bighorn sheep in the Mojave Desert. *The Journal of Wildlife Management* 71(5):1419–1426.
- Segal MR. 2003. Machine learning benchmarks and random forest regression. Available at <https://escholarship.org/uc/item/35x3v9t4>.

- Sellanes J, Salisbury RA, Tapia JM, Asorey CM. 2019. A new species of *Atrimitra* Dall, 1918 (Gastropoda: Mitridae) from seamounts of the recently created Nazca-Desventuradas Marine Park, Chile. *PeerJ* 7:e8279.
- Serratos J, Hyrenbach KD, Miranda-Urbina D, Portflitt-Toro M, Luna N, Luna-Jorquera G. 2020. Environmental drivers of seabird at-sea distribution in the Eastern South Pacific Ocean: assemblage composition across a longitudinal productivity gradient. *Frontiers in Marine Science* 6:838.
- Shepherd B, Pinheiro HT, Phelps TA, Easton EE, Pérez-Matus A, Rocha LA. 2020. A new species of *Chromis* (Teleostei: Pomacentridae) from Mesophotic Coral Ecosystems of Rapa Nui (Easter Island) and Salas y Gómez, Chile. *Copeia* 108(2):326–332.
- Shillinger GL, Palacios DM, Bailey H, Bograd SJ, Swithenbank AM, Wallace BP, Spotila JR, Paladino FV, Piedra R, Eckert SA, Block BA. 2008. Persistent leatherback turtle migrations present opportunities for conservation. *PLOS Biology* 6(7):e171.
- Smith JE, Schwarcz HP, Risk MJ, McConnaughey TA, Keller N. 2000. Paleotemperatures from deep-sea corals: overcoming ‘vital effects’. *Palaeos* 15(1):25–32.
- Steinacher M, Joos F, Frölicher TL, Plattner GK, Doney SC. 2009. Imminent ocean acidification in the Arctic projected with the NCAR global coupled carbon cycle-climate model. *Biogeosciences* 6(4):515–533.
- Steinberger B. 2002. Motion of the Easter hot spot relative to Hawaii and Louisville hot spots. *Geochemistry, Geophysics, Geosystems* 3(11):1–27.
- Syfert MM, Smith MJ, Coomes DA. 2013. The effects of sampling bias and model complexity on the predictive performance of MaxEnt species distribution models. *PLOS ONE* 8(2):e55158.
- Thiel M, Luna-Jorquera G, Álvarez-Varas R, Gallardo C, Hinojosa IA, Miranda-Urbina D, Morales N, Ory N, Pacheco AS, Portflitt-Toro M, Zavalaga C. 2018. Impacts of marine plastic pollution from continental coasts to subtropical gyres—fish, seabirds, and other vertebrates in the SE Pacific. *Frontiers in Marine Science* 5:238.
- Thresher RE, Tilbrook B, Fallon S, Wilson NC, Adkins J. 2011. Effects of chronic low carbonate saturation levels on the distribution, growth and skeletal chemistry of deep-sea corals and other seamount megabenthos. *Marine Ecology Progress Series* 442:87–99.
- Thuiller W, Georges D, Engler R, Breiner F, Georges MD, Thuiller CW. 2016. Package ‘biomod2’—species distribution modeling within an ensemble forecasting framework. *Ecography* 32:369–373.
- Tian RM, Sun J, Cai L, Zhang WP, Zhou GW, Qiu JW, Qian PY. 2016. The deep-sea glass sponge *Lophophysema eversa* harbours potential symbionts responsible for the nutrient conversions of carbon, nitrogen and sulfur. *Environmental Microbiology* 18(8):2481–2494.
- Tingley G, Dunn MR. 2018. *Global review of orange roughy (Hoplostethus atlanticus), their fisheries, biology and management*. Rome: Food and Agriculture Organization of the United Nations.
- Tittensor DP, Baco AR, Brewin PE, Clark MR, Consalvey M, Rowden AA, Schlacher T, Stocks KI, Rogers AD. 2009. Predicting global habitat suitability for stony corals on seamounts. *Journal of Biogeography* 36(6):1111–1128.
- Tong R, Purser A, Guinan J, Unnithan V. 2013. Modeling the habitat suitability for deep-water gorgonian corals based on terrain variables. *Ecological Informatics* 13:123–132.
- Ullah H, Nagelkerken I, Goldenberg SU, Fordham DA. 2018. Climate change could drive marine food web collapse through altered trophic flows and cyanobacterial proliferation. *PLOS Biology* 16(1):e2003446.

- UNGA. 2007. Sustainable fisheries, including through the 1995 agreement for the implementation of the provisions of the United Nations convention on the law of the sea of 10 December 1982 relating to the conservation and management of straddling fish stocks and highly migratory fish stocks, and related instruments. *United Nations General Assembly Resolution* **61(105)**:1–67.
- Van den Hove S, Moreau V. 2007. Deep-sea biodiversity and ecosystems: a scoping report on their socio-economy, management and governance (no. 184). UNEP/Earthprint. Available at <https://archive.org/details/deepseabiodivers07vand>.
- Van Dover CL, Ardron JA, Escobar E, Gianni M, Gjerde KM, Jaeckel A, Jones DOB, Levin LA, Niner HJ, Pendleton L, Smith CR, Thiele T, Turner PJ, Watling L, Weaver PPE. 2017. Biodiversity loss from deep-sea mining. *Nature Geoscience* **10(7)**:464–465 DOI 10.1038/ngeo2983.
- Van Dover CL, Aronson J, Pendleton L, Smith S, Arnaud-Haond S, Moreno-Mateos D, Barbier E, Billett D, Bowers K, Danovaro R, Edwards A, Kellert S, Morato T, Pollard E, Rogers A, Warner R. 2014. Ecological restoration in the deep sea: Desiderata. *Marine Policy* **44**:98–106 DOI 10.1016/j.marpol.2013.07.006.
- Vierod AD, Guinotte JM, Davies AJ. 2014. Predicting the distribution of vulnerable marine ecosystems in the deep sea using presence-background models. *Deep Sea Research Part II: Topical Studies in Oceanography* **99(9)**:6–18 DOI 10.1016/j.dsr2.2013.06.010.
- Visalli ME, Best BD, Cabral RB, Cheung WWL, Clark NA, Garilao C, Kaschner K, Kesner-Reyes K, Lam VWY, Maxwell SM, Mayorga J, Moeller HV, Morgan L, Crespo GOño, Pinsky ML, White TD, McCauley DJ. 2020. Data-driven approach for highlighting priority areas for protection in marine areas beyond national jurisdiction. *Marine Policy* **122**:103927 DOI 10.1016/j.marpol.2020.103927.
- Von Dassow P, Collado-Fabbri S. 2014. Biological oceanography, biogeochemical cycles, and pelagic ecosystem functioning of the east-central South Pacific Gyre: focus on Easter Island and Salas y Gómez Island. *Latin American Journal of Aquatic Research* **42(4)**:703–742 DOI 10.3856/vol42-issue4-fulltext-4.
- Wagner D, Friedlander AM, Pyle RL, Brooks CM, Gjerde KM, Wilhelm TA. 2020. Coral reefs of the high seas: hidden biodiversity hotspots in need of protection. *Frontiers in Marine Science* **7**:776 DOI 10.3389/fmars.2020.567428.
- Wagner H, Purser A, Thomsen L, Jesus CC, Lundälv T. 2011. Particulate organic matter fluxes and hydrodynamics at the Tisler cold-water coral reef. *Journal of Marine Systems* **85(1–2)**:19–29 DOI 10.1016/j.jmarsys.2010.11.003.
- Wagner D, Van der Meer L, Gorny M, Sellanes J, Gaymer CF, Soto EH, Easton EE, Friedlander AM, Lindsay DJ, Molodtsova TN, Boteler B, Durussel C, Gjerde KM, Currie D, Gianni M, Brooks CM, Shiple MJ, Wilhelm T, Quesada M, Thomas T, Dunstan PK, Clark NA, Villanueva LA, Pyle RL, Clark MR, Georgian SE, Morgan LE. 2021. The Salas y Gómez and Nazca ridges: a review of the importance, opportunities and challenges for protecting a global diversity hotspot on the high seas. *Marine Policy* **126(27)**:104377 DOI 10.1016/j.marpol.2020.104377.
- Walbridge S, Slocum N, Pobuda M, Wright DJ. 2018. Unified geomorphological analysis workflows with Benthic Terrain Modeler. *Geosciences* **8(3)**:94 DOI 10.3390/geosciences8030094.
- Wall M, Ragazzola F, Foster LC, Form A, Schmidt DN. 2015. Enhanced pH up-regulation enables the cold-water coral *Lophelia pertusa* to sustain growth in aragonite undersaturated conditions. *Biogeosciences Discussions* **12(17)**:6757–6781.
- Watling L, Norse EA. 1998. Disturbance of the seabed by mobile fishing gear: a comparison to forest clearcutting. *Conservation Biology* **12(6)**:1180–1197.

- Weichler T, Garthe S, Luna-Jorquera G, Moraga J. 2004. Seabird distribution on the Humboldt Current in northern Chile in relation to hydrography, productivity, and fisheries. *ICES Journal of Marine Science* 61(1):148–154.
- Weisz JB, Lindquist N, Martens CS. 2008. Do associated microbial abundances impact marine demosponge pumping rates and tissue densities? *Oecologia* 155(2):367–376.
- Whitney F, Conway K, Thomson R, Barrie V, Krautter M, Mungov G. 2005. Oceanographic habitat of sponge reefs on the Western Canadian Continental Shelf. *Continental Shelf Research* 25(2):211–226.
- Wild C, Mayr C, Wehrmann L, Schöttner S, Naumann M, Hoffmann F, Rapp HT. 2008. Organic matter release by cold water corals and its implication for fauna–microbe interaction. *Marine Ecology Progress Series* 372:67–75 DOI 10.3354/meps07724.
- Wiley EO, McNyset KM, Peterson AT, Robins CR, Stewart AM. 2003. Niche modeling and geographic range predictions in the marine environment using a machine learning algorithm. *Oceanography* 16(3):120–127 DOI 10.5670/oceanog.2003.42.
- Williams B, Risk MJ, Ross SW, Sulak KJ. 2006. Deep-water antipatharians: proxies of environmental change. *Geology* 34(9):773–776 DOI 10.1130/G22685.1.
- Winship AJ, Thorson JT, Clarke ME, Coleman HM, Costa B, Georgian SE, Gillett D, Grüss A, Henderson MJ, Hourigan TF, Huff DD, Kreidler N, Pirtle JL, Olson JV, Poti M, Rooper CN, Sigler MF, Viehman S, Whitmire CE. 2020. Good practices for species distribution modeling of deep-sea corals and sponges for resource management: data collection, analysis, validation, and communication. *Frontiers in Marine Science* 7:303 DOI 10.3389/fmars.2020.00303.
- Wood SN. 2017. *Generalized additive models: an introduction with R*. Second Edition. Boca Raton: CRC/Taylor & Francis.
- Wood S, Wood MS. 2015. Package ‘mgcv’. R package version 1.29. Available at <https://cran.r-project.org/web/packages/mgcv/index.html>.
- Yahel G, Whitney F, Reisinger HM, Eerkes-Medrano DI, Leys SP. 2007. In situ feeding and metabolism of glass sponges (Hexactinellida, Porifera) studied in a deep temperate fjord with a remotely operated submersible. *Limnology and Oceanography* 52(1):428–440 DOI 10.4319/lo.2007.52.1.0428.
- Yanez E, Silva C, Vega R, Espindola F, Alvarez L, Silva N, Palma S, Salinas S, Menschel E, Haeussermann V, Soto D, Ramirez N. 2009. Seamounts in the southeastern Pacific Ocean and biodiversity on Juan Fernandez seamounts, Chile. *Latin American Journal of Aquatic Research* 37(3):555–570.
- Yesson C, Bedford F, Rogers AD, Taylor ML. 2017. The global distribution of deep-water Antipatharia habitat. *Deep Sea Research Part II: Topical Studies in Oceanography* 145(23):79–86 DOI 10.1016/j.dsr2.2015.12.004.
- Yesson C, Taylor ML, Tittensor DP, Davies AJ, Guinotte J, Baco A, Black J, Hall-Spencer JM, Rogers AD. 2012. Global habitat suitability of cold-water octocorals. *Journal of Biogeography* 39(7):1278–1292.
- Zweng MM, Reagan JR, Antono JI, Locarnini RA, Mishonov AV, Boyer TP, Garcia HE, Baranova OK, Johnson DR, Seidov D, Biddle MM. 2013. World Ocean Atlas 2013, volume 2: salinity. In: Levitus S, Mishonov A, eds. *NOAA Atlas NESDIS 74*, 39. Available at <https://repository.library.noaa.gov/view/noaa/14848>.

Adding pieces to the puzzle: insights into diversity and distribution patterns of Cumacea (Crustacea: Peracarida) from the deep North Atlantic to the Arctic Ocean

Carolin Uhlir^{1,2}, Martin Schwentner^{1,3}, Kenneth Meland⁴,
Jon Anders Kongsrud⁵, Henrik Glenner^{4,6}, Angelika Brandt^{7,8},
Ralf Thiel¹, Jörundur Svavarsson⁹, Anne-Nina Lörz¹⁰ and Saskia Brix²

¹ Center of Natural History (CeNak), Universität Hamburg, Hamburg, Germany

² German Center for Marine Biodiversity Research (DZMB), Senckenberg Research Institute, Hamburg, Germany

³ Natural History Museum Vienna, Vienna, Austria

⁴ Department of Biological Sciences, University of Bergen, Bergen, Norway

⁵ Department of Natural History, University Museum of Bergen (ZMBN), Bergen, Norway

⁶ Centre of Macroecology, Evolution and Climate (CMEC), Globe Institute, University of Copenhagen, Copenhagen, Denmark

⁷ Senckenberg Research Institute and Natural History Museum, Frankfurt am Main, Germany

⁸ Institute for Ecology, Evolution and Diversity, Goethe University Frankfurt, Frankfurt am Main, Germany

⁹ Faculty of Life and Environmental Sciences, School of Engineering and Natural Sciences, University of Iceland, Reykjavik, Iceland

¹⁰ Institute for Marine Ecosystems and Fisheries Science, Center for Earth System Research and Sustainability (CEN), Universität Hamburg, Hamburg, Germany

ABSTRACT

The Nordic Seas have one of the highest water-mass diversities in the world, yet large knowledge gaps exist in biodiversity structure and biogeographical distribution patterns of the deep macrobenthic fauna. This study focuses on the marine bottom-dwelling peracarid crustacean taxon Cumacea from northern waters, using a combined approach of morphological and molecular techniques to present one of the first insights into genetic variability of this taxon. In total, 947 specimens were assigned to 77 morphologically differing species, representing all seven known families from the North Atlantic. A total of 131 specimens were studied genetically (16S rRNA) and divided into 53 putative species by species delimitation methods (GMYC and ABGD). In most cases, morphological and molecular-genetic delimitation was fully congruent, highlighting the overall success and high quality of both approaches. Differences were due to eight instances resulting in either ecologically driven morphological diversification of species or morphologically cryptic species, uncovering hidden diversity. An interspecific genetic distance of at least 8% was observed with a clear barcoding gap for molecular delimitation of cumacean species. Combining these findings with data from public databases and specimens collected during different international expeditions revealed a change in the composition of taxa from a Northern Atlantic-boreal to an Arctic community. The Greenland-Iceland-Scotland-Ridge (GIS-Ridge) acts as a geographical barrier and/or predominate water masses correspond well with cumacean taxa dominance.

Submitted 29 April 2021

Accepted 4 October 2021

Published 11 November 2021

Corresponding author

Carolin Uhlir,

carolin.uhlir@senckenberg.de

Academic editor

Tamar Guy-Haim

Additional Information and
Declarations can be found on
page 38

DOI [10.7717/peerj.12379](https://doi.org/10.7717/peerj.12379)

© Copyright

2021 Uhlir et al.

Distributed under

Creative Commons CC-BY 4.0

OPEN ACCESS

A closer investigation on species level revealed occurrences across multiple ecoregions or patchy distributions within defined ecoregions.

Subjects Biodiversity, Biogeography, Marine Biology, Molecular Biology, Taxonomy

Keywords Species delimitation, Integrative taxonomy, IceAGE project, 16S rDNA gene, Iceland, Benthic fauna, Deep sea, Biogeography

INTRODUCTION

The ocean surrounding Iceland and its adjacent waters have one of the world's highest diversities of water masses (*Hansen & Østerhus, 2000*). The hydrography of the area is rather complex as several primary water masses meet and often overlay each other (*Malmberg & Valdimarsson, 2003; Brix & Svavarsson, 2010; Meißner, Brenke & Svavarsson, 2014*). According to these hydrographic features, benthic habitats are characterized by depth gradients, water-mass parameters and habitat structure (*Meißner, Brenke & Svavarsson, 2014*). Thus, environmental data is important to help understand the driving forces of species' distribution patterns.

It is widely accepted that 'Arctic' water masses are distinguished from 'Subarctic' water masses by their origin from the upper 250–300 m of the Arctic Ocean, whereas the latter describe a mixture of polar and non-polar (Atlantic or Pacific) water masses (*Dunbar, 1951, 1972; Curtis, 1975*). Composition and distribution of benthic organisms in the Arctic Ocean is related to water masses, but also to the geological history (*Bluhm et al., 2011; Mironov, Dilman & Krylova, 2013*). The Fram Strait between North-East Greenland and Svalbard is the only deep-reaching connection to the Arctic Basin (sill depth > 2,200 m). In the Icelandic region, the Greenland-Iceland-Scotland Ridge (GIS-Ridge) is a natural border for benthic organisms extending from East Greenland to Scotland and forming a continuous barrier between the North Atlantic, the North European and Siberian Seas and the Arctic Ocean north of the ridge (*Hansen & Østerhus, 2000*). It acts as a transition region exhibiting major temperature differences between water masses of the warmer North Atlantic and colder Greenland, Iceland and Norwegian Sea (GIN-Seas, also termed the Nordic Seas; *Brix et al., 2018a*). Gaps along this ridge allow deep-water exchange between East Greenland and Iceland across the Denmark Strait and the Faroe Bank Channel between the Faroe Islands and the Faroe Bank, which, at 860 m, is the deepest connection between the >4,000 m deep basins separated by the GIS-Ridge (*Brix & Svavarsson, 2010*). Earlier studies in this region revealed a trend of north-south separation of benthic crustacean species distributions (*Weisshappel & Svavarsson, 1998; Weisshappel, 2000; Weisshappel, 2001*) and further outlined the ridge as a potential pathway for the dispersal of shelf fauna from Norway towards Iceland (*Brix et al., 2018a*).

Crustaceans of the taxon Peracarida Calman, 1904 often form a major fraction of macrobenthic communities in terms of diversity and abundance in Arctic and Subarctic waters (*Brandt, 1997; Conlan et al., 2008; Stransky & Svavarsson, 2010*). They are characterized by a marsupium, a brood pouch on the ventral side of the carapace of the mature female (*Westheide & Rieger, 1996; Silva, 2016*). Juveniles hatch as a manca stage by

skipping the planktonic stage. In this study, we will focus on the peracarid taxon Cumacea Krøyer, 1846, which are primarily marine bottom-dwelling benthic crustaceans, spending most of their life buried in or close to the sediment with an adapted morphology for a sediment-water-interface lifestyle. Thus, cumaceans are assumed to be restricted in their dispersal abilities and are most likely not able to drift over vast distances (Rex, 1981; Wilson & Hessler, 1987).

Most species have a specialized feeding strategy as detritus or filter feeders. Some more derived taxa have evolved in association with other epibenthic organisms such as sponges or corals and established a strategy as that of scavengers and micro-predators (e.g., *Campylaspis* G. O. Sars, 1865) with modified mouth parts as piercing organs (Foxon, 1936; Jones, 1976; Petrescu et al., 2009).

Currently there are over 1,800 accepted cumacean species recorded worldwide categorized into eight families (Watling & Gerken, 2019). Approximately 250 cumacean species are recorded in the high-latitude Arctic regions and at least 19 species are known as Arctic endemic species (Vassilenko, 1989). According to the most recent studies on biogeographical patterns of cumaceans in respect to water masses in the Arctic, the families Diastylidae Bate, 1856 and Nannastacidae Bates, 1966 are the most species rich and most widely distributed (Vassilenko, 1989; Watling & Gerken, 2005). The family Leuconidae G. O. Sars, 1878 is the second most species rich taxon and commonly found in colder waters (Vassilenko, 1989; Haye, Kornfield & Watling, 2004; Watling & Gerken, 2005). The predominantly warm-water family Bodotriidae Scott, 1901 and temperate cold-water family Lampropidae G. O. Sars, 1878 contain fewer representatives, but also some endemic Arctic species. Vassilenko (1989) divided the cumacean fauna in the Arctic Ocean into six biogeographic groups, listed in order of decreasing number of species: Boreal-Arctic, Arctic, Atlantic boreal, Pacific boreal, Atlantic subtropical-boreal and Amphiboreal species. In a later publication (Vassilenko, 2002), the Arcto-Atlantic bathyal species group was added to include widespread species from North Atlantic intermediate to near-bottom Arctic water at the continental slope of Arctic Ocean. A complete species list of biogeographic species' distributions is provided by Vassilenko (1989), Vassilenko & Brandt (1996), Watling & Gerken (2005) and Watling (2009). A reference catalogue of previous studies of the cumacean fauna in North Atlantic and the Atlantic sector of the Arctic Ocean is presented in Vassilenko (1989).

In Subarctic and Arctic Ocean regions, the typically patchy distribution patterns of many cumacean species correspond well with the distribution of major water masses (Gerken & Watling, 1999; Gage et al., 2004; Watling, 2009), as well as local sediment grain size as most cumaceans feed by scraping sand grains (Foxon, 1936). Distribution patterns are less controlled by depth; thus, most species are not restricted to deep-sea areas (Hansen, 1920; Haye, 2002; Watling & Gerken, 2005). The same pattern is assumed for another peracarid taxon, Tanaidacea Dana, 1849 (Błażewicz-Paszkwycz & Siciński, 2014), whereas species distributions of Isopoda Latreille, 1817 seem to be mostly driven by depth and related factors (Schnurr et al., 2014; Brix et al., 2018b). A recent study by Lörz et al. (2021) about amphipods supports water-mass properties to be the main factor shaping species distributions at the boundary between the North Atlantic and Arctic

waters as well as the prominent submarine Greenland-Iceland-Faroe Ridge playing a major role in hindering the exchange of deep-sea species between northern and southern deep-sea basins. Large numbers of cumaceans are assumed to remain undiscovered in greater depths, as shelf fauna has been studied to a larger extent and, thus, the abundance and diversity of cumaceans is probably underestimated (*Jones & Sanders, 1972; Vassilenko, 1989; Gage et al., 2004* and references therein).

This study aims to present a first insight into biogeographical species diversity of cumaceans from North Atlantic to Arctic waters. The integration of species occurrence records from public databases such as the Global Ocean Biogeographic Information System (OBIS) and the Marine Area database for Norwegian waters (MAREANO) will build the baseline for a species catalogue in the investigated area. New occurrence records provided by the present study will contribute to a better understanding of species distribution ranges for future research on cumacean distribution patterns. Morphological and molecular techniques are used for an integrative taxonomy approach and will increase the knowledge of genetic and morphological variability of this understudied taxon.

MATERIALS & METHODS

Sampling and study-area properties

The study area includes the northernmost part of the North Atlantic, extending across the GIN-Seas up to the Arctic Ocean. The main bulk of specimens included in this study was collected during the following international projects and expeditions: IceAGE (Icelandic marine Animals: Genetics and Ecology; Cruise M85/3 in 2011; *Brix et al., 2014a; Meißner et al., 2018*), which is a follow up of the BIOFAR (Biology of the Faroe Islands; *Nørrevang et al., 1994; Gerken & Watling, 1999*) and the BIOICE project (Benthic Invertebrates of Icelandic waters; *Omarsdottir et al., 2013*), and PASCAL (Physical feedbacks of Arctic PBL, Sea ice, Cloud and Aerosol; Cruise PS106/1 in 2017; *Macke & Flores, 2018*) onboard the RVs Meteor and Polarstern, focusing on remote shelf-break and deep-sea habitats within a depth range of 579–2,748 m (*Fig. 1*). Grant support and field permits are available under BR3843/3-1 and AWI_PS106_00. Additional specimens from the Norwegian Sea and waters off Svalbard sampled by the MAREANO program (*Thorsnes, 2009*) and the University of Bergen were included (*Table 1*). Cumaceans were sampled in large amounts in all projects.

Temperature and salinity were considered as hydrographic variables for the evaluation of water-mass characteristics, which were available for IceAGE areas (<http://www.vliz.be/en/imis?module=dataset&dasisid=6211>) and PASCAL stations (<https://doi.pangaea.de/10.1594/PANGAEA.881579>) measured just off the sea floor with a conductivity-temperature-depth profiler (CTD) (see *Brix et al. (2012); Brix & Devey (2019)*). Each area and station was allocated to a defined water mass according to the definition of *Schlichtholz & Houssais (2002)*, which is applicable for the Fram Strait region and, thus, the entrance to the deep Arctic Eurasian Basin. For the GIN-Seas around Iceland, the definitions as described by *Hansen & Østerhus (2000)*, *Brix & Svavarsson (2010)* and *Ostmann, Schnurr & Martínez Arbizu (2014)* have been used as baseline (*Table S1*). The records were manually divided into eight ecoregions based on their

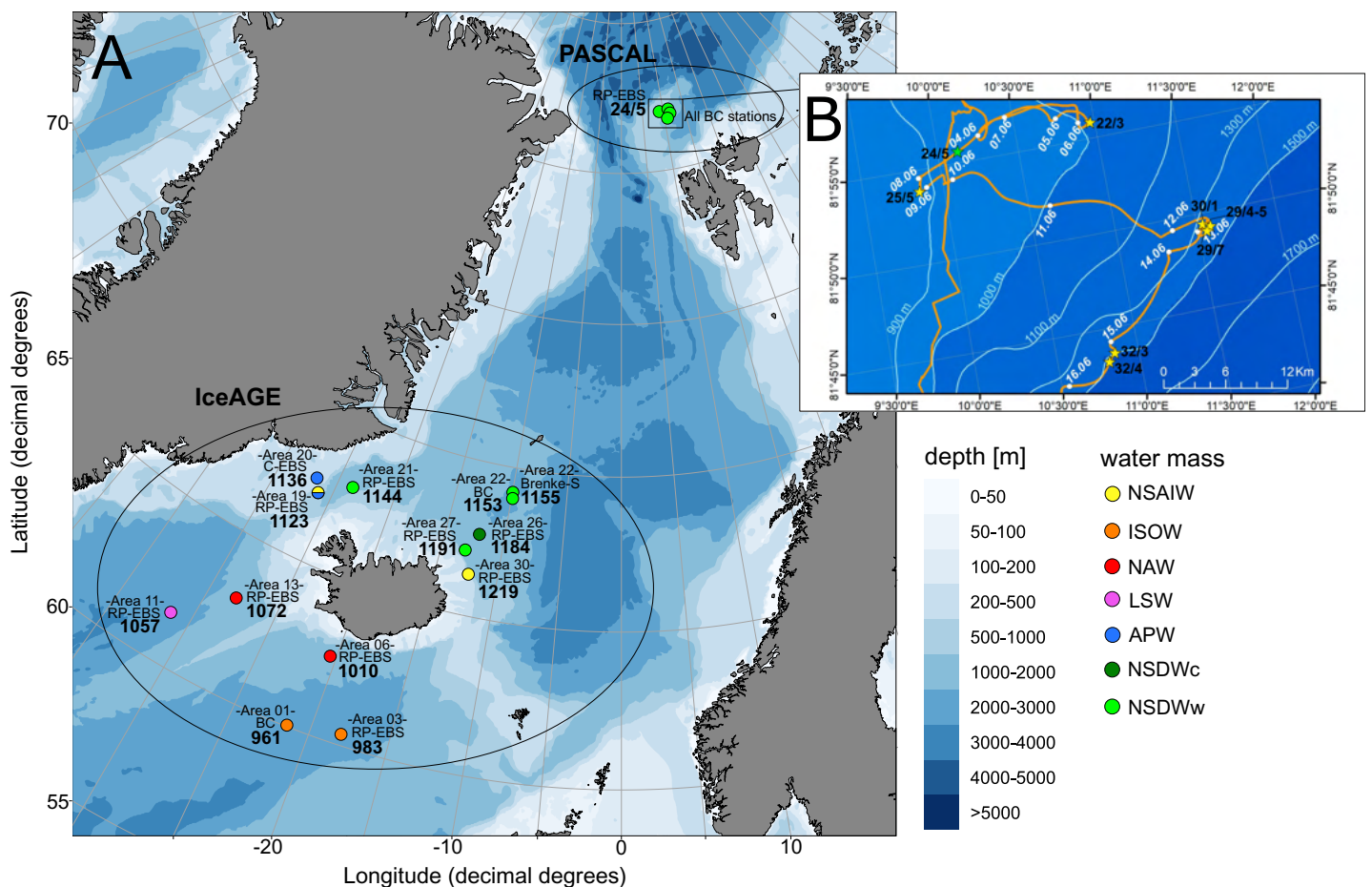


Figure 1 Station sites of investigated cumacean specimens sampled during IceAGE and PASCAL expedition. (A) All investigated station sites of cruise leg M85/3 (IceAGE) and PS106/1 (PASCAL) with information on the study area, deployed gear types and assigned water masses after Schlichtholz & Houssais (2002), Hansen & Østerhus (2000), Brix & Svavarsson (2010) and Ostmann, Schnurr & Martínez Arbizu (2014). (B) Drifting area of cruise leg PS106/1 marking the seven Box corer stations (BC; yellow stars) and the one Epibenthic sled station (EBS; green star; Macke & Flores, 2018).

Full-size DOI: 10.7717/peerj.12379/fig-1

predominate water-mass characteristics after the combined definitions of Curtis (1975), Spalding et al. (2007) and Piepenburg et al. (2011): Warm North Atlantic water mass (North Atlantic Ocean, ecoregion 4), intermediate Subarctic water mass (East Greenland Sea, 2; Norwegian Sea, 5; Barents Sea, 7) and cold Arctic water mass (Arctic Basin, 1; Kara Sea, 8; North Greenland Sea, 3; White Sea, 6).

Sampling data and sample treatment

Specimens were obtained using different types of benthic sampling gear. Most frequently applied was the Rothlisberg-Pearcy Epibenthic sled (RP-EBS, Rothlisberg & Pearcy, 1976; Brattegard & Fosså, 1991), equipped with a net of 500 μm mesh size and ending in a collecting cod end of 300 μm mesh size. Different from the standard deployment protocols as outlined in Brenke (2005), the sampling during the PASCAL expedition was conducted while the vessel was attached to an ice floe during a 2-week passive drifting according to the ocean's current with an average drift velocity of 0.12 kn. Furthermore, the

Table 1 Information on projects and sampled stations within the study area of Greenland, Iceland and Norwegian Sea (GIN-Seas). Information (if applicable) include start and end position of gear deployment (Latitude/Longitude) and calculated haul distance, deployed gear type, depth, CTD-data on near bottom temperature and salinity, drift velocity of the vessel during PASCAL and assigned water masses after *Schlichtholz & Houssais (2002)*, *Hansen & Østerhus (2000)*, *Brix & Svarvsson (2010)* and *Ostmann, Schurr & Martinez Arbizu (2014)*.

Project/ Expedition	Station	Area	Region	Habitat	Date	Latitude start	Longitude start	Latitude end	Longitude end	Gear	Depth (m)	Temp. bottom (°C)	Salinity bottom (ppt)	Haul distance (m)	Drift velocity (kn)	Water mass
Alaska	90,626	N/A	Juneau (Alaska)	shelf	26.06.2009	58.37,690	-134.56,69	N/A	N/A	RP-EBS	1	N/A	N/A	N/A	N/A	Alaska Coast
BIOICE	BIOICE3669	N/A	Iceland	shelf	25.04.2004	66.19,930	-23.30,780	N/A	N/A	RP-EBS	158	N/A	N/A	N/A	N/A	Modified North Atlantic Water (MNAW)
IceAGE	961	1	South Iceland Basin	deep sea	28.08.2011	60.0455	-21.50233	N/A	N/A	BC	2,748	2.53	34.99	N/A	N/A	ISOW
IceAGE	983	3	South Iceland Basin	deep sea	30.08.2011	60.35733	-18.135666	60.0455	-18.14183	RP-EBS	2,568	2.66	35	2,462	N/A	ISOW
IceAGE	1010	6	South Iceland Basin	slope	02.09.2011	62.55166	-20.39516	62.55366	-20.38116	RP-EBS	1,385	3.88	35.02	N/A	N/A	NAW
IceAGE	1057	11	South Iceland Irminger Basin	deep sea	07.09.2011	61.64166	-31.35616	61.654	-31.34916	RP-EBS	2,505	3.16	34.94	1,983	N/A	LSW
IceAGE	1072	13	South Iceland Irminger Basin	deep sea	08.09.2011	63.00766	-28.06816	63.01833	-28.0525	RP-EBS	1,594	4.28	34.99	1,673	N/A	NAW
IceAGE	1123	19	East Greenland Denmark Strait	slope	14.09.2011	67.21383	-26.2075	67.21466	-26.19216	RP-EBS	716.5	0.07	34.91	670	N/A	APW/ NSAIW
IceAGE	1136	20	East Greenland Denmark Strait	shelf	14.09.2011	67.63583	-26.7665	67.63266	-26.77366	CHSAP Sled	316	0.71	34.63	366	N/A	APW
IceAGE	1144	21	East Greenland Denmark Strait	deep sea	15.09.2011	67.86783	-23.69633	67.8595	-23.69616	RP-EBS	1,281	-0.67	34.91	1,340	N/A	NSDWW
IceAGE	1153	22	North-East Iceland Norwegian Basin	deep sea	17.09.2011	69.09333	-9.9335	N/A	N/A	BC	2,174	-0.75	34.91	N/A	N/A	NSDWW
IceAGE	1155	22	North-East Iceland Norwegian Basin	deep sea	17.09.2011	69.11483	-9.912	69.10616	-9.9205	Brenke Sled	2,204	-0.75	34.91	1,582	N/A	NSDWW
IceAGE	1184	26	Norwegian Sea Basin	deep sea	20.09.2011	67.64383	-12.162	67.63866	-12.138	RP-EBS	1,819	-0.85	34.91	1,885	N/A	NSDWC

Table 1 (continued)

Project/ Expedition	Station	Area	Region	Habitat	Date	Latitude start	Longitude start	Latitude end	Longitude end	Gear	Depth (m)	Temp. bottom (°C)	Salinity bottom (ppt)	Haul distance (m)	Drift velocity (kn)	Water mass
IceAGE	1191	27	North-East Iceland Norwegian Sea	deep sea	21.09.2011	67.07866	-13.06383	67.07516	-13.03816	RP-EBS	1,575	-0.74	34.91	1,795	N/A	NSDWw
IceAGE	1219	30	East Iceland Norwegian Sea	slope	22.09.2011	66.289	-12.347	66.2925	-12.355	RP-EBS	579	-0.4	34.9	760	N/A	NSAIW
MAREANO	R488-379, BT	N/A	Eggakanten (Norway)	deep sea	10.10.2009	69.43,760	15.11,110	N/A	N/A	Beam Trawl	2,241	N/A	N/A	N/A	N/A	Norwegian Coastal Current
MAREANO	R721-126, RP	N/A	Continental shelf (Norway)	shelf	25.07.2011	67.50,810	11.48,850	N/A	N/A	RP-EBS	183	N/A	N/A	N/A	N/A	Norwegian Coastal Current
MAREANO	R754-132, RP	N/A	Continental slope (Norway)	slope	22.09.2011	67.48,275	09.41,126	N/A	N/A	RP-EBS	823	N/A	N/A	N/A	N/A	Warm Atlantic Current
MAREANO	R814-22, RP	N/A	Continental shelf (Norway)	shelf	11.05.2012	67.39,220	10.18,580	N/A	N/A	RP-EBS	224	N/A	N/A	N/A	N/A	Norwegian Coastal Current
PASCAL	22-3	N/A	Yermak Plateau	deep sea	05.06.2017	81.93248	10.959499	N/A	N/A	BC	1,077	-0.55	34.91	N/A	0.1	NSDWw
PASCAL	24-5	N/A	Yermak Plateau	slope	07.06.2017	81.927034	10.13311	81.921801	10.055294	EBS	955	-0.48	34.92	1,345	0.3	NSDWw
PASCAL	25-5	N/A	Yermak Plateau	slope	08.06.2017	81.896594	9.855325	N/A	N/A	BC	931	N/A	N/A	N/A	0	NSDWw
PASCAL	29-4/5	N/A	Yermak Plateau	deep sea	12.06.2017	81.820493	11.566229	N/A	N/A	BC	1,564	-0.74	34.92	N/A	0.1	NSDWw
PASCAL	29-7	N/A	Yermak Plateau	deep sea	12.06.2017	81.815543	11.54354	N/A	N/A	BC	1,569	-0.74	34.92	N/A	0.1	NSDWw
PASCAL	30-1	N/A	Yermak Plateau	deep sea	13.06.2017	81.822024	11.538371	N/A	N/A	BC	1,547	-0.72	34.92	N/A	0.1	NSDWw
PASCAL	32-3	N/A	Yermak Plateau	deep sea	15.06.2017	81.728044	10.851854	N/A	N/A	BC	1,581	-0.7	34.92	N/A	0.1	NSDWw
PASCAL	32-4	N/A	Yermak Plateau	deep sea	15.06.2017	81.720718	10.811252	N/A	N/A	BC	1,543	-0.7	34.92	N/A	0.2	NSDWw
UoB	09.01.28-2	N/A	Fanaforde (Norway)	shelf	28.01.2009	60.16,440	05.11,050	N/A	N/A	RP-EBS	180	N/A	N/A	N/A	N/A	Fjord
UoB	11.01.19-1	N/A	Fensforde (Norway)	shelf	19.01.2011	60.50,856	04.51,702	N/A	N/A	RP-EBS	460	N/A	N/A	N/A	N/A	Fjord
UoB	11.01.21-1	N/A	Hjelteforde (Norway)	shelf	21.01.2011	60.37,600	04.52,400	N/A	N/A	RP-EBS	205	N/A	N/A	N/A	N/A	Fjord
UoB	11.03.09-1	N/A	Fensforde (Norway)	shelf	09.03.2011	60.51,935	04.54,384	N/A	N/A	RP-EBS	462	N/A	N/A	N/A	N/A	Fjord

(Continued)

Table 1 (continued)

Project/ Expedition	Station	Area	Region	Habitat	Date	Latitude start	Longitude start	Latitude end	Longitude end	Gear	Depth (m)	Temp. bottom (°C)	Salinity bottom (ppt)	Haul distance (m)	Drift velocity (kn)	Water mass
UoB	11.03.11-2	N/A	Hjeltefjorden (Norway)	shelf	11.03.2011	60.37,320	04.52,794	N/A	N/A	RP-EBS	239	N/A	N/A	N/A	N/A	Fjord
UoB	11.05.10-1	N/A	Sognesjøen (Norway)	shelf	10.05.2011	60.55,048	04.38,225	N/A	N/A	RP-EBS	550	N/A	N/A	N/A	N/A	Norwegian Coastal Current
UoB	11.05.10-3	N/A	Sognesjøen (Norway)	shelf	10.05.2011	60.57,986	04.40,912	N/A	N/A	RP-EBS	381	N/A	N/A	N/A	N/A	Norwegian Coastal Current
UoB	11.05.11-2C	N/A	Førdefjorden (Norway)	shelf	11.05.2011	61.29,106	05.21,497	N/A	N/A	RP-EBS	335	N/A	N/A	N/A	N/A	Fjord
UoB	11.05.15-1	N/A	Hjeltefjorden (Norway)	shelf	15.05.2011	60.37,600	04.52,300	N/A	N/A	RP-EBS	240	N/A	N/A	N/A	N/A	Fjord
UoB	BS 14-19	N/A	Skagerak (Norway)	shelf	13.05.2009	58.22,101	10.20,572	N/A	N/A	RP-EBS	407	N/A	N/A	N/A	N/A	Mixed Atlantic/ Baltic
UoB	BS 22-32	N/A	Skagerak (Norway)	shelf	14.05.2009	58.28,908	10.26,612	N/A	N/A	RP-EBS	301	N/A	N/A	N/A	N/A	Mixed Atlantic/ Baltic
UoB	BS 28-44	N/A	Skagerak (Norway)	shelf	14.05.2009	58.37,710	10.22,558	N/A	N/A	RP-EBS	251	N/A	N/A	N/A	N/A	Mixed Atlantic/ Baltic
UoB	BS 34-56	N/A	Skagerak (Norway)	shelf	15.05.2009	58.28,172	10.07,999	N/A	N/A	RP-EBS	513	N/A	N/A	N/A	N/A	Mixed Atlantic/ Baltic
UoB	BS 75-135	N/A	Skagerak (Norway)	shelf	19.05.2009	58.51,456	10.26,348	N/A	N/A	RP-EBS	246	N/A	N/A	N/A	N/A	Mixed Atlantic/ Baltic
UoB	BS 82-147	N/A	Skagerak (Norway)	shelf	20.05.2009	58.37,258	10.03,077	N/A	N/A	RP-EBS	484	N/A	N/A	N/A	N/A	Mixed Atlantic/ Baltic
UoB	BS 86-151	N/A	Skagerak (Norway)	shelf	20.05.2009	58.25,540	09.38,836	N/A	N/A	RP-EBS	710	N/A	N/A	N/A	N/A	Mixed Atlantic/ Baltic
UoB	H2DEEP- RP-1	N/A	Jan Mayen	deep sea	05.08.2009	75.35,340	07.45,390	N/A	N/A	RP-EBS	2,542	N/A	N/A	N/A	N/A	N/A
UoB	KV-09 2011	Sektor 4	Continental shelf (Norway)	shelf	03.06.2011	61.08,376	2.49,373	N/A	N/A	Grab	191	N/A	N/A	N/A	N/A	Norwegian Coastal Current
UoB	SFND-08R 2011	N/A	Continental shelf (Norway)	shelf	31.05.2011	61.48,140	1.85,231	N/A	N/A	Grab	273	N/A	N/A	N/A	N/A	Norwegian Coastal Current
UoB	UNIS 2007- 129	N/A	Svalbard	shelf	04.09.2007	80.05,008	22.11,834	N/A	N/A	RP-EBS	188	N/A	N/A	N/A	N/A	NSDw

Table 1 (continued)

Project/ Expedition	Station	Area	Region	Habitat	Date	Latitude start	Longitude start	Latitude end	Longitude end	Gear	Depth (m)	Temp. bottom (°C)	Salinity bottom (ppt)	Haul distance (m)	Drift velocity (kn)	Water mass
UoB	UNIS 2009- 27	N/A	Svalbard	shelf	01.09.2009	80.09,141	16.56,126	N/A	N/A	RP-EBS	340	N/A	N/A	N/A	N/A	NSDWw
UoB	UNIS 2009- 36	N/A	Svalbard	shelf	01.09.2009	79.36,693	18.55,051	N/A	N/A	RP-EBS	337	N/A	N/A	N/A	N/A	NSDWw
UoB	UNIS 2009- 4	N/A	Svalbard	shelf	25.08.2009	78.18,300	14.29,000	N/A	N/A	Dredge	56	N/A	N/A	N/A	N/A	NSDWw
UoB	UNIS 2009- 71	N/A	Svalbard	shelf	04.09.2009	80.27,453	12.20,208	N/A	N/A	RP-EBS	497	N/A	N/A	N/A	N/A	NSDWw
UoB	UNIS 2009- 73	N/A	Svalbard	shelf	04.09.2009	80.27,410	12.46,836	N/A	N/A	RP-EBS	452	N/A	N/A	N/A	N/A	NSDWw
UoB	UNIS 2007- 140	N/A	Svalbard	shelf	04.09.2007	80.38,915	22.06,067	N/A	N/A	RP-EBS	126	N/A	N/A	N/A	N/A	NSDWw
UoB	VGPT1-22 2009	Sektor 4	Continental shelf (Norway)	shelf	29.05.2009	61.23,724	02.07,254	N/A	N/A	Grab	295	N/A	N/A	N/A	N/A	Norwegian Coastal Current
UoB	VGPT2-10 2011	N/A	Continental shelf (Norway)	shelf	28.05.2011	61.22,632	02.06,582	N/A	N/A	Grab	284	N/A	N/A	N/A	N/A	Norwegian Coastal Current
UoB	VI-22 2011	Sektor 4	Continental shelf (Norway)	shelf	26.05.2011	61.22,140	02.26,688	N/A	N/A	Grab	334	N/A	N/A	N/A	N/A	Norwegian Coastal Current

Camera-Epibenthic sled (C-EBS; [Brandt et al., 2013](#)), the Brenke-Sled ([Brenke, 2005](#)) and the Giant Box corer (BC; [Hessler & Jumars, 1974](#)) were deployed. A detailed description of the sampling design is given in [Brix et al. \(2014a\)](#). Once the deployed gear was on board, the haul was carefully floated in seawater and evenly decanted gently over a series of sieves with mesh sizes of 1/0.5/0.3 mm, washed with sea water on a sieving table and bulk-fixed in precooled 96% undenatured ethanol. All samples were treated as described in [Riehl et al. \(2014\)](#), ensuring that the samples stayed consistently cooled. The samples were sorted either directly on board or afterwards in the laboratories of the German Center for Marine Biodiversity Research (DZMB, Senckenberg am Meer, Hamburg, Germany).

Morphological specimen identification

A total of 947 specimens ([Table S2](#)) were determined to the lowest possible taxonomic rank, based primarily on original species descriptions (e.g., [Hansen, 1920](#); [Sars, 1900](#)). Species identifications were conducted at the Department of Biological Sciences (University of Bergen, Norway) and DZMB Hamburg using either a ZEISS SteREO Discovery V8 or Leica MZ12.5 dissecting microscope. Dissected pereopods and mouth parts were assessed under a ZEISS Primo Star compound microscope. High quality pictures with depth of focus were taken with a Leica DFC400 digital compound microscope camera using the Z-stacking option in the Leica Application Suite imaging software. Current authoritative classification follows the catalogue World Cumacea Database (<http://www.marinespecies.org/cumacea/>, [Watling & Gerken, 2019](#)) in the World Register of Marine Species ([WoRMS Editorial Board, 2019](#)). Additionally, comparative museums' material has been obtained from the Center of Natural History Hamburg (CeNak) and the University Museum of Bergen (ZMBN).

Molecular methods

DNA extraction, PCR amplification and sequencing

To delimit putative species genetically, DNA extraction and PCR amplification were performed in the laboratories of UoB in Bergen and CeNak in Hamburg. To ascertain that a morphological voucher retained intact, DNA extraction was only performed if at least two individuals were morphologically assigned to the same species. Three different manual workflow kits (DNeasy® Blood and Tissue Kit, QIAGEN®; E.Z.N.A.® Mollusc DNA Kit, Omega Bio-tek, Inc., Norcross, GA, USA; Marine Animal Tissue Genomic DNA Extraction Kit, Neo-Biotech, Pasadena, CA, USA) and one chelating resin (Chelex® 100; Bio-Rad Laboratories, Hercules, CA, USA) were used by following the manufacturer's instructions, except for the subsequent cleanup step within the DNeasy Blood and Tissue Kit, which was conducted using the AMPure XP beads, ©Beckman Coulter.

All DNA extracts were stored immediately after processing at -20°C . Nucleic acid concentration (ng/ μL) and purity of one μL DNA extract was measured with a Thermo Scientific NanoDrop™ 2,000 Spectrophotometer for all extractions. When the measured concentration exceeded 20 ng/ μL , DNA template was diluted 1:10 with ddH₂O.

PCR reactions were performed in a reaction volume of 15 μL , consisting of 0.05 μL DreamTaq DNA Polymerase, 1.5 μL DreamTaq Buffer (Thermo Fisher Scientific,

Germany), 0.12 µL dNTPs mix (25 mM each), 1.5 µL of each primer (10 mM each) and 1–2 µL DNA extract. Two different sets of 16S rRNA gene primers were utilized, 16Sar-L (5'-CGCCTGTTTATCAAAAACAT-3', *Palumbi, Martin & Romano, 1991*) and 16Sb (5'-CTCCGGTTTGAAGTCAAGATCA-3', *Xiong & Kocher, 1991*), which was particularly successful for species of the families Diastylidae, Lampropidae and Leuconidae, and 16SALh (5'-GTACTAAGGTAGCATA-3') and 16SCLr (5'-ACGCTGTTAYCCC TAAAGTAATT-3', *Rehm, 2007; Rehm et al., 2020*), which yielded better results for the Bodotriidae, the Ceratocumatidae Calman, 1905 and some Nannastacidae. However, the latter results in a ~ 200 bp shorter DNA fragment, thus these short sequences were included only in the phylogenetic analyses and were excluded from genetic distance analyses. PCR program had a reaction profile of 94 °C (2 min.), 38 cycles of 94 °C (20 s), 46 °C (10 s) and 65 °C (1 min.) and final extension step of 65 °C (8 min.) was applied. PCR products were purified by incubating 11–13 µL PCR product with 0.8 µL FastAP (one U/µL) and 0.4 µL Exonuclease I (20 U/µL) (both Thermo Fisher ScientificTM, Waltham, MA, USA) in 37 °C for 15 min and 80 °C for 15 min. Bidirectional sequencing was performed with the respective PCR primer set, either with Macrogen Europe, Inc (Amsterdam-Zuidoost, Netherlands) or Eurofins Genomics Germany GmbH. Out of 123 extracted specimens, 80 yielded sequence data of sufficient quality to be included in the molecular species delimitation ([Table 2](#)). These sequences can be accessed *via* GenBank and BoLD (dx.doi.org/10.5883/DS-ICECU).

Phylogenetic analyses

Raw sequences were assembled and manually curated in Geneious® version 9.8.1 (*Kearse et al., 2012*). Consensus sequences were generated and blasted against GenBank database to identify potential contaminant sequences (*e.g.*, bacterial sequences). We further included 67 cumacean sequences published on GenBank, 51 sequences originating from North Atlantic cumaceans currently studied at the University Bergen as well as 16 from outside the study area ([Table 2](#)).

Due to the large number of substitutions and indels, the alignment of all sequenced species included many long, ambiguously aligned regions, which would compromise the following analyses. For this reason, we split the data into four subsets of more closely related (and thus more similar) sequences, based on morphological family taxa and a preliminary phylogenetic analysis on the complete dataset (dataset 1 in [Fig. 2](#); [Table 3](#)). These family-based alignments had fewer ambiguities and gaps and were thus used for subsequent analyses. Alignments were calculated separately for each of these four subsets with MAFFT 7.402 (*Katoh, 2002; Katoh & Standley, 2013*) on the CIPRES Science Gateway version 3.3 (*Miller, Pfeiffer & Schwartz, 2010*) using the L-INS-I algorithm and subsequently trimmed manually in BioEdit© version 7.0.5.3 (*Hall, 1999*). One outgroup species (represented by a member of one of the respective other cumacean families) was included in the alignments for the phylogenetic analyses but removed to further improve the alignment for genetic distance analyses.

The best-fitting evolutionary model was identified in MEGA X (*Kumar et al., 2018*), resulting in the General Time Reversible Model with invariable sites and gamma

Table 2 Information on cumacean specimens included in the molecular species delimitation based on 16S rRNA gene region sequences. Species ID groups specimens assigned morphologically to the same species and letters (A–C) show separated lineages by genetic analyses. Sequence ID identifies each specimen in the conducted phylogenetic analyses. Outgroup sequences of other peracarids (Amphipoda, Isopoda, Tanaidacea) are highlighted in grey.

Species ID	Project	Station	Sample ID	GenBank Accession	Higher taxon	Putative species	Sequence ID (Field ID)
NA	NA	NA	NA	HQ450558	Bodotriidae	<i>Atlantocuma</i> sp.	HQ450558
Bod01	IceAGE	983	DZMB-HH-68412	MZ402659	Bodotriidae	<i>Bathycuma brevirostre</i>	ICE1-Bod004
Bod03	IceAGE	1072	DZMB-HH-68361	MZ402660	Bodotriidae	Bodotriidae sp. 1	ICE1-Bod003
NA	NA	NA	NA	AJ388111	Bodotriidae	<i>Cumopsis fagei</i>	AJ388111
Bod05-B	IceAGE	983	DZMB-HH-68410	MZ402681	Bodotriidae	<i>Cyclaspis longicaudata</i>	ICE1-Bod001
Bod05-B	IceAGE	983	DZMB-HH-68411	MZ402680	Bodotriidae	<i>Cyclaspis longicaudata</i>	ICE1-Bod002
Bod05-A	UoB	11.05.15-1	Bio material=4-6	MK613872.1	Bodotriidae	<i>Cyclaspis longicaudata</i>	seq2
Bod05-A	UoB	VI-22 2011	Bio material=7-8	MK613873.1	Bodotriidae	<i>Cyclaspis longicaudata</i>	seq3
NA	NA	NA	NA	HQ450557	Bodotriidae	<i>Cyclaspis</i> sp.	HQ450557
Bod06	UoB	KV-09 2011	Bio material=146	MK613886.1	Bodotriidae	<i>Iphinoe serrata</i>	seq4
Cer01	IceAGE	1057	DZMB-HH-68388	MZ402679	Ceratocumatidae	<i>Cimmerius reticulatus</i>	ICE1-Cer001
Cer01	IceAGE	1072	DZMB-HH-68362	MZ402678	Ceratocumatidae	<i>Cimmerius reticulatus</i>	ICE1-Cer002
Cer01	IceAGE	1072	DZMB-HH-68349	MZ402677	Ceratocumatidae	<i>Cimmerius reticulatus</i>	ICE1-Cer003
Dia01	UoB	09.01.28-2	Bio material=160409-8	MK613898.1	Diastylidae	<i>Diastylis cornuta</i>	seq25
Dia01	UoB	VGPT1-22 2009	Bio material=9-13	MK613897.1	Diastylidae	<i>Diastylis cornuta</i>	seq26
Dia03	UoB	UNIS 2007- 129	Bio material=031109-12	MK613904.1	Diastylidae	<i>Diastylis goodsiri</i>	seq31
Dia04	UoB	BS 14-19	Bio material=21-22	MK613901.1	Diastylidae	<i>Diastylis laevis</i>	seq33
Dia05	UoB	BS 14-19	Bio material=26-28	MK613911.1	Diastylidae	<i>Diastylis lucifera</i>	seq35
Dia06	IceAGE	1144	DZMB-HH-68295	MZ402685	Diastylidae	<i>Diastylis polaris</i>	ICE1-Dia010
Dia06	IceAGE	1144	DZMB-HH-68297	MZ402686	Diastylidae	<i>Diastylis polaris</i>	ICE1-Dia016
Dia06	IceAGE	1184	DZMB-HH-68262	MZ402683	Diastylidae	<i>Diastylis polaris</i>	ICE1-Dia003
Dia06	IceAGE	1184	DZMB-HH-68263	MZ402682	Diastylidae	<i>Diastylis polaris</i>	ICE1-Dia006
Dia06	IceAGE	1184	DZMB-HH-68234	MZ402684	Diastylidae	<i>Diastylis polaris</i>	ICE1-Dia009
Dia06	IceAGE	1191	DZMB-HH-68259	MZ402687	Diastylidae	<i>Diastylis polaris</i>	ICE1-Dia019
Dia06	UoB	H2DEEP- RP-1	Bio material=29-31	MK613902.1	Diastylidae	<i>Diastylis polaris</i>	seq39
Dia06	MAREANO	R488-379, BT	Bio material=32-33	MK613903.1	Diastylidae	<i>Diastylis polaris</i>	seq40
Dia07	UoB	UNIS 2009- 73	Bio material=031109-19	MK613905.1	Diastylidae	<i>Diastylis rathkei</i>	seq36
NA	NA	NA	NA	HQ450555	Diastylidae	<i>Diastylis rathkei</i>	HQ450555
NA	NA	NA	NA	U81512	Diastylidae	<i>Diastylis sculpta</i>	U81512
Dia08	UoB	UNIS 2007- 140	Bio material=031109-16	MK613906.1	Diastylidae	<i>Diastylis cf. spinulosa</i>	seq38
Dia09	UoB	11.05.15-1	Bio material=35-37	MK613899.1	Diastylidae	<i>Diastylis tumida</i>	seq42
Dia09	MAREANO	R721-126, RP	Bio material=152-153	MK613900.1	Diastylidae	<i>Diastylis tumida</i>	seq43
Dia10	IceAGE	983	DZMB-HH-68413	MZ402689	Diastylidae	<i>Diastylodes atlanticus</i>	ICE1-Dia011

Table 2 (continued)

Species ID	Project	Station	Sample ID	GenBank Accession	Higher taxon	Putative species	Sequence ID (Field ID)
Dia10	IceAGE	983	DZMB-HH-68434	MZ402688	Diastylidae	<i>Diastylodes atlanticus</i>	ICE1-Dia024
Dia11	UoB	11.03.11-2	Bio material=D4-D6	MK613910.1	Diastylidae	<i>Diastylodes biplicatus</i>	seq44
Dia12	UoB	11.05.10-3	Bio material=38-40	MK613907.1	Diastylidae	<i>Diastylodes serratus</i>	seq47
Dia12	UoB	11.05.11-2C	Bio material=159, 174	MK613909.1	Diastylidae	<i>Diastylodes serratus</i>	seq48
Dia12	UoB	BS 82-147	Bio material=1004-1006	MK613908.1	Diastylidae	<i>Diastylodes serratus</i>	seq49
NA	NA	NA	NA	HQ450556	Diastylidae	<i>Diastylopsis</i> sp.	HQ450556
Dia14	IceAGE	1123	DZMB-HH-68456	MZ402704	Diastylidae	<i>Leptostylis ampullacea</i>	ICE1-Dia018
Dia14	IceAGE	1123	DZMB-HH-68443	MZ402711	Diastylidae	<i>Leptostylis ampullacea</i>	ICE1-Dia001
Dia14	IceAGE	1123	DZMB-HH-68445	MZ402708	Diastylidae	<i>Leptostylis ampullacea</i>	ICE1-Dia007
Dia14	IceAGE	1136	DZMB-HH-68266	MZ402710	Diastylidae	<i>Leptostylis ampullacea</i>	ICE1-Dia002
Dia14	IceAGE	1136	DZMB-HH-68267	MZ402709	Diastylidae	<i>Leptostylis ampullacea</i>	ICE1-Dia005
Dia14	IceAGE	1136	DZMB-HH-68268	MZ402707	Diastylidae	<i>Leptostylis ampullacea</i>	ICE1-Dia008
Dia14	IceAGE	1144	DZMB-HH-68296	MZ402706	Diastylidae	<i>Leptostylis ampullacea</i>	ICE1-Dia013
Dia14	IceAGE	1191	DZMB-HH-68258	MZ402705	Diastylidae	<i>Leptostylis ampullacea</i>	ICE1-Dia014
Dia15	IceAGE	1136	DZMB-HH-68269	MZ402712	Diastylidae	<i>Leptostylis borealis</i>	ICE1-Dia015
Dia15	IceAGE	1219	DZMB-HH-68403	MZ402713	Diastylidae	<i>Leptostylis borealis</i>	ICE1-Dia017
Dia16-A	UoB	11.05.10-1	Bio material=41-43	MK613921.1	Diastylidae	<i>Leptostylis longimana</i>	seq52
Dia16-A	UoB	BS 82-147	Bio material=49-50	MK613922.1	Diastylidae	<i>Leptostylis longimana</i>	seq53
Dia16-B	PASCAL	24/5	DZMB-HH-63369	MZ402723	Diastylidae	<i>Leptostylis</i> cf. <i>longimana</i>	P-Dias001
Dia16-B	PASCAL	24/5	DZMB-HH-63370	MZ402714	Diastylidae	<i>Leptostylis</i> cf. <i>longimana</i>	P-Dias002
Dia16-B	PASCAL	24/5	DZMB-HH-59943	MZ402722	Diastylidae	<i>Leptostylis</i> cf. <i>longimana</i>	P-Dias028
Dia16-B	PASCAL	24/5	DZMB-HH-63371	MZ402717	Diastylidae	<i>Leptostylis</i> cf. <i>longimana</i>	P-Dias032
Dia16-B	PASCAL	25/5	DZMB-HH-59218	MZ402718	Diastylidae	<i>Leptostylis</i> cf. <i>longimana</i>	P-Dias007
Dia16-B	PASCAL	30/1	DZMB-HH-63337	MZ402716	Diastylidae	<i>Leptostylis</i> cf. <i>longimana</i>	P-Dias003
Dia16-B	PASCAL	30/1	DZMB-HH-59533	MZ402719	Diastylidae	<i>Leptostylis</i> cf. <i>longimana</i>	P-Dias027
Dia16-B	PASCAL	30/1	DZMB-HH-63343	MZ402720	Diastylidae	<i>Leptostylis</i> cf. <i>longimana</i>	P-Dias031
Dia16-B	PASCAL	32/3	DZMB-HH-63330	MZ402721	Diastylidae	<i>Leptostylis</i> cf. <i>longimana</i>	P-Dias004
Dia16-B	PASCAL	32/3	DZMB-HH-63331	MZ402724	Diastylidae	<i>Leptostylis</i> cf. <i>longimana</i>	P-Dias029
Dia16-B	PASCAL	32/3	DZMB-HH-63334	MZ402715	Diastylidae	<i>Leptostylis</i> cf. <i>longimana</i>	P-Dias030
Dia17	IceAGE	983	DZMB-HH-68414	MZ402702	Diastylidae	<i>Leptostylis</i> sp. 1	ICE1-Dia012
Dia17	IceAGE	983	DZMB-HH-68418	MZ402701	Diastylidae	<i>Leptostylis</i> sp. 1	ICE1-Dia025
Lam01	Alaska	90626	Bio material=200912-9	MK613925.1	Lampropidae	<i>Alamprops augustinensis</i>	seq87
Lam02	IceAGE	983	DZMB-HH-68421	MZ402676	Lampropidae	<i>Chalarostylis elegans</i>	ICE1-Lam009
Lam02	IceAGE	983	DZMB-HH-68424	MZ402675	Lampropidae	<i>Chalarostylis elegans</i>	ICE1-Lam017
Lam04	UoB	BIOICE3669	Bio material=187-188, ma6	MK613924.1	Lampropidae	<i>Hemilamprops assimilis</i>	seq80
Lam05-A	UoB	BS 86-151	Bio material=63-64	MK613913.1	Lampropidae	<i>Hemilamprops cristatus</i>	seq81
Lam05-A	UoB	BS 86-151	Bio material=65	MK613914.1	Lampropidae	<i>Hemilamprops cristatus</i>	seq82
Lam05-B	IceAGE	983	DZMB-HH-68420	MZ402695	Lampropidae	<i>Hemilamprops</i> cf. <i>cristatus</i>	ICE1-Lam002
Lam05-B	IceAGE	983	DZMB-HH-68436	MZ402696	Lampropidae	<i>Hemilamprops</i> cf. <i>cristatus</i>	ICE1-Lam008
Lam05-A	IceAGE	1123	DZMB-HH-68446	MZ402697	Lampropidae	<i>Hemilamprops</i> cf. <i>cristatus</i>	ICE1-Lam018

(Continued)

Table 2 (continued)

Species ID	Project	Station	Sample ID	GenBank Accession	Higher taxon	Putative species	Sequence ID (Field ID)
Lam06	IceAGE	983	DZMB-HH-68419	MZ402692	Lampropidae	<i>Hemilamprops</i> cf. <i>diversus</i>	ICE1-Lam001
Lam06	IceAGE	983	DZMB-HH-68435	MZ402693	Lampropidae	<i>Hemilamprops</i> cf. <i>diversus</i>	ICE1-Lam006
Lam06	IceAGE	983	DZMB-HH-68422	MZ402694	Lampropidae	<i>Hemilamprops</i> cf. <i>diversus</i>	ICE1-Lam010
Lam06	IceAGE	983	DZMB-HH-68423	MZ402691	Lampropidae	<i>Hemilamprops</i> cf. <i>diversus</i>	ICE1-Lam011
Lam07	IceAGE	1072	DZMB-HH-68363	MZ402698	Lampropidae	<i>Hemilamprops</i> <i>pterini</i>	ICE1-Lam005
Lam07	IceAGE	1072	DZMB-HH-68364	MZ402699	Lampropidae	<i>Hemilamprops</i> <i>pterini</i>	ICE1-Lam013
Lam08	UoB	BS 28-44	Bio material=66-67	MK613923.1	Lampropidae	<i>Hemilamprops</i> <i>roseus</i>	seq83
Lam10	IceAGE	1072	DZMB-HH-68365	MZ402690	Lampropidae	<i>Hemilamprops</i> sp. 2	ICE1-Lam015
Lam11	IceAGE	1136	DZMB-HH-68270	MZ402700	Lampropidae	<i>Hemilamprops</i> <i>uniplicatus</i>	ICE1-Lam003
Lam11	UoB	11.05.15-1	Bio material=68-70	MK613915.1	Lampropidae	<i>Hemilamprops</i> <i>uniplicatus</i>	seq84
Lam11	UoB	SFND-08R 2011	Bio material=71-72	MK613916.1	Lampropidae	<i>Hemilamprops</i> <i>uniplicatus</i>	seq85
Lam12	UoB	VGPT1-22 2009	Bio material=61-62	MK613917.1	Lampropidae	<i>Mesolamprops</i> <i>denticulatus</i>	seq88
Lam13	IceAGE	1072	DZMB-HH-68366	MZ402737	Lampropidae	<i>Platysympus</i> <i>typicus</i>	ICE1-Lam016
Lam13	IceAGE	1136	DZMB-HH-68271	MZ402736	Lampropidae	<i>Platysympus</i> <i>typicus</i>	ICE1-Lam004
Lam13	UoB	UNIS 2009-71	Bio material=031109-15	MK613918.1	Lampropidae	<i>Platysympus</i> <i>typicus</i>	seq89
Lam13	MAREANO	R814-22, RP	Bio material=ma14	MK613919.1	Lampropidae	<i>Platysympus</i> <i>typicus</i>	seq90
Leu01	UoB	BS 75-135	Bio material=79-82	MK613870.1	Leuconidae	<i>Eudorella</i> <i>emarginata</i>	seq59
Leu02	UoB	BS 34-56	Bio material=88-93	MK613887.1	Leuconidae	<i>Eudorella</i> <i>hirsuta</i>	seq62
Leu02	UoB	11.03.09-1	Bio material=94-96, 102	MK613888.1	Leuconidae	<i>Eudorella</i> <i>hirsuta</i>	seq63
NA	NA	NA	NA	U81513	Leuconidae	<i>Eudorella</i> <i>pusilla</i>	U81513
Leu04-A	UoB	BS 28-44	Bio material=97, 99	MK613881.1	Leuconidae	<i>Eudorella</i> <i>truncatula</i>	seq64
Leu04-A	UoB	BS 75-135	Bio material=200	MK613882.1	Leuconidae	<i>Eudorella</i> <i>truncatula</i>	seq67
Leu04-B	UoB	11.01.19.1	Bio material=100-101	MK613884.1	Leuconidae	<i>Eudorella</i> <i>truncatula</i>	seq65
Leu04-B	UoB	11.01.21-1	Bio material=1007-1008	MK613883.1	Leuconidae	<i>Eudorella</i> <i>truncatula</i>	seq68
Leu04-C	MAREANO	R754-132, RP	Bio material=ma5	MK613885.1	Leuconidae	<i>Eudorella</i> <i>truncatula</i>	seq69
Leu05	IceAGE	1123	DZMB-HH-68457	MZ402728	Leuconidae	<i>Leucon</i> (<i>Alytoleucon</i>) <i>pallidus</i>	ICE1-Leu019
Leu05	IceAGE	1136	DZMB-HH-68274	MZ402729	Leuconidae	<i>Leucon</i> (<i>Alytoleucon</i>) <i>pallidus</i>	ICE1-Leu002
Leu05	IceAGE	1136	DZMB-HH-68276	MZ402731	Leuconidae	<i>Leucon</i> (<i>Alytoleucon</i>) <i>pallidus</i>	ICE1-Leu005
Leu05	IceAGE	1136	DZMB-HH-68278	NA	Leuconidae	<i>Leucon</i> (<i>Alytoleucon</i>) <i>pallidus</i>	ICE1-Leu008
Leu05	IceAGE	1144	DZMB-HH-68298	MZ402730	Leuconidae	<i>Leucon</i> (<i>Alytoleucon</i>) <i>pallidus</i>	ICE1-Leu003
Leu05	IceAGE	1144	DZMB-HH-68299	MZ402725	Leuconidae	<i>Leucon</i> (<i>Alytoleucon</i>) <i>pallidus</i>	ICE1-Leu006
Leu05	IceAGE	1144	DZMB-HH-68300	MZ402726	Leuconidae	<i>Leucon</i> (<i>Alytoleucon</i>) <i>pallidus</i>	ICE1-Leu009

Table 2 (continued)

Species ID	Project	Station	Sample ID	GenBank Accession	Higher taxon	Putative species	Sequence ID (Field ID)
Leu05	IceAGE	1219	DZMB-HH-68404	MZ402727	Leuconidae	<i>Leucon (Alytoleucon) pallidus</i>	ICE1-Leu010
Leu05	UoB	BS 82-147	Bio material=1001-1003	MK613892.1	Leuconidae	<i>Leucon (Alytoleucon) pallidus</i>	seq77
Leu05	UoB	11.01.19.1	Bio material=117-119	MK613891.1	Leuconidae	<i>Leucon (Alytoleucon) pallidus</i>	seq78
NA	NA	NA	NA	HQ450522	Leuconidae	<i>Leucon (Crymoleucon) antarcticus</i>	HQ450522
NA	NA	NA	NA	HQ450543	Leuconidae	<i>Leucon (Crymoleucon) intermedius</i>	HQ450543
NA	NA	NA	NA	HQ450549	Leuconidae	<i>Leucon (Crymoleucon) intermedius</i>	HQ450549
NA	NA	NA	NA	HQ450550	Leuconidae	<i>Leucon (Crymoleucon) intermedius</i>	HQ450550
NA	NA	NA	NA	HQ450537	Leuconidae	<i>Leucon (Crymoleucon) rossi</i>	HQ450537
Leu07	UoB	BS 22-32	Bio material=103-108	MK613889.1	Leuconidae	<i>Leucon (Leucon) acutirostris</i>	seq70
NA	NA	NA	NA	HQ450551	Leuconidae	<i>Leucon (Leucon) assimilis</i>	HQ450551
NA	NA	NA	NA	HQ450552	Leuconidae	<i>Leucon (Leucon) assimilis</i>	HQ450552
NA	NA	NA	NA	HQ450553	Leuconidae	<i>Leucon (Leucon) assimilis</i>	HQ450553
Leu08	UoB	09.01.28-2	Bio material=109-111	MK613895.1	Leuconidae	<i>Leucon (Leucon) nathorsti</i>	seq72
Leu08	UoB	BS 75-135	Bio material=112-114	MK613893.1	Leuconidae	<i>Leucon (Leucon) nathorsti</i>	seq73
Leu09	UoB	UNIS 2009-27	Bio material=031109-9	MK613894.1	Leuconidae	<i>Leucon (Leucon) aff. nathorsti</i>	seq75
Leu10	UoB	UNIS2009-4	Bio material=115-116	MK613890.1	Leuconidae	<i>Leucon (Leucon) nasicooides</i>	seq74
Leu11	IceAGE	1136	DZMB-HH-68273	MZ402734	Leuconidae	<i>Leucon (Leucon) profundus</i>	ICE1-Leu001
Leu11	IceAGE	1136	DZMB-HH-68275	MZ402732	Leuconidae	<i>Leucon (Leucon) profundus</i>	ICE1-Leu004
Leu11	IceAGE	1136	DZMB-HH-68277	MZ402733	Leuconidae	<i>Leucon (Leucon) profundus</i>	ICE1-Leu007
Leu14	IceAGE	1123	DZMB-HH-68449	MZ402735	Leuconidae	<i>Leucon (Macrauloleucon) spinulosus</i>	ICE1-Leu018
NA	NA	NA	NA	HQ450554	Leuconidae	<i>Leucon sp.</i>	HQ450554
Nan03	UoB	BS 86-151	Bio material=120-122	MK613876.1	Nannastacidae	<i>Campylaspis costata</i>	seq6
Nan04	UoB	BS 34-56	Bio material=1-3	MK613874.1	Nannastacidae	<i>Campylaspis globosa</i>	seq9
Nan04	IceAGE	1057	DZMB-HH-68390	MZ402662	Nannastacidae	<i>Campylaspis cf. globosa</i>	ICE1-Nann014
Nan05	IceAGE	1057	DZMB-HH-68389	MZ402663	Nannastacidae	<i>Campylaspis horrida</i>	ICE1-Nann013
Nan05	MAREANO	R721-126, RP	Bio material=123	MK613877.1	Nannastacidae	<i>Campylaspis horrida</i>	seq10
Nan06	PASCAL	24/5	DZMB-HH-63414	MZ402664	Nannastacidae	<i>Campylaspis intermedia</i>	P-Nann009
Nan07	PASCAL	24/5	DZMB-HH-63399	MZ402666	Nannastacidae	<i>Campylaspis rubicunda</i>	P-Nann001
Nan07	PASCAL	24/5	DZMB-HH-63400	MZ402665	Nannastacidae	<i>Campylaspis rubicunda</i>	P-Nann002
Nan07	PASCAL	24/5	DZMB-HH-63401	MZ402670	Nannastacidae	<i>Campylaspis rubicunda</i>	P-Nann003
Nan07	PASCAL	24/5	DZMB-HH-63402	MZ402669	Nannastacidae	<i>Campylaspis rubicunda</i>	P-Nann004

(Continued)

Table 2 (continued)

Species ID	Project	Station	Sample ID	GenBank Accession	Higher taxon	Putative species	Sequence ID (Field ID)
Nan07	PASCAL	24/5	DZMB-HH-63405	MZ402667	Nannastacidae	<i>Campylaspis rubicunda</i>	P-Nann006
Nan07	PASCAL	24/5	DZMB-HH-59833	MZ402668	Nannastacidae	<i>Campylaspis rubicunda</i>	P-Nann011
Nan07	PASCAL	24/5	DZMB-HH-63357	MZ402671	Nannastacidae	<i>Campylaspis rubicunda</i>	P-Nann012
Nan09	IceAGE	1072	DZMB-HH-68369	MZ402661	Nannastacidae	<i>Campylaspis</i> sp. 2	ICE1-Nann005
Nan10	IceAGE	1136	DZMB-HH-68280	MZ402672	Nannastacidae	<i>Campylaspis sulcata</i>	ICE1-Nann002
Nan10	IceAGE	1136	DZMB-HH-68281	MZ402674	Nannastacidae	<i>Campylaspis sulcata</i>	ICE1-Nann004
Nan10	IceAGE	1136	DZMB-HH-68282	MZ402673	Nannastacidae	<i>Campylaspis sulcata</i>	ICE1-Nann006
Nan10	UoB	11.05.15-1	Bio material=134-139	MK613875.1	Nannastacidae	<i>Campylaspis sulcata</i>	seq14
Nan11	UoB	11.05.15-1	Bio material=140-145	MK613878.1	Nannastacidae	<i>Campylaspis undata</i>	seq21
Nan18	IceAGE	1072	DZMB-HH-68370	MZ402738	Nannastacidae	<i>Styloptocuma gracillimum</i>	ICE1-Nann008
Pse01	UoB	UNIS 2009-36	Bio material=156-158	MK613871.1	Pseudocumatidae	<i>Petalosarsia declivis</i>	seq5
NA	NA	NA	NA	AJ388110	Tanaidacea	<i>Apseudopsis latreillii</i>	AJ388110
NA	NA	NA	NA	DQ305106	Isopoda	<i>Asellus (Asellus) aquaticus</i>	DQ305106
NA	NA	NA	NA	AF260869	Isopoda	<i>Colubotelson thompsoni</i>	AF260869
NA	NA	NA	NA	AF260870	Isopoda	<i>Crenoicus buntiae</i>	AF260870
NA	NA	NA	NA	AY693421	Isopoda	<i>Haploniscus</i> sp.	AY693421
NA	NA	NA	NA	AF259533	Isopoda	<i>Paramphisopus palustris</i>	AF259533
NA	NA	NA	NA	DQ305111	Isopoda	<i>Proasellus remyi remyi</i>	DQ305111
NA	NA	NA	NA	MK813124	Amphipoda	<i>Amphipoda</i> sp.	MK813124

distribution (GTR + G + I; [Lanave et al., 1984](#); [Rodriguez et al., 1990](#); [Nylander et al., 2004](#)) for all data sets. Subsequent phylogenetic analyses were performed with MrBayes version 3.2.7a ([Ronquist et al., 2012](#)) with 'nrns = 4' and 'nchains = 6', 50×10^6 generations and a sample frequency of 5,000. The first 25% of sampled trees were discarded as burn-in. The resulting consensus trees were visualized with FigTree version 1.4.4 ([Rambaut, 2018a](#)).

Two different species delimitation methods were employed, one tree-based (general mixed Yule coalescent, GMYC, [Pons et al., 2006](#)) and one distance-based (automatic barcode gap discovery, ABGD, [Puillandre et al., 2012](#)). The single threshold model of GMYC was performed in R (R Core Team) for each of the four subsets. The required ultrametric trees were calculated with BEAST 2.5 ([Bouckaert et al., 2019](#)), employing the Yule coalescent prior, enforcing the ingroup as monophyletic and running the analyses for 30×10^6 generations and sampling every 3,000th generation. Convergence was assessed in Tracer ([Rambaut et al., 2018b](#)) and the final tree produced with TreeAnnotator ([Bouckaert et al., 2019](#)), removing the first 25% of generations as burn-in.

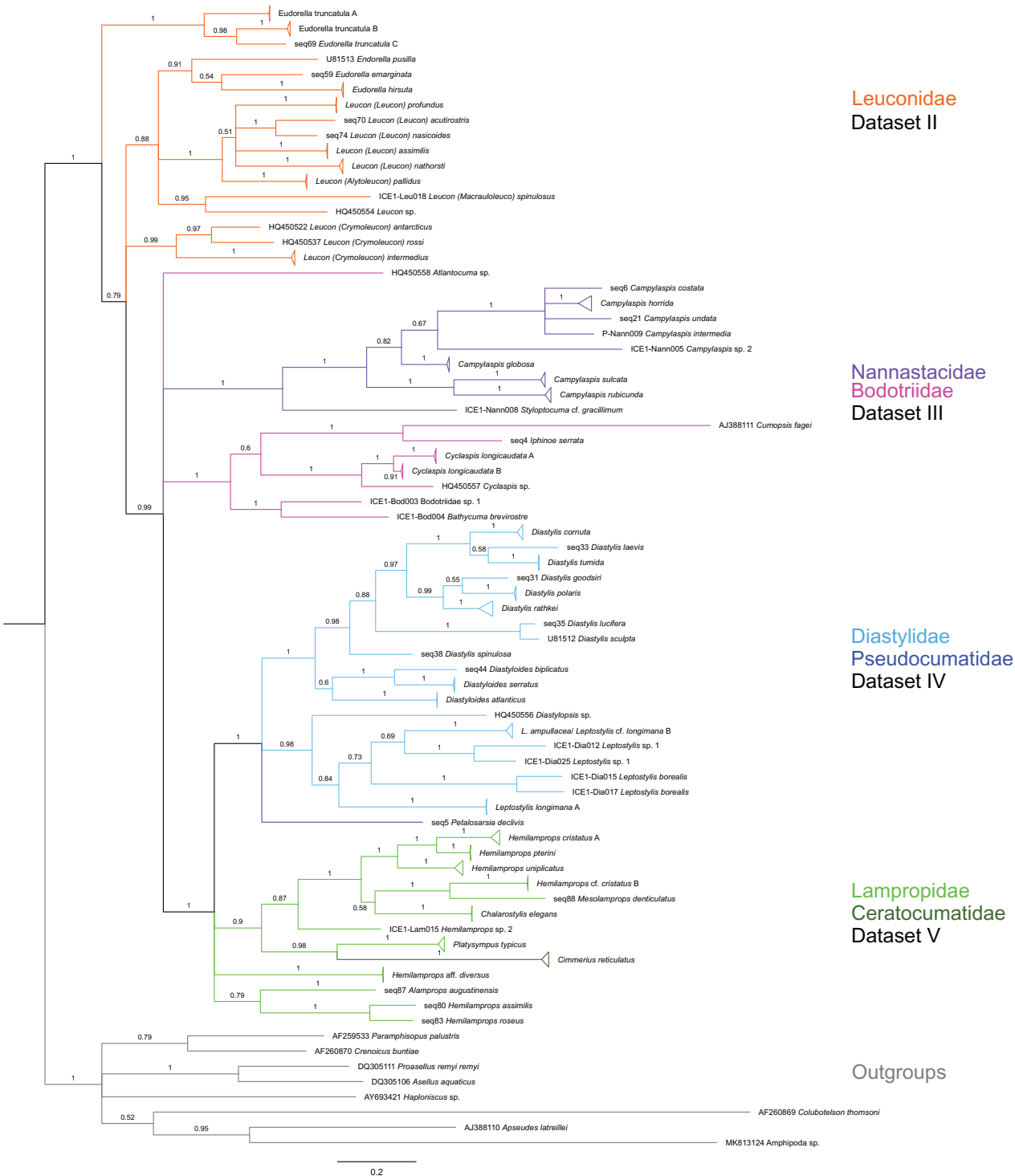


Figure 2 Dataset I-Phylogenetic analyses based on the 16S rRNA gene region of Cumacea from Northern Atlantic to Arctic waters. Included in the Bayesian analysis were 80 sequences of all morphologically determined cumacean species, 67 sequences published on GenBank of which 51 sequences are originating from North Atlantic cumaceans currently studied at the University Bergen as well as 16 from outside the study area and eight other peracarid outgroup sequences (Isopoda, Amphipoda, Tanaidacea). The branch labels indicate posterior probability scores in percent decimal values (1 = absolute support in all calculated trees). The scale bar at the bottom of the tree shows nucleotide substitutions per site of sequence. Colours are representing family taxa, which were split into dataset II-V for subsequent genetic distance analyses. Genetic lineages are separated by assigned letters A/B/C.

Full-size DOI: [10.7717/peerj.12379/fig-2](https://doi.org/10.7717/peerj.12379/fig-2)

Table 3 Summary of datasets 1–5. Number of sequences and the resulting alignment length in base pairs integrated in the Bayesian phylogenetic analyses.

Dataset	Taxa	Sequences for topology (n)	Outgroup sequences (n)	Alignment length (bp)
1	All Cumacea cumulative set	155	8	598
2	Leuconidae	38	1	525
3	Bodotriidae and Nannastacidae	31	1	524
4	Diastylidae and Pseudocumatidae	53	1	549
5	Ceratocumatidae and Lampropidae	29	1	525

The relatively large number of potential singleton taxa could be problematic for tree-based species delimitation approaches. For ABGD, uncorrected p -distances were precomputed without an evolutionary substitution model in MEGA X including transitions and transversions as substitution mutations and missing data was treated by pairwise deletion. Sequences shorter than 300 bp were excluded. The web-based version of ABGD was used (<https://bioinfo.mnhn.fr/abi/public/abgd/abgdweb.html>), setting $P_{min} = 0.01$, $P_{max} = 0.1$, the relative gap width (X) to 0.5 and the number of steps to 100.

Distribution maps

For a general occurrence range overview, distribution maps were created using the software R version 3.5.3 and the PlotSvalbard package version 0.8.5 (Vihtakari, 2019) for each species. A single map incorporates the available georeferenced records from the open-access portal OBIS (OBIS, 2019; <https://mapper.obis.org/>, accessed 19/09/2019) and either the type locality or reference localities from earlier publications. Additionally, new occurrence records, not integrated in the OBIS platform, were added from published literature (e.g., Watling & Gerken, 2005) as well as records from other publicly accessible occurrence record libraries (e.g., MAREANO platform, Table S3). The new OBIS dataset Icelandic Cumacea (ICECU) was created for IceAGE and PASCAL specimens (Uhlir et al., 2021; http://ipt.vliz.be/eurobis/resource?r=cumacea_pascal_iceage). Information on cumacean species sampled and identified by the MAREANO project are accessible for specific taxa via the species-list portal (http://webprod1.nodc.no:8080/marbunn_web/viewspecies).

RESULTS

Combined approach: morphological and molecular species delimitation

The 947 investigated specimens were assigned to 77 morphological species, representing all seven known families (Table S4). For 58 species, identification to a known species taxon was possible. In all other 19 cases, specimens were assigned to genus or family level, but clearly differed morphologically from all other species of these genera or families identified in our study. The largest number of species were assigned to the Nannastacidae (20 species), followed by the Diastylidae (19), the Lampropidae (14) and the Leuconidae

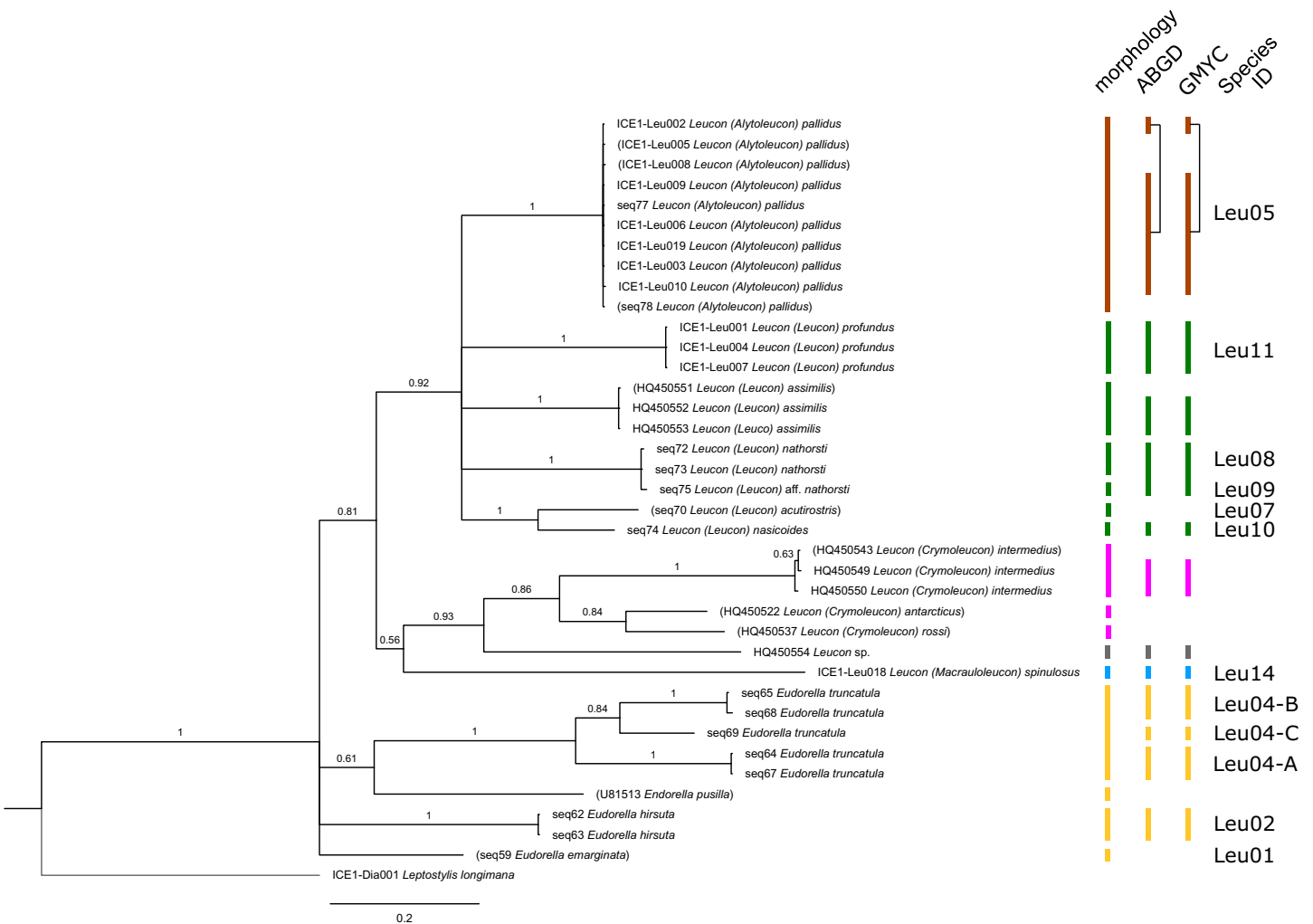


Figure 3 Dataset 2-Phylogenetic relationships inferred by Bayesian analysis of the Leuconidae. The branch labels indicate posterior probability scores. The scale bar at the bottom of the tree shows nucleotide substitutions per site of sequence. Sequences in parentheses were excluded from genetic distance analyses due to insufficient sequence length. Vertical bars indicate the species delimited based on morphology, ABGD and GMYC with colors representing genera. Genetic lineages are separated by assigned letters A/B/C. [Full-size !\[\]\(4857b3cfe28231a8bbb65a50eb4a14dd_img.jpg\) DOI: 10.7717/peerj.12379/fig-3](https://doi.org/10.7717/peerj.12379/fig-3)

(15). In terms of DNA quality and success rate, the Marine Animal Tissue Genomic DNA kit yielded the best results for the cumaceans and can, thus, be recommended for further studies on this taxon.

In total, 131 specimens were included in the genetic analyses, representing 54 of the 77 morphologically identified species (Table 2). The Bayesian phylogenetic analysis of dataset 1 in Fig. 2 (all taxa) resulted in the monophyly of the Cumacea (posterior probability (pp) = 1). Except for the Nannastacidae (pp = 1), families were not recovered as monophyletic (Figs. 3–6), but this was not surprising, as a single fastly evolving marker like 16S is not suitable to properly resolve such deep nodes.

The ABGD analyses delimited 53 genetic lineages (representing putative species). With few exceptions, lineages were separated by a clear barcoding gap, with the vast majority of intra-lineage distances being <1% and inter-lineage distances > 8% (mostly 15–45%)

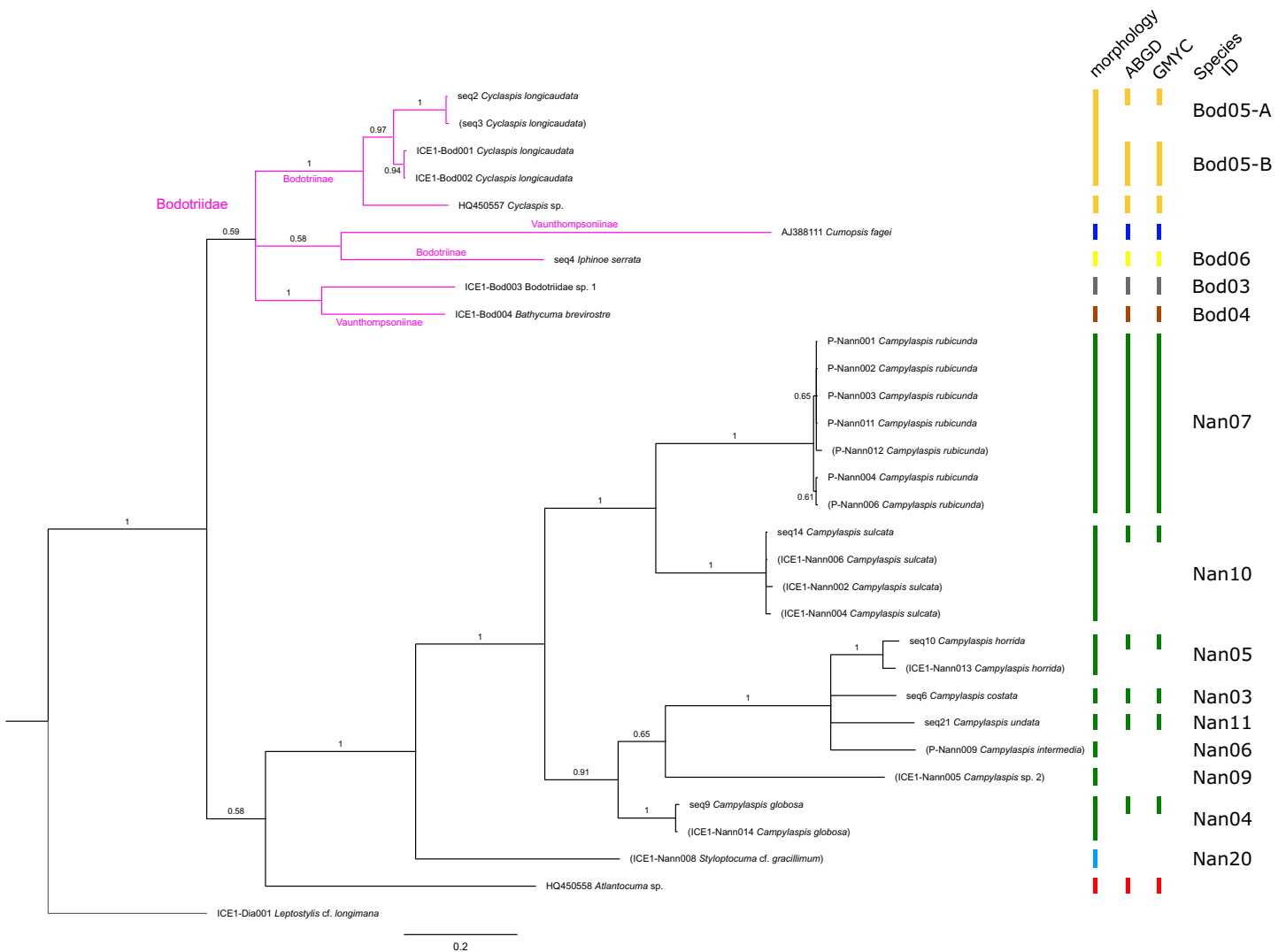


Figure 4 Dataset 3-Phylogenetic relationships inferred by Bayesian analysis of the Bodotriidae and Nannastacidae. The branch labels indicate posterior probability scores. The scale bar at the bottom of the tree shows nucleotide substitutions per site of sequence. Sequences in parentheses were excluded from genetic distance analyses due to insufficient sequence length. Vertical bars indicate the species delimited based on morphology, ABGD and GMYC with colors representing genera. Genetic lineages are separated by assigned letters A/B.

Full-size DOI: [10.7717/peerj.12379/fig-4](https://doi.org/10.7717/peerj.12379/fig-4)

(Fig. S1; Tables S5–S12). Cases of intra-lineage p -distance exceeding 1% were *Diastylis rathkei* Krøyer, 1841 (Dia07, 4%; Tables S5, S6) and *Hemilamprops cristatus* G. O. Sars, 1870 (Lam05-A, 2%; Tables S7, S8). GMYC resulted in nearly identical species delimitation, only *Diastylodes biplicatus* G. O. Sars, 1865 (Dia11) and *Diastylodes serratus* G. O. Sars, 1865 (Dia12) were grouped together (because these are separated by a genetic distance of 18%, we consider this to be an artifact due to the high number of singletons (*D. biplicatus* is also singleton) and treat them separately in the following as suggested by ABGD).

Inconsistencies between morphological and molecular species delimitation occurred in eight cases, which are summarized in Table 4. In four cases, genetic divergence was higher

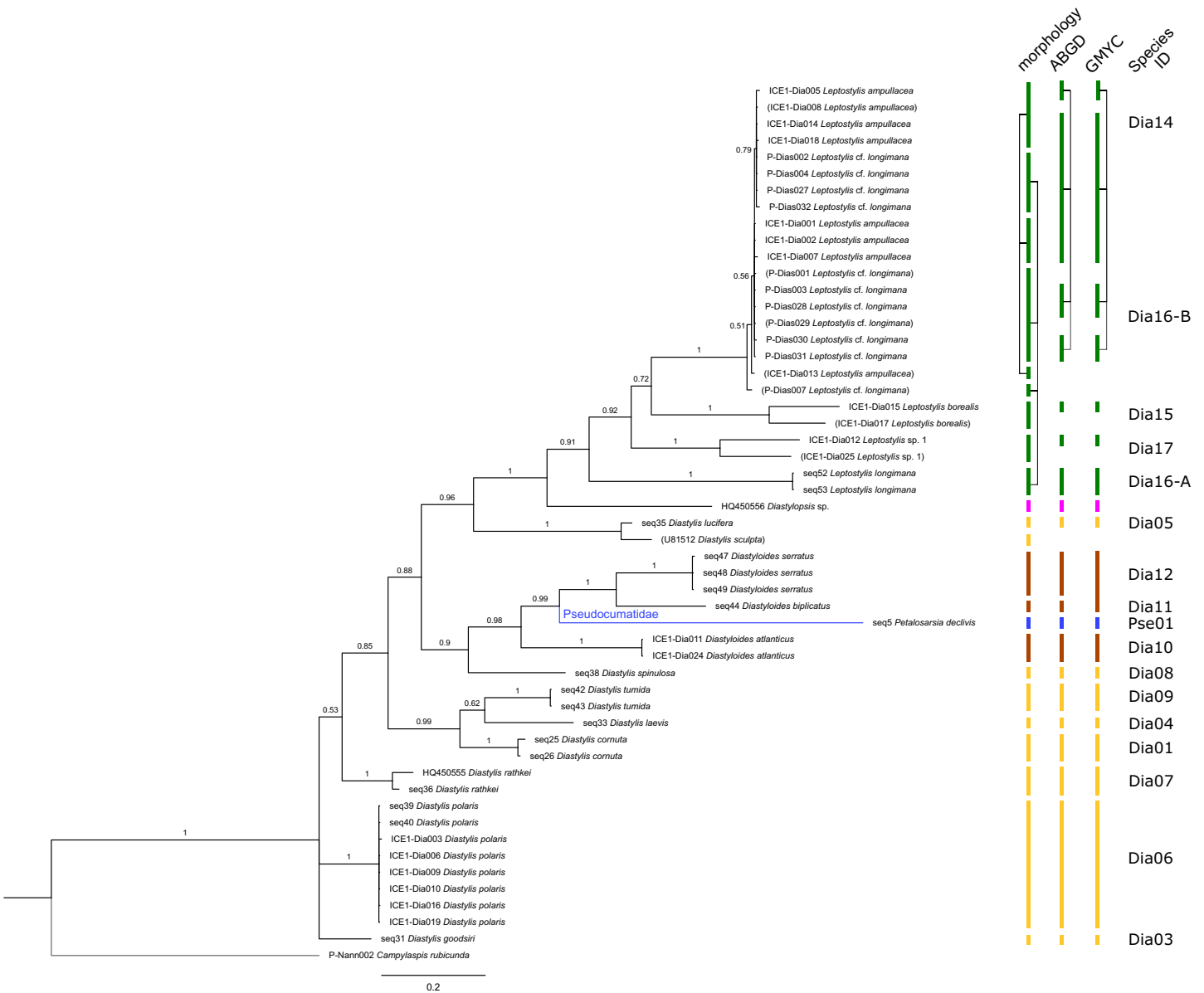


Figure 5 Dataset 4-Phylogenetic relationships inferred by Bayesian analysis of the Diastylidae and the Pseudocumatidae. The branch labels indicate posterior probability scores. The scale bar at the bottom of the tree shows nucleotide substitutions per site of sequence. Sequences in parentheses were excluded from genetic distance analyses due to insufficient sequence length. Vertical bars indicate the species delimited based on morphology, ABGD and GMYC with colors representing genera. Connecting line in Dia14, -16-A, -16-B indicates the same putative species based on morphological identification. Genetic lineages are separated by assigned letters A/B. [Full-size !\[\]\(98c911c074a0e29fafec169cbfa7248d_img.jpg\) DOI: 10.7717/peerj.12379/fig-5](https://doi.org/10.7717/peerj.12379/fig-5)

than expected by prior morphological determination suggesting cryptic diversity. *Cyclaspis longicaudata* Sars, 1865 was split into two distinct lineages (Bod05, A–B; [Table S9, S10](#)) as were *Leptostylis borealis* Stappers, 1908 (Dia15, A–B; [Tables S5, S6](#)) and *Leptostylis* sp. 1 (Dia17, A–B; [Tables S5, S6](#)). *Eudorella truncatula* Bate, 1856 was split into three lineages (Leu04, A–C; [Tables S11, S12](#)). Conversely, *Leucon* (*Leucon*) aff. *nathorsti* [Ohlin, 1901](#) (Leu09) and *L. (L.) nathorsti* (Leu08) were treated as two morphologically differing species based on prior determination following [Hansen \(1920\)](#)

Table 4 Summary of taxonomic incongruences, morphological variability, and potential cryptic diversity cases.

Species ID	Putative species	Sequence ID (Field ID)	Region	Depth range (m)	Water mass
Taxonomic incongruences					
Dia06 (Fig. 11C)	<i>Diastylis polaris</i> aka ' <i>Diastylis stygia</i> '	seq39	Jan Mayen (Norway)	2,542	Arctic, Subarctic
		seq40	Eggakanten (Norway)	2,241	Subarctic
		ICE1-Dia003, ICE1-Dia006, ICE1-Dia009	Norwegian Sea Basin	1,819	Subarctic
		ICE1-Dia010, ICE1-Dia016	East Greenland Denmark Strait	1,281	Arctic, Subarctic
		ICE1-Dia019	North-East Iceland Norwegian Sea	1,574	Subarctic
Lam13 (Fig. 11E)	<i>Platysympus typicus</i> aka ' <i>Platysympus tricarinatus</i> '	ICE1-Lam004	East Greenland Denmark Strait	315	Arctic, Subarctic
		ICE1-Lam016	South Iceland Irminger Basin	1,593	North Atlantic
		seq89	Svalbard	497	Arctic
		seq90	Continental Shelf (Norway)	224	North Atlantic
Morphological variability					
Dia14 (Fig. 11B) & Dia16-B (Fig. 11A)	<i>Leptostylis ampullacea</i> <i>Leptostylis cf. longimana</i> B	ICE1-Dia018, ICE1-Dia002, ICE1-Dia005, ICE1-Dia008, ICE1-Dia001, ICE1-Dia004, ICE1-Dia007, ICE1-Dia013, ICE1-Dia014	North East Iceland	700–1,500	Arctic, Subarctic
		P-Dias001, P-Dias002, P-Dias028, P-Dias032, P-Dias007, P-Dias027, P-Dias031, P-Dias003, P-Dias029, P-Dias030	Yermak-Plateau (Svalbard)	700–1,500	Arctic
Leu08 & Leu09 (Fig. S2W)	<i>Leucon nathorsti</i> <i>Leucon aff. nathorsti</i>	seq72, seq 73	Fanafjorden, Skagerak	180–246	North Atlantic
		seq75	Svalbard	56	Subarctic
Morphological & molecular data: cryptic diversity					
Leu04-A/- B/-C (Fig. S2U)	<i>Eudorella truncatula</i> A <i>Eudorella truncatula</i> B <i>Eudorella truncatula</i> C	seq64, seq67	Skagerak	250	North Atlantic
		seq65, seq68	Fensfjorden, Hjeltefjorden	200–400	North Atlantic
		seq69	Northern Norway	800	Subarctic
Bod05-A/-B (Fig. 13E)	<i>Cyclaspis longicaudata</i> A <i>Cyclaspis longicaudata</i> B	seq2, seq3	Hjeltefjorden	240–330	North Atlantic
		ICE1-Bod001, ICE1-Bod002	South Iceland Basin	2,500	North Atlantic
Dia15-A/-B (Fig. 12A)	<i>Leptostylis borealis</i> A <i>Leptostylis borealis</i> B	ICE1-Dia015	Greenland shelf	300	Subarctic
		ICE1-Dia017	North East Iceland	500	Subarctic
Dia17-A/-B (Fig. S2L)	<i>Leptostylis</i> sp. 1 A <i>Leptostylis</i> sp. 1 B	ICE1-Dia012	South Iceland Basin	2,500	North Atlantic
		ICE1-Dia025	South Iceland Basin	2,500	North Atlantic
Dia16-A/-B (Fig. 11A)	<i>Leptostylis cf. longimana</i> B <i>Leptostylis longimana</i> A	P-Dias001, P-Dias002, P-Dias028, P-Dias032, P-Dias007, P-Dias027, P-Dias031, P-Dias003, P-Dias029, P-Dias030	Yermak-Plateau (Svalbard)	700–1,500	Arctic, Subarctic
		seq52, seq53	Sognesjøen & Skagerak	500	North Atlantic
Lam05-A/-B (Fig. 11F)	<i>Hemilamprops cristatus</i> / <i>Hemilamprops cf. cristatus</i>	seq81, seq82, ICE1-Lam018	Skagerak & Greenland slope	700	North Atlantic, Subarctic
Lam05-B (Fig. 11F)	<i>Hemilamprops cf. cristatus</i>	ICE1-Lam002, ICE1-Lam008	South Iceland Basin	2,500	North Atlantic

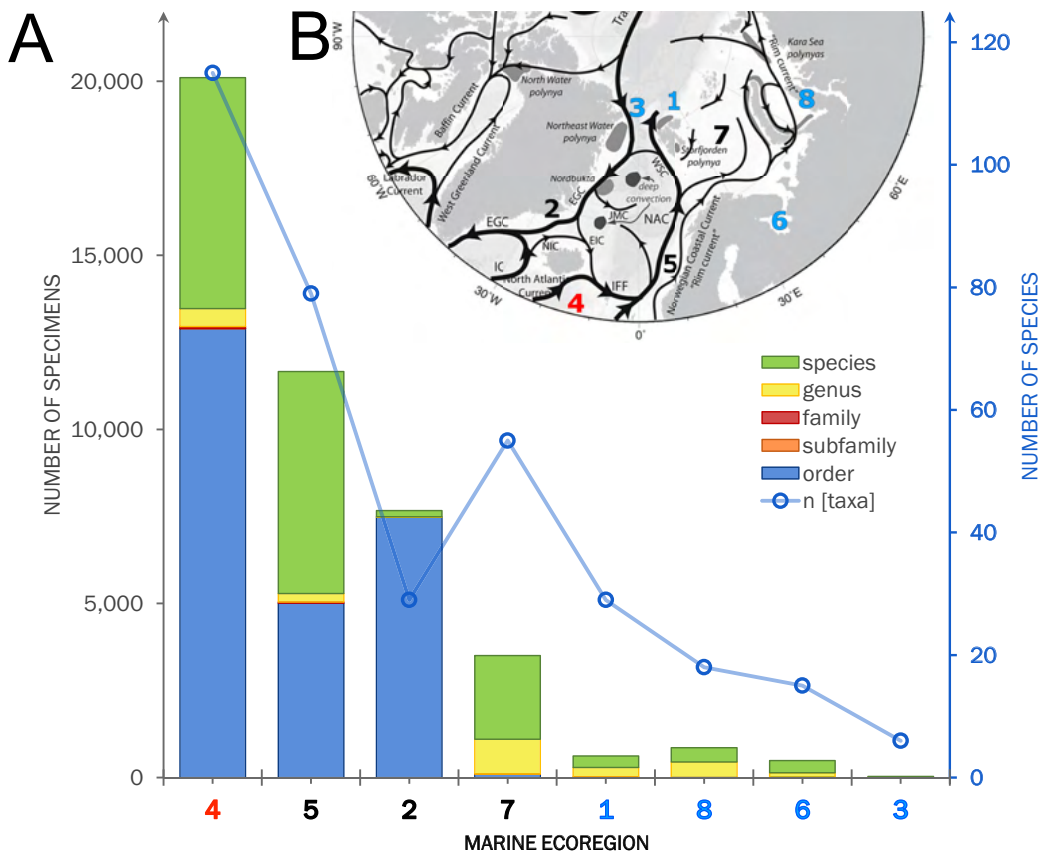


Figure 7 Summarized occurrence records of ‘Cumacea’ and their taxonomic level of determination. (A) Occurrence data of present (OBIS) and newly added records (MAREANO, ICECU, literature) summarized and separated into the predefined marine ecoregions (1–8) and water masses (red: North Atlantic; black: Sub-Arctic; blue: Arctic). Bar plots show the total number of specimens and their taxonomic level of determination (see legend) in relation to the total number of determined taxa. (B) Surface current branching of the North Atlantic current (4) entering the Arctic Ocean via the Norwegian Sea (5) up to Arctic water masses in the Kara Sea (8) and the outflow off the Greenland coast (3) passing the Denmark Strait (2) off Iceland (modified from *Townsend, 2012*). [Full-size DOI: 10.7717/peerj.12379/fig-7](https://doi.org/10.7717/peerj.12379/fig-7)

Leptostylis longimana (Dia16-A). Second, one species (*Hemilamprops cf. cristatus*; Lam05-B) morphologically very closely resembled *Hemilamprops cristatus* (Lam05-A) but was eventually differentiated based on a shorter rostrum and smaller, but more teeth within the serrated dorsal crest in Lam05-A. Also, genetic analyses suggested two lineages with strong divergence (23% *p*-distance), however, the Lam05-A specimen (sequence ID ICE1-Lam018) from the Greenland slope in Subarctic waters (APW-NSAIW), morphologically assigned to Lam05-B, clustered together with Lam05-A from the Norwegian continental shelf. All other Lam06 specimens were from Iceland Sea Overflow Water (ISOW) in the Iceland Basin.

Biogeographical data mining in OBIS

Within the investigated area, a total of 11,714 occurrence records including 44,933 individual specimens were extracted from OBIS (9,151 records), literature and other databases (2,270), and the new ICECU dataset added 293 records (Fig. 7). Out of these, about 6,200 records are in shelf regions up to 250 m depth, about 3,900 records in

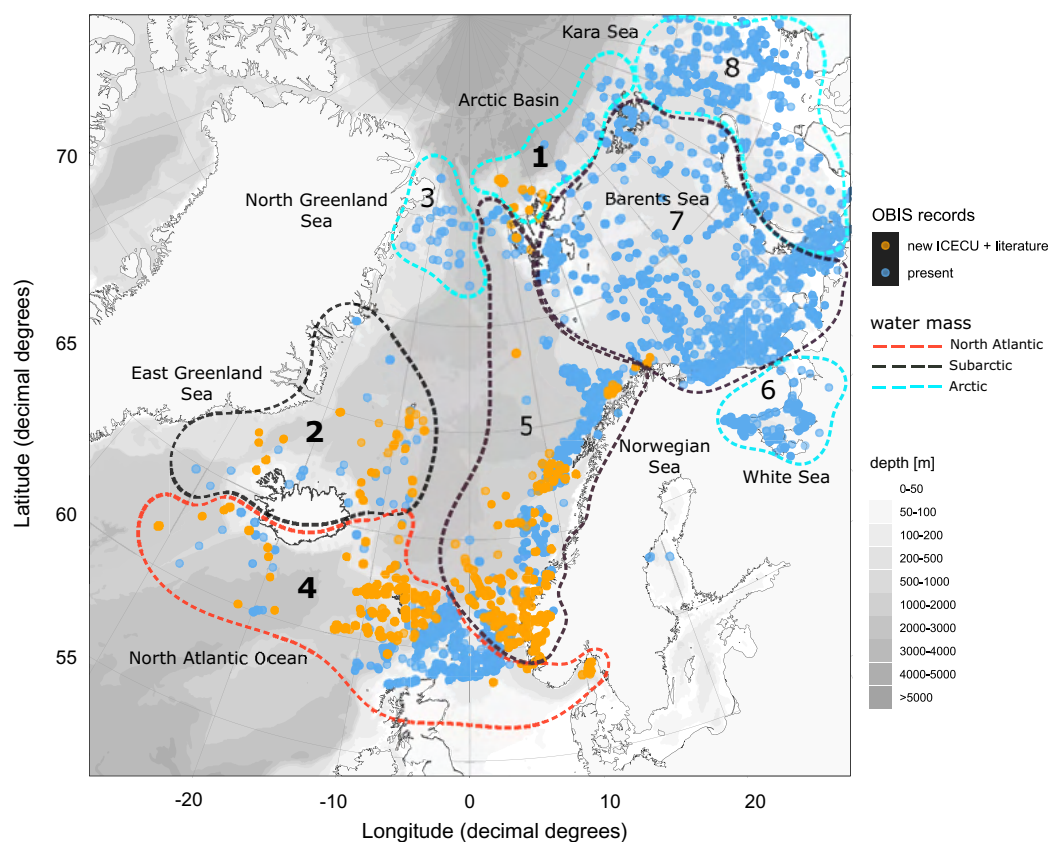


Figure 8 Occurrence records within defined ecoregions for the order Cumacea publicly accessible and additional records contributed by the new ICECU dataset. Overview map for the order Cumacea of present occurrence records (blue), which are publicly accessible on the OBIS platform, and new records (orange), which were contributed by the MAREANO platform, the ICECU dataset and literature data within predefined water masses (red, North Atlantic; black, Sub-Arctic; cyan, Arctic) and ecoregions (1, Arctic Basin; 2, East Greenland Sea; 3, North Greenland Sea; 4, North Atlantic Ocean; 5, Norwegian Sea; 6, White Sea; 7, Barents Sea; 8, Kara Sea) after *Curtis (1975)*, *Hansen & Østerhus (2000)* and *Schlichtholz & Houssais (2002)*. Main focus of this study is on specimens from the bold highlighted ecoregions 1, 2 and 4. [Full-size !\[\]\(9911f9f4a1611a62ffdac539328fb6e0_img.jpg\) DOI: 10.7717/peerj.12379/fig-8](https://doi.org/10.7717/peerj.12379/fig-8)

shelf-break regions between 250–1,000 m and 639 records below 1,000 m in the deep sea, excluding about 780 records with no available depth information. More than half of the specimens (25,496) were classified on order level as ‘Cumacea indet.’, whereas 19,437 specimens were identified to family or a lower taxonomic level. In total, 109 known species are recorded, of which 18 species of five families were recorded for the first time on the OBIS platform within the ecoregions 1, 2, 4, 5 and 7 (Fig. 8). The amount of data and specimen records varied remarkably among the predefined ecoregions 1–8. Ecoregion 4 was assigned to North Atlantic water mass characteristics comprising the highest specimen count (20,101), followed by ecoregion 5 (11,664), 2 (7,667) and 7 (3,505), which are composed of a mixture of North Atlantic and Arctic water masses and were, thus, assigned to Subarctic water-mass characteristics. Arctic water-mass ecoregions 8 (858 specimens), 1 (232), 6 (490) and 3 (29) contributed the lowest specimen sampling effort. There was a general trend of decreasing number of taxa (species diversity) with fewer

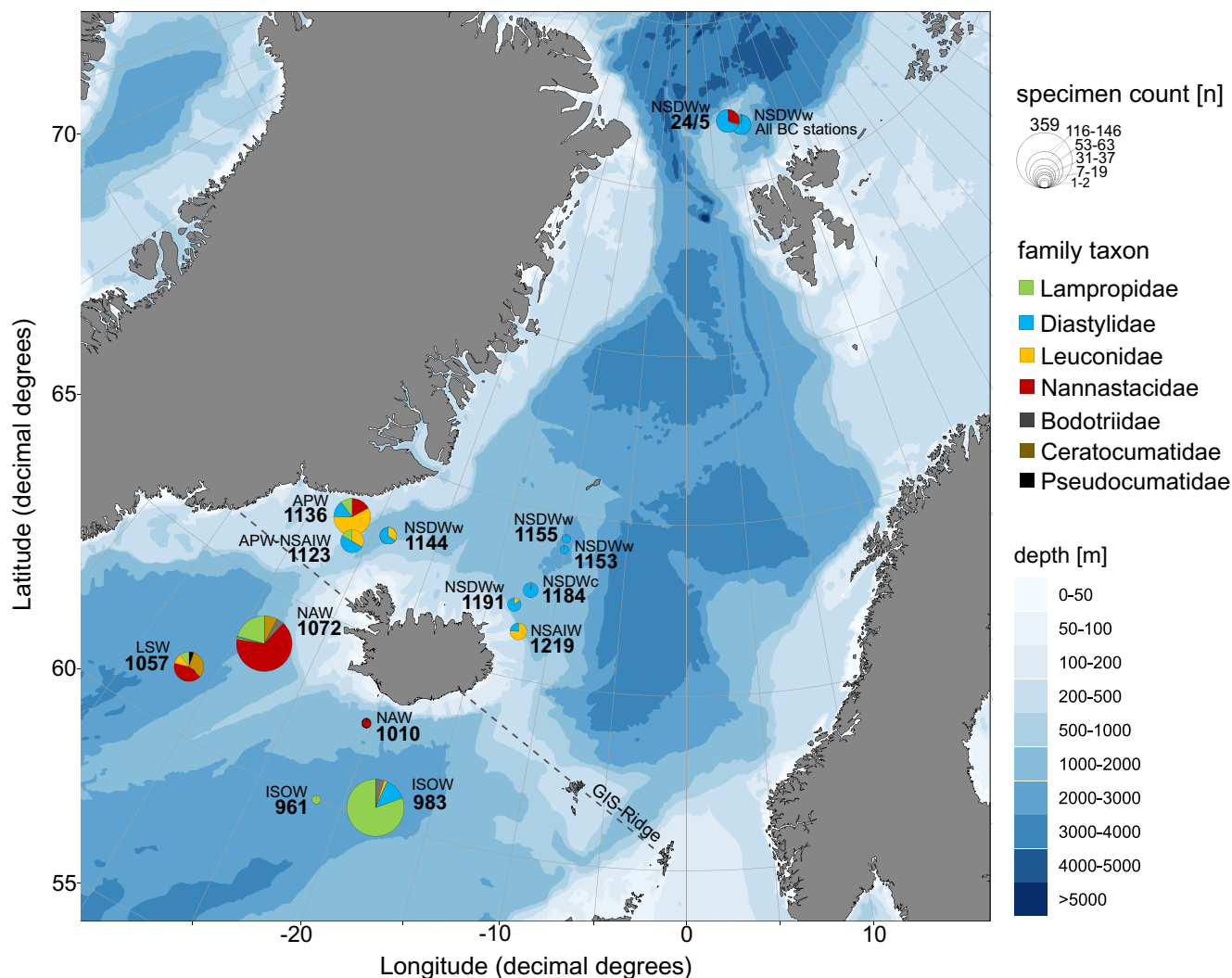


Figure 9 Relative family taxa composition, specimen count and predominating water masses at investigated stations of the ICECU dataset. Each station was assigned to the predominating water mass (APW, Arctic Polar Water; ISOW, Iceland Sea Overflow Water; LSW, Labrador Sea Water; NAW, North Atlantic Water; NSAIW, Norwegian Sea Arctic Intermediate Water; NSDWc/w, cold/warm Norwegian Sea Deep Water). Circle size represents number of specimens and family taxa are distinguished by colors. [Full-size DOI: 10.7717/peerj.12379/fig-9](https://doi.org/10.7717/peerj.12379/fig-9)

specimens following the northern extension of the North Atlantic Current (NAC). For example, out of 232 individual specimens in ecoregion 1, 203 were assigned to 30 different species, while ecoregion 8, one of the last ecoregions influenced by the NAC, had a higher sampling effort with 858 specimens, but a lower species diversity with 407 individuals assigned to 18 species.

Species distribution patterns within ecoregions

Overall, the composition of taxa was observed to change from a Northern Atlantic-boreal (ecoregion 4, 5, 7) to a typical Arctic community (2, 1, 8, 6, 3; Fig. 9). Investigating the composition of the most frequently occurring taxa in OBIS revealed that the taxon *Diastylis rathkei* was recorded in all ecoregions, followed by *Campylaspis rubicunda*

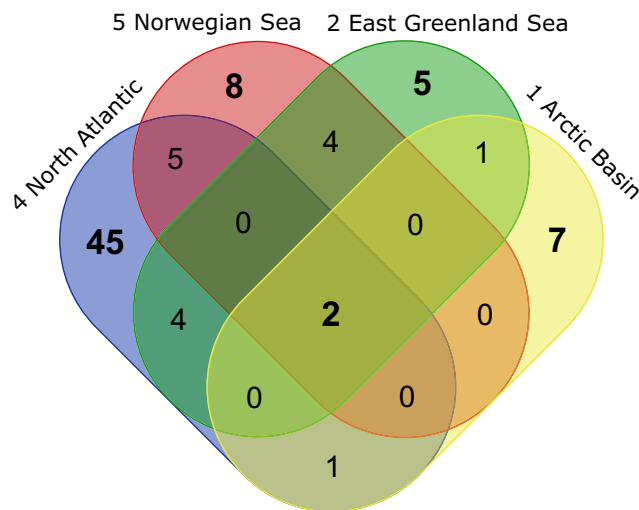


Figure 10 VENN-Diagram showing the total number of representative species per ecoregion as well as shared representatives occurring within several ecoregions. Ecoregions are sorted by the extension of the North Atlantic Current from south to north. Created using the web-tool <http://bioinformatics.psb.ugent.be/webtools/Venn/>. Full-size DOI: 10.7717/peerj.12379/fig-10

Liljeborg, 1855, *Diastylis goodsiri* Bell, 1855 and *Brachydiastylis resima* Krøyer, 1846, which were recorded in seven of eight regions. Compared to other ecoregions of the same size, the Arctic Ocean and the area around Iceland are underrepresented in cumacean occurrence records. Currently available records in these ecoregions are restricted to 90 entries of 32 species. Within these records, the most frequently occurring species are *Diastylis polaris*, Sars, 1871, *Leptostylis longimana*, *Platytyphlops semiornatus* Fage, 1929, *Campylaspis globosa* Hansen, 1920, *C. vallecuate* Jones, 1974, *Leucon (Epileucon) spiniventris* Hansen, 1920 and *Platycuma holti* Calman, 1905.

Faunistic mix in ICECU material

The morphologically and genetically investigated material of the ICECU dataset corresponded well with the earlier observed trend in the OBIS dataset of high species diversity in the North Atlantic (ecoregion 4) with 45 representative, ecoregion-specific species (Fig. 10; Table 5). With the northern extension of the NAC, the representative species number decreases to seven in ecoregion 1 (Arctic Basin) and five in ecoregion 2 (East Greenland Sea). The number of shared species occurring in more than one ecoregion decreases with distance: While the adjacent ecoregion 4 and 5 share five species, ecoregion 4 and 1 only share one species (*Campylaspis intermedia* Hansen, 1920). The two species *Platysympus typicus* G. O. Sars, 1870 and *Leucon (Alytoleucon) pallidus* G. O. Sars, 1865 were recorded in all ecoregions. Comparing regional distribution patterns of families, a seamless shift in the relative composition along the GIS-Ridge could be observed (Fig. 9). The highest number of investigated specimens and species was recorded in stations located south of the Ridge in the Icelandic and Irminger Basins, which have warmer and more saline water masses (ISOW, Labrador Sea Water (LSW), North Atlantic Water (NAW); ecoregion 4) and were characterized by the families Lampropidae and

Table 5 Table related to Fig.10: total number of representative species per ecoregion as well as shared representatives occurring within several ecoregions.

Ecoregions	Total	Representative species
1 Arctic Basin 2 East Greenland Sea 4 North Atlantic Ocean 5 Norwegian Sea	2	<i>Platysympus typicus</i> , <i>Leucon (Alytoleucon) pallidus</i>
1 Arctic Basin 2 East Greenland Sea	1	<i>Diastylis spinulosa</i>
1 Arctic Basin 4 North Atlantic Ocean	1	<i>Campylaspis intermedia</i>
2 East Greenland Sea 4 North Atlantic Ocean	4	<i>Hemilamprops</i> sp.1 (juv.), <i>Hemilamprops</i> cf. <i>crustatus</i> , <i>Leucon (Macrauloleucon) spinulosus</i> , <i>Leptostylis ampullacea</i>
2 East Greenland Sea 5 Norwegian Sea	4	<i>Hemilamprops uniplicatus</i> , <i>Diastylis polaris</i> , <i>Campylaspis sulcata</i> , <i>Campylaspis undata</i>
4 North Atlantic Ocean 5 Norwegian Sea	6	<i>Leptostylis longimana</i> , <i>Diastylis serratus</i> , <i>Leucon (Leucon) nathorsti</i> , <i>Eudorella hirsuta</i> , <i>Campylaspis horrida</i> , <i>Eudorella truncatula</i>
1 Arctic Basin	7	<i>Diastylis goodsiri</i> , <i>Petalosarsia declivis</i> , <i>Leucon (Leucon) nasicooides</i> , <i>Diastylis rathkei</i> , <i>Leptostylis</i> cf. <i>longimana</i> , <i>Campylaspis rubicunda</i> , <i>Leucon (Leucon)</i> aff. <i>nathorsti</i>
2 East Greenland Sea	5	<i>Leucon (Leucon) profundus</i> , <i>Campylaspis</i> sp.1, <i>Hemilamprops assimilis</i> , <i>Diastylis echinata</i> , <i>Leptostylis borealis</i>
4 North Atlantic Ocean	42	<i>Bathycuma brevirostre</i> , <i>Campylaspides</i> sp.1, <i>Diastylis lucifera</i> , <i>Chalarostylis</i> sp.1, <i>Cumellopsis</i> cf. <i>puritani</i> , <i>Eudorella emarginata</i> , <i>Hemilamprops</i> cf. <i>diversus</i> , <i>Hemilamprops pterini</i> , <i>Leucon (Crymoleucon) tener</i> , <i>Eudorella</i> sp.1, <i>Diastylis atlanticus</i> , <i>Hemilamprops roseus</i> , <i>Bodotriidae</i> sp.1, <i>Leptostylis</i> sp.2, <i>Cimmerius reticulatus</i> , <i>Campylaspis</i> sp.2, <i>Styloptocuma</i> sp.1, <i>Leptostylis</i> sp.1, <i>Leucon</i> sp.1, <i>Cyclaspis longicaudata</i> B, <i>Bodotriidae</i> sp.2, <i>Procampylaspis ommidion</i> , <i>Styloptocuma gracillimum</i> , <i>Leucon (Leucon) acutirostris</i> , <i>Leucon (Leucon)</i> cf. <i>robustus</i> , <i>Leucon (Macrauloleucon) siphonatus</i> , <i>Procampylaspis</i> sp.1, <i>Makrokyllindrus (Makrokyllindrus) spiniventris</i> , <i>Chalarostylis elegans</i> , <i>Styloptocuma erectum</i> , <i>Hemilamprops</i> sp.2, <i>Platytyphlops semiornatus</i> , <i>Nannastacidae</i> sp.1, <i>Campylaspis alba</i> , <i>Bathycuma</i> sp.1, <i>Styloptocuma</i> sp. 2, <i>Diastylis laevis</i> , <i>Diastylis</i> sp.1, <i>Campylaspis globosa</i> , <i>Campylaspis costata</i> , <i>Pseudocuma</i> sp.1, <i>Cumella (Cumella)</i> cf. <i>decepiens</i>
5 Norwegian Sea	6	<i>Iphinoe serrata</i> , <i>Diastylis biplicatus</i> , <i>Cyclaspis longicaudata</i> A, <i>Mesolamprops denticulatus</i> , <i>Diastylis cornuta</i> , <i>Diastylis tumida</i>

Nannastacidae. Stations north of the Iceland-Faroe Ridge, the Denmark Strait and on the Yermak Plateau north of Svalbard are influenced by colder and less saline water masses (APW, NSAIW, cold & warm Norwegian Sea Deep Water NSDWc & NSDWw; ecoregion 1, 2) and were mostly characterized by the families Diastylidae and Leuconidae.

Representatives of the family Bodotriidae were only recorded in southern stations (Station 983, ISOW; 1,057, LSW; 1,072, NAW), as well as the Ceratocumatidae (1,057, LSW; 1,072, NAW) and the only representative specimen of the Pseudocumatidae G. O. Sars, 1878 (1,057, LSW).

In correspondence with the OBIS data, *Leptostylis* cf. *longimana* (Dia16-B; Fig. 11A) and *Leptostylis ampullacea* (Dia14; Fig. 11B) were the most frequently recorded species, occurring at 13 out of 21 stations, followed by *Diastylis polaris* (Dia06; Fig. 11C) and *Leucon* (*Alytoleucon*) *pallidus* (Leu05; Fig. 11D) recorded at five stations each. Other wide-ranging species, such as *Platysympus typicus* (Lam13; Fig. 11E) and *Hemilamprops cristatus* (Lam05; Fig. 11F) were found across multiple ecoregions. A majority of the species were only present in samples from one or two stations. For characteristic boreal and Arctic taxa investigated in this study, such as *Leptostylis borealis* (Dia15; Fig. 12A), *L. (A.) pallidus* (Leu05) or *Hemilamprops pterini* Shalla & Bishop, 2007 (Lam07; Fig. 12B), additional occurrence records were contributed within the expected ranges. The species *Cimmerius reticulatus* Jones, 1973 (Cer01; Fig. 12C) was the first record for the family Ceratocumatidae to be found in the North Atlantic. Interesting new records of species in Icelandic waters such as *Hemilamprops* cf. *diversus* Hale, 1946 (Lam06; Fig. 12D), previously only known from off South-eastern Australia, and *Cumellopsis* cf. *puritani* Calman, 1906 (Nan13), mostly recorded in the Mediterranean Sea, might either represent unexpected wide distribution ranges for these species or presence of morphologically closely related species, but new to science.

In order to minimize the taxonomic knowledge gap, especially in ecoregion 2, the focus of this study is on specimens collected within the regions 1, 2, 4 and 5, which represent all three water-mass categories (North Atlantic, Subarctic, Arctic) and differed remarkably in their taxa composition.

Representatives of the Arctic Ocean (ecoregion 1)

One representative specimen of the circumpolar species *Diastylis spinulosa* Heller, 1875 (Dia08; Fig. 12E) was detected from north of Spitzbergen. In congruence with the OBIS occurrence records, ecoregion 1 was dominated by representatives of the families Diastylidae, Leuconidae and Nannastacidae. The morphologically examined material from the Arctic Ocean included only four species: *Leptostylis* cf. *longimana* (Dia16-B) dominated in specimen number, followed by *Campylaspis rubicunda* (Nan08; Fig. 12F), *Campylaspis intermedia* (Nan06; Fig. 13A) and one specimen of *Leucon* (*Alytoleuco*) *pallidus* (Leu05). *Campylaspis intermedia* is known to be widely distributed in the whole Atlantic Ocean but was not recorded in the Arctic yet. Thus, the occurrence records in the present study from north of Svalbard extend the previously assumed distribution range significantly. *Campylaspis rubicunda* is known from the North Pacific, the North Atlantic and the Arctic Oceans and *Leptostylis longimana* is widely distributed in the cold areas of the Northern Atlantic. Nevertheless, none of the previously mentioned species is found strictly in ecoregion 1, but rather widely distributed and occurring in other ecoregions.

Representatives of East Greenland Sea (ecoregion 2)

The most common species in ecoregion 2 was *Diastylis polaris* (Dia06), which was sampled at five IceAGE stations composed of NSDWw and NSDWc. This observation corresponds with the occurrence records found in OBIS, which also include the morphologically

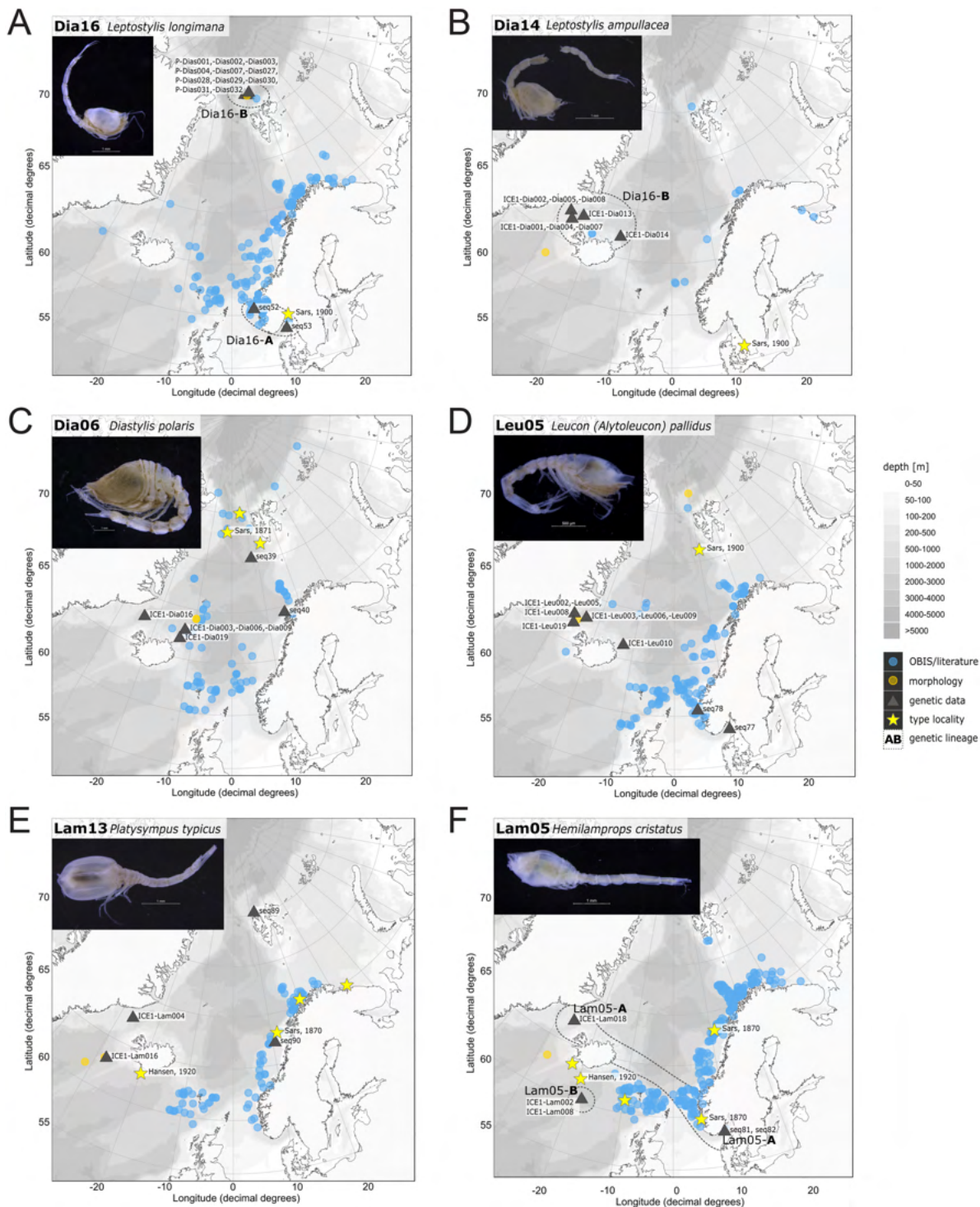


Figure 11 Distribution maps of species integrated in morphological and molecular analyses representing the families Diastylidae (A–C), Leuconidae (D) and Lampropidae (E–F). Occurrences of morphologically identified species integrated in genetic analyses. Occurrence records are shown from the MAREANO and OBIS platform as well as literature data (blue), specimens morphologically investigated in this study (orange) and subsequently genetically investigated (grey triangle with sequence ID) and type and/or syntype locality of putative species (yellow star with reference literature). Genetic lineages are highlighted with dotted circles and separated by assigned letters A–C.

Full-size DOI: 10.7717/peerj.12379/fig-11

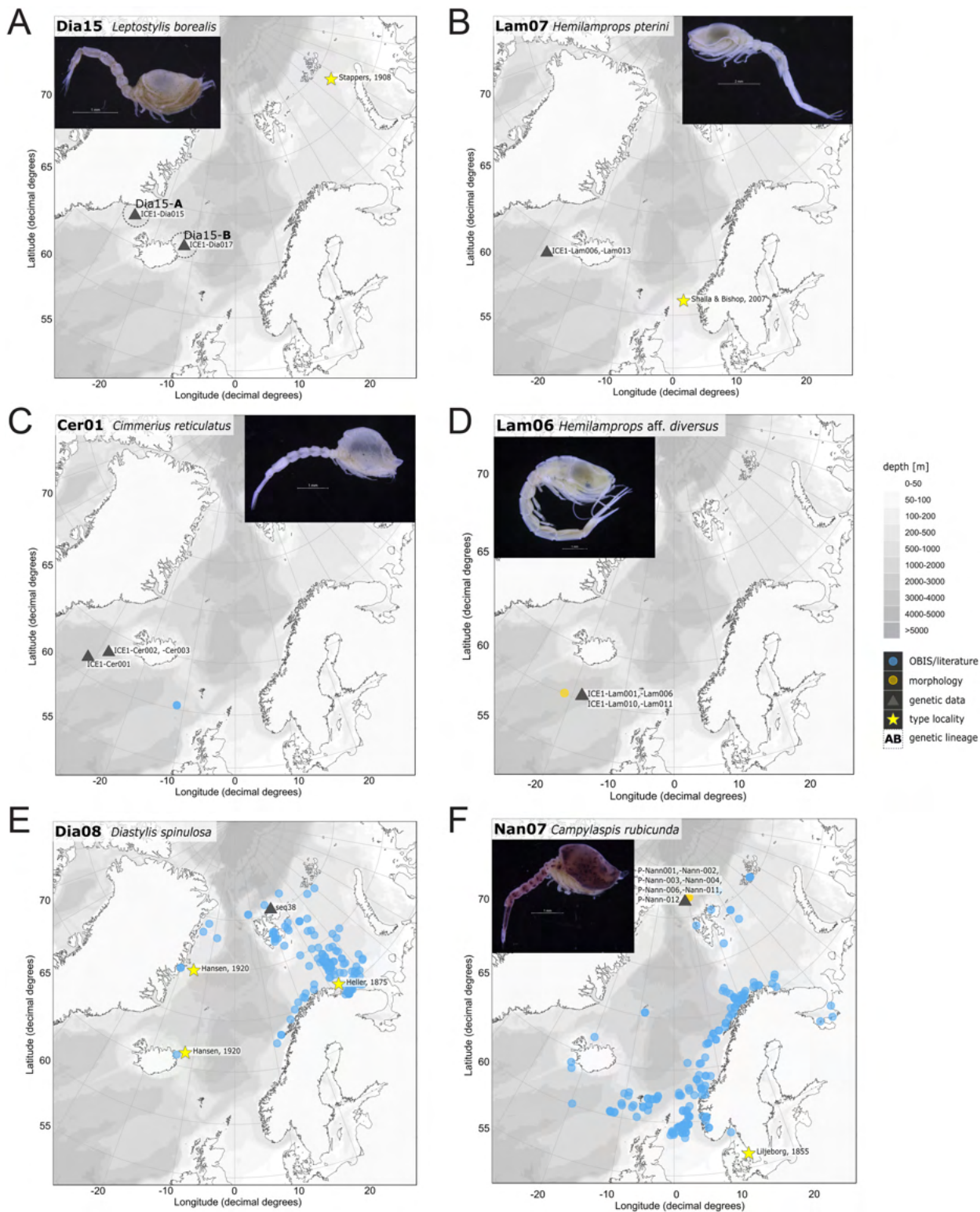


Figure 12 Distribution maps of species integrated in morphological and molecular analyses representing the families Diastylidae (A, E), Lampropidae (B, D), Ceratocumatidae (C) and Nannastacidae (F). [Full-size DOI: 10.7717/peerj.12379/fig-12](https://doi.org/10.7717/peerj.12379/fig-12)

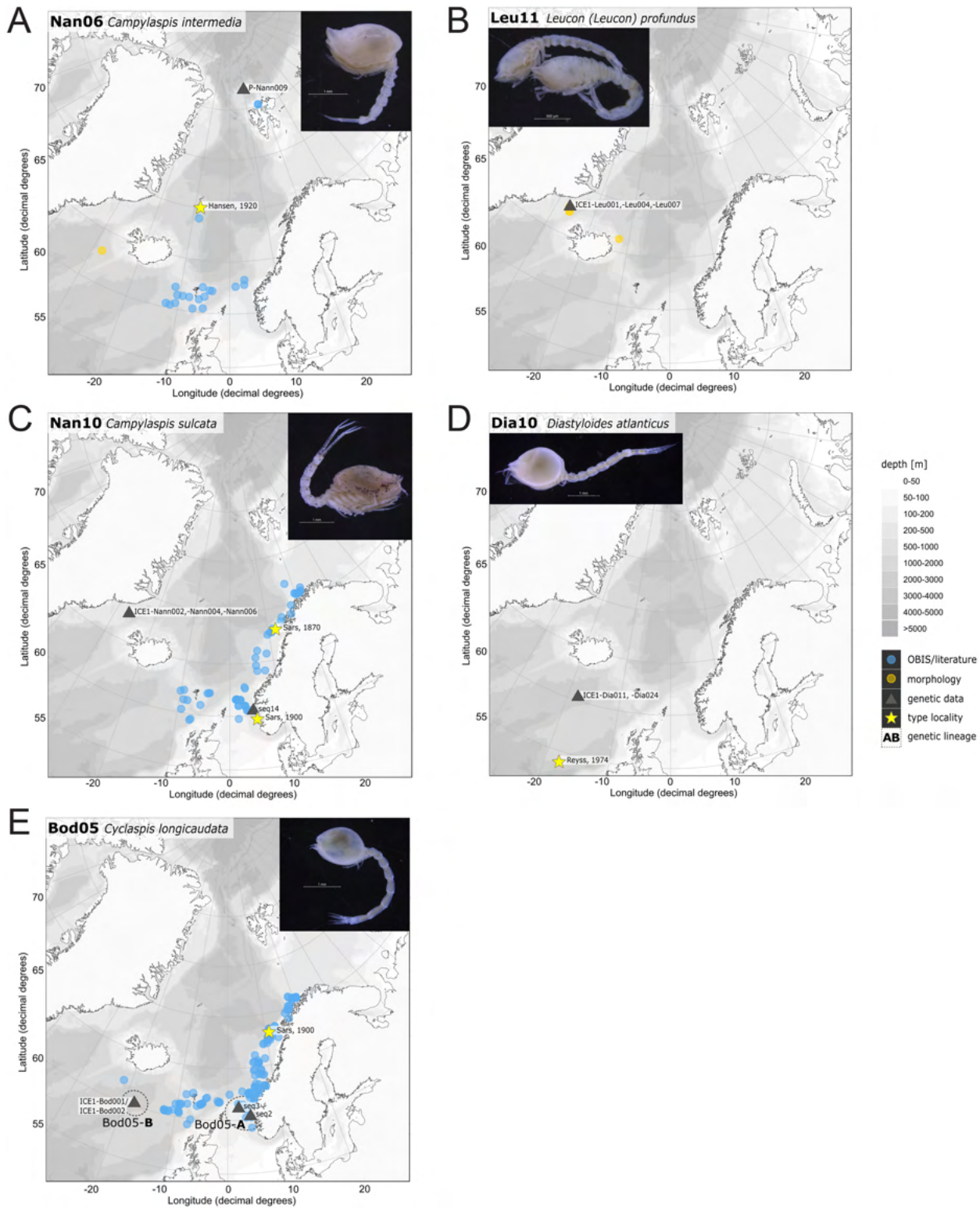


Figure 13 Distribution maps of species integrated in morphological and molecular analyses representing the families Nannastacidae (A, C), Leuconidae (B), Diastylidae (D) and Bodotriidae (E).

Full-size DOI: 10.7717/peerj.12379/fig-13

closely related *Diastylis stygia* G. O. Sars, 1871, both being described as true Arctic species. The species *Leptostylis borealis* (Dia15), originally described south of Franz-Josef-Land, was recorded for the first-time off Iceland. Most representatives of the family Leuconidae in the IceAGE material were sampled in ecoregion 2, north of the Iceland-Faroe Ridge. This result suggested a restricted distribution range of sampled representatives of the family Leuconidae to colder and fresher water masses (e.g., APW, NSAIW and NSDW). The species *Leucon (Leucon) profundus* Hansen, 1920 (Leu11; Fig. 13B) and *Leucon (Alytoleucon) pallidus* (Leu05) were the most common species of this family in the investigated material. Vassilenko (1989) and Gerken & Watling (1999) described both with a circumpolar distribution range from the North Atlantic Ocean to the Canadian Arctic Ocean, but mostly found in cold-water stations (Watling & Gerken, 2005). However, by our samples, new occurrence records of these species were added in the Norwegian Sea waters influenced by the North-Atlantic current, suggesting an extension of the distribution range for warmer waters of the previously assumed cold-water species.

Representatives of the North Atlantic and Norwegian Sea (ecoregion 4 and 5)

Ecoregion 4 was dominated in specimens by *Hemilamprops cf. diversus* (Lam07) and *Hemilamprops pterini* (Lam08), which are taxa found predominantly in warmer waters, as well as *Campylaspis* sp. 2 (Nan10; Fig. 13C). In general, the genera *Hemilamprops* and *Campylaspis* reached highest record numbers both in terms of taxa and specimen count. The widely distributed boreal Atlantic species *Hemilamprops cf. cristatus* (Lam05-B) is recorded to occur in high abundances within ecoregion 4 and 5, though it was also sampled at one station in the Denmark Strait. Specimens in ecoregion 4 were mostly sampled in deep-sea habitats, while specimens in ecoregion 5 were mostly sampled in coastal and fjord habitats. Typical Atlantic Ocean species of other families only recorded south of the GIS-Ridge in warmer waters were *Diastylodes atlanticus* Reyss, 1974 (Dia10; Diastylidae; Fig. 13D), *Bathycuma brevirostre* Norman, 1879 (Bod01; Bodotriidae) and *Cyclaspis longicaudata* Sars, 1865 (Bod05; Bodotriidae; Fig. 13E), as well as *Pseudocuma* sp. 1 (Pse02), the only representative of the Pseudocumatidae in the ICECU dataset. *Cimmerius reticulatus* (Cer01), expanding its distribution northward from the Bay of Biscay, is the only representative of the Ceratocumatidae. The specimens of *Eudorella truncatula* sampled in ecoregion 4 (Leu04-A/-B; Fig. S2-U) and ecoregion 5 (Leu04-C) were all separated into distinct lineages, which was also observed in *Cyclaspis longicaudata* from ecoregion 4 (Bod05-B) and ecoregion 5 (Bod05-A).

DISCUSSION

Combined species delimitation approach - morphology and genetics

As only a handful of studies applied molecular methods for species delimitation within cumaceans, the combined approach in this study highlights the high quality and overall congruence in most cases of morphological and genetic analyses. Even though delimiting species based solely on one mitochondrial marker like 16S rDNA has been questioned as there is no universal threshold for species delimitation (Meyer & Paulay,

2005; Meier et al., 2006; Wiemers & Fiedler, 2007; Schwentner, Timms & Richter, 2011; Collins & Cruickshank, 2013), in our study a clear barcoding gap between 2% and 8% was observed among most inferred species, corresponding nicely with morphological taxonomic characters in the vast majority of cases. The 4% genetic distance observed between the geographically widely separated (>3,000 km) *Diastylis rathkei* (Dia07) individuals cannot be easily interpreted as either intra- or interspecific and might hint at a recent and/or ongoing speciation event. Similar observations have been made previously for 16S rDNA of cumaceans and other peracarids like isopods (Brökeland & Raupach, 2008; Held & Wägele, 2005; Rehm, 2007; Rehm et al., 2020; Riehl, Lins & Brandt, 2018). Herein, intraspecific distances were usually below 1%, though geographically widely distributed species featured up to 3% or 5%, respectively. Conversely, interspecific distances exceeded 7%. Also, here the higher intraspecific genetic distances of 5% were tentatively suggested to represent potential cryptic species (Rehm, 2007). Based on these findings we suggest that the rare cases of conflict between morphological and genetic data represent cases of cryptic diversity or extensive morphological variability.

Examples of morphologically cryptic diversity

The incongruence of 16S sequence data revealing high genetic diversity within a species (or even cryptic species) was observed in six cases (Table 4). This affects *Hemilamprops cristatus* (Lam05, A–B), *Eudorella truncatula* (Leu04, A–C), *Cyclaspis longicaudata* (Bod05, A–B), *Leptostylis borealis* (Dia15, A–B) and *Leptostylis* sp. 1 (Dia18, A–B; Fig. S2L). The intraspecific genetic distances observed within each of these taxa greatly exceeded those commonly observed within species of Cumacea and other peracarids. We therefore conclude that all of these cases indicate presence of morphologically cryptic species. Moreover, some of these cryptic species were not even recovered as sister species, but widely separated (Fig. 2). Further taxonomic studies will be needed to prove these cases.

In *Cyclaspis longicaudata* (Bod05, A–B), *Eudorella truncatula* (Leu04, A–C) and *Leptostylis borealis* (Dia15, A–B) the respective cryptic species were geographically well separated and usually occurred in different water masses. In the case of *Hemilamprops cristatus* (Lam05, A–B), morphological re-examinations showed weak differences in the rostrum length and the serration of the dorsal crest on the carapace (shorter rostrum and smaller, but more teeth in Lam05-A). However, one specimen (ICE1-Lam018) sampled on the Greenland slope in Subarctic waters and morphologically corresponding to Lam05-B, clustered genetically together with Lam05-A from the Norwegian continental shelf.

Our cumacean examples do support the finding in other peracarid taxa (amphipods and isopods) of either overestimations (Lörz et al., 2020) or underestimations of intraspecific divergence (Brix, Svavarsson & Leese, 2014b; Jennings, Golovan & Brix, 2019; Paulus et al., in press). This emphasizes that sampling from a geographically limited portion of a species' range only risks missing relevant genetic variation, which blurs an important line between species-level and population-level diversity. Molecular species

delimitation should, thus, include specimens sampled in the widest possible distribution range of the examined taxon (Knox, 2012).

Examples of morphological variability and taxonomic incongruence

Specimens identified as *Diastylis polaris* (Dia06) and *Diastylis stygia* were identical in 16S. Interestingly, Zimmer (1926) synonymized these species based on Ohlin's (1901) and Stebbing's (1913) conclusion of their conspecificity. In Zimmer, 1980 re-examined a specimen of *D. stygia* collected by the Russian Sadko Expedition (Zimmer, 1943) and separated it again from *D. polaris* as a valid species. Our study lays additional support for *D. stygia* being a synonym of *D. polaris*. Similarly, after re-examination of *Platysympus typicus* (Lam14) sampled off East Greenland and *P. tricarinatus* Hansen, 1920 from the Norwegian shelf, these two species names are probably representing the same species. Gerken (2018) called the assumed differentiating characters of more or less conspicuous folds on the carapace into doubt and suggested that less prominent characters might be owed to juvenile stages. Therefore, *P. tricarinatus* is assumed to be a synonym of *P. typicus*. Similarly, *Leucon* (*Leucon*) aff. *nathorsti* (Leu09) differed morphologically from *L. (L.) nathorsti* (Leu08) by the presence of two dorsolateral teeth on the frontal lobe of the carapace and a more acute rostrum and, thus, identified as a possible separate species. However, in this 16S analyses these two morphotypes proved to be identical, suggesting the presence of a single, morphologically variable species. As Leu08-specimens were sampled on the Norwegian continental shelf in North Atlantic waters and Leu09 was collected off Svalbard in Subarctic waters, an ecologically-driven morphological population variation might be implied.

Further, we found that the two morphologically almost indistinguishable species *Leptostylis longimana* (Dia16-B) and *L. ampullacea* (Dia14) grouped into a large unresolved clade forming a "*Leptostylis longimana/ampullacea*" species complex. Species in the genus *Leptostylis* are rather difficult to distinguish as there is a certain degree of phenotypic plasticity tied to sex and growth stages, and some morphological distinctions are quite subjective, such as 'clumsier' body form of *L. ampullacea* compared to *L. longimana* (Sars, 1900). A second "*Leptostylis longimana*"-clade was retrieved, based on specimens from coastal Norway, genetically well separated from the Iceland/Arctic "*L. longimana/ampullacea*"-clade by 26–27% *p*-distance. Based on the present data, the Iceland/Arctic specimens should be referred to *L. ampullacea*, originally described from Kullaberg (off Sweden). This further implies that the "true" *L. longimana*, originally described from the Oslofjord, a more coastal and/or southern distribution. Further studies including additional specimens and gene markers, as well as museum type material will be necessary to resolve the taxonomy in more detail.

Biogeographic integration

Data-mining implications

This study contributed with the ICECU dataset first occurrence records of 18 species representing five families within the investigated ecoregions (Fig. 8). Additionally, about 25% of morphologically determined taxa could not be assigned to species level, which

might either constitute known species from originally other regions or new species to science. The extension of distribution ranges of ecoregional representative species clearly shows our knowledge gaps on estimated distribution patterns of cumaceans. By monitoring the impact of a changing climate on species distributions based on time series of the first occurrences of this species, the benefits of publicly accessible distribution data of marine animals on platforms such as OBIS are undeniable. The linkage to WoRMS ensures verified taxonomic name information following the Darwin Core standard and connection to other sources ([Costello et al., 2007](#); [Wieczorek et al., 2012](#)). Still, the determination of species demands knowledge of taxonomy, ecology, and morphological characters of the investigated taxon. Especially molecular species delimitation depends on prior morphological identification and database confidence. The importance of such reliable species name assignments was especially observed in the genus *Leptostylis*, in which hidden diversity was found when integrating genetic data. Thus, caution should be taken when using public distribution databases due to their restricted possibilities to present hidden diversity. This study showed that species identifications of a large dataset based only on morphological delimitation may underestimate true diversity. For example, in the case of the species *Hemilamprops cristatus* and *Eudorella truncatula*, which are assumed to be a widely distributed species in the boreal Arctic as well as in the North American basin ([Watling, 2009](#)), genetic analyses revealed either a cryptic speciation due to geographical separation and different water-mass conditions or species from distinct populations with separated geographical origins.

Are ecoregions reflected in species distribution?

The results of this study support the suggestion of [Hansen \(1920\)](#) and [Watling & Gerken \(2005\)](#) that water-mass characteristics are an important controlling variable for cumacean species occurrences. The community composition was observed to change from warm-water dominating families in ecoregion 4 south of the GIS-Ridge (Lampropidae, Bodotriidae, Nannastacidae) to families dominating in colder and less saline Subarctic and Arctic water masses found in ecoregion 1 and 2 (Diastylidae, Leuconidae; [Fig. 9](#)).

Closer investigation of cumacean distributions on species level revealed that most species occurred in multiple ecologically similar ecoregions ([Fig. 10](#); [Table 5](#)). Even though typical ecoregion-specific representatives could be determined, in many cases these also occurred in other ecoregions. This pattern was also corroborated by the genetic data. For example, [Vassilenko \(2002\)](#) categorized the species *Campylaspis globosa* (Nan04) and *Hemilamprops uniplicatus* G. O. Sars, 1872 (Lam11) as widely distributed Arcto-Atlantic bathyal species of Atlantic origin. This study supported the preceding assumption, as specimens inhabiting Arctic and Subarctic waters in the Denmark Strait (ecoregion 2) and Atlantic waters on the Norwegian continental shelf (ecoregion 4 & 5) were morphologically and genetically identical within the species ([Figs. S2Q, S2α](#)). The same case was observed in *Platysympus typicus* (Lam13) and *Diastylis polaris* (Dia06) from Atlantic to Arctic water influenced ecoregions (1, 2, 4, 5; [Figs. 11C, 11E](#)).

Some species revealed hidden diversity reflected by patchy distribution patterns within ecoregions. *Cyclaspis longicaudata* Bod05-B was sampled in the Iceland Basin (ecoregion 4) and was genetically differentiated and geographically separated by the GIS-Ridge to Bod05-A from the Norwegian continental shelf (ecoregion 5; Fig. 13E). A similar case was observed between the species *Hemilamprops cristatus* Lam05-B from a deep Iceland Basin station (2,500 m) and Lam05-A, which was sampled close to the type locality from Skagerrak (700 m depth; Fig. 11F). As this species is reported as a widely distributed boreal Atlantic species, cryptic speciation might be considered due to the geographical separation by the GIS-Ridge. It would seem that *H. cristatus* in the Iceland basin might be a hidden, putative species new to science. Simultaneously, the *Leptostylis longimana/ampullacea* complex Dia14/-16-B from cold-water masses (NSDWw, APW, APW/NSAIW) was revealed to be widely distributed from Iceland to Arctic regions (ecoregions 1 and 2) over a distance of more than 2,500 km. Dia16-A, though, was revealed to be a distinct genetically differentiated population in ecoregion 4. Earlier records of this species complex are from the same distribution area, and described as a predominantly bathyal-Atlantic, boreal-Arctic species (Jones, 1976; Vassilenko, 1989). Watling & Gerken (2005) observed *L. longimana* to be present over a wide temperature range. Another example in ecoregion 2 for potentially disrupted gene flow between populations by geographical barriers is the species *Leptostylis borealis* Dia15-A from the East Greenland shelf and Dia15-B from East Iceland Norwegian Sea, separated by the Denmark Strait (Fig. 12A). In contrast, *Leucon (A.) pallidus* (Leu05) sampled at these stations showed no genetic differentiation between specimens, despite the Denmark Strait as a potential barrier. For the investigation of distinct cumacean distribution patterns as proposed by Watling & Gerken (2005), a larger sample size is needed as many morpho- and genospecies were represented as singletons or were sampled in higher numbers, but at solely one station.

CONCLUSIONS

This study confirmed the advantage of a combined approach of traditional morphological and modern molecular techniques to delimit cumacean species and uncover hidden diversity, compared to delimitations based solely on one method. Some species may need more taxonomic attention and re-evaluation. We have shown examples of underestimated diversity as well as overestimated diversity. However, the advantage of molecular investigations for testing important questions of species diversity correlates significantly with prior species identifications and emphasizes the importance of a robust basis of taxonomic knowledge and morphological examination.

For example, in ecoregion 2, 98% of the specimens could only be determined to order level. When the resolution of identification only gets to order level, the species occurrence data is influenced as the species level information is not shown in public databases (for example). Thus, with more species level identifications in ecoregion 2, it is a high likelihood to find more species new to science or even more ecoregion-representative species. While this ecoregion was characterized by five representative species, ecoregion 4

revealed high species diversity with 45 representative species correlating with the highest sampling effort of all investigated regions.

As for other peracarid groups, the GIS-Ridge plays an important role as a geographical barrier and separates ecoregion-specific cumacean communities between the North Atlantic Ocean in the south and the Subarctic seas in the north. Although the biogeographic results of this study furthermore support the assumption of earlier studies that water-mass characteristics are important controlling variables for cumacean species occurrences, this remains a hypothesis unless a more detailed ecological observation of factors shaping cumacean distribution with statistical analyses including not only water masses, but further abiotic factors (*e.g.*, depth, sedimentary characteristics, potential geographical barriers) is undertaken.

ACKNOWLEDGEMENTS

Firstly, we would like to emphasize that the base of this study is formed by excellent international collaboration, fruitful discussions, and trust-based exchange of experience and knowledge. It would not have been possible without team- and networking, starting with those, who invest many days to sample at sea, preserve, catalogue and sort benthic samples for further analyses. We owe an immense debt to Karen Jeskulke, Nicole Gatzemeier, Antje Fischer, Sven Hoffmann and the whole team of DZMB HH for the technical support at all levels. We warmly thank Kathrin Philipps-Bussau, Petra Wagner, Nancy Mercado Salas and Alexandra Kerbl for maintenance of the CeNak collection material. Many thanks to Simon Bober, Johanna Bober, Mariam Dunker and Oliver Hawlitschek for the help on laboratory issues. Our sincere thanks go to the Captains and Crew of RV Meteor and RV Polarstern during M85/3 (IceAGE) and PS106/1 (PASCAL). Big thanks to Team 'SIEMO' for their help and efficient work at sea. Special thanks go to Sarah Gerken and Ute Mühlenhardt-Siegel for taxonomical expertise and advice. We are grateful to Louise Lindblom for guidance and assistance in the Biodiversity laboratory at University of Bergen.

ADDITIONAL INFORMATION AND DECLARATIONS

Funding

Carolin Uhlir received a grant from the Universität Hamburg to travel to Bergen. Lab work was funded *via* internal funds of the Universität Hamburg and the Center of Natural History. Kenneth Meland and Henrik Glenner were supported by the Norwegian Taxonomic Initiative (NTI). Angelika Brandt and Saskia Brix received grant support from AWI_PS106_00 for the PASCAL and from the DFG BR3843/3-1 for the IceAGE expedition. The funders had no role in study design, data collection and analysis, decision to publish, or preparation of the manuscript.

Grant Disclosures

The following grant information was disclosed by the authors:
Universität Hamburg.

Universität Hamburg and the Center of Natural History.
Norwegian Taxonomic Initiative (NTI).
Angelika Brandt and Saskia Brix: AWI_PS106_00.
DFG BR3843/3-1.

Competing Interests

The authors declare that they have no competing interests.

Author Contributions

- Carolin Uhlir conceived and designed the experiments, performed the experiments, analyzed the data, prepared figures and/or tables, authored or reviewed drafts of the paper, and approved the final draft.
- Martin Schwentner conceived and designed the experiments, analyzed the data, authored or reviewed drafts of the paper, and approved the final draft.
- Kenneth Meland conceived and designed the experiments, analyzed the data, authored or reviewed drafts of the paper, and approved the final draft.
- Jon Anders Kongsrud conceived and designed the experiments, authored or reviewed drafts of the paper, and approved the final draft.
- Henrik Glenner conceived and designed the experiments, authored or reviewed drafts of the paper, and approved the final draft.
- Angelika Brandt conceived and designed the experiments, authored or reviewed drafts of the paper, and approved the final draft.
- Ralf Thiel conceived and designed the experiments, authored or reviewed drafts of the paper, and approved the final draft.
- Jörundur Svavarsson conceived and designed the experiments, authored or reviewed drafts of the paper, and approved the final draft.
- Anne-Nina Lörz conceived and designed the experiments, authored or reviewed drafts of the paper, and approved the final draft.
- Saskia Brix conceived and designed the experiments, analyzed the data, authored or reviewed drafts of the paper, and approved the final draft.

Field Study Permissions

The following information was supplied relating to field study approvals (*i.e.*, approving body and any reference numbers):

Field permits are available with the following cruise codes: M85/3 (IceAGE; BR3843/3-1) and PS106/1 (PASCAL; AWI_PS106_00).

DNA Deposition

The following information was supplied regarding the deposition of DNA sequences:

Aligned sequences are available in the [Supplemental File](#). The ICECU BoLD project is available at: dx.doi.org/10.5883/DS-ICECU.

The sequences included in this study are available at GenBank: [HQ450558](#), [MZ402659](#), [MZ402660](#), [AJ388111](#), [MZ402681](#), [MZ402680](#), [MK613872.1](#), [MK613873.1](#), [HQ450557](#), [MK613886.1](#), [MZ402679](#), [MZ402678](#), [MZ402677](#), [MK613898.1](#), [MK613897.1](#),

MK613904.1, MK613901.1, MK613911.1, MZ402685, MZ402686, MZ402683, MZ402682, MZ402684, MZ402687, MK613902.1, MK613903.1, MK613905.1, HQ450555, U81512, MK613906.1, MK613899.1, MK613900.1, MZ402689, MZ402688, MK613910.1, MK613907.1, MK613909.1, MK613908.1, HQ450556, MZ402704, MZ402711, MZ402708, MZ402710, MZ402709, MZ402707, MZ402706, MZ402705, MZ402712, MZ402713, MK613921.1, MK613922.1, MZ402723, MZ402714, MZ402722, MZ402717, MZ402718, MZ402716, MZ402719, MZ402720, MZ402721, MZ402724, MZ402715, MZ402702, MZ402701, MK613925.1, MZ402676, MZ402675, MK613924.1, MK613913.1, MK613914.1, MZ402695, MZ402696, MZ402697, MZ402692, MZ40269, MZ402694, MZ402691, MZ402698, MZ402699, MK613923.1, MZ402690, MZ402700, MK613915.1, MK613916.1, MK613917.1, MZ402737, MZ402736, MK613918.1, MK613919.1, MK613870.1, MK613887.1, MK613888.1, U81513, MK613881.1, MK613882.1, MK613884.1, MK613883.1, MK613885.1, MZ402728, MZ402729, MZ402731, MZ402730, MZ402725, MZ402726, MZ402727, MK613892.1, MK613891.1, HQ450522, HQ450543, HQ450549, HQ450550, HQ450537, MK613889.1, HQ450551, HQ450552, HQ450553, MK613895.1, MK613893.1, MK613894.1, MK613890.1, MZ402734, MZ402732, MZ402733, MZ402735, HQ450554, MK613876.1, MK613874.1, MZ402662, MZ402663, MK613877.1, MZ402664, MZ402666, MZ402665, MZ402670, MZ402669, MZ402667, MZ402668, MZ402671, MZ402661, MZ402672, MZ402674, MZ402673, MK613875.1, MK613878.1, MZ402738, MK613871.1, AJ388110, DQ305106, AF260869, AF260870, AY693421, AF259533, DQ305111, MK813124.

Data Availability

The following information was supplied regarding data availability:

Occurrence data of the ICECU dataset is available at the OBIS platform: Uhlir, C.; Meland, K.; Glenner, H.; Brandt, A.; Brix, S. (2021). North Atlantic and Arctic Cumacea sampled during the IceAGE (2011) and PASCAL (2017) project. Marine Data Archive.

http://ipt.vliz.be/eurobis/resource?r=cumacea_pascal_iceage.

Supplemental Information

Supplemental information for this article can be found online at <http://dx.doi.org/10.7717/peerj.12379#supplemental-information>.

REFERENCES

- Bluhm BA, Ambrose WG, Bergmann M, Clough LM, Gebruk AV, Hasemann C, Iken K, Klages M, MacDonald IR, Renaud PE, Schewe I. 2011. Diversity of the arctic deep-sea benthos. *Marine Biodiversity* 41(1):87–107 DOI 10.1007/s12526-010-0078-4.
- Bouckaert R, Vaughan TG, Barido-Sottani J, Duchêne S, Fourment M, Gavryushkina A, Heled J, Jones G, Kühnert D, De Maio N, Matschiner M. 2019. BEAST 2.5: an advanced software platform for Bayesian evolutionary analysis. *PLOS Computational Biology* 15(4):e1006650 DOI 10.1371/journal.pcbi.1006650.
- Brandt A. 1997. Biodiversity of peracarid crustaceans (Malacostraca) from the shelf down to the deep Arctic Ocean. *Biodiversity & Conservation* 6(11):1533–1556 DOI 10.1023/A:1018318604032.

- Brandt A, Elsner N, Brenke N, Golovan O, Malyutina MV, Riehl T, Schwabe E, Würzberg L. 2013.** Epifauna of the Sea of Japan collected via a new epibenthic sledge equipped with camera and environmental sensor systems. *Deep Sea Research Part II: Topical Studies in Oceanography* **86(4)**:43–55 DOI [10.1016/j.dsr2.2012.07.039](https://doi.org/10.1016/j.dsr2.2012.07.039).
- Brattegard T, Fosså JH. 1991.** Replicability of an epibenthic sampler. *Journal of the Marine Biological Association of the United Kingdom* **71(1)**:153–166 DOI [10.1017/S0025315400037462](https://doi.org/10.1017/S0025315400037462).
- Brenke N. 2005.** An epibenthic sledge for operations on marine soft bottom and bedrock. *Marine Technology Society Journal* **39(2)**:10–21 DOI [10.4031/002533205787444015](https://doi.org/10.4031/002533205787444015).
- Brix S, Bauernfeind W, Brenke N, Błażewicz-Paszkowycz M, Borges V, Buldt K, Cannon JT, Díaz-Agras G, Fiege D, Fiorentino D, Haraldsdóttir S. 2012.** Overflow, circulation and biodiversity-cruise no. M85/3-August 27-September 28, 2011-Reykjavik (Iceland)-Cuxhaven (Germany). *Meteor-Berichte M85/3* **1**:41 DOI [10.2312/cr_m85_3](https://doi.org/10.2312/cr_m85_3).
- Brix S, Devey CW. 2019.** Stationlist of the IceAGE project (Icelandic marine animals: genetics and ecology) expeditions. Marine Data Archive DOI [10.14284/349](https://doi.org/10.14284/349).
- Brix S, Lörz AN, Jażdżewska AM, Hughes L, Tandberg AHS, Pabis K, Stransky B, Krapp-Schickel T, Sorbe JC. 2018a.** Amphipod family distributions around Iceland. *ZooKeys* **731(1–2)**:41–53 DOI [10.3897/zookeys.731.19854](https://doi.org/10.3897/zookeys.731.19854).
- Brix S, Meißner K, Stransky B, Halanych KM, Jennings RM, Kocot KM, Svavarsson J. 2014a.** Preface: The IceAGE project-a follow up of BIOICE. *Polish Polar Research* **35(2)**:141–150 DOI [10.2478/popore-2014-0010](https://doi.org/10.2478/popore-2014-0010).
- Brix S, Stransky B, Malyutina M, Pabis K, Svavarsson J, Riehl T. 2018b.** Distributional patterns of isopods (Crustacea) in Icelandic and adjacent waters. *Marine Biodiversity* **48(2)**:783–811 DOI [10.1007/s12526-018-0871-z](https://doi.org/10.1007/s12526-018-0871-z).
- Brix S, Svavarsson J. 2010.** Distribution and diversity of desmosomatid and nannoniscid isopods (Crustacea) on the Greenland-Iceland-Faeroe Ridge. *Polar Biology* **33(4)**:515–530 DOI [10.1007/s00300-009-0729-8](https://doi.org/10.1007/s00300-009-0729-8).
- Brix S, Svavarsson J, Leese F. 2014b.** A multi-gene analysis reveals multiple highly divergent lineages of the isopod chelator *insignis* (Hansen, 1916) south of Iceland. *Polish Polar Research* **35(2)**:225–242 DOI [10.2478/popore-2014-0015](https://doi.org/10.2478/popore-2014-0015).
- Brökeland W, Raupach MJ. 2008.** A species complex within the isopod genus *Haplomis* (Crustacea: Malacostraca: Peracarida) from the Southern Ocean deep sea: a morphological and molecular approach. *Zoological Journal of the Linnean Society* **152(4)**:655–706 DOI [10.1111/j.1096-3642.2008.00362.x](https://doi.org/10.1111/j.1096-3642.2008.00362.x).
- Błażewicz-Paszkowycz M, Siciński J. 2014.** Diversity and distribution of Tanaidacea (Crustacea) along the Victoria Land Transect (Ross Sea, Southern Ocean). *Polar Biology* **37(4)**:519–529 DOI [10.1007/s00300-014-1452-7](https://doi.org/10.1007/s00300-014-1452-7).
- Collins RA, Cruickshank RH. 2013.** The seven deadly sins of DNA barcoding. *Molecular Ecology Resources* **13(6)**:969–975 DOI [10.1111/1755-0998.12046](https://doi.org/10.1111/1755-0998.12046).
- Conlan K, Aitken A, Hendrycks E, McClelland C, Melling H. 2008.** Distribution patterns of Canadian beaufort shelf macrobenthos. *Journal of Marine Systems* **74(3–4)**:864–886 DOI [10.1016/j.jmarsys.2007.10.002](https://doi.org/10.1016/j.jmarsys.2007.10.002).
- Costello MJ, Stocks K, Zhang Y, Grassle JF, Fautin DG. 2007.** About the Ocean biogeographic information system. Available at <https://obis.org/> (accessed 19 September 2019).
- Curtis MA. 1975.** The marine benthos of arctic and sub-arctic continental shelves. *Polar Record* **17(111)**:595–626 DOI [10.1017/S0032247400032691](https://doi.org/10.1017/S0032247400032691).
- Dunbar MJ. 1951.** Eastern Arctic waters. *Journal of the Fisheries Research Board Bulletin* **88**:1–131.

- Dunbar MJ. 1972.** The nature and definition of the marine subarctic, with a note on the sea-life area of the Atlantic salmon. *Transactions of the Royal Society of Canada* **10**:249–257.
- Foxon GEH. 1936.** Notes on the natural history of certain sand-dwelling Cumacea. *Journal of Natural History* **17(99)**:377–393 DOI [10.1080/00222933608655133](https://doi.org/10.1080/00222933608655133).
- Gage JD, Lamshead PJD, Bishop JDD, Stuart CT, Jones NS. 2004.** Large-scale biodiversity pattern of Cumacea (Peracarida: Crustacea) in the deep Atlantic. *Marine Ecology Progress Series* **277**:181–196 DOI [10.3354/meps277181](https://doi.org/10.3354/meps277181).
- Gerken S. 2018.** The Lampropidae (Crustacea: Cumacea) of the world. *Zootaxa* **4428(1)**:1–192 DOI [10.11646/zootaxa.4428.1.1](https://doi.org/10.11646/zootaxa.4428.1.1).
- Gerken S, Watling L. 1999.** Cumacea (Crustacea) of the Faroe Islands Region. *Froedskaparrit* **47**:199–227.
- Hall TA. 1999.** BioEdit: a user-friendly biological sequence alignment editor and analysis program for windows 95/98/NT. *Nucleic Acids Symposium Series* **41**:95–98 DOI [10.14601/PHYTOPATHOL_MEDITERR-14998U1.29](https://doi.org/10.14601/PHYTOPATHOL_MEDITERR-14998U1.29).
- Hansen HJ. 1920.** The Order Cumacea. In: *Crustacea Malacostraca. Danish Ingolf-Expedition* **3(6)**:1–86 DOI [10.5962/bhl.title.10100](https://doi.org/10.5962/bhl.title.10100).
- Hansen B, Østerhus S. 2000.** North Atlantic-Nordic Seas exchanges. *Progress in Oceanography* **45(2)**:109–208 DOI [10.1016/S0079-6611\(99\)00052-X](https://doi.org/10.1016/S0079-6611(99)00052-X).
- Haye PA. 2002.** Systematics of the Cumacea (Crustacea). Doctoral dissertation. University of Maine.
- Haye PA, Kornfield I, Watling L. 2004.** Molecular insights into Cumacean family relationships (Crustacea, Cumacea). *Molecular Phylogenetics and Evolution* **30(3)**:798–809 DOI [10.1016/j.ympev.2003.08.003](https://doi.org/10.1016/j.ympev.2003.08.003).
- Held C, Wägele JW. 2005.** Cryptic speciation in the giant Antarctic isopod *Glyptonotus antarcticus* (Isopoda, Valvifera, Chaetiliidae). *Scientia Marina* **69(2)**:175–181 DOI [10.3989/scimar.2005.69s2175](https://doi.org/10.3989/scimar.2005.69s2175).
- Hessler RR, Jumars PA. 1974.** Abyssal community analysis from replicate box cores in the central North Pacific. *Deep-Sea Research* **21**:185–209 DOI [10.1016/0011-7471\(74\)90058-8](https://doi.org/10.1016/0011-7471(74)90058-8).
- Jennings RM, Golovan O, Brix S. 2019.** Integrative species delimitation of desmosomatid and nannoniscid isopods from the Kuril-Kamchatka trench, with description of a hadal species. In: *Progress in Oceanography*. Amsterdam, Netherlands: Elsevier.
- Jones NS. 1976.** British Cumaceans. Synopses of the British Fauna (new series). *Linnaean Society of London* **7**:1–62.
- Jones NS, Sanders HL. 1972.** Distribution of Cumacea in the deep Atlantic. *Deep-Sea Research* **19(10)**:737–745 DOI [10.1016/0011-7471\(72\)90066-6](https://doi.org/10.1016/0011-7471(72)90066-6).
- Katoh K. 2002.** MAFFT: A novel method for rapid multiple sequence alignment based on fast fourier transform. *Nucleic Acids Research* **30(14)**:3059–3066 DOI [10.1093/nar/gkf436](https://doi.org/10.1093/nar/gkf436).
- Katoh K, Standley DM. 2013.** MAFFT multiple sequence alignment software version 7: improvements in performance and usability. *Molecular Biology and Evolution* **30(4)**:772–780 DOI [10.1093/molbev/mst010](https://doi.org/10.1093/molbev/mst010).
- Kearse M, Moir R, Wilson A, Stones-Havas S, Cheung M, Sturrock S, Buxton S, Cooper A, Markowitz S, Duran C, Thierer T. 2012.** Geneious Basic: an integrated and extendable desktop software platform for the organization and analysis of sequence data. *Bioinformatics* **28(12)**:1647–1649 DOI [10.1093/bioinformatics/bts199](https://doi.org/10.1093/bioinformatics/bts199).
- Knox MA. 2012.** Diversity of New Zealand Deep-sea Amphipoda. Doctoral dissertation. University of Waikato.

- Kumar S, Stecher G, Li M, Knyaz C, Tamura K. 2018.** MEGA X: molecular evolutionary genetics analysis across computing platforms. *Molecular Biology and Evolution* **35(6)**:1547–1549 DOI [10.1093/molbev/msy096](https://doi.org/10.1093/molbev/msy096).
- Lanave C, Preparata G, Sacone C, Serio G. 1984.** A new method for calculating evolutionary substitution rates. *Journal of Molecular Evolution* **20(1)**:86–93 DOI [10.1007/BF02101990](https://doi.org/10.1007/BF02101990).
- Lörz AN, Brix S, Jażdżewska AM, Hughes LE. 2020.** Diversity and distribution of North Atlantic Lepechinellidae (Amphipoda: Crustacea). *Zoological Journal of the Linnean Society* **190(4)**:1095–1122 DOI [10.1093/zoolinnean/zlaa024](https://doi.org/10.1093/zoolinnean/zlaa024).
- Lörz A-N, Kaiser S, Oldeland J, Stolter C, Kürzel K, Brix S. 2021.** Biogeography, diversity and environmental relationships of shelf and deep-sea benthic Amphipoda around Iceland. *PeerJ* **9(2)**:e11898 DOI [10.7717/peerj.11898](https://doi.org/10.7717/peerj.11898).
- Macke A, Flores H. 2018.** The expeditions PS106/1 and 2 of the research vessel POLARSTERN to the Arctic Ocean in 2017. *Reports on polar and marine research, Bremerhaven, Alfred Wegener Institute for Polar and Marine Research*, 719 DOI [10.2312/BzPM_0719_2018](https://doi.org/10.2312/BzPM_0719_2018).
- Malmberg S-A, Valdimarsson H. 2003.** Hydrographic conditions in Icelandic waters, 1990–1999. *ICES Marine Science Symposia* **219**:50–60.
- Meier R, Shiyang K, Vaidya G, Ng PK. 2006.** DNA barcoding and taxonomy in Diptera: a tale of high intraspecific variability and low identification success. *Systematic Biology* **55(5)**:715–728 DOI [10.1080/10635150600969864](https://doi.org/10.1080/10635150600969864).
- Meißner K, Brenke N, Svavarsson J. 2014.** Benthic habitats around Iceland investigated during the IceAGE expedition. *Polish Polar Research* **35(2)**:177–202 DOI [10.2478/popore-2014-0016](https://doi.org/10.2478/popore-2014-0016).
- Meißner K, Brix S, Halanych KM, Jażdżewska AM. 2018.** Preface-biodiversity of Icelandic waters. *Marine Biodiversity* **48(2)**:715–718 DOI [10.1007/s12526-018-0884-7](https://doi.org/10.1007/s12526-018-0884-7).
- Meyer CP, Paulay G. 2005.** DNA barcoding: error rates based on comprehensive sampling. *PLOS Biology* **3(12)**:e422 DOI [10.1371/journal.pbio.0030422](https://doi.org/10.1371/journal.pbio.0030422).
- Miller MA, Pfeiffer W, Schwartz T. 2010.** Creating the CIPRES science gateway for inference of large phylogenetic trees. In: *Proceedings of the Gateway Computing Environments Workshop (GCE)*, New Orleans, LA1–8.
- Mironov AN, Dilman AB, Krylova EM. 2013.** Global distribution patterns of genera occurring in the Arctic Ocean deeper 2,000 m. *Invertebrate Zoology* **10(1)**:167–194 DOI [10.15298/invertzool.10.1.08](https://doi.org/10.15298/invertzool.10.1.08).
- Nylander JA, Ronquist F, Huelsenbeck JP, Nieves-Aldrey J. 2004.** Bayesian phylogenetic analysis of combined data. *Systematic Biology* **53(1)**:47–67 DOI [10.1080/10635150490264699](https://doi.org/10.1080/10635150490264699).
- Nørrevang A, Brattegard T, Josefson AB, Sneli JA, Tendal OS. 1994.** List of BIOFAR stations. *Sarsia* **79(3)**:165–180 DOI [10.1080/00364827.1994.10413557](https://doi.org/10.1080/00364827.1994.10413557).
- OBIS. 2019.** Ocean biodiversity information system. Intergovernmental Oceanographic Commission of UNESCO. Available at www.obis.org (accessed 19 September 2019).
- Ohlin A. 1901.** Arctic Crustacea collected during the Swedish Arctic Expeditions 1898 and 1899 under the direction of Professor A.G. Nathorst. I. Leptostraca, Isopoda, Cumacea. *Bihang till Svenska Vetenskaps-Akademiens Handlingar* **26(Afd IV, No. 12)**:1–54.
- Omarsdóttir S, Einarsdóttir E, Ögmundsdóttir HM, Freysdóttir J, Olafsdóttir ES, Molinski TF, Svavarsson J. 2013.** Biodiversity of benthic invertebrates and bioprospecting in Icelandic waters. *Phytochemistry Reviews* **12(3)**:517–529 DOI [10.1007/s11101-012-9243-7](https://doi.org/10.1007/s11101-012-9243-7).
- Ostmann A, Schnurr S, Arbizu PM. 2014.** Marine environment around Iceland: hydrography, sediments and first predictive models of Icelandic deep-sea sediment characteristics. *Polish Polar Research* **35(2)**:151–176 DOI [10.2478/popore-2014-0021](https://doi.org/10.2478/popore-2014-0021).

- Palumbi S, Martin A, Romano S. 1991.** 16s RNA primers. In: *The Simple Fool's Guide to PCR, Version 2*. Honolulu: University of Hawaii Press, 28.
- Paulus E, Brix S, Siebert A, Martínez Arbizu P, Rossel S, Peters J, Svavarsson J, Schwentner M.** (in press). Recent speciation and hybridization in Icelandic deep-sea isopods: an integrative approach using genomics and proteomics. *Molecular Ecology*
DOI 10.22541/au.161773761.10234925/v1.
- Petrescu I, Heard RW, Vargas R, Breedy O. 2009.** Cumaceans. In: Wehrtmann IS, Cortés J, eds. *Marine Biodiversity of Costa Rica, Central America. Monographiae Biologicae*. Vol. 86. Berlin: Springer & Business Media BV, 237–244.
- Piepenburg D, Archambault P, Ambrose WG, Blanchard AL, Bluhm BA, Carroll ML, Conlan KE, Cusson M, Feder HM, Grebmeier JM, Jewett SC. 2011.** Towards a pan-Arctic inventory of the species diversity of the macro-and megabenthic fauna of the Arctic shelf seas. *Marine Biodiversity* 41(1):51–70 DOI 10.1007/s12526-010-0059-7.
- Pons J, Barraclough TG, Gomez-Zurita J, Cardoso A, Duran DP, Hazell S, Kamoun S, Sumlin WD, Vogler AP. 2006.** Sequence-based species delimitation for the DNA taxonomy of undescribed insects. *Systematic Biology* 55(4):595–609 DOI 10.1080/10635150600852011.
- Puillandre N, Lambert A, Brouillet S, Achaz G. 2012.** ABGD, automatic barcode gap discovery for primary species delimitation. *Molecular Ecology* 21(8):1864–1877
DOI 10.1111/j.1365-294X.2011.05239.x.
- Rambaut A. 2018a.** FigTree version 1.4.4. Computer program and documentation distributed by the author. Available at <http://tree.bio.ed.ac.uk/software/figtree/> (accessed 15 December 2019).
- Rambaut A, Drummond AJ, Xie D, Baele G, Suchard MA. 2018b.** Posterior summarisation in Bayesian phylogenetics using Tracer 1.7. *Systematic Biology* 67(5):901–904
DOI 10.1093/sysbio/syy032.
- Rehm P. 2007.** Cumacea (Crustacea; Peracarida) of the Antarctic shelf-diversity, biogeography, and phylogeny. Doctoral dissertation, University of Bremen.
- Rehm P, Thatje S, Leese F, Held C. 2020.** Phylogenetic relationship within Cumacea (Crustacea: Peracarida) and genetic variability of two Antarctic species of the family Leuconidae. *Scientia Marina* 84(4):385–392 DOI 10.3989/scimar.05053.17A.
- Rex MA. 1981.** Community structure in the deep-sea benthos. *Annual Review of Ecology and Systematics* 12(1):331–353 DOI 10.1146/annurev.es.12.110181.001555.
- Riehl T, Brenke N, Brix S, Driskell A, Kaiser S, Brandt A. 2014.** Field and laboratory methods for DNA studies on deep-sea isopod crustaceans. *Polish Polar Research* 35(2):203–224
DOI 10.2478/popore-2014-0018.
- Riehl T, Lins L, Brandt A. 2018.** The effects of depth, distance, and the Mid-Atlantic Ridge on genetic differentiation of abyssal and hadal isopods (Macrostylidae). *Deep Sea Research Part II: Topical Studies in Oceanography* 148(6):74–90 DOI 10.1016/j.dsr2.2017.10.005.
- Rodriguez FJLOJ, Oliver JL, Marin A, Medina JR. 1990.** The general stochastic model of nucleotide substitution. *Journal of Theoretical Biology* 142(4):485–501
DOI 10.1016/S0022-5193(05)80104-3.
- Ronquist F, Teslenko M, Van Der Mark P, Ayres DL, Darling A, Höhna S, Larget B, Liu L, Suchard MA, Huelsenbeck JP. 2012.** MrBayes 3.2: efficient Bayesian phylogenetic inference and model choice across a large model space. *Systematic Biology* 61(3):539–542
DOI 10.1093/sysbio/sys029.
- Rothlisberg P, Percy WG. 1976.** An epibenthic sampler used to study the ontogeny of vertical migration of *Pandalus dordani* (Decapoda, Caridea). *Fishery Bulletin, National Oceanic and Atmospheric Administration of the United States* 74:994–997.

- Sars GO. 1900.** *An account of the Crustacea of Norway, Ill. Cumacea*. Vol. 3. Bergen, Norway: Bergen Museum, 1–115.
- Schlichtholz P, Houssais MN. 2002.** An overview of the y-S correlations in Fram Strait based on the MIZEX 84 data. *Oceanologia* **44**:243–272.
- Schnurr S, Brandt A, Brix S, Fiorentino D, Malyutina M, Svavarsson J. 2014.** Composition and distribution of selected munnopsid genera (Crustacea, Isopoda, Asellota) in Icelandic waters. *Deep Sea Research Part I: Oceanographic Research Papers* **84(7142)**:142–155 DOI [10.1016/j.dsr.2013.11.004](https://doi.org/10.1016/j.dsr.2013.11.004).
- Schwentner M, Timms BV, Richter S. 2011.** An integrative approach to species delineation incorporating different species concepts: a case study of Limnadopsis (Branchiopoda: Spinicaudata). *Biological Journal of the Linnean Society* **104(3)**:575–599 DOI [10.1111/j.1095-8312.2011.01746.x](https://doi.org/10.1111/j.1095-8312.2011.01746.x).
- Silva CDLA. 2016.** Taxonomy, systematics, morphological and molecular phylogeny of the order Tanaidacea (Crustacea: Peracarida), from the Antarctic, Atlantic and Pacific Oceans. Doctoral dissertation, University of Porto.
- Spalding MD, Fox HE, Allen GR, Davidson N, Ferdaña ZA, Finlayson MAX, Halpern BS, Jorge MA, Lombana AL, Lourie SA, Martin KD. 2007.** Marine ecoregions of the world: a bioregionalization of coastal and shelf areas. *Bioscience* **57(7)**:573–583 DOI [10.1641/B570707](https://doi.org/10.1641/B570707).
- Stebbing TRR. 1913.** Cumacea (Symphoda). In: *Das Tierreich*. Vol. 39. Berlin: R. Fiedlander and Son, 1–210.
- Stransky B, Svavarsson J. 2010.** Diversity and species composition of peracarids (Crustacea: Malacostraca) on the South Greenland Shelf: spatial and temporal variation. *Polar Biology* **33(2)**:125–139 DOI [10.1007/s00300-009-0691-5](https://doi.org/10.1007/s00300-009-0691-5).
- Thorsnes T. 2009.** MAREANO—an introduction. *Norwegian Journal of Geology*. **89(3)**, ISSN 029-196X.
- Townsend DW. 2012.** *Oceanography and marine biology. An introduction to marine science*. Sunderland: Sinauer Associates.
- Uhlir C, Meland K, Glenner H, Brandt A, Brix S. 2021.** North Atlantic and Arctic Cumacea sampled during the IceAGE (2011) and PASCAL (2017) project. Marine data archive. Available at http://ipt.vliz.be/eurobis/resource?r=cumacea_pascal_iceage.
- Vassilenko SV. 1989.** Arctic Ocean Cumacea. In: Herman Y, ed. *The Arctic Seas-Climatology, Oceanography, Geology, and Biology*. Berlin: Springer, 431–444.
- Vassilenko SV. 2002.** Cumaceans as indicators of Atlantic Waters over the continental slope of the Arctic Ocean. *Russian Journal of Marine Biology* **28(1)**:1–6 DOI [10.1023/A:1014444029044](https://doi.org/10.1023/A:1014444029044).
- Vassilenko SV, Brandt A. 1996.** Composition and biogeographic structure of the cumacean fauna of the Northeast Water Polynya, Greenland (Crustacea, Peracarida, Cumacea). *Arthropoda Selecta* **5**:27–38.
- Vihtakari M. 2019.** PlotSvalbard: PlotSvalbard–plot research data from Svalbard on maps. R package version 0.8.5. Available at <https://github.com/MikkoVihtakari/PlotSvalbard> (accessed 11 November 2019).
- Watling L. 2009.** Biogeographic provinces in the Atlantic deep sea determined from cumacean distribution patterns. *Deep Sea Research Part II: Topical Studies in Oceanography* **56(19–20)**:1747–1753 DOI [10.1016/j.dsr2.2009.05.019](https://doi.org/10.1016/j.dsr2.2009.05.019).
- Watling L, Gerken S. 2005.** The Cumacea of the Faroe Islands region: water mass relationships and North Atlantic biogeography. In: *BIOFAR Proceedings*. 137–149.

- Watling L, Gerken S. 2019. World cumacea database. Available at <http://www.marinespecies.org/cumacea> (accessed 12 November 2019).
- Weisshappel JB. 2000. Distribution and diversity of the hyperbenthic amphipod family Eusiridae in the different seas around the Greenland-Iceland-Faeroe-Ridge. *Sarsia* **85**(3):227–236 DOI [10.1080/00364827.2000.10414575](https://doi.org/10.1080/00364827.2000.10414575).
- Weisshappel JB. 2001. Distribution and diversity of the hyperbenthic amphipod family Calliopiidae in the different seas around the Greenland-Iceland-Faeroe-Ridge. *Sarsia* **86**(2):143–151 DOI [10.1080/00364827.2001.10420469](https://doi.org/10.1080/00364827.2001.10420469).
- Weisshappel J, Svavarsson J. 1998. Benthic amphipods (Crustacea: Malacostraca) in Icelandic waters: diversity in relation to faunal patterns from shallow to intermediate deep Arctic and North Atlantic Oceans. *Marine Biology* **131**(1):133–143 DOI [10.1007/s002270050304](https://doi.org/10.1007/s002270050304).
- Westheide W, Rieger R. 1996. *Spezielle zoologie, teil 1: einzeller und wirbellose tiere*. Stuttgart: Gustav Fischer, 582–600.
- Wieczorek J, Bloom D, Guralnick R, Blum S, Döring M, Giovanni R, Robertson T, Vieglais D. 2012. Darwin core: an evolving community-developed biodiversity data standard. *PLOS ONE* **7**(1):e29715 DOI [10.1371/journal.pone.0029715](https://doi.org/10.1371/journal.pone.0029715).
- Wiemers M, Fiedler K. 2007. Does the DNA barcoding gap exist? A case study in blue butterflies (Lepidoptera: Lycaenidae). *Frontiers in Zoology* **4**:8 DOI [10.1186/1742-9994-4-8](https://doi.org/10.1186/1742-9994-4-8).
- Wilson GD, Hessler RR. 1987. Speciation in the deep sea. *Annual Review of Ecology and Systematics* **18**(1):185–207 DOI [10.1146/annurev.es.18.110187.001153](https://doi.org/10.1146/annurev.es.18.110187.001153).
- WoRMS Editorial Board. 2019. World register of marine species. Available at <http://www.marinespecies.org> at VLIZ (accessed 23 November 2019).
- Xiong B, Kocher TD. 1991. Comparison of mitochondrial DNA sequences of seven morphospecies of black flies (Diptera: Simuliidae). *Genome* **34**(2):306–311 DOI [10.1139/g91-050](https://doi.org/10.1139/g91-050).
- Zimmer C. 1926. Northern and Arctic invertebrates in the collection of the Swedish State Museum, X Cumaceen. *Kongliga Svenska Vetenskaps-Akademiens Förhandlingar* **3**(2):1–88.
- Zimmer C. 1943. Über neue und weniger bekannte Cumaceen. *Zoologischer Anzeiger* **141**(7–8):148–167.
- Zimmer C. 1980. Cumaceans of the American Atlantic boreal coast region (Crustacea: Peracarida). *Smithsonian Contributions to Zoology* **302**:1–29.



Microplastic ingestion by commercial marine fish from the seawater of Northwest Peninsular Malaysia

Yuen Hwei Foo^{1,*}, Sharnietha Ratnam², Er Vin Lim², Masthurah Abdullah^{1,2}, Vincent J. Molenaar³, Aileen Tan Shau Hwai^{1,2}, Shoufeng Zhang⁴, Hongjun Li⁴ and Norlaila Binti Mohd Zanuri^{2,*}

¹ School of Biological Sciences, Universiti Sains Malaysia (USM), Gelugor, Pulau Pinang, Malaysia

² Centre for Marine and Coastal Studies (CEMACS), Universiti Sains Malaysia (USM), Gelugor, Pulau Pinang, Malaysia

³ Athena Institute for Research on Innovation and Communication in Health and Life Sciences, VU University Amsterdam, De Boelelaan, Amsterdam, Netherlands

⁴ National Marine Environmental Monitoring Center, Dalian, China

* These authors contributed equally to this work.

ABSTRACT

Over the past decade, concerns over microplastic pollution in the marine ecosystem has increasingly gained more attention, but research investigating the ingestion of microplastics by marine fish in Malaysia is still regrettably lacking. This study investigated the microplastic presence, abundance, and morphological types within the guts of four species of commercial marine fish (*Atule mate*, *Crenimugil seheli*, *Sardinella fimbriata* and *Rastrelliger brachysoma*) caught in seawater off the coast of Malaysia's Northwest Peninsular. A total of 72 individual commercial marine fish guts from four species (fish per species $n = 18$) were examined. Remarkably, this study found that 100% of the samples contained microplastics. A total number of 432 microplastics (size < 5 mm) from the four species were found in the excised marine fish guts. The most common type of microplastic discovered was fragment, which accounted for 49.5% of all microplastics present. The gut microplastic content differed between species. *Sardinella fimbriata* recorded the greatest amount of microplastic ingestion, with an average microplastic count of $6.5 (\pm 4.3)$ items per individual fish. However, there were no statistically significant differences found when comparing study species and different locations. SEM-EDX analysis confirmed the presence of microplastic particles by identifying the chemical elements found in the samples. Since the four studied species of commercial marine fish are popular protein sources in Malaysians' daily diet, this study suggests potential microplastic exposure to humans via contaminated fish consumption in Malaysia, which was previously unknown. Based on previous scientific evidence, this study also demonstrates the high probability of microplastic ingestion in marine fish in the Malaysian seawater, which could have an adverse effect on fish health as well as marine biota.

Submitted 6 April 2021

Accepted 7 March 2022

Published 19 April 2022

Corresponding author
Norlaila Binti Mohd Zanuri,
lailazanuri@usm.my

Academic editor
Isabella Bordon

Additional Information and
Declarations can be found on
page 18

DOI 10.7717/peerj.13181

© Copyright
2022 Foo et al.

Distributed under
Creative Commons CC-BY 4.0

OPEN ACCESS

Subjects Aquaculture, Fisheries and Fish Science, Marine Biology, Ecotoxicology, Environmental Contamination and Remediation, Environmental Impacts

Keywords Microplastic ingestion, Commercial marine fish, Northwest Peninsular Malaysia seawater

INTRODUCTION

Plastic pollution in the marine ecosystem has sparked increasing interest and research over the past decades, emphasizing the ecological and biological consequences for marine biota (Andrady, 2011). Global plastic production has surged since the early 1950s, reaching 360 million tonnes by 2018. Substantial demand from various sectors is driving this trend, among which domestic usage is an important source (Cole et al., 2011). Plastic is mass-produced on a large scale due to its high durability, resistance to degradation, relative ease of production and low production cost. Plastics are extremely resistant to biodegradation. They do, however, degrade into smaller particles over time when exposed to several natural factors, such as sunlight and wave action (Wang et al., 2016). The increased use of plastics in society has led to an exponential growth in plastic production, which is expected to continue. Plastics will increasingly reach all areas of the environment due to this increase in production and associated mismanagement during production, distribution, use and final disposal (Azoulay et al., 2019; Lusher et al., 2017). Eriksen et al. (2014), based on 24 expeditions, estimated that at least 5.25 trillion buoyant particles, weighing around 268.940 tons, are in the Earth's oceans.

The National Oceanic and Atmospheric Administration (NOAA) has defined microplastics as tiny plastic fragments smaller than five mm in diameter (Barboza & Gimenez, 2015). This means that most microplastics are difficult to identify with the naked eye, requiring microscopic observation. According to Li, Liu & Paulchen (2018), microplastics can be divided into two major types—primary and secondary microplastics. Primary types of microplastics include moulded plastic powders, 'scrubbers' for surface blast cleaning, industrial plastic nanoparticles, and microbeads found in cosmetic products. Also, spherical or cylindrical virgin resin pellets that are usually five mm in diameter are widely used before and during the plastic manufacturing processes (Koehler et al., 2015). Secondary microplastics are formed after the degradation or fragmentation of larger plastic debris (Fok & Cheung, 2015).

Primary and secondary microplastics have the potential to be ingested among a wide range of marine ecosystem taxa, such as benthic organisms, corals, plankton, fish and large marine mammals (Sharma & Chatterjee, 2017). The extremely small size of microplastics (between 0.1 μm and 5 mm in diameter) makes them highly bioavailable. Due to their buoyancy and appealing colours, they can be easily ingested by fish (Jovanović, 2017). Marine fish might mistakenly ingest microplastics, with detrimental effects, as they look like natural prey. Marine fish play a vital role in the marine ecosystem, linking both lower and higher trophic levels, acting as both prey and predator. Ultimately, trophic transfers can occur from lower to higher levels within a food chain, potentially causing relatively greater exposure to microplastics among apex predators (Santillo, Miller & Johnston, 2017).

A recent study by Karami et al. (2017a) in which packets of dried fish (*C. subviridis*, *J. belangerii*, *R. kanagurta* and *S. waitei*) were purchased from local markets in Malaysia, found that microplastics were present in the edible flesh of these four commercial marine fish species. The authors estimated that 246 microplastic particles from these dried fish sources are consumed annually by humans. Fish is an important natural protein source in

the daily diet of many nations, including the majority of Malaysians (Teh, 2012). Although microplastic ingestion by fish has previously been reported worldwide, there is relatively limited information on Malaysia's commercial coastal species. Based on statistics from 2000, annual per capita fish consumption in Malaysia was 58 kg per person (Nurnadia, Azrina & Amin, 2011). The 2008 Malaysian Adult Nutrition Survey (MANS) found that the daily consumption prevalence of marine fish in Malaysia was 51% for rural adults and 34% for urban adults (Norimahak et al., 2008). Thus, the hypotheses for this study were that plastic ingestion rates do not differ between species of fish and the habitats in which the fish were caught. Therefore, this research is crucial in highlighting the significant consumption of commercial marine fish as a potentially important source of microplastics exposure in Malaysia.

MATERIALS AND METHODS

Sample Collection

In this study, four commercial marine fish species, *Atule mate* (Yellowtail scad), *Crenimugil seheli* (Bluespot mullet), *Sardinella fimbriata* (Fringscale sardinella) and *Rastrelliger brachysoma* (Short mackerel) with a total number of 72 fish [fish per species $n = 18$] were attained from the fishermen at Teluk Bahang and Penaga fish market, Penang. The GPS coordinates of the fishing locations were obtained from the fishermen. *Crenimugil seheli* were collected on November 27th, 2019 at the Teluk Bahang fish market from fishing site GPS coordinates $5^{\circ}25'38.33''N$ $100^{\circ}8'54.23''E$ (Fig. 1). *Atule mate*, *Sardinella fimbriata* and *Rastrelliger brachysoma* were collected on December 3rd, 2019 at Penaga fish market from fishing location $5^{\circ}35'30.3''N$ $100^{\circ}15'38.0''E$. Both fishing sites are located in Northwest Peninsular Malaysia seawater. The animals were kept on ice during transportation to the laboratory at the Centre for Marine and Coastal Studies (CEMACS), Universiti Sains Malaysia.

Laboratory Procedures

Laboratory procedures were carried out at the microplastic laboratory, Centre for Marine and Coastal Studies (CEMACS), Universiti Sains Malaysia. Several laboratory steps were conducted in processing the samples before further microplastic observation and identification, including (1) measurement of biometric parameters of each fish sample, (2) isolating, which included steps of (i) depuration, (ii) dissection and (iii) digestion, (3) digestant filtering and (4) density separation and filtering.

Measurement of Biometric Parameters

Biometric parameters of the samples were obtained by measuring their standard lengths, total lengths and total wet weight. The standard length was measured from the fish mouth until tail muscle while the total length was measured from mouth to tail.

Isolating

The isolation process was done by the extraction of microplastics from biotic materials. The process included depuration, dissection and digestion of biological tissues with chemical processes (Lusher et al., 2017).

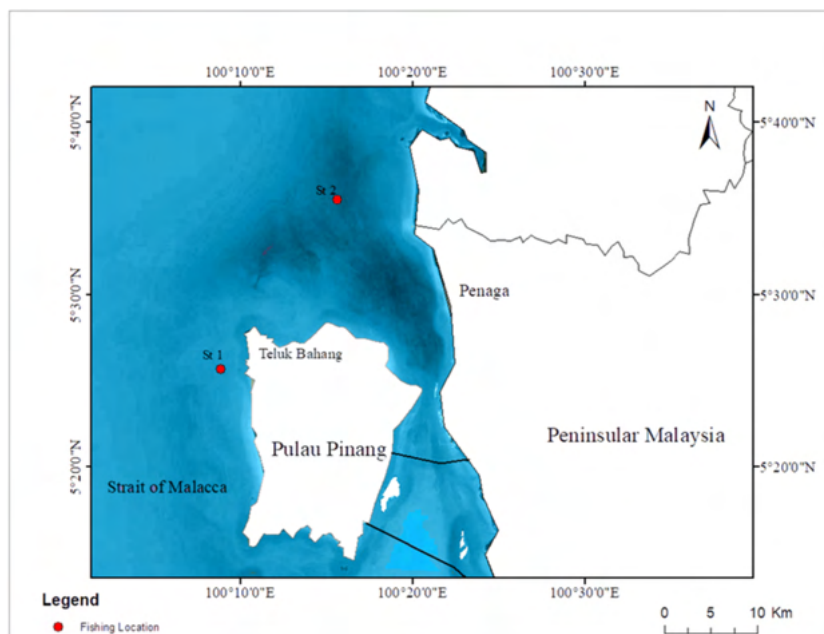


Figure 1 Map of fishing locations. St 1: fishing location of *Crenimugil seheli*; St 2: fishing location of *Atule mate*, *Sardinella fimbriata* and *Rastrelliger brachysoma*.

Full-size  DOI: [10.7717/peerj.13181/fig-1](https://doi.org/10.7717/peerj.13181/fig-1)

Depuration

To ensure that the study focused primarily on fish ingestion of microplastics, external adhering (micro)plastics were removed by washing with filtered distilled water. This process was to ensure that only microplastics retained within the tissues or collected in the intestinal tract were included, and findings were not confounded by other adhering microplastics (Lusher *et al.*, 2017).

Dissection

All dissection equipment such as scalpel, dissecting scissors and tweezers were rinsed with filtered distilled water to prevent contamination. A total of 72 fish samples were dissected with a scalpel and dissecting scissors from the anus to the upper part near the gills to obtain the fish guts. The guts were then excised using tweezers. The excised guts were weighed on an electronic balance, recorded and kept in 200 mL clean covered glass jars.

Digestion

Microplastics might be masked as they can be disguised by biological materials through encapsulation by the mucosae. Thus, digestion was done using 10% potassium hydroxide (KOH) as a base to denature protein and hydrolyse chemical bonds. KOH pellet (100 g) was dissolved in distilled filtered water (1,000 mL) to get a 10% KOH solution (Karami *et al.*, 2017a). A total of 5,000 mL of KOH was prepared to digest the four species of fish guts. Upon usage, KOH was filtered through Whatman GF/C glass microfibre filter membrane (pore size: 1.2 μm) to prevent plastic and other debris contamination. 30% volume of 10% KOH (1:3 v/v) was then added to each glass jar containing extracted fish gut

([Karami et al., 2017a](#)). One blank sample was prepared and processed simultaneously for each fish species (total four blanks). All the glass jars with covers containing extracted fish guts in 10% KOH solution were left in the incubator at 60 °C for 24 h until the gut digestion was completed ([Dehaut et al., 2016](#)).

Digestant filtering

The gut specimens were taken out from the incubator after 24 h of digestion. The presence of a clear digestant showed that the digestion process had been completed. Only guts from *Crenimugil seheli* obtained clear digestant and proceeded with the direct vacuum filtration process using Whatman GF/C glass microfibre filter membrane (pore size: 1.2 µm). Each filter was kept individually in a clean petri dish for further processing.

For *Atule mate*, *Sardinella fimbriata* and *Rastrelliger brachysoma*, a little digestion-resistance was found where some particles sank at the bottom of the glass jar. A density separation process was performed on these guts for further processing.

Density separation and filtering

Indigestible particles from the guts of *Atule mate*, *Sardinella fimbriata* and *Rastrelliger brachysoma* samples were density separated using potassium iodide (KI) solution. A 1:1 ratio of distilled water to KI was used to obtain a solution density of 1.52 g/mL (adaptation of [Karami et al., 2017a](#)). KI was used due to its non-hazardous and high-density properties and to allow less dense microplastic particles to separate from denser inorganic large particles such as fish bones and sand ([Bergmann, Gutow & Klages, 2015](#)). A density separator consisting of 200 mL filter funnels, 100–125 mL conical flasks, retort stands, rubber tubes, hinged and binder clips was set up. Filter funnels and conical flasks were covered with aluminium foil to prevent airborne contamination. KI was filtered through Whatman GF/C glass microfibre filter membrane (pore size: 1.2 µm) to prevent contamination. 100 mL of KI was added to each gut sample of *Atule mate*, *Sardinella fimbriata* and *Rastrelliger brachysoma* containing indigestible particles in KOH, which were then poured into the filter funnels. Samples were then allowed to settle for one hour. After the denser materials settled, the rubber tubes were unclipped slowly to discharge settled and unwanted particles. The remaining supernatant was collected in a clean conical flask and unwanted particles were discarded. Supernatant in the conical flasks was filtered through Whatman GF/C, and each filter was kept individually in glass petri dishes for further observation processing.

MICROPLASTIC ANALYSIS

Visual identification of microplastics on filter membranes was carried out by using an MDSI-40X dissecting stereomicroscope and a DM4 (1000x) USB digital electronic microscope. Microplastics were analysed and classified into different types based on their morphological characteristics, *i.e.*, fibre, pellet, film and fragment ([Crawford & Quinn, 2016](#); [Karami et al., 2017a](#)). Significant microplastics found from filters were photographed. The number of microplastics on the filter membranes was then recorded and expressed as items per individual fish. Due to the high susceptibility of error with visual identification, additional physical and characterization on microplastics using SEM-EDX technique was performed to reduce the risk of incorrect interpretation.

Table 1 Mean biometric parameters (\pm SD) of four studied fish species ($n = 18$ per species).

Species	Commonname	Total length (cm)	Standard length (cm)	Wetweight (g)	Gut weight (g)
<i>Atule mate</i>	Yellowtail scad/Pelata	16.68 (\pm 0.47)	13.02 (\pm 0.55)	40.17 (\pm 5.24)	1.58 (\pm 0.43)
<i>Crenimugil seheli</i>	Bluespot mullet/Kedera	16.99 (\pm 0.68)	14.32 (\pm 0.52)	45.67 (\pm 4.03)	2.60 (\pm 0.64)
<i>Sardinella fimbriata</i>	Fringescale sardinella/Tamban	14.74 (\pm 0.91)	12.09 (\pm 0.78)	29.17 (\pm 6.26)	1.28 (\pm 0.31)
<i>Rastrelliger brachysoma</i>	Short mackerel/ Kembung	16.30 (\pm 0.55)	13.33 (\pm 0.33)	43.61 (\pm 2.93)	2.95 (\pm 0.55)

SEM-EDX analysis

A Scanning Electron Microscope (SEM) was used to examine the characterization of the surface composition of the microplastic particles. Ten pieces of microplastic samples with different morphology were randomly selected and analyzed using SEM. Several shapes of microplastics were found, including regular sphere, flat fragments, film and fibre. The quality of the microstructure element (chemical characteristics) was assessed using the Energy-Dispersive Spectroscopy (EDX) analysis.

Statistical analysis

All statistical analyses were performed using SPSS (v23). The number of microplastics was log-transformed for analysis. All data were back-transformed for presentation. The total plastic ingestion rates across different species and habitat were determined by analysis of variance (ANOVA) when assumptions for normality and homoscedasticity were met (Shapiro–Wilk and Levene test, respectively). The significance level was set at $\alpha = 0.05$. Later, the Tukey's post hoc test was used to identify the differences among species. Data that did not meet normality and homoscedasticity were subjected to non-parametric Kruskal-Wallis tests followed by a Wilcoxon-Mann–Whitney post hoc test. Lastly, to investigate the differences in ingestion rate in two habitats, an independent samples T -test was conducted.

RESULTS

Biometric parameters of fish samples

Table 1 shows the mean biometric parameters (\pm SD) of the 72 individual fish for four species ($n = 18$ per species) investigated. *Crenimugil seheli* had the highest mean total length and standard length, at 16.99(\pm 0.68) cm and 14.32(\pm 0.52) cm respectively. *Sardinella fimbriata* had the lowest mean total length and standard length at 14.74(\pm 0.91) cm and 12.09(\pm 0.78) cm respectively. *Crenimugil seheli* was ranked the highest mean wet weight (whole fish) with 45.67(\pm 4.03) g while the lowest mean wet weight species was *Sardinella fimbriata* with 29.17(\pm 6.26) g. For extracted fish gut weight, the highest mean weight was attributed to *Rastrelliger brachysoma* with 2.95(\pm 0.55) g while *Sardinella fimbriata* was ranked with the lowest mean of 1.28(\pm 0.31) g.

Presence, abundance and morphological types of microplastics found

A total of 432 pieces of microplastic (size <5 mm) were observed in 72 excised marine fish guts of four commercial species ($n = 18$ per species) (**Table 2**). Among the samples

Table 2 Total number of microplastics (MPs), average microplastic number per individual fish (\pm SD), and frequency of occurrence of plastic ingestion (FO) per individual fish in four studied species ($n = 18$ per species).

Fish species	FO (%)	Average MPs/individual fish (\pm SD)	Total number of MPs found
<i>Atule Mate</i>	100	6.3 (\pm 4.9)	114
<i>Crenemugil seheli</i>	100	5.0 (\pm 3.7)	90
<i>Sardinella fimbriata</i>	100	6.5 (\pm 4.3)	117
<i>Rastrelliger brachysoma</i>	100	6.2 (\pm 3.3)	111
Total			432

of fish guts examined, microplastics were present in 100% of the samples (FO = 100%, Table 2). *Sardinella fimbriata* had the highest average microplastic number (abundance), at 6.5(\pm 4.3) items per individual fish. *Crenemugil seheli* had the lowest average microplastic number, at 5.0(\pm 3.7) items per individual fish.

There were four morphological types of microplastics found: fragment, fibre, pellet and film. Figure 2 shows that fragment was the most frequent type of microplastic found in this study (49.5%), followed by fibre (41.9%) and pellet (7.6%). The film was the least frequent type of microplastic found (0.9%) overall.

Comparison of the abundance and morphological types of microplastics in four selected commercial marine fish guts

The microplastic abundance in the excised marine fish guts of *Crenimugil seheli*, *Atule mate*, *Sardinella fimbriata* and *Rastrelliger brachysoma* are shown in Fig. 3. ANOVA indicated no significant difference when all species were considered ($F = 0.408$, $p = 0.748$). Figure 4 shows the average microplastic abundance per individual fish according to two different locations. In our study population, *Crenimugil seheli* caught at location 1 showed fewer microplastic concentrations in the gut content compared to the other species caught at location 2. However, independent sample T -test found no significant difference between these two locations ($t = 0.804$, $p = 0.424$).

Crenimugil seheli was observed with the lowest numbers of microplastics in the gut samples among the 4 commercial marine fish species, which were 90 pieces of microplastics in total ($n = 18$) or 5.0(\pm 3.7) items per individual on average. Relatively similar abundances were found among the three species collected from location 2, although amounts were slightly greater in *Sardinella* in which there were 117 pieces of microplastics in total ($n = 18$) or an average of 6.5(\pm 4.3) items per individual fish. By comparison, there were a total of 111 pieces of microplastic found in *Atule mate* gut samples ($n = 18$) or 6.3(\pm 4.9) items per individual fish and 114 pieces of microplastics found in guts of *Rastrelliger brachysoma* ($n = 18$) with an average of 6.2(\pm 3.3) items per individual fish.

Figure 5 shows that fragments were the most abundant microplastics found in *Sardinella fimbriata* and *Rastrelliger brachysoma* with an average number of 4.3(\pm 3.5) items and 3.9(\pm 2.2) items per individual fish, respectively. For *Atule mate* and *Crenimugil seheli*, there were an average of 3.5(\pm 2.5) and 3.0(\pm 2.2) fibres per individual sample fish gut respectively, which was the most abundant morphological type of microplastics found

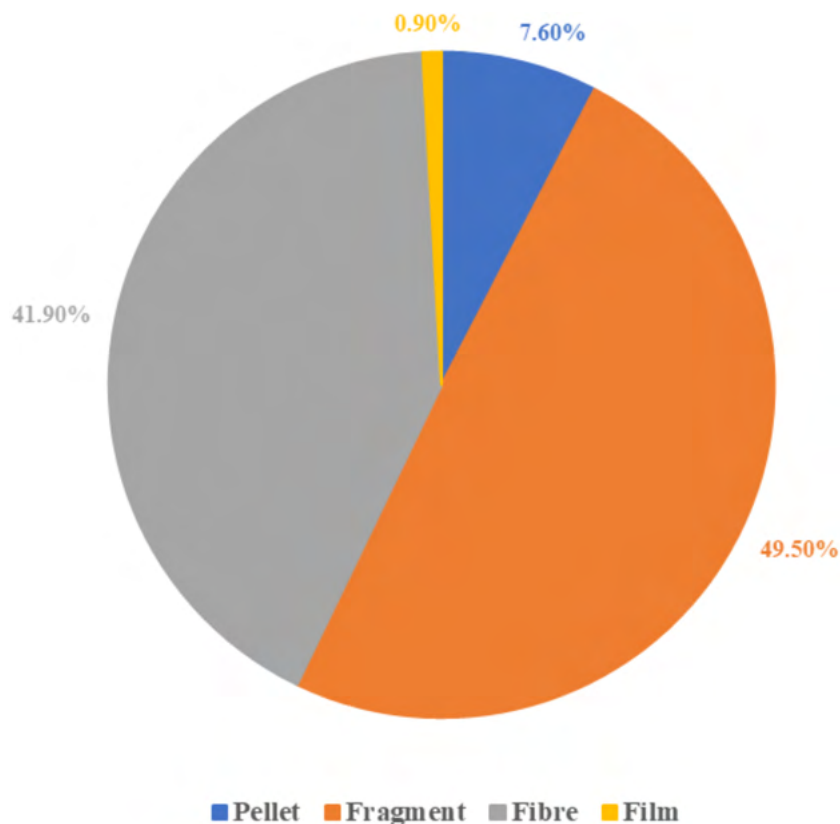


Figure 2 Microplastic classification by the morphological types.

[Full-size](#) [DOI: 10.7717/peerj.13181/fig-2](https://doi.org/10.7717/peerj.13181/fig-2)

in the two species. For all four fish species, film was the least frequent microplastic type present with maximum average numbers of $0.1(\pm 0.3)$ items per individual fish found in *Crenimugil seheli*. [Figures 6](#) and [7](#) shows the images of microplastic particles found using two different types of microscopes.

The SEM-EDX image ([Fig. 8](#)) shows the morphology of the microplastics isolated from the fish guts. EDX analysis showed the presence of carbon, chlorine, iron, sodium, aluminium, calcium, silicon and oxygen in the sample particles. The elements found on the surface of the samples support the identification of the samples as microplastics.

DISCUSSION

Chemical characteristics of microplastic by EDX

Each analysed microplastic has different percentages of elements that characterize the material ([Gniadek & Dabrowska, 2019](#)). In the present study, the SEM-EDX analysis provides qualitative and quantitative results on the composition of the samples observed. Plastics commonly consist of elements such as carbon, hydrogen, nitrogen, oxygen, chlorine and sulphur. The quantitative analysis shows the morphological observation of the microplastic being studied. The microplastics observed in this research are marine debris that has undergone physical, chemical and biological weathering ([Wang et al., 2017](#)).

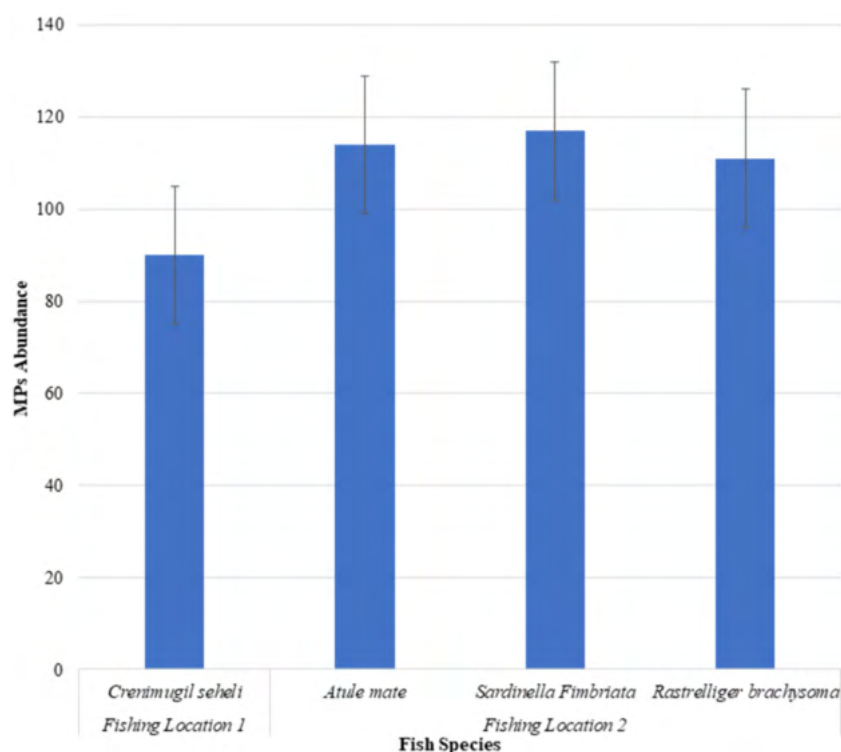


Figure 3 Microplastic abundance (number) in the excised marine fish guts of *Crenimugil seheli*, *Atule mate*, *Sardinella fimbriata* and *Rastrelliger brachysoma* caught from the two fishing locations.

Full-size DOI: 10.7717/peerj.13181/fig-3

Thus, the SEM-EDX analysis can represent any form of degradation undergone by the microplastic.

Microplastics are classified into different types based on their morphological characteristics, *i.e.*, fibre, pellet, *film and fragment*. The SEM-EDX analysis of the samples in this study identified them as (a) fibre, (b) film and (c) fibre. The common observation of all microplastic observed under SEM-EDX was the degradation of the microplastic. The surface of the microplastic was rough with cracked and porous surfaces. Degradation of the microplastics could occur due to weathering, microbial action and chemical actions (*Shahnawaz, Sangale & Ade, 2019*).

The greatest percentage of elements found in the EDX analysis was potassium (K). The occurrence of K indicates the chemical deposition of KOH which was used in the digestion process, as described above (*O'Donovan et al., 2018*). Moreover, the presence of carbon (C) distinguishes the element as a plastic, as most of the plastics produced are primarily made up of C. The highest component of samples (a) and (b) are K, C and oxygen (O). Sample (c) is slightly different, comprised predominantly of C, K and calcium (Ca). The presence of C and O in samples (a) and (c) indicates that the microplastic is typically a polyethylene terephthalate (PET) (*Kohutiar, 2020 #132*). PET is a commonly used plastic material in the textile industry (*Wang et al., 2017*). The structure type of microplastics observed in samples (a) and (c) is fibre which is basically made up of PET. The presence of Ca also indicates the

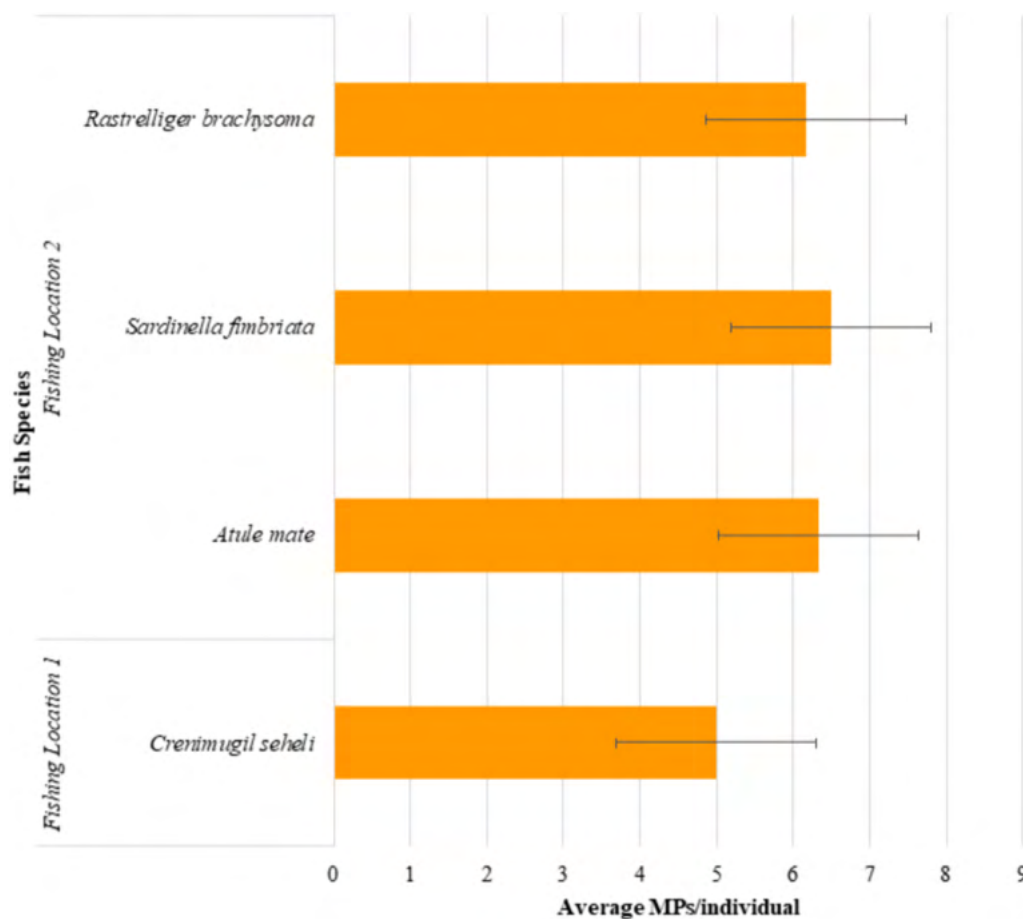


Figure 4 Average microplastic abundance per individual fish in the excised marine fish guts of *Crenimugil seheli*, *Atule mate*, *Sardinella fimbriata* and *Rastrelliger brachysoma* caught from the two fishing locations.

Full-size DOI: [10.7717/peerj.13181/fig-4](https://doi.org/10.7717/peerj.13181/fig-4)

filler material that is used in the production of original plastics, which is the source of the microplastics observed in this research. Calcium carbonate (CaCO_3) is the most popular filler material used in plastic compounds such as polyethylene where it reduces surface energy, enhancing the surface gloss and opacity (Elleithy et al., 2010).

Microplastic ingestion by marine fish

The present study contributes to the knowledge base on the presence of microplastics within the human food chain by providing data on the ingestion of microplastics by four commercially available fish species in the Peninsular Malaysia seawater of the Strait of Malacca. A remarkable and significant finding of this study was 100% of the individual fish gut samples (FO = 100%) were found to contain microplastics. This FO is remarkably high compared to a similar study conducted in Malaysia on plastic ingestion among commercial fish (collected from the fish market in Sri Kembangan, Malaysia), where researchers found an average FO of 26% (Karbalaei et al., 2019). A similar study conducted in Indonesia and the United States (US) showed a plastic uptake of 28% and 9%, respectively. These results

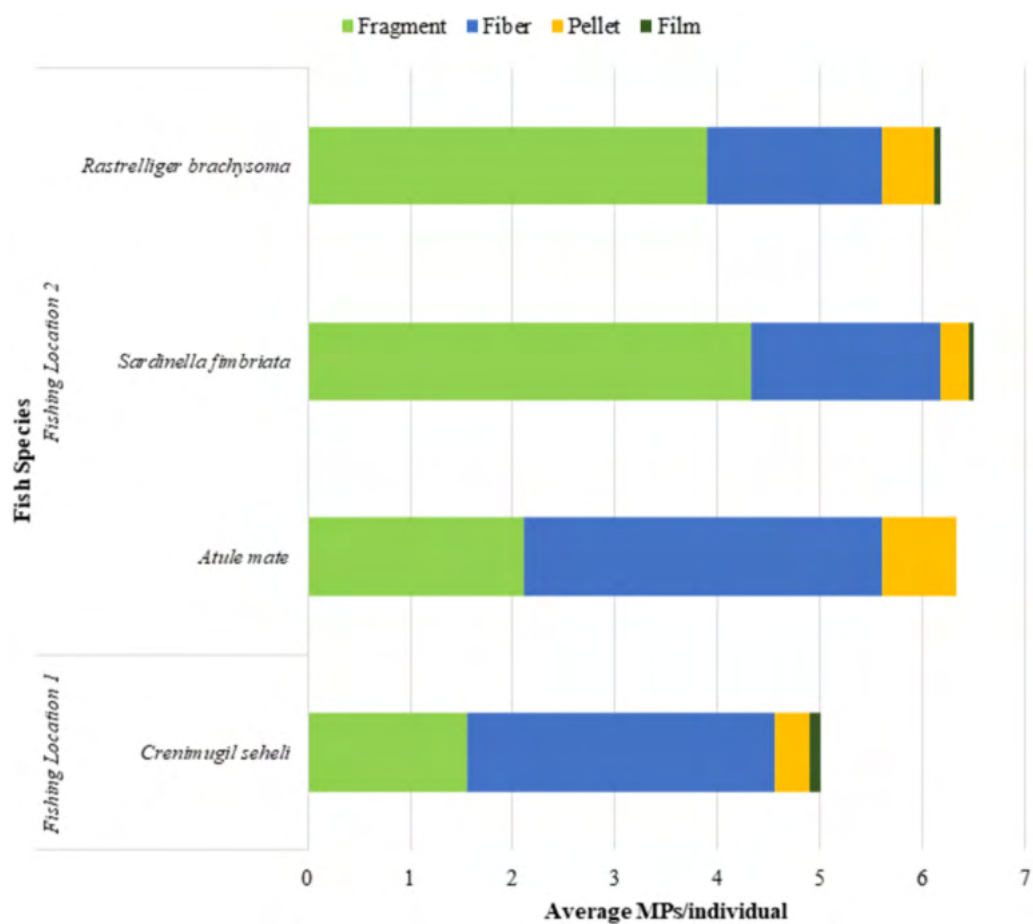


Figure 5 Microplastic classification by morphological types in *Crenimugil seheli*, *Atule mate*, *Sardinella fimbriata* and *Rastrelliger brachysoma* gut samples from two fishing locations.

Full-size DOI: [10.7717/peerj.13181/fig-5](https://doi.org/10.7717/peerj.13181/fig-5)

may not be surprising given that the US (20th), Malaysia (8th), and Indonesia (2nd) are among the top 20 countries mismanaging plastic waste (Jameck *et al.*, 2015). Thus, the results of the present study provide leading evidence of microplastic contamination in commercial marine fish guts from the Northwest Peninsular Malaysia seawater. This also indicates that marine fish in the studied area are exposed to and interact with microplastics in the marine environment. A recent dissertation by Hastuti, Lumbanbatu & Wardiatno (2019) showed similar results where 97.13% of FO in the sample fish guts were contaminated by microplastic. Similarly, Jabeen *et al.* (2017) found 100% of FO in marine fish using μ FTIR and chemical digestion in the Yangtze estuary, China.

The Strait of Malacca is known for its high anthropocentric activity, and it is expected that greater plastic concentrations will occur, however, no research was available previously and the present study aimed to fill this knowledge gap. It is known that Southeast Asia is one of the worst plastic polluters (Jameck *et al.*, 2015). Considering that there is a paucity of research in Asian seawaters, which is emphasized by the review of Markic *et al.* (2020), there could well be an unknowingly high FO of microplastics in this region. The available studies

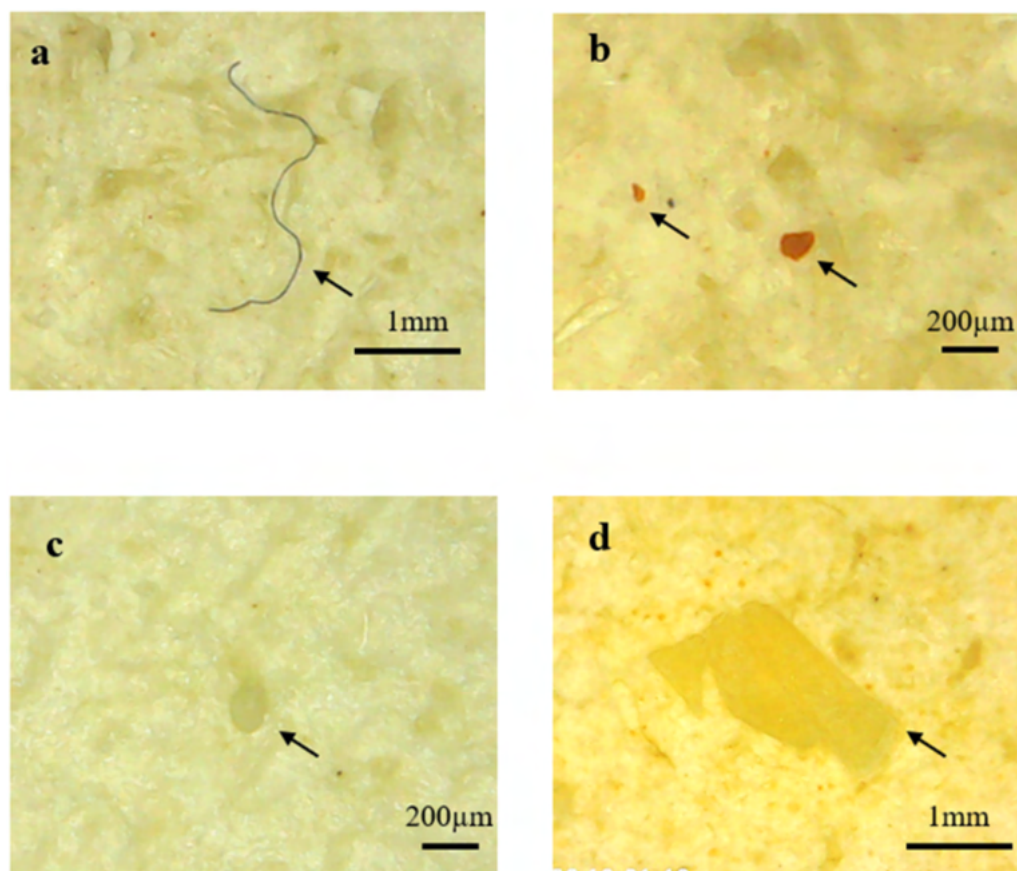


Figure 6 Images of different microplastic morphological types found in fish guts by using DM4 (1000x) USB digital electronic microscope. Particles identified as (A) fibre (B) fragment (C) pellet (D) film.

Full-size [DOI: 10.7717/peerj.13181/fig-6](https://doi.org/10.7717/peerj.13181/fig-6)

in Southeast Asia found high FO (100%) for *Crenimugil seheli* and *Sardinella fimbriata* (Hastuti, Lumbanbatu & Wardiatno, 2019), 33% for *Rastrelliger brachysoma* (Azad et al., 2018) and 11.4% for *Atule mate* (Klangnurak & Chunniyom, 2020). However, small sample sizes were used, increasing the margin of error. Acknowledging these shortcomings, the magnitude of marine plastic ingestion in Southeast Asia could well be underestimated, possibly inducing vast exposure on its citizens with unknown health effects. However, further research is needed to validate this statement.

The comparison of microplastic data with other studies still has a large research gap due to differences across sample size, fish species, temporal and spatial scale as well as sampling methods. Despite that, the results of this study support the growing literature documenting microplastic ingestion by fish under natural conditions (Karbalaei et al., 2019; Akhbarizadeh, Moore & Keshavarzi, 2018; Barboza, Vieira & Guilhermino, 2018b; Neves et al., 2015; Nabr et al., 2015). These studies reveal that microplastic ingestion by marine fish from different species and feeding habitats is common nowadays (Lusher, Mchugh & Thompson, 2013).

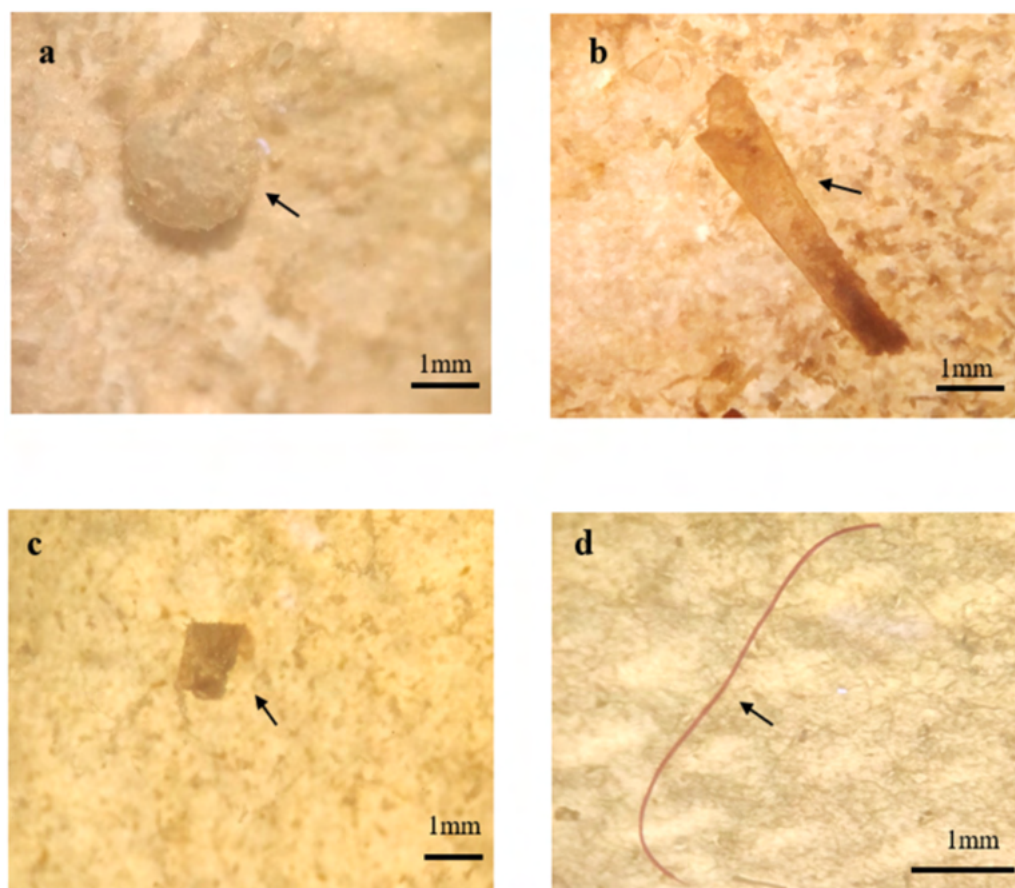


Figure 7 Images of different microplastic morphological types found in fish guts by using MDSI-40X dissecting stereomicroscope. Particles identified as (A) pellet (B) film (C) fragment (D) fibre.

Full-size  DOI: [10.7717/peerj.13181/fig-7](https://doi.org/10.7717/peerj.13181/fig-7)

The main type of microplastic found in the fish sample guts in the present study was fragment (49.5%), which is another remarkable finding in this study. This result supports the studies of *Eriksen et al. (2014)* which found that this type of isolated microplastic was most abundant. The results also indicate the widespread problem of micro-fragments in the marine ecosystem. Percentages of fibre (41.9%) were similar to fragment and ranked as the second-highest microplastic type found in this study. The result of this study was partly complemented by the result of other studies by *Boerger et al. (2010)*, *Lusher, Mchugh & Thompson (2013)* and *Pazos et al. (2017)*, which found that fibres were the predominant microplastic, indicating the high probability of fish ingesting microfibrils. Together, these findings suggest that the difference in microplastics morphological types, sizes and polymers found in organisms are likely caused by different strategies of waste management, contamination sources and sampling locations.

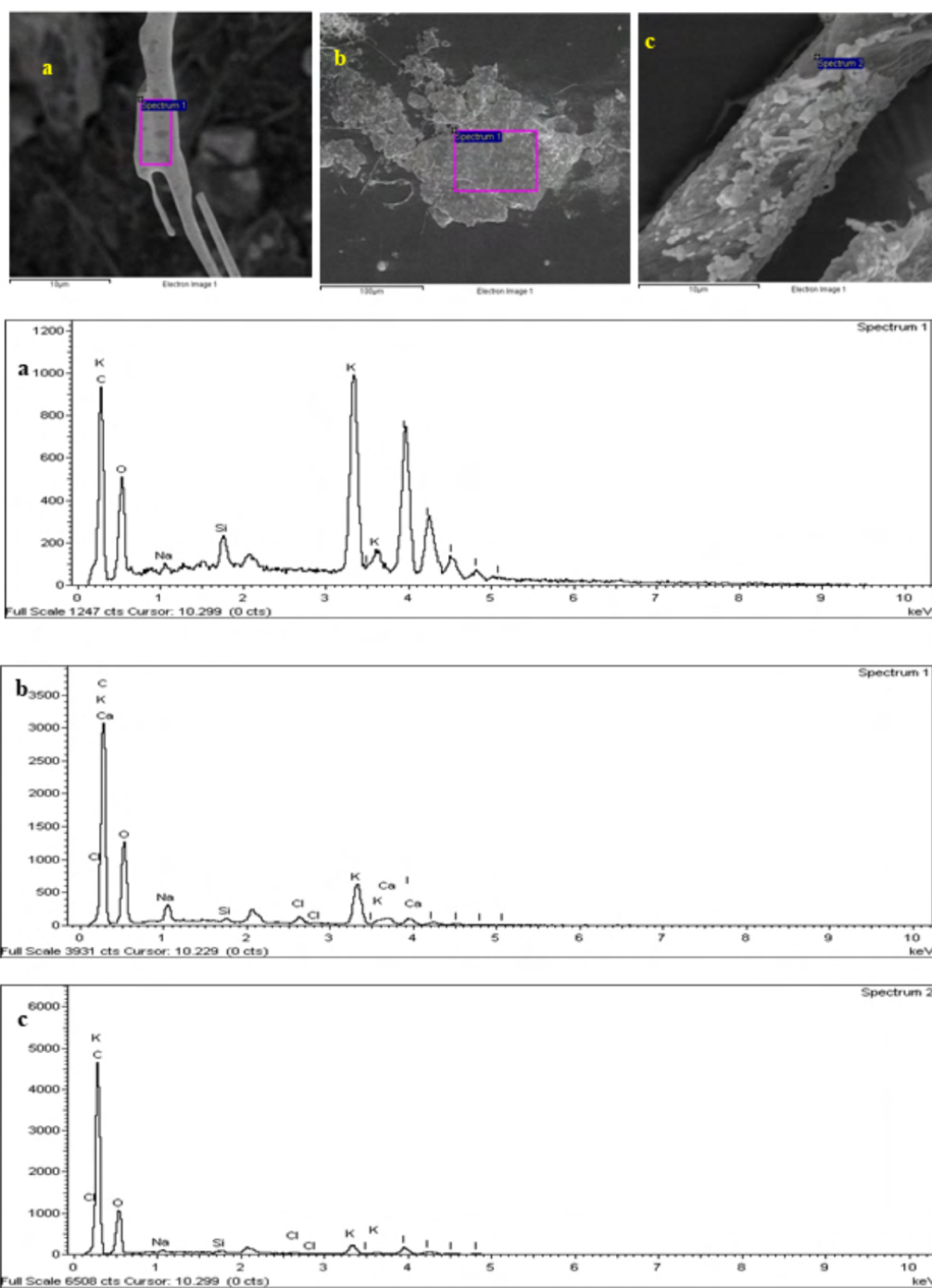


Figure 8 The SEM-EDX imaging and spectrum of microplastic studied. Particles identified as (A) fibre (B) film (C) fibre.

Full-size DOI: 10.7717/peerj.13181/fig-8

Variation of microplastic ingestion among the four marine fish species

In this study, microplastics were present in all the sampled fish guts. Microplastic ingestion numbers varied among the four different species of commercial marine fish from two different locations. The overall finding of this study suggests bony commercial marine fish species from the Northwest Peninsular Malaysia seawater are ingesting significant quantities of microplastic particles. However, there might be risks of underestimation (loss of microplastics during sampling or lab processing) or overestimation (net feeding, background and airborne contamination) of microplastics, which could lead to misrepresentation of the data (Nadal, Alomar & Deudero, 2016; Rummel et al., 2016). Despite these risks, the sample blanks of each commercial species in this study were identified with negligible contamination levels (range 1–2 particles with mean = 1.25 particles per blank), indicating minimal airborne contamination during the processing of the fish gut samples.

According to Froese & Pauly (2000), all four species in this study (*Atule mate*, *Crenimugil seheli*, *Sardinella fimbriata* and *Rastrelliger brachysoma*) are pelagic fish with a habitat range between shallow marine and brackish water. They are commercial marine fish that are commonly found in Malaysia's wet markets and popular as daily meals among Malaysians. A previous study by Lusher, Mchugh & Thompson (2013) reported the presence of microplastics in pelagic fish species in the English Channel. The difference in microplastic ingestion (occurrence in fish guts) in the four species in the present study might be influenced by several factors such as the prevalence of microplastic found in two different fishing locations, fish feeding behaviour and strategies, ecological range and population density (Liboiron et al., 2016). Pelagic-feeding fish are more vulnerable to microplastic particle ingestion compared to demersal feeders due to the characteristics of microplastic polymers (high buoyancy, low density) which are abundant and highly dispersed on the marine surface (HHidalgo-ruz et al., 2012). Microplastic ingestion by marine fish at a particular location may not necessarily be from local sources, due to marine currents which play a vital role in transporting microplastics over very long distances (Nadal, Alomar & Deudero, 2016).

In the present study, *Sardinella fimbriata* was recorded with the highest amount of microplastic ingestion, with a total number of 117 for all samples or $6.5(\pm 4.3)$ items per individual fish. These results are supported by a recent study by Hastuti, Lumbanbatu & Wardiatno (2019) in which the highest microplastic numbers were found in *Sardinella fimbriata* with 20 ± 8 particles per individual fish. *Sardinella fimbriata* are filter feeders, feeding on planktonic organisms; they inhabit the marine pelagic zone and filter water while they are feeding (Hastuti, Lumbanbatu & Wardiatno, 2019). Fish with filter-feeding behaviour are more susceptible to microplastic ingestion compared to other marine fish as they are generalists in term of feeding behaviour (Rummel et al., 2016). Also, the high microplastic ingestion of this species might due to the feeding habitat at the shallow pelagic marine zone. Floating and buoyant microplastic are highly bioavailable for this species as they are extremely small and similar to natural prey which can be found within the water column's plankton (Lima, Costa & Barletta, 2014). The finding that *Sardinella fimbriata*

ingests a significant quantity of microplastics suggests the potential of this species as an indicator for further studies on microplastic ingestion in marine fish. The present study also suggests the possibility that plankton- and pelagic-feeding fish such as *Sardinella fimbriata* could be a major sink species for the floating microplastics in the marine waters of Malaysia.

Crenimugil seheli was shown to ingest the lowest amount of microplastics with a total number of 90 for all samples or an average number of $5.0(\pm 3.7)$ items per individual fish. Although this species is a pelagic feeder like *Atule mate*, *Sardinella fimbriata* and *Rastrelliger brachysoma*, the *Crenimugil seheli* was fished at a different site to the other three sample species of this study. The fishing location of *Crenimugil seheli* was nearby the coast of Teluk Bahang while the *Atule mate*, *Sardinella fimbriata* and *Rastrelliger brachysoma*'s fishing location was nearby the coast of Penaga. This suggests that the marine environment of the fishing location at Teluk Bahang (located at the Penang National Park) might be less polluted by microplastic debris compared to the fishing location of Penaga. When considering feeding behaviour, *Crenimugil seheli* is herbivorous while *Sardinella fimbriata* is carnivorous (Hastuti, Lumbanbatu & Wardiatno, 2019). According to Froese & Pauly (2000), *Atule mate* and *Rastrelliger brachysoma* feed mostly on small crustaceans, planktonic invertebrates and microzooplankton, and can be classified as carnivorous. Hastuti, Lumbanbatu & Wardiatno (2019) found that herbivorous fish have a lower average microplastic number than carnivorous fish, indicating that carnivorous fish might accumulate more microplastic particles. This is due to trophic transfer during which the microplastics transfer from prey to carnivorous fish or are mistakenly ingested as natural prey (Lusher, Mchugh & Thompson, 2013; Markic et al., 2018; Boerger et al., 2010). Our results support this finding, showing that *Crenimugil seheli*, as a herbivorous fish, ingested less microplastics compared to the other three carnivorous fish species. However, robust evidence regarding the influence of trophic transfer on the microplastic ingestion rate in marine fish is still lacking. The multispecies survey of Güven et al. (2017) found a contradictory result in which there was no correlation of microplastic ingestion with fish biological parameters and the fish species' trophic level. Güven et al. (2017) also proposed that only the habitat types or ranges (benthic or pelagic fish) will influence microplastic ingestion by marine fish. Thus, many different factors need to be taken into consideration when comparing microplastic ingestion across different fish species, such as the differences in biological and physiological characteristics, ecological range, feeding behaviour and food retention time in the gut (Grigorakis, Mason & Drouillard, 2017; Ory et al., 2018; Hastuti, Lumbanbatu & Wardiatno, 2019).

Negative impacts of microplastics ingestion

Microplastic pollution also negatively affects a wide range of taxonomic groups in the marine biota including zooplankton, sea urchins, sea turtles and corals (Browne et al., 2008). The finding of microplastic ingestion in marine fish could be a starting point for further investigations on the impacts and toxicity of microplastics to fish health and the further risks of exposure to the marine biota *via* trophic transfer. The consumption of fish and other seafood contaminated with microplastics could potentially impact human health,

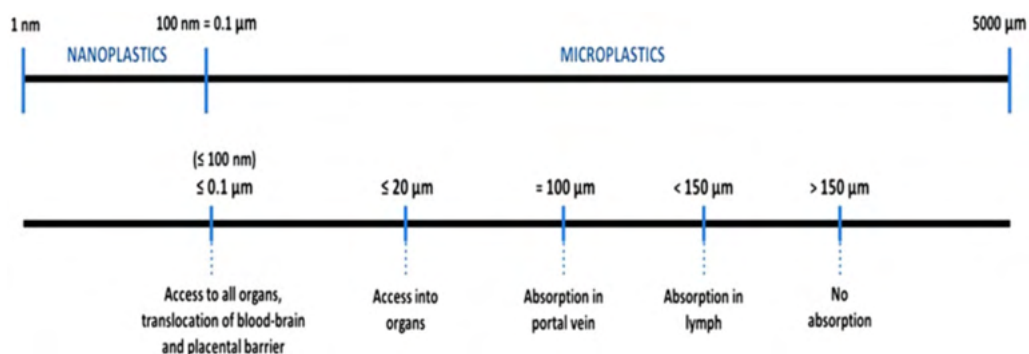


Figure 9 Particle sizes and transferability. Data source: *Lusher et al. (2017)*.

Full-size DOI: [10.7717/peerj.13181/fig-9](https://doi.org/10.7717/peerj.13181/fig-9)

although this assumption is not proven. More dynamic studies regarding microplastics in marine organisms are needed to have a better understanding of the impacts of microplastics on fish, the whole marine biota and humans.

Human health implications

Numerous pathways of microplastic exposure in humans exist, however, knowledge on the human health effects is largely unknown (*Wright & Kelly, 2017*). The human health implications research field is in the early stages (*Koelmans et al., 2017*). Nevertheless, there are sundry commercial fish species bringing seafood safety into question. Additionally, a recent study found that microplastics are capable of penetrating root systems and contaminating fruit and vegetables (*Oliveri Conti et al., 2020*). The food we consume and the omnipresence of microplastics increasingly affect the very foundation of our lives. Microplastics are increasingly revealed as a potential public health concern.

According to a literature review by *Barboza et al. (2018a)*, there is no consensus on microplastics size that can transfer from the gut cavity to the lymph and circulatory system of humans. Currently, it is speculated that microplastics bigger than 150 μm cannot be absorbed in the human body and will be egested (*Fig. 9*). Smaller particles would be able to penetrate human organs. The smaller their sizes, the higher the ability.

Plastics are expected to be toxic and could disrupt human hormones, but the real toxic effects are mostly unknown (*Wright & Kelly, 2017*). Nevertheless, we know from the literature that plastics toxicity increases with dose and smaller particle sizes (*MATTSSON et al., 2017*). Microplastics have been found in the edible part of the fish (*Abbasi et al., 2018; Karami et al., 2017b*). In two species, the fish fillet contained higher plastic loads than the gastrointestinal tract. De-gutting before cooking is common practice for the four fish species (*Atule mate, Crenimugil seheli, Sardinella fimbriata, and Rastrelliger brachysoma*) in this study. Thus, the guts of the four species are generally not consumed by humans, and only the fish fillet is consumed. There might be an accumulation of microplastics in consumer food, but what this means for human health remains a challenge based on limited data to date. Exposure to plastics and additives in our society are ubiquitous, but

the specific impacts on human health are not entirely understood, and many knowledge gaps prevail.

CONCLUSIONS

In conclusion, the results of this study indicate that microplastic ingestion by commercial fish from the Northwest Peninsular Malaysia seawater does occur, suggesting a potential route of microplastic exposure to humans. The most abundant microplastics found in this study were fragments and fibres, with chemical microplastic composition was confirmed by SEM-EDX. The fish gut are often discarded before human consumption, thus further investigation of microplastic contamination of edible and commercial fish tissue is recommended to assess potential microplastic pollution in human food. Thus, further research is needed for a deeper understanding and risk assessment of marine food safety and security in Malaysia.

ACKNOWLEDGEMENTS

We would like to thank the staff of the Centre for Marine and Coastal Studies (CEMACS) and the School of Biological Sciences, Universiti Sains Malaysia for infrastructure and technical support. Thank you also to the National Marine Environmental Monitoring Centre (NMEMC), China, for knowledge sharing regarding this research.

ADDITIONAL INFORMATION AND DECLARATIONS

Funding

This work was supported by the Ministry of Higher Education Malaysia for Fundamental Research Grant Scheme with project code: FRGS/1/2020/STG03/USM/02/6 and Universiti Sains Malaysia, Bridging Incentive Grant project code 304/PPANTAI/6316350. The funders had no role in study design, data collection and analysis, decision to publish, or preparation of the manuscript.

Grant Disclosures

The following grant information was disclosed by the authors:

The Ministry of Higher Education Malaysia for Fundamental Research Grant Scheme: FRGS/1/2020/STG03/USM/02/6.

Universiti Sains Malaysia.

Bridging Incentive Grant project: 304/PPANTAI/6316350.

Competing Interests

The authors declare there are no competing interests.

Author Contributions

- Yuen Hwei Foo conceived and designed the experiments, performed the experiments, prepared figures and/or tables, authored or reviewed drafts of the paper, and approved the final draft.

- Sharnietha Ratnam and Masthurah Abdullah performed the experiments, prepared figures and/or tables, authored or reviewed drafts of the paper, and approved the final draft.
- Er Vin Lim performed the experiments, authored or reviewed drafts of the paper, and approved the final draft.
- Vincent J. Molenaar analyzed the data, prepared figures and/or tables, authored or reviewed drafts of the paper, and approved the final draft.
- Aileen Tan Shau Hwai, Shoufeng Zhang and Hongjun Li analyzed the data, authored or reviewed drafts of the paper, and approved the final draft.
- Norlaila Binti Mohd Zanuri conceived and designed the experiments, prepared figures and/or tables, authored or reviewed drafts of the paper, and approved the final draft.

Data Availability

The following information was supplied regarding data availability:

The raw data measurements are available in the [Supplementary Files](#).

Supplemental Information

Supplemental information for this article can be found online at <http://dx.doi.org/10.7717/peerj.13181#supplemental-information>.

REFERENCES

- Abbasi S, Soltani N, Keshavarzi B, Moore F, Turner A, Hassanaghaei M. 2018.** Microplastics in different tissues of fish and prawn from the Musa Estuary, Persian Gulf. *Chemosphere* **205**:80–87 DOI [10.1016/j.chemosphere.2018.04.076](https://doi.org/10.1016/j.chemosphere.2018.04.076).
- Akhbarizadeh R, Moore F, Keshavarzi B. 2018.** Investigating a probable relationship between microplastics and potentially toxic elements in fish muscles from northeast of Persian Gulf. *Environmental Pollution* **232**:154–163 DOI [10.1016/j.envpol.2017.09.028](https://doi.org/10.1016/j.envpol.2017.09.028).
- Andrady AL. 2011.** Microplastics in the marine environment. *Marine Pollution Bulletin* **62**:1596–1605 DOI [10.1016/j.marpolbul.2011.05.030](https://doi.org/10.1016/j.marpolbul.2011.05.030).
- Azad S, Towatana P, Pradit S, Patricia BG, Hue HT, Jualaong S. 2018.** First evidence of existence of microplastics in stomach of some commercial fishes in the lower gulf of Thailand. *Applied Ecology and Environmental Research* **16**:7345–7360 DOI [10.15666/aeer/1606_73457360](https://doi.org/10.15666/aeer/1606_73457360).
- Azoulay D, Villa P, Arellamo Y, Gordon M, Moon D, Miller K, Thompson K. 2019.** *Plastic and Health: the hidden costs of a plastic planet*. United State: University of Michigan.
- Barboza LGA, Dickvethaak A, Lavorante BRBO, Lundebye A-KL, Guilhermino L. 2018a.** Marine microplastic debris: an emerging issue for food security. *Food Safety and Human Health. Marine Pollution Bulletin* **133**:336–348 DOI [10.1016/j.marpolbul.2018.05.047](https://doi.org/10.1016/j.marpolbul.2018.05.047).

- Barboza LGA, Gimenez BCG. 2015.** Microplastics in the marine environment: current trends and future perspectives. *Marine Pollution Bulletin* **97**:5–12 DOI [10.1016/j.marpolbul.2015.06.008](https://doi.org/10.1016/j.marpolbul.2015.06.008).
- Barboza LGA, Vieira LR, Guilhermino L. 2018b.** Single and combined effects of microplastics and mercury on juveniles of the European seabass (*Dicentrarchus labrax*): changes in behavioural responses and reduction of swimming velocity and resistance time. *Environmental Pollution* **236**:1014–1019 DOI [10.1016/j.envpol.2017.12.082](https://doi.org/10.1016/j.envpol.2017.12.082).
- Bergmann M, Gutow L, Klages M. 2015.** *Marine anthropogenic litter*. Cham: Springer.
- Boerger CM, Lattin GL, Moore SLB, Moore CJ. 2010.** Plastic ingestion by planktivorous fishes in the North Pacific Central Gyre. *Marine Pollution Bulletin* **60**:2275–2278 DOI [10.1016/j.marpolbul.2010.08.007](https://doi.org/10.1016/j.marpolbul.2010.08.007).
- Browne MA, Dissanayake A, Galloway TS, Lowe DM, Thompson RC. 2008.** Ingested microscopic plastic translocates to the circulatory system of the mussel, *Mytilus Edulis* (L.). *Environmental Science & Technology* **42**:5026–5031 DOI [10.1021/es800249a](https://doi.org/10.1021/es800249a).
- Cole M, Lindeque P, Halsband C, Galloway TS. 2011.** Microplastics as contaminants in the marine environment: a review. *Marine Pollution Bulletin* **62**:2588–2597 DOI [10.1016/j.marpolbul.2011.09.025](https://doi.org/10.1016/j.marpolbul.2011.09.025).
- Crawford CBC, Quinn B. 2016.** *Microplastic pollutants*. Amsterdam: Elsevier Limited.
- Dehaut B, Cassone A-L, Frère L, Hermabessiere L, Himber C, Rinnert E, Rivière G, Lambert C, Soudant P, Huvet A, Duflos G, Paul-pont I. 2016.** Microplastics in seafood: benchmark protocol for their extraction and characterization. *Environmental Pollution* **215**:223–233 DOI [10.1016/j.envpol.2016.05.018](https://doi.org/10.1016/j.envpol.2016.05.018).
- Elleithy RH, Ali I, Ali MA, Al-Zahrani SM. 2010.** High density polyethylene/micro calcium carbonate composites: A study of the morphological, thermal, and viscoelastic properties. *Journal of Applied Polymer Science* **117**(4):2413–2421 DOI [10.1002/app.32142](https://doi.org/10.1002/app.32142).
- Eriksen M, Lebreton LCM, Carson HS, Thiel M, Moore CJ, Borerro JC, Galgani F, Ryan PG, Reisser J. 2014.** Plastic Pollution in the World's Oceans: more than 5 trillion plastic pieces weighing over 250,000 Tons Afloat at Sea. *PLOS ONE* **9**:e111913 DOI [10.1371/journal.pone.0111913](https://doi.org/10.1371/journal.pone.0111913).
- Fok L, Cheung PK. 2015.** Hong Kong at the pearl river estuary: a hotspot of microplastic pollution. *Marine Pollution Bulletin* **99**:112–118 DOI [10.1016/j.marpolbul.2015.07.050](https://doi.org/10.1016/j.marpolbul.2015.07.050).
- Froese R, Pauly D. 2000.** *Fishbase 2000*. Makati City (Philippines): International Center for Living Aquatic Resources Management.
- Grigorakis S, Mason SA, Drouillard KG. 2017.** Determination of the gut retention of plastic microbeads and microfibers in goldfish (*Carassius auratus*). *Chemosphere* **169**:233–238 DOI [10.1016/j.chemosphere.2016.11.055](https://doi.org/10.1016/j.chemosphere.2016.11.055).
- Güven O, Gökdağ K, Jovanović B, Kıdeys AE. 2017.** Microplastic litter composition of the Turkish territorial waters of the Mediterranean Sea, and its occurrence in the gastrointestinal tract of fish. *Environmental Pollution* **223**:286–294 DOI [10.1016/j.envpol.2017.01.025](https://doi.org/10.1016/j.envpol.2017.01.025).

- Hastuti AYU, Lumbanbatu DTF, Wardiatno Y. 2019.** The presence of microplastics in the digestive tract of commercial fishes off Pantai Indah Kapuk coast, Jakarta, Indonesia. *Biodiversitas* **20**:1233–1242.
- Hidalgo-ruz V, Gutow L, Thompson RC, Thiel M. 2012.** Microplastics in the marine environment: a review of the methods used for identification and quantification. *Environmental Science & Technology* **46**:3060–3075 DOI [10.1021/es2031505](https://doi.org/10.1021/es2031505).
- Jabeen K, SU L, LI J, Yang D, Tong C, MU J, Shi H. 2017.** Microplastics and mesoplastics in fish from coastal and fresh waters of China. *Environmental Pollution* **221**:141–149 DOI [10.1016/j.envpol.2016.11.055](https://doi.org/10.1016/j.envpol.2016.11.055).
- Jambeck JR, Geyer R, Wilcox C, Siegler TR, Perryman M, Andrady A, Narayan R, Law KL. 2015.** Plastic waste inputs from land into the ocean. *Science* **347**:768 DOI [10.1126/science.1260352](https://doi.org/10.1126/science.1260352).
- Jovanović B. 2017.** Ingestion of microplastics by fish and its potential consequences from a physical perspective. *Integrated Environmental Assessment and Management* **13**:510–515 DOI [10.1002/ieam.1913](https://doi.org/10.1002/ieam.1913).
- Karami A, Golieskardi A, Choockromano N, HO YB, Salamatinia B. 2017a.** A high-performance protocol for extraction of microplastics in fish. *Science of the Total Environment* **578**:485–494 DOI [10.1016/j.scitotenv.2016.10.213](https://doi.org/10.1016/j.scitotenv.2016.10.213).
- Karami A, Golieskardi A, Hoyblarat V, Salamatinia B. 2017b.** Microplastics in eviscerated flesh and excised organs of dried fish. *Scientific Reports* **7**:5473–5471 DOI [10.1038/s41598-017-05828-6](https://doi.org/10.1038/s41598-017-05828-6).
- Karbalaei S, Golieskardi A, Hamzah HB, Abdulwahid S, Hanachi P, Walker TR, Karami A. 2019.** Abundance and characteristics of microplastics in commercial marine fish from Malaysia. *Marine Pollution Bulletin* **148**:5–15 DOI [10.1016/j.marpolbul.2019.07.072](https://doi.org/10.1016/j.marpolbul.2019.07.072).
- Klangnurak W, Chunnuyom S. 2020.** Screening for microplastics in marine fish of Thailand: the accumulation of microplastics in the gastrointestinal tract of different foraging preferences. *Environmental Science and Pollution Research* **27**:27161–27168 DOI [10.1007/s11356-020-09147-8](https://doi.org/10.1007/s11356-020-09147-8).
- Koehler A, Anderson A, Andrady A, Arthur C, Baker J, Bouwman H, Gall S, Hidalgo-Ruz V, Koehler A, Law K, Leslie H, Kershaw P, Pahl S, Potemra J, Ryan P, Shim W, Thompson R, Takada H, Turra A, Wyles K. 2015.** *Sources, fate and effects of microplastics in the marine environment: a global assessment*. London: International Maritime Organization.
- Koelmans AA, Besseling E, Foekema E, Kooi M, Mintenig S, Ossendor PB, Credondohasselerharm PE, Verschoor A, Van Wezel AP, Scheffer M. 2017.** Risks of plastic debris: unravelling fact, opinion, perception, and belief. *Environmental Science & Technology* **51**:11513–11519 DOI [10.1021/acs.est.7b02219](https://doi.org/10.1021/acs.est.7b02219).
- Kohutiar M, Janík R, Pajtášová M, Ondrušová D, Labaj I, Zvolánková Mezenecová V. 2020.** Study of structural changes in thermoplastics using dynamic mechanical analysis. *IOP Conference Series: Materials Science and Engineering* **776**(1):012092 DOI [10.1088/1757-899x/776/1/012092](https://doi.org/10.1088/1757-899x/776/1/012092).

- Li J, Liu H, Paulchen J. 2018.** Microplastics in freshwater systems: a review on occurrence, environmental effects, and methods for microplastics detection. *Water Research* **137**:362–374 DOI [10.1016/j.watres.2017.12.056](https://doi.org/10.1016/j.watres.2017.12.056).
- Liboiron M, Liboiron F, Wells E, Richárd N, Zahara A, Mather C, Bradshaw H, Murichi J. 2016.** Low plastic ingestion rate in Atlantic cod (*Gadus morhua*) from Newfoundland destined for human consumption collected through citizen science methods. *Marine Pollution Bulletin* **113**:428–437 DOI [10.1016/j.marpolbul.2016.10.043](https://doi.org/10.1016/j.marpolbul.2016.10.043).
- Lima A, Costa M, Barletta M. 2014.** Distribution patterns of microplastics within the plankton of a tropical estuary. *Environmental Research* **132**:146–155 DOI [10.1016/j.envres.2014.03.031](https://doi.org/10.1016/j.envres.2014.03.031).
- Lusher AL, Mchugh M, Thompson RC. 2013.** Occurrence of microplastics in the gastrointestinal tract of pelagic and demersal fish from the English Channel. *Marine Pollution Bulletin* **67**:94–99 DOI [10.1016/j.marpolbul.2012.11.028](https://doi.org/10.1016/j.marpolbul.2012.11.028).
- Lusher A, Welden N, Sobral P, Cole M. 2017.** Sampling, isolating and identifying microplastics ingested by fish and invertebrates. *Analytical Methods* **9**:1346–1360.
- Gniadek M, Dąbrowska A. 2019.** The marine nano- and microplastics characterisation by SEM-EDX: the potential of the method in comparison with various physical and chemical approaches. *Marine Pollution Bulletin* **148**:210–216 DOI [10.1016/j.marpolbul.2019.07.067](https://doi.org/10.1016/j.marpolbul.2019.07.067).
- Markic A, Gaertner J-C, Gaertner-mazouni N, Koelmans AA. 2020.** Plastic ingestion by marine fish in the wild. *Critical Reviews in Environmental Science and Technology* **50**:657–697 DOI [10.1080/10643389.2019.1631990](https://doi.org/10.1080/10643389.2019.1631990).
- Markic A, Niemand C, Bridson JH, Mazouni-Gaertner N, Gaertner J-C, Eriksen M, Bowen M. 2018.** Double trouble in the South Pacific subtropical gyre: increased plastic ingestion by fish in the oceanic accumulation zone. *Marine Pollution Bulletin* **136**:547–564 DOI [10.1016/j.marpolbul.2018.09.031](https://doi.org/10.1016/j.marpolbul.2018.09.031).
- Mattsson K, Johnson EV, Malmendal A, Linse S, Hansson L-A, Cedervall T. 2017.** Brain damage and behavioural disorders in fish induced by plastic nanoparticles delivered through the food chain. *Scientific Reports* **7**:11452–11451 DOI [10.1038/s41598-017-10813-0](https://doi.org/10.1038/s41598-017-10813-0).
- Nadal M, Alomar C, Deudero S. 2016.** High levels of microplastic ingestion by the semipelagic fish bogue *Boops boops* (L.) around the Balearic Islands. *Environmental Pollution* **214**:517–523 DOI [10.1016/j.envpol.2016.04.054](https://doi.org/10.1016/j.envpol.2016.04.054).
- Neves D, Sobral P, Ferreira JL, Pereira T. 2015.** Ingestion of microplastics by commercial fish off the Portuguese coast. *Marine Pollution Bulletin* **101**:119–126 DOI [10.1016/j.marpolbul.2015.11.008](https://doi.org/10.1016/j.marpolbul.2015.11.008).
- Nobre CR, Santana MFM, Maluf A, Cortez FS, Cesar A, Pereira CDS, Turra A. 2015.** Assessment of microplastic toxicity to embryonic development of the sea urchin *Lytechinus variegatus* (Echinodermata: Echinoidea). *Marine Pollution Bulletin* **92**:99–104 DOI [10.1016/j.marpolbul.2014.12.050](https://doi.org/10.1016/j.marpolbul.2014.12.050).
- Norimahak JR, Safiah M, Jamal K, Haslinda S, Zuhaida H, Rohida S, Fatimah S, Norazlin S, Poh BK, Kandiah M, Zalilah MS, Wan Manan WM, Fatimah S, Azmi**

- MY. 2008.** Food consumption patterns: findings from the Malaysian adult nutrition survey (MANS). *Malaysian Journal of Nutrition* **14**:25–39.
- Nurnadia A, Azrina A, Amin I. 2011.** Proximate composition and energetic value of selected marine fish and shellfish from the West coast of Peninsular Malaysia. *International Food Research Journal* **18**:137–148.
- O'Donovan S, Mestre NC, Abel S, Fonseca TG, Carteny CC, Cormier B, Keiter SH, Bebianno MJ. 2018.** Ecotoxicological effects of chemical contaminants adsorbed to microplastics in the clam *Scrobicularia plana*. *Frontiers in Marine Science* **5**:143 DOI [10.3389/fmars.2018.00143](https://doi.org/10.3389/fmars.2018.00143).
- Oliveri Conti G, Ferrante M, Banni M, Favara C, Nicolosi I, Cristaldi A, Fiore M, Zuccarello P. 2020.** Micro- and nano-plastics in edible fruit and vegetables, the first diet risks assessment for the general population. *Environmental Research* **187**:109677 DOI [10.1016/j.envres.2020.109677](https://doi.org/10.1016/j.envres.2020.109677).
- Ory NC, Gallardo C, Lenz M, Thiel M. 2018.** Capture, swallowing, and egestion of microplastics by a planktivorous juvenile fish. *Environmental Pollution* **240**:566–573 DOI [10.1016/j.envpol.2018.04.093](https://doi.org/10.1016/j.envpol.2018.04.093).
- Pazos R, Maiztegui T, Colautti D, Paracampo A, Gómez N. 2017.** Microplastics in gut contents of coastal freshwater fish from Río de la Plata estuary. *Marine Pollution Bulletin* **122**:85–90.
- Rummel CD, Löder MG, Fricke NF, Lang T, Griebeler E-M, Janke M, Gerdtz G. 2016.** Plastic ingestion by pelagic and demersal fish from the North Sea and Baltic Sea. *Marine Pollution Bulletin* **102**:134–141 DOI [10.1016/j.marpolbul.2015.11.043](https://doi.org/10.1016/j.marpolbul.2015.11.043).
- Santillo D, Miller K, Johnston P. 2017.** Microplastics as contaminants in commercially important seafood species. *Integr Environ Assess Manag* **13**:516–521 DOI [10.1002/ieam.1909](https://doi.org/10.1002/ieam.1909).
- Shahnawaz M, Sangale MK, Ade AB. 2019.** Analysis of the plastic degradation products. In: *Bioremediation technology for plastic waste*. Singapore: Springer Singapore.
- Sharma S, Chatterjee S. 2017.** Microplastic pollution, a threat to marine ecosystem and human health: a short review. *Environmental Science and Pollution Research* **24**:21530–21547 DOI [10.1007/s11356-017-9910-8](https://doi.org/10.1007/s11356-017-9910-8).
- Teh E. 2012.** *Fisheries in Malaysia: can resources match demand?* Kuala Lumpur: Maritime Institute of Malaysia (MIMA).
- Wang J, Tan Z, Peng J, Qiu Q, Li M. 2016.** The behaviors of microplastics in the marine environment. *Marine Environmental Research* **113**:7–17 DOI [10.1016/j.marenvres.2015.10.014](https://doi.org/10.1016/j.marenvres.2015.10.014).
- Wang ZM, Wagner J, Ghosal S, Bedi G, Wall S. 2017.** SEM/EDS and optical microscopy analyses of microplastics in ocean trawl and fish guts. *Science of the Total Environment* **603–604**:616–626.
- Wright SL, Kelly FJ. 2017.** Plastic and human health: a micro issue? *Environmental Science & Technology* **51**:6634–6647 DOI [10.1021/acs.est.7b00423](https://doi.org/10.1021/acs.est.7b00423).



Habitat variability and faunal zonation at the Ægir Ridge, a canyon-like structure in the deep Norwegian Sea

Saskia Brix¹, Stefanie Kaiser^{2,3}, Anne-Nina Lörz⁴, Morgane Le Saout⁵, Mia Schumacher⁵, Frederic Bonk¹, Hronn Egilsdottir⁶, Steinunn Hilma Olafsdottir⁶, Anne Helene S. Tandberg⁷, James Taylor¹, Simon Tewes⁸, Joana R. Xavier^{9,10} and Katrin Linse¹¹

¹ Senckenberg am Meer, German Center for Marine Biodiversity Research (DZMB), Senckenberg Nature Research Society, Hamburg, Germany

² Faculty of Biology and Environmental Protection, Department of Invertebrate Zoology and Hydrobiology, Łódź, Poland

³ INES Integrated Environmental Solutions UG, Wilhelmshaven, Niedersachsen, Germany

⁴ Institute for Marine Ecosystems and Fisheries Science, Center for Earth System Research and Sustainability (CEN), University of Hamburg, Hamburg, Germany

⁵ GEOMAR Helmholtz Centre for Ocean Research, Kiel, Germany

⁶ Marine and Freshwater Research Institute, Hafnarfjörður, Iceland

⁷ University Museum, University of Bergen, Bergen, Norway

⁸ Bundesamt für Seeschifffahrt und Hydrographie, Hamburg, Germany

⁹ CIIMAR—Interdisciplinary Centre of Marine and Environmental Research of the University of Porto, Matosinhos, Portugal

¹⁰ Department of Biological Sciences, University of Bergen, Bergen, Norway

¹¹ British Antarctic Survey, Cambridge, United Kingdom

ABSTRACT

The Ægir Ridge System (ARS) is an ancient extinct spreading axis in the Nordic seas extending from the upper slope east of Iceland (~550 m depth), as part of its Exclusive Economic Zone (EEZ), to a depth of ~3,800 m in the Norwegian basin. Geomorphologically a rift valley, the ARS has a canyon-like structure that may promote increased diversity and faunal density. The main objective of this study was to characterize benthic habitats and related macro- and megabenthic communities along the ARS, and the influence of water mass variables and depth on them. During the IceAGE3 expedition (Icelandic marine Animals: Genetics and Ecology) on RV Sonne in June 2020, benthic communities of the ARS were surveyed by means of a remotely-operated vehicle (ROV) and epibenthic sledge (EBS). For this purpose, two working areas were selected, including abyssal stations in the northeast and bathyal stations in the southwest of the ARS. Video and still images of the seabed were used to qualitatively describe benthic habitats based on the presence of habitat-forming taxa and the physical environment. Patterns of diversity and community composition of the soft-sediment macrofauna, retrieved from the EBS, were analyzed in a semiquantitative manner. These biological data were complemented by producing high-resolution bathymetric maps using the vessel's multi-beam echosounder system. As suspected, we were able to identify differences in species composition and number of macro- and megafaunal communities associated with a depth gradient. A biological canyon effect became evident in dense aggregates of megafaunal filter feeders and elevated macrofaunal densities. Analysis of videos and still images from the ROV transects also led to

Submitted 20 April 2021

Accepted 16 April 2022

Published 15 June 2022

Corresponding author

Saskia Brix,
Saskia.Brix-Elsig@senckenberg.de

Academic editor

Blanca Figuerola

Additional Information and
Declarations can be found on
page 30

DOI 10.7717/peerj.13394

© Copyright
2022 Brix et al.

Distributed under
Creative Commons CC-BY 4.0

OPEN ACCESS

the discovery of a number of Vulnerable Marine Ecosystems (VMEs) dominated by sponges and soft corals characteristic of the Arctic region. Directions for future research encompass a more detailed, quantitative study of the megafauna and more coherent sampling over the entire depth range in order to fully capture the diversity of the habitats and biota of the region. The presence of sensitive biogenic habitats, alongside seemingly high biodiversity and naturalness are supportive of ongoing considerations of designating part of the ARS as an “Ecologically and Biologically Significant Area” (EBSA).

Subjects Biodiversity, Conservation Biology, Ecology, Marine Biology, Environmental Impacts

Keywords Iceland, Deep sea, Marine invertebrates, Arctic circle, EBSA, VME, ROV transects, Banana hole, Sponge gardens, Soft corals

INTRODUCTION

Life on the deep seafloor beyond the shelf break is undoubtedly rich and contains a significant fraction of the global marine biodiversity (*Appeltans et al., 2012; Danovaro, Snelgrove & Tyler, 2014*). The deep sea also holds an abundance of geomorphic features, including seamounts, canyons, troughs, ridges, trenches, and abyssal plains that are anticipated to represent distinct types of benthic habitats (*Ramirez-Llodra et al., 2010; Harris & Baker, 2011*). A combination of factors and processes are considered to have shaped the diversity and distribution of today’s deep-sea fauna. Among these, bathymetry, temperature, salinity, oxygen, hydrostatic pressure, organic matter flux, substrate type, and seabed geomorphology stand out as key environmental descriptors (*Levin et al., 2001*). The variety of geological features (or geodiversity) creates a heterogeneous environment that promotes high diversity of habitats and species on a range of scales. Bathymetric discontinuities, such as seamounts, submarine canyons, and ridges, can have a significant impact on hydrodynamics by diverting current flow or changing current velocity. For example, unique hydrographic features of canyons can lead to increased flux and channeling of organic matter from surface waters to the sea floor, making them areas of augmented benthic biomass and productivity, but also promoting biodiversity in several faunal taxa (*Schlacher et al., 2007; De Leo et al., 2010; Vetter, Smith & De Leo, 2010; Leduc et al., 2020*). Furthermore, topographical and biogenic structures, such as boulders or corals, as well as disturbance or ephemeral food patches contribute to increased local-scale heterogeneity and thus biodiversity in the deep sea (*McClain & Barry, 2010; Vanreusel et al., 2010; Riehl et al., 2020*).

Understanding species’ spatial distributions and their relationships to the abiotic seafloor environment makes a fundamental contribution to marine spatial planning and serves as a basis for monitoring potential future shifts in biodiversity and biogeographic ranges (*Costello, 2009*). Typical conservation management ensures sustainable use of marine resources while safeguarding marine life, their habitats, and functions, *i.e.*, preserving the biological and geological heritage of the marine realm (*Ware & Downie, 2020*). However, there remains a general lack of knowledge about the biological and physical components

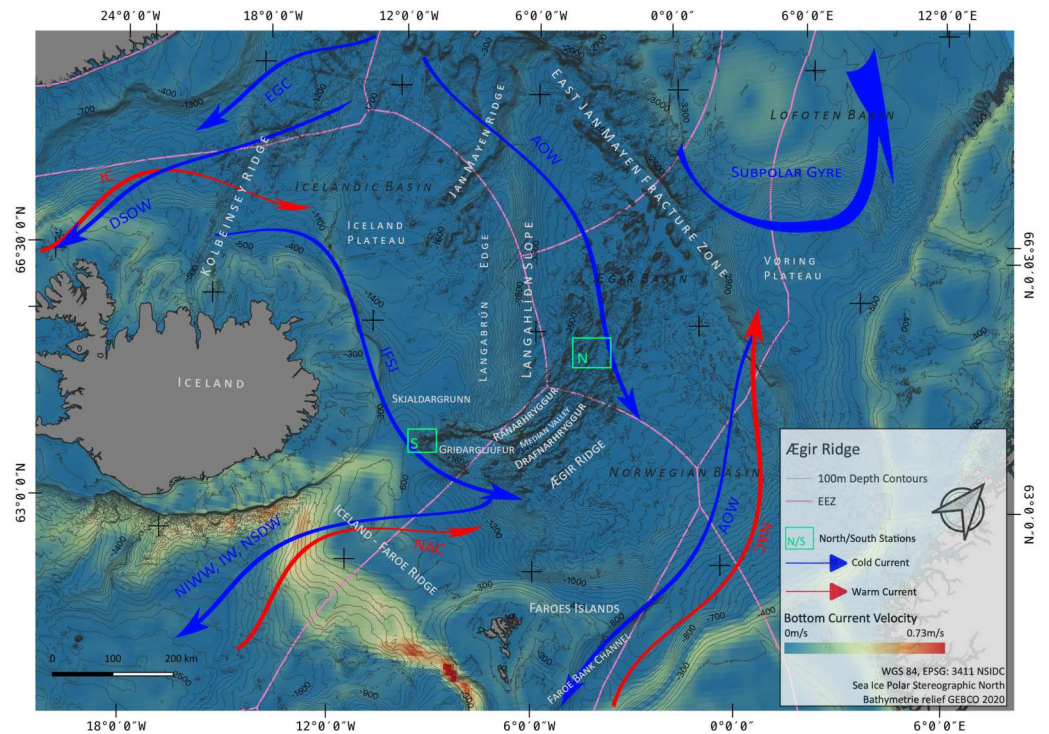


Figure 1 Overview map. Map of the study region. Green boxes ‘N’ and ‘S’ indicated the sampling areas ‘North’ and ‘South’ at the Ægir Ridge. Blue arrows indicate dense, cold water currents, red arrows indicate warmer water currents. AOW—Arctic Overflow Water, DSO—Denmark Strait Overflow Water, EGC—East Greenland Current, NAC—North Atlantic Current. Map produced with software QGIS 3.16.4.; bathymetry obtained from GEBCO Compilation Group; bottom current velocity obtained from Copernicus locator model (*Copernicus Marine Service, 2021*).

Full-size DOI: 10.7717/peerj.13394/fig-1

of deep-sea ecosystems, also due to the fact that a mere fraction of the seabed has been thoroughly mapped to date (*Wölfl et al., 2019*). To remedy this deficiency, national and international initiatives, including the Seabed 2030 (<http://seabed2030.org>) project or the Norwegian MAREANO (Marine Areal Database for Norwegian Coasts and Sea Areas) program (*Buhl-Mortensen et al., 2015a*), are now underway. As part of the German IceAGE3 (SO276) expedition in summer 2020, efforts were made to expand the bathymetry data of the Norwegian basin particularly along the Ægir Ridge system (ARS, *Fig. 1*) nested therein, and to characterize its associated habitats and macro- and megafaunal communities (*Brix et al., 2020*). MAREANO is making efforts to collate data in the Norwegian EEZ and beyond, making them publicly available. One focus here is area-wide high-resolution mapping of the Nordic and Barents Seas, with a vast multibeam coverage having already been achieved. The ARS has been mapped at its center and northern rim during the recent bathymetric mappings (2018–2020) of the Norwegian Sea by the Norwegian Mapping authorities (*Kartverket, 2007*). Using these existing bathymetric data, IceAGE3 intends to fill data gaps and expand the overall high-resolution bathymetric knowledge.

The Nordic seas, including the deep basin of the Norwegian Sea and neighbouring Greenland and Iceland seas, as well as the Barents Sea, with the Greenland-Scotland Ridge

(GSR) (including *i.e.*, the Greenland-Iceland Ridge [GIR] and the Iceland-Faroe Ridge [IFR]) as a boundary towards the Atlantic, are known to host various kinds of different water masses. The prevailing current systems are supplied by the upstreaming North Atlantic Current (NAC) and the Irminger Current (IC) that transport warm, saline water from the Atlantic into the Nordic seas (Fig. 1). The branch of IC that reaches to the northern part of Iceland is often referred as NIIC (North Icelandic Irminger Current). These currents become subject to heat loss and mixing with dense Arctic waters, forming the subpolar gyre as well as boundary current systems (Mauritzen, 1996; Chatterjee *et al.*, 2018; Puerta *et al.*, 2020). The Norwegian Basin region is known to be a deep-water formation area and, although most of the water is trapped here, parts of it return to the northern Atlantic as intermediate overflow plumes (Mauritzen, 1996; Swift & Aagaard, 1982) or as deep boundary currents (Våge *et al.*, 2011), thereby playing a major role for the Atlantic Meridional Overturning Circulation (AMOC) (Semper *et al.*, 2020; Puerta *et al.*, 2020).

The two major downstream (southward transport) pathways are through the Denmark Strait, a deep passage in the GIR, and over the IFR (Swift & Aagaard, 1982; Hansen & Østerhus, 2000; Våge *et al.*, 2011; Semper *et al.*, 2020). The Denmark Strait Overflow Current (DSOC) is a well-studied (*e.g.*, Mauritzen, 1996; Våge *et al.*, 2011; Mastropole *et al.*, 2017) water mass bulk transport comprised of the two East Greenland Current (EGC) branches and the deep North Iceland Jet (NIJ), streaming westward along the continental shelf of Iceland. The Iceland-Scotland Overflow is formed by Arctic Intermediate water masses mainly originated in the Iceland Sea, whereas deep water formed in the Norwegian sea leaves the basin through the Faroe Bank Channel (FBC) (Mauritzen, 1996; Semper *et al.*, 2020). At the southern tip of ARS, called Gríðargljúfur Gorge, it is mainly the newly discovered deep Iceland Faroe Slope Jet (IFSJ) that supplies the local deep-water masses with cold and dense water, streaming eastward along the northern slope of the Greenland-Iceland Ridge (Semper *et al.*, 2020). The upstreaming North Atlantic Current contributes to the local surface water masses at the location and over the extent of ARS, transporting warm and saline water into the Norwegian basin, which itself is part of the subpolar gyre (*e.g.*, Chatterjee *et al.*, 2018).

The ARS (Fig. 1) is an extinct spreading axis in the Nordic seas west of the Norwegian Basin, located south-east of the Jan Mayen microcontinent, bound by the East-Jan-Mayen-Fracture-Zone at its northern flank and the GSR at its southern end on the Iceland Plateau (Blischke *et al.*, 2016). Politically, the northern half of the ARS (Figs. 1 and 2) is located in the high seas in an area beyond national jurisdiction (ABNJ). The southern half of the median valley is within the Faroe exclusive economic zone (EEZ) (Figs. 1 and 3) and the southern extremity belongs to the Iceland EEZ. Together with the Mohns Ridge further north, the ARS represents the first spreading center linked to the continental breakup between Norway and Greenland from 55 Ma to its abortion approximately 25 Ma ago (Talwani & Eldholm, 1977; Gaina, Gernigon & Ball, 2009; MacLeod *et al.*, 2017). Reflection seismic surveys (Uenzelmann-Neben *et al.*, 1992) reveal that the median valley is covered by between 900 and 1,400 m of sediment. Following the global geomorphic features map by Harris *et al.* (2014), the ARS is a 1,000 km spreading segment with a well-defined 830 km

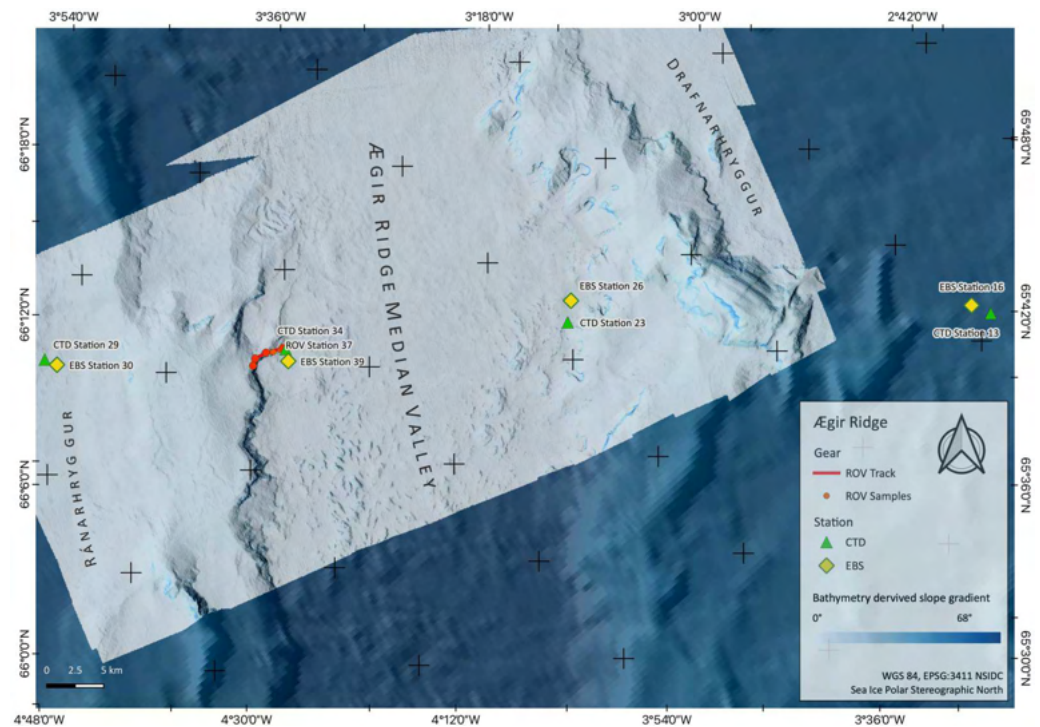


Figure 2 **Sampling Area North.** Detailed map of sampling area ‘North’ at the Aegir Ridge, including locations of ROV dives, CTD and EBS deployments. Map produced with software QGIS 3.16.4; bathymetry obtained multibeam survey and processed with QPS Qimera 2.0.

Full-size DOI: [10.7717/peerj.13394/fig-2](https://doi.org/10.7717/peerj.13394/fig-2)

long and 30–70 km wide median valley. Its southern tip (Gríðargljúfur Gorge, Fig. 1) belongs to the extinct spreading center while being slow spreading (when the segment was active) and becoming the “fanning” extension. However, both sides of the valley are surrounded by abyssal hills and plains and situated within the Norwegian Basin. The valley rims lay 700 m below sea level at the southern tip near Iceland and deepen towards the north to reach a depth of 3,800 m in the Norwegian Basin.

The ARS is interesting from both a geological and biological point of view, as it is geomorphologically a rift valley, but biologically reminiscent of a canyon-like structure with steep walls and large bathymetric differences linking the upper slope of the GIF and the abyss of the Norwegian Sea. The heterogeneous environment in terms of substrate, hydrography, and depth is likely to support distinct faunal communities. The northern part of the ARS, being located in international waters in an area called “Banana hole” nested between the Norwegian, Icelandic, Faroe’s, and United Kingdom’s EEZs, is under consideration as a candidate for an Ecologically and Biologically Significant Area (EBSA) under the Convention on Biological Diversity by Norway, as it is in the area beyond the 200 nautical mile baseline area that Norway claims under its Continental Shelf Submission for the United Nations Convention for the Law of the Sea (*Norwegian Petroleum Directorate, 2006*). Its “fanning” extension is located in the Icelandic EEZ, and is not included in the Norwegian efforts of describing an EBSA area. The EBSA

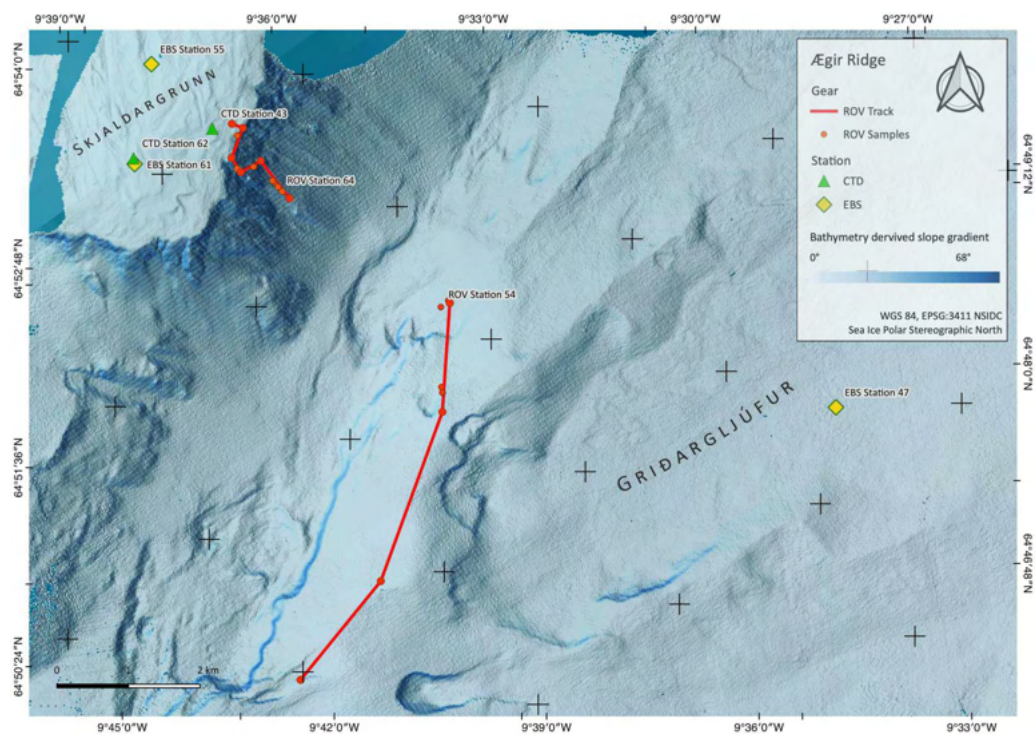


Figure 3 Sampling Area South. Detailed map of the sampling area ‘South’ at the Aegir Ridge, including locations of ROV dives, CTD and EBS deployments. Map produced with software QGIS 3.16.4.; bathymetry obtained multibeam survey and processed with QPS Qimera 2.0.

Full-size DOI: [10.7717/peerj.13394/fig-3](https://doi.org/10.7717/peerj.13394/fig-3)

criteria provided by the CBD may thus create the prerequisites for a protection status of the region in the long term. VME indicator species as defined by the Food and Agriculture Organization of the United Nations criteria (FAO, 2009; ICES, 2020) can be modelled for the areas in the vicinity of mapped findings using species distribution models such as used by Burgos *et al.* (2020). Morato *et al.* (2018) and Morato *et al.* (2021), suggest these models are vastly improved by areas adding new data.

In this study, we present a description of the physical and biological components of the ARS based on data collated during the IceAGE3 expedition (Brix *et al.*, 2020). As knowledge about depth zonation is rather scarce, our focus is more on the depth gradient than on community analysis. Specific objectives were to describe the area’s seafloor topography at 20–50 m resolution using multi-beam bathymetry. Furthermore, to analyze the epifaunal mega- and macrofauna composition of the ARS and its adjacent abyssal plain and infer its relationships to environmental variables. We expected the canyon-like topography of the ARS to promote a fauna with corresponding biological characteristics such as higher densities and diversity compared to the adjacent flat and sediment-dominated abyssal plain (De Leo *et al.*, 2010; Riehl *et al.*, 2020). In addition, we assumed that the physical environment, especially water mass and depth, had a major impact on community composition and distribution. In particular, we hypothesize that faunal communities shifted in relation to changes in environmental factors, notably depth, temperature,

salinity, oxygen, and productivity, along the ARS. Finally, we discuss our findings in light of international agreements established to protect vulnerable marine ecosystems in the North Atlantic and Arctic oceans.

MATERIALS & METHODS

Sampling

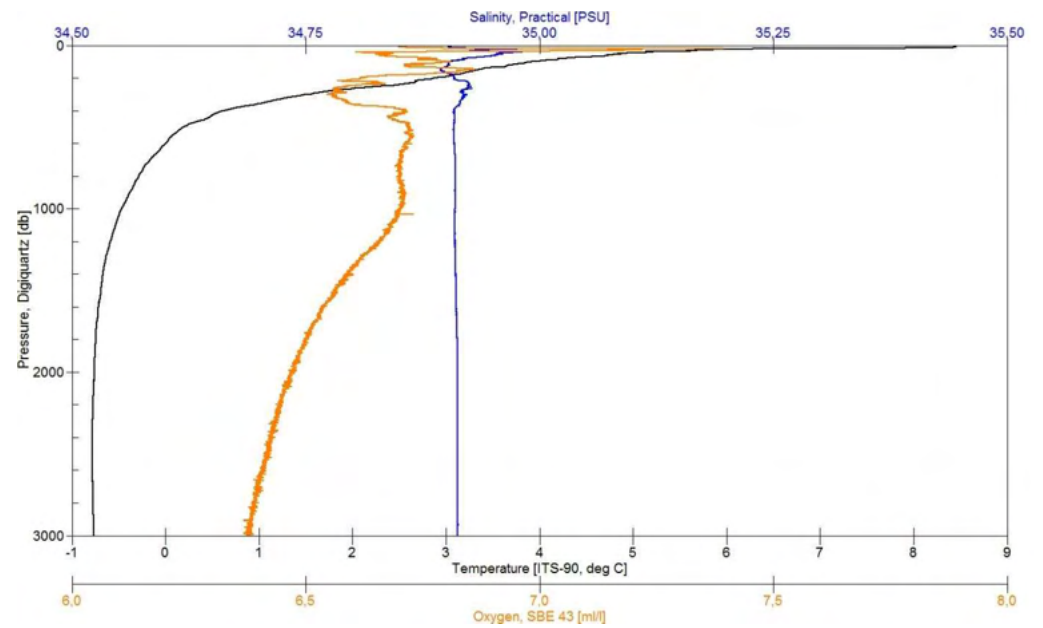
During the IceAGE3 expedition (Icelandic marine Animals: Genetics and Ecology) on RV Sonne as SO276 (MerMet17-06) in June/July 2020, we investigated the central and southern sections of the ARS, referred to as Ægir Ridge ‘North’/‘N’ and Ægir Ridge ‘South’/‘S’, using multibeam hydroacoustics, CTDs, an epibenthic sled (EBS), and the remotely operated vehicle (ROV) Kiel 6000 (Figs. 2 and 3; *Brix et al., 2020*). The sampling design of the IceAGE project places a CTD into the center of each working area to link all benthic gear deployed with abiotic data from the water column is outlined in *Brix et al. (2014)*. Abiotic variables analyzed from the CTD are temperature, salinity, and oxygen. In particular salinity and temperature are used as variables to define the water masses around Iceland to receive background information for biology (*Brix & Svavarsson, 2010; Brix et al., 2018a; Brix et al., 2018b*).

Bathymetry

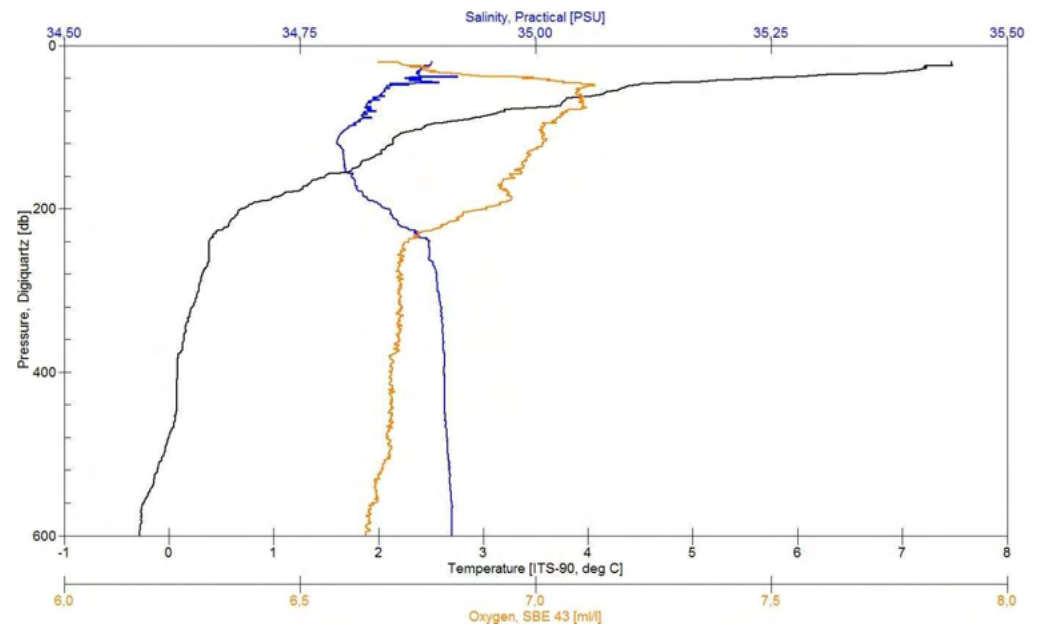
Prior to sampling, multibeam bathymetry surveys of the areas were carried out using the RV Sonne’s hull mounted Kongsberg SIMRAD EM122 multibeam echo sounder system (MBES) to create high resolution maps of the sampling sites. This MBES operates at a frequency of 12 kHz and can therefore reach down to water depths of 12,000 m. With the automatic ping rate, varying with depth from 0.2–0.06 pings/second between –1,000 m and –4,000 m, a vessel speed of ~8 kn during the surveys and swath widths of 90°–110° (depending on the data quality), bathymetric maps with a grid resolution of 20 m (at the shallower southern ridge end called Gríargljúfur Gorge, Fig. 3) and 50 m (in the valley center called median valley between Ránarhryggur Ridge and Drafnarhryggur Ridge) were achieved (Fig. 2). The raw data point cloud was post-processed, *i.e.*, cleaned for outliers and gridded, with QPS Qimera 2.0 software. The processed data products were exported as interpolated grids to be visualized as maps with the open-source software QGIS 3.16.4.

Oceanography

In total five CTD casts were deployed in the described area, ranging from 246–3,571 m in the maximum profile depth, which is represented by Fig. 4A for deep- and Fig. 4B for shallow profiles. The CTD stations visible on the map (Figs. 2 and 3) indicate the RV Sonne ship’s owned SBE 911plus CTD unit (Seabird Electronics). It was mounted approximately 1 m below the water sampler equipped with double conductivity, temperature, oxygen, chlorophyll (Chl), and turbidity sensors (Table 1). The water sampler was equipped with 24 × 10 l Niskin bottles that were electronically triggered to close at given depths on the upcast of the CTD profiles. The sampling rate of the sensors amounts to 24 Hz with 41 Bytes per scan. Data recording and Niskin bottle triggering was controlled with SEASAVE V7 software from a ship mounted computer. The GPS positions during each profile were



A



B

Figure 4 CTD plots. Environmental variables water column profiles of Station 013 (A) a deep, abyssal plain CTD location casting to 3,008 m depth and Station 043 (B) shallow profile, ridge top CTD location casting to 603 m depth.

Full-size  DOI: 10.7717/peerj.13394/fig-4

logged from an NMEA-string of the RV Sonne. Each cast was processed by using SBE Data Processing to convert the binary (.hex) data to ASCII (.cnv) data.

The CTD data, as well as the plots (Figs. 4A and 4B) were untreated when used for first on board analyses of the sediment and further station work decisions. Depending on the weather conditions, some profiles started at a depth of approximately 20 m below surface for safety reasons (Fig. 4B). The quality control of the salinity values was done by taking water samples from the Niskin bottles during the upcast to analyze them in a land-based laboratory, using a Guildline 4800B Lab Salinometer. The samples were taken from the maximum depth and in homogenous water layers.

Habitat characterization and megafaunal sampling by ROV

The ROV Kiel 6000 was deployed for three dives with a total of 26:08 h deployment time at the ARS (Table 2). For seafloor imagery (photos, video, and frame grabs of videos) ROV Kiel 6000 was equipped with two HDTV cameras (Sulis and ALPHA +) and two SD-color zoom video cameras OE14-366 MKII, the latter mounted on pan and tilt units. The footage of all of these were permanently recorded. Additionally, ROV Kiel 6000 is equipped with four black and white video observation cameras. Lighting for the video cameras is provided by two 400 W HMI SeaArc[®]2, two 70 W HID SeaArc[®]5000, and eight dimmable 250 W halogen SMulti-SeaLite[®] lights. Additionally, two Alpha Cam lasers, 6.7 cm apart, were mounted parallel to the focal axis of the video camera to provide scale in images.

ROV dive 37 investigated the abyssal plain in the central ARS median valley (Fig. 2) along a line from 3,700 m to 3,450 m depth (Fig. 2, Table 3). The ROV dives 54 (2,030 m to 1,700 m) and 64 (1,400 m to 740 m) investigated the southwestern end of the ARS along bathyal transects from the foot of the Grí argljúfur Gorge to its plateau called Skjaldargrunn Bank (Fig. 3). Digital still images taken during the dives were used for the identification of selected prominent or abundant megafauna and the identification followed the best practice for the use of open nomenclature signs to image-based faunal analyses (Horton *et al.*, 2021) (Table 4). Observed species were assessed as to their VME indicator status following NEAFC 2014 and the latest lists of VME indicators defined by the ICES Working group on Deep-Water Ecology (WGDEC, ICES 2019, ICES, 2020).

For horizontal megafauna zonation analysis, ROV footage was reviewed with the deepest and shallowest occurrences of selected taxa extracted (see Table 4). Additionally, five frame grabs per 25 m of depth were randomly selected from the ROV videos to assess presence and dominance of the selected taxa for the habitat schematics. This process involved extracting screen grabs from each depth zone, ascertained by the corresponding metadata files generated by the ROV, at 10 s intervals, assigning them a randomly generated number and then generating random numbers to select the corresponding images. This was done to eliminate observer bias. No individual abundance numbers of taxa per defined area analysis was done as the distance defining lasers were not on throughout the dives.

No statistical analyses could be conducted, because of the lack of replicates at the three sites.

Table 1 Water variables. Summary of environmental water column variables measured at the Ægir Ridge System by SBE 911 CTD used in this study.

Station	Date	Position		Bottom	SBE911						Turbidity (NTU)		
		Latitude	Longitude	Depth (m)	CTD Depth (m)	Temperature (°C)	Salinity (PSU)	O ₂ (ml/l)	max. O ₂ (ml/l)	max. Chl a (mg/m ³)			
13	28.06.2020	65°42.676'N	002°57.153'W	3,341	3,008	-0.763	34.912	6.386	Depth (m) 26	7.200	Depth (m) 26	2.097	0.078
23	29.06.2020	65°55.471'N	003°33.628'W	3,692	3,571	-0.717	34.913	6.338	Depth (m) 30	7.400	Depth (m) 44	1.600	0.080
29	30.06.2020	66°10.152'N	004°21.613'W	3,423	3,403	-0.737	34.917	6.343	Depth (m) 42	7.165	Depth (m) 42	1.420	0.078
34	01.07.2020	66°03.138'N	003°59.896'W	3,675	3,010	-0.762	34.913	6.370	Depth (m) 42	7.059	Depth (m) 29	1.314	0.077
41	02.07.2020	65°16.296'N	007°56.559'W	1,413	246	0.764	34.878	6.775	Depth (m) 43	7.300	Depth (m) 34	3.112	0.081
43	03.07.2020	64°52.862'N	009°37.831'W	716	603	-0.291	34.911	6.633	Depth (m) 49	7.112	Depth (m) 34	2.635	0.080
62	06.07.2020	64°53.019'N	009°39.247'W	686	674	-0.342	34.911	6.613	Depth (m) 68	7.134	Depth (m) 10	2.943	0.085

Table 2 ROV dives. Summary of ROV Kiel 6000 dive locations at the Ægir Ridge System as used in this study.

Station	Dive No. Kiel 6000	Date	Latitude Start	Longitude Start	Latitude End	Longitude End	Depth Start (m)	Depth End (m)
37	298	01.07.2020	66°03.170'N	003°59.914'W	66°03.684'N	004°01.952'W	3,700	3,419
54	299	04.07.2020	64°50.818'N	009°36.219'W	64°50.080'N	009°37.720'W	2,030	1,838
64	300	05.07.2020	64°52.180'N	009°37.471'W	64°52.835'N	009°37.548'W	1,411	740

Table 3 EBS stations. Summary of epibenthic sledge stations conducted during the IceAGE3 (MerMet 17-6/SO276) expedition along the Ægir Ridge System as used in this study. Information includes area, latitude and longitude (in degree), depth (m), time and trawling distance.

Station	Date	Latitude start	Longitude start	Depth start (m)	Trawling distance (m)
16	28.06.2020	65°43.552'N	002°58.158'W	3,363	576
26	29.06.2020	65°56.122'N	003°31.727'W	3,702	648
30	30.06.2020	66°09.596'N	004°20.937'W	3,467	612
39	01.07.2020	66°02.682'N	004°00.570'W	3,678	486
47	03.07.2020	64°48.515'N	009°31.816'W	2,289	540
55	04.07.2020	64°53.509'N	009°38.047'W	681	360
61	05.07.2020	64°52.979'N	009°39.289'W	686	198

Taxonomic identifications of megafauna from ROV *in-situ* images

Taxonomic identification of megafaunal groups were made to the lowest taxonomic rank possible, from images obtained with the ROV, using the authors' taxonomic expertise and recent revisions of specific groups (e.g., on sponges, [Cárdenas et al., 2013](#); [Hestetun, Tompkins-Macdonald & Rapp, 2017](#)) of the bathyal fauna of the boreo-Arctic region. When a particular taxon could not be confidently identified to species level, higher taxonomic ranks combined with open nomenclature signs (e.g., 'sp.', 'stet.', 'indet.') were implemented following the standards proposed by [Horton et al. \(2021\)](#).

Macrofauna sampling by epibenthic sledge (EBS)

The macrofauna were examined with an EBS ([Table 2](#)) with just an epibenthic sampling unit such as is in the EBS by [Rothlisberg & Percy \(1977\)](#) and corresponding to the epi-samplers of related EBS types, which have an epibenthic and a suprabenthic sample unit ([Brandt & Barthel, 1995](#); [Brenke 2005](#); [Brandt et al., 2013](#)). We deployed one EBS at each depth, where it was possible to deploy an EBS. This is a trawled gear and can only be deployed where there is enough space/room for it on the seafloor. Thus, the macrofauna data cannot cover the "wall", which has been sampled/observed via ROV dives. The aim was to deploy the EBS on each side of the Ægir Ride in the north and on the shallower part and deeper parts in the south. A detailed description of the sampling procedures is given in [Brix et al. \(2020\)](#). In total (both, North and South samples as indicated on the overview map in [Fig. 1](#)) seven EBS were deployed in the ARS area ranging in depth from 681 m to 3,702 m ([Table 3](#)). Three stations were taken from the bottom of the median valley (stations 26, 39, and 47) and four stations from shallower parts (Ránarhryggur and Skjaldargrunn; [Table 3](#)). Trawling distance (d) was standardized to a trawled distance of 1,000 m for calculation of

Table 4 Taxa. Selected, noticeable megafauna elements and their depth occurrences on *in-situ* ROV imagery on the Ægir Ridge used in this study. Phyla and VME indicator taxa marked in bold.

Phylum class	Order	Family	Lower rank	Label in habitat schematics	Depth min. (m)	Depth max. (m)
Porifera						
Demospongiae	Axinellida	Axinellidae	<i>Phakellia</i> sp. indet	<i>Phakellia</i>	1,230	2,000
Demospongiae	Poecilosclerida	Cladorhizidae	<i>Asbestopluma furcata</i>	<i>Asbestopluma</i>	1,220	2,000
Demospongiae	Poecilosclerida	Cladorhizidae	<i>Chondrocladia grandis</i>	<i>Chondrocladia</i>	750	900
Demospongiae	Poecilosclerida	Geodiidae	<i>Geodia hentscheli</i>	<i>Geodia</i>	1,030	1,970
Demospongiae	Poecilosclerida	Coelosphaeridae	<i>Lissodendoryx complicata</i>	<i>Lissodendoryx</i>	1,850	1,950
Hexactinellida	Lyssacinosa	Rossellidae	<i>Caulophacus arcticus</i>	<i>Caulophacus</i>	3,530	3,700
Hexactinellida	Lyssacinosa	Rossellidae	<i>Schaudinna rosea</i>	<i>Schaudinna</i>	850	1,970
Mollusca						
Chephalopoda	Octopoda	Opisthotheuthidae	<i>Grimptotheuthis</i> sp. indet			3,600
Gastropoda	Neogastropoda	indet	Neogastropod sp. indet.			1,930
Echinodermata						
Asteroidea	Velatidae	Pterasteridae	<i>Hymenaster</i> sp. indet	<i>Hymenaster</i>	1,100	1,950
Crinoidea	Comatulida		Comatulid sp. indet	Crinoid	750	1,220
Ophiuroidea	Euryalida	Gorgonocephalinae	<i>Gorgonocephalus</i> sp. indet		750	1,300
Echiuroidea			Echiuroid indet	Echiuroid	1,450	3,700
Arthropoda						
Pycnogonida	Pantopoda	indet	Pycnogonid sp. indet			3,700
		Colossendeidae	<i>Colossendeis</i> sp. indet		840	1,330
Malacostraca	Decapoda	Bythocaridae	<i>Bythocaris</i> cf. <i>leucopis</i>	<i>Bythocaris</i>	1,900	3,700
	Amphipoda	Calliopiidae	Calliopiid sp. indet	Calliopiid	1,900	3,700
Cnidaria						
Anthozoa	Alcyonacea	Nephtheidae	<i>Drifa glomerata</i>	Soft coral	750	1,450
	Alcyonacea	Nephtheidae	<i>Gersemia</i> sp.	Soft coral	1,340	2,000
	Actinaria	Actinostolidae	Actinostolid sp. A indet	Actinostolid	3,530	3,530
	Actinaria	Actinostolidae	Actinostolid sp. B indet	Actinostolid	1,930	3,680
	Actinaria	Actinostolidae	Actinostolid sp. C indet	Actinostolid	750	820

1,000 m² sampled seabed area, as the epibenthic sample unit is 1 m wide. We therefore used the following formula: $d = (V_1 \times T_1) + (V_2 \times T_2) + (V_3 \times T_3)$ (V_1 : ship velocity during trawling; T_1 : trawling time; V_2 : ship velocity during haul; T_2 : haul time (sled off bottom), V_3 : winch velocity; T_3 : haul time [sled off bottom]). As soon as the EBS arrived on deck, the cod end was retrieved and immediately taken to the cold room (+4 °C). The sample processing mostly followed protocols for a cold chain that enable later molecular analyses (Riehl et al., 2014). Specimens visible to the naked eye were picked from the bulk sample, photographically documented, and separately fixed (RNAlater and undenaturated 96% ethanol) or frozen for genetic, genomic or biochemical analysis. The remaining sample was carefully elutriated in pre-chilled filtered seawater, then sieved through a 300- μ m mesh, fixed in pre-chilled (-20 °C) 96% denaturated ethanol and stored at -20 °C for at least 48 h. Sorting of the samples began on board and was continued in the Senckenberg laboratory

(DZMB, Hamburg) and due to pandemic restrictions finished in “home office”. Specimens were assigned to major taxonomic units (phylum, class, order level).

Analysis of macrofaunal taxa

Comparisons of macrofaunal abundances obtained from the EBS were made based on density data. Therefore, total abundances were standardized to individuals per 1,000 m² seabed area.

PRIMER v6 (*Clarke & Gorley, 2006*) was used for the multivariate statistical analysis. A one-way Analysis of Variance (ANOVA) was used to test for differences in macrofaunal densities between stations using SigmaPlot Version 12.5. To test for homogeneity of variance Levene’s test was used, while we used Shapiro–Wilk test to test for normality. In case assumption of normality and homogeneity of variance were not met, a non-parametric Kruskal-Wallis test was applied. Sample size between EBS deployments may differ (see [Table 3](#)), and thus samples provide arguably only semiquantitative data (*Kaiser & Brenke, 2016*). To assess differences in macrofauna community composition between samples, Bray–Curtis similarities were calculated for non-transformed relative abundance (percentage) data of total macrofauna obtaining a similarity matrix (*Clarke & Gorley, 2006*). Relative abundances for the multivariate analysis were used to account for this. Non-metric multi-dimensional scaling (nMDS) implemented in PRIMER v6 was used to visualize differences between stations and depth.

Relationships between macrofaunal densities, environmental factors (T, S and O₂), and depth were explored using Spearman rank correlation coefficient in Sigmaplot 12.0 for total macrofauna. Furthermore, relationships between macrofaunal composition and environmental variables were explored using the Biota and Environment matching (BIO-ENV) procedure based on normalized Euclidean distance. All parameters were previously tested for collinearity using a draftsman plot calculated in Primer v6.

RESULTS

Bathymetry

The two regions of the ARS investigated and mapped during the IceAGE3 expedition present a contrasted ridge morphology. In the central region (named North) near 66° N, the ARS is a ~27 km wide axial valley at a depth of 3,700 m–3,800 m. The eastern and western valley walls Ránarhryggur Ridge and Drafnarhryggur Ridge have gentle slopes (less than 15°). The valley is bound by two broad shoulders (16–18 km wide), a relict of a split volcanic ridge. They culminate at a depth of 3,000 m and 2,000 m for the western and eastern shoulder, respectively. These shoulders separate the median valley from the surrounding abyssal plain at ~3,400 m. South, at Griargljúfur Gorge (southern end of the ridge), the axial valley is wider (67 km) with a shallower valley floor laying at 2,300 m–2,600 m below sea level. The section map (at ~64.8° N) shows that the valley walls become steeper (1–60°). In this region, which lays between 700 and 1,100 m below sea level, there is no shoulder between the valley and the surrounding seafloor.

Backscatter analyses ([Fig. 5](#)) in both sampling areas (North and South as indicated in [Fig. 5C](#)) revealed that the seafloor along and across the ARS does not have a homogeneous

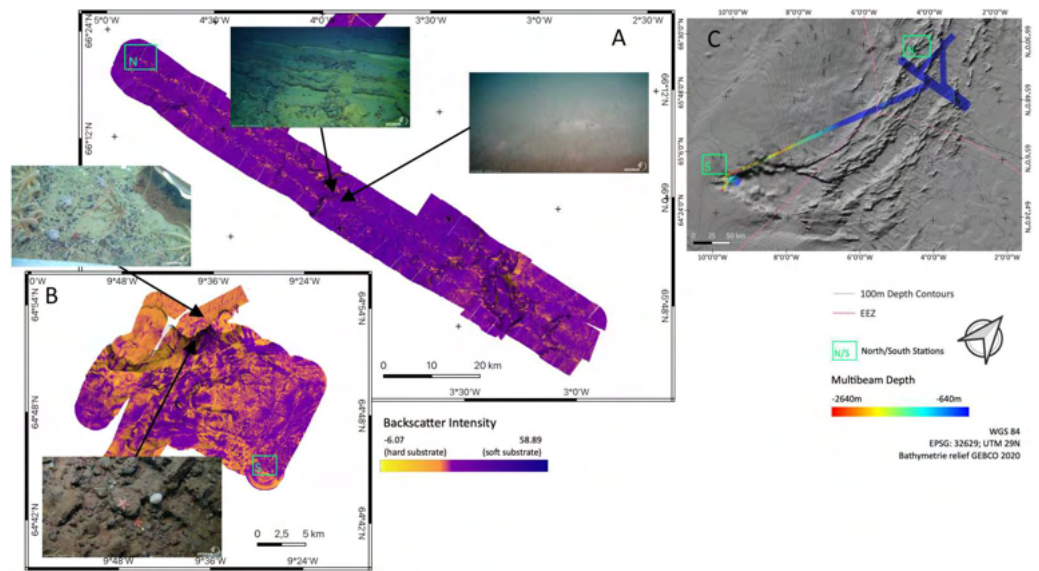


Figure 5 Backscatter data. Detailed maps of sediment backscatter information maps of sampling areas (A) ‘North’ and (B) ‘South’ at the Ægir Ridge including an overview map as orientation (C). *In-situ* images show representative hard and soft substrates observed. Maps produced with software QGIS 3.16.4.

Full-size [DOI: 10.7717/peerj.13394/fig-5](https://doi.org/10.7717/peerj.13394/fig-5)

acoustic characterization and systematic variations are evidenced. The valley floor has always a lower backscatter amplitude than the surrounding abyssal plain. The shallowest southern end of the ridge has a higher backscatter amplitude than the deeper central section of the ridge. The highest amplitude is found on a wall where the depth gradient exceeds 30° . Variations in the intensity of the acoustic signal, reflect change in the substrate hardness. Low backscatter amplitudes are attributed to soft substrate and high backscatter to hard substrate. Correlation between backscatter signal and substrate is observed from ROV footage, especially between the between north and south region. Images of the seafloor show that rock fragment, mostly dark grey and black, up to few decimeters in diameter are predominant on the southern section of the ridge. Similarly, steeper slope on the valley wall exposed larger blocks or compacted sediment layers.

Environmental parameters–CTD

Each of the CTD profiles shows water masses with different properties of temperature and salinity (Figs. 4A and 4B) in the upper layer (0–600 m), creating an inhomogeneous mixed layer with a relatively strong thermocline. The range in temperature (*e.g.*, Station 13: 8 to 0 °C) and salinity (35.05 to 34.89 PSU) shows the impact of the colder and denser Artic-origin water from the south and Atlantic-origin water from the north (Puerta *et al.*, 2020). The 0 °C point was reached after 600 m and is generally considered as an indicator for Artic-water masses (Semper *et al.*, 2019). At this depth down to the bottom the change in temperature (*e.g.*, Station 34: 0 to -0.77 °C) and salinity (34.91 to 34.92 PSU) slightly decreases, developing a more homogenous water mass. The minimum water temperature for each profile was reached at a depth of 1,500 m (*e.g.*, Station 29: -0.77 °C) turning into a homogenous water mass. The minimum salinity value was found in the described upper

mixed layer (e.g., Station 43: 34.78 PSU). The change in salinity decreases with depth and reaches a constant level after 1,800 m (e.g., overall: 34.88 to 34.92 PSU).

Although some variables were strongly correlated (Spearman rank correlation, $\rho > 0.9$), in particular salinity, oxygen, and chlorophyll, we kept all of them in the analysis, since the combination of water mass properties has been identified as important to explain differences in benthic community structure in the Nordic seas/North Atlantic (Weisshappel & Svavarsson, 1998; Puerta et al., 2020; Roberts et al., 2018).

The maximum oxygen value was located in the upper 70 m (e.g., 7.06 to 7.40 ml/l). The effect of mixing water masses shows in the upper 500 m with the change of oxygen (e.g., station 013: 7.20 to 6.55 ml/l) until it constantly decreases with the depth (Fig. 4A).

Megafauna based on ROV imagery

During three ROV Kiel 6000 dives, *in-situ* video footage was taken at three sites with different depth ranges on the ARS and its adjacent abyssal plain and rise (Table 4, Figs. 2, 6, 7 and 8). The deepest ROV transect at station 37 (3,700 m to 3,450 m) from the sedimented plain in the median valley towards the rise of the ridge (Ránarhryggur) showed a highly sedimented habitat with sparse rocky outcrops in the abyssal plain area (Fig. 9). The sedimented areas showed Lebensspuren, including echiuroid mounts (Figs. 6A, 6B), irregular presences of burrowing cerianthid anemones, stalked crinoids (currently on the FAO NW Atlantic VME indicator taxa list), and the occasional rocks colonized by the glass sponge *Caulophacus arcticus* (Hansen 1885) (Figs. 6C, 6D). The *C. arcticus* colonies provide a habitat for aggregations of caridean shrimp (*Bythocaris* cf. *leucopis* GO Sars 1879) and amphipod species of different size classes, most prominently large amphipods from the family Calliopiidae, which are at present stage not identified as any described species and need further taxonomic attention (Fig. 6D). Ascending along the rise, the habitats changed from a sedimented seafloor to an area of hard rock outcrops separated by sediment flows, (Fig. 9C) to steep, consolidated sediment layers (Fig. 9D) and areas with drop stones, ending in a further sedimented area on the upper rise. The hard rock outcrops surrounded by sediment flows were colonized by occasional, single specimens of *C. arcticus*, while some drop stones were covered by dense colonies of this sponge. The consolidated sediment layers appeared bare of megafauna.

The two ROV dives in Gríargljúfur Gorge (southwestern end of the ARS) and the plateau Skjaldargrunn Bank started at the foot of the ridge structure in a flat, sediment covered bathyal area at 2,030 m depth and ended on the top edge of the ridge plateau (Skjaldargrunn Bank) at 740 m (Figs. 3, 7, 8 and 10; Table 4). The second ROV track at station 54, ascending from 2,030 m to 1,700 m depth, started in coarse sedimented areas which were interrupted intermittently by sediment blocks of various sizes, providing diverse habitats for epifaunal taxa, as well as cobbles and pebbles (Figs. 7A–7D). These hard rock surfaces were frequently colonized by various species of sponges, including the carnivorous sponge *Asbestopluma* (*Asbestopluma*) *furcata* Lundbeck, 1905 (Fig. 8G), with the regular presence of crustaceans, gastropods, and echinoderms. The sedimented areas were colonized by soft corals, sponges, and epifaunal pterasterid starfish. Closer to the steeper foot area of the ridge, consolidated sediment layers, densely colonized

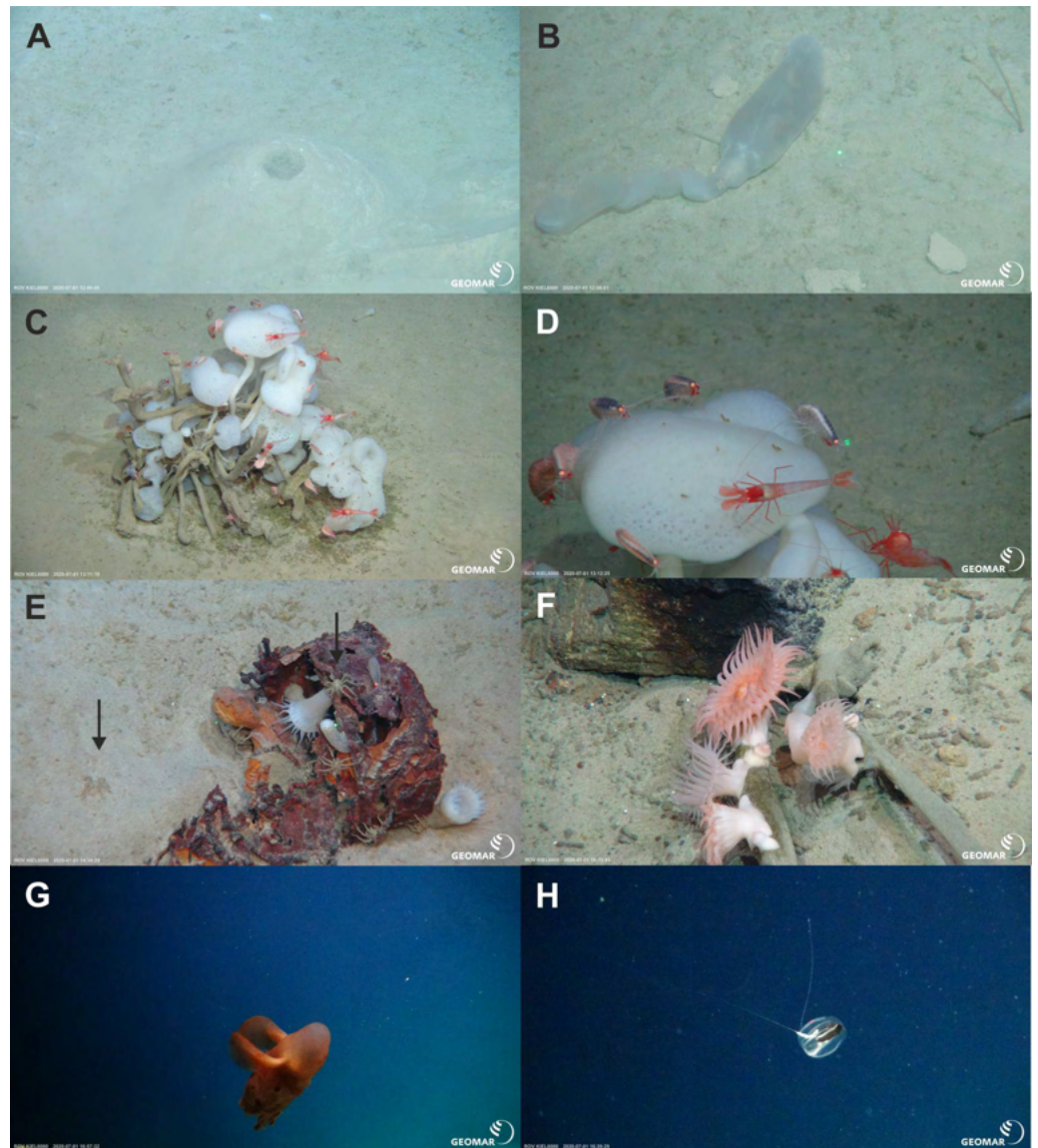


Figure 6 Megafaunal elements. *In-situ* images of characteristic megafauna of the Ægir Ridge at 3,400–3,700 m. (A) Echiurid mount. (B) Echiurid. (C & D) Glass sponge *Caulophacus arcticus* with caridean decapods and amphipod peracarids. (E) Actinostolid sp. A anemones and Pycnogonida sp. seaspiders (arrows). (F) Actinostolid sp. B anemones on *Caulophacus* stalks. (G) Dumbo octopus, *Grimpotheuthis* sp. (H) Ctenophore. Image source credits: GEOMAR/Senckenberg.

Full-size DOI: [10.7717/peerj.13394/fig-6](https://doi.org/10.7717/peerj.13394/fig-6)

by sponges were seen (Figs. 7E, 7F). The third survey at station 64 ascended from the steep part of the ridge foot in 1,400 m to the ridge top (740 m) (Table 4, Fig. 10). The sediment layer became thinner to non-existent with increased steepness of slope (*i.e.*, a thick sediment layer at the bottom, only rocks and no sediment at the top, just rocks, see Fig. 5). Frequent steep hard rock outcrops and walls alternated with less steep areas, which then had thin sediment covers (Figs. 7G, 7H). These hard rock structures were densely covered by habitat forming sponges of different morphospecies including demosponges

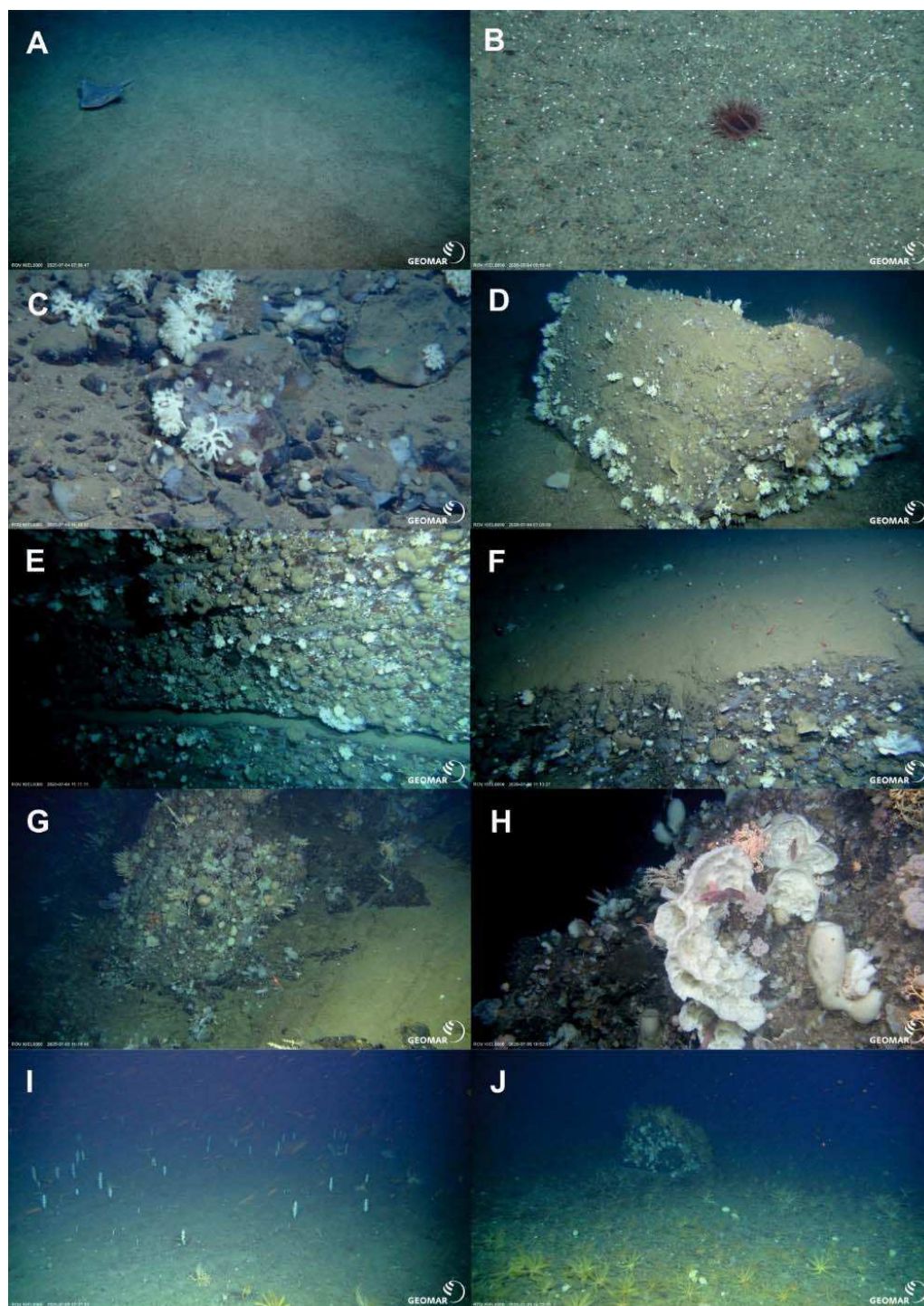


Figure 7 **Geomorphology.** *In-situ* images of geomorphology types of the Ægir Ridge at 2,000 m–600 m. (A & B) Coarse soft sediments. (C) Cobbles and pebbles on soft sediment (D) Sediment block on soft sediment. (E) Steep consolidated sediment layers. (F) Sedimented, flat steps of consolidated sediment layers. (G & H) Steep hard rock outcrops. (I & J) Flattened ridge top with sedimented areas and sediment blocks. Image source credits: GEOMAR/Senckenberg.

Full-size  DOI: [10.7717/peerj.13394/fig-7](https://doi.org/10.7717/peerj.13394/fig-7)

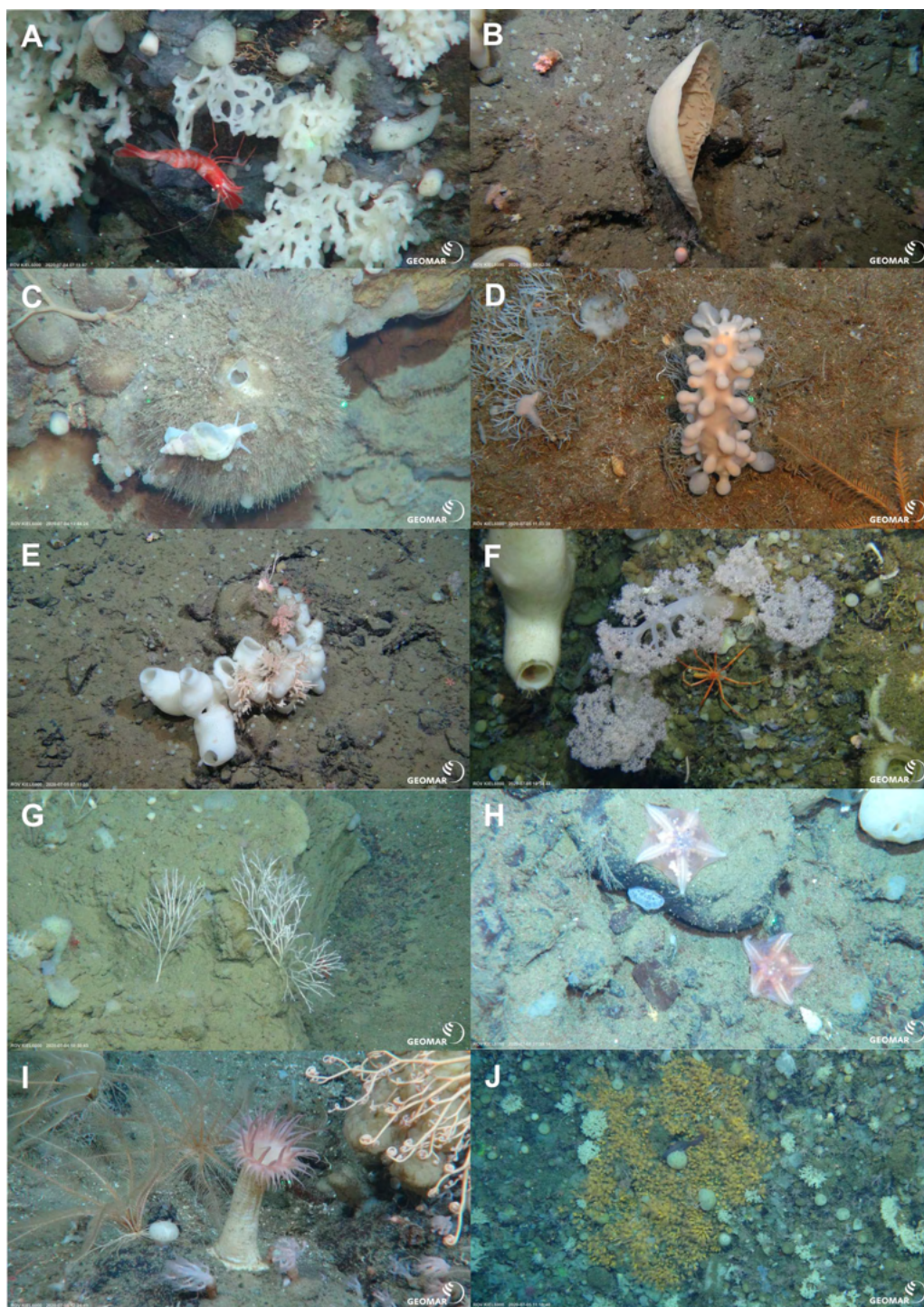


Figure 8 Characteristic megafauna. *In-situ* images of characteristic megafauna of the Ægir Ridge at 2,000–600 m. (A) Demosponge *Lissodendoryx* (*Lissodendoryx*) *complicata* with caridean decapod. (B) Flabellate demosponge *Phakellia* sp. indet. (C) The tetractinellid sponge *Geodia hentscheli* with neogastropod. (D) Carnivorous sponge *Chondrocladia* (*Chondrocladia*) *grandis*. (E) Glass sponge *Schaudinna rosea* (F) Soft coral with *Colossendeis* sp. seaspider. (G) Carnivorous sponge *Asbestopluma* (*Asbestopluma*) *furcata*. (H) Pterasterid starfish *Hymenaster* sp. (I) Commatulid crinoids, basket star *Gorgonocephalus* sp. and actinostolid sp. C anemone. (J) Aggregations of demosponges and zoanthid cnidarians. Image source credits: GEOMAR/Senckenberg.

Full-size  DOI: 10.7717/peerj.13394/fig-8

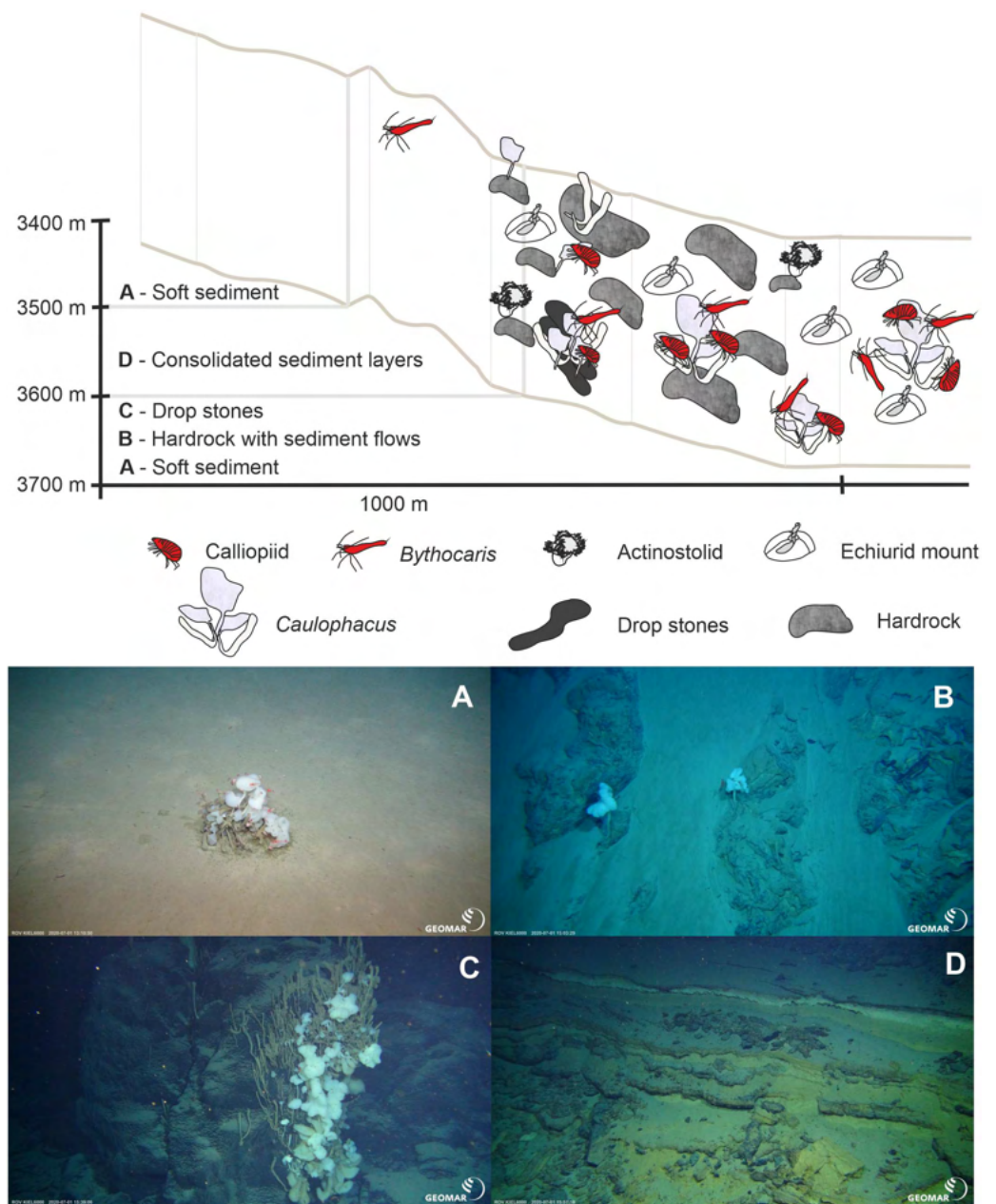


Figure 9 Schematic 1. The Ægir Ridge System at sampling area 'N': (A) Habitat schematic for the Ægir Ridge System sampling area 'N'. *In-situ* images represent: (B) Soft sediment. (C) Hardrock with sediment flows. (D) Drop stones. (E) Consolidated sediment layers. Image source credits: BAS/Senckenberg.

Full-size DOI: [10.7717/peerj.13394/fig-9](https://doi.org/10.7717/peerj.13394/fig-9)

belonging to the families Cladorhizidae and Coelosphaeridae, as well as hexactinellids of the family Rossellidae. These sponges provided diverse habitats for aggregations of cnidarians, molluscs, pycnogonids, crustaceans, and echinoderms (Table 4). The flattened top of the ridge (Figs. 7I, 7J) was densely covered by comatulid crinoids, actinostolid actinians and sponges like the “club-shaped” *Chondrocladia* (*C.*) *grandis* (Verrill, 1879) (Fig. 8D).

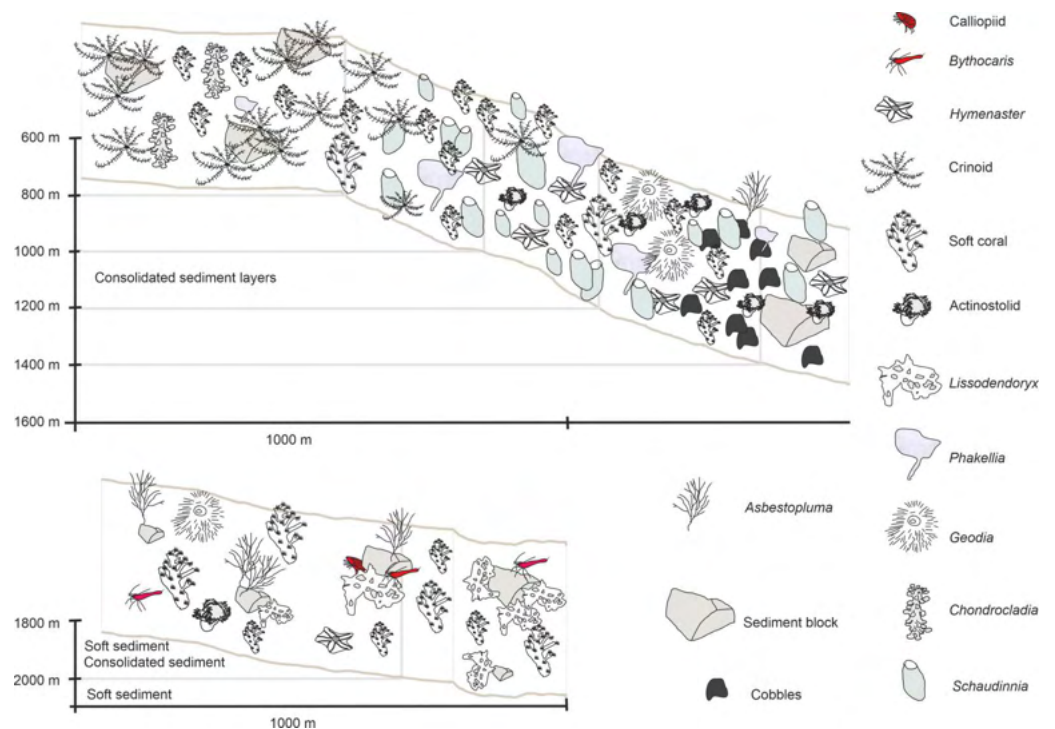


Figure 10 Schematic 2. Habitat schematic for the Ægir Ridge System in sampling area 'S'. (A) Based on ROV Kiel 6000 dive 300. (B) Based on ROV Kiel 6000 dive 299.

Full-size [DOI: 10.7717/peerj.13394/fig-10](https://doi.org/10.7717/peerj.13394/fig-10)

The habitat heterogeneity and dominant megafaunal elements are characterized in schematics to visualize the change of sediment structure and faunal zonation along a depth gradient (Figs. 9 and 10). The first and last depth appearance of the dominant megafauna, as well as their status as VME indicators for NEAFC (ICES, 2020), was noted (Table 4) and indicates zonation of megafaunal communities along depth. The rossellid sponge *Caulophacus arcticus* was only observed in depths of 3,530 m–3,700 m, while the associated crustaceans were also observed on a different species of sponge until 1,900 m depth. Echiurid mounts were present in soft sedimented areas from 1,450 m to 3,700 m depth. The nephtheid soft coral *Gersemia* sp. was present at 1,340 m to 2,000 m, while *Drifa glomerata* (Verrill, 1869) was present at 750 m to 1,450 m but was most dense at 1,000 m to 1,250 m. The sponges *Phakellia* sp. indet and *A. (A) furcata* were present at 1,220 m to 2,000 m, while the rossellid *Schaudinnia rosea* (Fristedt 1887) was observed from 850 m to 1,970 m. The carnivorous *C. (C.) grandis* first appeared at 900 m depth and was more frequent on the ridge top at 750 m depth. The large, multiarmed ophiuroid *Gorgonocephalus* sp. indet and the comatulid sp. indet crinoids, were first recorded on the upslope ROV dive around 1,250 m depth and were present to the ridge top at 750 m depth, where the comatulids showed their highest densities.

The ARS valley abyssal plain hosted VME indicator species (Figs. 6–10, Table 4) especially sponges indicating habitat like “deep sea sponge aggregations” as well as “sediment emergent fauna”. In the sedimented areas Cerianthidae were observed, they are listed as

VME indicators of “tube-dwelling anemone” patches (Fig. 7B). The gentle and steep slopes of the southwestern ARS of hard-bottom and soft-sedimented substrate showed a variety of VME taxa, including the soft coral family Nephtheidae, with the species *Gersemia* sp. abundant at 1,340 m to 2,000 m depth indicating “cauliflower coral fields”. The hard bottom areas, especially on steep slopes, provided habitat to dense, species rich deep-sea sponge aggregations. Habitat forming species like the rossellid and poecilosclerid sponges hosted dense communities and harboring numerous fauna. While not a VME indicator taxon, high species richness and abundance of carnivorous sponge taxa including *A. (A.) furcata*, and *C. (C.) grandis* was noted at all depths investigated by ROV surveys at the southwestern ARS site, which suggests the presence of rich supra-benthic food resources, like swimming crustacean taxa, e.g., Amphipoda, Copepoda, or Isopoda (Table S1).

Macrofauna based on EBS collections

For the entire macrofauna there seems to be a slight trend towards higher densities at the shallow sites (stations 55 and 61) compared to the deeper ones (Table S1). However, this is largely due to the high proportion of calanoid copepods at epibenthic depths at these stations, which make up between 53.0% and 75.8% of the total macrofauna there (Fig. 11). The mechanism of the EBS, which closes the sample unit as soon as seafloor contact is lost, and remains closed through the water column, precludes collection in the pelagic zone. When removing calanoids from the analysis, macrofauna densities at the deeper part of the ARS (stations, 26, 39, and 47) were significantly higher compared to the other stations (one-way ANOVA, $F_{1,6} = 35.6$; $p < 0.002$). Overall, Polychaeta was the most dominant taxon with 41.9% of the total macrofauna, followed by the Isopoda (14.2%), Ophiuroidea (9.0%), Bivalvia (7.1%) and Tanaidacea (6.2%). Yet, the relative abundance of each taxon varied between stations and depth. While polychaetes showed high relative abundances at the deep stations, where they contributed between 30.8% and 69.4% to total macrofauna, they were only poorly represented at the two shallow stations (4.7–5.3%). Here, isopods and ophiuroids were more dominant. Differences in macrofaunal densities could not be related to any of the measured environmental, also water mass defining variables or depth (Spearman rank; $p > 0.05$). For polychaetes, however, depth was identified as the most important factor explaining density variation densities (Spearman rank; $\rho = 0.89$, $p = 0.0000002$), whereas the remaining factors were revealed as not significant (Spearman rank; $p > 0.05$).

Community analysis of the total macrofauna, as visualized by nMDS, showed a clear division between shallow parts of the ARS (Stations 55 and 61) and the deeper ones (Fig. 12). Since calanoid copepods made up a large fraction at these stations, analyses were repeated without them, but the same pattern remained. The correlated environmental variables T, S, and O_2 gave evidence for the presence of water masses of North Atlantic origin at the shallower stations, while the deep-sea stations were under Arctic water mass influence. These water mass differences and especially the presence of their associated mesozooplankton community is likely have an effect on the benthic community composition.

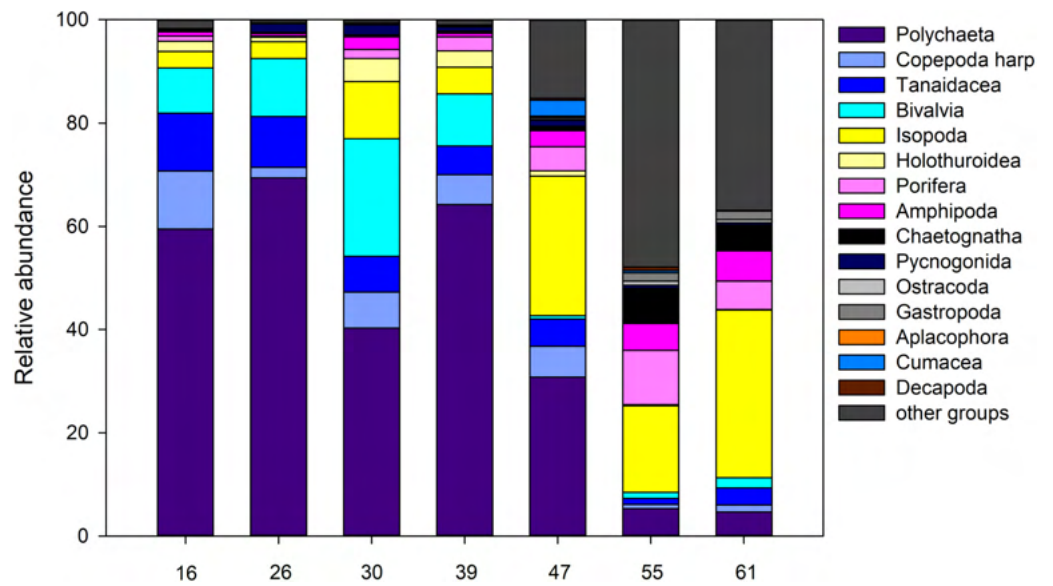


Figure 11 Abundance. Relative abundance (%) of macrofauna collected from the Ægir Ridge by means of an epibenthic sledge.

Full-size [DOI: 10.7717/peerj.13394/fig-11](https://doi.org/10.7717/peerj.13394/fig-11)

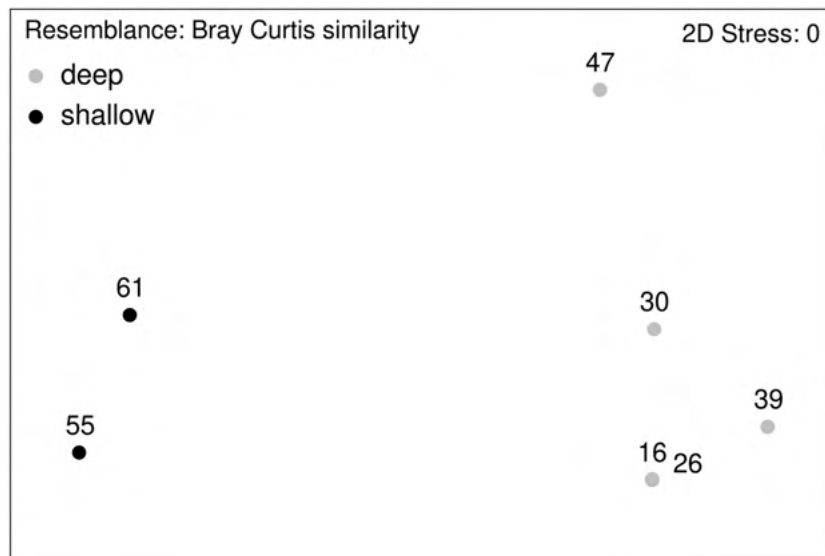


Figure 12 nMDS plot. Macrofauna assemblage analyses of EBS samples (nMDS plots).

Full-size [DOI: 10.7717/peerj.13394/fig-12](https://doi.org/10.7717/peerj.13394/fig-12)

DISCUSSION

The deep-sea floor is increasingly being used for its living and non-living resources. With the cumulative effects of pollution from litter and waste, and climate-related impacts, the deep-sea benthic fauna are being seriously affected (*Ramirez-Llodra et al., 2010*). Given the impediment of fragmentary knowledge about deep-sea ecosystems, it is clear that we cannot protect what has only been sparsely sampled, mapped, and described (*Glover et al., 2018; Ficetola, Canedoli & Stoch, 2019*). Therefore, concerted efforts not only to incorporate but also to produce new scientific knowledge into decision-making processes are essential and not to be delayed in order to develop sustainable management practices to conserve a representative range of deep-sea habitat types and communities. In this study, we investigated macro- and megabenthic communities along the ARS in the deep Norwegian Sea. In the following, we discuss the various components of the ridge's geological and biological diversity, starting with a characterization of the physical environment through its biotic mega- and macrofaunal components towards assessing its ecological and biological value. This will be valuable data for the Faroese, Icelandic, and Norwegian managements of the deep sea, and will support the ongoing work with describing vulnerable areas and possibly VMEs.

Environmental and geological and settings of the Ægir Ridge System

The geologically and environmentally unique ARS offers a large variability of environment over short and long distances associated with rapid changes in depth and sea floor substrates. In its relatively shallow southern end (Gríðargljúfur Gorge), the ARS has steep (up to 60°) and indented valley walls that do not follow typical fault lines. Similar morphologies are observed along at the head of submarine canyons, where water and turbidity current incise the continental shelf (*Maier Johnson & Hart, 2018*). In addition to the variations in the morphology and depth, the ARS displays variations in the substrate. Backscatter analysis has shown a change in the proportion of hard substrate associated with water depth and slope. The correlation between slope and backscatter intensity indicates that the abundance of soft substrate is related to the steepness of slopes, with no coherent soft sediment layer found on slope steeper than 30°. As the average seafloor deepens in the Norwegian Basin, the median valley become less deep compared to the surrounding seafloor and the valley walls (Ránarhryggur Ridge, Drafnarhryggur Ridge) which is typical of heavily sedimented fault scarps. There is also an increase of soft substrate in the deepest section of the ARS that can be associated with: 1/ an increase in sediment thickness: ~200 cm at the southern rim (*Straume et al., 2019*), up to 1,400 cm in the valley center (*Uenzelmann-Neben et al., 1992*) and 2/ a decrease of the amount of pebbles (4–64 mm in diameters) and cobbles (64 to 256 mm in diameters) that cover the shallow rim of the Gríðargljúfur Gorge, which are absent in the central section N of the ridge. These fragments contribute to increase the sediment grain size and offer hard substrate for organisms. The difference of sediment thickness could indicate that the sediment is transported from the shoulders to the valley center, but also along the ARS valley from the south to north where sediments accumulate.

In addition to morphology and substrate variation, the ARS is affected by different currents and water masses. The oceanographic CTD profiles ([Fig. 4](#)) taken in the middle

(North square in Fig. 1) and southwestern areas of the ARS showed the influence of different water masses of both Atlantic and Arctic origin, with the warmer, less dense Atlantic water in the upper water column and the colder, denser Arctic water in waters from the upper bathyal (600 m to 1,000 m) to abyssal range (>3,000 m). These observations were in line with the current knowledge of the oceanographic settings in the Norwegian Basin and wider Nordic seas as being a mixing zone of different water masses (e.g., *Semper et al., 2019; Semper et al., 2020*). Especially the southern end of the ARS is influenced by several circulation systems including the Iceland-Faroe Slope Jet (IFSJ), the warm and saline North Atlantic Current (NAC), and the Faroe Current (*Huang et al., 2020; Semper et al., 2020*) and is still of interest for studies on sources and upstream pathways of dense overflow water in the Nordic seas and the on the AMOC (Atlantic Meridional Overturning Circulation) (*Huang et al., 2020; Chafik et al., 2020*). The deep and strong IFSJ on the southern tip of the ARS could be a major inducer of sediment erosion at the shallow edges of the ridge. To find evidence for this suggestion however, further studies must be made to observe local and fine scale currents.

In recent decades, the AMOC's importance to the Earth's climate has been identified (*Boers, 2021*). Studies observed its overall weakening (e.g., *Ceasar et al., 2018; Liu et al., 2020; Boers, 2021*), as well as a stable partition of subpolar overturning in the eastern North Atlantic basins (*Fu et al., 2020*). Additionally, faster, warm Atlantic currents have been observed, driving the poleward extension of temperate marine fauna into the Arctic (e.g., *Oziel et al., 2020; Caspó, Grabowski & Weslawski, 2021*), a phenomenon termed "Atlantification". The analyses of our CTD casts showed evidence of Atlantic-origin, warmer waters in the upper layers (0–600 m) at all sites. *Gislason & Silva (2012)* showed how the Arctic and North Atlantic different water masses define the composition and abundance of the zooplankton communities. To study and understand the effects and extent of Atlantification, *Caspó, Grabowski & Weslawski (2021)* highlighted that both needed to be known, the distribution of pelagic and benthic animals in the North Atlantic/Arctic areas and the evolutionary history of the fauna. The southwestern end of the ARS is neighboring the northern end of the IFR, while the more northerly part of the ARS is rising from the abyssal Norwegian Basin (*Hjartarson, Erlendsson & Blischke, 2017*). This area is at the boundary of benthic cold-temperate boreal Atlantic and subpolar/polar Arctic faunal elements (e.g., *Olafsdóttir & Gudmundsson, 2019*). Along the Norwegian shelf northwards range extensions for about 200 species in the last three decades has been observed by *Narayanaswamy, Bett & Hughes (2010)*. Less is known on the diversity and species ranges of the bathyal and abyssal fauna of the Norwegian Basin and the ARS within.

What type of megafauna communities do we see?

The ROV footage from the ARS showed different deep-water communities where sponges and soft corals play a role as habitat-forming elements. The images revealed the dominance of cold-water sponge fauna. *Hestetun, Tompkins-Macdonald & Rapp (2017)* that showed that cold-water carnivorous sponges of the family Cladorhizidae were represented with seventeen species belonging to *Cladorhiza*, *Lycopodina*, *Asbestopluma*, and *Chondrocladia* in the Greenland-Iceland-Norwegian (GIN) Seas. Many of them were close to the IFR, like

the amphi-Atlantic *C. a. (C.) grandis* that is distributed in the cold-water mass north and northeast of Iceland (north of the GIF) (Hestetun, Tompkins-Macdonald & Rapp, 2017). Furthermore, *Geodia hentscheli* (Cárdenas et al., 2010), observed here, was considered an Arctic species and was commonly found in the Denmark Strait and in the Nordic seas (Cárdenas et al., 2013). Other cold related species found were the hexactinellids *S. rosea* and *C. arcticus*, that were dominant in the northern part of ARS. A large-scale predictive mapping of possible distribution of VMEs in the Nordic seas show that the sponges *C. (C.) arcticus*, *Cladorhiza* sp., *C. (C.) grandis*, and *Lycopodina* sp. as well as *Geodia parva* Hansen 1885 and *G. hentscheli* are highly likely to be present in the sea north of the GSR as supported in Cárdenas et al. (2013) and Hestetun, Tompkins-Macdonald & Rapp (2017).

The sponge species and assemblages found in the ARS are characteristic of the Nordic seas or wider Arctic (Klitgaard & Tendal, 2004; Murillo et al., 2018), although a few species (e.g., *C. (C.) grandis*) are also found at lower latitudes, particularly in the western part of the North Atlantic (Hestetun, Tompkins-Macdonald & Rapp, 2017). Their distribution in the various sections of the ARS is very likely driven by the prevailing water masses, with the deeper areas dominated by a few structural species (e.g., *C. arcticus*) and their associates adapted to comparatively colder Arctic water; and shallower areas with a more diverse megafauna likely benefiting from a dynamic mixing between water masses supplying oxygen and nutrients, as well as preventing high sedimentation. The findings in the ARS are supported by previous observations from neighboring ridges and straits (Meyer et al., 2016; Roberts et al., 2018; Meyer et al., 2019; Ramirez-Llodra et al., 2020).

The soft nephteidae corals, *Gersemia fruticosa* (Sars, 1860), *G. clavata* (Danielssen, 1887), *G. rubiformis* (Ehrenberg 1834), *Drifa glomerata* and *Duva florida* (Rathke, 1806) are widely distributed around Iceland. The records date back to the year 1900 at a depth range of 630–184 m (Jungersen, 1917; Madsen, 1944a; Madsen, 1944b), 1993 at a depth range 495–1,350 m (unpublished BIOICE data, SH Olafsdottir & S Brix 2021 pers. obs.) and most recently in 2016 and 2017 at 460–760 m depth (Olafsdóttir & Gudmundsson, 2019). Although not observed by the ROV in this survey, the sea pens *Umbellula encrinus* (Linnaeus, 1758) and *Virgularia glacialis* Kolliker 1870 have also been reported in the area at 746–790 m depth (Olafsdóttir & Gudmundsson, 2019).

As stated earlier, Arctic influenced fauna (mostly sponges) was observed during the ROV dives. No cold-water "gorgonian corals" (Alcyonacea), reef-forming corals (like *Desmophyllum pertusum* (Linnaeus, 1758) or *Madrepora oculata* Linnaeus, 1758, Scleractinia) were observed. These are, however, known from the nearby Lónsdjúp trough and the slope off Papagrúnn bank (Brix et al., 2020; Ragnarsson & Burgos, 2018; Olafsdottir et al., 2020) and around the Faroe Islands (Frederiksen, Jensen & Westerberg, 1992; Tendal, 1992). Scleractinia and the various "gorgonian corals" have their distributional boundaries at the IFR and are not in the deep cold waters north of the ridge (Buhl-Mortensen et al., 2015b) although Burgos et al. (2020) models show potential occurrence around the Faroes and in the Aegir Ridge area

This region is known for its strong currents and overflow regions (Hansen & Østerhus, 2000) as also indicated by the velocities in Fig. 1. We may conclude that the water bodies have an important influence shaping the operational habitat for these corals. Thus, it

is important to mention here that these “typical” elements of the North Atlantic, the corals like *Paragorgia* and *Desmophyllum* were not observed along the investigated parts of the ARS. The occurrence of these corals seems to be associated with depth and suitable habitats and currents along the thermocline, which also plays an important role in other invertebrates (Høisæter, 2010; Brix et al., 2018a; Brix et al., 2018b).

For the megafauna, we have derived habitat zonation along the ARS from abyssal to the upper bathyal depth on the ridge top, recorded the presence of VME indicator taxa, especially at the steep hard-sedimented slopes. These vertical steeps of canyon-like walls had only become accessible for investigations with the availability of deep-water ROVs (Huvenne et al., 2011; Johnson et al., 2013). The soft sedimented areas of the neighboring abyssal plain or the ridge top were suitable for the investigation by towed EBS for the investigation of macrofauna.

Macrofauna

Community composition of the soft sediment linked macrofauna in our study were largely driven by depth and to a lesser extent water mass properties. A depth zonation between a shallow (upper slope) and abyssal fauna was evident in total macrofauna. Generally, the composition of the fauna of the deep Nordic seas is influenced by cold temperatures of the prevailing water masses and the presence of the GSR, which represents a distribution barrier for fauna from the North Atlantic (Schnurr et al., 2018; Brix et al., 2018a; Jöst et al., 2019; Lörz et al., 2021; Uhlir et al., 2021). Accordingly, taxa that live in the deep Nordic basins are derived from those with broad bathymetric distributions enabling species to cross the ridge from the south (e.g., Svavarsson, Strömberg & Brattegard, 1993; Weisshappel, 2000; Weisshappel, 2001). That means for peracarid crustaceans, that taxa found in the deeper parts are likely to appear shallower too, but not necessarily vice versa. Nevertheless, in our study depth had been revealed as an important factor in the differentiation of communities for all taxa investigated and at all taxonomic levels, as shown by the BIO-ENV analysis.

It has been found that many macro- and megabenthic species in the region are restricted to distinct water masses (Weisshappel & Svavarsson, 1998; Brix & Svavarsson, 2010; Schnurr et al., 2018; Lörz et al., 2018; Roberts et al., 2021). Hydrographic conditions in the region, particularly in the vicinity of the GIF, are complex and reveal considerable variation in temperature, salinity and other physical properties, that strongly shape benthic communities. The fact that we found little influence of water mass on macrofaunal patterns in our study was likely due to biologically insignificant differences between these variables; in other words, the variation in environmental parameters, such as salinity, or temperature are only minor and may have not a strong effect on faunal communities. However, the presence of certain isopod species at the upper slope sites in our study, such as *Chelator insignis* (Hansen, 1916)—a predominant North Atlantic species (Brix et al., 2014)—suggested at least an Atlantic influence for these stations. Similar to the megafauna, the deep abyssal stations, by contrast, consisted exclusively of Arctic isopod species (Svavarsson, Strömberg & Brattegard, 1993). Shallower stations were located at the lower limit of the thermocline, which was between 400 and 700 m for the region (Bett, 2001; Høisæter, 2010).

Faunal densities are often related to the amount of nutrient input and generally decrease with increasing depth (Rex *et al.*, 2006; Rex & Etter, 2010). Patterns of total macrofauna in our study appeared to be following this trend, but only when including calanoid copepods. If copepods are removed from the analysis, a different picture emerged of elevated densities of the ARS deep-sea floor stations.

We could rule out that the high number of copepods found in each EBS sample was due to a sampling error; that is, the EBS closing mechanism worked properly at all stations and only epifauna occurred in the catch. It is likely that calanoids contained in the cold, deep Arctic water become trapped in these deeper water masses and thus “hang” off the wall of the southern end of the ARS in the Grjóðargljúfur Gorge. In reality our data offered only a small glimpse in time and space, and more sampling is needed to corroborate this pattern.

Implications for conservation

The sustainable management and conservation of deep-sea habitats and their protection from anthropogenic pressures (bottom fishing, deep-sea mining, climate change) has been high in the global scientific and political agendas (Norwegian Ministry of Fisheries and Industry, 2019). Increasing recognition of the spatial and temporal extent of such impacts on biodiversity and ecosystem function, led to the development and implementation of area-based management tools (*e.g.*, MPA networks and EBSAs designation) and other effective conservation measures (*e.g.*, closure areas) at national and international levels.

In 2010, the Conference of the Parties (COP) to the Convention on Biological Diversity (CBD) committed to conserve at least 10% of coastal and marine areas through “effectively and equitably managed, ecologically representative and well-connected systems of protected areas and other effective area-based conservation measures” (Aichi Target 11) as part of the Strategic Plan for Biodiversity 2011–2020 (CBD, 2010). Since then, great advances have been made to identify and protect a set of ecologically or biologically significant areas, following the established EBSAs scientific criteria (SC) of: (1) uniqueness or rarity; (2) special importance for life-history stages; (3) importance for threatened, endangered or declining species and/or habitats; (4) vulnerability, fragility, sensitivity, or slow recovery; (5) biological productivity; (6) biological diversity; and (7) naturalness (CBD, 2008).

The Arctic-Intermediate Water (AIW) between 400 and 1,500 m depth over ARS are an overwintering area for the key-ecosystem species *Calanus finmarchicus* (Gunnerus, 1770) (Bagøien, Melle & Kaartvedt, 2012; Melle *et al.*, 2014a; Melle *et al.*, 2014b), an important resource that supports higher trophic levels (SC2). In addition, sponge aggregations and coral gardens as those found are listed as threatened and/or declining species and habitats (SC3) by the OSPAR convention (OSPAR Convention, 1992; OSPAR, 2008) and as VMEs (SC4) on account of life-history traits (*e.g.*, slow growth, high longevity) of its constituent species (FAO, 2009).

The sponge aggregations observed during our study of the ARS are similar to the ones found on the Schulz Bank located on the transition between the Mohn and Knipovich ridges (Roberts *et al.*, 2018; Meyer *et al.*, 2019) as well as on the Mohn’s Ridge (Ramirez-Llodra *et al.*, 2020), and, to some extent, in the eastern Fram Strait (Meyer *et al.*, 2016). These Arctic deep-sea habitats are known to have particular ecological significance, playing key

roles both in the recycling of major nutrients ([Rooks et al., 2020](#)), and serving as refuge and nursery areas for several demersal fish species such as the Arctic skate (*Amblyraja hyperborean* [Collett, 1879]), the Roughhead grenadier (*Macrourus berglax* Lacepède, 1801) and the Greenland halibut (*Reinhardtius hippoglossoides* [Walbaum, 1792]) ([Meyer et al., 2019](#)). Unlike other types of sponge habitats, these Arctic sponge grounds, commonly known as cold-water “Ostur” are not currently protected under area-based management tools such as MPAs, either at national or international levels.

Sponge grounds are considered threatened and declining and slowly recovering. They are even considered “habitat” forming, as we observed for the rossellid sponge *Caulophacus arcticus* in the deep sedimented plains with the species interactions of pantopods, the caridean shrimp *Bythocaris*, and so far on genus or species level unidentifiable calliopiid amphipods. These amphipods are representing most probably a species new to science. Thus, the associated macrofauna—although rarely always observed in ROV video data—may play an important role and at least in the sedimented plains the little “oases” do link the macrofauna of the sedimented plain with the easily visible megafauna. The connections and species interactions still need to be studied in more detail and this may also be true for some of the sampled isopod species. Overall macrofaunal patterns will need to be further assessed and compared with other Arctic and Atlantic locations, especially with regard to the EBSA criteria, in order to identify areas with high biodiversity and a high proportion of rare or threatened species. For instance, some isopod species found in our study have been demonstrated to represent species complexes (e.g., *Chelator insignis* Hansen, 1916, *Eurycope producta* GO Sars, 1866, *Oecidiobranthus nansenii* Just, 1980, *Haploneiscus bicuspis* (GO Sars, 1877) as figured out in ([Brix et al., 2014](#); [Jennings et al., 2018](#); [Schnurr et al., 2018](#); [Paulus et al., 2022](#)), where effective population size and range extent of undescribed species within most complexes is still unknown.

While a considerable number of MPAs and EBSAs have been designated in the North Atlantic to protect deep-sea VMEs, at present the only MPAs established in the Nordic seas fall within the Icelandic and Norwegian EEZs. Notably, none of these currently encompass sponge aggregations or soft coral gardens in their conservation targets, although some are focused on cold-water coral reefs (another VME type). Thus, the potential designation of part of the ARS as an EBSA would provide a good opportunity to augment the representativity by increasing the range of ecosystems (a ridge system) and habitats (sponge aggregations and coral gardens) under protection for a biogeographical area which is currently under-represented in the context of the wider North Atlantic. This would also be well aligned with Norwegian ongoing discussions of defining an area “the deep Norwegian Sea” including the parts of the ARS within the “Banana hole” as a “Particularly Valuable and Vulnerable Area” (Særlig verdifult og sårbart område – “SVO”) ([Eriksen et al., 2021](#)).

CONCLUSIONS

Our research was conducted on the boundary of the Arctic Ocean close to the Atlantic Overflow, an area of complex water masses and bathymetry that is also of great importance

to deep-water formation and the AMOC globally. With advancing Atlantification of the Nordic seas and accompanying effects of this and additional anthropogenic stressors (*e.g.*, pollution, fishing etc.), protection of seafloor habitats and related fauna is a pressing concern. First and foremost, however, it demands an understanding of how the fauna is structured and which factors play a role in it.

The great variation in seabed topography that defines the ARS, particularly in relation to the steep, canyon-like walls of its southern part, as well as differences in depth and water mass features let us ask if this is reflected in the diversity and composition of the macro- and megafaunal biota. Here, in particular, the use of different sampling devices provided insights into different types of fauna (macro- and megafauna) and environments (hard and soft substrate). In brief, we discovered a clear faunal zonation along the ARS from the abyssal sediment plain to the ridge top, both in macro- and megafauna communities, albeit slight variations between taxonomic groups. According to our expectations, water mass and depth were the main factors responsible for (macro-) faunal patterns. The vertical steep walls of the ridge, described as canyon-like structures, only became accessible for surveying with the availability of a deep-water ROV (*Huvenne et al., 2011; Johnson et al., 2013*). A biological canyon effect was evident in dense aggregates of megafaunal filter feeders and elevated macrofaunal densities. Analysis of videos and still images from the ROV also led to the discovery of a number of VME habitats and taxa in the megafaunal communities of the ARS.

As our study covered only a small portion of the ARS in two disjunct sampling areas, more work and sampling are needed to more thoroughly analyse the benthic communities along the ARS. Nonetheless, our results indicate that the depth and canyon-like topography of the ARS appear to strongly influence faunal patterns in both macro and megafauna, and further promoting the presence of VME elements. With regard to the EBSA criteria for naturalness and biodiversity, our findings are moreover in line with the ongoing calls to consider parts of the ARS as candidate locations for an EBSA.

ACKNOWLEDGEMENTS

We thank the captain, Oliver Meyer, the RV Sonne crew and the participants of SO276 (MerMet17-6) for their logistical and practical support. Special thanks go to the ROV team from GEOMAR, the EBS and DZMB team for their help with sampling. Also special thanks to Karen Jeskulke and Antje Fischer for all database entries. Colin Devey kindly verified the sediment identifications, *e.g.*, drop stones, on the extinct Ægir Ridge. We would like to thank our reviewers for their valuable, constructive contributions, greatly improving our manuscript

ADDITIONAL INFORMATION AND DECLARATIONS

Funding

The IceAGE3 expedition was supported by the German Science Foundation (MerMet17-6) and the Bundesministerium für Bildung und Forschung (SO276). Stefanie Kaiser received a grant from the Narodowa Agencja Wymiany Akademickiej (NAWA, Poland) under the ULAM program. Anne-Nina Lörz was funded by the DFG project "IceAGE Amphipoda" (LO2543/1-1). Anne Helene S Tandberg was funded through the Norwegian Biodiversity Information Centre project 16_18_NORAMPH2. Joana R Xavier's research is supported by national funds through FCT, the Portuguese Foundation for Science and Technology within the scope of UIDB/04423/2020, UIDP/04423/2020, and CEECIND/00577/2018. This study is a contribution to EU Horizon 2020 iAtlantic project. The funders had no role in study design, data collection and analysis, decision to publish, or preparation of the manuscript.

Competing Interests

The authors declare there are no competing interests.

Author Contributions

- Saskia Brix conceived and designed the experiments, performed the experiments, analyzed the data, prepared figures and/or tables, authored or reviewed drafts of the paper, compiled all data and manuscript pieces, and approved the final draft.
- Stefanie Kaiser performed the experiments, analyzed the data, prepared figures and/or tables, authored or reviewed drafts of the paper, performed the Primer analyses, and approved the final draft.
- Anne-Nina Lörz performed the experiments, analyzed the data, prepared figures and/or tables, authored or reviewed drafts of the paper, was responsible for determining amphipods, and approved the final draft.
- Morgane Le Saout performed the experiments, analyzed the data, prepared figures and/or tables, authored or reviewed drafts of the paper, identified geological features, and approved the final draft.
- Mia Schumacher performed the experiments, analyzed the data, prepared figures and/or tables, authored or reviewed drafts of the paper, created maps and bathymetry data, and approved the final draft.
- Frederic Bonk analyzed the data, prepared figures and/or tables, worked on the video data and frame grabs, and approved the final draft.
- Hronn Egilsdottir conceived and designed the experiments, analyzed the data, prepared figures and/or tables, authored or reviewed drafts of the paper, worked on the video data and frame grabs, and approved the final draft.
- Steinunn Hilma Olafsdottir conceived and designed the experiments, analyzed the data, prepared figures and/or tables, authored or reviewed drafts of the paper, worked on the video data and frame grabs, and approved the final draft.

- Anne Helene S. Tandberg conceived and designed the experiments, analyzed the data, prepared figures and/or tables, authored or reviewed drafts of the paper, co-responsible for amphipod determination and working on the video data and frame grabs, and approved the final draft.
- James Taylor conceived and designed the experiments, performed the experiments, analyzed the data, prepared figures and/or tables, authored or reviewed drafts of the paper, led the work on the video data and frame grabs, and approved the final draft.
- Simon Tewes performed the experiments, analyzed the data, prepared figures and/or tables, did the CTD profiles, and approved the final draft.
- Joana R. Xavier analyzed the data, prepared figures and/or tables, authored or reviewed drafts of the paper, was responsible for sponge species identification, and approved the final draft.
- Katrin Linse conceived and designed the experiments, performed the experiments, prepared figures and/or tables, illustrated the habitat schematics, and approved the final draft.

Field Study Permissions

The following information was supplied relating to field study approvals (i.e., approving body and any reference numbers):

We did sample with RV Sonne in international waters (ABNJ) and within the Icelandic EEZ during SO (MerMet 17-06). All diplomatic formulars with Iceland were received prior expedition.

Data Availability

The following information was supplied regarding data availability:

The cruise report for IceAGE3 including all station information is available in PANGEA under http://doi.org/10.48433/cr_so276.

The original photographs and plates are available at figshare:

Kaiser, Stefanie; Taylor, James; Lörz, Anne-Nina; Le Saout, Morgane; Schumacher, Mia; Bonk, Frederik; et al. (2022): Fig. 6 Aegir Ridge N megafaunal elements. figshare. Figure. <https://doi.org/10.6084/m9.figshare.19665243.v2>.

Kaiser, Stefanie; Brix, Saskia; Lörz, Anne-Nina; Le Saout, Morgane; Schumacher, Mia; Bonk, Frederik; et al. (2022): Fig. 7 Aegir Ridge 2000 m to 600m. figshare. Figure. <https://doi.org/10.6084/m9.figshare.19665255.v2>.

Kaiser, Stefanie; Brix, Saskia; Lörz, Anne-Nina; Le Saout, Morgane; Schumacher, Mis; Bonk, Frederik; et al. (2022): Fig. 8 Aegir Ridge S megafaunal elements. figshare. Figure. <https://doi.org/10.6084/m9.figshare.19665267.v2>.

Kaiser, Stefanie; Brix, Saskia; Lörz, Anne-Nina; Le Saout, Morgane; Schumacher, Mia; Bonk, Frederik; et al. (2022): Fig. 9 Aegir Ridge N_figure_final_revised. figshare. Figure. <https://doi.org/10.6084/m9.figshare.19665273.v2>.

Kaiser, Stefanie; Brix, Saskia; Lörz, Anne-Nina; Le Saout, Morgane; Schumacher, Mia; Bonk, Frederik; et al. (2022): Fig. 10 Aegir Ridge S_ROV3&4_final_revised. figshare. Figure. <https://doi.org/10.6084/m9.figshare.19665300.v2>.

Kaiser, Stefanie; Brix, Saskia; Lörz, Anne-Nina; Le Saout, Morgane; Schumacher, Mia; Bonk, Frederik; et al. (2022): **Fig. 6** Original photos. figshare. Media. <https://doi.org/10.6084/m9.figshare.19665309.v2>.

Kaiser, Stefanie; Brix, Saskia; Lörz, Anne-Nina; Le Saout, Morgane; Schumacher, Mia; Bonk, Frederik; et al. (2022): **Fig. 7** Original photos. figshare. Media. <https://doi.org/10.6084/m9.figshare.19665318.v2>.

Kaiser, Stefanie; Brix, Saskia; Lörz, Anne-Nina; Le Saout, Morgane; Schumacher, Mia; Bonk, Frederik; et al. (2022): **Fig. 8** Original photos. figshare. Media. <https://doi.org/10.6084/m9.figshare.19665321.v2>.

Kaiser, Stefanie; Brix, Saskia; Lörz, Anne-Nina; Le Saout, Morgane; Schumacher, Mia; Bonk, Frederik; et al. (2022): **Fig. 9** Original photos. figshare. Media. <https://doi.org/10.6084/m9.figshare.19665324.v2>.

Supplemental Information

Supplemental information for this article can be found online at <http://dx.doi.org/10.7717/peerj.13394#supplemental-information>.

REFERENCES

- Appeltans W, Ahyong ST, Anderson G, Angel MV, Artois T, Bailly N, Bamber R, Barber A, Bartsch I, Berta A, Błażewicz-Paszkowycz M, Bock P, Boxshall G, Boyko CB, Brandão SN, Bray RA, Bruce NL, Cairns SD, Chan T-Y, Cheng L, Collins AG, Cribb T, Curini-Galletti M, Dahdouh-Guebas F, Davie PJF, Dawson MN, De Clerck O, Decock W, De Grave S, de Voogd NJ, Domning DP, Emig CC, Erséus C, Eschmeyer W, Fauchald K, Fautin DG, Feist SW, Franssen CHJM, Furuya H, Garcia-Alvarez O, Gerken S, Gibson D, Gittenberger A, Gofas S, Gómez-Daglio L, Gordon DP, Guiry MD, Hernandez F, Hoeksema BW, Hopcroft RR, Jaume D, Kirk P, Koedam N, Koenemann S, Kolb JB, Kristensen RM, Kroh A, Lambert G, Lazarus DB, Lemaitre R, Longshaw M, Lowry J, Macpherson E, Madin LP, Mah C, Mapstone G, McLaughlin PA, Mees J, Meland K, Messing CG, Mills CE, Molodtsova TN, Mooi R, Neuhaus B, Ng PKL, Nielsen C, Norenburg J, Opresko DM, Osawa M, Paulay G, Perrin W, Pilger JF, Poore GCB, Pugh P, Read GB, Reimer JD, Rius M, Rocha RM, Saiz-Salinas JI, Scarabino V, Schierwater B, Schmidt-Rhaesa A, Schnabel KE, Schotte M, Schuchert P, Schwabe E, Segers H, Self-Sullivan C, Shenkar N, Siegel V, Sterrer W, Stöhr S, Swalla B, Tasker ML, Thuesen EV, Timm T, Todaro MA, Turon X, Tyler S, Uetz P, van der Land J, Vanhoorne B, van Ofwegen LP, van Soest RWM, Vanaverbeke J, Walker-Smith G, Walter TC, Warren A, Williams GC, Wilson SP, Costello MJ. 2012. The magnitude of global marine species diversity. *Current Biology* 22(23):2189–2202 DOI 10.1016/j.cub.2012.09.036.
- Bagøien E, Melle W, Kaartvedt S. 2012. Seasonal development of mixed layer depths, nutrients, chlorophyll and *Calanus finmarchicus* in the Norwegian Sea—a basin-scale habitat comparison. *Progress in Oceanography* 103:58–79 DOI 10.1016/j.pocean.2012.04.014.

- Bett BJ. 2001.** UK Atlantic Margin Environmental Survey: introduction and overview of bathyal benthic ecology. *Continental Shelf Research* **21(8-10)**:917–956 DOI [10.1016/S0278-4343\(00\)00119-9](https://doi.org/10.1016/S0278-4343(00)00119-9).
- Blischke A, Gaina C, Hopper JR, Péron-Pinvidic G, Brandsdóttir B, Guarnieri P, Erlendsson Ö, Gunnarsson K. 2016.** The Jan Mayen microcontinent: an update of its architecture, structural development and role during the transition from the Ægir Ridge to the mid-oceanic Kolbeinsey Ridge. *Geological Society, London, Special Publications* **447**:299–337.
- Boers N. 2021.** Observation-based early-warning signals for a collapse of the Atlantic Meridional Overturning Circulation. *Nature Climate Change* **11**:680–688 DOI [10.1038/s41558-021-01097-4](https://doi.org/10.1038/s41558-021-01097-4).
- Brandt A, Barthel D. 1995.** An improved supra- and epibenthic sledge for catching Peracarida (Crustacea, Malacostraca). *Ophelia* **43(1)**:15–23 DOI [10.1080/00785326.1995.10430574](https://doi.org/10.1080/00785326.1995.10430574).
- Brandt A, Elsner N, Brenke N, Golovan O, Malyutina MV, Riehl T, Schwabe E, Würzberg L. 2013.** Epifauna of the Sea of Japan collected via a new epibenthic sledge equipped with camera and environmental sensor systems. *Deep-Sea Research Part II* **86–87**:43–55.
- Brenke N. 2005.** An epibenthic sledge for operations on marine soft bottom and bedrock. *Marine Technology Society Journal* **39(2)**:10–21 DOI [10.4031/002533205787444015](https://doi.org/10.4031/002533205787444015).
- Brix S, Lörz A-N, Jazdzewska AM, Hughes L, Tandberg AHS, Pabis K, Stransky B, Rapp-Schickel T, Corbe JC, Hendryks E, Vader W, Frutos I, Horton T, Jazdzewsky K, Peart R, Beerman J, Coleman CO, Buhl-Mortensen L, Corbari L, Havermans C, Tato R, Campean AJ. 2018b.** Amphipod family distributions around Iceland. *ZooKeys* **731**:1–53.
- Brix S, Meißner K, Stransky B, Halanych KM, Jennings RM, Kocot KM, Svavarsson J. 2014.** The IceAGE project—a follow up of BIOICE. *Polish Polar Research* **35**:141–150 DOI [10.2478/popore-2014-0010](https://doi.org/10.2478/popore-2014-0010).
- Brix S, Stransky B, Malyutina M, Pabis K, Svavarsson J, Riehl T. 2018a.** Distributional patterns of isopods (Crustacea) in Icelandic and adjacent waters. *Marine Biodiversity* **48**:783–811 DOI [10.1007/s12526-018-0871-z](https://doi.org/10.1007/s12526-018-0871-z).
- Brix S, Svavarsson J. 2010.** Distribution and diversity of desmosomatid and nannoniscid isopods (Asellota) on the Greenland-Iceland-Faeroe Ridge. *Polar Biology* **33**:515–530 DOI [10.1007/s00300-009-0729-8](https://doi.org/10.1007/s00300-009-0729-8).
- Brix S, Taylor J, Le Saout M, Mercado-Salas N, Kaiser S, Lörz A-N, Gatzemeier N, Jeskulke K, Kürzel K, Neuhaus J. 2020.** *Depth transects and connectivity along gradients in the North Atlantic and Nordic seas in the frame of the IceAGE project (Icelandic marine Animals: genetics and Ecology), Cruise No. SO276 (MerMet17-06), 22.06.2020-26.07.2020, Emden (Germany) - Emden (Germany).* Bonn: SONNE-Berichte DOI [10.48433/cr_so276](https://doi.org/10.48433/cr_so276).
- Buhl-Mortensen L, Buhl-Mortensen P, Dolan MJF, Gonzalez-Mirelis G. 2015a.** Habitat mapping as a tool for conservation and sustainable use of marine resources: some

- perspectives from the MAREANO Programme, Norway. *Journal of Sea Research* **100**:46–61 DOI [10.1016/j.seares.2014.10.014](https://doi.org/10.1016/j.seares.2014.10.014).
- Buhl-Mortensen L, Olafsdottir SH, Buhl-Mortensen P, Burgos JM, Ragnarsson SA. 2015b.** Distribution of nine cold-water coral species (Scleractinia and Gorgonacea) in the cold temperate North Atlantic: effects of bathymetry and hydrography. *Hydrobiologia* **759**:39–61 DOI [10.1007/s10750-014-2116-x](https://doi.org/10.1007/s10750-014-2116-x).
- Burgos JM, Buhl-Mortensen L, Buhl-Mortensen P, Ólafsdóttir SH, Steingrund P, Ragnarsson S, Skagseth Á, Skagseth Ø. 2020.** Predicting the distribution of indicator taxa of vulnerable marine ecosystems in the Arctic and Sub-arctic Waters of the Nordic seas. *Frontiers in Marine Science* **7**:131 DOI [10.3389/fmars.2020](https://doi.org/10.3389/fmars.2020).
- Cárdenas P, Rapp HT, Klitgaard AB, Best M, Thollessen M, Tendal OS. 2013.** Taxonomy, biogeography and DNA barcodes of *Geodia* species (Porifera, Demospongiae, Tetractinellida) in the Atlantic boreo-arctic region.
- Cárdenas P, Rapp HT, Schander C, Tendal OS. 2010.** Molecular taxonomy and phylogeny of the Geodiidae (Porifera, Demospongiae, Astrophorida)—combining phylogenetic and Linnaean classification. *Zoologica Scripta* **39**(1):89–106 DOI [10.1111/j.1463-6409.2009.00402.x](https://doi.org/10.1111/j.1463-6409.2009.00402.x).
- Caspó HK, Grabowski M, Weslawski JM. 2021.** Coming home –Boreal ecosystem claims Atlantic sector of the Arctic. *Science of the Total Environment* **771**:144817 DOI [10.1016/j.scitotenv.2020.144817](https://doi.org/10.1016/j.scitotenv.2020.144817).
- Ceasar L, Rahmstorf S, Robinson A, Feulner G, Saba V. 2018.** Observed fingerprint of a weakening Atlantic Ocean overturning circulation. *Nature* **556**:191–196 DOI [10.1038/s41586-018-0006-5](https://doi.org/10.1038/s41586-018-0006-5).
- Chafik L, Hátún H, Kjellsson J, Larsen KMH, Rossby T, Berx B. 2020.** Discovery of an unrecognized pathway carrying overflow waters toward the Faroe Bank Channel. *Nature Communications* **11**:3721 DOI [10.1038/s41467-020-17426-8](https://doi.org/10.1038/s41467-020-17426-8).
- Chatterjee S, Raj RP, Bertino L, Skagseth Ø, Ravichandran M, Johannessen OM. 2018.** Role of Greenland Sea gyre circulation on Atlantic Water temperature variability in the Fram Strait. *Geophysical Research Letters* **45**:8399–8406 DOI [10.1029/2018GL079174](https://doi.org/10.1029/2018GL079174).
- Clarke KR, Gorley RN. 2006.** PRIMER v6: user manual/tutorial. In: *PRIMER-E. Convention on biological diversity 2008; Decision IX/20 annex 1*. Plymouth; PRIMER-E. Available at <http://www.cbd.int/decision/cop/default.shtml?id=11663> (accessed on June 2013).
- Convention on Biological Diversity (CBD). 2008.** Decision adopted by the conference of the parties to the Convention on Biological diversity at its tenth meeting IX/20. Marine and coastal biodiversity. Bonn. Available at <https://www.cbd.int/doc/decisions/cop-09/cop-09-dec-20-en.pdf>.
- Convention on Biological Diversity (CBD). 2010.** Decision adopted by the conference of the parties to the Convention on Biological diversity at its tenth meeting. X/2. In: *The Strategic Plan for Biodiversity 2011-2020 and the Aichi Biodiversity Targets*. Nagoya. Available at <https://www.cbd.int/doc/decisions/cop-10/cop-10-dec-02-en.pdf>.

- Copernicus Marine Service (CMES).** 2021. Operational Mercator global ocean analysis and forecast system; Global Ocean 1/12° Physics Analysis and Forecast. Available at https://resources.marine.copernicus.eu/?option=com_csw&view=details&product_id=GLOBAL_ANALYSIS_FORECAST_PHY_001_024 (accessed on March 2021).
- Costello MJ.** 2009. Distinguishing marine habitat classification concepts for ecological data management. *Marine Ecology Progress Series* **397**:253–268 DOI [10.3354/meps08317](https://doi.org/10.3354/meps08317).
- Danovaro R, Snelgrove PV, Tyler P.** 2014. Challenging the paradigms of deep-sea ecology. *Trends in Ecology & Evolution* **29**(8):465–475 DOI [10.1016/j.tree.2014.06.002](https://doi.org/10.1016/j.tree.2014.06.002).
- De Leo FC, Smith CR, Rowden AA, Bowden DA, Clark MR.** 2010. Submarine canyons: hotspots of benthic biomass and productivity in the deep sea. *Proceedings of the Royal Society B: Biological Sciences* **277**(1695):2783–2792 DOI [10.1098/rspb.2010.0462](https://doi.org/10.1098/rspb.2010.0462).
- Eriksen E, van der Meeren GI, Nilsen BM, von Quillfeldt CH, Johnsen H.** 2021. Particularly valuable and vulnerable areas (SVO) in Norwegian seas - Environmental values. Assessment of environmental values and borders of present SCOs and proposals of new areas. Rapport fra havforskningen 2021-26. 308 pp. Available at <https://www.hi.no/hi/nettrapporter/rapport-fra-havforskningen-2021-26#sec-1>.
- FAO.** 2009. Report of the Technical Consultation on International Guidelines for the Management of Deep-sea Fisheries in the High Seas, Rome, 4-8 February and 25-29 August 2008. Food and Agriculture Organization of the United Nations Fisheries and Agriculture Report 991. Rome: FAO, 86.
- Ficetola GF, Canedoli C, Stoch F.** 2019. The Racovitza impediment and the hidden biodiversity of unexplored environments. *Conservation Biology* **33**(1):214–216 DOI [10.1111/cobi.13179](https://doi.org/10.1111/cobi.13179).
- Frederiksen R, Jensen A, Westerberg H.** 1992. The distribution of the scleractinian coral *Lophelia pertusa* around the Faroe Islands and the relation to intertidal internal mixing. *Sarsia* **77**:157–171 DOI [10.1080/00364827.1992.10413502](https://doi.org/10.1080/00364827.1992.10413502).
- Fu Y, Li F, Karstensen J, Wang C.** 2020. A stable Atlantic meridional overturning circulation in a changing North Atlantic Ocean since the 1990s. *Science Advances* **6**:eabc7836 DOI [10.1126/sciadv.abc7836](https://doi.org/10.1126/sciadv.abc7836).
- Gaina C, Gernigon L, Ball P.** 2009. Palaeocene–recent plate boundaries in the NE Atlantic and the formation of the Jan Mayen microcontinent. *Journal of the Geological Society* **166**:601–616 DOI [10.1144/0016-76492008-112](https://doi.org/10.1144/0016-76492008-112).
- Gislason A, Silva T.** 2012. Abundance, composition, and development of zooplankton in the Subarctic Iceland Sea in 2006, 2007, and 2008. *ICES Journal of Marine Science* **69**:1263–1276 DOI [10.1093/icesjms/fss070](https://doi.org/10.1093/icesjms/fss070).
- Glover AG, Wiklund H, Chen C, Dahlgren TG.** 2018. Point of view: managing a sustainable deep-sea ‘blue economy’ requires knowledge of what actually lives there. *eLife* **7**:e41319 DOI [10.7554/eLife.41319](https://doi.org/10.7554/eLife.41319).
- Hansen B, Østerhus S.** 2000. North Atlantic–Nordic seas exchanges. *Progress in Oceanography* **45**:109–208 DOI [10.1016/S0079-6611\(99\)00052-X](https://doi.org/10.1016/S0079-6611(99)00052-X).
- Harris P, Baker E (eds.)** 2011. *Seafloor geomorphology as benthic habitat: geohab atlas of seafloor geomorphic features and benthic habitats*. Amsterdam: Elsevier.

- Harris PT, Macmillan-Lawler M, Rupp J, Baker EK. 2014.** Geomorphology of the oceans. *Marine Geology* 352:4–24 DOI 10.1016/j.margeo.2014.01.011.
- Hestetun JT, Tompkins-Macdonald G, Rapp HT. 2017.** A review of carnivorous sponges (Porifera: Cladorhizidae) from the Boreal North Atlantic and Arctic. *Zoological Journal of the Linnean Society* 181(1):1–69 DOI 10.1093/zoolinnean/zw022.
- Hjartarson A, Erlendsson Ö, Blischke A. 2017.** The Greenland-Iceland-Faroe ridge complex. *Geological Society, London, Special Publications* 447:127–148 DOI 10.1144/SP447.14.
- Høisæter T. 2010.** The shell-bearing, benthic gastropods on the southern part of the continental slope off Norway. *Journal of Molluscan Studies* 76(3):234–244 DOI 10.1093/mollus/eyq003.
- Horton T, Marsh L, Bett BJ, Gates AR, Jones DOB, Benoist NMA, Pfeifer S, Simon-Lledó E, Durden JM, Vandepitte L, Appeltans W. 2021.** Recommendations for the standardisation of open taxonomic nomenclature for image-based identifications. *Frontiers in Marine Science* 8:620702 DOI 10.3389/fmars.2021.620702.
- Huang J, Pickart RS, Huang RX, Lin P, Brakstad A, Xu F. 2020.** Sources and upstream pathways of the densest overflow water in the Nordic seas. *Nature Communications* 11:5389 DOI 10.1038/s41467-020-19050-y.
- Huvenne VAI, Tyler PA, Masson DG, Fisher EH, Hauton C, Hühnerbach V, Le Bas TP, Wolff GA, Roberts JM. 2011.** A picture on the wall: innovative mapping reveals cold-water coral refuge in Submarine Canyon. *PLOS ONE* 6(12):e28755 DOI 10.1371/journal.pone.0028755.
- International Council for the Exploration of the Sea (ICES). 2020.** ICES/NAFO Joint Working Group on EU regulatory area options for VME protection (WKEUVME). Deep-water Ecology (WGDEC). *ICES Scientific Reports* 2:62 DOI 10.17895/ices.pub.6095.
- Jennings RM, Brix S, Bober S, Svarvarsson J, Driskell A. 2018.** More diverse than expected: distributional patterns of *Oecidiobranthus* Hessler, 1970 (Isopoda, Asellota) on the Greenland-Iceland-Faeroe Ridge based on molecular markers. *Marine Biodiversity* 48:845–857 DOI 10.1007/s12526-018-0857-x.
- Johnson MP, White M, Wilson A, Würzberg L, Schwabe E, Folch H, Allcock AL, Roberts JM. 2013.** A Vertical Wall Dominated by *Acesta excavata* and *Neopycnodonte zibrowii*, an undersampled Group of Deep-Sea Habitats. *PLOS ONE* 8(11):e79917 DOI 10.1371/journal.pone.0079917.
- Jöst AB, Yasuhara M, Wei C-L, Okahashi H, Ostmann A, Martinez Arbizu P, Mamo B, Svavarsson J, Brix S. 2019.** North Atlantic Gateway: test bed of deep-sea macroecological patterns. *Journal of Biogeography* 46(9):2056–2066 DOI 10.1111/jbi.13632.
- Jungersen HFE. 1917.** Alcyonarian and Madreporarian corals in the Museum of Bergen collected by the FRAM-Expedition 1898-1902 and by the ‘Michael Sars’ 1900-1906. *Bergens Museums Aarbok* 1915-1916(6):44 pp.
- Kaiser S, Brenke N. 2016.** Epibenthic sledges. In: *Biological sampling in the Deep Sea*. West Sussex: Wiley Blackwell, 184–206.

- Kartverket. 2007.** Kartverket (Norwegian Mapping Authority). Available at <http://www.kartverket.no>.
- Klitgaard AB, Tendal OS. 2004.** Distribution and species composition of mass occurrences of large-sized sponges in the northeast Atlantic. *Progress in Oceanography* 61:57–98 DOI 10.1016/j.pocean.2004.06.002.
- Leduc D, Nodder SD, Rowden AA, Gibbs M, Berkenbusch K, Wood A, De Leo F, Smith C, Brown J, Bury SJ, Pallentin A. 2020.** Structure of infaunal communities in New Zealand submarine canyons is linked to origins of sediment organic matter. *Limnology and Oceanography* 65(10):2303–2327 DOI 10.1002/lno.11454.
- Levin LA, Etter RJ, Rex MA, Goody AJ, Smith CR, Pineda J, Stuart CT, Hessler RR, Pawson D. 2001.** *Annual Review of Ecology and Systematics* 32(1):51–93 DOI 10.1146/annurev.ecolsys.32.081501.114002.
- Liu W, Federov AV, Xie S-P, Hu S. 2020.** Climate impacts of a weakened Atlantic Meridional Overturning Circulation in a warming climate. *Science Advances* 6:eaz4876 DOI 10.1126/sciadv.aaz4876.
- Lörz A-N, Kaiser S, Oldeland J, Stolter C, Kürzel K, Brix S. 2021.** Biogeography, diversity and environmental relationships of shelf and deep-sea benthic Amphipoda around Iceland. *PeerJ* 9:e11898 DOI 10.7717/peerj.11898.
- Lörz A-N, Tandberg AHS, Willassen E, Driskell A. 2018.** Rhachotropis (Eusiroidea, Amphipoda) from the North East Atlantic. Pp. 75–101 In: Brix S, Lörz A-N, Stransky B, Svavarsson J. (Eds) Amphipoda from the IceAGE-project (Icelandic marine Animals: Genetics and Ecology). *ZooKeys* 731:1–173.
- MacLeod SJ, Williams SE, Matthews KJ, Müller RD, Qin X. 2017.** A global review and digital database of large-scale extinct spreading centers. *Geosphere* 13(3):911–949 DOI 10.1130/GES01379.1.
- Madsen FJ. 1944a.** Octocorallia (Stolonifera –Telestacea –Xeniidea –Alcyonacea –Gorgonacea). *The Danish Ingolf Expedition* V(13).
- Madsen FJ. 1944b.** Octocorallia. *The Danish Ingolf Expedition. Copenhagen* 5(13):1–65.
- Maier KL, Johnson SY, Hart P. 2018.** Controls on submarine canyon head evolution: Monterey Canyon, offshore central California. *Marine Geology* 404:24–40 DOI 10.1016/j.margeo.2018.06.014.
- Mastropole D, Pickart RS, Valdimarsson H, Våge K, Jochumsen K, Girton J. 2017.** On the hydrography of Denmark Strait. *Journal of Geophysical Research: Oceans* 122:306–321 DOI 10.1002/2016JC012007.
- Mauritzen C. 1996.** Production of dense overflow waters feeding the North Atlantic across the Greenland-Scotland- Ridge. Part 1: evidence for a revised circulation scheme. *Deep Sea Research Part I* 43(6):769–806 DOI 10.1016/0967-0637(96)00037-4.
- McClain CR, Barry JP. 2010.** Habitat heterogeneity, disturbance, and productivity work in concert to regulate biodiversity in deep submarine canyons. *Ecology* 91(4):964–976 DOI 10.1890/09-0087.1.
- Melle W, Runge J, Head E, Plourde S, Castellani C, Licandro P, Pierson J, Jonasdottir S, Johnson C, Broms CMFL. 2014a.** The North Atlantic Ocean as habitat for *Calanus*

- finmarchicus*: environmental factors and life history traits. *Progress in Oceanography* **129**:244–284 DOI [10.1016/j.pocean.2014.04.026](https://doi.org/10.1016/j.pocean.2014.04.026).
- Melle W, Runge J, Head E, Plourde S, Castellani C, Licandro P, Pierson J, Jonasdottir S, Johnson C, Broms C, Debes H, Falkenhaus T, Gaard E, Gislason A, Heath M, Niehoff B, Nielsen TG, Pepin P, Stenevik EK, Chust G. 2014.** The North Atlantic Ocean as habitat for *Calanus finmarchicus*: environmental factors and life history traits. *Progress in Oceanography* **129**:224–284.
- Meyer HK, Roberts EM, Rapp HT, Davies AJ. 2019.** Spatial patterns of arctic sponge ground fauna and demersal fish are detectable in autonomous underwater vehicle (AUV) imagery. *Deep-Sea Research I* **153**:103137 DOI [10.1016/j.dsr.2019.103137](https://doi.org/10.1016/j.dsr.2019.103137).
- Meyer KS, Young CM, Sweetman AK, Taylor J, Soltwedel T, Bergmann M. 2016.** Rocky islands in a sea of mud: biotic and abiotic factors structuring deep-sea dropstone communities. *Marine Ecology Progress Series* **556**:45–57 DOI [10.3354/meps11822](https://doi.org/10.3354/meps11822).
- Morato T, Pham CK, Fauconnet L, Taranto GH, Chimienti G, Cordes E, Carreiro-Silva M, et al. 2021.** North atlantic basin-scale multi-criteria assessment database to inform effective management and protection of vulnerable marine ecosystems. *Frontiers in Marine Science* **8**:255 DOI [10.3389/fmars.2021.637078](https://doi.org/10.3389/fmars.2021.637078).
- Morato T, Pham CK, Pinto C, Golding N, Ardron JA, Duran Munoz P, Neat F. 2018.** A multi criteria assessment method for identifying Vulnerable Marine Ecosystems in the North-East Atlantic. *Frontiers in Marine Science* **5**:460 DOI [10.3389/fmars.2018.00460](https://doi.org/10.3389/fmars.2018.00460).
- Murillo FJ, Kenchington E, Tompkins G, Beazley L, Baker E, Knudby A, Walkusz W. 2018.** Sponge assemblages and predicted archetypes in the eastern Canadian Arctic. *Marine Ecological Progress Series* **597**:115–135 DOI [10.3354/meps12589](https://doi.org/10.3354/meps12589).
- Narayanaswamy BE, Bett BJ, Hughes DJ. 2010.** Deep-water macrofaunal diversity in the Faroe-Shetland region (NE Atlantic): a margin subject to an unusual thermal regime. *Marine Ecology* **31**(1):237–246 DOI [10.1111/j.1439-0485.2010.00360.x](https://doi.org/10.1111/j.1439-0485.2010.00360.x).
- Norwegian Ministry of Fisheries and Industry. 2019.** Forskrift om endring i forskrift om regulering av fiske med bunnredskap i Norges økonomiske sone, fiskerisone rundt Jan Mayen og i fiskerisone ved Svalbard, FOR-2019-03-29-416. Available at <https://lovdata.no/dokument/LTI/forskrift/2019-03-29-416>.
- Norwegian Petroleum Directorate. 2006.** Continental Shelf Submission of Norway in respect of areas in the Arctic Ocean, the Barents Sea and the Norwegian Sea. Available at https://www.un.org/depts/los/clcs_new/submissions_files/nor06/nor_exec_sum.pdf.
- Olafsdottir SH, Burgos J, Ragnarsson SA, Karlsson H. 2020.** *Kóralsvæi við Ísland. Rannsóknir 2009-2012 lýsing – útbreislá – verndun./Coral areas in Iceland, Surveys 2009-2012 description – distribution – protection.* Reykjavík: Marine and Freshwater Research Institute HV 2020-31, 84 pp. (in Icelandic).
- Olafsdóttir SH, Gudmundsson G. 2019.** *Vöktun botndýra á djúpslóumhverfis Ísland./Monitoring of benthos in deep waters around Iceland.* Reykjavík: Marine and Freshwater Research Institute HV 2019-41, 28pp. (in Icelandic).

- OSPAR. 2008. List of Threatened and/or Declining Species and Habitats. Reference number 2008-6. Available at <https://www.ospar.org/work-areas/bdc/species-habitats/list-of-threatened-declining-species-habitats>.
- OSPAR Convention. 1992. 1 Text as amended on 24 July 1998, updated 9 May 2002, 7 February 2005 and 18 May 2006. Amendments to Annexes II and III adopted at OSPAR 2007: convention for the protection of the marine environment of the North-East Atlantic. Available at https://www.ospar.org/site/assets/files/1169/pages_from_ospar_convention_a2.pdf.
- Oziel L, Baudena A, Ardyna M, Massicotte P, Randelhoff A, Sallee J-B, Ingvaldsen RB Devred, E, Babin M. 2020. Faster Atlantic currents drive poleward expansion of temperate phytoplankton in the Arctic Ocean. *Nature Communications* 11:1705 DOI 10.1038/s41467-020-15485-5.
- Paulus E, Brix S, Siebert A, Svavarsson J, Peters J, Rossel S, Martinez Arbizu P, Schwentner M. 2022. Recent speciation and hybridization in Icelandic deep-sea isopods: an integrative approach using genomics and proteomics. *Molecular Ecology* 31(1):313–330 DOI 10.1111/mec.16234.
- Puerta P, Johnson C, Carreiro-Silva M, Henry L-A, Kenchington E, Morato T, Kazanidis G, Rueda JL, Urrea J, Ross S, Wei C-L, González-Irusta JM, Arnaud-Haond S, Orejas C. 2020. Influence of water masses on the biodiversity and biogeography of Deep-Sea Benthic Ecosystems in the North Atlantic. *Marine Science* 7:239 DOI 10.3389/fmars.2020.00239.
- Ragnarsson SÁ, Burgos JM. 2018. Associations between fish and cold-water coral habitats on the Icelandic shelf. *Marine Environmental Research* 136:8–15 DOI 10.1016/j.marenvres.2018.01.019.
- Ramírez-Llodra E, Brandt A, Danovaro R, Mol BD, Escobar E, German CR, Levin LA, Martinez Arbizu P, Menot L, Buhl-Mortensen P, Narayanaswamy BE, Smith CR, Tittensor DP, Tyler PA, Vanreusel A, Vecchione M. 2010. Deep, diverse and definitely different: unique attributes of the world's largest ecosystem. *Biogeosciences* 7(9):2851–2899 DOI 10.5194/bg-7-2851-2010.
- Ramírez-Llodra E, Hilário A, Paulsen E, Costa CV, Bakken T, Johnsen G, Rapp HT. 2020. Benthic communities of the Mohn's Treasure Mound: implications for management of seabed mining in the Arctic Mid-Ocean Ridge. *Frontiers in Marine Science* 7:490 DOI 10.3389/fmars.2020.00490.
- Rex MA, Etter RK. 2010. Deep-Sea biodiversity: pattern and scale. *BioScience* 61(4):327–328.
- Rex MA, Etter RJ, Morris JS, Crouse J, McClain CR, Johnson NA, Stuart CT, Deming JW, Thies R, Avery R. 2006. Global bathymetric patterns of standing stock and body size in the deep-sea benthos. *Marine Ecology Progress Series* 317:1–8 DOI 10.3354/meps317001.
- Riehl T, Brenke N, Brix S, Driskell A, Kaiser S, Brandt A. 2014. Field and laboratory methods for DNA studies on deep-sea isopod crustaceans. *Polish Polar Research* 35(2):205–226.

- Riehl T, Wöfl AC, Augustin N, Devey CW, Brandt A. 2020.** Discovery of widely available abyssal rock patches reveals overlooked habitat type and prompts rethinking deep-sea biodiversity. *Proceedings of the National Academy of Sciences of the United States of America* **117**(27):15450–15459 DOI [10.1073/pnas.1920706117](https://doi.org/10.1073/pnas.1920706117).
- Roberts EM, Bowers DG, Meyer HK, Samuelsen A, Rapp HT, Cardenas P. 2021.** Water masses constrain the distribution of deep-sea sponges in the North Atlantic Ocean and Nordic seas. *Marine Ecology Progress Series* **659**:75–96 DOI [10.3354/meps13570](https://doi.org/10.3354/meps13570).
- Roberts EM, Mienis F, Rapp HT, Hanz U, Meyer HK, Davies AJ. 2018.** Oceanographic setting and short-timescale environmental variability at an Arctic seamount sponge ground. *Deep-Sea Research I* **138**:98–113 DOI [10.1016/j.dsr.2018.06.007](https://doi.org/10.1016/j.dsr.2018.06.007).
- Rooks C, Fang JKH, Mørkved PT, Zhao R, Rapp HT, Xavier JR, Hoffmann F. 2020.** Deep-sea sponge grounds as nutrient sinks: high denitrification rates in boreo-arctic sponges. *Biogeosciences* **17**:1231–1245 DOI [10.5194/bg-17-1231-2020](https://doi.org/10.5194/bg-17-1231-2020).
- Rothlisberg PC, Percy WG. 1977.** An epibenthic sampler used to study the ontogeny of vertical migration of *Pandalus jordani*, (Decapoda, Caridea). *Fishery Bulletin* **74**:994–997.
- Schlacher TA, Schlacher-Hoenlinger MA, Williams A, Althaus F, Hooper JNA, Kloser R. 2007.** Richness and distribution of sponge megabenthos in continental margin canyons off southeastern Australia. *Marine Ecology Progress Series* **340**:73–88 DOI [10.3354/meps340073](https://doi.org/10.3354/meps340073).
- Schnurr S, Osborn KJ, Malyutina M, Jennings R, Brix S, Driskell A, Svavarsson J, Arbizu PM. 2018.** Hidden diversity in two species complexes of munnopsid isopods (Crustacea) at the transition between the northernmost North Atlantic and the Nordic seas. *Marine Biodiversity* **48**(2):813–843 DOI [10.1007/s12526-018-0877-6](https://doi.org/10.1007/s12526-018-0877-6).
- Semper A, Våge KS, Pickart RS, Valdimarsson H, Torres DJ, Jónsson S. 2019.** The emergence of the North Icelandic jet and its evolution from Northeast Iceland to Denmark Strait. *American Meteorological Society* **49**:2499–2521.
- Semper S, Pickart RS, Våge K, Larsen KMH, Hátún H, Hansen B. 2020.** The Iceland-Faroe Slope Jet: a conduit for dense water toward the Faroe Bank Channel overflow. *Nature Communications* **11**:5390 DOI [10.1038/s41467-020-19049-5](https://doi.org/10.1038/s41467-020-19049-5).
- Straume EO, Gaina C, Medvedev S, Hochmuth K, Gohl K, Abdul Whittaker JM, Fattah R, Doornenbal JC, Hopper JR. 2019.** GlobSed: updated total sediment thickness in the world's oceans. *Geochemistry, Geophysics, Geosystems* **20**:1756–1772 DOI [10.1029/2018GC008115](https://doi.org/10.1029/2018GC008115).
- Svavarsson J, Strömberg J-O, Brattegard T. 1993.** The deep-sea asellote (Isopoda, Crustacea) fauna of the Northern Seas, species composition, distributional patterns and origin. *Journal of Biogeography* **20**:537–555 DOI [10.2307/2845725](https://doi.org/10.2307/2845725).
- Swift JH, Aagaard K. 1982.** Seasonal transitions and water mass formation in the Iceland and Greenland seas. In: *Deep Sea Research Part A: Oceanographic research papers*. vol. 28. 1107–1129 DOI [10.1016/0198-0149\(81\)90050-9](https://doi.org/10.1016/0198-0149(81)90050-9).
- Talwani M, Eldholm O. 1977.** Evolution of the Norwegian-Greenland Sea. *GSA Bulletin* **88**:969–999 DOI [10.1130/0016-7606\(1977\)88<969:EOTNS>2.0.CO;2](https://doi.org/10.1130/0016-7606(1977)88<969:EOTNS>2.0.CO;2).

- Tendal OS. 1992.** The North Atlantic distribution of the octocoral *Paragorgia arborea* (L. 1758) (Cnidaria, Anthozoa). *Sarsia* 77(3–4):213–217
DOI [10.1080/00364827.1992.10413506](https://doi.org/10.1080/00364827.1992.10413506).
- Uenzelmann-Neben G, Jokat W, Miller H, Steinmetz S. 1992.** The Ægir Ridge: structure of an extinct spreading axis. *Journal of Geophysical Research* 97:9203–9218
DOI [10.1029/91JB03096](https://doi.org/10.1029/91JB03096).
- Uhlir C, Schwentner M, Meland K, Kongsrud JA, Glenner H, Brandt A, Thiel R, Svavarsson J, Lörz A-N, Brix S. 2021.** Adding pieces to the puzzle: insights into diversity and distribution patterns of Cumacea (Crustacea: Peracarida) from deep northern waters. *PeerJ* 9:e12379 DOI [10.7717/peerj.12379](https://doi.org/10.7717/peerj.12379).
- Våge K, Pickart RS, Spall MA, Valdimarsson H, Jónsson S, Torres DJ, Østerhus S, Eldevik T. 2011.** Significant role of the North Icelandic Jet in the formation of Denmark Strait overflow water. *Nature Geoscience* 4:723–727 DOI [10.1038/ngeo1234](https://doi.org/10.1038/ngeo1234).
- Vanreusel A, Fonseca G, Danovaro R, Da Silva MC, Esteves AM, Ferrero T, Gad G, Galtsova V, Gambi C, Da Fonsêca Genevois V, Ingels J, Ingole B, Lampadariou N, Merckx B, Miljutin D, Miljutina M, Muthumbi A, Netto S, Portnova D, Radziejewska T, Raes M, Tchesunov A, Vanaverbeke J, Van Gaever S, Venekey V, Bezerra TN, Flint H, Copley J, Pape E, Zeppilli D, Martinez PA, Galeron J. 2010.** The contribution of deep-sea macrohabitat heterogeneity to global nematode diversity. *Marine Ecology* 31(1):6–20 DOI [10.1111/j.1439-0485.2009.00352.x](https://doi.org/10.1111/j.1439-0485.2009.00352.x).
- Vetter EW, Smith CR, De Leo FC. 2010.** Hawaiian hotspots: enhanced megafaunal abundance and diversity in submarine canyons on the oceanic islands of Hawaii. *Marine Ecology* 31(1):183–199.
- Ware S, Downie AL. 2020.** Challenges of habitat mapping to inform marine protected area (MPA) designation and monitoring: an operational perspective. *Marine Policy* 111:103717 DOI [10.1016/j.marpol.2019.103717](https://doi.org/10.1016/j.marpol.2019.103717).
- Weisshappel JBF. 2000.** Distribution and diversity of the hyperbenthic amphipod family Eusiridae in the different seas around the Greenland-Iceland-Faeroe-Ridge. *Sarsia* 85(3):227–236 DOI [10.1080/00364827.2000.10414575](https://doi.org/10.1080/00364827.2000.10414575).
- Weisshappel JBF. 2001.** Distribution and diversity of the hyperbenthic amphipod family Calliopiidae in the different seas around the Greenland-Iceland-Faeroe-Ridge. *Sarsia* 86(2):143–151 DOI [10.1080/00364827.2001.10420469](https://doi.org/10.1080/00364827.2001.10420469).
- Weisshappel JBF, Svavarsson J. 1998.** Benthic amphipods (Crustacea: Malacostraca) in Icelandic waters: diversity in relation to faunal patterns from shallow to intermediate deep Arctic and North Atlantic Oceans. *Marine Biology* 131:133–143
DOI [10.1007/s002270050304](https://doi.org/10.1007/s002270050304).
- Wöfl AC, Snaith H, Amirebrahimi S, Devey CW, Dorschel B, Ferrini V, Huvenne VAI, Jakobsson M, Jencks J, Johnston G, Lamarche G, Mayer L, Millar D, Pedersen TH, Picard K, Reitz A, Schmitt T, Visbeck M, Weatherall P, Wigley R. 2019.** Seafloor Mapping—the challenge of a truly global ocean bathymetry. *Frontiers in Marine Science* 6:283 DOI [10.3389/fmars.2019.00283](https://doi.org/10.3389/fmars.2019.00283).

Navigating paths through science as early career researchers: A WCMB panel discussion

Navigating the winding, complicated, uncertain path through science can be stressful even for seasoned scientists, and often completely overwhelming for early career researchers. A useful method to provide a roadmap for this path is to learn from those who have walked it before you. With this in mind, we hosted a panel at the 5th World Conference on Marine Biodiversity with Maria Dornelas, Graham Edgar, Madeleine van Oppen, and Moriaki Yasuhara to discuss their paths through marine science and offer advice to early career researchers. Here, we share the stories, recommendations, and advice they conveyed to the audience during the panel.

Trevyn Toone, Elin Thomas, Georgia Sarafidou, and Ariadna Nocera

Members of the WCMB Early Career Committee



Prof Madeleine van Oppen



Dr Maria Dornelas



Dr Moriaki Yasuhara



Prof Graham Edgar

The adage that one's journey through life is never straight was exemplified by our panellists' routes from their doctorates to their current positions. Dr. Edgar was quick to volunteer that he has never had a permanent job, rather bouncing between fellowships and contract positions. This path was not without its downsides including a lack of job security; however, he enjoys the freedom it allows to shift between different interesting ideas. Dr. Dornelas's career has also followed a winding path including a series of postdocs, a child, and multiple moves before her position at the University of St. Andrews. Dr. Yasuhara moved to the U.S. from Japan as a postdoc before moving back to East Asia to take up his current position in Hong Kong. This multi-national journey was shared by Dr. van Oppen who moved between the Netherlands, England, and Australia for various opportunities before ultimately negotiating her current Australian position.

All four panellists agreed that the most successful students were not necessarily the ones with the highest grades, but rather the ones who were curious about the world around them.

Along these paths each of our panellists identified key turning points in their career as largely being acts of serendipity that led them to discover their talents and passions. For Dr. van Oppen this was learning RNA sequencing in her masters which would be vital to future research, while for Dr. Edgar it was a trip to the Galapagos as a postdoc that broadened his perspectives. For Dr. Dornelas her career turning point was largely defined by discovering what she enjoyed (field work and modelling) and what she did not (lab work) and then building her career along those lines. Dr. Yasuhara, on the other hand, uncovered his skill and passion for deep-sea biology later in his career as a postdoc, a discovery which he credits as shaping the rest of his career.

Looking back on their careers, our panellists were largely in agreement about which skills were most useful to them. While hard skills were important, they unanimously identified soft skills - primarily creativity and drive - as the most useful to develop as an early career researcher. Dr. van Oppen specifically mentioned not being afraid to push the boundaries of science while Dr. Dornelas commented on the importance of building a space that allows for creativity to flourish. All four panellists agreed that the most successful students were not necessarily the ones with the highest grades, but rather the ones who were curious about the world around them.

Opening the door for others when you receive fortuitous opportunities, then, becomes not just a matter of kindness but of fairness.

When it came to the role of serendipity on their path through science our panellists were quick to point out the importance of luck, but also noted that taking advantage of opportunities is a skill itself. Being in the right place at the right time is important, but it takes skill to recognize which opportunities are the good ones, and how best to harness these. Dr. Dornelas also noted the role privilege plays in these discussions and the importance of considering who is even allowed into the right room. Opening the door for others when you receive fortuitous opportunities, then, becomes not just a matter of kindness but of fairness.

For many young scientists, particularly new Ph.D. students, starting a path in research can seem like one long stream of criticism and rejections. On this front our panellists were unanimous - science is a marathon not a sprint, and it is vital to focus on your successes and future rather than drowning in negative feedback. Dr. Dornelas connected this perceived 'cycle of failure' with imposter syndrome and noted that sometimes ideas that initially get

rejected blossom into successful projects years or even decades later. She also emphasized the importance of effectively filtering feedback.

The impact of a good mentor is impossible to overstate and many, if not most, researchers can point to mentors in their past who shaped their career in science. Our panellists were quick to note the wide range of relationships and interactions that can constitute mentorship, from fully supervisory positions to short conversations between colleagues at conferences. Dr. Dornelas suggested viewing mentors not as those opening doors for someone but rather as any flow of advice, meaning mentors can be anyone who is more familiar with certain systems, not just established researchers or older individuals. Dr. van Oppen suggested prioritizing mentors outside of your own field to avoid bias in perspectives, as well as noting the importance of peer-to-peer mentorship.

Science is a marathon not a sprint, and it is vital to focus on your successes and future rather than drowning in negative feedback.

For early career researchers just starting on their path through science, our panellists emphasized the importance of learning skills outside your comfort zone. For example, seeking colleagues within your lab who can help teach new techniques or connecting with someone outside the lab who can bring in new ideas.

Looking to the future, we asked our panellists how they stay positive in a field like conservation and marine biodiversity where trends can often be negative. The responses ranged from the metaphysical (“the Great Barrier Reef did not exist 2 million years ago and will not exist in 2 million years”) to the eminently practical (“go for a walk”). Overall, however, the panellists agreed that passion for the environment and the world around us can motivate any researcher to look past the negatives and embrace the future.

Finally, we offered each of our panellists the opportunity to provide one final piece of advice to early career researchers. Dr. van Oppen recommended studying statistics and developing the quantitative skills that are necessary for wrangling the large data sets that have come to define conservation science, while Dr. Moriaki advised having a strong skin and not worrying about rejection. Dr. Edgar recommended broadening horizons and generalizing results to larger audiences. Dr. Dornelas, on the other hand, was succinct: “be curious, and be stubborn”.

Our paths through life and through science are circuitous, but hopefully the thoughts and words of our panellists will be inspiring and helpful to early career researchers. We want to

offer our sincerest thanks to WCMB for organizing and allowing us to host this event and, of course, to the four wonderful panellists for sharing their time and thoughts.

Dr Maria Dornelas is the Deputy Director of the Centre of Biological Diversity at the University of St Andrews in the UK.

Professor Madeleine van Oppen is an Australian Research Council Laureate Fellow at the University of Melbourne and the Australian Institute of Marine Science.

Professor Graham Edgar is a Senior Research Fellow at the Institute for Marine and Antarctic Studies at the University of Tasmania.

Dr Moriaki Yasuhara is an Associate Professor of Environmental Science at the School of Biological Sciences and the Swire Institute of Marine Science at the University of Hong Kong.

Navigating Early Careers as Women in Marine Science:

A WCMB panel discussion

Every scientist transitions through the initial phases of their career as an early career researcher. It is a challenging career phase, marked by numerous transitions, short term contracts and a lot of uncertainty. In addition, navigating this phase as women in marine science can bring extra challenges of its own. To provide guidance and advice, the brilliant Dr. Suchana Apple Chavanich, Dr. Lisa Levin, Dr. Patricia Miloslavich, and Dr. Amanda Bates accepted our invitation to be panellists in a forum specifically for female early career researchers at the 5th World Conference of Marine Biodiversity. During an online panel discussion with over seventy participants, they answered moderator and audience questions relating to women's early careers in science. The four accomplished panellists shared their own experiences and thoughts on the early career process.

Emilee D. Benjamin, Erin Satterthwaite, Priscila M. Salloum, Jasmin M. Schuster

Members of the WCMB Early Career Committee



Dr. Suchana Apple
Chavanich



Dr. Lisa Levin



Dr. Patricia Miloslavich



Dr. Amanda Bates

What was your path from early career researcher to the permanent academic position you now hold?

The panellists shared their journey from their PhDs to their current position, which included overcoming challenges like moving to different places and failed job applications. Dr. Bates said she wanted to travel the world, so had some breaks from academia, but she always ended up returning to science. Dr. Miloslavich did not have such gaps, but moved to a number of different countries for postdocs and research, while raising her three children with her husband. Dr. Levin changed to a slightly different field, from zoology to oceanography,

after working as a consultant and realizing she was much happier in science. From their answers, it was clear that it can be hard to make decisions such as coming in and out of academia, moving places and changing fields, but the answers of all panellists echoed the essence of what has really driven them through their journeys: a passion for science.

How have you balanced life with your career?

Women in particular face a lot of pressure to balance life and career, and women scientists are no exception. The panellists agreed that it is hard to balance having enough time for your kids, spouse, students, and research, but Dr. Levin emphasized that it is important to not be hard on yourself and to understand that you are doing the best you can. Dr. Miloslavich added that having a supportive partner is important, but that Moms are priceless when it comes to childcare. She acknowledged that when your children are young it can be difficult to balance your life and your career, but she also said that, "It isn't going to be easy, but it can be done." Dr. Bates added that it is important to know yourself and to put energy into what is important for you, so you can enjoy those things.

What would be important on a CV for getting a postdoc?

A central piece of advice from panellists was to be open to opportunities and work in a collaborative way. The panellists suggested that building relationships, being open to opportunities, and making sure to work in a connected, networked way is essential. Dr. Bates also suggested that you often can't predict what someone is looking for by the job description. She encouraged recent grads to explore many career options in different sectors.

Do you have any advice for people that are trying to move from the postdoc loop to a permanent position?

The panellists highlighted the importance of multidimensionality in this context. Dr. Levin advised accepting opportunities that give you new skills, especially if you have multiple choices available to you; choose the ones that add something new to your skillset. She added that, "After all, a range of skills could lead to your dream job."

In times where you felt it was hard to be a woman in academia what kept you going?

It can be hard being a woman working among male colleagues, and Dr. Chavanich agrees with that. But she said that she was inspired by Sylvia Earle, and that having role models, as well as using whatever support from resources available in your institution can help. Dr. Levin said that there was not much institutional support when she was an early career researcher, and that women used to sacrifice everything, including family, for their careers. However, she had a close group of female friends that supported each other. Thus, regardless of where support is coming from, it is key to face those hard moments, and reach out for support - nobody should feel alone.

The audience brought to the discussion a recently retracted article that suggested female mentorship can negatively affect career paths, both for mentors and mentees.

Dr. Bates responded by emphasizing that people can have a great mentorship relationship regardless of gender. She went on to say that we often look for people we want to emulate

and, as women, we sometimes look to other women. She mentioned she has had both male and female mentors that have helped her in different ways.

How can we be more inclusive and diversify science in general?

A conscious effort to include underrepresented groups was highlighted as essential across the panellists. Diversity is something that we should consciously include in everything that we do since it is such an important, cross-cutting theme. The panellists emphasized the importance of enhancing the participation of underrepresented groups in all facets of our work as scientists, such as in guest lectures, working groups, publications, who we cite etc.

How do you deal with patronizing comments from male colleagues?

Early career researchers and especially women and minorities, often have to deal with patronizing comments. Whilst the panellists say there is no single answer for how to respond to being patronized, they highlight that responses need to be tailored to the situation, such as if you are being patronized by a professor, a colleague, or your advisor. Yet, regardless of the source, being honest and making your boundaries and standpoint clear, whilst remaining respectful was advised.

What can we do to be more inclusive of non-native English speakers?

As a non-native English speaker, Dr. Chavanich recognised how important it is to allow ourselves to be exposed to foreign scientists, and to eventually get in tune with different accents. She highlighted that collaboration with other countries is important, so we have to network and break the language barrier to move our research and career forward. She said that, in her experience, exposing herself to work more often with foreigners made communication become easier than expected. On the other side of the spectrum, Dr. Levin advised native English speakers to be conscious of the speed that they normally talk at, and give space for foreign speakers to talk as well.

Did you have to sacrifice anything throughout your career?

This question was answered first by Dr. Bates by advising attendees to decide what is most important to them. She shared that she was one of the first people in Canada to be given maternity leave and she was extremely grateful for that. She also shared that she spaced her kids out by 6 years which helped with her career. Dr. Levin shared that she luckily did not have to sacrifice anything for her family but that she regrets that she has not been to Antarctica.

If you had one piece of advice to early career researchers, what would it be?

When asked about one piece of advice for early career researchers, panellists agreed that being passionate, positive, and confident is critical. The panellists mentioned that it is important to be confident in your work, know your own worth and sustain a positive attitude. Dr. Chavanich added that having the skills to take great photos of your work is very important for scientists right now. To round the question off, Dr. Levin advised to be compassionate and take time to help others, which in some way, will have a big impact on yourself and others.

Any last-minute words of advice, specifically for women in science?

The session closed with some final words by Dr. Miloslavich who said: “Your body is strong now and you have the ability to do things that you won't be able to do in 20 years; enjoy your life, do sports, dance, read, go hiking, take time for yourself and keep your body young in spirit as long as you can.”

Dr. Suchana Apple Chavanich is an Associate Professor at the Centre of Excellence for Marine Biology at Chulalongkorn University in Thailand.

Dr. Lisa Levin is a Distinguished Professor at the Centre for Marine Biodiversity and Conservation at the Scripps Institution of Oceanography in San Diego (USA), and a founding member of the Deep-Ocean Stewardship Initiative.

Dr. Patricia Miloslavich is the Executive Director of the Scientific Committee on Oceanic Research (SCOR), based at the College of Earth, Ocean and Atmosphere at the University of Delaware, USA.

Dr. Amanda Bates is an Associate Professor and Canada Research Chair in Marine Physiological Ecology at Memorial University of Newfoundland, Canada.

[PeerJ Awards Winners at the 5th World Conference on Marine Biodiversity](#)

The PeerJ Awards program aims to support students and early career researchers by highlighting their work, as well as bringing continued awareness to the benefits that open access has in keeping science open and available to all.

PeerJ sponsored four Early Career Researchers awards at the 5th WCMB – two for presentations and two for posters – the winners of each receiving a free publication in any PeerJ journal (subject to peer review).



**5th World Conference
on Marine Biodiversity**
AUCKLAND | 13-16 DECEMBER 2020

Can you tell us a bit about yourself and your research interests?

I'm originally from Taiwan, now doing my PhD with Dr. Rebecca Fox and Dr. Michael Jennions at the Australian National University. I'm interested in the feeding preferences of reef fishes, and how much production they can access from epifaunal invertebrates in tropical seascapes.



Can you briefly explain the research you presented at the WCMB conference?

I've presented one chapter of my PhD thesis which was about the secondary production from macroalgae-associated epifaunal invertebrates. I've found that epifaunal production was positively correlated to macroalgal canopy size, and can be affected by predatory fish biomass and sea temperature. I've also found that epifaunal production was sensitive to environmental disturbances. Understanding how epifaunal production response to changing habitats can help us model the consequences of marine warming events.

What first interested you in this field of research?

I was born and raised in Taiwan, a beautiful island surrounded by seas which is famous for its amazing marine biodiversity. I've been obsessed with marine animals since I was a child.

How did you find the virtual conference experience?

I'm still trying to get used to this new trend. Missing the chance of attending the conference and meeting outstanding people in person was quite frustrating. But I did find that this time I was able to watch all the talks I was interested in. I was also motivated by everybody's passion for marine research that can not be stopped by COVID-19.

What are your next steps? How will you continue to build on this research?

My next step is to estimate how much epifaunal production can be consumed by carnivorous fishes, by conducting underwater caging experiments. Since most carnivorous fishes in tropical seascapes are fishery targets or recreational species, results of my study can be used to help marine habitat management and conservation.

Ariadna Nocera PhD candidate at the National University of Patagonia San Juan Bosco - CONICET, Argentina

Can you tell us a bit about yourself and your research interests?

I'm a marine biologist from Argentina who later specialized in biological oceanography in Canada. In 2018 I started my PhD focused on zooplankton dynamics in coastal marine ecosystems in northern Patagonia. I'm interested in how these organisms that are fundamental for marine food webs can change under future possible scenarios, but first it is important to update the baseline studies.



Can you briefly explain the research you presented at the WCMB conference?

I presented the most recent data from the Valdés Biosphere Reserve, corresponding to the composition and abundance of zooplankton in relation to environmental variables. This involved sampling at sea and the identification of hundreds of organisms under a stereo microscope.

What first interested you in this field of research?

I think I was always curious about how small organisms can have such a big influence on other larger organisms, and even on an entire marine ecosystem. I started the study through modeling and now looking more closely at their characteristics, morphologies and behavioral differences allow me to pose new questions that motivate even more my interest in these incredible organisms.

How did you find the virtual conference experience?

Even if there is still less interaction between researchers when compared to an in-person one, the virtual conference gave me the opportunity to participate at WCMB that otherwise would have been more difficult due to the distance and travel costs. It also allowed me to be part of the Early Career Researcher Committee, which organized two different panels during the conference, while interacting with young researchers from different countries. It was definitely a very positive experience and I recommend it!

What are your next steps? How will you continue to build on this research?

The next steps in my research are to continue gathering more data about plankton community composition and distribution over the coming year to strengthen and complete my thesis. In addition, I have planned to carry out experiments to evaluate the effect of atmospheric dust on zooplankton and, finally, to carry out a numerical model for the area with all the information gathered from the fieldwork and experiments.

Trevyn Toone Ph.D. Candidate at the University of Auckland, New Zealand

Can you tell us a bit about yourself and your research interests?

I'm a marine ecologist interested in how we can merge ecology, conservation, and restoration to improve coastal environments. I grew up in coastal North Carolina near salt marshes, shellfish reefs, and seagrass beds, inspiring a career in conserving these ecologically and culturally vital ecosystems. My current work focuses on mussel beds and how we can most successfully restore lost shellfish reefs via scientifically supported methods including harnessing positive species interactions, improving early life stage retention, and minimizing stressors.



Can you briefly explain the research you presented at the WCMB conference?

I presented the first stage of my work in Kenepuru Sound, an area at the top of New Zealand's South Island. The Kenepuru was historically an area with dense and healthy mussel reefs along much of the shoreline, but those populations have been decimated in the last fifty years leading to calls for restoration. My project sought to find the exact extent of this loss, as well as potential causes. We pinpointed the cause of the depletion to commercial handpicking, which began in the late 1960's. Our results also suggest a number of factors that may be responsible for a continued lack of recovery since the end of handpicking, including loss of settlement surfaces, predation, and sedimentation.

What first interested you in this field of research?

Growing up on the coast I've always been interested in the ocean and the fascinating ecosystems it creates. In my undergrad I was introduced to the world of ecology and how species interactions and connections build the world around us. From there I was hooked on research and finding out ways to use ecological principles to conserve and restore the ecosystems I first fell in love with growing up.

How did you find the virtual conference experience?

The virtual conference experience was never going to perfectly replicate an in-person event, but if 2020 has taught us anything it's that adaptability and change are sometimes necessary. I particularly liked being able to go back and rewatch talks after they initially aired as it opened the door to seeing talks in sessions I wasn't able to attend the first time. While the networking aspect of a virtual conference will never be the same as an in-person experience, I still

enjoyed WCMB and wouldn't have been able to create the presentation I did without the virtual environment.

What are your next steps? How will you continue to build on this research?

My next steps are building on the results of this project. Shoreline resurveys and interviews with residents have confirmed the need for successful restoration and provided valuable information on where to start these efforts. Specifically my next project will focus on improving recruitment success for mussels which was one of the most commonly identified problems during my interviews. After that I plan on trialing restoration methods for intertidal mussels and looking beyond shellfish to other coastal ecosystems.

If you want to watch Trevyn's presentation, it has been [uploaded to YouTube](#).

Ohad Peleg PhD candidate at the University of Auckland, New Zealand

Can you tell us a bit about yourself and your research interests?

I am a marine ecologist studying shallow temperate reef ecosystems. My study focuses on how human stressors, such as overfishing and sedimentation, affect kelp forest ecosystem health and stability.



Can you briefly explain the research you presented at the WCMB conference?

Phase shifts from kelp forests to unforested ecosystem states due to anthropogenic activities are widely considered a catastrophic decline in ecosystem health on temperate reefs. Using 20 years of monitoring data from inside and outside New Zealand's oldest marine reserve, I demonstrated that by protecting sea urchin predators, long-term marine reserve protection can promote more stable and healthier kelp forest ecosystems. In contrast, unprotected sites lacked stability and fluctuated between less healthy urchin barren and algal turf states. Remediation, however, can take decades, and it is unclear whether this will be possible under future climatic scenarios. Therefore, prompt protection of larger reef areas is strongly advised.

How did you find the virtual conference experience?

Given the current world pandemic, being able to meet and have an excellent conference cannot be taken for granted. With such an outstanding line-up of speakers and presenters communicating excellent top-notch science, I did not have any expectation to win a prize, and I am stoked and humbled to have won the award for the Best ECR presentation (speed-talk). I am also delighted to have won the best 'story' photograph for my photo titled 'the battlefield'

showing sea urchins grazing on kelp. I wish to thank the participants, organisers, and sponsors for an outstanding conference, and for these awards and prizes.

What are your next steps? How will you continue to build on this research?

I hope my study can promote marine protection and kelp forest ecosystem restoration and thereby its health. Communicating this work is, therefore, extremely important. Currently, I am looking for a postdoctoral opportunity on kelp forest ecosystem ecology and human impacts.

Dr. Shang Yin Vanson Liu discusses the role Dongsha Atoll plays in connecting the coral reefs of the South China Sea

Can you tell us a bit about yourself?

Hi, I am Dr. Shang Yin Vanson Liu, currently an associate professor at the Department of Marine Biotechnology and Resources, National Sun Yat-sen University. I am a molecular ecologist and have an interest in marine biodiversity and the evolutionary processes of reef organisms.



Can you briefly explain the research you published in PeerJ?

Well, this study is an international collaboration of marine biologists and students from Taiwan, the United States, Sweden and Indonesia funded by NSC (National Science Council, US) and MOST (Ministry of Science and Technology, Taiwan) who were interested in understanding the role that Dongsha Atoll plays in connecting the coral reefs of the South China Sea (SCS). Dongsha Atoll, located 340 km southeast of Hong Kong and 850 km southwest of Taipei, with an area of about 600 km², is the largest and oldest atoll in the South China Sea.

In this study, by comparing DNA sequences obtained from 9 reef species collected at Dongsha atoll with sequences from nearby populations in a database compiled by DIPnet, we found that species with larvae that spend a relatively short duration in the plankton (< 40 days) tend to rely on Dongsha as a critical stepping-stone that connects SCS reefs which indicate its' importance in term of marine connectivity in the SCS.

Do you have any anecdotes about this research?

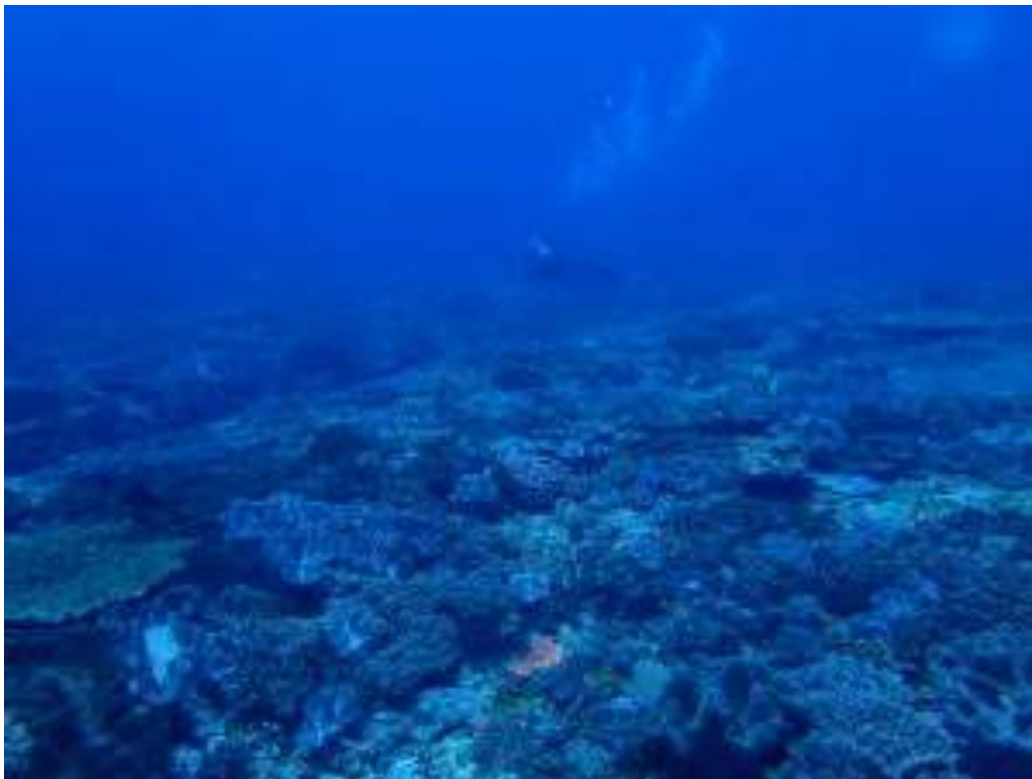
The data collecting of this study was done by a group of students from California State University, Monterey Bay and National Sun Yat-sen University under the supervision of Dr. Eric Crandall and I. It was fun to see how this joint project impacts their career and with interesting findings and fruitful results. The field trip led by scientists from three nations in 2017 to the Dongsha atoll was also amazing, Dongsha Atoll Research Station (DARS) is equipped with well-established facilities and equipment that we need for sampling with SCUBA (<https://dongsha-mr.nsysu.edu.tw/>) around the atoll and the diversity and coral coverage was stunning.

What kinds of lessons do you hope your readers take away from the research?

This multispecies study provides the most comprehensive examination of the role of Dongsha Atoll in marine connectivity in the South China Sea to date. Combining new and existing population genetic data for nine coral reef species in the region with a graph theoretical analysis, this study provides evidence that Dongsha Atoll is an important hub for sustaining connectivity for the majority of coral-reef species in the region.

Do you have any comments about your overall experience with us?

I have 4 papers published in PeerJ including this study, and definitely will submit again since the review process is transparent and fair under the handling editors in the field of aquatic biology.





PeerJ
Life & Environment